HYDRODYNAMIC LOADING AND DESIGN ASPECTS OF OFFSHORE JACKET PLATFORMS

by

MOHAMED ELNOUR ABDELRADI BSc CEng MIME

This thesis is submitted for the degree of Doctor of Philosophy in the Department of Naval Architecture and Ocean Engineering, University of Glasgow.

Great Britain November 1984

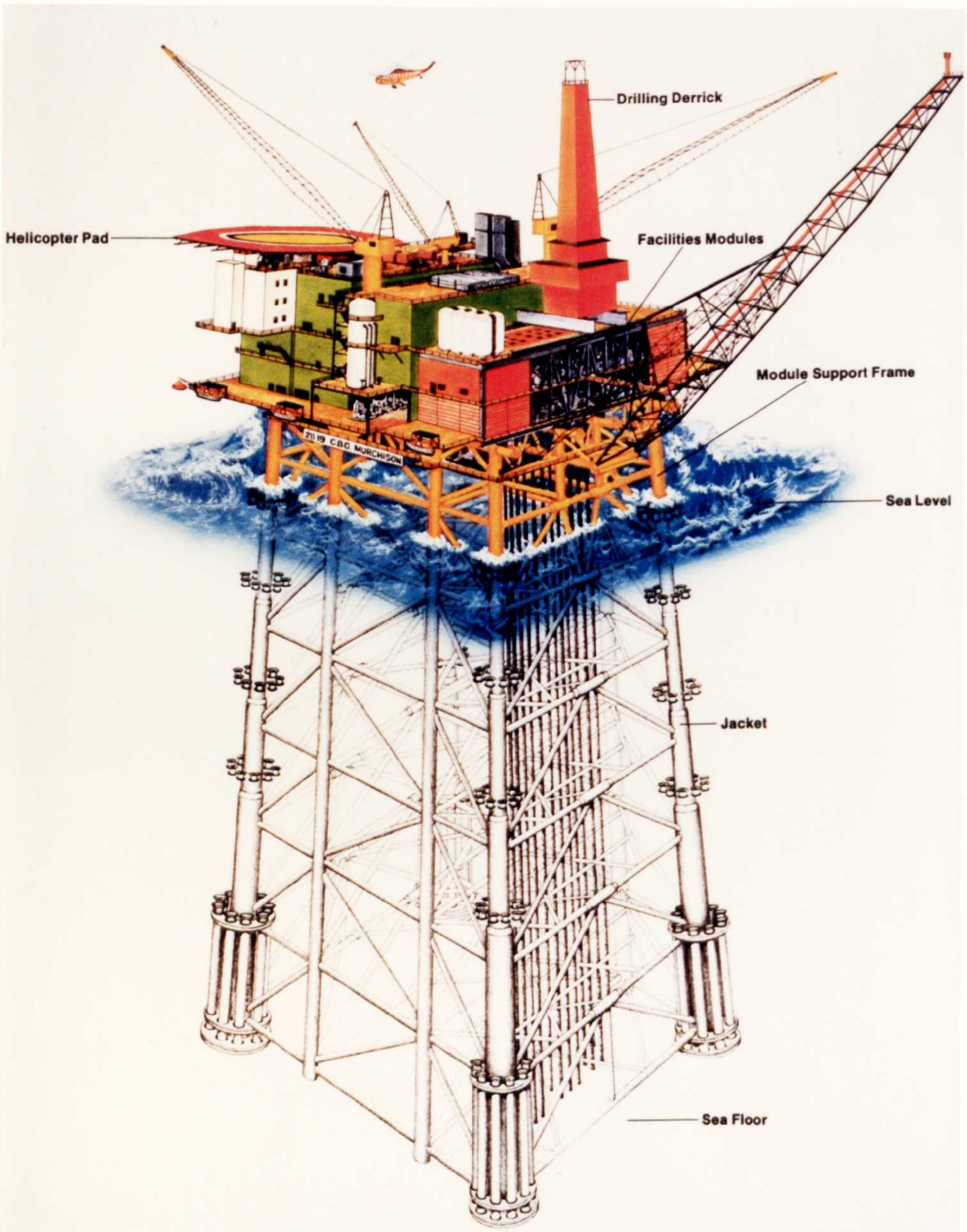

Murchison Field Production Platform

DEDICATION

TO THE MEMORY OF MY PARENTS

DECLARATION

Apart from reference to the work of others this thesis is believed to be original.

ACKNOWLEDGEMENT

I wish to thank Professor D Faulkner, head of the Department of Naval Architecture and Ocean Engineering, University of Glasgow for his assistance and the technical material he made available to me.

My deepest gratitude to my supervisor, Mr N S Miller for his help and advice in planning, carrying out and reviewing this thesis. Without his continuous encouragement, support and suggestions, this work could not have been achieved.

I would like also to thank Mrs Clare MacEachen, Computer Manager, Hydrodynamics Laboratory, for her help in developing the computer programs.

I am very grateful to Mr and Mrs E Peters for their patience and care in typing this thesis.

I wish also to express my thanks and appreciation to all teaching and research staff and technicians in the Hydrodynamics Laboratory who have contributed in one way or another to make this work possible.

Finally, I am greatly indebted to the Arab Maritime Transport Academy, Alexandria, Egypt who granted me the opportunity to do this work and has provided all the financial support during the course of the study.

CONTENTS

SUMMARY

The design aspects of offshore jacket structures are presented and discussed with a special emphasis on the different factors which affect wave loading calculations for these structures.

An up-to-date review of a large amount of data on the hydrodynamic coefficients obtained from Laboratory experiments and wave projects is presented and the main data are tabulated.

To assess the different aspects of the wave loading a set of computer programs were developed and used to perform various comparative studies for the existing methods of wave loading estimation. The analysis of the wave loading was carried out using a jacket structure of 119 members having 73m x 73m base representing a typical offshore platform, assumed to be working in 150m of water.

The general method of wave loading calculation is based on Morison's equation taking into account the phase differences between the velocities and accelerations of the wave particles. The relative positions of the different members in space and time when the wave passes through the jacket were also considered. Besides the drag and inertia forces, the lift (transverse) forces are also taken into account.

The kinematics of the flow can be determined using Airy (linear) wave theory, Stokes 2nd order theory or Stokes 5th order theory. Constant drag and inertia coefficients (C_D, C_M), as recommended by Lloyd's Register of Shipping (LR), Det Norkse Veritas (DnV) and Bureau Veritas (BV), can be used. Alternatively, variable

hydrodynamic coefficients (C_D, C_M, C_L) from Sarpkaya's experimental data for smooth and rough cylinders can be used. The drag interference effect and the current effect can be included in the calculations.

Various interpretations as to how to apply Morison's equation in the design were examined which have shown the importance of taking full account of both the relative positions in space and time of the different members of the structure as well as the phase relationships in the wave.

A comparison was made between the results of calculations using the recommended coefficients (C_D, C_M) of LR, DnV and BV which has shown that even small variations in these coefficients leads to appreciable differences in the loading estimation of up to 45%.

The approach using variable coefficients (Sarpkaya's data), which are related to the local Reynolds number (R_e) and Keulegan-Carpenter number (K) at the different points of the structure, was compared with the method of adopting constant coefficients (as recommended by LR) showed differences up to 26% in the wave loading estimation between the two methods. The effects of surface roughness, as well as the transverse (lift) forces, on the wave loading were also investigated and found to be very significant (eg 43% to 56% in the surge force) and should be considered in design.

Three wave theories (Airy, Stokes 2nd order, Stokes 5th order) were compared in terms of wave profile, horizontal and vertical velocities and accelerations. The results have shown that the differences in predicting the wave kinematics by Airy and Stokes theories are large. The wave forces on the individual members as well as the total forces and moments on the complete structure calculated by the fifth order theory, showed 30-60% differences when compared with the results based on Airy theory.

The experimental data on the interference effect between the cylindrical members were reviewed. The effect on the jacket loading was examined using some experimental data and found to be 6-9% reduction in the loading for rough cylinders. However, more experimental investigations are required in this area to deal with this problem properly.

The effect of current speed and direction on the wave loading was examined by the commonly used practice of adding the velocity of current vectorially to the wave particle velocity when calculating the drag and lift forces. The results showed that the total forces and moments could be increased by 16-37% for a 1 m/s current in the direction of the wave.

Several static analyses of the jacket were performed using constant and variable hydrodynamic coefficients and two wave theories (Airy and Stokes 5th order theory). The initial differences in the wave loading due to the different coefficients and wave theories appeared again as appreciable differences in the maximum stress on the different members. This supported the necessity of calculating the wave loading accurately from the beginning.

A general review of the reliability analysis method as applied to jacket structures indicated that the modelling of the wave loading needs further improvements to take account of the large uncertainties in the loading especially due to the hydrodynamic coefficients and non-linear loads.

NOTATION

Ax	horizontal acceleration
Axm	maximum horizontal acceleration
Ay	vertical acceleration
Aym	maximum vertical acceleration
B	bias
B_{33}, B_{35}, B_{55}	coefficients, Table C.5
C_1, C_2	coefficients, Tables C.5
C_D	drag coefficient
C_{D_i}	interference drag coefficient (Chapter 7)
C_F^*	total force coefficient (Chapter 2)
C_{in}	interference coefficient (Chapter 7)
C_L	lift coefficient
C_M	inertia coefficient
C_s	interference coefficient (side-by-side)
C_t	interference coefficient (tandem)
COV	coefficient of variation
D	depth of water
D_f	total damage at failure
D_i	fatigue damage per cycle
D_t	total damage, ΣD_i
d	diameter of cylinder
d	water depth (Chapter 6)
d_e	equivalent diameter (Chapter 7)
d_i	diameter for the individual cylinders in an array (Chapter 7)
d_p	pitch circle diamter (Chapter 7)
E	Young's modulus (Chapter 10)
e	gap between cylinder and wall (Chapter 2)
F	force per unit length of cylinder

F_y	maximum shearing force in Y-direction (Chapter 9)
F_z	maximum shearing force in Z-direction (Chapter 9)
F_{D_v}	drag force in 'v' direction
F_{D_w}	drag force in 'w' direction
F_{I_v}	inertia force in 'v' direction
F_{I_w}	inertia force in 'w' direction
F_L	lift force
F_{L_v}	lift force in 'v' direction
F_{L_w}	lift force in 'w' direction
F_{T_v}	total force in 'v' direction for any member
$F_{T_{v_i}}$	total force in 'v' direction for any member 'i' (Chapter 3)
F_{T_w}	total force in 'w' direction for any member
$F_{T_{w_i}}$	total force in 'w' direction for any member 'i' (Chapter 3)
f_v	frequency of vortex shedding
g	acceleration due to gravity
H	wave height
H_{max}	maximum Wave Height (Chapter 10)
H_s	significant wave height
I_D	drag interference coefficient (Chapter 7), $\frac{C_D d_p}{\Sigma C_{D_i} . d_i}$
K	Keulegan-Carpenter number, $U_m.T/d$
K*	Keulegan-Carpenter number (Chapter 2)
k	roughness height
k	wave number, $2\pi/L$ (Chapters 3, 6, 10)
k	constant (Chapter 10)
L	wave length
L_o	wave length by the linear theory, $g.T^2/2\pi$
ℓ	length of member
M	overturning moment
M_p	full plastic moment

M_y	maximum bending moment in Y-direction
M_z	maximum bending moment in Z-direction
M_{D_v}	moment of drag force in 'v' direction
M_{D_w}	moment of drag force in 'w' direction
M_{I_v}	moment of inertia force in 'v' direction
M_{I_w}	moment of inertia force in 'w' direction
M_{L_v}	moment of lift force in 'v' direction
M_{L_w}	moment of lift force in 'w' direction
M_{max}	maximum overturning moment
m	total number of members of the structure
N	maximum axial force
N_i	number of stress cycle at which failure occurs
P_f	probability of failure
$P(H_s, T_z)$	joint probability distribution of H_s and T_z
Q	maximum torsion
R	reliability
R_e	Reynolds number,
S	distance between centres of cylindrical members (Chapter 7)
S_L	length solidification (Chapter 7)
S_t	Strouhal number
SR	Surface roughness (relative roughness), k/d
s_F	constant (Chapter 10)
s_i	stress amplitude
s_y	yield stress
T	wave period
T_z	zero crossing period
$T_{M_{vi}}$	total moment of forces in 'v' direction
$T_{M_{wi}}$	total moment of forces in 'w' direction
T_{max}	instantaneous time of maximum force or moment on member

t	time
t	wall thickness of cylinder (Chapter 10)
t_r	relative time, T_{max}/T
U	horizontal component of water particle velocity
u	water particle horizontal velocity
$\dot{u}$	water particle horizontal acceleration
U_m	maximum water velocity in a cycle
U_v	component of water particle velocity in 'v' direction
U_w	component of water particle velocity in 'w' direction
U_x	horizontal component of water particle velocity in member reference system
Ux	horizontal velocity (Chapter 6)
Uxm	maximum horizontal velocity (Chapter 6)
$\dot{U}_x$	horizontal component of water particle acceleration
$\dot{U}_y$	vertical component of water particle acceleration in member reference system
Uy	vertical velocity (Chapter 6)
Uym	maximum vertical velocity (Chapter 6)
$\dot{U}_y$	vertical component of water particle velocity in member reference system
(u,v,w)	co-ordinates of member reference system
V_h	current velocity at a distance 'h' above sea bottom
V_R	relative current velocity (Chapter 2)
V_s	current velocity at the still water level
W	orbit width of water particle, $\dfrac{H}{\tanh \frac{2\pi D}{L}}$
$\overline{X}$	vector of basic random variables
(X,Y,Z)	co-ordinates of structure reference system
(X_E,Y_E,Z_E)	co-ordinates of the end point of member
(X_S,Y_S,Z_S)	co-ordinates of the starting point of member

(x,y,z)	co-ordinates of wave reference system
z	reliability function (Chapter 10)
α	wave steepness H/L
α_{ij}	correlation coefficient (Chapter 10)
α_{11}	cosine of the angle between X and u
α_{12}	cosine of the angle between X and v
α_{13}	cosine of the angle between X and w
α_{21}	cosine of the angle between Y and u
α_{22}	cosine of the angle between Y and v
α_{23}	cosine of the angle between Y and w
α_{31}	cosine of the angle between Z and u
α_{32}	cosine of the angle between Z and v
α_{33}	cosine of the angle between Z and w
β	incident angle of wave
β	frequency parameter, R_e/K (Chapter 2)
β	reliability (safety) index (Chapter 10)
β_{11}	cosine of the angle between x and X axes
β_{12}	cosine of the angle between x and Y axes
β_{13}	cosine of the angle between x and Z axes
β_{21}	cosine of the angle between y and X axes
β_{22}	cosine of the angle between y and Y axes
β_{23}	cosine of the angle between y and Z axes
β_{31}	cosine of the angle between z and X axes
β_{32}	cosine of the angle between z and Y axes
β_{33}	cosine of the angle between z and Z axes
Γ	gamma function (Chapter 10)
λ	coefficient (Chapter 6)
μ	mean value
ν	kinematic viscosity of water
ρ	water density

ρ	correlation coefficient (Chapter 10)
σ	standard deviation
σ^2	variance
σ_{max}	maximum tensile or compressive stress
τ_{max}	maximum shearing stress
ϕ	distribution function for normal (Gaussian) distribution
ω	wave frequency (rad/s)
θ	current direction (Chapter 8)

LIST OF FIGURES

CHAPTER 5

CHAPTER 6

CHAPTER 7

CHAPTER 10

APPENDIX A

APPENDIX E

LIST OF TABLES

CHAPTER 5

CHAPTER 6

CHAPTER 7

CHAPTER 8

CHAPTER 9

CHAPTER 10

APPENDIX C

CHAPTER 1

CHAPTER 1

INTRODUCTION AND GENERAL DESIGN OF JACKET PLATFORMS

1. BRIEF HISTORY OF FIXED OFFSHORE PLATFORMS

The offshore oil industry began off the coast of California (USA) in the late 1890s. Marine drilling in the Gulf of Mexico began in the 1930s in Louisiana using timber platforms. Since then, the design and construction of offshore platforms has developed from the early primitive timber platforms in 3-5 m of water to the most sophisticated steel structures in more than 300 m of water. A review of this development is given in Ref. (11) and the following are some of the historical highlights.

The first platform to be constructed in the Gulf of Mexico, 1.6 km offshore and in 4.3m water depth, was designed by Brown & Root Incorporated. The platform was constructed in 1938 from timber piles and had a 30 m x 90 m base from which conventional land drilling was performed. Also in 1938 a 15 m x 27 m timber platform was constructed in 3-4.5 m water depth, about 1.6 km off the coast of Texas.

In 1946, the Magnolia Oil Company (Mobil Oil Company) constructed the first steel platform in Louisiana. The platform (53 mx 23 m) was sited in 4.3 m of water, 8 km offshore. It was designed to withstand wind speeds up to 67 m/s and a maximum wave height of 5.5 m.

This was followed in 1947, by the Superior Oil Company who revolutionised the design and construction techniques to allow completely self-contained platforms to operate 29 km offshore in 6 m water. The total platform plan area was 53 m x 33 m. The drilling platform included drilling rig, equipment, pipe racks and all supporting facilities. Living quarters were placed on a separate platform connected to the drilling platform by a bridge. Six steel braced jackets were fabricated onshore and carried to the site by barge and then lowered into the water by a crane and fixed to the bottom by steel piles. The installation of the jacket in the water took about 9 days instead of the usual time of 2 months using the old methods.

It was not until 1955 that the Shell Oil Company installed the first platform in over 30 m of water. The deck area was 67 m x 32 m.

This was followed in 1957 by the introduction of derrick launching which replaced barge launching and the installation of platforms in deeper and deeper waters continued so that by 1967, platforms were being placed in over 100 m of water. In the early 1970s, Shell Oil Company installed a platform in the Gulf of Mexico in 114 m of water and the Tenneco Corporation placed another platform 208 km off the Louisiana coast, also in 114 m of water.

In 1976, Exxon installed a self-contained, drilling and production platform (Hondo) in Santa Barbara Channel, California. It was located 8 km offshore in 259 m of water.

Between July 1977 and September 1978, Shell Oil Company installed the world's tallest, self-contained, drilling and production platform (Cognac) in about 311 m of water in the Gulf of Mexico.

Since the late 1960's, jacket structures have been installed in the Northern North Sea for oil and gas productions starting with the Forties installation. The last major platform to be installed was Magnus in about 186 m of water and in very severe environmental conditions to the North East of Shetland. The total cost of this installation was £1.32 billion.

Thus in the span of 45 years fixed offshore structures for oil drilling and production have moved from timber framed structures carrying a few tons of pay load in shallow water to massive steel structures capable of withstanding the most severe wave loading in more than 300 m of water and with deck loads approaching 30000 tonnes.

2. TYPES OF PLATFORMS

In deep water (above 120 m) self-contained platforms are used combining all activities. In shallow water it is preferred to separate the functions using several separate platforms. The different types of platforms are shown in Fig. (1).

2.1 Jacket (Template) Platform

The modern production platform is a large, multi-decked structure which has adequate strength and space to support the entire drilling rig and production equipment with all auxiliary services and crew quarters and enough supplies and materials to last through the longest anticipated period of bad weather when supplies cannot be brought in.

A typical fixed platform consists of three major components: jacket (template), piles, and deck section. The jacket is a three-dimensional welded frame of tubular members. It can have different types of braces (K, X, horizontal, diagonal), Fig. (2).

The bracing system performs the following general functions (11):-

1. Assists in the transmission of the horizontal loads to the foundation.

2. Provides structural integrity during fabrication and installation.

3. Resists wrenching motion of the installed jacket-pile system.

4. Supports the corrosion anodes and well conductors, and carries the wave forces generated by these elements to the foundation.

In plan view the jacket legs form a rectangle. The inclination of the legs is usually 1/7 - 1/8 for legs on the long side and 1/10 - 1/12 for legs on the short side. In recent platform designs the lower portion of the legs are constructed of very large-diameter tubes (bottles) so that several piles may be driven through pile guide tubes provided in the large-diameter legs. Skirt piles may be added in-between the legs to assist in resisting the overturning moment on the structure.

3. CONSTRUCTION AND INSTALLATION OF JACKETS

3.1 Fabrication

Most of the fabrication occurs in a construction yard onshore.

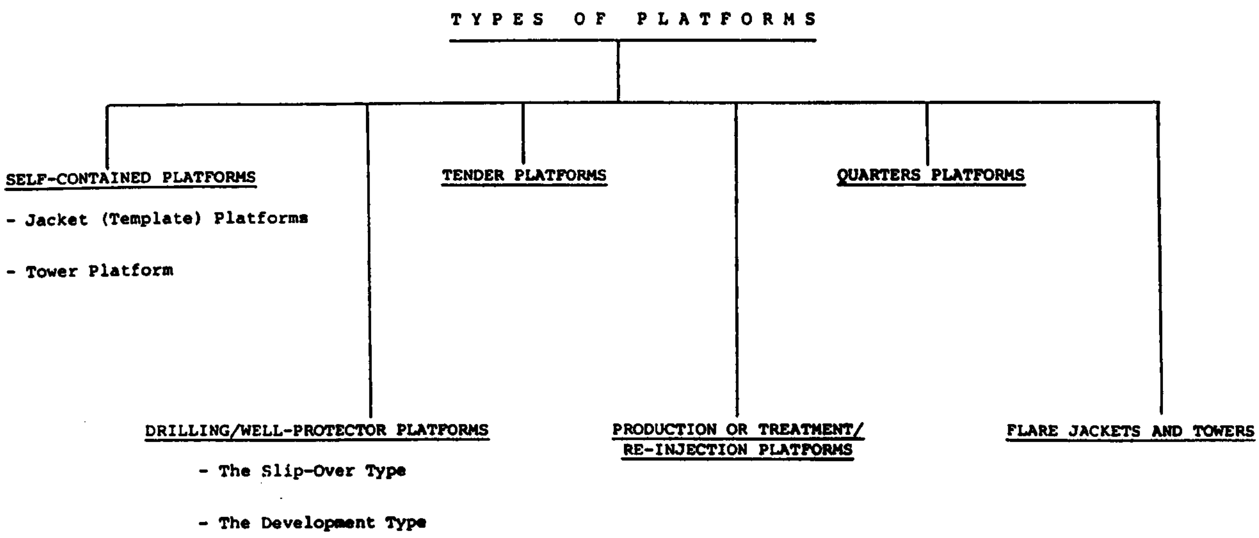

Fig. (1) Types of Fixed Steel Platforms

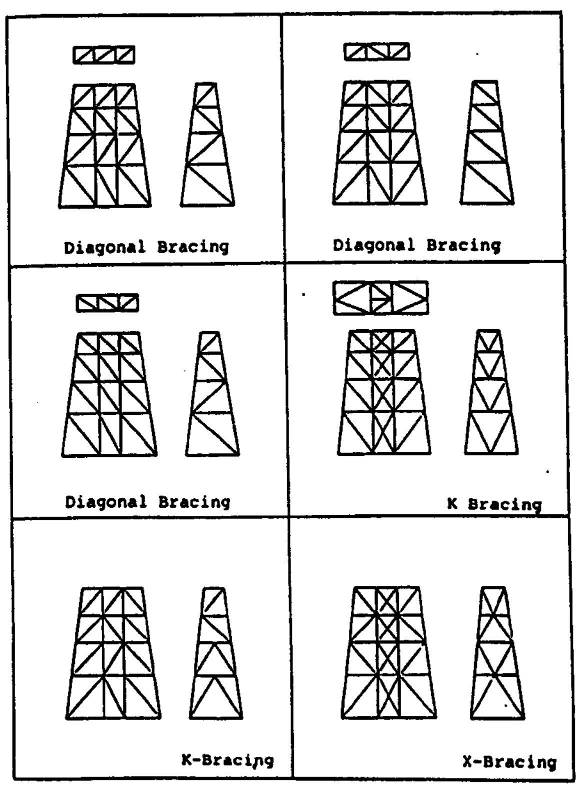

Fig. (2) Framing Configurations
(Courtesy of Brown & Root Inc) Ref (11)

On-site installation is limited to launching and upending the jacket, driving piles, placing the deck structure in a series of modules, and welding all of these into a single unit.

The components are prefabricated into the largest units that can be economically and quickly transported from the fabrication yard to the offshore site, thus minimising the amount of construction offshore. The recent introduction of very heavy lift cranes (5000 tonnes in one lift) has made big changes in the design of deck modules and greatly reduced hook up times.

The jacket is usually assembled by constructing its narrow dimension frames lying flat on the ground. These are then rotated by cranes into a vertical position where cross bracing, guides and other members are then added. Thus, when finished, the jacket will be lying on one of its long sides. The jacket is constructed with the two middle legs on the long side (launch runners) lying on the launch beams used to skid the jacket off the shore onto the barge. After the jacket and its deck sections have been completed, the components are pulled or lifted onto barges and transported to the offshore site.

3.2 Jacket Load-out and Installation

Generally, the jacket is built in one piece whose weight far exceeds practical derrick barge lifting capacities. Therefore, it must be erected through a sequence of operations that involve:-

a. launching (or sliding) from the deck of the cargo barge into the water.

b. floating on its own in a horizontal position, and

c. upending until the jacket rests in its upright position on the ocean floor either by lifting from the top while flooding the legs or by the controlled flooding of built-in compartments

Alternatively, the jacket is floated to its site attached to a flotation pontoon or it is built to float on its side with a minimum draft. The second method is generally used when multiple piles in a cluster at each corner are used to support the structure. Thus, the large diameter legs required for the attachment of the piles are used as buoyancy tanks.

For water depths less than about 45 m, the jacket may be launched from a launch barge or lifted from the transportation barge by derrick barges and lowered into the water.

Deck modules and major items of operational equipment are fabricated or assembled onshore and are installed on the platforms after the jacket has been piled to the ocean floor. Figures (3) to (6) show different methods of installing jackets.

4. DESIGN OF JACKET PLATFORMS

4.1 Design Procedure

The jacket designer will initially be faced with the problem of carrying a deck load of production equipment, a drilling module, accommodation etc which it is hoped can be specified accurately in terms of mass and required volume at an early stage in the design. He

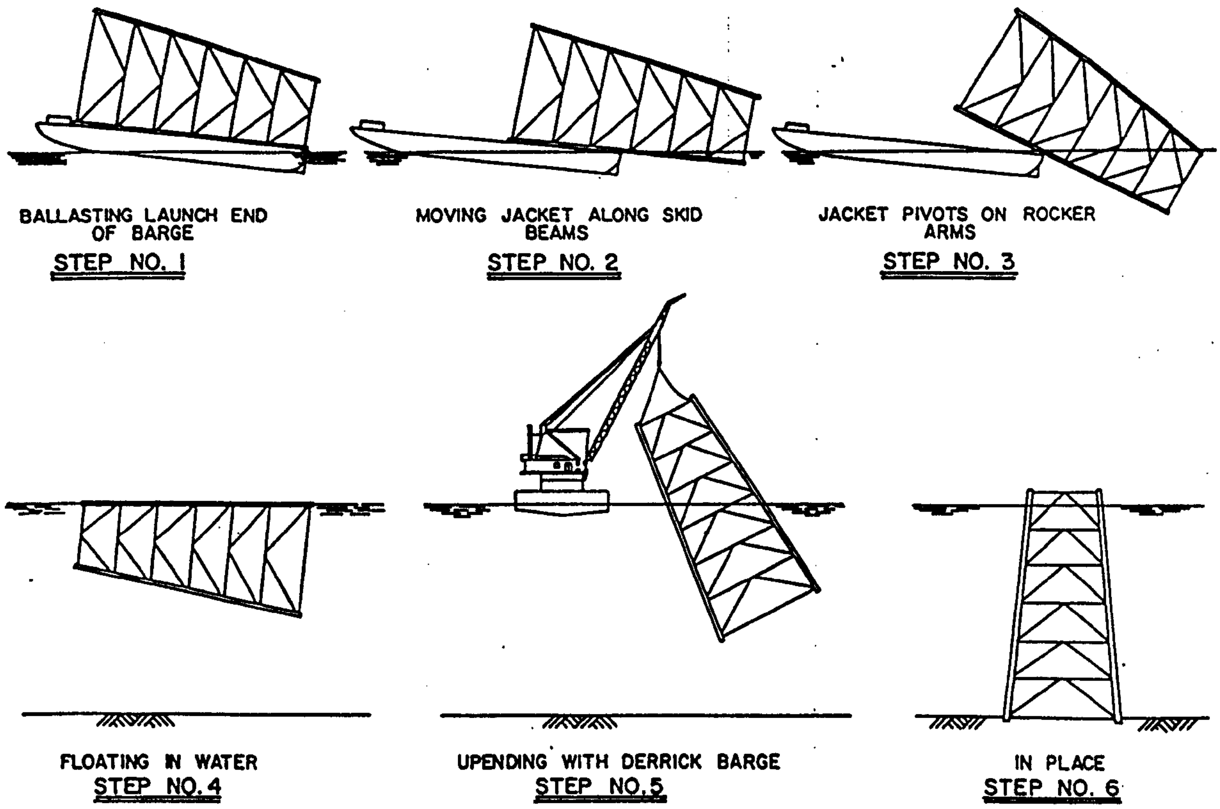

Fig. (3) Installation of a Jacket by Launching

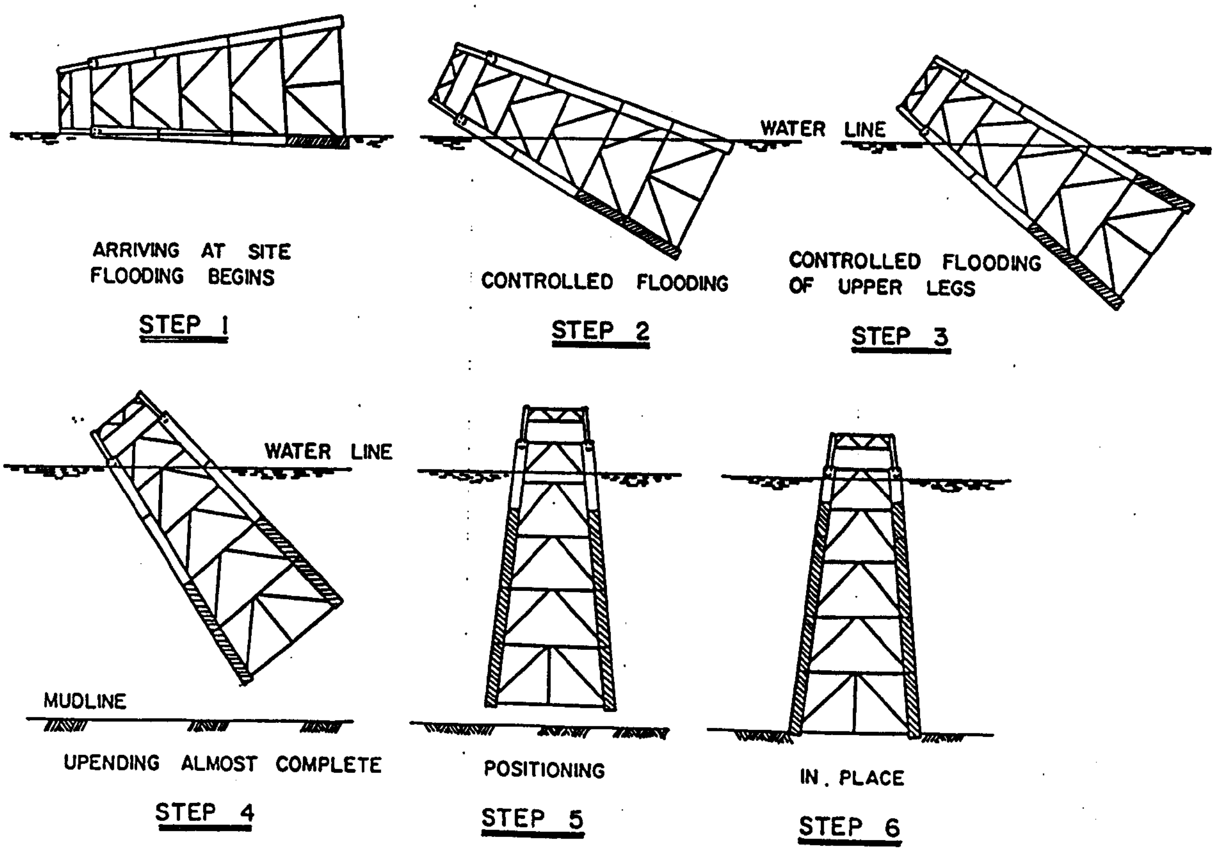

Fig. (4) Installation of a Self-Floating Jacket (Courtesy of J McDermott Inc)

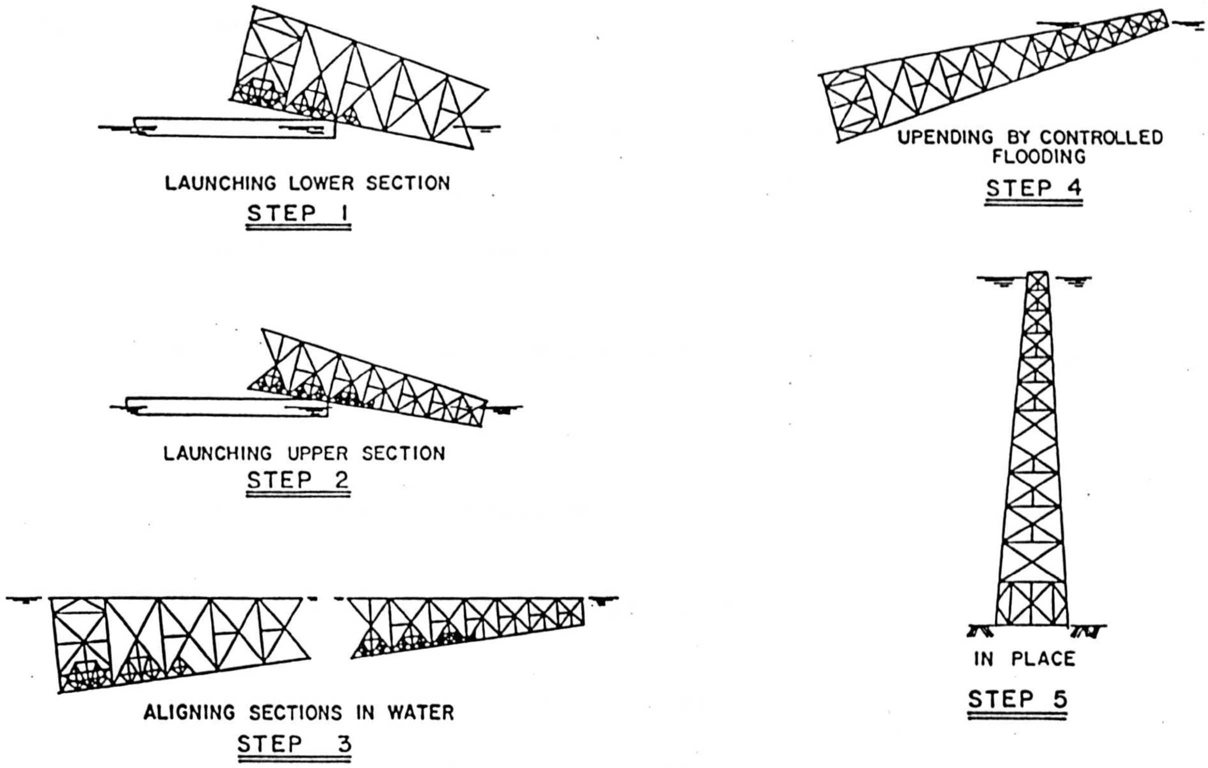

Fig. (5) Installation of a Horizontally Connected Sectionalised Jacket

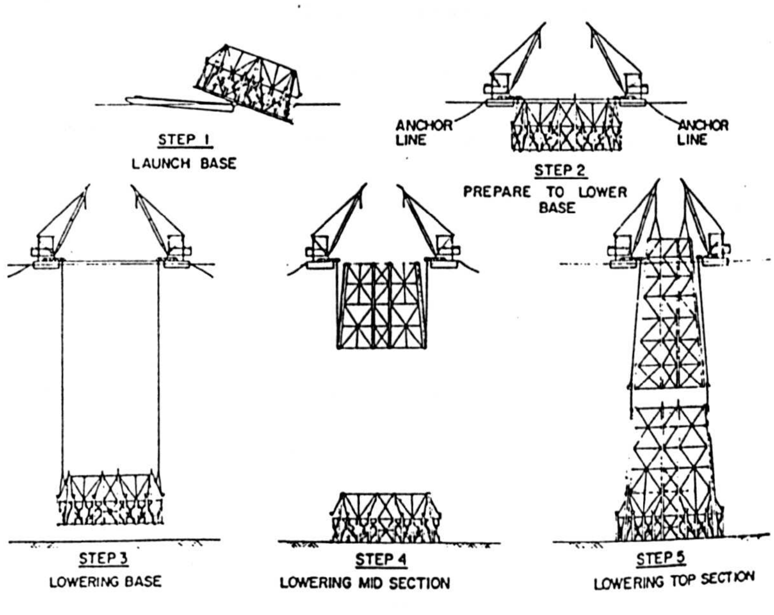

Fig. (6) Installation of a Vertically Connected Sectionalised Jacket
(Courtesy of J McDermott Inc) Ref.(11)

will also have environmental data on the wind, wave and current conditions to be expected in the area. The geologists will have provided some evaluation of the soil characteristics of the ocean floor where the platform is to be sited. He must also bear in mind the limitations of the construction sites such as:-

a. The water depth and tide variations outside the steel fabrication yards, which will limit the float-out draft for the self floating jackets.

b. The capacity and availability of material handling equipment.

c. Welding technology available.

d. Rolling and fabrication equipment, etc.

From this mass of data the designer must decide on a geometry of jacket which will enable him to carry the deck loading in a manner which is conducive to efficient operation of the production etc and minimise, as far as possible, wind loading etc. He will be aware that changes in technology or changes in the oilfield characteristics as these become better determined may require the addition of further modules which will add extra deck mass plus wind loading. Although undesirable such changes in specifications are somewhat inevitable and a prudent designer will make some allowance for them in his layout and structural design. The order of error in specifications might be expected to be around 500 tonnes in a total mass of the order of 10000 tonnes or about 5%.

Knowing the overall deck area which he derives the designer is able to consider the platform geometries and numbers of decks which will satisfy this area. Different framing configurations can be used for the bracing members to ensure sufficient redundancy and residual strength in the structure, Fig. (2).

The X-bracing is thought to have increased stiffness qualities over the K-bracing. It also offers less projected wave area because the bay heights can be increased, thereby reducing the secondary horizontal framing (10). However, the sizes of the bracing members may have to be increased and thus the wave loading may be increased again.

Single diagonal framing reduces the projected wave area and the number of joints in the structure and, consequently, fatigue problems but it reduces the redundancy significantly.

He will have in mind many other considerations such as:-

a. Whether the platform will be floated out or carried on a barge(s) and launched.

b. The craneage available in the construction yards from the point of view of both weight capacity and height of lift.

c. The material and sizes of steel tubes which are readily available or can be rolled and welded by the available equipment.

d. The number of joints which must be fabricated and eventually inspected and maintained in a hostile environment.

e. The bottom foundation conditions both in the building yard and the eventual site at sea.

f. He will wish to ensure that the natural vibration frequencies for the structure as a whole be above the range of wave frequencies

Thus, the eventual geometry will be fixed with only a limited regard for wave loading considerations.

However, when it comes to the all important decisions regarding the diameters and scantlings of the structure the wave loading assumes a predominant importance. As indicated above the direct loading from the deck mass can probably be predicted within 5% and the maximum wind loading on the above water structure to about the same level of accuracy. However, this is not the case for wave loading.

Having determined the dead and environmental loads, the forces and moments on the individual members, as well as the total forces and moments acting on the complete structure can be calculated. Preliminary estimates of the sizes of the various members can now be made. The design is then revised, the operational and environmental loads are again calculated, the foundation requirements are re-evaluated and new sizes for the members are determined. The overall process is repeated, including the structural analysis, until an adequate and safe design meeting all the criteria is obtained. The dynamic behaviour and fatigue life of the structural members and connections are of great importance. The designer should aim to get the first natural period of vibration of the platform well away from the high energy part of the wave spectrum. The platform must be designed to satisfy stiffness and fatigue criteria, thus, large scantlings, especially for the nodes and for long circular members may be required.

In order to obtain a reliable assessment of the fatigue life of the platform, the fatigue properties of the material and connections have to be known. An appropriate S - N (stress-cycles) curve for the joint under consideration should be selected. Suitable stress concentration factors should also be adopted when applying Miner's rule to calculate the fatigue damage.

The installation phase may, for some members, induce large fatigue loading, especially if the platform is to be towed for a long distance.

When the sizes of the main structural components have been determined, other details are designed such as: boat decks, stairs, hand railings, heliports, launch rails, lifting rigs, etc.

After the design phase has been completed, the construction and installation phases can be started.

The design, construction and installation of the platform involve many activities and require a variety of technologies. Figure (7) shows the principal technologies needed. For detailed information on the subject, see References (10-12, 17, 19, 23-25, 37, 43, 44).

4.2 Wave Loading Calculation

The hydrodynamic loading on offshore structures has been widely covered in the literature. (2, 8, 13-15, 20, 26, 29, 32, 33, 35, 36, 41).

JACKET PLATFORM DESIGN

TECHNOLOGY

OCEANOGRAPHY	FOUNDATION ENGINEERING	STRUCTURAL ENGINEERING	MARINE CIVIL ENGINEERING	NAVAL ARCHITECTURE
Wind Wave Current Tide Ice Earthquakes Forces	Soil Characteristics	Materials Selection and Corrosion	Installation Equipment	Flotation & Buoyancy
	Vertical Pile - Soil Characteristics	Structural Analysis	Installation Methods	Towing
	Lateral Pile - Soil Characteristics	Stress Analysis	Navigation Safety Instrumentation	Launching
		Fatigue		
	Scour	Welding		Controlled Flooding
		Design for Fabrication and Installation		
		Appurtenances		

Fig. (7) Technologies Involved in Jacket Platform Design, Ref. (11)

There are two basic approaches to calculate the hydrodynamic loading from a given sea state:-

a. Deterministic (Design Wave) Approach

The sea state is given in terms of a design wave of a specified height (H) and period (T) travelling in a specific direction relative to the structure with an average expected recurrence interval of 100 years.

This approach has been extensively used because:- 1) its simplicity in the design process; 2) the nonlinear loads (drag and lift) can be included in the wave loading calculations; and 3) nonlinear waves (eg Stokes' 5th order theory, stream function theory) can be used to calculate the wave kinematics. It is recommended that several possible single design waves of varying period be analysed to determine the worst loads experienced from any of these design waves. This approach has been used throughout the present study.

b. Non-Deterministic (Stochastic) Approach

The sea state, is mathematically described by statistical means in terms of an energy spectrum. The wave loads are determined by spectral analysis. In this approach all calculations are performed in the frequency domain rather than the time domain.

This stochastic method can only be justified if reliable transfer functions for the wave kinematics and load responses can be established. The implication is that nonlinear loads such as drag forces and others (lift forces) must be small in comparison with the linear loads such as inertia forces since this method is valid only when the linear superposition principle is applicable (2). Nonlinear wave theories cannot be used to calculate the wave kinematics. This approach has been fully described and presented in many references. See, for example, References (1, 3-7, 9, 16, 18, 21, 22, 28, 30, 31, 38-40).

4.2.1 Morison's Equation

The most widely used method to calculate the forces due to waves has been based on Morison's equation (27). This equation assumes that the wave force can be expressed as the linear sum of two independent components, one in phase with the velocity of the water particle known as the drag force and the other in phase with the acceleration of the water particles, known as the inertia force. The original Morison's equation for the force on a vertical cylinder reads:-

$$F = 0.5d\rho C_D\, U.\,|U| + 0.25\rho\pi d^2 C_M \frac{dU}{dt}$$

where F is the inline force per unit length on a cylinder of diameter d and U is the horizontal component of the water particle velocity. A critical assessment of this equation is presented by Sarpkaya (34).

The computation of wave forces by Morison's equation is only possible if the assumption is made that the wave characteristics are unaffected by the presence of the structure. This means that the size of the structure must be small compared with the wave length. The generally accepted limit is:-

$$\frac{d}{L} \leqslant 0.2$$

where d is the diameter of the cylindrical member and L is the wave length.

For larger structures, the scattering of the waves cannot be neglected and diffraction wave theory should be used.

When Morison's equation is applicable, the predominance of the individual forces is as follows:-

$d/W \simeq \pi/K > 0.2$	Inertia increasingly dominant
$d/W \simeq \pi/K < 0.6$	Incipience of drag (and lift)
$d/W \simeq \pi/K < 0.2$	Drag increasingly predominant

where K is Keulegan-Carpenter number and W is the orbit width of the water particle which is given by:-

$$W = \frac{H}{\tanh \frac{2\pi D}{L}}$$

H is the wave height and D is water depth.

In addition to the inline force calculated by the Morison's equation the transverse or lift force should be calculated also and added vectorially to the inline force to obtain the total resultant force on the cylinder. The transverse force (lift) per unit length is calculated by a similar expression to the drag force as follows:-

$$F = 0.5\rho C_L d.U.|U|$$

where C_L is the lift coefficient.

5. AIM OF THE STUDY

It is the purpose of this thesis to examine the variability in the wave and current loading mainly arising from our lack of knowledge of the hydrodynamic coefficients to be used in the equations for calculating the wave forces. When this thesis was commenced, Sarpkaya had recently published values for these coefficients which disagreed with the values recommended by classification societies by more than 100% in certain cases. There was a wealth of experimental data becoming available which had the chief characteristic that they showed a very wide scatter and it was clear that the hydrodynamics of wave flow past groups of cylinders were poorly understood.

It was felt necessary to present an up-to-date review of the data on the hydrodynamic coefficients especially those obtained in the last few years. In chapter 2 a large number of laboratory experiments and wave projects are described and their results are analysed. The main data from these experiments are summarised in a tabular form for easy reference.

Apart from the errors due to incorrect force coefficients there are considerable difficulties in specifying the sea conditions which will cause the most severe wave loading and the probability of occurrence of these conditions. The tendency of designers was to use a "design wave" for the determination of the principal scantlings and to check on fatigue properties by using spectral methods at frequencies higher than the design wave frequency. It was clear from the literature that there were several concepts as to how these design loads should be calculated, that few designers took account of the phasing between the loads on the various members and thus any approach to a reliability analysis of the structure was extremely difficult.

A large computer program (OSS) for calculating the wave loading on jacket structures was developed. The general method of wave loading estimation is based on Morison's equation taking into account the phase differences between the velocities and accelerations of the wave particles. The relative positions of the different members of the jacket in space and time when the wave passes through the jacket were also considered. The lift (transverse) force is included and calculated by an expression similar to the drag force. This program is described in chapter 3.

In chapter 4, various studies were performed to compare the accurate method of program OSS with other computer programs based on different methods of calculation where the phase relationships in the wave are neglected. A detailed study was also presented on the effects of the differences in drag and inertia coefficients as recommended by Lloyd's Register (LR), Det Norske Veritas (DnV) and Bureau Veritas (BV) on the wave loading for a typical jacket structure assumed to be working in 150 m of water.

The results of the study presented in chapter 4 showed the large influence of the hydrodynamic coefficients on the wave loading estimation and indicated the need for another study to investigate other aspects of the hydrodynamic coefficients. In chapter 5, the approach using variable coefficients (Sarpkaya's experimental results) which are related to the local Reynolds number (R_e), Keulegan-Carpenter number (K) and surface roughness, at the different points of the structure was compared with the commonly used method of specifying constant coefficients (eg LR) for the whole structure irrespective of the flow particulars, depth below surface, roughness...etc. Besides the surface roughness, it was also necessary to emphasise the importance of including the lift (transverse) forces in wave loading calculations.

Having established the fact that the hydrodynamic coefficients should be related to the local flow characteristics (ie, the velocities at different depths) it became apparent that the wave kinematics should be calculated as accurately as possible because not only are they included in the wave loading equations but they also affect the values of the hydrodynamic coefficients. To investigate this problem, three wave theories, commonly used in practice, (Airy (linear) theory, Stokes' 2nd order theory and Stokes' 5th order theory) were compared in terms of wave profile, horizontal and vertical velocities and accelerations. However, it was difficult from the results of the variations in the velocities and accelerations to draw concrete conclusions regarding the possible effects on the wave loading without carrying out the wave loading calculation. Therefore, the study was extended to compare the wave forces on individual members of the jacket as well as the total forces (surge, heave, sway) and moments (rolling, yawing, pitching) on the complete structure, calculated by Airy and Stokes' 5th order theories. These results are presented in chapter 6.

As mentioned before, the hydrodynamic coefficients have a very important role in the process of wave loading estimation. The more accurate these coefficients are determined, the more reliable will be the final results of the loading. One of the problems which, until now, is not accounted for properly is the intereference effects between the adjacent members in a jacket structure. The experimental data available are not sufficient and do not give any information about some cases, eg, the interference between inclined members or members of different diameters. It was necessary at least to develop a method to include the intereference information within the wave loading program.

The procedure developed was applied to assess the effect, on the wave loading for a typical jacket platform using some experimental data. The method of calculation and the results, together with a comprehensive review of experimental data on intereference effects are presented in chapter 7.

In chapter 8, the effect of current on the wave loading of the jacket was examined. The current velocity was added vectorially to the wave particle velocity and the combined flow velocity was used to calculate the drag and lift forces. Currents with different speeds and directions, relative to the wave direction, were used in the calculations.

The several comparative studies, as described before, showed significant differences in the wave loading for the complete jacket, and for the individual members, as a result of using different hydrodynamic coefficients, different wave theories ...etc. However, since the scantlings of the different structural members (diameter, wall thickness) are determined from the maximum stresses experienced by each member which, in turn, are induced by the local wave and current loading besides the structural loading transferred from the other members of the jacket, a detailed structural analysis was of absolute necessity.

Chapter 9 describes the set of computer programs used to perform the different static analyses of the jacket. The hydrodynamic coefficients recommended by LR, DnV and BV as well as Sarpkaya's data were used. Airy and Stokes' 5th order theories were used to evaluate the flow kinematics. The variation in the maximum stresses on the different members due to the variation in loading estimations indicated the importance of calculating the wave loading as accurately as possible.

The use of reliability analysis techniques in the design of jacket structures have developed over the last few years. Due to the limitation of time, it was not possible to discuss this big topic in detail. However, a general review of the methods applied to jacket structures with a special regard to the loading uncertainties was felt necessary. This subject is dealt with in chapter 10.

Finally, chapter 11 summarises design recommendations and the main conclusions drawn throughout this comprehensive study.

REFERENCES

1. BASU, A K, and SINGH, R P, 'Use of Generalised Coordinates in the Non-Linear Time-Domain Analysis of Steel Jackets', BOSS '79, London, 1979, pp97-104.

2. BEA, R G, and LAI, N W, 'Hydrodynamic Loading on Offshore Platforms', OTC Paper No 3064, Houston, Texas, 1978.

3. BORGMAN, L E, 'The Spectral Density for Ocean Wave Forces', Coastal Engineering Conf, ASCE, 1965.

4. BORGMAN, L E, 'Wave Forces on Piling for Narrow-Band Spectra', Jour of the Waterways and Harbors Div, ASCE, Vol 91, No WW3, 1965, pp65-90.

5. BORGMAN, L E, 'Spectral Analysis of Ocean Wave Forces on Piling', Jour of the Waterways and Harbors Div, ASCE, Vol 93, No WW2, 1967, pp129-165.

6. BORGMAN, L E, 'Ocean Wave Simulation for Engineering Design', Jour of the Waterways, Harbors and Coastal Engineering Div, ASCE, Vol 95, No WW4, 1969, pp557-583.

7. BORGMAN, L E, 'Statistical Models for Ocean Waves and Wave Forces', Recent Advances in Hydroscience, Vol 8, Academic Press, 1972, pp123-456.

8. CHAKRABARTI, S K, 'Impact of Analytical, Model, and Field Studies on the Design of Offshore Structures', Intl Symp on Ocean Engineering and Ship Handling, Gothenburg, 1980.

9. CHAKRABARTI, S K, 'Discussion on Reference (21), Jour of the Engineering Mechanics Div, ASCE, No EM3, Jun 71, pp1028-1029.

10. DOMINGUES, F J, 'Fixed Offshore Platforms, Design Considerations', Design-Inspection-Redundancy Symp, Ship Structure Committee, Williamsburg, Va, Paper No 7, 1983.

11. GRAFF, W J, 'Introduction to Offshore Structures', Gulf Publishing Company, Houston, Texas, 1981.

12. HARIHARAN, M, 'The Design Process for Offshore Structures - A Critical Review', Proc 2nd Intl Indian Conf on Ocean Engineering, Pune, India, Vol 1, Dec 83, pp478-488.

13. HOGBEN, N, 'Fluid Loading on Offshore Structures, a State of Art Appraisal: Wave Loads', Maritime Technology Monograph No 1, RINA, 1974.

14. HOGBEN, N, 'Wave Loads on Structures', BOSS '76, Trondheim, Vol 1, 1976.

15. HOGBEN, N, MILLER, B L, SEARLE, J W, and WARD, G, 'Estimation of Fluid Loading on Offshore Structures', NMI Report NMI-R11, Apr 77.

16. HUDSPETH, R T 'Wave Force Predictions from Nonlinear Random Sea Simulations', OTC Paper No 2193, Houston, Texas, 1975.

17. HUSLID, J M, GUDMESTAD, O T, and ALM-PAULSEN, A, 'Alternate Deep Water Concepts for Northern North Sea Extreme Conditions', BOSS '82, MIT, Cambridge, Mass, Vol 1, 1982.

18. KAPLAN, P, JIANG, C W, and DELLO STRITTO, F J, 'Determination of Total Base Shear and Bending Moment Power Spectra for an Offshore Structure at Sea', OTC Paper No 4228, Houston, Texas, 1982, pp737-748.

19. LEE, G C, 'Design and Construction of Deep Water Jacket Platforms', BOSS '82, MIT, Cambridge, Mass, Vol 1, 1982.

20. LIGHTHILL, J, 'Waves and Hydrodynamic Loading', BOSS '79, London, Vol 1, 1979, pp1-40.

21. MALHOTRA, A K, and PENZIEN, J, 'Response of Offshore Structures to Random Wave Forces', Journal of the Structural Division, ASCE, Vol 96, No ST 10, Oct 70, pp2155-2173.

22. MALHOTRA, A K and PENZIEN, J, 'Nondeterministic Analysis of Offshore Structures', Jour of the Engineering Mechanics Div, ASCE, Vol 96, EM6, Dec 70, pp985-1003.

23. MARSHALL, P W, 'Strategy for Monitoring, Inspection and Repair for Fixed Offshore Structures', BOSS '79, London, Vol 2, 1979, pp369-389.

24. McKINNEY, W M, 'The Effect of Variation in Design Criteria on Steel Offshore Structures', Paper No EVR 25, European Offshore Petroleum Conf and Exhibition, London, Oct 78.

25. METCALF, M F, PRAUGHT, M W, and MacDONELL, W O, 'On the Installation Planning of a Self-Floating Offshore Platform', Marine Technology, Vol 6, No 3, Jul 79, pp279-293.

26. MILGRAM, J H, 'Waves and Wave Forces', BOSS '76, Trondheim, Vol 1, 1976.

27. MORISON, R J, O'BRIEN, M P, JOHNSON, J W, and SCHOAF, S A, 'The Forces Exerted by Surface Waves on Piles', Petroleum Trans, AIME, Vol 189, 1950.

28. NAFDAY, A M, and WANG, H, 'Probabilistic Model of Wave Forces on Cylindrical Pile', Jour of Waterway, Port, Coastal and Ocean Engineering Div, ASCE, Vol 109, No 2, May 83, pp147-163.

29. OHMART, R D, 'Hydrodynamic Loading of Steel Structures', OTC Paper No 4612, Houston, Texas, 1983.

30. OLSEN, O A, and TORSET, O P, 'Hydrodynamic Loading on Jackets - Application of Linear Stochastic Methods', 2nd Intl Symp on Integrity of Offshore Structures, Glasgow, Jul 81, pp19-34.

31. PIERSON, W J, and HOLMES, P, 'Irregular Wave Forces on a Pile', Jour of the Waterways and Harbors Div, ASCE, Vol 91, No WW4, 1965.

32. RAHMAN, M, and CHAKRAVARTY, I C, 'Hydrodynamic Loading Calculations for Offshore Structures', Jour of Applied Mathematics, Vol 41, No 3, Dec 81.

33. RAMBERG, S E, and NIEDZWECKI, J M, 'Some Uncertainties and Errors in Wave Force Computations', OTC Paper No 3579, Houston, Texas, 1979.

34. SARPKAYA, T, 'A Critical Assessment of Morison's Equation', Intl Symp on Hydrodynamics in Ocean Engineering, Trondheim, Vol I, 1981.

35. SARPKAYA, T, and ISAACSON, M, 'Mechanics of Wave Forces on Offshore Structures', Van Nostrand Reinhold, New York, 1981.

36. SHAW, T L, (Editor), 'Mechanics of Wave-Induced Forces on Cylinders', Pitman Advanced Publishing Program, London, 1979.

37. STIANSEN, S G, 'Interrelation Between Design, Inspection and Redundancy in Marine Structures', Design-Inspection-Redundancy Symp, Ship Structure Committee, Williamsburg, Va, Paper No 2, 1983.

38. TICKELL, R G, 'Continuous Random Wave Loading on Structural Members', The Structural Engineer, Vol 55, No 5, May 1977.

39. TICKELL, R G, and HOLMES, P, 'Approaches to Fluid Loading, Probabilitic and Deterministic Analyses', Numerical Methods in Offshore Engineering, John Wiley and Sons, UK, 1979, pp43-85.

40. TUAH, H, and HUDSPETH, R T, 'Nondeterministic Wave Forces on Fixed Small Vertical Piles', Applied Ocean Research, Vol 5, No 2, 1983, pp63-68.

41. VUGTS, J H, 'A Review of Hydrodynamic Loads on Offshore Structures and their Formulations', BOSS '79, London, Vol 3, 1979.

42. WADE, B G and DWYER, M, 'On the Application of Morison's Equation to Fixed Offshore Platforms', OTC Paper No 2723, Houston, Texas, 1976.

43. WATT, B J, 'Basic Structural Systems - A Review of Their Design and Analysis REquirements', Numerical Methods in Offshore Engineering, John Wiley and Sons, UK, 1978, pp1-42.

44. WEIDLER, J B, and KARSAN, D I, 'Design, Inspection and Redundancy Investment Vs Risk for Pile Founded Offshore Structures', Design-Inspection-Redundancy Symp, Ship Structure Committee, Williamsburg, Va, Paper No 10, 1983.

CHAPTER 2

CHAPTER 2

HYDRODYNAMIC COEFFICIENTS - A REVIEW OF AVAILABLE DATA

1. INTRODUCTION

There have been numerous studies by several researchers to determine experimentally the values of the hydrodynamic coefficients applicable to circular cylinders in steady and wave flows, namely the drag coefficient C_D, the inertia coefficient C_M, and the lift coefficient C_L. These experimental investigations were conducted either in the laboratory or in the field.

Laboratory experiments involved circular cylinders either horizontal and totally submerged, or vertical and piercing the free surface. Some experiments were carried out for inclined cylinders. These experiments may be classified into:-

a. Steady flow experiments, eg Miller (43),

b. sinusoidal oscillating flow about fixed cylinders, eg Sarpkaya (47-59),

c. Harmonically oscillated cylinder in still water or in waves, eg Garrison (26), Matten (42), Chakrabarti (19),

d. Wave tank tests, eg Chakrabarti (14-20).

Laboratory experiments offer the following advantages:-

(1) Cheap to construct and to run; data can be obtained and analysed within a short time.

(2) The ability to derive the force coefficients systematically under controlled conditions.

(3) The ability to assess, separately, the different factors affecting the loading, eg interference effect, surface roughness, or inclination of the members.

(4) Errors and uncertainties in measurements and analysis of the data are relatively small.

However, laboratory tests do not accurately model or simulate the actual environment. Therefore, a degree of uncertainty regarding the validity and applicability of their results for full scale structures will remain. In this respect, the results from wave tank tests are more relevant to the actual conditions than those from steady or two dimensional sinusoidal flows. Unfortunately, they were limited in the range of Reynolds number or Keulegan-Carpenter number which could be achieved. (For jacket structures $10^5 < R_e < 10^8$ and $10 < K < 150$).

Ocean tests were conducted on single vertical piles or on large scale space structures. Data from these tests could be very valuable but unfortunately, field investigations are associated with the following disadvantages:-

(1) Very expensive to construct, run and maintain over the period of operation.

(2) Difficulties and uncertainties in the measured data due to random waves, wave spreading, current effect, uneven roughness distribution, wind effect, etc.

(3) Difficulty in obtaining systematic data for specified parameters, or when studying roughness or interference

effects. The derived data depend upon the method of analysis used.

(4) Tests on single vertical cylinders do not offer information for inclined members or interference effects which are present in actual structures.

(5) In experiments with space structures, part of the measured forces on a member is, in fact, due to structural loads transferred from other members in the structure.

An excellent and comprehensive review of the data on drag and inertia coefficients (C_D, C_M) from laboratory and field tests has been presented by the British Ship Research Association (13) and may be referred to also in Hogben et al (35). This paper reviews and summarises a very wide range of published data (up to 1976) for C_D and C_M. They are systematically documented with tabulated values of key parameters such as depth of water, dimensions of test cylinders, height and period of waves, Reynolds and Keulegan-Carpenter numbers. Useful information and recent reviews are also available in Refs. (22, 27, 55).

In this chapter, the next two sections review the data on hydrodynamic coefficients obtained from laboratory experiments and from field investigations. At the end, Table (1) summarises the main data on C_D, C_M and C_L presented in this chapter. The problem of the interference between the cylindrical members, its effect on the force coefficients, and also the available experimental data, will be discussed in Chapter 7.

2. LABORATORY EXPERIMENTS

2.1 Sarpkaya's Experiments

Sarpkaya has carried out extensive experimental investigations of the inline and transverse (lift) forces acting on smooth and rough circular cylinders in a sinusoidally oscillating flow in a U-shaped vertical water tunnel. Most of the data were obtained from tests with single, horizontal circular cylinders but data were also obtained for the cases of a single cylinder near or on a plane boundary (wall), inclined cylinders, and multiple cylinders. The complete description of the various experiments and the detailed analyses of the results were published in a number of papers and reports, Refs. (47 to 60).

2.1.1 Single Horizontal Cylinders

The initial phases of the comprehensive studies were carried out in a small U-shaped vertical tunnel, using small, smooth spheres and cylinders at low Reynolds numbers (47). The cross section of the tunnel measured 18" by 20" (46cm x 51cm) and the height was 100" (254cm). The spheres tested ranged from 1.125" to 3.398" in diameter, while the cylinders ranged from 1.0" to 2.5" in diameter.

The drag, inertia and lift coefficients (C_D, C_M, C_L) were determined using Fourier analysis of the force measurements and found to depend upon the Keulegan-Carpenter number (K).

Within the range of subcritical Reynolds numbers encountered, the results showed that the lift force was as large as the inline force and alternated at frequencies ranging from one to four times the frequency of the fluid (47).

To achieve larger Reynolds numbers, a larger U-shaped water tunnel was constructed. The length and height were 30ft and 16ft, respectively. The cross-section of the two vertical legs was 3ft by 6ft while the cross-section of the 30ft long test section measured 3ft by 3ft. The diameters of the test cylinders ranged from 2.0" to 6.5".

The extensive experimental investigations of the inline and transverse forces acting on smooth and artificially roughened cylinders covered a wide range of Reynolds number (up to 1.5×10^6), Keulegan-Carpenter number (up to 200) and relative roughness (k/d) from 1/800 to 1/50. Sand papers, sand and polystyrene beads were used as roughness elements.

The drag and inertia coefficients were determined through the use of Fourier analysis and the least squares method. The transverse (lift) force was analysed in terms of its maximum, semi-peak-to-peak, and root-mean-square values. In addition, the frequency of vortex shedding and the Strouhal numbers were determined.

Sarpkaya's results for cylinders in harmonic flow with zero mean velocity, Refs.(47 to 55) have shown that:-

a. For smooth cylinders, the drag, inertia, and lift coefficients (C_D, C_M, C_L) depend on both Reynolds number (R_e) and Keulegan-Carpenter number (K), particularly for $R_e > 2 \times 10^4$. As R_e increases, C_L decreases rapidly to a value of about 0.25.

b. For rough cylinders, the drag and inertia coefficients depend on R_e, K and k/d. The lift coefficient does not depend on R_e and becomes almost identical with those for smooth cylinders at very low Reynolds numbers.

c. The drag coefficient undergoes a 'drag crisis' (a steep fall) depending on the relative roughness (k/d) and then rises to an asymptotic value. The asymptotic values of the post-critical drag coefficient are larger than those corresponding to the smooth cylinder case. The larger the relative roughness, the larger is the asymptotic value of the drag coefficient.

d. The inertia coefficient also undergoes an 'inertia crisis' at R_e values corresponding to the 'drag crisis' at which C_M reaches a maximum value and then asympotically decreases. The terminal values of C_M depend, as in the case of C_D, on K and k/d.

e. The asymptotic values of the post-critical drag coefficient for $K < 100$ are larger than those corresponding to the steady flow over cylinders of similar roughness.

f. The drag and inertia coefficients become independent of k/d for roughness Reynolds numbers ($U_m k/\nu$) larger than about 300.

g. The transverse (lift) force is a significant fraction of the total force for both smooth and rough cylinders and must be considered in the design of offshore structures.

h. The Strouhal number ($S_t = f_v d/U_m$) for smooth cylinders depends on Reynolds and Keulegan-Carpenter numbers varying from 0.15 to 0.45. For rough cylinders it is essentially constant at about 0.22 for all Reynolds numbers larger than 2×10^4.

i. Suitable artificial roughness, eg sand, may be used to provoke and simulate supercritical flow in model tests in steady as well as oscillatory flows.

j. The similarity between the drag coefficients obtained from the field tests and those obtained with steady uniform flow over similar cylinders under controlled laboratory conditions is rather fortuitous and as a consequence of the reduced spanwise coherence in the ocean tests.

k. The force coefficients for wavy flows may differ (be reduced) somewhat from the oscillatory flow results partly due to the reduced spanwise coherence, partly due to the three-dimensionality of the flow and partly due to the nonlinear interaction of the current with the waves. Also, the marine-growth roughness may differ significantly from the organised sand roughness used in the tests.

2.1.2 Cylinder Near or on Plane Boundary

Sarpkaya (57, 58) reported the results of measurements of the inline and transverse forces acting on smooth cylinders near a wall in oscillatory flow in U-shaped water tunnels.

The first investigation (58) was carried out in the small tunnel. The Keulegan-Carpenter number (K) varied from 2 to 40, Reynolds number (R_e) from 4×10^3 to 2.5×10^4, and the gap between the cylinder (e) and the wall from 0.01d to 1.0d. The drag and inertia coefficients were determined using Morison's equation with Fourier analysis and the least squares methods. The lift coefficients were obtained for the forces toward and away from the wall. As K approaches zero, the force coefficients were found to approach those predicted by the potential theory (57).

The second investigation (58) was carried out in the large tunnel at high Reynolds numbers (up to 1.5×10^6) and Keulegan-Carpenter numbers (up to 100). The results show that:-

a. The effect of wall-proximity is to increase the drag and inertia coefficients for relative gaps (e/d) less than 0.5. Both coefficients depend on R_e, K and e/d.

b. The lift force toward the wall is relatively small and fairly independent of e/d. The lift force away from the wall is quite large and depends on e/d, particularly for $e/d < 0.5$.

c. For $e/d > 0.5$, the drag, inertia and lift coefficients nearly assume their free-cylinder values ($e/d = \infty$).

Sarpkaya and Rajabi (59) reported the experiments of measuring the inline and transverse (vertical) forces on bottom-mounted (no gap) smooth and rough cylinders in periodic flow in the modified tunnel. The axis of the cylinders was transverse to the direction of flow.

The length of the tunnel was increased from 30ft to 35ft and the height from 16ft to 22ft. The cross section of the 35ft long test section was increased from 3ft by 3ft to 3ft by 4.7ft.

The experiments were conducted with 5" and 6.5" diameter smooth and sand-roughened cylinders with $k/d = 0.01$. The results show that:-

a. Generally, the potential flow values of the inertia and lift coefficients tend to underestimate the forces on a bottom-mounted cylinder.

b. The drag coefficient for bottom-mounted cylinders can acquire very large values. The inertia coefficient at very low values of K is nearly identical to that obtained from the potential theory and increases with increasing K.

c. The lift force is always away from the wall ($e/d = 0.0$) and the lift coefficient decreases with increasing K and R_e. The lift coefficient for very small values of K (no separation) approaches that predicted theoretically.

2.1.3 Inclined Cylinders

Sarpkaya, Raines and Trytten (56), reported experiments on the forces on inclined smooth and rough cylinders in harmonic flow in the modified tunnel. Three smooth and three rough cylinders ($k/d = 0.01$) of 3", 4.5" and 6" in diameter at yaw angles of 45, 60, 90 degrees were used. Sarpkaya et al concluded that:-

a. The drag and inertia coefficients for the 45-degree and 60-degree smooth and rough yawed cylinders differ significantly from those of the 90-degree normal cylinder.

b. Fourier-averaged drag and inertia coefficients based on Morison's equation and the root-mean-square value of the lift coefficients are unique for each angle of yaw, R_e, K and k/d.

c. Morison's equation predicts the measured force with the same degree of accurary as that for the normal cylinder provided that the force coefficients appropriate to each yaw angle, R_e, and K are used.

d. The normal force acting on a smooth or rough inclined cylinder is significantly underestimated through the use of the 'independence principle' and the drag and inertia coefficients obtained from the 90-degree normal cylinder.

The independence principle states that the force normal to the axis of an inclined cylinder depends only on the normal component of the flow velocity and is independent of the tangential component. Recent research has shown that the independence principle applies to steady ambient flow about inclined cylinders when the boundary layer is wholly laminar or wholly turbulent, ie when the drag coefficient is nearly constant (subcritical and post-critical flow regimes). This principle allows the decomposition of forces and velocities into normal and tangential components, the tangential components being neglected in most loading analysis.

2.2 Chakrabarti's Experiments

2.2.1 Vertical Cylinders

Chakrabarti has carried out extensive experiments for the wave forces on vertical and inclined smooth cylinders and also on rough vertical cylinders, Refs. (14 to 20). The experiments were carried out in a wave tank 250ft (76m) long, 33ft (10m) wide, and 18ft (5.5m) deep.

In the first study (14), a 3" (76mm) diameter vertical cylinder was tested in 10ft (3m) of water. The total inline and tranverse forces on the cylinder as well as the local inline and transverse forces on two 1ft long instrumented sections were measured.

The wave periods ranged from 1.0 sec to 3.5 sec in 0.25 sec increments. At each period about three wave heights were generated. The Keulegan-Carpenter number (K) ranged from 0.0 to 16.0, while the maximum Reynolds number was 2.8×10^4. The drag and inertia coefficients were calculated from the inline forces on the two 1ft sections using the least squares method and were presented graphically against K. The wave kinematics were calculated by the linear wave theory.

The scatter in C_M values was relatively smaller than that of C_D values. The scatter in C_D was attributed to the variations in R_e and to the inaccurate estimate of wave kinematics by the linear wave theory.

The frequencies of the lift forces and the lift coefficients were investigated and presented as functions of K. For K = 15, the resultant wave force (inline and lift) on the cylinder was as much as 60% higher than the inline force alone.

Chakrabarti (15) re-analysed his data (14) and conducted further tests for the inline forces using 1.5" and 3" vertical cylinders. In the new tests, the value of K was extended to a value of about 85. However, R_e was still confined to the range of 2×10^4 to 3×10^4. The water depth in the wave tank was kept at 10ft (3m) except for one set of tests carried out in 5ft (1.5m) depth with the 1.5" cylinder.

The wave periods ranged from 1.5 sec to 3.5 sec in increments of 0.25 sec. For the 1.5" cylinder in 5ft water, wave periods up to 8 sec were generated.

The velocities and accelerations of the flow field were calculated from the measured wave profiles using the stream function theory (23).

The drag and inertia coefficients were found to be functions of Keulegan-Carpenter number (K). There was some scatter in the data attributed partly to the variations in Reynolds number (R_e) and partly to the use of calculated kinematics instead of the real ones.

At low K values, the values of C_M decreased as the C_D values increased. When the data were compared with Sarpkaya's results for the same range of R_e and K, the values of C_M were found to be larger at the small ($K < 15$) and high ($K > 55$) values of K. Within the range $15 < K < 55$, the drag and inertia coefficients are similar to the results of the two-dimensional oscillatory flow.

2.2.2 Inclined Cylinders

Chakrabarti, Tam and Wolbert (17, 18) reported the tests of the forces on smooth cylinders at different orientation in the wave tank.

In the first investigation (17), three cylinders of 3", 5" and 7.5" diameter were used. The water depth in the tank was 5ft. Each cylinder was tested at wave periods ranging from 1.5 sec to 3.0 sec in 0.25 sec intervals for about 3 wave heights at each period.

The average drag and inertia coefficients over the length of the cylinder were derived from the measurements of the total forces on the cylinder using Fourier analysis and the least squares methods.

The variations of the drag and inertia coefficients were presented graphically against Keulegan-Carpenter number (up to K = 17.5). However, these data are confined within the limits of the test and because of the averaging process they are not suitable for any scaling (17).

In the second investigation (18) forces on two 1ft sections of 3" diameter, 10ft long cylinder were measured at various orientations relative to the wave direction.

The drag and inertia coefficients were calculated from the measured inline forces by the least squares method and were found to depend on K without large scatter. It was not possible to correlate the data with Reynolds number (R_e) due to the narrow test range of R_e. The use of the coefficients is also limited by the small range of K (up to 16).

Recently Cotter and Chakrabarti (20) presented the results of the latest tests on vertical and inclined smooth cylinders in the wave tank.

The inline and transverse forces on 1ft instrumented section of 3" diameter, 10ft long cylinder were measured. Three inclinations, namely, 0^o, 30^o, and 45^o to the vertical were tested.

The wave periods ranged from 1.25 sec to 8 sec. At each period, three different wave heights ranging from 6" to 20" were generated. The average K varied from 1 to 39 while the average R_e varied from 1.5×10^3 to 9.1×10^4. The water particle velocities and accelerations were derived from measured wave profiles using the stream function theory (23).

The drag and inertia coefficients were computed from the measured inline forces on the instrumented section by the least squares technique. These coefficients were found to depend on K, but not on R_e, because of the limited range of R_e. The scatter in the data was shown in terms of coefficients of variation (COV) at various K regions.

Generally, the scatter in C_D was high at low K values, while the scatter in C_M was high at high K values.

Cotter and Chakrabarti argued that the relatively large scatter of C_D or C_M (at low or high values of K) would not affect the total load on the cylinder significantly, because the loading becomes inertia dominated at low K and drag dominated at high K.

The lift coefficients were presented in terms of the first five harmonics (by a Fourier analysis). These harmonic coefficients were found to be functions of K. The largest value of the lift coefficient ($C_L \doteq 0.8 - 1.0$) occurred at the second harmonic of the motion. The value of K at which a particular coefficient and harmonic of the lift force becomes dominant was found to increase with the order (first, second, etc) of the harmonic, ie, the higher the K, the higher the order of the dominating harmonic. Finally, it was concluded that the 'Independence Principle'for the inclined cylinders is valid if the normal components of the velocity and acceleration are used in Morison's equation.

2.2.3 Rough Vertical Cylinders

As a continuation for the experimental work on smooth cylinders (14, 15, 17, 18, 19, 20) Chakrabarti (16) presented the results of the wave force coefficients for rough vertical cylinders. Two cylinders 3" (76mm) and 1.5" (38mm) in diameter and 8.5ft (2.6m) long were tested.

To simulate marine fouling, the cylinders were sand-roughened at three different relative roughnesses (k/d), namely, 0.002, 0.007, and 0.02.

The total inline and transverse forces on each cylinder, as well as on two 1ft instrumented sections, were measured. The wave periods ranged from 1.5 sec to 8.0 sec, the Keulegan-Carpenter number ranged from 0.0 to 65 and the Reynolds number ranged from 0.1×10^4 to 3×10^4. The water particle velocities and accelerations were computed by the stream function theory (23).

Although the scatter in the coefficients was relatively large, the mean C_D, C_M, and C_L values showed a definite trend with K. The drag and lift coefficients increased with the increase of relative roughness, while the inertia coefficients were relatively unaffected. The values of C_L tended to peak in the K range of 10 to 15. The predominant lift frequency steadily increased in relation to the wave frequency as K increased.

The resultant force was found to increase, relative to the inline force, steadily up to a K value of about 15 and the increase was as much as 70%. At higher values of K, the percentage difference decreased.

2.3 Garrison et al

Garrison, Field and May (26) reported the experimental results of sinusoidally oscillated cylinders in still water. The experiments were carried out in a water channel 23" (0.584mm) wide, 16ft (4.9m) long and 4ft (1.2m) deep using smooth cylinders of 2.0" (51mm), 3.0" (76mm) and 4.5" (114.3mm) in diameter.

The Keulegan-Carpenter number (K) varied from about 6 to 35, while Reynolds number (R_e) ranged from about 10^4 to 6×10^5. The drag and inertia coefficients were determined from the measured forces using the least squares method.

At large R_e values, the data showed agreement with the results obtained from the Ocean Test Structure (OTS).

Garrison et al concluded that:-

a. The drag and inertia coefficients depend on both K and R_e in general but C_D and C_M become independent of K when it is large and they become independent of R_e when $R_e > 2 \times 10^5$.

b. When both K and R_e are large, C_D approaches a value of 0.61 and C_M approaches a value of 1.7.

c. As K decreases, C_M and C_D tend to their potential flow values of 2.0 and zero respectively.

The results for sand-roughened cylinders (k/d = 0.01) were presented by Garrison (27). The scatter in the drag and inertia coefficients was large at R_e of about 4×10^4. The value of C_D was found to increase rapidly with increasing R_e to a value less than 1.8

and then decreases rapidly with Reynolds number for $R_e > 2 \times 10^5$. This is in opposition to Sarpkaya's results which show that C_D becomes independent of Reynolds number and remains constant for $R_e > 1.5 \times 10^5$.

2.4 B L Miller (National Physical Laboratory)

Miller (43) carried out experiments on smooth and rough cylinders in two wind tunnels (steady flow) at the National Physical Laboratory, UK. The tested cyclinders were 0.5m, 0.10m and 0.15m in diameter with a variety of surface finish (smooth, real marine growth, sand roughness, and coarse grained roughness). The maximum Reynolds number was about 6×10^6.

The results showed that for relative roughness (k/d) between 0.002 and 0.005, the drag coefficient reaches a constant value of about 1.0 at the postcritical Reynolds numbers. For smaller relative roughnesses ($k/d < 0.002$), the drag coefficient reaches a maximum value, below 1.0, and then decreases.

Miller concluded that the rigid marine growths (barnacles) and sand roughness of similar physical size have similar effects on drag forces. He stated also that the wave loading could be significantly increased due to roughness.

2.5 R Matten (National Maritime Institute)

Matten (41) conducted experiments on rough vertical surface piercing cylinders in waves and the forces were compared with those of smooth cylinders. The experiments were carried out in the NMI towing tank which was 2.26m deep and 6.1m wide.

The marine roughnesses were simulated by attaching garnet paper to the surface of the cylinders. Two sizes of cylinders were tested having diameters of 0.05m and 0.10m with relative roughnesses 0.02 and 0.01, respectively. The waves generated in the tank ranged from 0.25m to 0.75m in height and from 2.0 sec to 3.0 sec in period. The wave steepness (H/L) varied from 0.04 to 0.05, with depth to wave length ratios of 0.4 and 0.17, respectively. The Keulegan-Carpenter number ranged from about 0.0 to 25.0 while Reynolds number ranged from 2×10^4 to 8×10^4.

Matten found that the wave force for rough cylinders increased significantly and indicated that the drag coefficient C_D increased by 60% due to roughness. He concluded that the transverse force on smooth vertical surface piercing cylinders may be up to 80% of the inline force even in fairly high irregular waves. Both the frequency and the maximum value of the transverse force are dependent on K, whilst roughness has little effect. Matten suggested that the results are relevant to full scale structures.

2.6 N J Heaf

Heaf (34) reported experiments with vertical cylinders in a towing tank where the wave loading was due to a highly irregular wave train. This work indicated that in the super-critical Reynolds number region of flow applicable to offshore structures, the surface roughness due to marine growth will increase the local value of C_D by 150% or more over the C_D value for a smooth cylinder.

Heaf has concluded that the values of C_D and C_M predicted by

Sarpkaya's work (54) seem to be the most appropriate data for predicting the effect of different heights of surface roughness on C_D and C_M and thereby on the wave loading. The fact that this data was obtained in two-dimensional harmonic flow probably means that such an approach would lead to a conservative design (34).

2.7 J H Nath (Oregon State University)

Nath (44, 45) reported experimental studies carried out on smooth and rough horizontal cylinders at Oregon State University in a flow visualisation flume, in a low speed wind tunnel and in the Wave Research Facility. The long term objective of the work was to determine the hydrodynamic coefficients in waves and currents for cylinders with heavy accumulations of marine growths.

2.7.1 Flow Visualisation

The flow visualisation flume was 4" wide, 8ft long and 2ft deep. Plexiglass cylinders of 2" diameter were positioned horizontally 8" above the bottom in 17" water depth.

The tests were performed for:-

a. A smooth cylinder

b. A sand roughened cylinder ($k/d = 0.05$)

c. Hand carved barnacles roughened cylinder ($k/d = 0.10$)

d. A cylinder covered with plastic strips to simulate kelp.

e. An artificially roughened cylinder simulating marine roughness ($k/d \approx 0.2$).

For the smooth cylinder, the Strouhal number ($S_t = f_v d/U$, f_v = frequency of vortex shedding, U = flow speed) was 0.21 in the range of Reynolds number (R_e) from 5×10^3 to 2×10^4. For the rough cylinders, vortex shedding was also noted but its frequency was reduced (44).

2.7.2 Wind Tunnel

The wind tunnel had a test section of 5ft wide, 4ft high and 30ft long. A 3" diameter plastic cylinder was mounted horizontally with a 2ft long test section at the mid length.

The root-mean-square values of the lift coefficients (C_L) were quite scattered and ranged from 0.27 to 0.48 for the smooth cylinder, 0.30 to 1.60 for the sand roughened cylinder and 0.17 to 0.48 for the marine roughened cylinder (44).

Within the range of Reynolds number from 2×10^4 to 10^5, the average value of the drag coefficient (C_D) was 1.2 for the smooth and sand roughened cylinders and 1.25 for the marine roughened cylinder.

2.7.3 Wave Flume

The wave flume was 12ft wide, 15ft deep and 340ft overall length, with a 128ft length for the test section.

A 5" diameter solid aluminium bar was rigidly suspended from a tow carriage. To the 5" bar were mounted six half-cylinders (skins) from a 8.625" diameter pipe such that the two centre semi-cylinders comprised the 2ft long test section. The whole arrangement was mounted 3.7ft below the still water surface in 11.5ft and 13.5ft of water (44).

Three sets of roughness specimens (skins) were prepared:-

1. A smooth aluminium surface.
2. A sand roughened surface (k/d = 0.02).
3. An artificially marine roughened surface (k/d ≐ 0.09).

The experiments were carried out by towing the cylinder at constant speed and by testing it in periodic waves.

a. Steady Towing

The initial results were reported in Nath (44). The carriage speed, the inline and transverse forces on the test section were measured. The maximum value of Reynolds number (R_e) was 5 x 10^5. The maximum lift coefficients (C_L) showed large scatter when plotted against R_e. For the smooth cylinder, the results of the drag coefficients (C_D) showed that the cylinder was not 'hydrodynamically' smooth, the value of the critical Reynolds number was reduced. For the rough cylinders, the critical flow region was virtually eliminated due to the limited value of R_e.

The drag coefficients for the roughened cylinders showed an independence from Reynolds number. At low Reynolds number, the values of the drag coefficient from the wave flume were somewhat less than those obtained from similar specimens in the wind tunnel. The average values of the drag coefficient for the marine and sand roughened cylinders were 1.16 and 0.93 respectively and for the smooth cylinder the average value was 0.90 (45).

b. Periodic Waves

The results of the experiments were presented in Nath (45). The waves ranged in period from 1 sec to 6 sec, the wave heights were up to 5ft. The Keulegan-Carpenter number (K) ranged from 2 to 26, while the maximum Reynolds number (R_e) was 2×10^5. The flow kinematics were calculated by stream function theory (23).

When the drag and inertia coefficients (C_D, C_M) were plotted against K, there was considerable scatter compared with the results from Sarpkaya (50) and Sarpkaya and Isaacson (55).

The results for $15 < K < 26$ were then compared with those from Sarpkaya and Isaacson (55) for $K = 20$ and with those from Holmes and Chaplin (36) for $K = 24$. For the smooth cylinder it was found that the values of C_D according to Sarpkaya form an upper bound for those from the wave flow, while the values of C_M fall between those from Refs. (55) and (36).

For the sand roughened cylinder, the values of C_D were much smaller than those from Sarpkaya and Isaacson (55), while the value of C_M was 0.8. For the marine roughened cylinder, the C_M values had large scatter ranging from 0.8 to 2.5. The C_D values ranged from 1.2 to 1.8.

3. FIELD INVESTIGATIONS

3.1. The Pacific Coast (Davenport, California)

Wiegel, Beebe and Moon (65) analysed the results of the experimental studies conducted by the University of California near

Davenport, California. Measurements were made of forces exerted by waves as high as 20ft in water varying in depth from 45ft to 50ft. The measured forces were presented in graphical form. The test sections were 6.625", 12.75", 2ft and 5ft in diameter.

The drag and inertia coefficients were computed from the measured data using linear wave theory to predict the water particle velocities and accelerations. The data showed considerable scatter. The drag coefficient was found to have no well-defined relationship to Reynolds number in the test range of Reynolds number from 3×10^4 to 9×10^5. The average value of the inertia coefficient was found to be 2.5 with a Gaussian distribution about this average value. No relationship was found between C_D and C_M, R_e, horizontal water acceleration, or the wave period.

Comparison between the maximum predicted and maximum measured forces, using the average values of C_D and C_M showed serious discrepancies and a trend for under-prediction was observed for the higher measured forces.

Large lateral vibrations for the 2ft test pile were noted under the action of high waves mainly due to the alternative breaking off of large vortices.

The reasons for the scatter in the data were attributed to the following (65):-

a. The large difference in wave shape from the theoretical one.

b. The varying degree of turbulence in the flow field.

c. The effects of roughness, lift forces, and current.

d. The effect of the locally generated wind waves.

e. The limits of accuracy of the tests.

3.2 Wave Projects (I) and (II) (Gulf of Mexico)

The wave measurement installations were located in the Gulf of Mexico. Wave Project I (1954-1958) was located in 30ft of water and data were obtained during three hurricanes and two tropical storms. The maximum wave height was 22ft. To obtain data from larger waves in deeper water, Wave Project II (1960-1963) was installed in 100ft of water. Data were obtained during Hurricane Carla (1961) and many smaller storms. The maximum wave height was 43ft.

More details of the projects and a summary of the storm data are given in Ref (62).

Evans (25) analysed the data of the two projects by two different methods. For Wave Project I, the drag coefficient was determined at the positions where the wave force is purely drag (wave crest and trough). Similarly, the inertia coefficient was determined where the wave force is predominantly inertial (at L/4). For Wave Project II, the least squares method was used.

The analysis of Project I data gave an average value of C_D of 0.585 for all analysed waves. The highest waves (H = 15 - 22ft) gave average value for C_D of 0.495. A histogram of C_M indicated a modal value of 1.2, but a value of 1.5 was used in force predictions (25). C_D was shown to decrease with both increasing wave period and height.

The correlation between C_D and Reynolds number (R_e) was generally poor and only the average values of C_D showed some correlation to the steady flow results.

For Project II, the mean value of C_D was 0.88 for all waves. For higher waves only ($H \geq 25$ft and $T \geq 10$ sec), the mean value was 0.578. Parametric analysis of the average drag coefficient for wave heights and periods showed that C_D decreases for increasing wave heights and increasing wave periods. It was also noted that C_D decreases with elevation above the sea bottom for most wave heights (25). For all waves, the mean C_M was 1.682 and for higher waves C_M was 1.765. The results showed that C_M increases with the distance above sea bottom. At the end, Evans (25) stated that C_D and C_M values would differ with varying wave theories and that the coefficients presented should be used cautiously for large diameter piles.

Dean and Aagaard (21) analysed the data of Wave Projects I and II by a deterministic, single-wave approach. The kinematics of the flow were calculated by the stream function theory (23).

In the range of Reynolds number (R_e) between 6×10^5 and 6×10^6, the drag coefficient (C_D) was found to decrease from about 1.3 to 0.5 with the increase of Reynolds number. The inertia coefficient (C_M) was constant at a value of 1.33 for all Reynolds numbers. In this analysis the effect of current was not taken into account.

Wheeler (64) used linear-filter techniques and a modified small-amplitude wave theory to analyse the data of force measurements in about 400 waves at various elevations along a 44" diameter pile during Hurricane Carla (1961).

When only the highest 50% of the peak wave forces measured at each height above bottom was considered, the drag coefficient ranged from 0.44 to 0.60 while the inertia coefficient varied between 0.0 and 2.0. Wheeler emphasised that these coefficients should be used only with the calculations procedures presented in his paper and that their application should be limited to the calculation of forces on members similar in size and surface properties to the test member used to obtain the measured forces (64).

3.3 Bass Straits Experiment (Australia, 1973)

Kim and Hibbard (40) presented and analysed the results of tests conducted on a single pile of 12.75" diameter and 38ft long. The pile had an 18" long load cell section to measure wave forces, positioned at about 7ft below the water surface.

The wave height ranged between 2.5ft and 10.0ft and the steady current speed was about 1.0ft/sec.

Drag and inertia coefficients were calculated for individual waves from the measured water-particle velocities and wave forces.

Over the range of Reynolds number from 2×10^5 to 8×10^5, the average drag coefficients was 0.61 with a standard deviation of $\pm$ 24%. The inertia coefficient showed a tendency to decrease with increasing water particle acceleration and had an average value of 1.2 wih a standard deviation of $\pm$ 22%.

3.4 Hurricane Edith Experiment

Ohmart and Gratz (46) reported the results obtained from wave forces and horizontal particle velocities measured on an offshore test platform during Hurricane Edith. The force transducers were 3ft diameter by 2ft long.

The determination of the force coefficients was based on Morison's equation using the least squares approach. Reynolds number ranged from 3×10^5 to 3×10^6. The best fit of the measured and predicted forces was obtained with a drag coefficient of 0.7 and an inertia coefficient of 1.5. For the peak forces, the best fit was obtained using $C_D = 0.7$ and $C_M = 1.7$.

3.5 The Ocean Test Structure (OTS), Gulf of Mexico (1976-1978)

The Ocean Test Structure (OTS) was a large scale experimental platform designed to evaluate wave forces calculation procedures for fixed jacket structures. The overall dimensions of the platform were 20 x 20 x 120 ft and it was installed in 66ft water depth in the Gulf of Mexico.

Storm wave data, modelling typical platform design conditions (at 1/3rd to 1/6th scale) were collected during two winter seasons and one hurricane season (Hurricane Anita, 1977).

The wave height ranged from 9ft to 24ft while the wave period ranged from 6 sec to 12 sec.

The data obtained included local wave forces on clean and barnacle-covered members, local wave kinematics, total base shearing force and overturning moment on the structure, forces on simulated group of well conductors, and impact forces on a member above mean water level (30).

The design, installation, calibration and operation of the OTS instrumentation system was described by Germinder and Pomonick (29). The evaluation of the OTS measurement program and applications of the data to the assessment of wave loading theories were presented by Haring et al (30).

The major storm events, the selection criteria for choosing individual wave force events for detailed analysis, and the marine growth development on the platform during its operating time were discussed by Haring and Spencer (31).

Data interpretations and analysis of the results by several investigators were reported in Refs. (9, 10, 11, 24, 27, 32, 33, 38, 60).

Heideman, Olsen and Johannson (33) analysed the data measured by clean and barnacle fouled wave force transducers (WFT) by two methods to evaluate the drag and inertia coefficients.

The first was the least squared error procedure for each half wave cycle. The instantaneous inline velocity in Morison's equation included both the wave velocity and the projection of the current velocity.

In the second method, the drag coefficient was evaluated over short segments of waves in which the drag force was dominant, while the inertia coefficient was evaluated over short segments in which inertia force was dominant, see Ref. 40.

The inline force was taken as the projection of the normal force (to the wave force transducer) on the velocity vector. The significant wave height ranged from 8ft to 14ft.

The drag and inertia coefficients showed large scatter, particularly for Keulegan-Carpenter number (K) < 20. The scatter decreased considerably in the range 20 < K < 45. In the drag-inertia regime (8 < K < 20), the drag coefficient for a 0.5" barnacle encrusted WFT ranged from 0.5 to about 2.5. The inertia coefficient ranged from 0.7 to 1.8.

The composite results of the two methods of analysis for all storms data showed that C_D seemed to approach an asymptotic value of about 0.68 for clean WFTs and about 1.0 for fouled WFTs. The mean value of C_M ranged from 1.51 to 1.65 with a standard deviation of about 0.30 for the clean WFTs. In the case of fouled WFTs, the mean value of C_M ranged from 1.25 to 1.43 with a standard deviation of about 0.34.

Heideman et al (33) attributed the scatter in C_D and C_M to random wake encounter concept, see Beckmann and McBride (12).

According to Beckmann and McBride (12), the 'true' drag coefficient in oscillatory flow should be the same as the drag coefficient in steady flow and the variations in the 'apparent' drag coefficient are caused by random wake encounters. So, if the cylinder, during the test, encounters its wake on the return half cycle but the velocity meter does not, then the actual incident velocity will be greater than measured and the 'apparent' C_D calculated from the measured force and velocity will be higher than the 'true' C_D. Conversely, if the velocity meter encounters the wake on the return half cycle but the cylinder does not, then the 'apparent' C_D will be lower than the 'true' C_D.

Heideman et al (33) concluded that:-

a. Morison's equation with constant coefficients can be made to fit the measured local forces and kinematics satisfactorily over individual half wave cycles.

b. Most of the scatter in the C_D results can be explained by the random wake encounter concept.

c. Local deviations in apparent C_D are not spatially correlated in any given wave.

d. C_D results from Sarpkaya's experiments represent an upper bound to C_D values that may be expected in random three-dimensional oscillatory flow.

e. For $R_e > 2 \times 10^5$, the apparent C_D depends on surface roughness and when the member cross section lies in the orbit plane, on K.

f. Asymptotic C_D results from the test data in random three-dimensional oscillatory flow are consistent with steady flow data for the same relative roughness.

g. C_M is greater for smooth cylinders than for rough cylinders, while the reverse is true for C_D.

Haring, Olsen and Johansson (32) compared the measured and the computed total forces (base shear) and overturning moments for different sets of data by two procedures. Stokes fifth order theory was used to calculate the flow kinematics.

In the first method, a constant C_M value of 1.68 was assumed together with one of three average values of C_D for each set of data, namely 0.81, 1.14 and 0.97. Each of these values of C_D, when used, was assumed to be uniform and constant over the whole structure. In this method a large scatter in results was found on a wave-by-wave basis.

An alternative analysis was conducted with the same data in which the drag coefficient was varied locally in the calculations to account for vertical surface roughness distribution, wake encounter effects and Keulegan-Carpenter number (K). Thus, C_D was in the order of 0.7 for clean members and 1.0 for fouled members while the C_M value was assumed as 1.5.

However, the use of variable drag coefficients did not improve the scatter in the results. The average bias in the base shear ranged from -1% to 19% and in the overturning moment from -4% to 14% (30). The -ve sign indicates that the calculated force (or moment) is smaller than the measured one.

Borgman and Yfantis (9) determined the spectral estimates of C_D and C_M for selected storm intervals from OTS data. They stated that these spectral estimates represent the average values of C_D and C_M simultaneously over the whole structure, which are required to determine the inline total force (base shear) spectra.

They argued that such average coefficients may be more relevant to determine the base shear (and overturning moment) than the local values since they take into account directional and random cancellations throughout the structure. Borgman and Yfantis also emphasised that these spectral estimates of C_D and C_M may not necessarily coincide with the hydrodynamic C_D and C_M values present locally along the individual members of the structure.

Sarpkaya and Cakal (60) re-analysed parts of the OTS data which were obtained with a 0.5" covering of barnacles on the wave force transducers (March 1977). The analysis was performed in terms of the sensitivity of the data to random disturbances imposed on the measured wave forces, velocities and accelerations. Sarpkaya and Cakal concluded that:-

a. The scatter observed in C_D and C_M obtained from OTS data is partly due to random disturbances superimposed on the recorded force and partly due to random disturbances superimposed on the kinematics of the flow field.

b. Neither type of disturbance, alone or in combination, is sufficient to explain the entire scatter.

c. For each frequency parameter, ($\beta = R_e/K$) there exists a relationship between C_D and K for various values of 'relative current velocity', V_R (V_R = VcT/d, Vc = current speed).

d. The effect of current is to reduce C_D for a given β and K.

e. In spite of the scatter, OTS data show that C_D and C_M must be somewhat below those obtained under laboratory conditions partly because of the effect of current and partly because of the reduced spanwise coherence due to all other disturbances ever present in the ocean environment.

Kaplan, Jiang and Dello Stritto (38) analysed the experimental data for 13 waves from the winter (1976-1977) storm series to evaluate the drag, inertia and lift coefficients for inclined members of OTS.

The data consisted of the measurements of the wave forces on an instrumented element of a member inclined at 45°, as well as the horizontal velocity components (inline and transverse), the vertical velocity and wave elevations measured at specific locations on the OTS.

The method of data analysis was based upon the use of the system identification technique, which has previously been applied to determine Morison's equation force coefficients for vertical members of the same structure (see Kaplan et al (39)).

The time histories of the variation of the velocities and forces showed good agreement between the measured and estimated results using Morison's equation although the degree of agreement (accuracy) for the forces was not as good as in the case of the vertical members as reported in Reference (39). However, the general agreement between theory and experiment indicated the validity of using Morison's equation to calculate wave forces on inclined members.

The mean values of Reynolds number and Keulegan-Carpenter number (based on the average velocities of wave crest and trough) ranged from 3.9×10^{5} to 4.8×10^{5} and from 33.1 to 50.4, respectively.

The drag coefficient C_D ranged from 0.835 to 1.128 while the inertia coefficient C_M ranged from 1.727 to 2.302. For some waves the lift coefficient C_L was 0.15 approximately.

The drag coefficient showed less scatter, when plotted against Reynolds number R_e, as compared with the values of Johansson (37) which were obtained using the analysis method of Kim and Hibbard (40).

3.6 Christchurch Bay Tower (1976)

The tower is a small offshore structure sited in 9.0m water depth, designed specifically for research into wave forces and gravity foundations with a reasonable modelling of North Sea conditions. The wave force experiments were intended to fill the gap between small scale laboratory work in rather simplified waves and the full-scale structures in the complex waves of the real sea(1).

The tower consists of a large central column of 2.8m diameter and a small column (wave staff) of 0.48m diameter. The large column was designed to lie mainly in the inertia regime except for the largest waves while the small column was drag dominated for wave heights larger than 2.5m. The data collected covered a series of storms with wave heights up to 7.0m. The full details of this project may be referred to in References (5) and (63).

The results of the wave project were analysed by the following methods:-

a. Examination of time histories.

b. Wave-by-wave analysis, Reference (61).

c. Mean square analysis, References (3, 6).

d. Statistical and spectral analyses, References (2, 8).

e. Analyses of directional spectra.

f. Analysis of pressure distributions.

Inspection of time histories of the initial data obtained indicated a reasonable correlation between the force on the large column and water particle motion. The force on the small column exhibited a strong vortex shedding influence with very large changes in the direction of the force (1).

Using the mean square analysis method of Bishop (6), the initial data indicated inertia coefficients C_M on the large column varying from 1.7 to 2.0. On the small column, the inertia coefficients varied between 1.1 and 1.7, while the drag coefficients varied between 0.65 and 0.8. The variations in the inertia coefficient were attributed to the effect of current.

Bishop and Holmes (2) analysed some data from the experiment in spectral and probabilistic terms. The preliminary results showed that the inline velocity field in random waves had Gaussian properties, as did the force on the inertia dominated main column. Force ranges were reasonably represented by a Rayleigh distribution function.

For the small column (wave staff), working in the drag-inertia regime, the Gaussian and Rayleigh assumptions for inline force and force ranges were not valid. These parameters were better represented by a probability density function which retained the non-linear drag term (2). More details were presented by Bishop (8).

Bishop (3) obtained the drag and inertia coefficients by fitting data of a 20 minute record of the wave forces to a mean square derivation of Morison's equation. The mean square method (6) utilises the relationship between the mean square value of force and corresponding parameters of water particle kinematics. The time record is divided into sections or intervals of a particular duration and the mean square values for each interval provide one data set. Multiple data sets from a long record (not less than 20 minutes) are then used to derive C_D and C_M values.

The force coefficients, obtained by this method, were found to be very stable for integration intervals larger than about 4 minutes and showed increasing variations as the integration interval was reduced. However, comparison with force coefficients derived for a different 20 minute recording indicated significant differences due to current effect.

Bishop (3) stated that the variations of the force coefficients could be attributed to genuine hydrodynamic effects and also to imperfections in the experimental and analytic techniques.

Bishop, Tickell and Gallagher (4) presented a comprehensive review of the results of the project. The mean square method was used in conjunction with a new total force coefficient $C_F{}^*$ defined as, Ref. (7):-

$$C_{F*} = \left[\frac{C_D{}^2 + C_M{}^2 \left(\frac{\pi^2}{0.866K_*}\right)^2}{1 + \left(\frac{\pi^2}{0.866K_*}\right)^2} \right]^{\frac{1}{2}}$$

where, K_* (Keulegan-Carpenter number, Reference (1)) $= \frac{2\pi}{0.866d}\left(\frac{u^{-4}}{\dot{u}^{-2}}\right)^{\frac{1}{2}}$

$u, \dot{u}$ = water particle horizontal velocity and acceleration.

The advantage of the total force coefficient is the ability to judge the degree of scatter or variability in the force data without the need to think about the relative contributions of drag and inertia forces (4). The analysis indicated significant variations of the force coefficients from one 20 minute recording to another which were thought to be due to differing tidal current. However, a considerable reduction in the variability of the coefficients was found if the individual data samples were long enough to contain about 7 waves. There was also a tendency for the variability to be less for the highest waves (4).

Wave-by-wave analysis demonstrated a variability of the fitting of measured forces to those predicted by Morison's equation. Part of this could be due to differing particle motion conditions at the velocity and force measuring stations and another part could be due to vortex shedding effect.

4. CONCLUDING REMARKS AND RECOMMENDATIONS

In spite of the extensive research effort which has been expended to determine the hydrodynamic coefficients, the presently available data are not sufficient and further work needs to be done to improve the quality of data. Due to the high costs of field tests, it is unlikely that any major wave project will be sponsored, at least in the near future. Therefore, the efforts should now be directed to the much cheaper laboratory experiments.

The data obtained from two-dimensional harmonic flow, eg Sarpkaya's results, are complete and well documented. This is not the case with wave tank experiments, although they should be more relevant to the actual environment than the two-dimensional tests.

A large testing facility is now required, capable of generating waves in sufficient depth of water to approach, as near as possible, the range of Reynolds and Keulegan-Carpenter numbers corresponding to full scale structures. With this facility in hand, large scale models representing complete or part of jacket structures can be tested. Tests with single cylinders are not enough. The problems of the forces on inclined members or interference effects must also be dealt with.

However, until this facility becomes available, designers of offshore stuctures have to rely on the available data to compute wave loading.

It is the opinion of the author that Sarpkaya's results seem to be the most suitable data, at least for the time being. The data cover a wide range of Reynold's number, Keulegan-Carpenter number, and surface roughness in such a way that they can be integrated into wave loading computer programs.

Data obtained from the real ocean are quite valuable. Unfortunately, until now they are not complete. However, they can be used, eg to check the calculations for certain individual members in critical parts of the structure, particularly when the dimensions and surface conditions of the checked member are similar to one of those used in the ocean tests.

The fact that Sarpkaya's data were obtained from two-dimensional sinusoidal flow means that the design procedure would probably be somewhat conservative. It must also be remembered that Morison's equation with its well-known limitations has been accepted and used by the engineers as a primary tool in designing offshore structures. This is simply because no other better alternative method or equation is yet available. The same argument goes also for the two-dimensional flow results.

REFERENCES

1. BISHOP, J R, 'Description of the UK Christchurch Bay Wave Force Project and Some Initial Results', Part 1 of Paper EVR 23, European Offshore Petroleum Conference and Exhibition, London, Oct 78.

2. BISHOP, J R, and HOLMES, P, 'Description of the UK Christchurch Bay Wave Force Project and Some Initial Results', Part 2 of Paper EUR, European Offshore Petroleum Conference and Exhibition, London, Oct 78.

3. BISHOP, J R, 'RMS Force Coefficients Derived from Christchurch Bay Wave Force Data', NMI Report NMI-R62, 1979.

4. BISHOP, J R, TICKELL, R G, and GALLAGHER, K A, 'The UK Christchurch Bay Project; A Review of Results', NMI Report NMI-R87, Jun 80.

5. BISHOP, J R, 'A Description of the Christchurch Bay Wave Force Project', NMI Report NMI-R33, 1978.

6. BISHOP, J R, 'The Mean Square Value of Wave Force Based on the Morison Equation', NMI Report NMI-R40, 1978.

7. BISHOP, J R, 'A Total Wave Force Coefficient Suited to Irregular Waves', NMI Report NMI-R77, Jan 80.

8. BISHOP, J R, 'A Spectral Analysis of Christchurch Bay Wave Force Data Recorded in September 1976', NMI Report NMI-R53, Jul 79.

9. BORGMAN, L E, and YFANTIS, E, 'Three-Dimensional Character of Waves and Forces', Civil Engineering in the Ocean IV, ASCE, 1979.

10. BENDAT, J S, RICHMAN, G, OSBORNE, A R and SILBERT, M N, 'Cross-Spectral and Coherence Analysis of OTS Data', Civil Engineering in the Oceans IV, ASCE, 1979.

11. BECKMAN, H, and MERWIN, J E, 'Wave Forces on Conductor Pipe Group', Civil Engineering in the Oceans IV, ASCE, 1979.

12. BECKMAN, H, and McBRIDE, C M, 'Inherent Scatter of Wave Forces on Submerged Structures', ASME Petroleum Div Joint Conf with Pressure Vessels and Piping Div in Dallas, Texas, 1968.

13. BRITISH SHIP RESEARCH ASSOCIATION, 'A Critical Evaluation of the Data on Wave Force Coefficients, BSRA Contract Report No W278, 1976.

14. CHAKRABARTI, S K, WOLBERT, A L and TAM, W A, 'Wave Forces on Vertical Circular Cylinder', Jour of the Waterways, Harbors and Coastal Engineering Div, ASCE, Vol 102, No WW2, May 76.

15. CHAKRABARTI, S K, 'In-Line Forces on Fixed Vertical Cylinder in Waves', Jour of the Waterway, Port, Coastal and Ocean Div, ASCE, Vol 106, No WW2, May 80.

16. CHAKRABARTI, S K, 'Wave Force Coefficients for Rough Vertical Cylinders', Jour of the Waterway, Port, Coastal and Ocean Div, ASCE, Vol 108, No WW4, Nov 82.

17. CHAKRABARTI, S K, TAM, W A and WOLBERT, A L, 'Wave Forces on a Randomly Oriented Tube', OTC Paper No 2190, Houston, Texas, 1975.

18. CHAKRABARTI, S K, TAM, W A and WOLBERT, A L, 'Total Forces on a Submerged Randomly Oriented Tube Due to Waves', OTC Paper No 2495, Houston, Texas, 1976.

19. CHAKRABARTI, S K, COTTER, D C and LIBBY, A R, 'Hydrodynamic Coefficients of a Harmonically Oscillated Tower', Applied Ocean Research, Vol 5, No 4, 1983.

20. COTTER, D C and CHAKRABARTI, S K, 'Wave Force Tests on Vertical and Inclined Cylinders', Jour of the Waterway, Port, Coastal and Ocean Div, ASCE, Vol 110, No 1, Feb 84.

21. DEAN, R G and AAGAARD, P M,'Wave Forces: Data Analysis and Engineering Calculation Method', Jour of Petroleum Technology, Mar 70.

22. DEAN, R G, 'Methodology for Evaluating Suitability of Wave and Wave Force Data for Determining Drag and Inertia Coefficients', BOSS 76, Trondheim, Vol 2, 1976, pp40-64.

23. DEAN, R G, 'Stream Function Representation of Nonlinear Ocean Waves', Jour of Geophysical Research, Vol 70, No 18, 1965, pp4561-4572.

24. DEAN, R G, LO, J-M, and JOHANSSON, P I, 'Rare Wave Kinematics versus Design Practice', Civil Engineering in the Oceans IV, ASCE, 1979, pp1030-1049.

25. EVANS, D J, 'Analysis of Wave Force Data', Jour of Petroleum Technology, Mar 70.

26. GARRISON, C J, FIELD, J B and MAY, M D, 'Drag and Inertia Forces on a Cylinder in Periodic Flow', Jour of the Waterway, Port, Coastal and Ocean Div, ASCE, Vol 103, No WW2, May 1977.

27. GARRISON, C J, 'A Review of Drag and Inertia Forces on Circular Cylinders', OTC Paper No 3760, Houston, Texas, 1980.

28. GASTON, J D and OHMART, R D, 'Effects of Surface Roughness on Drag Coefficients', Civil Engineering in the Oceans IV, ASCE, 1979, pp611-621.

29. GERMINDER, R E and POMONICK, G M, 'The Ocean Test Structure Measurement System', Civil Engineering The Oceans IV, ASCE, 1979, pp1010-1029.

30. HARING, R E, SHUMWAY, D H, SPENCER, L P, and PEARCE, B K, 'Operation of an Ocean Test Structure', Paper EUR22, European Offshore Petroleum Conference and Exhibitions, London, Oct 78.

31. HARING, R E, and SPENCER, L P, 'The Ocean Test Structure Data Base', Civil Engineering in the Oceans IV, ASCE, 1979, pp69-683.

32. HARING, R E OLSEN, O A, and JOHANSSON, P I, 'Total Wave Force and Moment versus Design Practice', Civil Engineering in the Oceans IV, ASCE, 1979, pp805-819.

33. HEIDEMAN, J C, OLSEN, O A, and JOHANSSON, P I, 'Local Wave Force Coefficients', Civil Engineering in the Oceans IV, ASCE, 1979, pp684-699.

34. HEAF, N J, 'The Effect of Marine Growth on the Performance of Fixed Offshore Platforms in the North Sea', OTC Paper No 3386, Houston, Texas, 1979.

35. HOGBEN, N, MILLER, B L, SEARLE, J W, and WARD, G, 'Estimation of Fluid Loading on Offshore Structures', NMI Report NMI-R11, Apr 77.

36. HOLMES, P, and CHAPLIN, J R, 'Wave Loading on Horizontal Cylinders', Proc 16th Coastal Engineering Conf, Hamburg, West Germany, 27 Aug-3 Sep 78, pp372-387.

37. JOHANSSON, P I, 'Ocean Test Structure Data Interpretation', Part 4 - Task II-C, DnV Report No 78-531, 1978.

38. KAPLAN, P, JIANG, C W, and DELLO STRITTO, F J, 'Force Coefficient Evaluation for Offshore Structure Inclined Members', BOSS '82, MIT, Cambridge, Mass, 1982.

39. KAPLAN, P, JIANG, C W and DELLO STRITTO, F J, 'Determination of Offshore Structure Morison Equation Force Coefficients via System Identification Techniques', Proc Hydrodynamics in Ocean Engineering, Trondheim, Norway, Vol 1, 1981, pp469-489.

40. KIM, Y Y and HIBBARD, H C, 'Analysis of Simultaneous Wave Force and Water Particle Velocity Measurements', OTC Paper No 2192, Houston, Texas, 1975.

41. MATTEN, R B, 'The Influence of Surface Roughness Upon the Drag of Circular Cylinders in Waves', OTC Paper No 2902, Houston, Texas, 1977.

42. MATTEN, R B, HOGBEN, N and ASHLEY, R M, 'A Circular Cylinder Oscillating in Still Water, in Waves and in Currents', NMI Report NMI-R63, Jul 79.

43. MILLER, B L, 'The Hydrodynamic Drag of Roughened Circular Cylinders', Trans RINA, Vol 119, 1977, pp55-70.

44. NATH, J H, 'Hydrodynamic Coefficients for Macro-Roughnesses', OTC Paper No 3989, Houston, Texas, 1981.

45. NATH, J H, 'Heavily Roughened Horizontal Cylinders in Waves', BOSS '82, MIT, Cambridge, Mass, 1982.

46. OHMART, R D and GRATZ, R L, 'Drag Coefficients from Hurricane Wave Data', Civil Engineering in the Oceans IV, ASCE, 1979, pp260-272.

47. SARPKAYA, T, 'Forces on Cylinders and Spheres in a Sinusoidally Oscillating Fluid', Jour of Applied Mechanics, Vol 42, Mar 75.

48. SARPKAYA, T, 'In-Line and Transverse Forces on Smooth and Sand-Roughened Cylinders in Oscillatory Flow at High Reynolds Numbers', Naval Postgraduate School, Technical Report No NPS-69SL76062, Monterey, CA, Jun 76.

49. SARPKAYA, T, 'Vortex Shedding and Resistance in Harmonic Flow about Smooth and Rough Circular Cylinders at High Reynolds Numbers', Naval Postgraduate School, Technical Report No NPS-59SL76021, Monėterey, CA, Feb 76.

50. SARPKAYA, T, 'Vortex Shedding and Resistance in Harmonic Flow about Smooth and Rough Circular Cylinders', BOSS 76, Trondheim, Vol I, 1976, pp220-235.

51. SARPKAYA, T, 'In-Line and Transverse Forces on Cylinders in Oscillatory Flow at High Reynolds Numbers', OTC Paper No 2533, Houston, Texas, 1976.

52. SARPKAYA, T, 'In-Line and Transverse Forces on Cylinders in Oscillatory Flow at High Reynolds Numbers', Jour of Ship Research, Vol 21, No 4, Dec 77, pp200-216.

53. SARPKAYA, T, 'The Hydrodynamic Resistance of Roughened Cylinders in Harmonic Flow', Trans RINA, 1977.

54. SARPKAYA, T, COLLINS, N J, and EVANS, S R, 'Wave Forces on Rough-Walled Cylinders at High Reynolds Numbers', OTC Paper No 2901, Houston, Texas, 1977.

55. SARPKAYA, T, and ISAACSON, M, 'Mechanics of Wave Forces on Offshore Structures', Van Nostrand Reinhold, New York, 1981.

56. SARPKAYA, T, RAINES, T S, and TRYTTEN, D O, 'Wave Forces on Inclined Smooth and Rough Circular Cylinders', OTC Paper No 4227, Houston, Texas, 1982.

57. SARPKAYA, T, "Forces on Cylinders Near a Plane Boundary in a Sinusoidaly Oscillating Fluid', Jour of Fluids Engineering, ASME, Vol 98, Ser 1, No 3, 1976, pp499-505.

58. SARPKAYA, T, 'In-Line and Transverse Forces on Cylinders Near a Wall in Oscillatory Flow at High Reynolds Numbers', OTC Paper No 2898, Houston, Texas, 1977.

59. SARPKAYA, T, RAJABI, F, 'Hydrodynamic Drag on Bottom-Mounted Smooth and Rough Cylinders in Periodic Flow', OTC Paper No 3761, 1979.

60. SARPKAYA, T, and CAKAL, I, 'A Comprehensive Sensitivity Analysis of the OTS Data', OTC Paper No 4616, Houston, Texas, 1983.

61. STANDING, R G, 'Wave-by-Wave Analysis of Data from the Christchurch Bay Wave Force Experiment', NMI Report NMI-R86, Sep 80.

62. THRASHER, I W and AAGAARD, P M, 'Measured Wave Force Data on Offshore Platforms', Jour of Petroleum Technology, Mar 70, pp339-346.

63. WHEATLEY, J H W, 'A British Offshore Research Facility', Trans RINA, Vol 118, 1976.

64. WHEELER, J D, 'Method for Calculating Forces Produced by Irregular Waves', Jour of Petroleum Technology, Mar 70.

65. WIEGEL, R L, BEEBE, K E, and MOON, J, 'Ocean Wave Forces on Circular Cylindrical Piles', Jour of the Hydraulics Div, ASCE, Vol 83, HY2, 1957.

Reference	Location	Flow Particulars	Test Structure	Wave Theory	R_e	K	C_D	C_M	C_L
LABORATORY EXPERIMENTS									
CHAKRABARTI et al (14)	Wave Tank	T=1.0-3.5 sec	Vert Cylinder Smooth d=3"	Airy	Up to 2.8×10^4	0.0-16.0	0.0-0.7	1.7-2.7	0.0-0.66
CHAKRABARTI (15)	Wave Tank	T=1.5-8.0 sec	Vert cyl smooth d=1.5", 3"	Stream Function	$2\times10^4-3\times10^4$	0.0-85	0.2-1.75	0.6-2.5	-
COTTER AND CHAKRABARTI (20)	Wave Tank	T=1.25-8.0sec H=6"-20"	Vert cyl smooth d=3"	Stream Function	$1.5\times10^3-9.1\times10^4$	1.0-39	0.5-1.9	0.5-2.1	0.0-1.0
CHAKRABARTI et al (18)	Wave Tank	T=1.5-8.0sec	Vert cyl d=1.5", 3". Rough (k/d =0.002,0.007,0.02	Stream Function	$0.1\times10^4-3\times10^4$	0.0-65	0.0-2.0	1.3-2.4	0.2-1.9
CHAKRABARTI et al (18)	Wave Tank	T=1.0-3.5 sec	Inclined cyl d=3" smooth	Airy		0.0-16			
			45° along the tank				0.65-4.0	1.5-2.2	
			60° along the tank				1.5-3.3	1.6-2.2	
			75° along the tank				1.0-4.0	1.4-2.3	
			45° across the tank				0.0-1.0	1.3-2.3	
			60° across the tank				0.0-1.0	1.5-2.2	
			45° down tank				1.0-5.6	1.3-2.3	
			60° to horizontal @ 45° to down tank				0.7-3.0	1.5-2.6	
COTTER AND CHAKRABARTI (20)	Wave Tank	T=1.25-8.0sec H=6"-20"	Inclined cyl Smooth	Stream Function	$1.5\times10^3-9.1\times10^4$	1.0-39.0			
			30° to the Vert				0.10-1.90	1.0-2.0	0.0-0.83
			45° to the vert				1.10-2.5	0.75-2.5	0.0-0.85
GARRISON et al(26)	Water Channel	Still Water	Sinu Oscillating Horizontal smooth cyl d=2", 3", 4.5"		$10^4-6\times10^5$	6-35	0.3-1.65	0.6-1.93	-
GARRISON et al(27)	Water Channel	Still Water	Rough, k/d=0.01		$2\times10^4-6\times10^5$	5-22	0.7-2.10	0.8-1.90	-
MILLER (43)	Wind Tunnel	Steady Flow	Horiz cyl d=0.05m, 0.10m, 0.15m smooth		Up to 6×10^6		0.2-1.25		
			Rough k/d=0.0004-0.063				0.45-1.30		

Table (1.1) Summary of Data on Hydrodynamic Coefficients

Reference	Location	Flow Particulars	Test Structure	Wave Theory	R_e	K	C_D	C_M	C_L
LABORATORY EXPERIMENTS									
NATH (44)	Wind Tunnel	Steady Flow	Horiz Cyl d=3"		$2x10^4-10^5$				
			Smooth				1.2		0.27-0.48
			Sand Roughened				1.2		0.3 -1.60
			Marine Roughened				1.25		0.17-0.48
NATH (45)	Wave Tank	Steady Towing	Horiz Cyl d=$8\frac{5}{8}$"		$5x10^5$				
			Smooth				0.9		
			Sand Roughened k/d=0.02				0.93		
			Marine Roughened k/d=0.09				1.16		
NATH (45)	Wave Tank	T=1-6 sec H up to 5ft	Horiz Cyl d=$8\frac{5}{8}$"	Stream Function	Up to $2x10^5$	2-26			
			Smooth					0.8	
			Sand Roughened				1.2-1.8	0.8-2.5	-
SARPKAYA (47)	U-Tunnel	2-Dim Sinu-soidal Flow	Horiz Cyl Smooth d=1"-2.5"		$2.5x10^3-5x10^4$	0-50	0.5-2.3	0.7-2.2	1-2.9 (max)
SARPKAYA (48-55)	U-Tunnel	2-Dim Sinu-soidal Flow	Horiz Cyl d=2"-6.5"		$10^4-1.5x10^6$				
			Smooth			6-100	0.5-2.0	0.65-1.96	0.2-3.4
			Rough k/d=$\frac{1}{800}-\frac{1}{50}$			20-100	0.6-1.9	1.0-1.98	0.3-3.4
SARPKAYA et al (56)	U-Tunnel	2-Dim Sinu-soidal Flow	Inclined Cyl θ=45°, 60°			2-4.0			
			d=3", 4.5", 6"						
			Smooth θ=45°				0.68-1.38	2.50-3.10	0.11-0.30
			θ=60°				0.68-1.30	1.90-2.50	0.11-0.33
			θ=90° normal				0.65-1.78	0.58-2.0	0.15-1.70
			Rough k/d=1/100						
			θ=45°				1.45-2.10	2.80-3.40	0.20-1.20
			θ=60°				1.40-2.30	1.60-2.50	0.30-1.55
			θ=90° normal				1.10-2.10	0.89-1.90	0.65-1.85
WAVE PROJECTS									
BISHOP (1-4)	Christchurch Bay Wave Project	H=2-3m	Main Column d=2.8m				1.0	1.8-2.0	
			Wave Staff d=0.48m Smooth				0.65-0.8	1.1-1.7	

Table (1.2) Summary of Data on Hydrodynamic Coefficients

Reference	Location	Flow Particulars	Test Structure	Wave Theory	R_e	K	C_D	C_M	C_L
DEAN and AAGAARD(21)	Gulf of Mexico Wave Project I	H_{max} = 22ft		Stream Function	$6\times10^5-6\times10^6$		0.5-1.3	1.33	
	Wave Project II	H_{max} = 43ft							
EVANS(25)	Gulf of Mexico Wave Project I	H_{max} = 22ft							
		All Waves 15<H<22					0.59 0.50	1.5 1.5	
	Wave Project II	H_{max} = 43ft							
		All Waves					0.88	1.68	
		H>25ft and T>10sec					0.58	1.77	
HEIDEMANN et al(33)	Gulf of Mexico OTS	H = 8-14ft	0.5" Barnacle Fouled WFT			8-20	0.5-2.5	0.7-1.8	
		All Waves H=9-24ft T=6-12sec	Clean WFTS				0.68 (Assymptotic Value)	1.51-1.65 σ = 0.30	
			Fouled WFTS				1.0	1.25-1.43 σ = 0.34	
KAPLAN et al(38)			45^o Inclined Cylinders		$3.9\times10^5-4.8\times10^5$	33-50	0.84-1.13	1.73-2.3	0.15
KIM and HIBBARD (40)	Bass Straits (Australia)	H = 2.5-10ft Current Speed = 1.0ft/sec	Vertical cyl d = 12.75"		$2\times10^5-8\times10^5$		0.61 $\sigma\pm0.24$	1.2 $\sigma\pm0.22$	
OHMART and GRATZ(46)		Hurricane Edith	Test Platform WFT d=3ft		$3\times10^5-3\times10^6$		0.7	1.5-1.7	
WHEELER(64)	Gulf of Mexico Wave Project II	Hurricane Carla	d = 44"				0.44-0.60	0.0-2.0	
WIEGEL et al(65)	Davenport (California)	H_{max} = 20ft	Vert Cyl D=$6\frac{5}{8}$", $12\frac{3}{4}$", 2ft, 5ft	Airy	$3\times10^4-9\times10^5$			2.5	

Table (1.3) Summary of Data on Hydrodynamic Coefficients

CHAPTER 3

CHAPTER 3

OSS - A COMPUTER PROGRAM TO CALCULATE WAVE LOADING FOR JACKET STRUCTURES

1. INTRODUCTION

The majority of the work on the methods of wave loading analysis of jacket structures rests on the use of Morison's equation(7)

$$F = 0.5d\rho C_D\, U|U| + 0.25\, \pi\rho d^2 C_M \frac{dU}{dt}$$

where F is the force per unit length on a cylinder of diameter d and U is the horizontal component of the water velocity. As generally applied, it is assumed that the maximum acceleration and velocity occur at the same time (whereas according to wave theory they are 90° out of phase) and it is also common to assume that the maximum values occur on all members of the structure at the same time, i.e. no account is taken of the phase difference between the acceleration and velocity for the distance between different members of the structure in the directions of wave travel. The decay in the acceleration and velocity below the surface is accounted for by the usual exponential term but few, if any, programs seem to take account of the changes in Reynolds Number which this implies and adjust the drag and inertia coefficients to take account of this. Interference effects between adjacent members are rarely considered and especially their variation with R_e.

The following computer program was written to allow an examination of the differences in wave loading which could be obtained by using different assumptions about the way in which the accelerations and velocities are calculated and the C_M and C_D coefficients are obtained for a particular geometry of jacket structure. In particular the program performs the following:-

a. Calculates the forces and moments assuming that the maximum acceleration and velocity occurs at the same time on each member for the C_M and C_D values recommended by three Classification Societies: Lloyd's Register of Shipping (LR), Det norske Veritas (DnV), and Bureau Veritas (BV). However, any other coefficients specified by the user can be used.

b. Repeats the above calculation but taking account of the phase angle between the acceleration and velocity.

c. Analyses the Reynolds Number and Keulegan-Carpenter Number on each member and derives the C_M and C_D coefficients appropriate to these numbers from the work of Sarpkaya (Refs. (8) to (15)).

d. Using method (b) or (c) above taking account of interference effects between adjacent members on the drag coefficient.

e. The effect of current on the fluid loading can be taken into account.

f. The kinematics of the flow can be calculated by Airy wave theory, Stokes' 2nd order theory, or Stokes' 5th Order theory.

In this chapter, only the general method of calculation based on the Airy wave theory and the main features of the program will be discussed. The other features of the program which deal with specific problems such as the interference effects, current effect, or the use of Stokes wave theories will be presented and discussed in the subsequent chapters.

The program has been used to assess the level of 'accuracy' of existing methods of wave load estimation.

2. CALCULATION OF WAVE LOADING

2.1. General Procedure

The general method used follows an earlier program developed by Incecik (5).

The inertia and drag forces are calculated using Morison's equation, but taking into account the relative positions of the different members with respect to the structure reference system, Fig. (1). The time variation is also considered and the calculations are repeated at intervals of time of 0.1 x wave period. The transverse forces (lift forces) are taken into account and are calculated by a similar procedure.

The kinematics of the flow field are evaluated using linear wave theory (or Stokes 2nd and 5th order theories). The velocities and accelerations are first transferred from the wave reference system (x, y, z), see Fig. (1), to the member reference system and the forces and moments are calculated in the (u, v, w) directions. The forces and moments are then transferred to the structure reference system (X, Y, Z) and resolved to estimate the surge, heave and sway forces and also the rolling, yawing and pitching moments at the base of the structure.

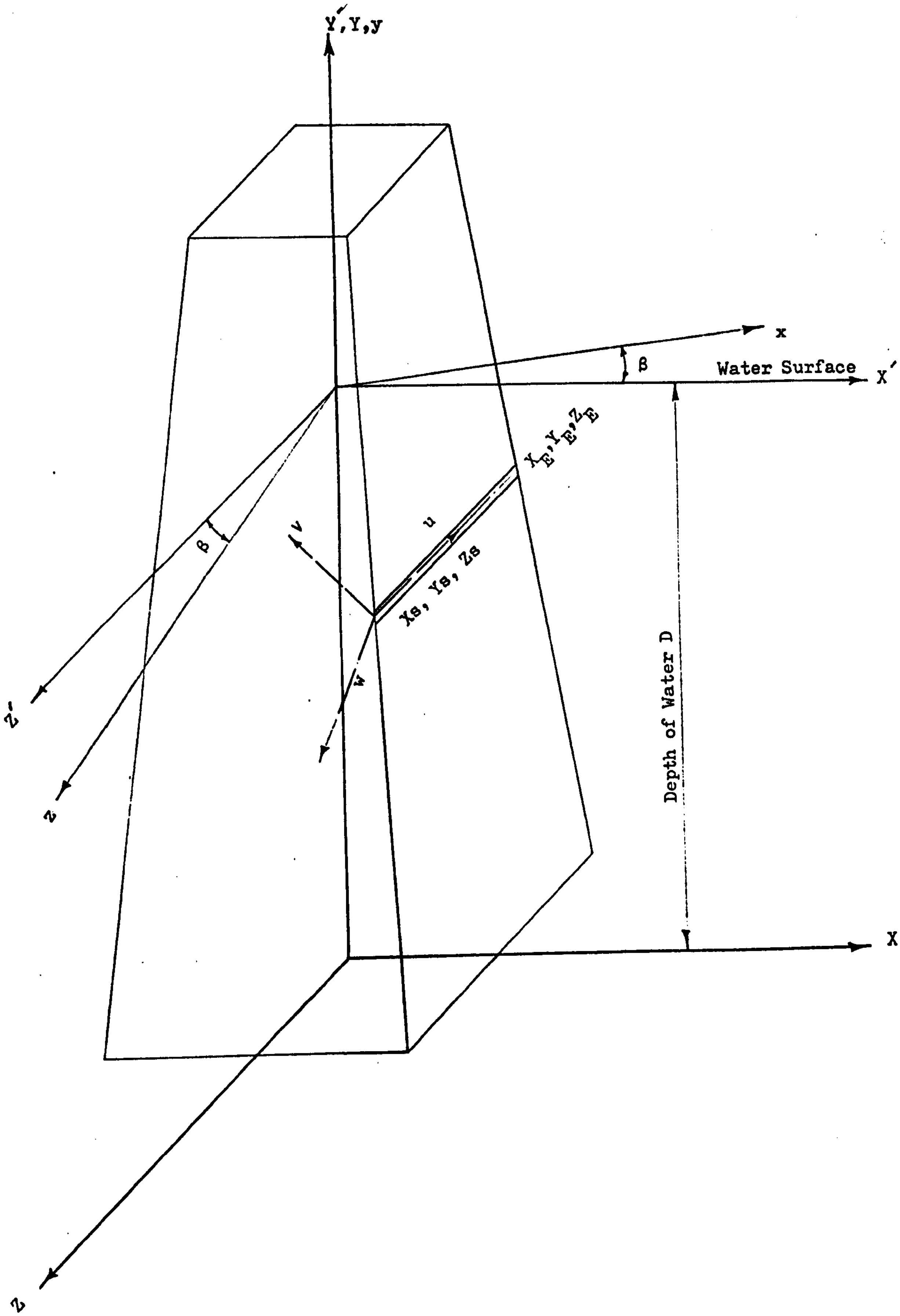

Fig. (1) Reference Systems

2.2. Kinematics of the Flow Field (Airy Theory)

The wave profile, the horizontal and vertical components of the water particle velocity and acceleration, written in the wave reference system, (x, y, z), are given by the following equations:-

$$y = 0.5H \operatorname{Cos}(k.x-\omega.t) \tag{1}$$

$$U_x = 0.5\omega.He^{ky} \operatorname{Cos}(k.x - \omega.t) \tag{2}$$

$$U_y = 0.5\omega\, He^{ky} \operatorname{Sin}(k.x - \omega.t) \tag{3}$$

$$\dot{U}_x = 0.5\omega^2He^{ky} \operatorname{Sin}(k.x - \omega.t) = \omega.U_y \tag{4}$$

$$\dot{U}_y = - 0.5\omega^2He^{ky} \operatorname{Cos}(k.x - \omega.t) = -\omega.U_x \tag{5}$$

To transfer the velocities and accelerations, equations (2) to (5), to the structure reference system, (X, Y, Z), the following matrix equation is used:-

$$\begin{bmatrix} x \\ y \\ z \end{bmatrix} = \begin{bmatrix} \beta_{11} & \beta_{12} & \beta_{13} \\ \beta_{21} & \beta_{22} & \beta_{23} \\ \beta_{31} & \beta_{32} & \beta_{33} \end{bmatrix} \begin{bmatrix} X \\ Y \\ Z \end{bmatrix} + \begin{bmatrix} 0.0 \\ -D \\ 0.0 \end{bmatrix} \tag{6}$$

where,

β_{11} : is the cosine of the angle between x and X axes = $\operatorname{Cos}\beta$

β_{12} : is the cosine of the angle between x and Y axes = 0.0

β_{13} : is the cosine of the angle between x and Z axes = $-\operatorname{Sin}\beta$

β_{21} : is the cosine of the angle between y and X axes = 0.0

β_{22} : is the cosine of the angle between y and Y axes = 1.0

β_{23} : is the cosine of the angle between y and Z axes = 0.0

β_{31} : is the cosine of the angle between z and X axes = $\operatorname{Sin}\beta$

β_{32} : is the cosine of the angle between z and Y axes = 0.0

β_{33} : is the cosine of the angle between z and Z axes = $\operatorname{Cos}\beta$

(0.0, -D, 0.0) : are the coordinates of the origin of the structure reference system relative to the wave reference system.

From equation (6), we get:-

$$x = X\cos\beta - Z\sin\beta \tag{7.a}$$

$$y = Y - D \tag{7.b}$$

$$z = X\sin\beta + Z\cos\beta \tag{7.c}$$

To transfer the velocities and accelerations from the structure reference system, (X, Y, Z), to the member reference system, (u, v, w), the following matrix equation is used:-

$$\begin{bmatrix} X \\ Y \\ Z \end{bmatrix} = \begin{bmatrix} \alpha_{11} & \alpha_{12} & \alpha_{13} \\ \alpha_{21} & \alpha_{22} & \alpha_{23} \\ \alpha_{31} & \alpha_{32} & \alpha_{33} \end{bmatrix} \begin{bmatrix} u \\ v \\ w \end{bmatrix} + \begin{bmatrix} X_s \\ Y_s \\ Z_s \end{bmatrix} \tag{8}$$

where,

α_{11} : is the cosine of the angle between X and u

α_{12} : is the cosine of the angle between X and v

α_{13} : is the cosine of the angle between X and w

α_{21} : is the cosine of the angle between Y and u

α_{22} : is the cosine of the angle between Y and v

α_{23} : is the cosine of the angle between Y and w

α_{31} : is the cosine of the angle between Z and u

α_{32} : is the cosine of the angle between Z and v

α_{33} : is the cosine of the angle between Z and w

(X_s, Y_s, Z_s) : are the coordinates of the starting point of the member Fig. (1).

From equations (8), we get:-

$$X = \alpha_{11}u + \alpha_{12}v + \alpha_{13}w + X_S \qquad (9.a)$$

$$Y = \alpha_{21}u + \alpha_{22}v + \alpha_{23}w + Y_S \qquad (9.b)$$

$$Z = \alpha_{31}u + \alpha_{32}v + \alpha_{33}w + Z_S \qquad (9.c)$$

Since the diameter of the member is assumed to be small relative to its length, the wave height and wave length, an approximation can be made by neglecting the terms including v or w and equations (9) now become:-

$$X = \alpha_{11}u + X_S \qquad (10.a)$$

$$Y = \alpha_{21}u + Y_S \qquad (10.b)$$

$$Z = \alpha_{31}u + Z_S \qquad (10.c)$$

Now equations (7) can be written as:-

$$x = (\alpha_{11} u + X_s)\cos\beta - (\alpha_{31} u + Z_s)\sin\beta \qquad (11.a)$$

$$y = \alpha_{21}u + Y_S - D \qquad (11.b)$$

$$z = (\alpha_{11}u + X_S)\sin\beta + (\alpha_{31}u + Z_S)\cos\beta \qquad (11.c)$$

Substituting from equations (11) into equations (2) and (3), the horizontal and vertical components of the water particle velocity, written in the member reference system but in a direction parallel to the wave propagation, are calculated by the following equations, Reference (5):-

$$U_x = 0.5\omega H e^{k(\alpha_{21}u + Y_s - D)} \cos\left[k\{(\alpha_{11}u + X_s)\cos\beta - (\alpha_{31}u + Z_s)\sin\beta\} - \omega.t\right] \quad (12)$$

$$U_y = 0.5\omega H e^{k(\alpha_{21}u + Y_s - D)} \sin\left[k\{\alpha_{11}u + X_s)\cos\beta - (\alpha_{31}u + Z_s)\sin\beta\} - \omega.t\right] \quad (13)$$

where α_{11}, α_{21}, α_{31} are the direction cosines between the direction of wave travel and the local axis of the member.

The horizontal and vertical components of water acceleration are calculated by the following relations:-

$$\dot{U}_x = \omega.U_y \quad (14)$$

$$\dot{U}_y = -\omega.U_x \quad (15)$$

Resolving the velocities and accelerations, (U_x, U_y, $\dot{U}_x$, $\dot{U}_y$), along the structure reference system, the following equations are obtained:-

$$U_{(X)} = U_x \cos\beta \quad (16.a)$$

$$U_{(Y)} = U_y \quad (16.b)$$

$$U_{(Z)} = -U_x \sin\beta \quad (16.c)$$

$$\dot{U}_{(X)} = \dot{U}_x \cos\beta \quad (16.d)$$

$$\dot{U}_{(Y)} = \dot{U}_y \quad (16.e)$$

$$\dot{U}_{(Z)} = - \dot{U}_x \text{Sin}\beta \tag{16.f}$$

The components of the wave velocities and accelerations in (v, w) directions can be calculated from the following equations:-

$$U_v = U_{(X)}\alpha_{12} + U_{(Y)}\alpha_{22} + U_{(Z)}\alpha_{32} \tag{17.a}$$

$$= U_x(\alpha_{12}\ \text{Cos}\beta - \alpha_{32}\ \text{Sin}\beta) + U_y\alpha_{22} \tag{17.b}$$

$$U_w = U_{(X)}\alpha_{13} + U_{(Y)}\alpha_{23} + U_{(Z)}\alpha_{33} \tag{17.c}$$

$$= U_x(\alpha_{13}\ \text{Cos}\beta - \alpha_{33}\ \text{Sin}\beta) + U_y\alpha_{23} \tag{17.d}$$

$$\dot{U}_v = \dot{U}_{(X)}\alpha_{12} + \dot{U}_{(Y)}\alpha_{22} + \dot{U}_{(Z)}\alpha_{32} \tag{17.e}$$

$$= \dot{U}_x(\alpha_{12}\ \text{Cos}\beta - \alpha_{32}\ \text{Sin}\beta) + \dot{U}_y\alpha_{22} \tag{17.f}$$

$$\dot{U}_w = \dot{U}_{(X)}\alpha_{13} + \dot{U}_{(Y)}\alpha_{23} + \dot{U}_{(Z)}\alpha_{33} \tag{17.g}$$

$$= \dot{U}_x(\alpha_{13}\ \text{Cos}\beta - \alpha_{33}\text{Sin}\beta) + \dot{U}_y\alpha_{23} \tag{17.h}$$

2.3 Calculation of the inertia force

The inertia forces in the (v, w) directions, for a member of length ℓ, are calculated by the following equations:-

$$F_{I_w} = \pi/4\rho d^2 \int_{0.0}^{\ell} C_M\{\dot{U}_x(\alpha_{13}\text{Cos}\beta - \alpha_{33}\text{Sin}\beta) + \dot{U}_y\alpha_{23}\}du \tag{18}$$

$$F_{I_v} = \pi/4\rho d^2 \int_{0.0}^{\ell} C_M\{\dot{U}_x(\alpha_{12}\text{Cos}\beta - \alpha_{32}\text{Sin}\beta) + \dot{U}_y\alpha_{22}\}du \tag{19}$$

2.4 Calculation of the drag force

The drag forces in the (v, w) directions are calculated by the following equations:-

$$F_{D_v} = 0.5\ \rho d \int_{0.0}^{\ell} C_D.U_v|U_v|du \tag{20}$$

$$F_{D_w} = 0.5\,\rho\, d \int_{0.0}^{\ell} C_D . U_w |U_w| du \qquad (21)$$

2.5 Calculation of the transverse (lift) force

The lift forces in the (v, w) directions are calculated by the following equations:-

$$F_{L_v} = 0.5\,\rho\, d \int_{0.0}^{\ell} C_L . U_w |U_w| du \qquad (22)$$

$$F_{L_w} = 0.5\,\rho\, d \int_{0.0}^{\ell} C_L . U_v |U_v| du \qquad (23)$$

2.6 Calculation of surge, heave, and sway forces

The total forces in the (v,w) directions for any member 'i' are given by:-

$$F_{T_{vi}} = F_{I_v} + F_{D_v} + F_{L_v} \qquad (24)$$

$$F_{T_{wi}} = F_{I_w} + F_{D_w} + F_{L_w} \qquad (25)$$

The surge, heave and sway forces acting at the base of the structure of 'm' members are calculated by the following equations:-

$$\text{Surge Force} = \sum_{i=1}^{m} (F_{T_{wi}} \alpha_{13} + F_{T_{vi}} \alpha_{12}) \qquad (26)$$

$$\text{Heave Force} = \sum_{i=1}^{m} (F_{T_{wi}} \alpha_{23} + F_{T_{vi}} \alpha_{22}) \qquad (27)$$

$$\text{Sway Force} = \sum_{i=1}^{m} (F_{T_{wi}} \alpha_{33} + F_{T_{vi}} \alpha_{32}) \qquad (28)$$

2.7 Calculation of Rolling, Yawing and Pitching Moments

The total moments of the forces in the (v,w) directions for any member 'i', taken about its starting point, see Appendix (A), are given by:-

$$T_{M_{vi}} = M_{I_v} + M_{D_v} + M_{L_v} \tag{29}$$

$$T_{M_{wi}} = M_{I_w} + M_{D_w} + M_{L_w} \tag{30}$$

where:

M_{I_v} is the moment of the inertia force in the 'v' direction for the member about its starting point

M_{D_v} is the moment of the drag force in the 'v' direction for the member about its starting point

M_{L_v} is the moment of the lift force in the 'v' direction for the member about its starting point

M_{I_w}, M_{D_w} and M_{L_w} have the same definitions in the 'w' direction.

The rolling, yawing and pitching moments acting at the base of the structure of 'm' members are calculated by the following equations:-

$$\text{Rolling Moment} = \sum_{i=1}^{m} \{\alpha_{13}.T_{M_{vi}} - \alpha_{12}\, T_{M_{wi}} + F_{T_{wi}}(Y_s.\alpha_{33} - Z_s.\alpha_{23}) + F_{T_{vi}}(Y_s\alpha_{32} - Z_s\alpha_{22})\} \tag{31}$$

$$\text{Yawing Moment} = \sum_{i=1}^{m} \{\alpha_{23}.T_{M_{vi}} - \alpha_{22}\, T_{M_{wi}} + F_{T_{wi}}(Z_s.\alpha_{13} - X_s.\alpha_{33}) + F_{T_{vi}}(Z_s\alpha 12 - X_s.\alpha_{32})\} \tag{32}$$

$$\text{Pitching Moment} = \sum_{i=1}^{m} \{\alpha_{33}.T_{M_{vi}} - \alpha_{32}.T_{M_{wi}} + F_{T_{wi}}(X_s.\alpha_{23} - Y_s.\alpha_{13}) + F_{T_{vi}}(X_s.\alpha_{22} - Y_s.\alpha_{12})\} \tag{33}$$

3. DESCRIPTION OF THE COMPUTER PROGRAMS

3.1 Main Program OSS

This program calculates the wave loading on steel jacket offshore structures. Program OSS uses another two programs, XYZ and DATA, to create a data file containing the information regarding the geometry of the structure. OSS also calls the following subroutines: SIMP, DIRCOS, MAX2, MAX4, COEF and CDCMCL, see Fig. (2).

Each member of the structure is divided into 10 sections and the numerical integration of the forces and moments is carried out by Simpson's first rule using 11 ordinates.

To run OSS the following input data are required:-

(a) Wave frequency ω (rad/s) and wave height H(m)

(b) Depth of water D (m)

(c) Incident angle of wave β (rad)

(d) Lift coefficient C_L (option when using subroutine COEFF)

(e) Water density ρ (Kg/m^3) and kinematic viscosity ν (m^2/s)

(f) The code of the classification society required.

The following output data can be obtained from the program:-

(1) The actual length and the direction cosines of each member, see Figs. (A.1) and (A.2), Appendix A.

(2) The distribution of velocities and accelerations of the flow field along the member length in the x and y directions (or (v,w) directions).

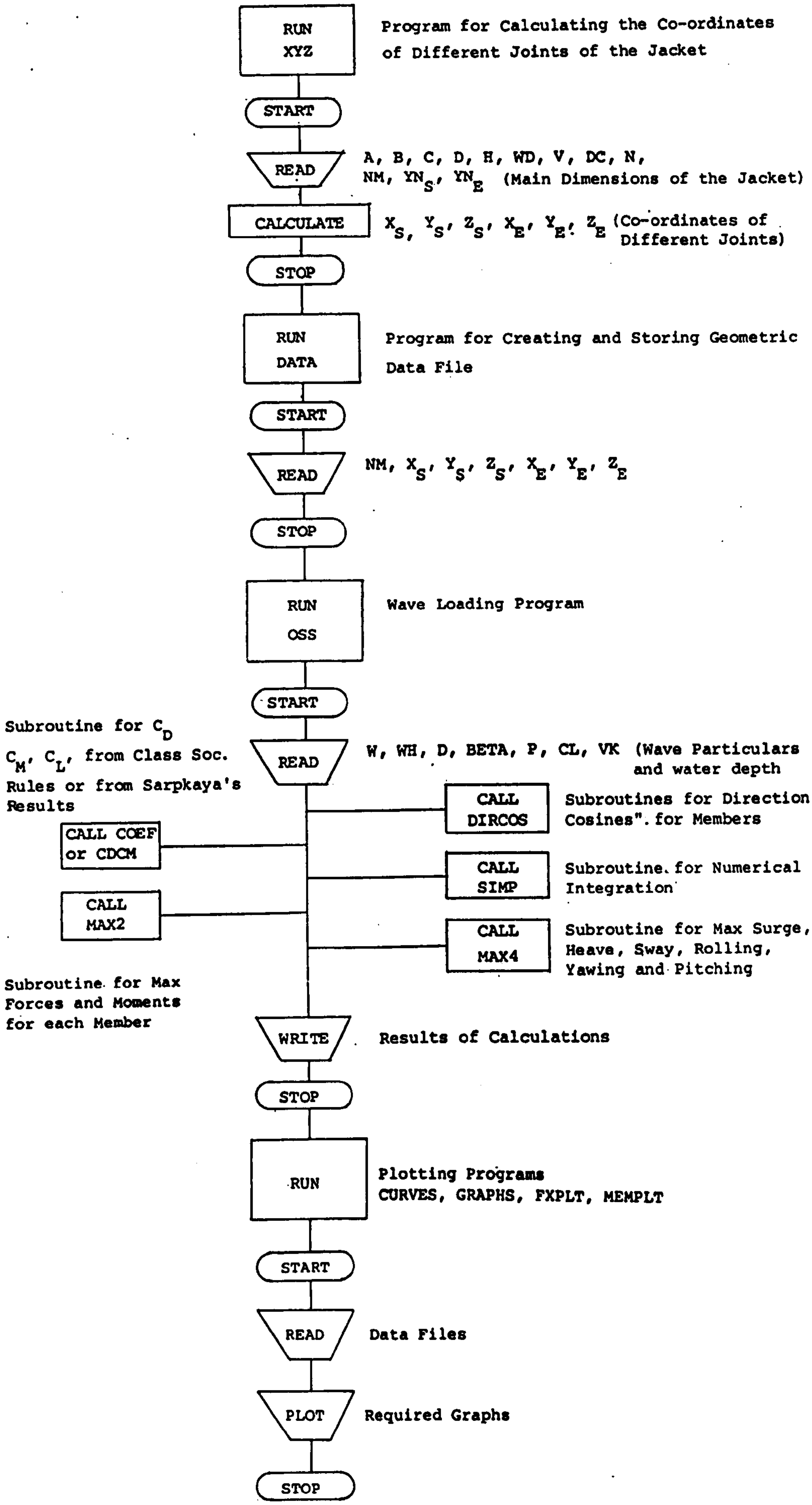

Fig. (2) Flow Chart for the Programs

(3) The distribution of forces (inertia, drag and lift) along the member length in the (v, w) directions.

(4) The resultant force and the total moment about the starting point of the member in the (v, w) directions.

(5) The total forces acting at the base of the structure at any interval of time within one complete wave cycle:-

(i) Surge Force in X direction

(ii) Heave Force in Y direction

(iii) Sway Force in Z direction.

(6) The total moments acting at the base of the structure at any interval of time within one complete wave cycle:-

(i) Rolling Moment about X axis

(ii) Yawing Moment about Y axis

(iii) Pitching Moment about Z axis.

(7) The maximum forces and maximum moments in the (v, w) directions for each member within one complete wave cycle and the correponding instantaneous time for each.

(8) The maximum values of surge force, heaving force, and sway force within the wave cycle.

(9) The maximum values of rolling moment, yawing moment, and pitching moment within the wave cycle.

3.2 Program XYZ

This program is used to determine the co-ordinates of the starting and end points for each member in the structure. The input data are:-

(a) The main dimensions (length and breadth) at the base of the structure.

(b) The main dimensions (length and breadth) at the top of the structure.

(c) The height of the structure and the depth of water.

(d) YN_S and YN_E for each member. (See Appendix A).

The output data of this program are used by program DATA.

3.3 Program DATA

This program is used to create a data file containing the co-ordinates of the different joints and the external diameters of the members of the structure. It is assumed that the structure is rectangular in plan form and that the axes are taken at the centre with X and Z horizontally and Y vertically, see Fig. (1). The input data are:-

a. The total number of members.

b. The co-ordinates of the starting point (X_s, Y_s, Z_s) of each member (determined from Program XYZ).

c. The external diameter of each member.

3.4 Subroutine DIRCOS

This subroutine determines the direction cosines of each member α_{11}, α_{12}, α_{13}, α_{21}, α_{22}, α_{23}, α_{31}, α_{32} and α_{33}.

3.5 Subroutine SIMP

This subroutine is used to carry out the numerical integration of the forces and moments for each member in (v,w) directions.

Simpson's first rule is used with 11 ordinates. However, more ordinates could be used if necessary by slight modification in this subroutine.

3.6 Subroutine MAX2

This subroutine is used to determine the maximum values of the forces and the moments in (v,w) directions and also the relative time defined as,

$$\frac{T_{max}}{\text{wave period}} \quad \text{for each member}$$

T_{max} is the instantaneous time at which the maximum force (or moment) occurs.

3.7 Subroutine MAX4

This subroutine determines the maximum values of the total forces (surge, heave, sway) and the total moments (rolling, yawing, pitching) acting at the base of the structure within one complete wave cycle.

3.8 Subroutine COEF

This subroutine determines the inertia and drag coefficients as recommended by three Classification Societies, namely:-

(a) Lloyd's Register of Shipping (LR, code number 1), Ref. (6)

(b) Det Norske Veritas (DnV, code number 2), Refs. (2-4)

(c) Bureau Veritas (BV, code number 3), Ref. (1)

When running the main program OSS, the values of drag and inertia coefficients (C_D and C_M) can be chosen by selecting the corresponding 'code number' of the Classification Society.

The values of C_D and C_M as obtained from steady flow data could also be used by selecting code number 4. In this case:-

$$C_D = 0.6$$

$$C_M = 2.0$$

3.9 Subroutine CDCMCL

This subroutine determines the drag, inertia and lift coefficients according to the work of Sarpkaya. The data are determined from a series of polynomials obtained by curve fitting the results given in Refs. (8) to (15). The full description of this work will be given in Chapter 5.

3.10 Programs CURVES, GRAPHS, FXPLT, MEMPLT

These are various plotting programs to present the output data graphically such as:-

(a) The variation of the total forces (surge, heave and sway) and total moments, (rolling, yawing and pitching) with time for one complete wave cycle.

(b) The variation of the maximum surge force, heave force, etc, with frequency.

(c) The variation of the member forces with frequency.

REFERENCES

1. BUREAU VERITAS, 'Rules and Regulations for the Construction and Classification of Offshore Platforms', 1975.

2. DET NORSKE VERITAS, 'Rules for the Design, Construction and Inspection of Mobile Offshore Units', 1974.

3. DET NORSKE VERITAS, 'Rules for the Construction and Classification of Mobile Offshore Units', 1975.

4. DET NORSKE VERITAS, 'Rules for the Design, Construction and Inspection of Offshore Structures', Appendix B, 1977.

5. INCECIK, A, 'A General Method and a Computer Program to Calculate Wave Loading on the Circular Cylindrical Members of Fixed and of Floating Offshore Structures', Dept of Naval Architecture and Ocean Engineering, University of Glasgow, Report No NAOE-HL-80-19, 1980.

6. LLOYD'S REGISTER OF SHIPPING, 'Rules for the Construction and Classification of Mobile Offshore Units', 1972.

7. MORISON, J R, et al, 'The Force Exerted by Surface Waves on Piles', Petroleum Trans, AIME, Vol 189, 1950, pp149-157.

8. SARPKAYA, T, 'In-Line and Transverse Forces on Smooth and Sand-Roughened Cylinders in Oscillatory Flow at High Reynolds Numbers', Naval Postgraduate School, Technical Report No NPS-69SL76062, Monterey, CA, Jun 76.

9. SARPKAYA, T, 'Vortex Shedding and Resistance in Harmonic Flow about Smooth and Rough Circular Cylinders at High Reynolds Numbers', Naval Postgraduate School, Technical Report No NPS-59SL76021, Moneterey, CA, Feb 76.

10. SARPKAYA, T, 'In-Line and Transverse Forces on Cylinders in Oscillatory Flow at High Reynolds Numbers', OTC Paper No 2533, Houston, Texas, May 76.

11. SARPKAYA, T, 'Vortex Shedding and Resistance in Harmonic Flow about Smooth and Rough Circular Cylinders', BOSS '76, Trondheim, Vol I, 1976, pp220-235.

12. SARPKAYA, T, 'In-Line and Transverse Forces on Cylinders in Oscillatory Flow at High Reynolds Numbers', Jour of Ship Research, Vol 24, No 4, Dec 77, pp200-216.

13. SARPKAYA, T, 'The Hydrodynamic Resistance of Roughened Cylinders in Harmonic Flow', Trans RINA, Vol 120, 1978, pp41-55.

14. SARPKAYA, T, COLLINS, N J, and EVANS, S R, 'Wave Forces on Rough-Walled Cylinders at High Reynolds Numbers', OTC Paper No 2901, Houston, Texas, 1977.

15. SARPKAYA, T, and ISAACSON, M, 'Mechanics of Wave Forces on Offshore Structures', Van Nostrand Reinhold, New York, 1981.

CHAPTER 4

CHAPTER 4

THE INFLUENCE OF DRAG AND INERTIA COEFFICIENTS ON WAVE LOADING

1. INTRODUCTION

A steel jacket offshore platform generally consists of circular members connected together in various planes. To design such a space structure, the forces and moments due to waves and currents on the individual members should be estimated, as well as the resultant forces and moments acting on the whole structure at its base.

The most widely used method to calculate the forces due to waves has been based on Morison's equation (6).

The original Morison's equation for the force on a vertical cylinder reads:

$$F = 0.5\ d\ \rho\ C_D\ U.\ |U| + 0.25\ \pi\ d^2 \rho\ \ C_M \frac{dU}{dt}$$

where F is the force per unit length on a cylinder of diameter d and U is the horizontal component of the water particle velocity.

A particular difficulty in applying the equation for design purposes has been the selection of the appropriate coefficients, namely, the drag coefficient C_D and the inertia coefficient C_M. The selection of the coefficients generally depends on Reynolds number R_e, Keulegan-Carpenter number K, and the surface roughness of the cylinder. Strictly speaking, the coefficients should also be considered as time-dependent and varying along the length of the cylinder, although in most current design methods only constant values are assumed.

The rules of the Classification Societies for offshore structures, recommend values of C_D and C_M for wave loading calculations. The recommended values by the different classification rules are constant and are related mainly to the diameter of the cylinder and do not reflect the variation with Reynolds number, Keulegan-Carpenter number and roughness mentioned above.

The purpose of the current chapter is to show the effect of the differences in C_D and C_M values as given by Lloyd's Register of Shipping (LR), Det Norske Veritas (DnV) and Bureau Veritas (BV) rules on the wave loading estimation.

Chapter (5) will compare these results with the results of calculations where the C_M and C_D values are related directly to the Reynolds number and Keulegan-Carpenter number for each member using the experimental results of Sarpkaya.

The design load for each member will be a combination of the above wave loads, the loads induced by the mass of decks and equipment and the elastic response of the structure to these loads. Thus in members far below the surface where the wave action is slight, the dominant loads will come purely from the transmission of the loads applied higher up to the foundations. In reliability studies it is important to know not only how the load in each member arrives but also the probability of that maximum load occuring at the same time as the maxima in other members. This study may help answer some of these questions.

2. METHODS OF CALCULATION

2.1 General

For the purpose of calculations and comparison between the three different classification rules, a jacket structure of 119 members was chosen representing a typical offshore platform. The structure is symmetrical with respect to the X axis and Z axis (See Fig. (1)). The base and top of the structure were assumed to be square. The main particulars are shown in Fig. (2). A three dimensional representation of the jacket structure with its member numbering is shown in Figs. (3) and (4).

The sizes of the members were selected so as to cover the range of diameters where viscous forces form a significant proportion of the total force and where there is considerable dispute as to the appropriate inertia and drag coefficients. Thus the main columns have a diameter of 4m and the bracing are of 1.5 and 2.0m diameter.

The calculations were carried out for nine wave frequencies varying from 0.37 rad/s ($L = 450.01$m) to 1.6 rad/s ($L = 54.83$m).

Since the structure is square in planform, two values for the incident angle of wave (β) were considered, namely 0^{o} and 45^{o}.

A summary of the particulars of the waves is given in Table (1) and a summary of the recommended values of C_D and C_M by LR, DnV and BV is given in Table (2).

The calculations were performed for the bracing members

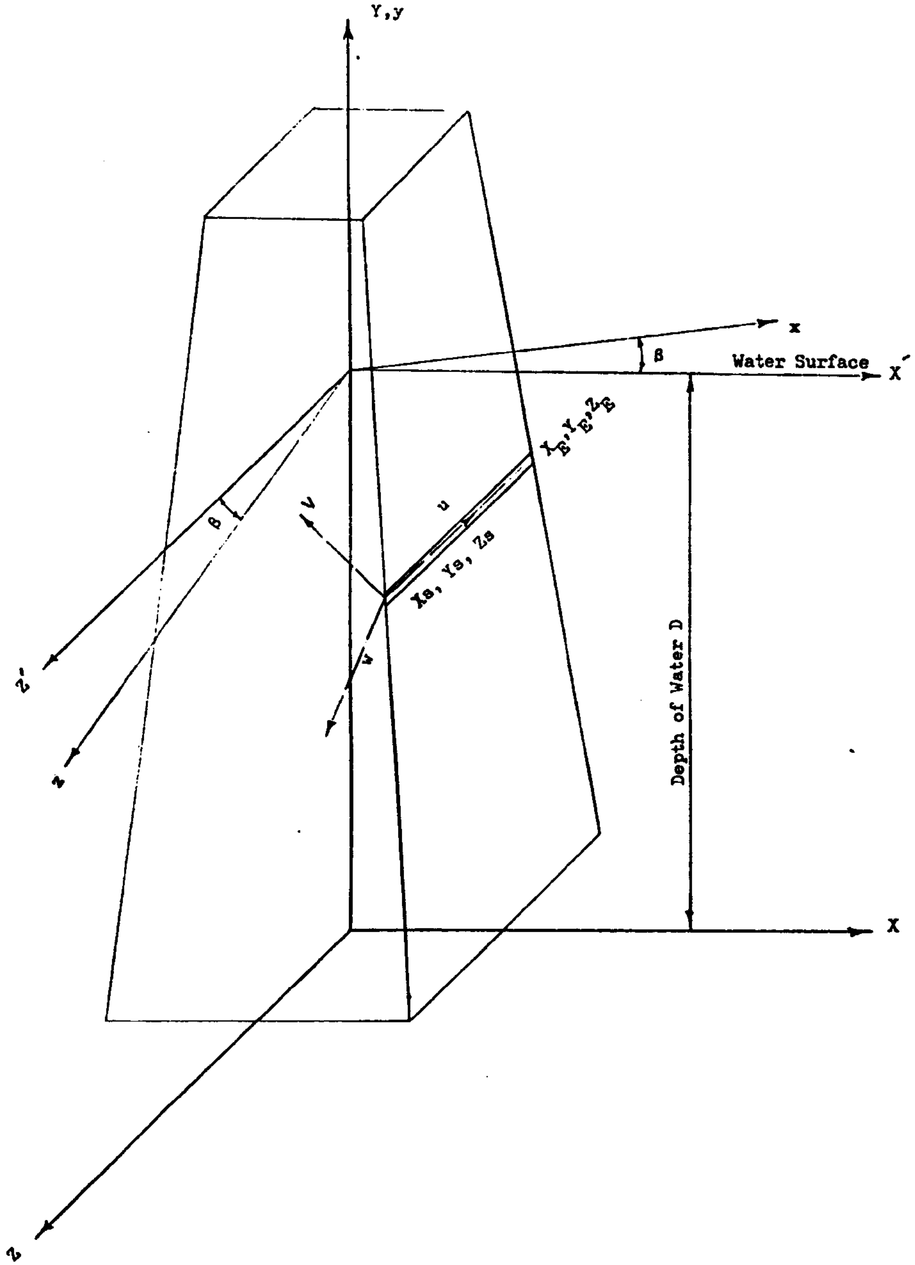

Fig. (1) Reference Systems

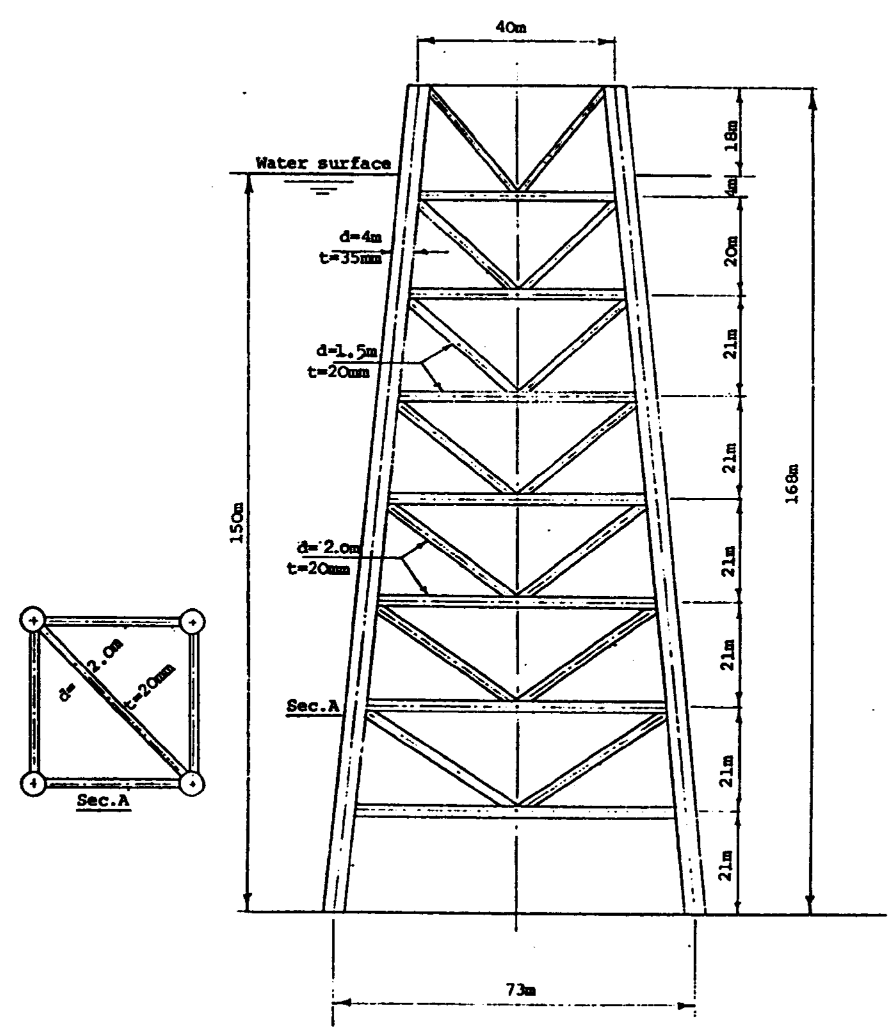

Fig. (2) Main Particulars of the Jacket Structure

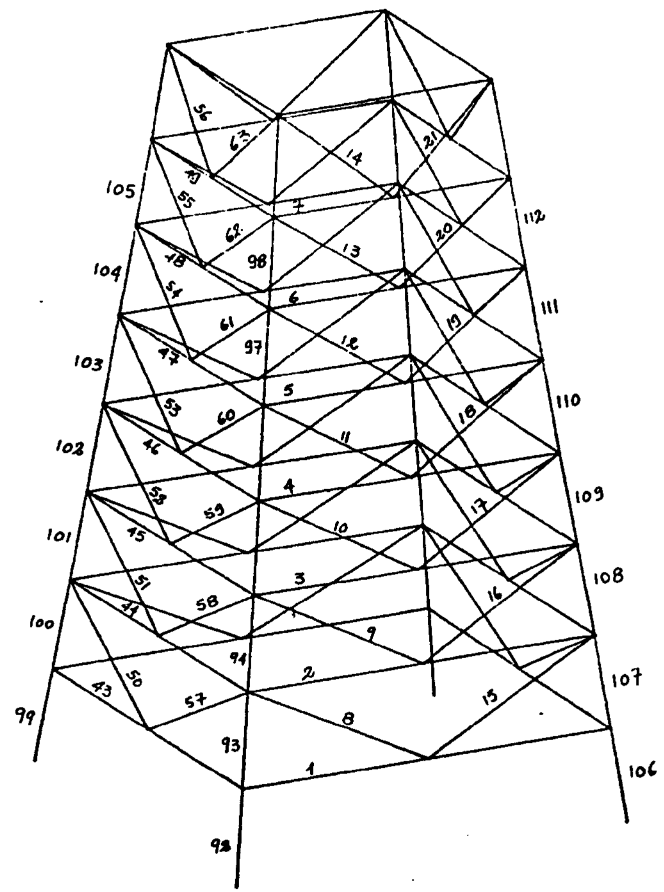

BASE DIMENSIONS=73X73 m　　TOP DIMENSIONS=40X40 m
HEIGHT=168 m　　NUMBER OF MEMBERS=119
FIG.(3) 3-DIM. REPRESENTATION OF THE JACKET STRUCTURE

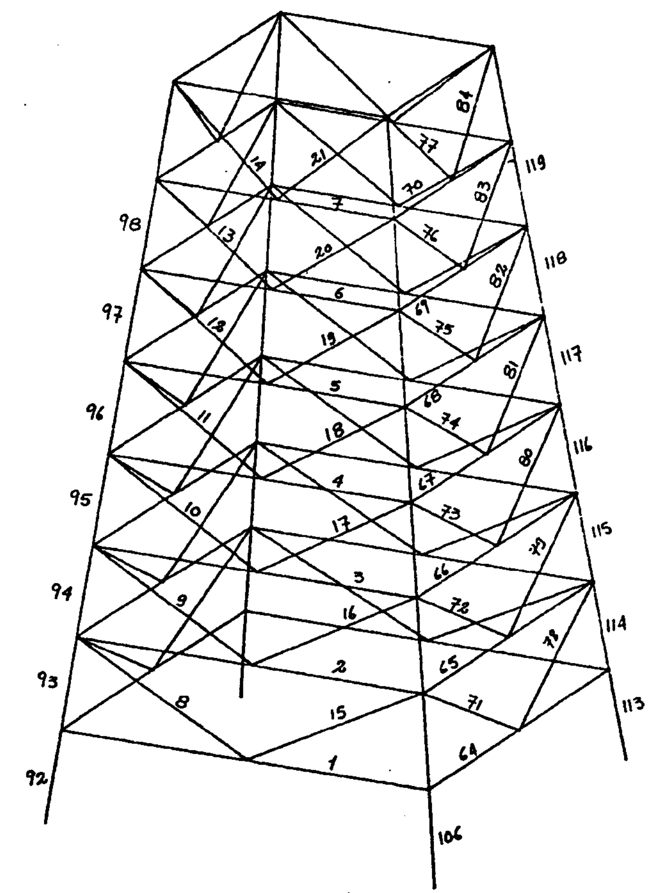

BASE DIMENSIONS=73X73 m　　TOP DIMENSIONS=40X40 m
HEIGHT=168 m　　NUMBER OF MEMBERS=119
FIG.(4) 3-DIM. REPRESENTATION OF THE JACKET STRUCTURE

Wave Length L(m)	Wave Height H(m)	Wave Period T(s)	Frequency ω(rad/s)
54.83	6	5.92	1.06
69.72	7	6.68	0.94
109.52	11	8.37	0.75
150.40	15	9.81	0.64
196.45	20	11.21	0.56
246.43	20	12.56	0.50
304.23	20	13.96	0.45
349.24	20	14.95	0.42
450.01	30	16.97	0.37

Table (1) Particulars of Waves

Classi-cation Society	Drag Co-efficient C_D	Inertia Coefficient C_M	Notes
LR	0.5	1.5 ($d \leq$ 3.5m) 2.0 ($d \geq$ 3.5m)	smooth cylinders d=dia of cylinder
DnV	$\geq$ 0.7	1.5 ($d/\ell = 1.0$) 2.0 ($d/\ell \leq 0.1$)	$R_e > 3 \times 10^6$ ℓ=length of cylinder if $0.1 < d/\ell < 1$ interpolate for C_M
BV	0.75	1.6 ($d \leq$ 1.45m) $C_M = 1 + \sqrt{\log_{10}(10d) - 0.8}$	($d >$ 1.45m)

Table (2) Values of C_D and C_M as recommended by LR, DnV and BV assuming that the starting and end points of the member are the nodes resulting from the intersection of the centre line of the member with the other members at each end.

Therefore, the length of the member used in the calculations is in fact larger than the actual length exposed to the waves by about 8%. However, for the main columns, the actual lengths were used.

When the exact lengths of all members of the structure were used and the calculations were repeated for some sample frequencies, the values of the maximum forces and maximum moments were reduced by about 10%.

It should be noted that all the results given in this chapter are related to the approximate lengths used in calculations.

2.2 Program OSS

This program calculates the wave forces and moments in each member and sums them algebraically for the complete structure using the velocities and accelerations at eleven points along the member. The basic formula is similar to Morison's approach except that the phase angles between wave displacement, velocity and acceleration are allowed for assuming linear wave theory and deep water throughout.

For each wave frequency the calculations were performed for one complete wave cycle with increments of time of 0.1 x period. For each member the maximum forces and moments in (v, w) directions were printed out, together with the corresponding relative times. For the complete structure the maximum values of the total forces (surge, heave and sway) as well as the total moments (rolling, yawing and pitching) were also printed. The graphs representing the variation of the total forces and moments with time and frequency were also drawn. A summary of the results of these calculations is given in the attached tables.

2.3 Program MRSEQ

This program is a modified version of program OSS. It repeats the above mentioned calculations with the same sequence but after eliminating the time dependent terms from the equations and assuming that the maximum drag force and maximum inertia force for all members of the structure occur simultaneously. When applying Morison's equation in this case, the inertia and drag forces are added **vectorially**, i.e. taking into consideration the actual directions of forces. The results of the calculations are summarised in the attached tables.

2.4 Program MRSEQ2

This program is similar to program MRSEQ but it shows another method of applying Morison's equation for design purposes.

In this case, the maximum drag force and maximum inertia force for the different members are assumed to occur at the same time but the absolute values are added together, ie, the actual directions of forces are not considered. The results of calculations are summarised in the attached tables.

3. ANALYSIS OF RESULTS FOR THE INDIVIDUAL MEMBERS

To analyse the results, the values of forces and moments obtained when using LR coefficients were taken as the basis for the comparison.

3.1 C_D and C_M Coefficients

Table (3) summarises the recommended values of C_D and C_M coefficients as applied to the jacket structure under consideration. According to DnV, the drag coefficient C_D is larger by 40% and the inertia coefficient C_M is larger by 33% compared to the LR values when the diameter of the cylinder is either 1.5m or 2.0m.

According to BV, the drag coefficient C_D is larger by 50% and the inertia coefficient C_M is larger by 7.5% and 14% for the 1.5m and 2.0m diameters respectively.

For the 4.0m diameter, C_M is smaller by 5%.

Classification Society	d = 1.5m		d = 2.0m		d = 4.0m	
	C_D	C_M	C_D	C_M	C_D	C_M
LR	0.5	1.5	0.5	1.5	0.5	2.0
DnV	0.7	2.0	0.7	2.0	0.7	2.0
BV	0.75	1.613	0.75	1.708	0.75	1.896

Table (3) Recommended Values of C_D and C_M for the Jacket Structure

3.2 Position of Wave Relative to the Structure

When a wave passes through the structure, the various members of the structure will be at different positions relative to the wave crest and thus will experience different velocities and accelerations relative to one another.

Figures (5) and (6) show the varying position of the wave relative to the jacket structure for two frequencies (ω = 0.37 rad/s, ω = 0.64 rad/s). The graphs show 4 positions at different times as a ratio of the wave period. The starting time (t = 0.0) is that when the crest of the wave is at the centre line of the structure. The graphs show also the ratio between the wave height and length and the overall dimensions of the structure.

Figures (7), (8) and (9) show the position of the wave relative to the upper part of the structure near to the water surface for all frequencies from 1.06 rad/s to 0.37 rad/s. The graphs also compare the dimensions of the waves (length and height) at the different frequencies.

In the shortest waves there can be complete reversal of sign of velocity and acceleration from one side of the structure to the other while in long waves the majority of the structure will be experiencing the same directions of flow at any given time. Although this latter condition is likely to produce the highest overall bending moment and shear force, it may not produce the highest load in individual members.

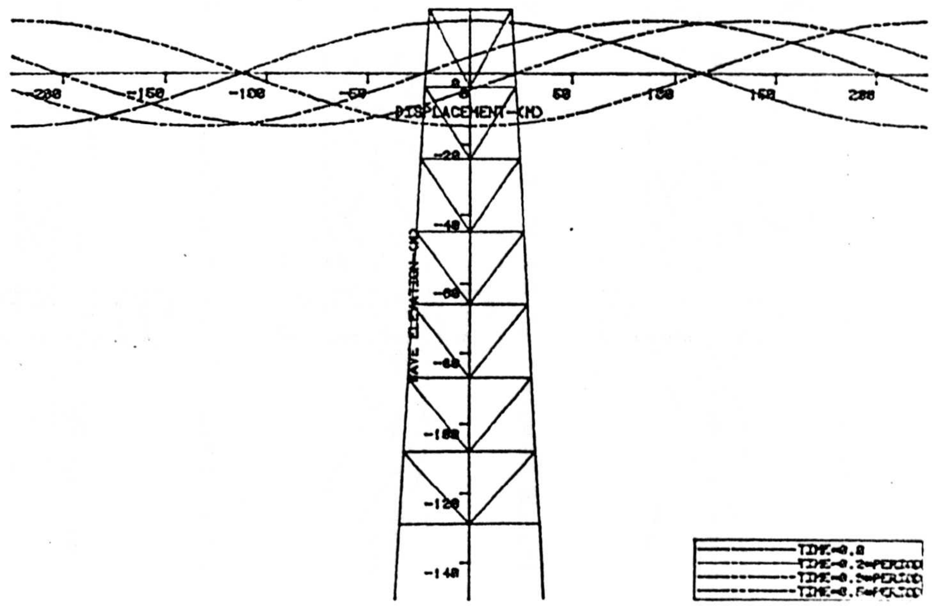

FIG.(5)POSITION OF WAVE RELATIVE TO THE STRUCTURE, ω =0.37 R/S, L = 450.01 M

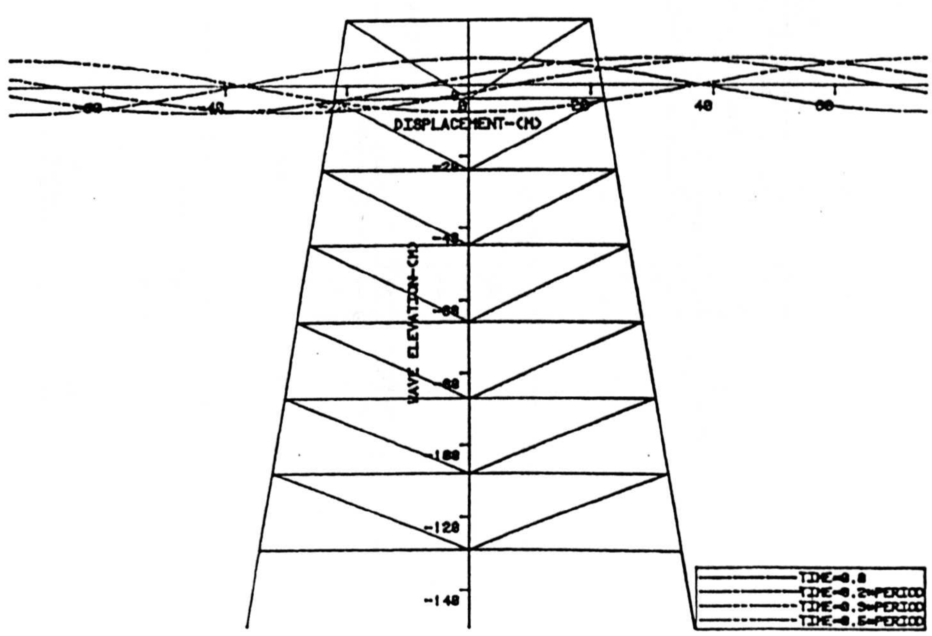

FIG.(6)POSITION OF WAVE RELATIVE TO THE STRUCTURE, ω =0.64 R/S, L = 150.4 M

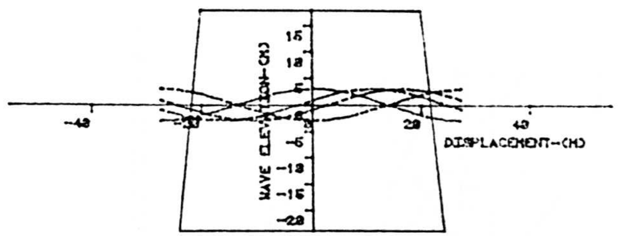

(a) FREQUENCY=1.06 R/S, WAVE LENGTH= 54.83 M

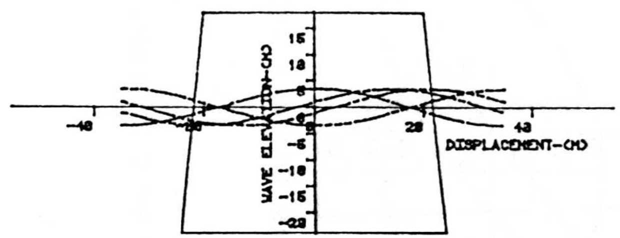

(b) FREQUENCY= 0.94 R/S, WAVE LENGTH= 69.72 M

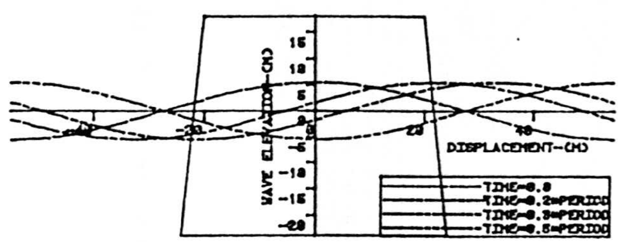

(c) FREQUENCY=0.75 R/S, WAVE LENGTH= 109.52 M

FIG.(7)POSITION OF WAVE RELATIVE TO THE STRUCTURE AT DIFFERENT FREQUENCIES

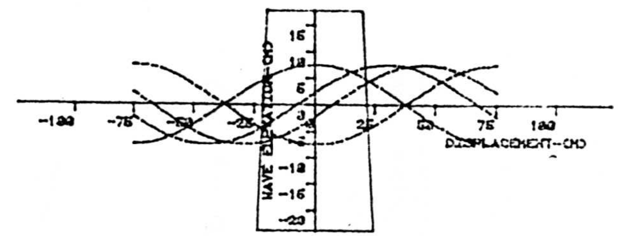

(a) FREQUENCY= 0.64R/S, WAVE LENGTH=150.4 M

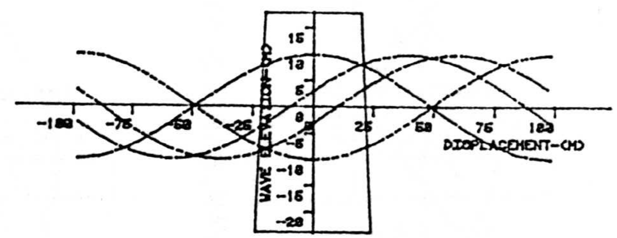

(b) FREQUENCY= 0.56R/S, WAVE LENGTH= 196.4 M

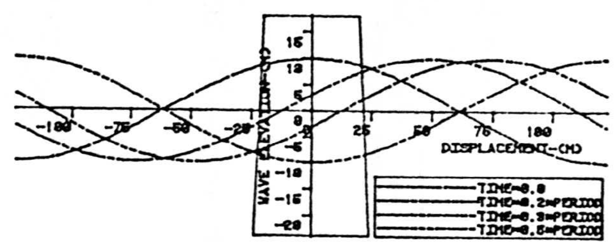

(c) FREQUENCY= 0.5 R/S, WAVE LENGTH= 246.53 M

FIG.(8)POSITION OF WAVE RELATIVE TO THE STRUCTURE AT DIFFERENT FREQUENCIES

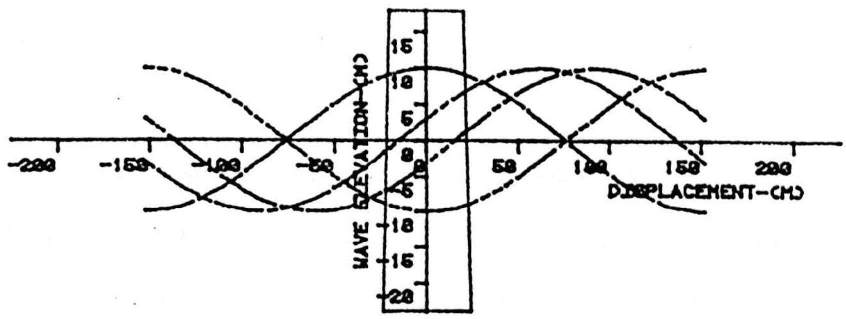

(a) FREQUENCY= 0.45R/S, WAVE LENGTH= 304.23 M

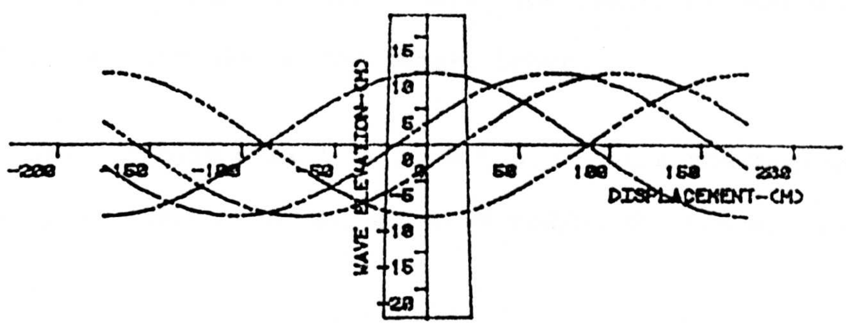

(b) FREQUENCY= 0.42 R/S, WAVE LENGTH= 349.24 M

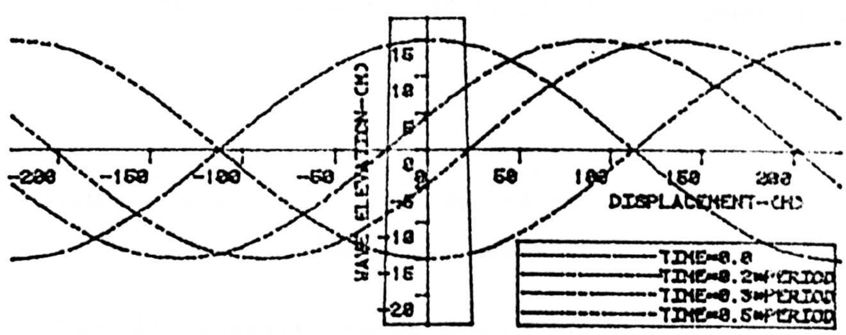

(c) FREQUENCY= 0.37 R/S, WAVE LENGTH= 450.01 M

FIG.(9)POSITION OF WAVE RELATIVE TO THE STRUCTURE AT DIFFERENT FREQUENCIES

3.3 Maximum Forces on Members and the Relative Time

As an illustrative example, the results of the maximum forces (in w direction) for the different members of the structure at two frequencies (0.37 rad/s and 0.64 rad/s) were analysed and are summarised in Table (4).

In the case of LR, the results show that when $\omega = 0.37$ rad/s, a maximum number of 35 out of 119 (29.4%) had their maximum forces occuring at the same relative time. The relative time is defined as the instantaneous time at which the maximum force occurs divided by the wave period. When $\omega = 0.64$ rad/s, the number of members increased to 44 representing 37% of the total number.

DnV results show that at $\omega = 0.37$ rad/s the maximum number of members is 34 (28.6%) and at $\omega = 0.64$ rad/s, the number increased to 44 (37%).

In the case of BV, the maximum number of members at $\omega = 0.37$ rad/s is 35 (29.4%) and at $\omega = 0.64$ rad/s the maximum number is 38 (31.9%).

3.4 Maximum Forces (F_{T_w}), OSS Vs. MRSEQ

Table (5) compares the values of the maximum forces in the 'w' direction (F_{T_w}) for 36 different members, as calculated by Programs OSS and MRSEQ for three different frequencies and using the LR coefficients. The comparison is limited to these two programs only because both of them sum the drag and inertia forces algebraically i.e. taking the correct signs into account, which is not the case for Program, MRSEQ2. From the given results the following is noted:

Classification Society	Relative time $t_r = \frac{T_{max}}{Period}$	ω = 0.37 rad/s		ω = 0.64 rad/s	
		number of members	% of the total number	number of members	% of the total number
LR	0.0	23	19.3%	44	37%
	0.1	32	26.9%	20	16.8%
	0.2	35	29.4%	22	18.5%
	0.3	23	19.3%	18	15.1%
	0.4	6	5%	15	12.6%
	0.5	23	19.3%	44	37%
DnV	0.0	21	17.6%	44	37%
	0.1	32	26.9%	20	16.8%
	0.2	34	28.6%	22	18.5%
	0.3	26	21.8%	18	15.1%
	0.4	6	5%	15	12.6%
	0.5	21	17.6%	44	37%
BV	0.0	18	15.1%	38	31.9%
	0.1	32	26.9%	24	20.2%
	0.2	35	29.4%	22	18.5%
	0.3	31	26.1%	20	16.8%
	0.4	3	2.5%	15	12.6%
	0.5	18	15.1%	38	31.9%

Table (4):

Maximum Forces on Members (F_{T_w}) and Relative Time (OSS, β = 0.0)

Member No.	ω = 0.37 rad/s		ω = 0.64 rad/s		ω = 1.06 rad/s	
	$F_{T_w} \times 10^{-5}$ (N)		$F_{T_w} \times 10^{-4}$ (N)		$F_{T_w} \times 10^{-2}$ (N)	
	OSS	MRSEQ	OSS	MRSEQ	OSS	MRSEQ
1	1.086	0.8315	0.3225	0.4661	0.0008	0.0043
3	1.732	0.9408	1.792	2.328	0.0434	0.4640
5	2.008	0.2074	5.422	5.592	1.309	27.620
7	4.837	2.356	33.400	3.182	573.8	1877.0
8	0.7216	0.214	0.3824	0.1198	0.0064	0.0030
10	1.210	1.051	2.092	0.3085	0.7871	0.2366
12	1.630	2.801	6.134	2.906	55.590	5.202
14	2.187	1.259	16.860	1.150	1379.0	820.6
15	0.7146	0.9966	0.3814	0.5802	0.0064	0.0140
17	1.205	1.656	2.085	3.089	0.7876	1.581
19	1.653	1.545	6.281	9.186	55.340	100.0
21	2.194	0.8379	17.240	2.303	1330.0	1010.0
43	1.109	0.8315	0.4604	0.4661	0.0042	0.0043
45	1.770	0.9408	2.378	2.328	0.4434	0.4640
47	2.091	0.2074	6.556	5.592	27.410	27.620
49	4.710	2.356	36.760	3.182	2566.0	1877.0
50	0.611	0.4962	0.3477	0.3654	0.0085	0.0088
52	0.9546	0.6358	1.780	1.828	0.8866	0.9577
54	1.052	0.1798	4.880	4.420	52.250	57.100
56	2.097	0.0613	17.150	8.796	1196.0	1380.0
64	1.123	0.8315	0.460	0.4661	0.0042	0.0043
66	1.783	0.9408	2.378	2.328	0.4438	0.4640
68	2.048	0.2074	6.616	5.592	27.420	27.620
70	4.688	2.356	36.800	3.182	2565.0	1877.0
71	0.616	0.4191	0.3474	0.3361	0.0085	0.0081
73	0.969	0.4381	1.780	1.625	0.886	0.8596
75	1.027	0.1918	4.925	3.386	52.370	49.000
77	2.211	2.208	17.630	8.799	1239.0	412.300
92	1.146	1.389	0.3497	0.4287	0.0018	0.0022
94	2.053	2.560	2.079	2.480	0.2320	0.2743
96	3.658	4.802	12.170	14.470	28.600	33.690
98	7.547	10.89	84.390	109.3	5026.0	6145.0
99	1.146	1.001	0.350	0.2882	0.0018	0.0015
101	2.056	1.938	2.078	1.674	0.2321	0.1843
103	3.683	3.932	12.170	9.989	28.600	22.640
105	7.734	10.040	85.370	85.470	5012.0	4350.0

Table (5)

Maximum Forces (F_{T_w}), OSS Vs MRSEQ (LR, β = 0.0)

a. At $\omega = 0.37$ rad/s, the forces calculated by MRSEQ were underestimated for 27 members representing 75% of the total number (36), 12 of them being horizontal members. The largest error was 97% at member No. 47 which is horizontal.

b. At $\omega = 0.64$ rad/s, the forces were underestimated for 21 members (58.3%), 7 of them being horizontal members. The largest error was 91.4% at the horizontal member No. 70.

c. At $\omega = 1.06$ rad/s, the forces were underestimated for 14 members (38.9%), 2 of which are horizontal members. The largest error was 90.6% at member No. 12 which is an inclined member.

In general, the underestimation of the forces is mainly for the horizontal members followed by the members at large inclinations. Although both the inertia force (F_{I_w}) and the drag force (F_{D_w}) according to MRSEQ are larger than those obtained when using program OSS, the vector sum (F_{T_w}) may be smaller.

In the case of the vertical members, the inertia and drag forces are generally in the same direction, therefore, the forces calculated by MRSEQ will be larger than those of OSS.

3.5 Maximum Forces per Unit Wave Height

To find out the effect of frequency on the maximum force per unit wave height for the individual members of the structure, 21 members were chosen representing the jacket structure, Fig. (10). The first 7 of these members are horizontal members at different levels below the water surface; the second set consists of 7 inclined bracing

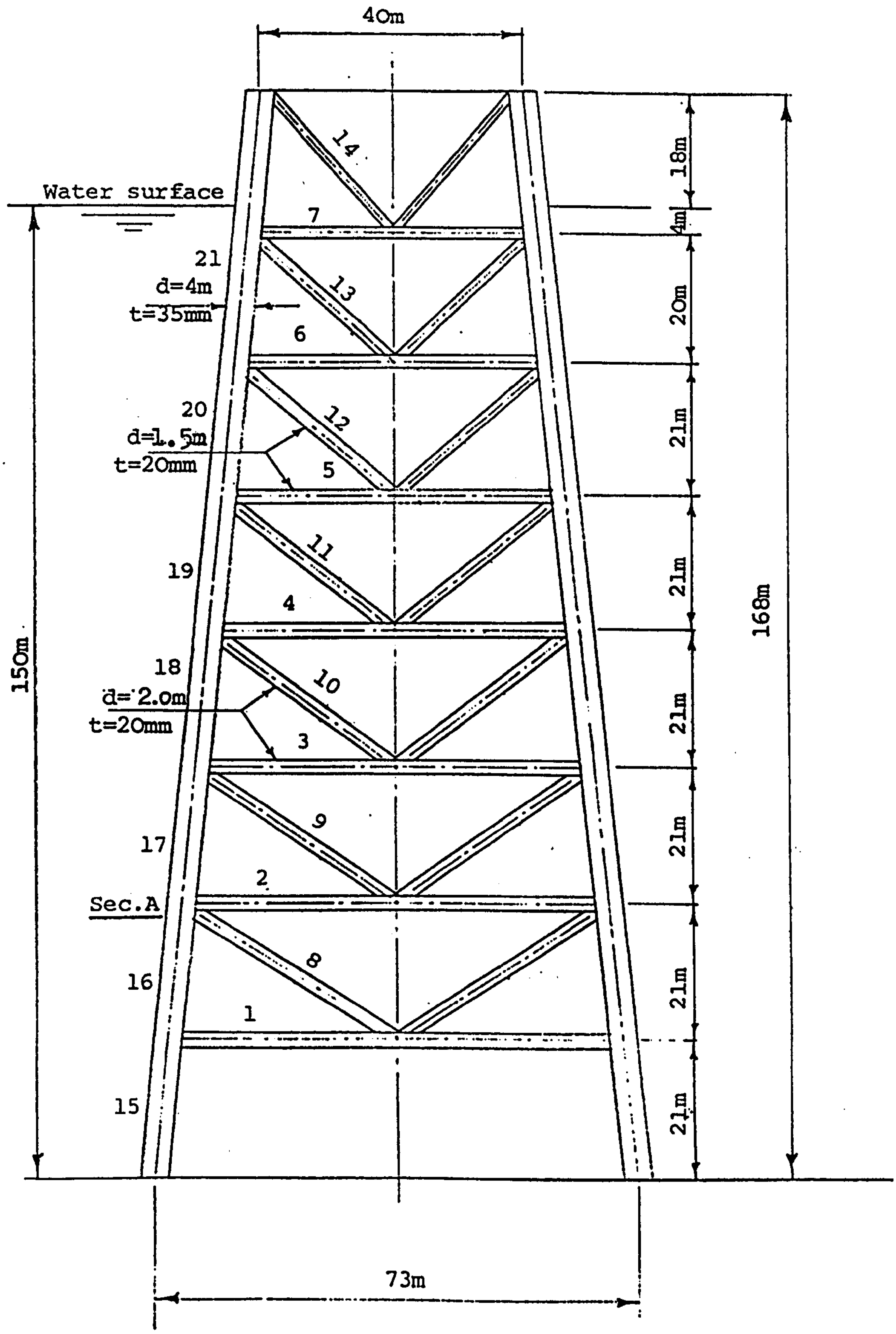

Fig. (10) Locations of the 21 Members of the Structure members and the third set consists of 7 members constituting one of the main columns of the structure

For each group of members the maximum forces in the (v, w), directions, i.e. normal to the member axis in two planes at 90^{o} to one another, were calculated at the different frequencies by three methods:-

First Method:

The forces were calculated using the wave heights given in table (1) and the force was obtained by dividing the maximum force at each frequency by the corresponding wave height, Figs. (11) to (13). This ignores the non-linear term in the viscous forces and will lead to an overestimation of the force per unit height.

Second Method:

The maximum forces were calculated using 1m wave height for the different frequencies, Figs. (14) to (16).

Third Method:

The forces were calculated as in the first method but using waves of constant steepness of 1/15, table (6), Figs. (17) to (19).

The above mentioned calculations were carried out using the C_D and C_M coefficients recommended by LR, DnV and BV rules. The graphs (Figs. (11) to (19)) show some general trends, applicable to all the above methods of calculation, which may be summarised as follows:-

a.(i) The forces on the horizontal members, Nos (1) to (7) in 'w' direction are largely inversely proportional to the frequency except member No (7) which shows an unsteady

Wave Length L(m)	Wave Height H(m)	Wave Period T(s)	Frequency ω (rad/s)
54.83	3.66	5.92	1.06
69.72	4.65	6.68	0.94
109.52	7.30	8.37	0.75
150.40	10.03	9.81	0.64
196.45	13.10	11.21	0.56
246.43	16.43	12.56	0.50
304.23	20.30	13.96	0.45
349.24	23.28	14.95	0.42
450.01	30.00	16.97	0.37

Table (6) Particulars of Waves with Constant Steepness $\frac{H}{L} = \frac{1}{15}$

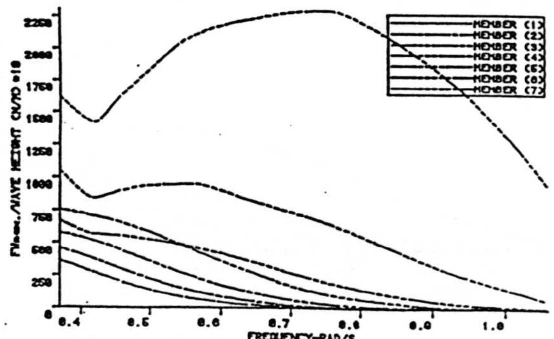

(a) MAX. FORCES ON MEMBERS IN w DIRECTION

PROGRAM: OSS ,COEFFICIENTS: LR , β = 0.0
FIG.(11.1) MAX. FORCES/UNIT WAVE HEIGHT Vs. FREQUENCY

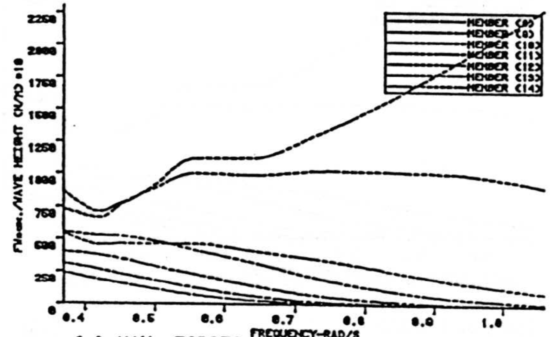

(a) MAX. FORCES ON MEMBERS IN w DIRECTION

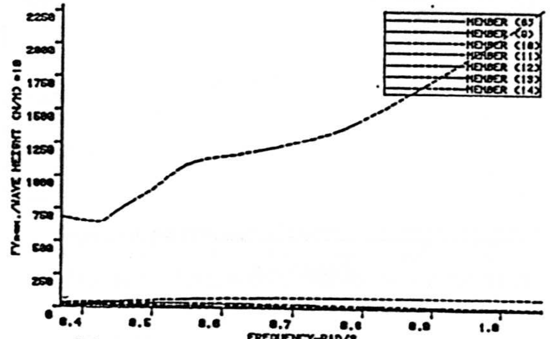

(b) MAX. FORCES ON MEMBERS IN v DIRECTION

PROGRAM: OSS ,COEFFICIENTS: LR , β = 0.0
FIG.(11.2) MAX. FORCES/UNIT WAVE HEIGHT Vs. FREQUENCY

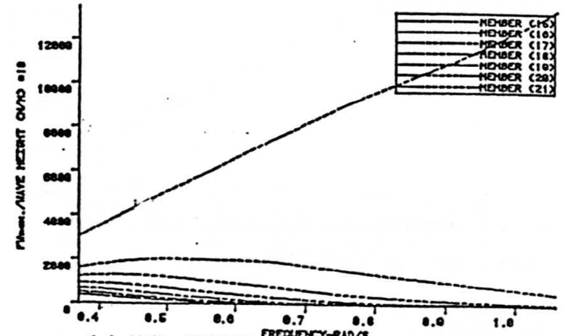

(a) MAX. FORCES ON MEMBERS IN w DIRECTION

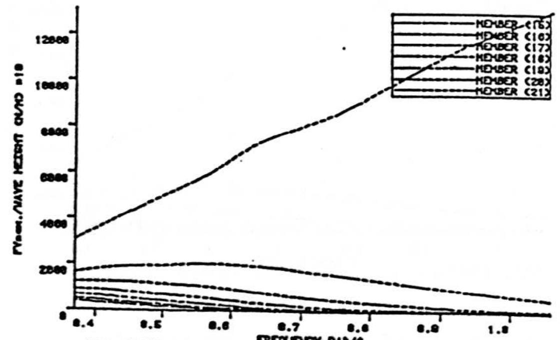

(b) MAX. FORCES ON MEMBERS IN v DIRECTION

PROGRAM: OSS ,COEFFICIENTS: LR , β = 0.0
FIG.(11.3) MAX. FORCES/UNIT WAVE HEIGHT Vs. FREQUENCY

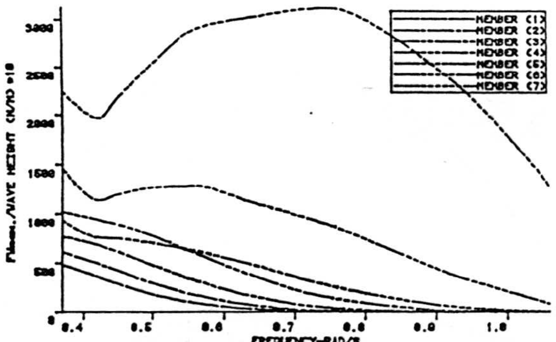

(a) MAX. FORCES ON MEMBERS IN w DIRECTION

PROGRAM: OSS ,COEFFICIENTS: DnV , β = 0.0
FIG.(12.1) MAX. FORCES/UNIT WAVE HEIGHT Vs. FREQUENCY

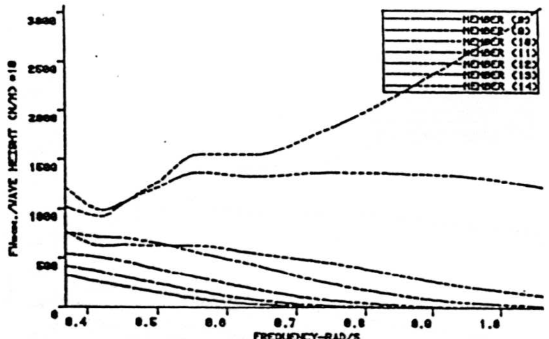

(a) MAX. FORCES ON MEMBERS IN w DIRECTION

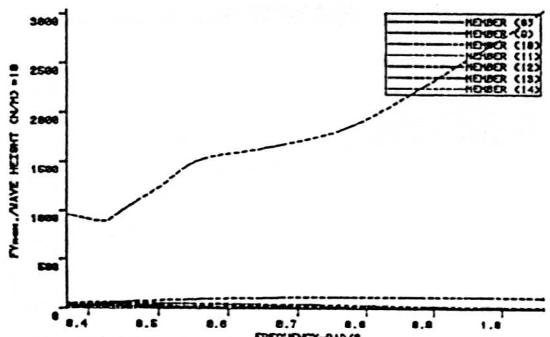

(b) MAX. FORCES ON MEMBERS IN v DIRECTION

PROGRAM: OSS ,COEFFICIENTS: DnV , β = 0.0
FIG.(12.2) MAX. FORCES/UNIT WAVE HEIGHT Vs. FREQUENCY

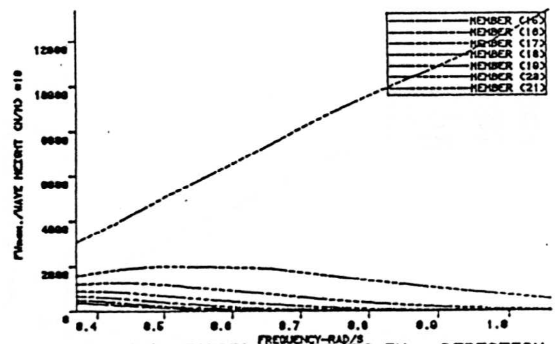

(a) MAX. FORCES ON MEMBERS IN w DIRECTION

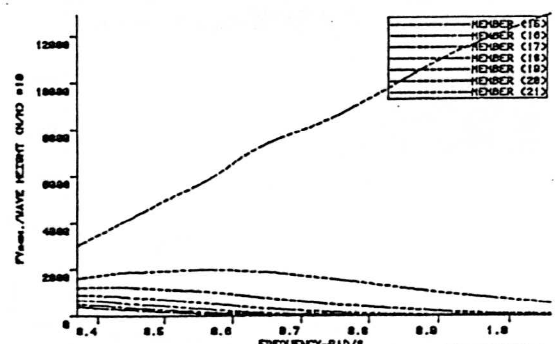

(b) MAX. FORCES ON MEMBERS IN v DIRECTION

PROGRAM: OSS ,COEFFICIENTS: DnV , β = 0.0
FIG.(12.3) MAX. FORCES/UNIT WAVE HEIGHT Vs. FREQUENCY

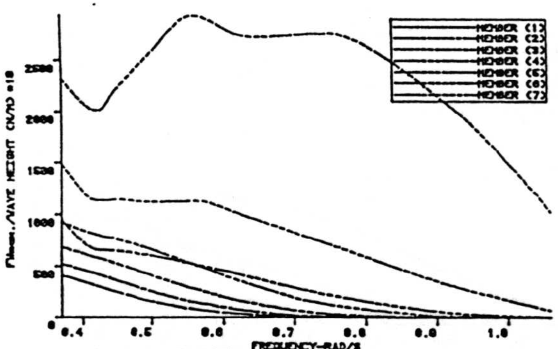

(a) MAX. FORCES ON MEMBERS IN w DIRECTION

PROGRAM: OSS ,COEFFICIENTS: BV , β = 0.0
FIG.(B.1) MAX. FORCES/UNIT WAVE HEIGHT Vs. FREQUENCY

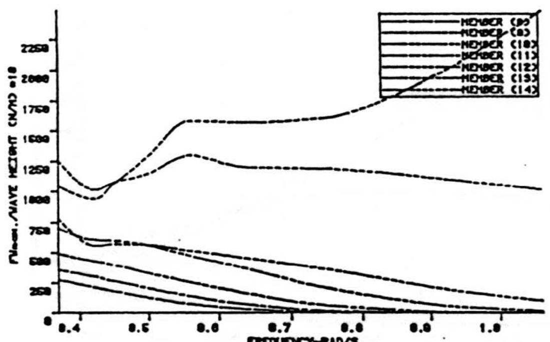

(a) MAX. FORCES ON MEMBERS IN w DIRECTION

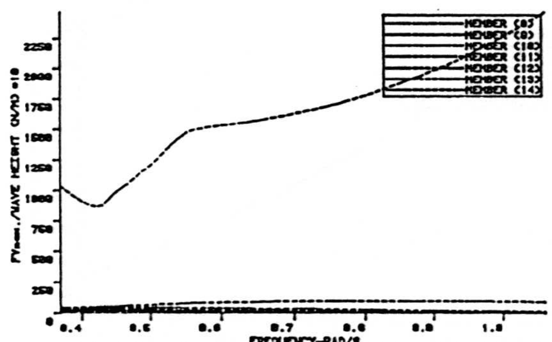

(b) MAX. FORCES ON MEMBERS IN v DIRECTION

PROGRAM: OSS ,COEFFICIENTS: BV , β = 0.0
FIG.(B.2) MAX. FORCES/UNIT WAVE HEIGHT Vs. FREQUENCY

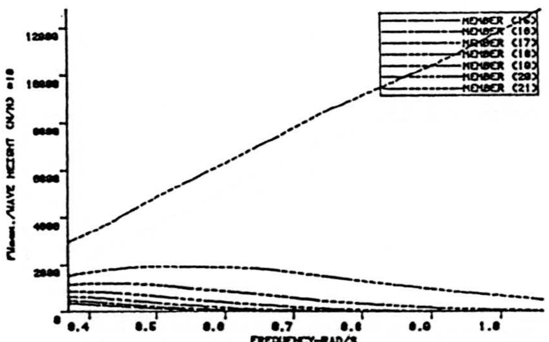

(a) MAX. FORCES ON MEMBERS IN w DIRECTION

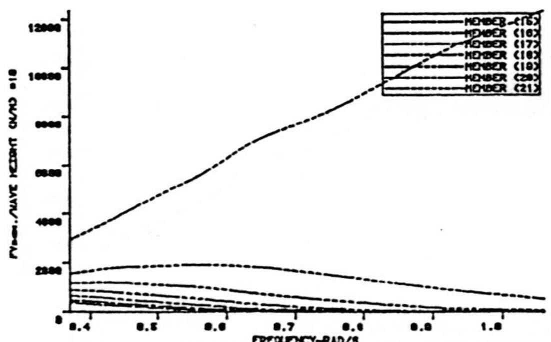

(b) MAX. FORCES ON MEMBERS IN v DIRECTION

PROGRAM: OSS ,COEFFICIENTS: BV , β = 0.0
FIG.(B.3) MAX. FORCES/UNIT WAVE HEIGHT Vs. FREQUENCY

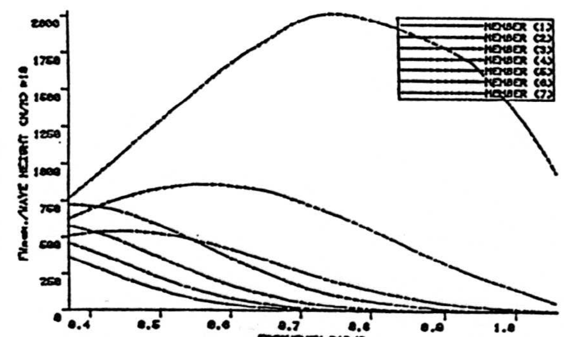

(a) MAX. FORCES ON MEMBERS IN w DIRECTION

PROGRAM: OSS ,COEFFICIENTS: LR , β = 0.0
FIG.(14.1) MAX. FORCES/UNIT WAVE HEIGHT Vs. FREQUENCY

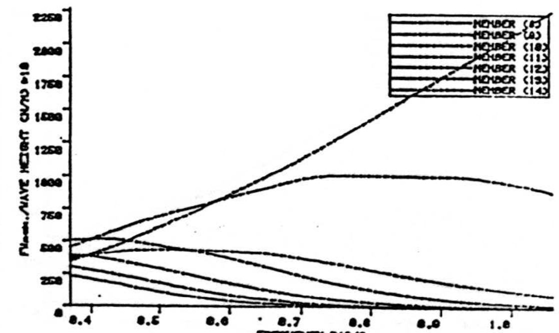

(a) MAX. FORCES ON MEMBERS IN w DIRECTION

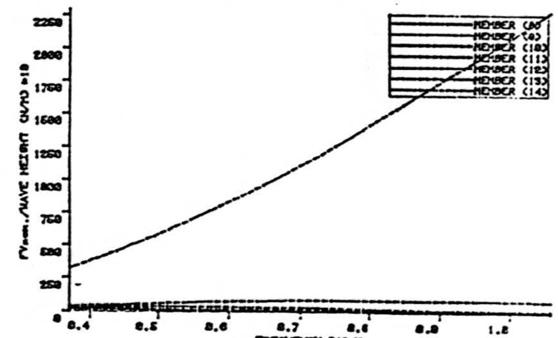

(b) MAX. FORCES ON MEMBERS IN v DIRECTION

PROGRAM: OSS ,COEFFICIENTS: LR , β = 0.0
FIG.(14.2) MAX. FORCES/UNIT WAVE HEIGHT Vs. FREQUENCY

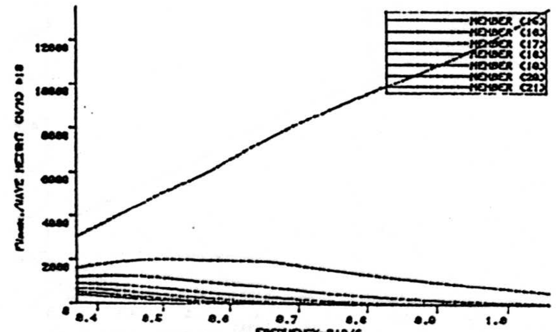

(a) MAX. FORCES ON MEMBERS IN w DIRECTION

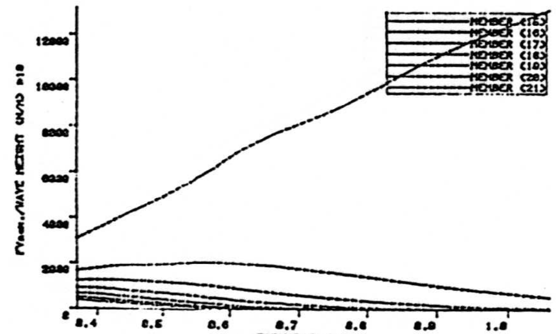

(b) MAX. FORCES ON MEMBERS IN v DIRECTION

PROGRAM: OSS ,COEFFICIENTS: LR , β = 0.0
FIG.(14.3) MAX. FORCES/UNIT WAVE HEIGHT Vs. FREQUENCY

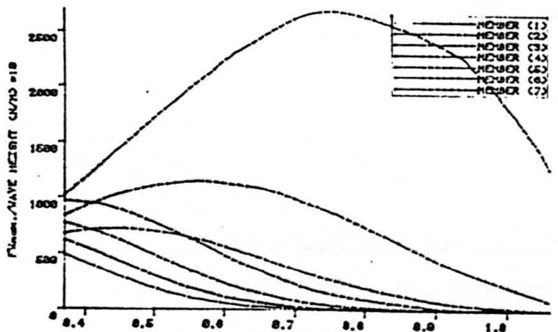

(a) MAX. FORCES ON MEMBERS IN w DIRECTION

PROGRAM: OSS ,COEFFICIENTS: DnV , β = 0.0
FIG.(5.1) MAX. FORCES/UNIT WAVE HEIGHT Vs. FREQUENCY

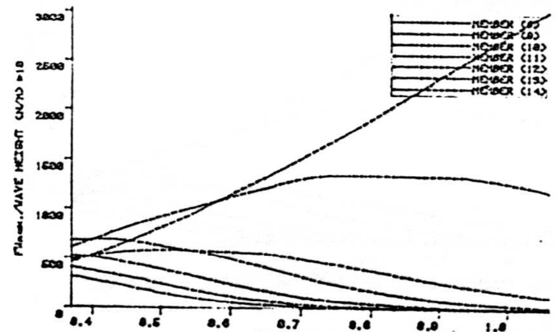

(a) MAX. FORCES ON MEMBERS IN w DIRECTION

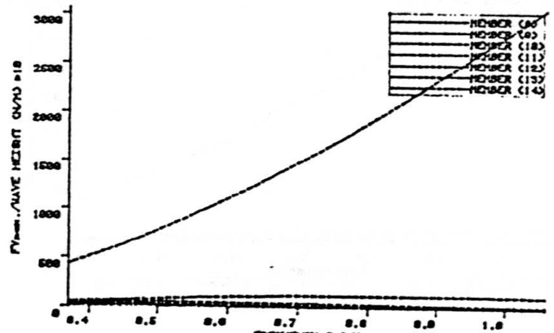

(b) MAX. FORCES ON MEMBERS IN v DIRECTION

PROGRAM: OSS ,COEFFICIENTS: DnV , β = 0.0
FIG.(5.2) MAX. FORCES/UNIT WAVE HEIGHT Vs. FREQUENCY

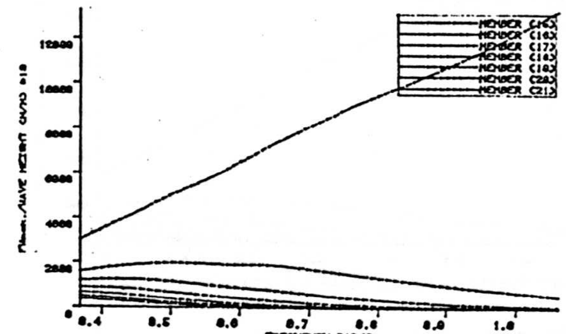

(a) MAX. FORCES ON MEMBERS IN w DIRECTION

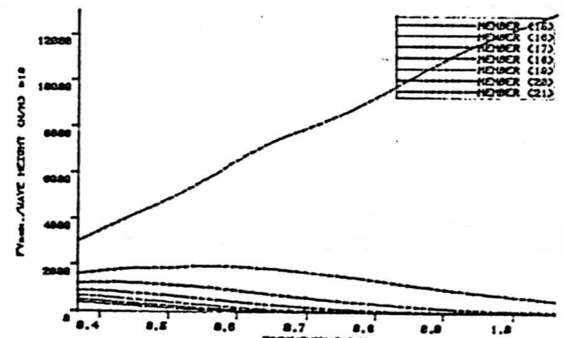

(b) MAX. FORCES ON MEMBERS IN v DIRECTION

PROGRAM: OSS ,COEFFICIENTS: DnV , β = 0.0
FIG.(5.3) MAX. FORCES/UNIT WAVE HEIGHT Vs. FREQUENCY

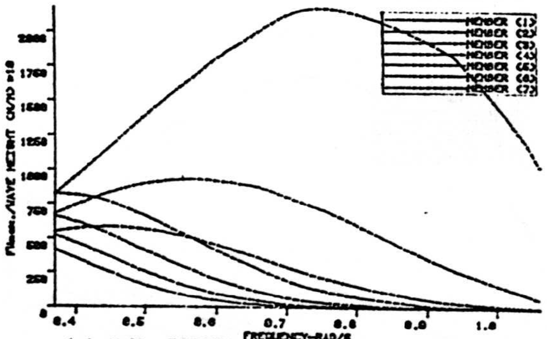

(a) MAX. FORCES ON MEMBERS IN w DIRECTION

PROGRAM: OSS ,COEFFICIENTS: BV ,β = 0.0
FIG.(161) MAX. FORCES/UNIT WAVE HEIGHT Vs. FREQUENCY

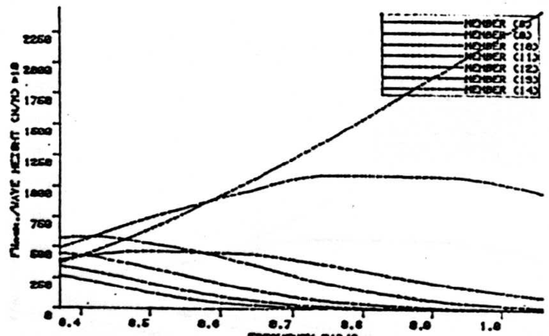

(a) MAX. FORCES ON MEMBERS IN w DIRECTION

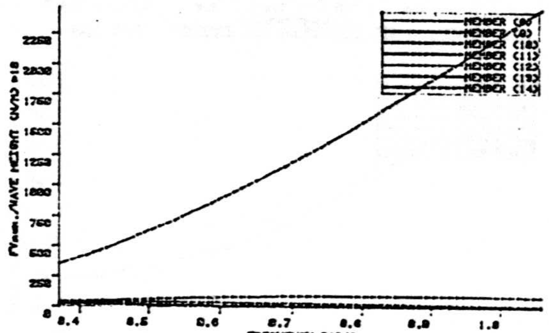

(b) MAX. FORCES ON MEMBERS IN v DIRECTION

PROGRAM: OSS ,COEFFICIENTS: BV , β= 0.0
FIG.(16.2) MAX. FORCES/UNIT WAVE HEIGHT Vs. FREQUENCY

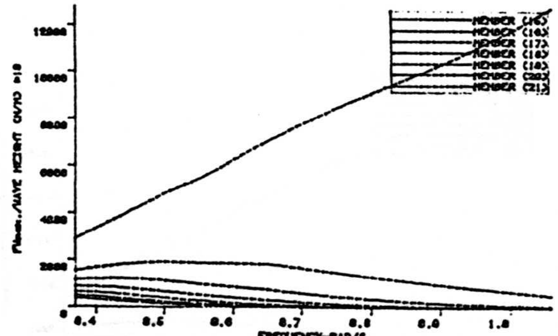

(a) MAX. FORCES ON MEMBERS IN w DIRECTION

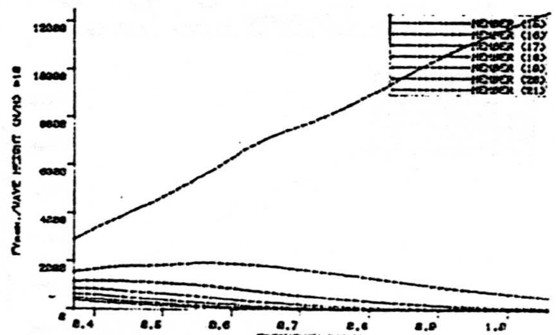

(b) MAX. FORCES ON MEMBERS IN v DIRECTION

PROGRAM: OSS ,COEFFICIENTS: BV ,β = 0.0
FIG.(163) MAX. FORCES/UNIT WAVE HEIGHT Vs. FREQUENCY

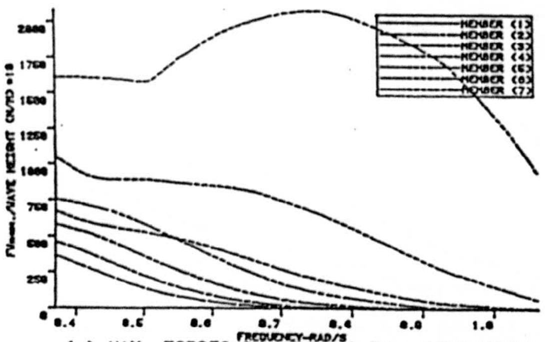

(a) MAX. FORCES ON MEMBERS IN w DIRECTION

PROGRAM: OSS ,COEFFICIENTS: LR , β = 0.0
FIG. (17.1) MAX. FORCES/UNIT WAVE HEIGHT Vs. FREQUENCY

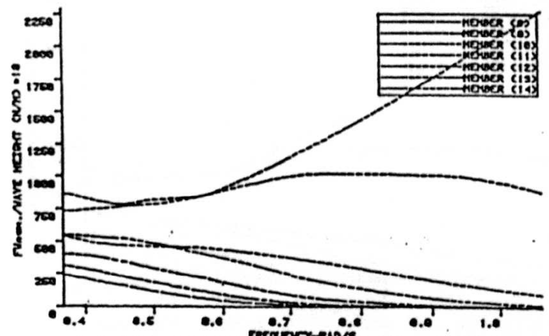

(a) MAX. FORCES ON MEMBERS IN w DIRECTION

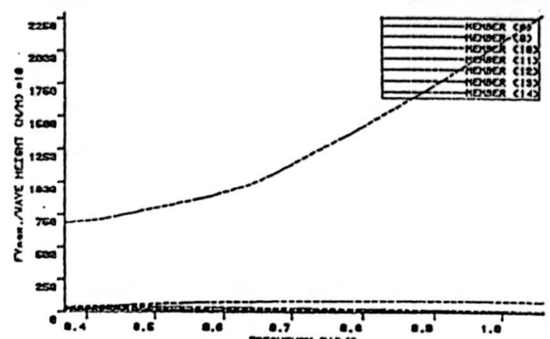

(b) MAX. FORCES ON MEMBERS IN v DIRECTION

PROGRAM: OSS ,COEFFICIENTS: LR , β = 0.0
FIG. (17.2) MAX. FORCES/UNIT WAVE HEIGHT Vs. FREQUENCY

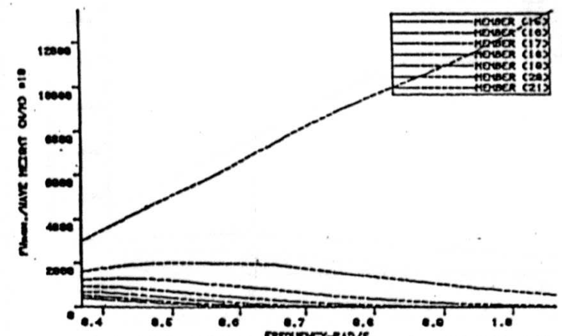

(a) MAX. FORCES ON MEMBERS IN w DIRECTION

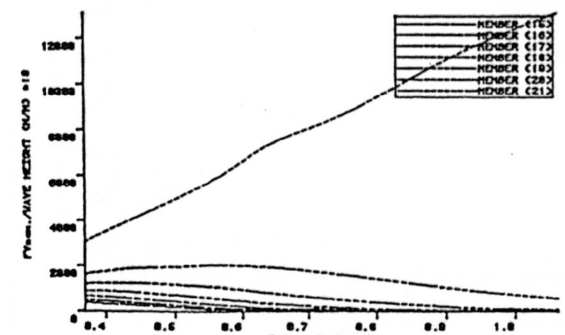

(b) MAX. FORCES ON MEMBERS IN v DIRECTION

PROGRAM: OSS ,COEFFICIENTS: LR , β = 0.0
FIG. (17.3) MAX. FORCES/UNIT WAVE HEIGHT Vs. FREQUENCY

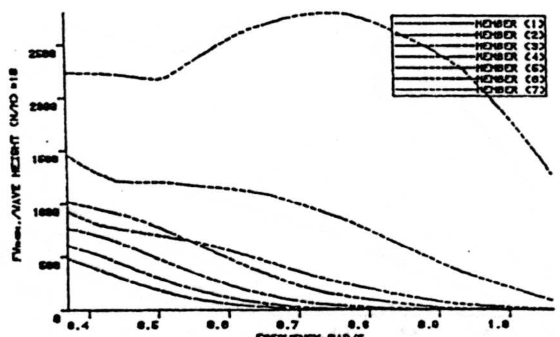

(a) MAX. FORCES ON MEMBERS IN w DIRECTION

PROGRAM: OSS ,COEFFICIENTS: DnV , β = 0.0
FIG.(18.1) MAX. FORCES/UNIT WAVE HEIGHT Vs. FREQUENCY

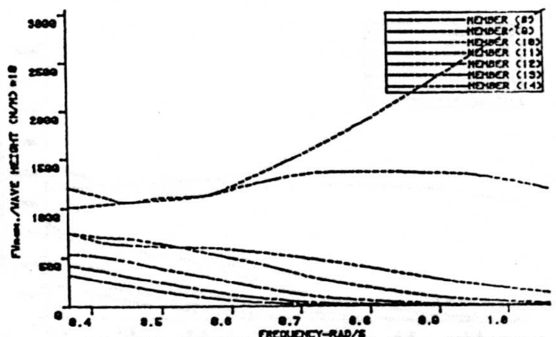

(a) MAX. FORCES ON MEMBERS IN w DIRECTION

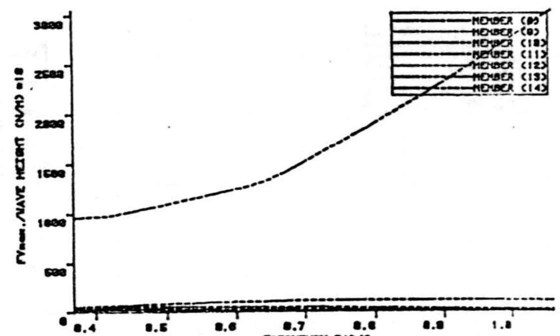

(b) MAX. FORCES ON MEMBERS IN v DIRECTION

PROGRAM: OSS ,COEFFICIENTS: DnV , β = 0.0
FIG.(18.2) MAX. FORCES/UNIT WAVE HEIGHT Vs. FREQUENCY

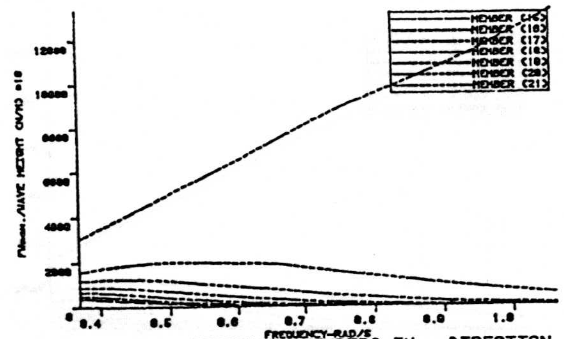

(a) MAX. FORCES ON MEMBERS IN w DIRECTION

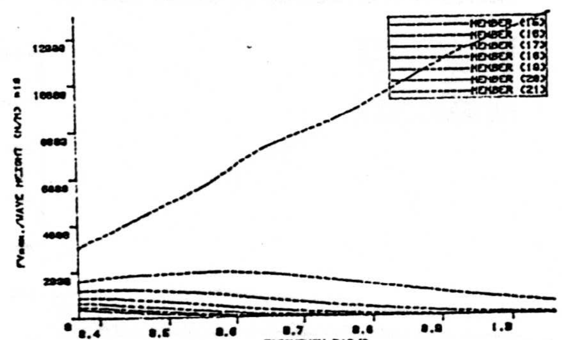

(b) MAX. FORCES ON MEMBERS IN v DIRECTION

PROGRAM: OSS ,COEFFICIENTS: DnV , β = 0.0
FIG.(18.3) MAX. FORCES/UNIT WAVE HEIGHT Vs. FREQUENCY

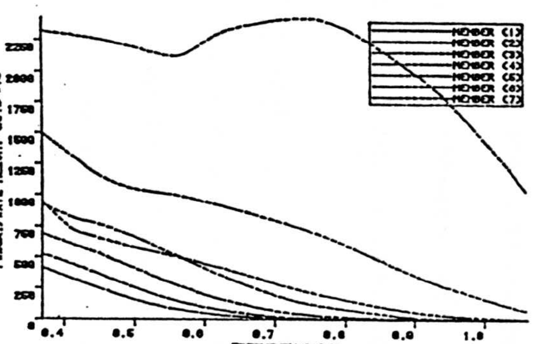

(a) MAX. FORCES ON MEMBERS IN w DIRECTION

PROGRAM: OSS ,COEFFICIENTS: BV , β = 0.0
FIG.(13.1) MAX. FORCES/UNIT WAVE HEIGHT Vs. FREQUENCY

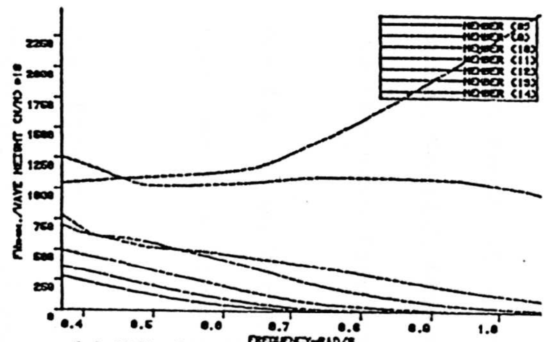

(a) MAX. FORCES ON MEMBERS IN w DIRECTION

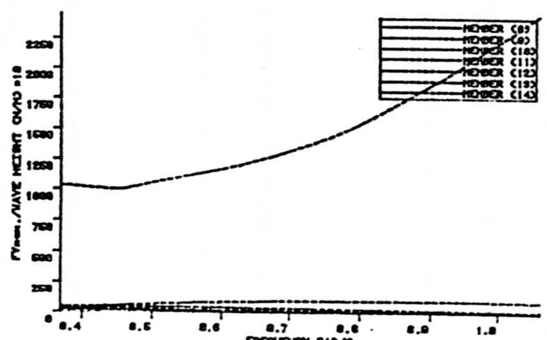

(b) MAX. FORCES ON MEMBERS IN v DIRECTION

PROGRAM: OSS ,COEFFICIENTS: BV , β = 0.0
FIG.(13.2) MAX. FORCES/UNIT WAVE HEIGHT Vs. FREQUENCY

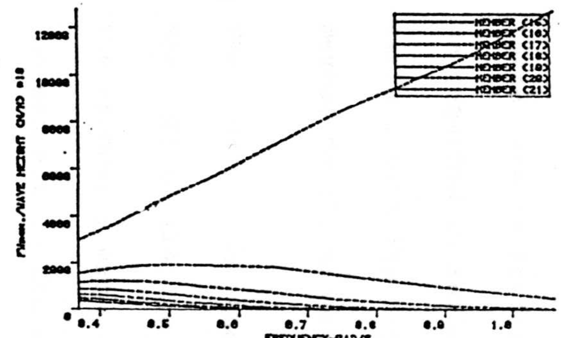

(a) MAX. FORCES ON MEMBERS IN w DIRECTION

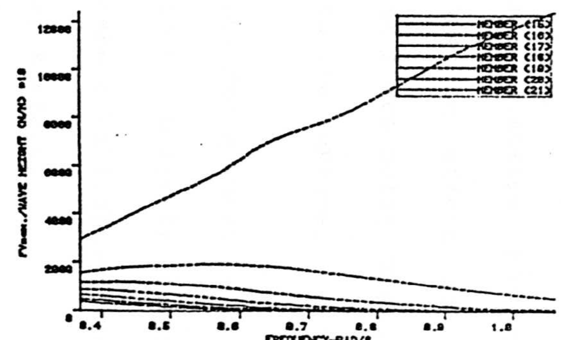

(b) MAX. FORCES ON MEMBERS IN v DIRECTION

PROGRAM: OSS ,COEFFICIENTS: BV , β = 0.0
FIG.(13.3) MAX. FORCES/UNIT WAVE HEIGHT Vs. FREQUENCY

relation between the force and the frequency with a maximum value at ω = 0.7 - 0.8 rad/s. For all members there are no forces in v direction. The graph may also be regarded as reflecting the effect of depth below surface with the highest force being experienced by the member No (7) nearest to the surface.

(ii) The forces on the inclined members in 'w' direction, Nos (8) to (14) tend to be inversely proportional to the frequency except members No (13) and (14) which are the nearest to the water surface.

In 'v' direction, the forces per unit wave height are almost constant in magnitude for all members except member No (14) where the force is directly proportional to the wave frequency.

(iii) The forces on the third group of members Nos (15 to 21) have the same trend in both 'v' and 'w' directions.

The forces per unit wave height decrease slightly with frequency for all members except No (21) which is a surface piercing member.

b. As far as the difference in force estimation by LR, DnV and BV, the results for the members near the water surface (which had the largest forces) show that:

<u>First Method:</u>

(1) For the horizontal member No (7), the maximum force per unit wave height was increased by about 38% in the case of DnV and by 30% in the case of BV (relative to LR).

(2) For the inclined member No (14), the maximum force was increased by about 33% in the case of DnV and by about 11% in the case of BV.

(3) For member No (21), the maximum force is the same for both LR and DnV but it is reduced by about 6% in the case of BV.

Second Method:

(1) For the horizontal member No (7), the maximum force per unit wave height was increased by 35% in the case of DnV and by 10% in the case of BV.

(2) For the inclined member No (14), the maximum force was increased by 33% in the case of DnV and by 9% in the case of BV.

(3) For member No (21), the maximum force is the same for both LR and DnV but it is reduced by about 5% in the case of BV.

Third Method:

(1) For the horizontal member No (7), the maximum force was increased by 35% in the case of DnV and by 17% in the case of BV.

(2) For the inclined member No (14), the maximum force was increased by 35% in the case of DnV and by 8% in the case of BV.

(3) For member No (21), the maximum force is the same for LR and DnV but it is reduced by 7% in the case of BV.

These calculations demonstrate that the majority of the differences between the classification societies arise from the differences in their recommended C_M value, rather than the C_D value. Since the latter is associated with the square of the wave height one would have expected large differences between the first and second method alone, especially for the smaller diameter members. It will be seen that the differences are not large. Also, for member No (21) there is no significant difference between LR and DnV, although the C_D values are respectively 0.5 and 0.7 for this member. The BV result for this member is lower because its C_M value is 1.896 compared to 2.0 for the other two.

4. ANALYSIS OF RESULTS FOR THE WHOLE STRUCTURE

In the following analysis, each wave frequency has a particular wave height as given in Table (1).

4.1 Maximum Surge, Heave and Sway Forces (OSS, $\beta = 0.0$)

Table (7) summarises the results of the maximum total forces, from which the following was noted:-

a. The variation in the maximum surge force ranged from -3.3% to 14.9% according to DnV, while it ranged from -3.8% to 5.3% according to BV. The -ve sign indicates reduction in the force compared to LR values.

Class. Society	Surge Force x 10^{-8} (N) ω (rad/s)					Heave Force x 10^{-7} (N) ω (rad/s)					Sway Force x 10^{-6} (N) ω (rad/s)				
β = 0.0	0.37	0.42	.45	0.50	0.56	0.37	0.42	.45	0.50	0.56	0.37	0.42	.45	0.50	0.50
LR	0.2087	0.1382	0.1377	0.1332	0.1229	1.274	0.7665	0.7649	0.7533	0.7303	0.1392	0.09205	0.1058	0.1320	0.1673
DnV	0.2362	0.1552	0.1547	0.1499	0.1387	1.741	1.043	1.043	1.031	1.005	0.1915	0.1262	0.1451	0.1811	0.2294
Diff.	13.2%	12.3%	12.4%	12.5%	12.9%	36.7%	36.1%	36.4%	36.9%	37.6%	37.6%	37.1%	37.2%	37.2%	37.1%
BV	0.2197	0.1436	0.1432	0.1389	0.1287	1.760	0.9287	0.9285	0.9191	0.8993	0.2012	0.1196	0.1379	0.1726	0.2190
Diff.	5.3%	3.9%	4%	4.3%	4.7%	38.2%	21.2%	21.4%	22%	23.1%	44.5%	29.9%	30.3%	30.8%	30.9%

Class. Society	ω (rad/s)				ω (rad/s)				ω (rad/s)			
	0.64	0.75	0.94	1.06	0.64	0.75	0.94	1.06	0.64	0.75	0.94	1.06
LR	0.07423	0.03105	0.01225	0.02558	0.4669	0.2594	0.05904	0.01125	0.1404	0.1277	0.07461	0.03751
DnV	0.08379'	0.03567	0.01185	0.02605	0.6475	0.3650	0.08908	0.01625	0.1901	0.1715	0.09985	0.05010
Diff.	12.9%	14.9%	-3.3%	1.8%	38.7%	40.7%	50.9%	44.4%	35.4%	34.3%	33.8%	33.4%
BV	0.07728	0.03232	0.01178	0.02480	0.5711	0.3157	0.07222	0.01605	0.1776	0.1446	0.08257	0.04091
Diff.	4.1%	4.1%	-3.8%	-3.1%	22.3%	21.7%	22.3%	42.7%	26.5%	13.2%	10.7%	9.1%

Table (7) Maximum Surge, Heave and Sway Forces (OSS, β = 0.0)

Class. Society	Rolling Moment x 10^{-8} (N.M) ω (rad/s)					Yawing Moment x 10^{-7} (N.M) ω (rad/s)					Pitching Moment x 10^{-9} (N.M) ω (rad/s)				
β = 0.0	0.37	0.42	.45	0.50	0.56	0.37	0.42	.45	0.50	0.56	0.37	0.42	.45	0.50	0.50
LR	0.2091	0.1457	0.1717	0.2197	0.2824	0.09685	0.07592	0.09567	0.1407	0.2172	1.981	1.386	1.428	1.454	1.411
DnV	0.2900	0.2000	0.2357	0.3014	0.3873	0.1328	0.1039	0.1311	0.1929	0.2978	2.254	1.548	1.595	1.625	1.581
Diff.	38.7%	37.3%	37.3%	37.2%	37.2%	37.1%	36.9%	37%	37.1%	37.1%	13.8%	11.7%	11.7%	11.8%	12.1%
BV	0.3106	0.1911	0.2255	0.2885	0.3707	0.1264	0.09721	0.1235	0.1829	0.2824	2.22	1.434	1.479	1.511	1.473
Diff.	48.5%	31.2%	31.3%	31.3%	31.3%	30.5%	28%	29.1%	30%	30%	12.1%	3.5%	3.6%	3.9%	4.4%

Class. Society	ω (rad/s)				ω (rad/s)				ω (rad/s)			
	0.64	0.75	0.94	1.06	0.64	0.75	0.94	1.06	0.64	0.75	0.94	1.06
LR	0.2418	0.2217	0.1412	0.08591	0.2318	0.2577	0.2939	0.2976	0.8910	0.3758	0.1950	0.3777
DnV	0.3254	0.2978	0.1890	0.1148	0.3159	0.3485	0.3918	0.3969	0.9959	0.4237	0.1998	0.3920
Diff.	34.6%	34.3%	33.9%	33.6%	36.3%	35.2%	33.3%	33.4%	11.8%	12.8%	2.5%	3.8%
BV	0.3036	0.2520	0.1563	0.09421	0.2907	0.3073	0.3158	0.3201	0.9234	0.3882	0.1921	0.3695
Diff.	25.6%	13.7%	10.7%	9.7%	25.4%	19.3%	7.5%	7.6%	3.6%	3.3%	-1.5%	-2.2%

Table (8) Maximum Rolling, Yawing and Pitching Moments (OSS, β = 0.0)

b. The vertical heave force showed the largest deviation which ranged from 36.1% to 50.9% in the case of DnV and from 21.2% to 42.7% in the case of BV.

c. The sway force varied from 33.4% to 37.6% in the case of DnV, while the deviation was from 9.1% to 44.5% in the case of BV.

4.2 Maximum Rolling, Yawing and Pitching Moments (OSS, $\beta = 0.0$)

Table (8) summarises the results of the maximum total moments from which the following was noted:-

a. The rolling moment showed the largest deviation ranging from 33.6% to 38.7% in the case of DnV and from 9.7% to 48.5% in the case of BV.

b. The yawing moment varied from 33.3% to 37.1% in the case of DnV, while in the case of BV, the differences ranged from 7.5% to 30.5%.

c. The pitching moment varied from 2.5% to 13.8% in the case of DnV. In the case of BV, the difference varied from -2.2% to 12.1%.

4.3 Maximum Surge, Heave and Sway Forces (MRSEQ, $\beta = 0.0$)

From Table (9), it is evident that the percentages of the maximum differences in surge and heave forces are much larger than those obtained from Table (7). They can be summarised as follows:-

a. The differences in the surge force varied from 14.3% to 21% in the case of DnV and from 4.9% to 18% in the case of BV.

Class. Society	Surge Force x 10^{-8} (N)					Heave Force x 10^{-7} (N)					Sway Force x 10^{-6} (N)				
	ω (rad/s)					ω (rad/s)					ω (rad/s)				
β = 0.0	0.37	0.42	0.45	0.50	0.56	0.37	0.42	.45	0.50	0.56	0.37	0.42	.45	0.50	0.50
LR	0.3219	0.1980	0.2011	0.2043	0.2063	0.04245	0.2474	0.2473	0.2336	0.2046	0.2252	0.1515	0.1750	0.2216	0.2884
DnV	0.3895	0.2339	0.2373	0.2408	0.2430	0.1430	0.2881	0.2872	0.2675	0.2267	0.3065	0.2074	0.2397	0.3036	0.3950
Diff.	21%	18.1%	18%	17.9%	17.8%	236.9%	16.5%	16.1%	14.5%	10.8%	37.4%	36.9%	37%	37%	37%
BV	0.3798	0.2241	0.2272	0.2303	0.2324	0.5045	0.0611	0.05493	0.02823	0.02069	0.2976	0.1948	0.2260	0.2871	0.3740
Diff.	18%	13.2%	13%	12.7%	12.7%	1088.5%	-75.3%	-77.8%	-87.9%	-90.2%	32.2%	28.6%	29.1%	29.6%	29.7%
Class. Society	ω (rad/s)					ω (rad/s)					ω (rad/s)				
	0.64	0.75	0.94	1.06		0.64	0.75	0.94	1.06		0.64	0.75	0.94	1.06	
LR	0.1459	0.1022	0.06293	0.05419		0.2413	0.2414	0.2246	0.2237		0.2549	0.2328	0.1982	0.1972	
DnV	0.1699	0.1178	0.07195	0.06197		0.2927	0.3038	0.2903	0.2909		0.3477	0.3159	0.2672	0.2652	
Diff.	16.5%	15.3%	14.3%	14.4%		21.3%	25.9%	29.3%	30%		36.4%	35.7%	34.8%	34.5%	
BV	0.1607	0.1104	0.06639	0.05685		0.1111	0.1687	0.1975	0.2058		0.3219	0.2847	0.2316	0.2265	
Diff.	10.1%	8%	5.5%	4.9%		-54%	-30.1%	-12.1%	-8%		26.3%	22.3%	16.9%	14.9%	

Table (9) Maximum Surge, Heave and Sway Forces (MRSEQ, β = 0.0)

Class. Society	Rolling Moment x 10^{-8} (N.M)					Yawing Moment x 10^{-1} (N.M)					Pitching Moment x 10^{-10} (N.M)				
	ω (rad/s)					ω (rad/s)					ω (rad/s)				
β = 0.0	0.37	0.42	0.45	0.50	0.56	0.37	0.42	.45	0.50	0.56	0.37	0.42	.45	0.50	0.50
LR	0.3181	0.2248	0.2658	0.3421	0.4456	0.0	3.4	0.8	0.6	3.2	0.3347	0.214	0.2243	0.2389	0.2530
DnV	0.4382	0.3081	0.3642	0.4686	0.6099	0.4	0.4	3.6	2.400	0.4	0.4095	0.2552	0.2671	0.2839	0.3005
Diff.	37.8%	37.1%	37%	37%	36.9%		-88.2%	350%	300%	-87.5%	22.4%	19.3%	19.1%	18.8%	18.8%
BV	0.4267	0.2917	0.3449	0.4438	0.5771	2.8	3.4	2.2	0.0	0.0	0.4016	0.2457	0.2569	0.2727	0.2882
Diff.	34.1%	29.8%	29.8%	29.7%	29.5%		-	175%	-100%	-100%	20%	14.8%	14.5%	14.2%	13.9%
Class. Society	ω (rad/s)					ω (rad/s)					ω (rad/s)				
	0.64	0.75	0.94	1.06		0.64	0.75	0.94	1.06		0.64	0.75	0.94	1.06	
LR	0.3910	0.3520	0.2948	0.2913		0.6	0.6	1.0	0.8		0.1869	0.1367	0.08762	0.07655	
DnV	0.5329	0.4775	0.3973	0.3918		0.6	0.4	0.4	0.2		0.2189	0.1583	0.1005	0.08780	
Diff.	36.3%	35.7%	34.8%	34.5%		-	-33.3%	-60%	-75%		17.1%	15.8%	14.7%	14.7%	
BV	0.4927	0.4298	0.3441	0.3345		1.600	0.6	0.4	1.0		0.2076	0.1483	0.09272	0.08049	
Diff.	26%	22.1%	16.7%	14.8%		166.7%	-	-60%	25%		11.1%	8.5%	5.8%	5.2%	

Table (10) Maximum Rolling, Yawing and Pitching Moments (MRSEQ, β = 0.0)

b. In general, the heave force gave considerable irregular differences. In the range of frequencies from 0.37 rad/s to 0.56 rad/s, the percentage differences were decreasing in the case of DnV, while they were increasing in the case of BV. In the range from 0.56 rad/s to 1.06 rad/s the opposite behaviour was obtained. The deviation varied from 10.8% to 237% in the case of DnV and from -90.2% to 1089% in the case of BV. The maximum differences occured at a frequency of 0.37 rad/s.

c. The differences in the sway force varied from 34.5% to 37.4% in the case of DnV, with smaller deviations in the case of BV, ranging from 14.9% to 32.2%.

4.4 Maximum Rolling, Yawing and Pitching Moments (MRSEQ, $\beta = 0.0$)

The pitching moments from Table (10) have larger differences than those obtained from Table (8). However, similarly to Table (8), the pitching moment had the smallest differences compared to the yawing and rolling moments as shown below:-

a. The differences in the rolling moment varied from 34.5% to 37.8% in the case of DnV and from 14.8% to 34.1% in the case of BV.

b. The values of the yawing moments are negligible. This is due to the symmetry of the jacket structure and the method of calculation which ignores the different instantaneous times and relative positions of the members.

c. The differences in the pitching moment varied from 14.7% to 22.4% in the case of DnV and from 5.2% to 20% in the case of BV.

4.5 Maximum Surge, Heave and Sway Forces (MRSEQ2, $\beta = 0.0$)

The results in Table (11) show that:-

a. The percentage differences in the surge force ranged from 19.3% to 24.7% according to DnV and from 7.8% to 20.7% in the case of BV. In the range of frequencies from 0.42 rad/s to 0.56 rad/s, the percentage differences are constant.

b. The variations in the heaving force are much smaller than those obtained from Table (9). In the case of DnV, the percentage differences are almost the same for the whole range of frequencies varying only from 34.8% to 36.7%. According to BV, smaller differences were obtained ranging from 17.2% to 30.7%.

c. The sway force gave the results with the smallest differences. In the case of DnV, the variation was between 3.7% and 6.6% while in the case of BV, the variation was between -1% and 5.6%.

4.6 Maximum Rolling, Yawing and Pitching Moments (MRSEQ2, $\beta = 0.0$)

The results in Table (12) show that:-

a. The rolling moment gave better agreement between the classification societies in comparison with yawing and pitching moments. The percentage differences ranged from 3.7% to 8.9% in the case of DnV and from -0.8% to 9.7% in the case of BV.

Class Society	Surge Force x 10^{-8} (N)					Heave Force x 10^{-7} (N)					Sway Force x 10^{-7} (N)				
	ω (rad/s)					ω (rad/s)					ω (rad/s)				
	0.37	0.42	.45	0.50	0.56	0.37	0.42	.45	0.50	0.56	0.37	0.42	.45	0.50	0.56
LR	0.2133	0.1296	0.1317	0.1340	0.1359	0.4673	0.2819	0.2956	0.3193	0.3505	0.8353	0.5536	0.5673	0.5839	0.5974
DnV	0.2659	0.1584	0.1608	0.1635	0.1659	0.6390	0.3838	0.4026	0.4352	0.4782	0.8902	0.5771	0.5917	0.6100	0.6262
Diff.	24.7%	22.2%	22.1%	22%	22.1%	35.7%	36.2%	36.2%	36.3%	36.4%	6.6%	4.2%	4.3%	4.5%	4.8%
BV	0.2575	0.1503	0.1525	0.1550	0.1572	0.6106	0.3574	0.3754	0.4068	0.4484	0.8821	0.5670	0.5810	0.5985	0.6137
Diff.	20.7%	16%	15.8%	15.7%	15.7%	30.7%	26.8%	27%	27.4%	27.9%	5.6%	2.4%	2.4%	2.5%	2.7%
Class Society	ω (rad/s)					ω (rad/s)					ω (rad/s)				
	0.64	0.75	.0.94	1.06		0.64	0.75	0.94	1.06		0.64	0.75	0.94	1.06	
LR	0.09587	0.06729	0.04184	0.0364		0.2620	0.2007	0.1428	0.1344		0.4419	0.3217	0.2050	0.1775	
DnV	0.1159	0.08073	0.04991	0.04348		0.3567	0.2724	0.1929	0.1812		0.4599	0.3337	0.2126	0.1844	
Diff.	20.9%	20%	19.3%	19.5%		36.2%	35.6%	35.1%	34.8%		4.1%	3.7%	3.7%	3.9%	
BV	0.1086	0.07471	0.04538	0.03925		0.3292	0.2468	0.1695	0.1575		0.4480	0.3228	0.2035	0.1757	
Diff.	13.3%	11%	8.5%	7.8%		25.7%	23%	18.7%	17.2%		1.4%	0.3%	-0.7%	-1%	

Table (11) Maximum Surge, Heave and Sway Forces (MRSEQ2, $\beta = 0.0$)

Class Society	Rolling Moment x 10^{-9} (N.M)					Yawing Moment x 10^{-8} (N.M)					Pitching Moment x 10^{-10} (N.M)				
	ω (rad/s)					ω (rad/s)					ω (rad/s)				
	0.37	0.42	.45	0.50	0.56	0.37	0.42	.45	0.50	0.56	0.37	0.42	.45	0.50	0.56
LR	0.8353	0.5689	0.6029	0.6529	0.7035	0.8210	0.4440	0.4348	0.4146	0.3869	0.2230	0.1412	0.1482	0.1583	0.1686
DnV	0.9093	0.6003	0.6360	0.6893	0.7442	1.124	0.6043	0.5916	0.5639	0.5262	0.2799	0.1736	0.1820	0.1943	0.2069
Diff.	8.9%	5.5%	5.5%	5.6%	5.8%	36.9%	36.1%	36.1%	36%	36%	25.5%	23%	22.8%	22.7%	22.7%
BV	0.9163	0.5979	0.6324	0.6837	0.7363	1.085	0.5658	0.5525	0.5247	0.4883	0.2728	0.1657	0.1736	0.1851	0.1970
Diff.	9.7%	5.1%	4.9%	4.7%	4.7%	32.2%	27.4%	27.1%	26.6%	26.2%	22.3%	17.4%	17.1%	16.9%	16.8%
Class Society	ω (rad/s)					ω (rad/s)					ω (rad/s)				
	0.64	0.75	0.94	1.06		0.64	0.75	0.94	1.06		0.64	0.75	0.94	1.06	
LR	0.5436	0.4136	0.2754	0.2424		0.2365	0.1386	0.06602	0.04996		0.1244	0.09122	0.05911	0.05217	
DnV	0.5689	0.4302	0.2856	0.2518		0.3207	0.1874	0.08888	0.06715		0.1510	0.1098	0.07068	0.06242	
Diff.	4.7%	4%	3.7%	3.9%		35.6%	35.2%	34.6%	34.4%		21.4%	20.4%	19.6%	19.7%	
BV	0.5581	0.4182	0.2742	0.2405		0.2914	0.1665	0.07658	0.05725		0.1418	0.1017	0.06423	0.05631	
Diff.	2.7%	1.1%	-0.4%	-0.8%		23.2%	20.1%	16%	14.6%		14%	11.5%	8.7%	7.9%	

Table (12) Maximum Rolling, Yawing and Pitching Moments (MRSEQ2, $\beta = 0.0$)

b. The percentage differences in the yawing moment are more or less the same in the case of DnV varying from 34.4% to 36.9%. In the case of BV, the differences are inversely proportional to the frequency and vary from 14.6% to 32.2%.

c. The differences in the pitching moment are inversely proportional to the frequency. In the case of DnV, the differences ranged from 19.6% to 25.5% and in the case of BV, they ranged from 7.9% to 22.3%.

4.7 Maximum Surge, Heave and Sway Forces (OSS, $\beta = \pi/4$)

Table (13) shows that the heave force gave the largest differences followed by the surge and sway forces which are identical. This is shown below:-

a. The differences in the surge force varied from 12.3% to 28.8% in the case of DnV. In the case of BV, the differences varied from 3% to 7.8%.

b. The differences in the heave force ranged from 29.9% to 38.5% in the case of DnV and from 14% to 38.6% in the case of BV.

c. Similarly to the surge force, the differences in the sway force ranged from 12.3% to 28.8% in the case of DnV. BV had better agreement with smaller differences ranging from 3% to 7.8%.

Class. Society	Surge Force x 10^{-7} (N)					Heave Force x 10^{-7} (N)					Sway Force x 10^{-7} (N)				
	ω (rad/s)					ω (rad/s)					ω (rad/s)				
β = π/4	0.37	0.42	0.45	0.50	0.56	0.37	0.42	.45	0.50	0.56	0.37	0.42	.45	0.50	0.50
LR	1.472	0.9807	0.9788	0.9518	0.8890	1.268	0.7641	0.7626	0.7514	0.7305	1.47	0.9799	0.9781	0.9511	0.8883
DnV	1.663	1.101	1.099	1.071	1.003	1.738	1.039	1.039	1.027	1.003	1.662	1.100	1.098	1.070	1.002
Diff.	13%	12.3%	12.3%	12.5%	12.8%	37.1%	36%	36.2%	36.7%	37.3%	13.1%	12.3%	12.3%	12.5%	12.8%
BV	1.561	1.014	1.013	0.9856	0.9223	1.757	0.9245	0.924	0.9145	0.8962	1.560	1.013	1.012	0.9849	0.9216
Diff.	6.1%	3.4%	3.5%	3.6%	3.8%	38.6%	21%	21.2%	21.7%	22.7%	6.1%	3.4%	3.5%	3.6%	3.8%
Class. Society	ω (rad/s)					ω(rad/s)					ω(rad/s)				
	0.64	0.75	0.94	1.06		0.64	0.75	0.94	1.06		0.64	0.75	0.94	1.06	
LR	0.5631	0.292	0.07335	0.05711		0.4754	0.2804	0.107	0.06487		0.5627	0.2918	0.07332	0.05708	
DnV	0.6371	0.3363	0.09445	0.07304		0.6555	0.3882	0.1457	0.08426		0.6367	0.3361	0.09442	0.07301	
Diff.	13.1%	15.2%	28.8%	27.9%		37.9%	38.5%	36.2%	29.9%		13.2%	15.2%	28.8%	27.9%	
BV	0.5806	0.3006	0.0791	0.06142		0.5783	0.3376	0.1249	0.07392		0.5801	0.3004	0.07907	0.06138	
Diff.	3.1%	3%	7.8%	7.6%		21.6%	20.4%	16.7%	14%		3.1%	3%	7.8%	7.5%	

Table (13) Maximum Surge, Heave and Sway Forces (OSS, $\beta = \frac{\pi}{4}$)

Class. Society	Rolling Moment x 10^{-10} (N.M)					Yawing Moment x 10^{-5} (N.M)					Pitching Moment x 10^{-10} (N.M)				
	ω (rad/s)					ω (rad/s)					ω (rad/s)				
β = π/4	0.37	0.42	.45	0.50	0.56	0.37	0.42	.45	0.50	0.56	0.37	0.42	.45	0.50	0.50
LR	0.1395	0.09828	0.1014	0.1038	0.1021	0.1705	0.1211	0.1515	0.2174	0.3267	0.1396	0.09836	0.1015	0.1039	0.1022
DnV	0.1614	0.1096	0.1131	0.1159	0.1143	0.2287	0.1560	0.1925	0.2707	0.3988	0.1616	0.1097	0.1132	0.1160	0.1143
Diff.	15.7%	11.5%	11.5%	11.7%	12%	34.1%	28.8%	27.1%	24.5%	22%	15.8%	11.6%	11.5%	11.7%	11.8%
BV	0.1589	0.1011	0.1044	0.1069	0.1053	0.2402	0.1612	0.1979	0.2761	0.4032	0.1590	0.1012	0.1044	0.107	0.1054
Diff.	13.9%	2.9%	3%	3%	3.1%	40.9%	33.1%	30.6%	27%	23.4%	13.9%	2.9%	2.9%	3%	3.1%
Class. Society	ω (rad/s)					ω (rad/s)					ω (rad/s)				
	0.64	0.75	0.94	1.06		0.64	0.75	0.94	1.06		0.64	0.75	0.94	1.06	
LR	0.06802	0.0366	0.008996	0.007345		0.3572	0.4458	0.7476	0.9791		0.06807	0.03662	0.008998	0.007347	
DnV	0.07619	0.04155	0.01133	0.009229		0.4167	0.4958	0.7783	0.1019		0.07624	0.04157	0.01133	0.009229	
Diff.	12%	13.5%	25.9%	25.7%		16.7%	11.2%	4.1%	4.1%		12%	13.5%	25.9%	25.6%	
BV	0.06970	0.03739	0.009584	0.00783		0.4126	0.4793	0.7252	0.9493		0.06975	0.03742	0.009586	0.007831	
Diff.	2.5%	2.2%	6.54%	6.6%		15.5%	7.5%	-3%	-3%		2.5%	2.2%	6.5%	6.6%	

Table (14) Maximum Rolling, Yawing and Pitching Moments (OSS, $\beta = \frac{\pi}{4}$)

4.8 Maximum Rolling, Yawing and Pitching Moments (OSS, $\beta = \pi/4$)

Table (14) shows that the rolling moment and the pitching moment are identical. The rolling moment had large differences as follows:-

a. The rolling moment had differences ranging from 11.5% to 25.9% in the case of DnV. In the case of BV, the differences varied only from 2.2% to 13.9%.

b. The differences in the yawing moment ranged from 4.1% to 34.1% in the case of DnV and from -3% to 40.9% in the case of BV. (See note on p.182).

c. The differences in the pitching moment ranged from 11.5% to 25.9% in the case of DnV and from 2.2% to 13.9% in the case of BV.

4.9 Maximum Surge, Heave and Sway Forces (MRSEQ, $\beta = \pi/4$)

From Table (15), the following was noted:-

a. The differences in the surge force ranged from 14.9% to 21% in the case of DnV and from 5.2% to 18% in the case of BV.

b. The behaviour of the heave force is similar to that of Table (9). The differences in the heave force ranged from 11% to 251% in the case of DnV and from -91.2% to 1165% in the case of BV. The maximum differences were obtained when $\omega = 0.37$ rad/s.

c. Similarly to the surge force, the differences in the sway force ranged from 14.9% to 21.1% in the case of DnV and from 5.2% to 18.1% in the case of BV.

Class. Society	Surge Forc x 10^{-8} (N)					Heave Force x 10^{-7} (N)					Sway Force x 10^{-8} (N)				
	ω (rad/s)					ω (rad/s)					ω (rad/s)				
β = π/4.	0.37	0.42	.45	0!50	0.56	0.37	0.42	.45	0.50	0.56	0.37	0.42	.45	0.50	0.50
LR	0.2292	0.1411	0.1436	0.1461	0.148	0.03955	0.2487	0.2486	0.2349	0.2059	0.2291	0.141	0.1434	0.146	0.1479
DnV	0.2774	0.1668	0.1696	0.1725	0.1747	0.1389	0.29	0.289	0.2693	0.2286	0.2774	0.1668	0.1695	0.1724	0.1746
Diff.	21%	18.2%	18.1%	18.1%	18%.	251.2%	16.6%	16.3%	14.6%	11%	21.1%	18.3%	18.2%	18.1%	18.1%
BV	0.2705	0.1599	0.1623	0.165	0.167	0.5001	0.06306	0.05689	0.03019	0.01813	0.2705	0.1598	0.1622	0.1649	0.1669
Diff.	18%	13.3%	13%	12.9%	12.8%	1164.5%	-74.6%	-77.1%	-87.2%	-91.2%	18.1%	13.3%	13.1%	13%	12.9%

Class. Society	ω (rad/s)				ω (rad/s)				ω (rad/s)			
	0.64	0.75	0.94	1.06	0.64	0.75	0.94	1.06	0.64	0.75	0.94	1.06
LR	0.105	0.07388	0.04583	0.03964	0.242	0.2418	0.2248	0.2239	0.1049	0.07382	0.0458	0.03961
DnV	0.1226	0.08548	0.05267	0.04556	0.2937	0.3043	0.2905	0.2911	0.1225	0.08541	0.05263	0.04556
Diff.	16.8%	15.7%	14.9%	14.9%	21.4%	25.9%	29.2%	30%	16.8%	15.7%	14.9%	15%
BV	0.1159	0.07995	0.04848	0.04169	0.1122	0.1693	0.1978	0.206	0.1158	0.07989	0.04844	0.04166
Diff.	10.4%	8.2%	5.8%	5.2%	-53.6%	-30%	-12%	-8%	10.4%	8.2%	5.8%	5.2%

Table (15) Maximum Surge, Heave and Sway Forces (MRSEQ, $\beta = \frac{\pi}{4}$)

Class. Society	Rolling Moment x 10^{-10} (N.M)					Yawing Moment x 10^{-1} (N.M)					Pitching Moment x 10^{-10} (N.M)				
	ω (rad/s)					ω (rad/s)					ω (rad/s)				
β = π/4	0.37	0.42	.45	0.50	0.56	0.37	0.42	.45	0.50	0.56	0.37	0.42	.45	0.50	0.50
LR	0.2387	0.1528	0.1604	0.1712	0.1819	1.403	0.1112	0.415	1.858	1.164	0.2389	0.1529	0.1605	0.1713	0.1820
DnV	0.2923	0.1825	0.1913	0.2039	0.2165	4.216	1.282	1.033	3.360	0.6035	0.2925	0.1827	0.1915	0.2041	0.2167
Diff.	22.5%	19.4%	19.3%	19.1%	19%	200.5%	1052.9%	148.9%	80.8%	-48.2%	22.4%	19.5%	19.31%	19.2%	19.1%
BV	0.2867	0.1757	0.1839	0.1958	0.2076	3.088	1.509	2.744	0.4114	2.022	0.2869	0.1758	0.1841	0.1959	0.2078
Diff.	20.1%	15%	14.7%	14.4%	14.1%	120.1%	1257%	561.2%	-77.9%	73.7%	20.1%	15%	14.7%	14.4%	14.2%

Class. Society	ω (rad/s)				ω (rad/s)				ω (rad/s)			
	0.64	0.75	0.94	1.06	0.64	0.75	0.94	1.06	0.64	0.75	0.94	1.06
LR	0.1347	0.09891	0.06388	0.05604	0.4067	0.3095	0.06943	0.1778	0.1348	0.09899	0.06393	0.05608
DnV	0.1583	0.115	0.07368	0.06464	0.8737	0.06592	0.7618	0.2682	0.1584	0.1151	0.07374	0.06469
Diff.	17.5%	16.3%	15.3%	15.4%	114.8%	-78.7%	997.2%	50.8%	17.5%	16.3%	15.3%	15.4%
BV	0.15	0.1076	0.06776	0.05908	0.04824	0.1297	0.03887	0.3036	0.1501	0.1077	0.06781	0.0591
Diff.	11.4%	8.8%	6.1%	5.4%	-88.1%	-58.1%	-44%	70.8%	11.4%	8.8%	6.1%	5.4%

Table (16) Maximum Rolling, Yawing and Pitching Moments (MRSEQ, $\beta = \frac{\pi}{4}$)

4.10 Maximum Rolling, Yawing and Pitching Moments (MRSEQ, $\beta = \pi/4$)

In this case, the yawing and pitching moments, Table (16) had larger differences than the rolling moment as shown below:-

a. The variations in the rolling moment ranged from 15.3% to 22.5% in the case of DnV and from 5.4% to 20.1% in the case of BV.

b. The values of the yawing moments are negligible for the same reasons mentioned earlier in 4.4(b). (See note on p182)..

c. Similarly to the rolling moment, the differences in the pitching moment ranged from 15.3% to 22.4% in the case of DnV and from 5.4% to 20.1% in the case of BV.

4.11 Maximum Surge, Heave and Sway Forces (MRSEQ2, $\beta = \pi/4$)

The results in Table (17) show that:-

a. The differences in the surge force ranged from 15.2% to 20.5% according to DnV and from 5.4% to 17.3% according to BV.

b. The differences in the heave force are almost the same throughout the whole range of frequencies in the case of DnV, varying from 36% to 38%. According to BV, the differences are inversely proportional to the frequency and vary from 17.8% to 33.1%.

c. The differences in the sway force ranged from -0.3% to 7.3% in the case of DnV and from -1.4% to 10.8% in the case of BV.

Class Society $\beta=\frac{\pi}{4}$	Surge Force x 10^{-8} (N)					Heave Force x 10^{-7} (N)					Sway Force x 10^{-7} (N)				
	ω (rad/s)					ω (rad/s)					ω (rad/s)				
	0.37	0.42	.45	0.50	0.56	0.37	0.42	.45	0.50	0.56	0.37	0.42	.45	0.50	0.50
LR	0.2063	0.1282	0.1306	0.1334	0.1357	0.4932	0.2893	0.3023	0.3247	0.3545	1.266	0.7966	0.8161	0.8399	0.8595
DnV	0.2486	0.1509	0.1537	0.1570	0.1599	0.6807	0.3979	0.4158	0.4468	0.4878	1.358	0.8216	0.8417	0.8676	0.8907
Diff.	20.5%	17.7%	17.7%	17.7%	17.8%	38%	37.5%	37.6%	37.6%	37.6%	7.3%	3.1%	3.1%	3.3%	3.6%
BV	0.2420	0.1444	0.1470	0.1500	0.1527	0.6565	0.3735	0.3904	0.4201	0.4597	1.403	0.8419	0.8615	0.8863	0.9080
Diff.	17.3%	12.6%	12.6%	12.4%	12.5%	33.1%	29.1%	29.1%	29.4%	29.7%	10.8%	5.7%	5.6%	5.5%	5.6%
Class Society	ω (rad/s)					ω (rad/s)					ω (rad/s)				
	0.64	0.75	0.94	1.06		0.64	0.75	0.94	1.06		0.64	0.75	0.94	1.06	
LR	0.09705	0.06888	0.04325	0.03764		0.2616	0.1984	0.1402	0.1318		0.6215	0.4434	0.2754	0.2362	
DnV	0.1131	0.07972	0.04981	0.04344		0.3590	0.2714	0.1906	0.1788		0.6339	0.4471	0.2748	0.2356	
Diff.	16.5%	15.7%	15.2%	15.4%		37.2%	36.8%	36%	35.7%		2%	0.8%	-0.2%	-0.3%	
BV	0.1070	0.07453	0.04582	0.03968		0.3327	0.2462	0.1674	0.1553		0.6417	0.4490	0.2729	0.2329	
Diff.	10.3%	8.2%	5.9%	5.4%		27.2%	24.1%	19.4%	17.8%		3.3%	1.3%	-0.9%	-1.4%	

Table (17) Maximum Surge, Heave and Sway Forces (MRSEQ2, $\beta=\frac{\pi}{4}$)

Class Society $\beta=\frac{\pi}{4}$	Rolling Moment x 10^{-9} (N.M)					Yawing Moment x 10^{-8} (N.M)					Pitching Moment x 10^{-10} (N.M)				
	ω (rad/s)					ω (rad/s)					ω (rad/s)				
	0.37	0.42	.45	0.50	0.56	0.37	0.42	.45	0.50	0.56	0.37	0.42	.45	0.50	0.50
LR	1.329	0.8588	0.9066	0.9760	1.045	0.7491	0.4133	0.4051	0.3865	0.3607	0.2129	0.1380	0.1453	0.1559	0.1666
DnV	1.463	0.9030	0.9522	1.024	1.097	1.023	0.5613	0.5500	0.5245	0.4896	0.2591	0.1640	0.1725	0.1850	0.1978
Diff.	10.1%	5.2%	5%	4.9%	5%	36.6%	35.8%	35.8%	35.7%	35.7%	21.7%	18.8%	18.7%	18.7%	18.7%
BV	1.526	0.9337	0.9828	1.054	1.126	0.9768	0.5198	0.5078	0.4826	0.4491	0.2535	0.1575	0.1656	0.1773	0.1894
Diff.	14.8%	8.7%	8.4%	8.0%	7.9%	30.4%	25.8%	25.4%	24.9%	24.5%	19.1%	14.1%	14%	13.7%	13.7%
Class Society	ω (rad/s)					ω (rad/s)					ω (rad/s)				
	0.64	0.75	0.94	1.06		0.64	0.75	0.94	1.06		0.64	0.75	0.94	1.06	
LR	0.7839	0.5807	0.3749	0.3267		0.2232	0.1324	0.06413	0.04883		0.1246	0.09240	0.06048	0.05342	
DnV	0.8060	0.5876	0.3741	0.3255		0.3020	0.1787	0.08623	0.06557		0.1462	0.1075	0.06993	0.06185	
Diff.	2.8%	1.2%	-0.2%	-0.4%		35.3%	35%	34.5%	34.3%		17.3%	16.3%	15.6%	15.8%	
BV	0.8205	0.5930	0.3729	0.3229		0.2715	0.1572	0.07373	0.05555		0.1383	0.1005	0.06424	0.05642	
Diff.	4.7%	2.1%	-0.5%	-1.2%		21.6%	18.7%	15%	13.8%		11%	8.8%	6.2%	5.6%	

Table (18) Maximum Rolling, Yawing and Pitching Moments (MRSEQ2, $\beta=\frac{\pi}{4}$)

4.12 Maximum Rolling, Yawing and Pitching Moments (MRSEQ2, $\beta = \pi/4$)

The results in Table (18) show that:

a. The differences in the rolling moment ranged from -0.4% to 10.1% according to DnV and from -1.2% to 14.8% according to BV.

b. The differences in the yawing moment are almost the same according to DnV, varying from 34.3% to 36.6%. In the case of BV, the differences are inversely proportional to the frequency and varying from 13.8% to 30.4% (See note on p182).

c. The differences in the pitching moment ranged from 15.6% to 21.7% according to DnV and from 5.6% to 19.1% according to BV.

5. ANALYSIS OF LR RESULTS BY PROGRAMS OSS, MRSEQ AND MRSEQ2

Tables (19) to (22) summarise the results of LR calculation as carried out by the different methods (OSS, MRSEQ and MRSEQ2). These results were analysed, as shown below, taking OSS as the basis for comparison.

5.1 LR Maximum Surge, Heave and Sway Forces ($\beta = 0.0$)

Table (19) shows that:-

a. According to program MRSEQ, the values of the surge force were overestimated compared with the OSS results for all frequencies. The differences ranged from 43.3% to 414%. However, for the program MRSEQ2, the surge forces were underestimated at $\omega = 0.42$ rad/s and at $\omega = 0.45$ rad/s

LR $\beta = 0.0$ Program	Surge Force x 10^{-8} (N)					Heave Force x 10^{-7} (N)					Sway Force x 10^{-6} (N)				
	ω (rad/s)					ω (rad/s)					ω (rad/s)				
	0.37	0.42	.45	0.50	0.56	0.37	0.42	.45	0.50	0.56	0.37	0.42	.45	0.50	0.56
OSS	0.2087	0.1382	0.1377	0.1332	0.1229	1.274	0.7665	0.7649	0.7533	0.7303	0.1392	0.09205	0.1058	0.1320	0.1673
MRSEQ	0.3219	0.1980	0.2011	0.2043	0.2063	0.04245	0.2474	0.2473	0.2336	0.2046	0.2252	0.1515	0.1750	0.2216	0.2884
Diff.	54.2%	43.3%	46%	53.4%	67.9%	-96.7%	-67.7%	-67.7%	-69%	-72%	61.8%	64.6%	65.4%	67.9%	72.4%
MRSEQ2	0.2133	0.1296	0.1317	0.1340	0.1359	0.4673	0.2819	0.2956	0.3193	0.3505	8.353	5.536	5.673	5.839	5.974
Diff.	2.2%	-6.2%	-4.4%	0.6%	10.6%	-63.3%	-63.2%	-61.4%	57.6%	-52%					
Program	ω (rad/s)					ω (rad/s)					ω (rad/s)				
	0.64	0.75	0.94	1.06		0.64	0.75	0.94	1.06		0.64	0.75	0.94	1.06	
OSS	0.07423	0.03105	0.01225	0.02558		0.4669	0.2594	0.05904	0.01125		0.1404	0.1277	0.07461	0.03751	
MRSEQ	0.1459	0.1022	0.06293	0.05419		0.2413	0.2414	0.2246	0.2237		0.2549	0.2328	0.1982	0.1972	
Diff.	96.6%	229%	414%	112%		-48.3%	-6.9%	280%			81.5%	82.3%	166%	426%	
MRSEQ2	0.09587	0.06729	0.04184	0.0364		0.2620	0.2007	0.1428	0.1344		4.419	3.217	2.050	1.775	
Diff.	29.2%	117%	242%	42%		-43.9%	-22.6%	142%							

Table (19) LR Maximum Surge, Heave and Sway Forces (β= 0.0)

LR $\beta = 0.0$ Program	Rolling Moment x 10^{-8} (N.M.)					Yawing Moment x 10^{-7} (N.M)					Pitching Moment x 10^{-10} (N.M)				
	ω (rad/s)					ω (rad/s)					ω (rad/s)				
	0.37	0.42	.45	0.50	0.56	0.37	0.42	.45	0.50	0.56	0.37	0.42	.45	0.50	0.56
OSS	0.2091	0.1457	0.1717	0.2197	0.2824	0.09685	0.07592	0.09567	0.1407	0.2172	0.1981	0.1386	0.1428	0.1454	0.1411
MRSEQ	0.3181	0.2248	0.2658	0.3421	0.4456	negligible values					0.3347	0.214	0.2243	0.2389	0.253
Diff.	52.1%	54.3%	54.8%	55.7%	57.8%						69%	54.4%	57.1%	64.3%	79.3%
MRSEQ2	8.553	5.689	6.029	6.529	7.035	8.210	4.440	4.348	4.146	3.869	0.2230	0.1412	0.1482	0.1583	0.1686
Diff.	very large					very large					12.6%	1.9%	3.8%	8.9%	19.5%
Program	ω (rad/s)					ω (rad/s)					ω (rad/s)				
	0.64	0.75	0.94	1.06		0.64	0.75	0.94	1.06		0.64	0.75	0.94	1.06	
OSS	0.2413	0.2217	0.1412	0.08591		0.2318	0.2577	0.2939	0.2976		0.08910	0.03758	0.01950	0.03777	
MRSEQ	0.3910	0.3520	0.2948	0.2913		negligible values					0.1869	0.1367	0.08762	0.07655	
Diff.	61.7%	58.8%	109%	239%							110%	264%	349%	103%	
MRSEQ2	5.436	4.136	2.754	2.424		2.365	1.386	0.6602	0.4996		0.1244	0.09122	0.05911	0.05217	
Diff.	very large					920%	438%	125%	68%		39.6%	143%	203%	38%	

Table (20) LR Maximum Rolling, Yawing and Pitching Moments (β= 0.0) by 6.2% and 4.4% respectively. At the other frequencies, the forces were overestimated. The differences ranged from about 2.2% to 242%.

b. According to MRSEQ, the heave forces were underestimated up to ω = 0.75 rad/s, with a maximum difference of 96.7% while at ω = 0.94 rad/s the force was overestimated by 280%. Using program MRSEQ2, the heave forces were underestimated up to ω = 0.75 rad/s with a maximum difference of 63.3%. At ω = 0.94 rad/s, the force was overestimated by 142%. At ω = 1.06 rad/s MRSEQ and MRSEQ2 gave big differences.

c. According to MRSEQ, the sway forces were overestimated. The differences ranged from 61.8% to 426%. Program MRSEQ2 gave much larger differences throughout the whole range of frequencies.

5.2 LR Maximum Rolling, Yawing and Pitching Moments (β = 0.0)

Table (20) shows that:-

a. According to MRSEQ, the rolling moments were overestimated by differences ranging from 52.1% to 239%. Using MRSEQ2, the differences are much larger for all frequencies.

b. The values of the yawing moment calculated by MRSEQ are negligible. According to MRSEQ2 the values of the yawing moment are much larger than those of program OSS.

c. Using program MRSEQ, the pitching moments are overestimated by differences ranging from 54.4% to 349%. According to MRSEQ2, the moments were overestimated by differences ranging from 1.9% to 203%.

5.3 LR Maximum Surge, Heave and Sway Forces ($\beta = \pi/4$)

Table (21) shows that:-

a. Program MRSEQ overestimated the surge forces by differences ranging from 43.9% to 594%, while MRSEQ2 overestimated the forces by differences ranging from 30.7% to 559%.

b. MRSEQ underestimated the heave forces up to $\omega = 0.75$ rad/s with maximum differences of 96.9%. At $\omega = 0.94$ rad/s and $\omega = 1.06$ rad/s, the forces were overestimated by 110% and 245% respectively. According to MRSEQ2 the heave forces were underestimated up to $\omega = 0.75$ rad/s with a maximum difference of 62.1%. At $\omega = 0.94$ rad/s and $\omega = 1.06$ rad/s, the forces were overestimated by 31% and 103% respectively.

c. MRSEQ overestimated the sway forces by differences ranging from 43.9% to 594% while MRSEQ2 underestimated the forces up to $\omega = 0.56$ rad/s with a maximum difference of 18.7%. At the other frequencies, the forces were overestimated with differences ranging from 10.4% to 314%.

5.4 LR Maximum Rolling, Yawing and Pitching Moments ($\beta = \pi/4$)

Table (22) shows that:-

a. Program MRSEQ overestimated the rolling moments by differences ranging from 55.5% to 663% while for program MRSEQ2, the moments were underestimated up to $\omega = 0.5$ rad/s with a maximum difference of 12.6% and then the moments

LR $\beta = \frac{\pi}{4}$ Program	Surge Force x 10^{-8} (N) ω (rad/s)					Heave Forcex 10^{-7} (N) ω (rad/s)					Sway Force x 10^{-7} (N) ω (rad/s)				
	0.37	0.42	.45	0.50	0.56	0.37	0.42	.45	0.50	0.56	0.37	0.42	.45	0.50	0.56
OSS	0.1472	0.09807	0.09788	0.09518	0.08890	1.268	0.7641	0.7626	0.7514	0.7305	1.47	0.9799	0.9781	0.9511	0.8883
MRSEQ	0.2292	0.1411	0.1436	0.1461	0.148	0.03955	0.2487	0.2486	0.2349	0.2059	2.291	1.411	1.434	1.46	1.479
Diff.	55.7%	43.9%	46.7%	53.5%	66.5%	-96.9%	-67.5%	-67.4%	-68.7%	-71.8%	55.9%	43.9%	46.6%	53.5%	66.5%
MRSEQ2	0.2063	0.1282	0.1306	0.1334	0.1357	0.4932	0.2893	0.3023	0.3247	0.3545	1.266	0.7966	0.8161	0.8399	0.8595
Diff.	40.1%	30.7%	33.4%	40.2%	52.6%	-61.1%	-62.1%	-60.4%	-56.8%	-51.5%	-13.9%	-18.7%	-16.6%	-11.7%	-3.2%

Program	ω (rad/s)				ω (rad/s)				ω (rad/s)			
	0.64	0.75	0.94	1.06	0.64	0.75	0.94	1.06	0.64	0.75	0.94	1.06
OSS	0.05631	0.0292	0.007335	0.005711	0.4754	0.2804	0.107	0.06487	0.5627	0.2918	0.07332	0.05708
MRSEQ	0.105	0.07388	0.04583	0.03964	0.242	0.2418	0.2248	0.2239	1.049	0.7382	0.458	0.3961
Diff.	86.5%	153%	525%	594%	-49.1%	-13.8%	110%	245%	86.4%	153%	525%	594%
MRSEQ2	0.09705	0.06888	0.04325	0.03764	0.2616	0.1984	0.1402	0.1318	0.6215	0.4434	0.2754	0.2362
Diff.	72.3%	136%	490%	559%	-45%	-29.2%	31%	103%	10.4%	52%	276%	314%

Table (21) LR Maximum Surge, Heave and Sway Forces ($\beta \frac{\pi}{4}$)

LR $\beta = \frac{\pi}{4}$ Program	Rolling Moment x 10^{-9} (N.M) ω (rad/s)					Yawing Moment x 10^{-5} (N.M) ω (rad/s)					Pitching Moment x 10^{-10} (N.M) ω (rad/s)				
	0.37	0.42	.45	0.50	0.56	0.37	0.42	.45	0.50	0.56	0.37	0.42	.45	0.50	0.56
OSS	1.395	0.9828	1.014	1.038	1.021	0.1705	0.1211	0.1515	0.2174	0.3267	0.1396	0.09836	0.1015	0.1039	0.1022
MRSEQ	2.387	1.528	1.604	1.712	1.819	negligible values					0.2389	0.1529	0.1605	0.1713	0.1820
Diff.	71.1%	55.5%	58.2%	64.9%	78.2%						71.1%	55.4%	58.1%	64.9%	78.1%
MRSEQ2	1.329	0.8588	0.9066	0.976	1.045	749.1	413.3	405.1	386.5	360.7	0.2129	0.138	0.1453	0.1559	0.1666
Diff.	-4.7%	-12.6%	-10.6%	-6%	2.4%	very large					52.5%	40.3%	43.2%	50%	63.1%

Program	ω (rad/s)				ω (rad/s)				ω (rad/s)			
	0.64	0.75	0.94	1.06	0.64	0.75	0.94	1.06	0.64	0.75	0.94	1.06
OSS	0.6802	0.366	0.08996	0.07345	0.3572	0.4458	0.7476	0.9791	0.06807	0.03662	0.008998	0.007347
MRSEQ	1.347	0.9891	0.6388	0.5604	negligible values				0.1348	0.09899	0.06393	0.05608
Diff.	98%	170%	610%	663%					98%	170%	611%	663%
MRSEQ2	0.7839	0.5807	0.3749	0.3267	223.2	132.4	64.13	48.83	0.1246	0.0924	0.06048	0.05342
Diff.	15.2%	58.7%	317%	345%	very large				83%	152%	572%	627%

Table (22) LR Maximum Rolling, Yawing and Pitching Moments ($\beta = \frac{\pi}{4}$)

were overestimated by differences ranging from 2.4% to 345%.

b. The values of the yawing moments calculated by MRSEQ are negligible. According to MRSEQ2, the yawing moments are much larger than those of OSS. (See note on p.182).

c. MRSEQ overestimated the pitching moments by differences ranging from 55.4% to 663% while MRSEQ2 over-estimated the moments by differences ranging from 40.3% to 627%

6. EFFECT OF WAVE HEIGHT

So far, the analysis of the results of the calculations performed by the different methods and using different C_D and C_M coefficients has been related to the variation of the wave frequency. For each frequency, a corresponding wave height was assumed. To examine the effects of wave height on loading estimation, the calculations were carried out at a selected constant frequency of 0.37 rad/s and 4 wave heights of 1.0, 10.0, 20.0 and 30.0m. The results of calculations are given in Tables (23) to (28) and are analysed as shown below.

6.1 Maximum Forces and Moments (OSS, $\beta = 0.0$)

The results in Table (23) show the following:

a. The percentage differences in the surge force due to the change in wave height ranged from 10.4% to 13.2% according to DnV and from 0.6% to 5.3% according to BV.

b. The percentage differences in the heave force ranged from 34.1% to 36.7% according to DnV and from 11.3% to 38.2% according to BV.

β = 0.0 ω = 0.37	Surge Force x 10^{-7} (N)				Heave Force x 10^{-7} (N)				Sway Force x 10^{-5} (N)			
Class Society	Wave Height (m)				Wave Height (m)				Wave Height (m)			
	1.0	10.0	20.0	30.0	1.0	10.0	20.0	30.0	1.0	10.0	20.0	30.0
LR	0.06304	0.6506	1.3460	2.0870	0.03474	0.3474	0.7536	1.2740	0.02725	0.2888	0.7303	1.3920
DnV Diff.	0.06959 10.4%	0.7242 11.3%	1.5110 12.3%	2.3620 13.2%	0.0466 34.1%	0.4660 34.1%	1.0220 35.6%	1.7410 36.7%	0.03635 33.4%	0.3863 33.80%	1.0000 36.9%	1.9150 37.6%
BV Diff.	0.06344 0.6%	0.6648 2.2%	1.3970 3.8%	2.1970 5.3%	0.03866 11.3%	0.3866 11.3%	0.9127 21.1%	1.7600 38.2%	0.02836 4.1%	0.3220 11.5%	0.9405 28.8%	2.0120 44.5%
Class Society	Rolling Moment x 10^{-7} (N.M)				Yawing Moment x 10^{-6} (N.M)				Pitching Moment x 10^{-9} (N.M)			
	Wave Height (m)				Wave Height (m)				Wave Height (m)			
	1.0	10.0	20.0	30.0	1.0	10.0	20.0	30.0	1.0	10.0	20.0	30.0
LR	0.03555	0.3850	1.0740	2.0910	0.01733	0.2012	0.5240	0.9685	0.05939	0.6146	1.2750	1.9810
DnV Diff.	0.04742 33.4%	0.5155 33.9%	1.4750 37.3%	2.9000 38.7%	0.02311 33.4%	0.2723 35.3%	0.7149 36.4%	1.3280 37.1%	0.06514 9.7%	0.6803 10.7%	1.4250 11.8%	2.2540 13.8%
BV Diff.	0.03680 3.5%	0.4641 20.6%	1.4070 31%	3.1060 48.5%	0.01823 5.2%	0.2389 18.7%	0.6602 26%	1.2640 30.5%	0.05933	0.6243 1.6%	1.3170 3.3%	2.2200 12.1%

Table (23) Maximum Forces and Moments at Different Wave Heights (OSS, β = 0.0)

β = 0.0 ω = 0.37	Surge Force x 10^{-7} (N)				Heave Force x 10^{-7} (N)				Sway Force x 10^{-5} (N)			
Class Society	Wave Height (m)				Wave Height (m)				Wave Height (m)			
	1.0	10.0	20.0	30.0	1.0	10.0	20.0	30.0	1.0	10.0	20.0	30.0
LR	0.07092	0.8221	1.895	3.219	0.03597	0.2437	0.2295	0.04245	0.03059	0.4440	1.195	2.252
DnV Diff.	0.07888 11.2%	0.9469 15.2%	2.245 18.5%	3.895 21%	0.04757 32.3%	0.3133 28.6%	0.2656 15.7%	0.1430 237%	0.04089 33.7%	0.6022 35.6%	1.634 36.7%	3.095 37.4%
BV Diff.	0.07202 1.6%	0.8896 8.2%	2.156 13.8%	3.798 18%	0.03926 9.2%	0.2186 -10.3%	0.05041 -78%	0.5045 1089%	0.03245 6.1%	0.5316 19.7%	1.523 27.5%	2.976 32.2%
Class Society	Rolling Moment x 10^{-7} (N.M.)				Yawing Moment (N.M)				Pitching Moment x 10^{-9} (N.M)			
	Wave Height (m)				Wave Height (m)				Wave Height (m)			
	1.0	10.0	20.0	30.0	1.0	10.0	20.0	30.0	1.0	10.0	20.0	30.0
LR	0.03805	0.5915	1.652	3.181	0.5625	2.000	6.000	0.0	0.0689	0.8214	1.937	3.347
DnV Diff.	0.05089 33.8%	0.8043 36%	2.265 37.1%	4.382 37.8%	0.9375	3.000 negligible values	14.000	4.00	0.07674 11.4%	0.9528 16%	2.318 19.7%	4.095 22.4%
BV Diff.	0.04027 5.8%	0.7191 21.6%	2.141 29.6%	4.267 34.1%	0.625	10.000 negligible values	30.000	28.000	0.06984 1.4%	0.8971 9.2%	2.236 15.4%	4.016 20%

Table (24) Maximum Forces and Moments at Different Wave Heights (MRSEQ, β = 0.0)

c. The percentage differences in the sway force ranged from 33.4% to 37.6% according to DnV which is similar to those for heave force. In the case of BV, the differences ranged from 4.1% to 44.5%.

d. The differences in the rolling moment ranged from 33.4% to 38.7% according to DnV and from 3.5% to 48.5% for BV.

e. The differences in the yawing moment ranged from 33.4% to 37.1% according to DnV which is similar to the case of the rolling moment. Using the BV values, the differences ranged from 5.2% to 30.5%.

f. The differences in the pitching moment ranged from 9.7% to 13.8% in the case of DnV and from 1.6% to 12.1% for BV.

6.2 Maximum Forces and Moments (MRSEQ, $\beta = 0.0$)

Table (24) shows that:-

a. The percentage differences in the surge force ranged from 11.2% to 21% according to DnV and from 1.6% to 18% according to BV.

b. The differences in the heave force are irregular. They ranged from 15.7% to 237% using DnV values and from -78% to 1089% in the case of BV.

c. The differences in the sway force ranged from 33.7% to 37.4% according to DnV and from 6.1% to 32.2% for BV.

d. The differences in the rolling moment ranged from 33.8% to 37.8% for DnV and from 5.8% to 34.1% according to BV.

e. The values of the yawing moment are negligible.

f. The differences in the pitching moment ranged from 11.4% to 22.4% for DnV and from 1.4% to 20% in the case of BV.

6.3 Maximum Forces and Moments (MRSEQ2, β = 0.0)

Table (25) shows that:-

a. The percentage differences in the surge force ranged from 15.8% to 24.7% according to DnV and from 3.7% to 20.7% for BV.

b. The differences in the heave force according to DnV are similar to those of Table (22), ranging from 33.6% to 36.7%. In the case of BV, the differences ranged from 11.8% to 30.7%.

c. The differences in the sway force are the smallest. Using DnV values, they ranged from -1% to 6.6% and for BV values the differences ranged from -4.5% to 5.6%.

d. The rolling moment gave the smallest differences compared to both the yawing and pitching moments. The differences ranged from -2.6% to 8.9% for DnV and from -5.2% to 9.7% for BV.

e. The differences in the yawing moment ranged from 33.5% to 36.9% according to DnV and from 13.2% to 32.2% for BV.

f. The differences in the pitching moment ranged from 15.5% to 25.5% using DnV values and from 3.2% to 22.3% according to BV.

β = 0.0 ω = 0.37	Surge Force x 10^{-7} (N)				Heave Force x 10^{-7} (N)				Sway Force x 10^{-7} (N)			
Class Society	Wave Height (m)				Wave Height (m)				Wave Height (m)			
	1.0	10.0	20.0	30.0	1.0	10.0	20.0	30.0	1.0	10.0	20.0	30.0
LR	0.04497	0.5308	1.2420	2.1330	0.007875	0.1027	0.2584	0.4673	0.02269	0.2429	0.5213	0.8353
DnV	0.05206	0.6342	1.5210	2.6590	0.01052	0.1386	0.3516	0.6390	0.02246	0.2470	0.5437	0.8902
Diff.	15.8%	19.5%	22.5%	24.7%	33.6%	35%	36.1%	36.7%	-1%	1.7%	4.3%	6.6%
BV	0.04663	0.5880	1.4460	2.5750	0.008802	0.1239	0.3274	0.6106	0.02168	0.2407	0.5348	0.8821
Diff.	3.7%	10.8%	16.4%	20.7%	11.8%	20.6%	26.7%	30.7%	-4.5%	-0.9%	2.6%	5.6%
Class Society	Rolling Moment x 10^{-9} (N.M)				Yawing Moment x 10^{-8} (N.M)				Pitching Moment x 10^{-9} (N.M)			
	Wave Height (m)				Wave Height (m)				Wave Height (m)			
	1.0	10.0	20.0	30.0	1.0	10.0	20.0	30.0	1.0	10.0	20.0	30.0
LR	0.02033	0.2267	0.5051	0.8353	0.0133	0.1766	0.4503	0.8210	0.04391	0.5335	1.277	2.230
DnV	0.0198	0.2306	0.5337	0.9093	0.01776	0.2387	0.6133	1.1240	0.05073	0.6394	1.5720	2.7990
Diff.	-2.6%	1.7%	5.7%	8.9%	33.5%	35.2%	36.2%	36.9%	15.5%	19.9%	23.1%	25.5%
BV	0.01928	0.2278	0.5332	0.9163	0.01505	0.2160	0.5775	1.085	0.04532	0.5947	1.5040	2.7280
Diff.	-5.2%	0.5%	5.6%	9.7%	13.2%	22.3%	28.3%	32.2%	3.2%	11.5%	17.8%	22.3%

Table (25) Maximum Forces and Moments at Different Wave Heights (MRSEQ2, β = 0.0)

β = $\frac{\pi}{4}$ ω = 0.37	Surge Force x 10^{-7} (N)				Heave Force x 10^{-7} (N)				Sway Force x 10^{-7} (N)			
Class Society	Wave Height (m)				Wave Height (m)				Wave Height (m)			
	1.0	10.0	20.0	30.0	1.0	10.0	20.0	30.0	1.0	10.0	20.0	30.0
LR	0.04506	0.4630	0.9535	1.4720	0.03477	0.3477	0.7513	1.2680	0.04503	0.4626	0.9528	1.4700
DnV	0.04984	0.5157	1.07	1.663	0.04662	0.4662	1.019	1.738	0.0498	0.5153	1.069	1.662
Diff.	10.6%	11.4%	12.2%	13%	34.1%	34.1%	35.6%	37.1%	10.6%	11.4%	12.2%	13.1%
BV	0.04537	0.4723	0.9859	1.561	0.03863	0.3868	0.9089	1.757	0.04534	0.4719	0.9852	1.560
Diff.	0.7%	2%	3.4%	6.1%	11.3%	11.3%	21%	38.6%	0.7%	2%	3.4%	6.1%
Class Society	Rolling Moment x 10^{-9} (N.M)				Yawing Moment x 10^{-4} (N.M)				Pitching Moment x 10^{-9} (N.M)			
	Wave Height (m)				Wave Height (m)				Wave Height (m)			
	1.0	10.0	20.0	30.0	1.0	10.0	20.0	30.0	1.0	10.0	20.0	30.0
LR	0.04247	0.4372	0.9022	1.3950	0.01236	0.2562	0.8241	1.7050	0.0425	0.4375	0.9029	1.3960
DnV	0.04666	0.4842	1.007	1.6140	0.01321	0.3251	1.087	2.287	0.04670	0.4845	1.008	1.616
Diff.	9.9%	10.8%	11.6%	15.7%	6.9%	26.9%	31.9%	34.1%	9.9%	10.7%	11.6%	15.8%
BV	0.04243	0.4431	0.9281	1.5890	0.0122	0.3326	1.134	2.402	0.04247	0.4435	0.9288	1.590
Diff.		1.4%	2.9%	13.9%	-1.3%	29.8%	37.6%	40.9%		1.4%	2.9%	13.9%

Table (26) Maximum Forces and Moments at Different Wave Heights (OSS, β = $\frac{\pi}{4}$)

6.4 Maximum Forces and Moments (OSS, $\beta = \pi/4$)

Table (26) shows that:-

a. The values of the surge force and sway force are identical and the percentage differences are much smaller than those for the heave force. In the case of DnV, the differences ranged from 10.6% to 13.1% and in the case of BV, the differences ranged from 0.7% to 6.1%.

b. The differences in the heave force ranged from 34.1% to 37.1% for DnV values and from 11.3% to 38.6% according to BV.

c. The values of the rolling moment and the pitching moment are identical and the percentage differences are much smaller than those of the yawing moment. According to DnV, the differences ranged from 9.9% to 15.7% and for BV, the differences ranged from 1.4% to 13.9%.

d. The differences in the yawing moment ranged from 6.9% to 34.1% for DnV and from -1.3% to 40.9% according to BV. (See note on p.182).

6.5 Maximum Forces and Moments (MRSEQ, $\beta = \pi/4$)

Table (27) shows that:-

a. The values of the surge and sway forces are identical and the percentage differences are much smaller than those of the heave force. Using DnV values the differences ranged from 11.3% to 21.1% while for BV, the differences ranged from 1.6% to 18.1%.

$\beta = \frac{\pi}{4}$ $\omega = 0.37$	Surge Force x 10^{-7} (N)				Heave Force x 10^{-7} (N)				Sway Force x 10^{-7} (N)			
Class Society	Wave Height (m)				Wave Height (m)				Wave Height (m)			
	1.0	10.0	20.0	30.0	1.0	10.0	20.0	30.0	1.0	10.0	20.0	30.0
LR	0.05038	0.5846	1.349	2.292	0.03597	0.2440	0.2308	0.03955	0.05034	0.5842	1.348	2.291
DnV	0.05609	0.6740	1.599	2.776	0.04757	0.3137	0.2674	0.1389	0.05604	0.6735	1.598	2.774
Diff.	11.3%	15.3%	18.5%	21.1%	32.3%	28.6%	15.9%	251%	11.3%	15.3%	18.6%	21.1%
BV	0.05118	0.633	1.535	2.707	0.03926	0.2191	0.05235	0.5001	0.05114	0.6325	1.534	2.705
Diff.	1.6%	8.3%	13.8%	18.1%	9.2%	-10.2%	-77.3%	1164%	1.6%	8.3%	13.8%	18.1%
Class Society	Rolling Moment x 10^{-9} (N.M)				Yawing Moment (N.M)				Pitching Moment x 10^{-9} (N.M)			
	Wave Height (m)				Wave Height (m)				Wave Height (m)			
	1.0	10.0	20.0	30.0	1.0	10.0	20.0	30.0	1.0	10.0	20.0	30.0
LR	0.04897	0.5846	1.380	2.387	0.07126	10.000	8.7570	14.030	0.04901	0.5851	1.381	2.389
DnV	0.05460	0.6789	1.653	2.923	0.04883	6.355	0.7412	42.16	0.05464	0.6795	1.655	2.925
Diff.	11.5%	16.1%	19.8%	22.5%		negligible values			11.5%	16.1%	19.8%	22.4%
BV	0.04965	0.6389	1.594	2.867	0.4345	4.398	2.690	30.880	0.04969	0.6394	1.596	2.869
Diff.	1.4%	9.3%	15.5%	20.1%		negligible values			1.4%	9.3%	15.6%	20.1%

Table (27) Maximum Forces and Moments at Different Wave Heights (MRSEQ, $\beta = \frac{\pi}{4}$)

$\beta = \pi/4$ $\omega = 0.37$	Surge Force x 10^{-7} (N)				Heave Force x 10^{-7} (N)				Sway Force x 10^{-7} (N)			
Class Society	Wave Height (m)				Wave Height (m)				Wave Height (m)			
	1.0	10.0	20.0	30.0	1.0	10.0	20.0	30.0	1.0	10.0	20.0	30.0
LR	0.04632	0.5329	1.2210	2.0630	0.007496	0.1027	0.2671	0.4932	0.02885	0.3299	0.7519	1.2660
DnV	0.05144	0.6119	1.4410	2.4860	0.01017	0.1405	0.3674	0.6807	0.02659	0.3239	0.7766	1.3580
Diff.	11.1%	14.8%	18%	20.5%	35.7%	36.8%	37.6%	38%	-7.8%	-1.8%	3.3%	7.3%
BV	0.04697	0.5742	1.3810	2.4200	0.008467	0.1263	0.3452	0.6565	0.02675	0.3297	0.7973	1.4030
Diff.	1.4%	7.8%	13.1%	17.3%	13%	23%	29.2%	33.1%	-7.3%		6%	10.8%
Class Society	Rolling Moment x 10^{-9} (N.M)				Yawing Moment x 10^{-8} (N.M)				Pitching Moment x 10^{-9} (N.M)			
	Wave Height (m)				Wave Height (m)				Wave Height (m)			
	1.0	10.0	20.0	30.0	1.0	10.0	20.0	30.0	1.0	10.0	20.0	30.0
LR	0.02714	0.3247	0.7678	1.3290	0.01322	0.1686	0.4184	0.7491	0.04495	0.5303	1.2400	2.1290
DnV	0.02474	0.3220	0.8099	1.4630	0.01765	0.2276	0.5686	1.0230	0.04994	0.6125	1.4760	2.5910
Diff.	-8.8%	-0.8%	5.5%	10.1%	33.5%	35%	35.9%	36.6%	11.1%	15.5%	19%	21.7%
BV	0.02512	0.3311	0.8399	1.5260	0.01493	0.2040	0.5296	0.9768	0.04546	0.5757	1.4210	2.5350
Diff.	-7.4%	2%	9.4%	14.8%	12.9%	21%	26.6%	30.4%	1.1%	8.6%	14.6%	19.1%

Table (28) Maximum Forces and Moments at Different Wave Heights (MRSEQ2, $\beta = \frac{\pi}{4}$)

b. The heave force gave an irregular and wide range of differences. In the case of DnV, the differences ranged from 15.9% to 251%, while in the case of BV, the differences ranged from -77.3% to 1164%.

c. The values of the rolling moment and pitching moment are identical. According to DnV, the differences ranged from 11.5% to 22.5% and for BV, the differences ranged from 1.4% to 20.1%.

d. The values of the yawing moment are negligible (See note on p.182).

6.6 Maximum Forces and Moments (MRSEQ2, $\beta = \pi/4$)

Table (28) shows that:-

a. The differences in the surge force ranged from 11.1% to 20.5% using DnV values and from 1.4% to 17.3% for BV values.

b. The differences in the heave force ranged from 35.7% to 38% according to DnV and from 13% to 35.1% for BV.

c. The sway force gave the smallest differences compared to the surge and heave forces. According to DnV, the differences ranged from -7.8% to 7.3% and for BV, the differences ranged from -7.3% to 10.8%.

d. The rolling moment gave closer agreement than both the yawing and pitching moments. With DnV values, the differences ranged from -8.8% to 10.1% and for BV, the differences ranged from -7.4% to 14.8%.

e. The differences in the yawing moment ranged from 33.5% to 36.6% in the case of DnV and from 12.9% to 30.4% in the case of BV (see note below).

f The differences in the pitching moment ranged from 11.1% to 21.7% according to DnV and from 1.1% to 19.1% for BV.

Note:

It should be noted that, throughout this chapter, theoretically all the yawing moments when $\beta = \pi/4$ should be zero due to the symmetry of the structure. The values of the yawing moments which are negligible compared with the rolling and pitching moments, merely reflect the accuracy of the calculations by the different methods. This applies also to the corresponding data in Chapters 5 and 6.

7. CONCLUSIONS

a. The drag coefficient C_D and the inertia coefficient C_M have large influences on wave loading calculations. Even small differences in the coefficients, as given by the different classification rules, lead to significant effects. Great care should be taken when selecting these coefficients.

b. The forces on the individual members could be underestimated when applying Morison's equation by the method of program MRSEQ. Taking the instantaneous time and the relative position of the members into consideration could lead to larger forces and determine the actual forces more accurately.

c. Although the use of Morison's equation as described in programs MRSEQ and MRSEQ2 generally tends to overestimate the maximum total forces and moments, there are some exceptions. For example, the heave force shows a reverse behaviour. This point should be taken into account, especially in the case of semi-submersible platforms, where the motion response is quite important.

d. The design approach which assumes that the maximum forces and moments on the structure occur simultaneously would be generally unrealistic and would result in overweight structures. Figs. (20) to (31) show the phase differences among the forces and moments. Even for the individual members, Table (4) shows that a maximum of 37% of the members examined had their maximum values occurring at the same time.

REFERENCES

1. BUREAU VERITAS, 'Rules and Regulations for the Construction and Classification of Offshore Platforms', 1975.

2. DET NORSKE VERITAS, 'Rules for the Design, Construction and Inspection of Mobile Offshore Units', 1974.

3. DET NORSKE VERITAS, 'Rules for the Construction and Classification of Mobile Offshore Units', 1975.

4. DET NORSKE VERITAS, 'Rules for the Design, Construction and Inspection of Offshore Structures', Appendix B, 1977.

5. LLOYD'S REGISTER OF SHIPPING, 'Rules for the Construction and Classification of Mobile Offshore Units', 1972.

6. MORISON, J R, et al, 'The Force Exerted by Surface Waves on Piles', Petroleum Trans, AIME, Vol 189, 1950, pp149-157.

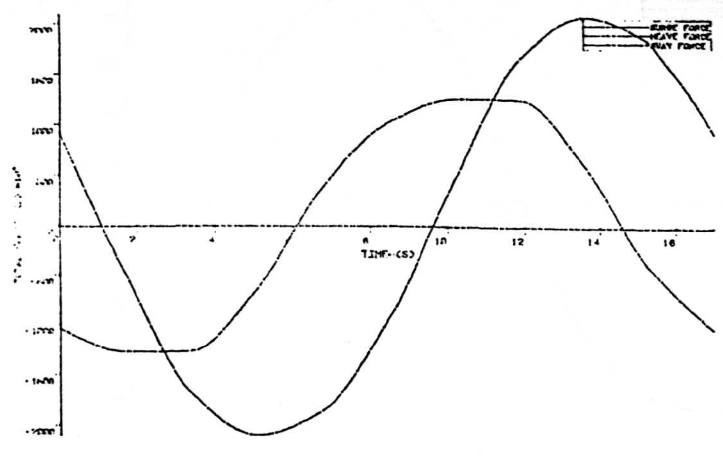

COEFFICIENTS FROM: LR , ω = 0.37, β = 0.0
FIG.(20) TOTAL FORCES Vs. TIME FOR OSS

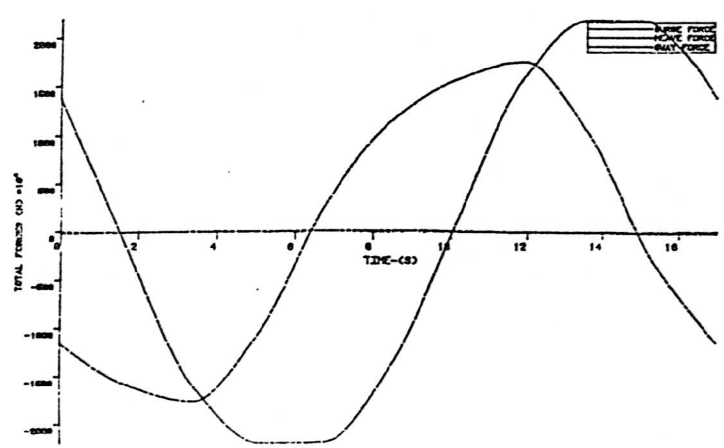

COEFFICIENTS FROM: DnV , ω = 0.37, β = 0.0
FIG.(21) TOTAL FORCES Vs. TIME FOR OSS

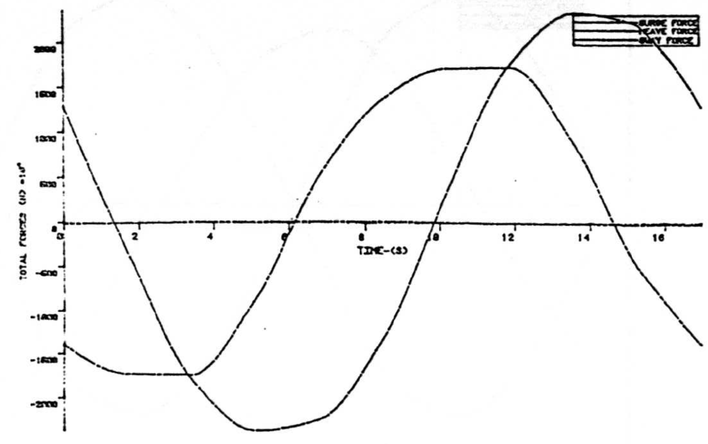

COEFFICIENTS FROM: BV , ω = 0.37, β = 0.0
FIG.(22) TOTAL FORCES Vs. TIME FOR OSS

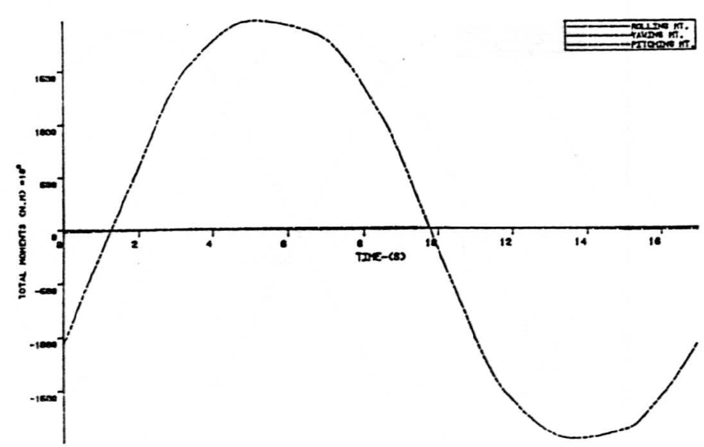

COEFFICIENTS FROM: LR , ω = 0.37, β = 0.0
FIG.(23) TOTAL MOMENTS Vs. TIME FOR OSS

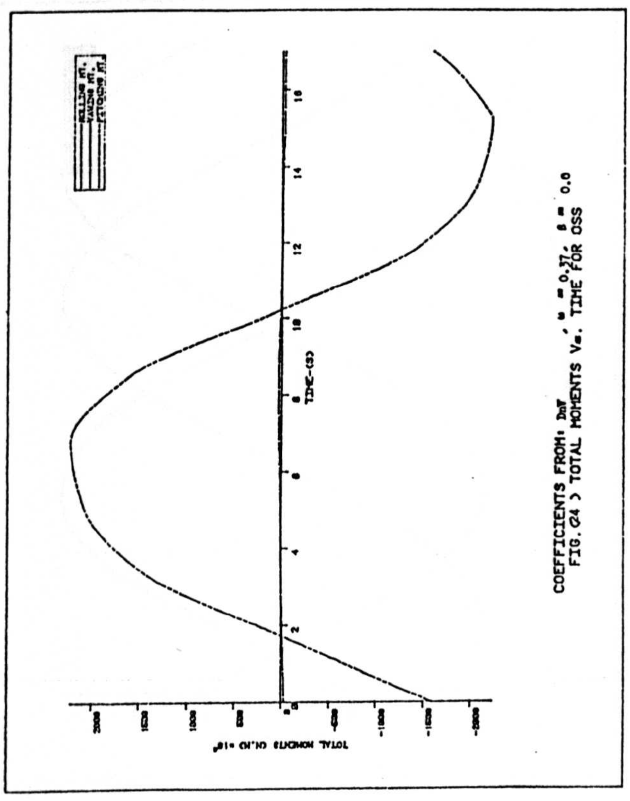

COEFFICIENTS FROM: DnV , ω = 0.37, β = 0.0
FIG.(24) TOTAL MOMENTS Vs. TIME FOR OSS

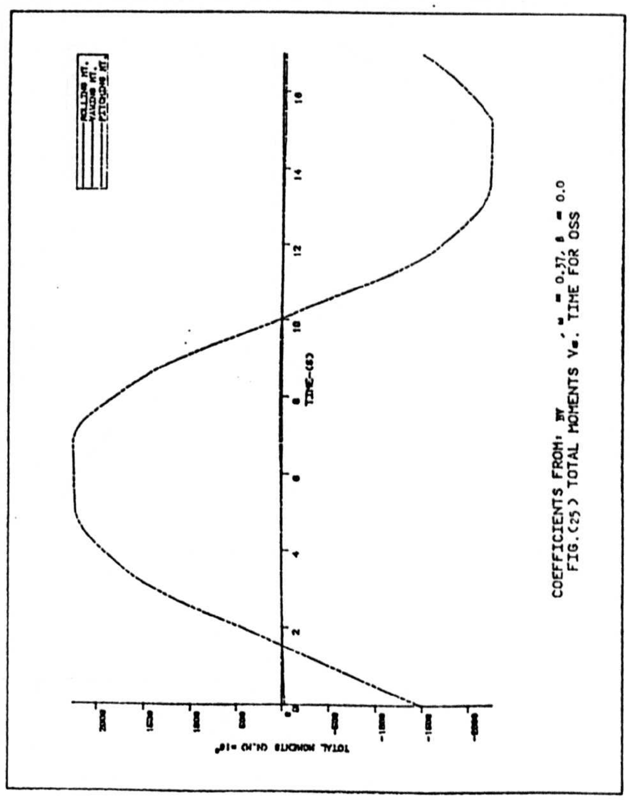

COEFFICIENTS FROM: BV , ω = 0.37, β = 0.0
FIG.(25) TOTAL MOMENTS Vs. TIME FOR OSS

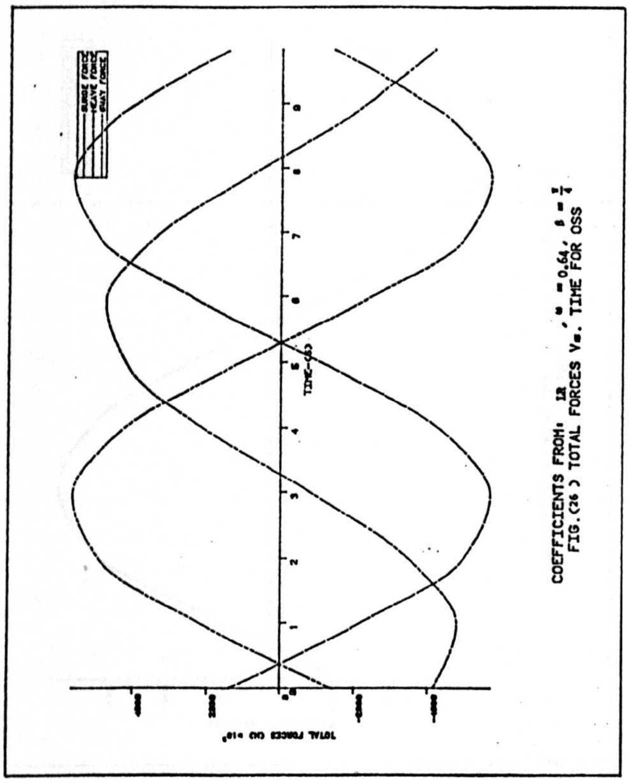

COEFFICIENTS FROM: IR , ω = 0.64, β = π/4
FIG.(26) TOTAL FORCES Vs. TIME FOR OSS

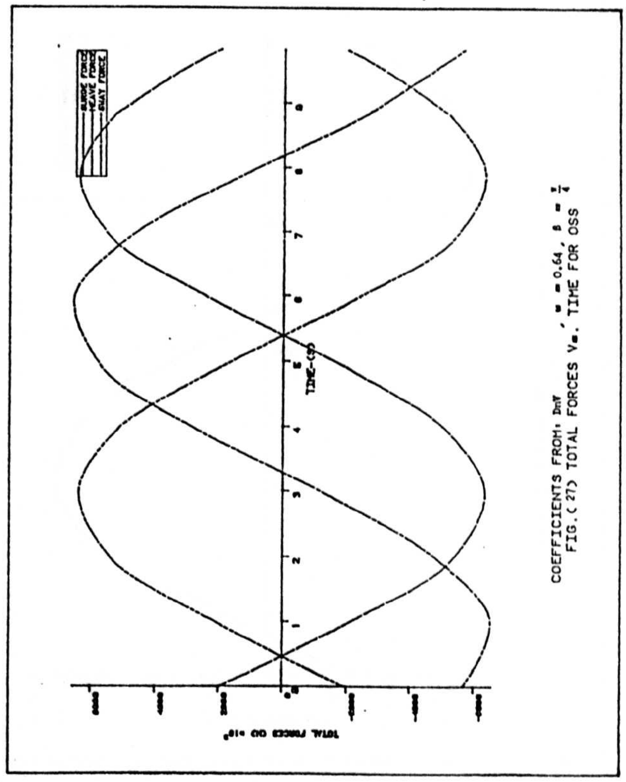

COEFFICIENTS FROM: DnV , ω = 0.64, β = π/4
FIG.(27) TOTAL FORCES Vs. TIME FOR OSS

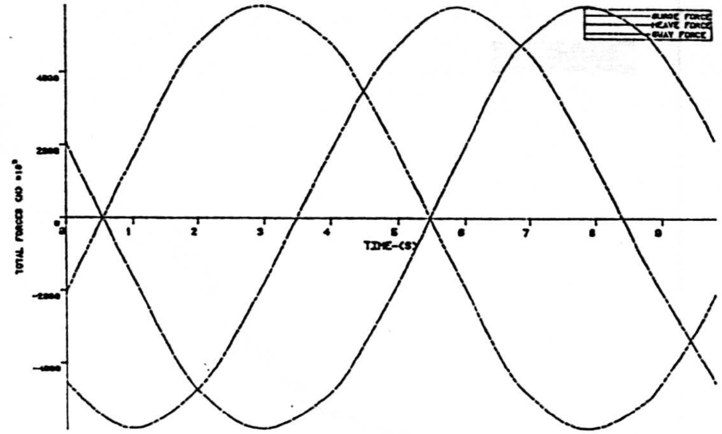

COEFFICIENTS FROM: BV , ω = 0.64 $\beta = \frac{\pi}{4}$
FIG.(28) TOTAL FORCES Vs. TIME FOR OSS

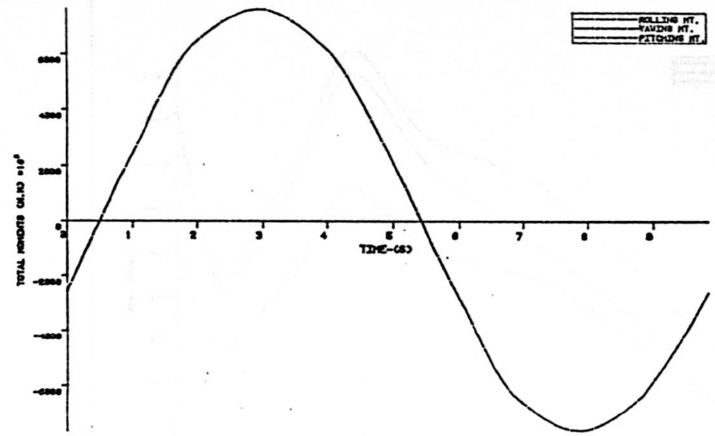

COEFFICIENTS FROM: DnV , ω = 0.64 $\beta = \frac{\pi}{4}$
FIG.(30) TOTAL MOMENTS Vs. TIME FOR OSS

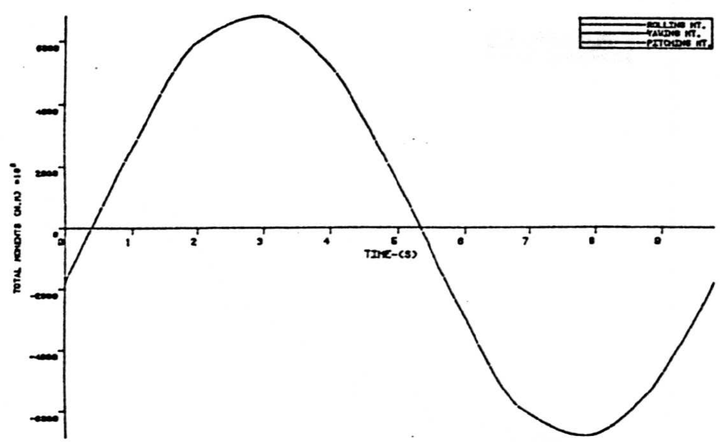

COEFFICIENTS FROM: LR , ω = 0.64 $\beta = \frac{\pi}{4}$
FIG.(29) TOTAL MOMENTS Vs. TIME FOR OSS

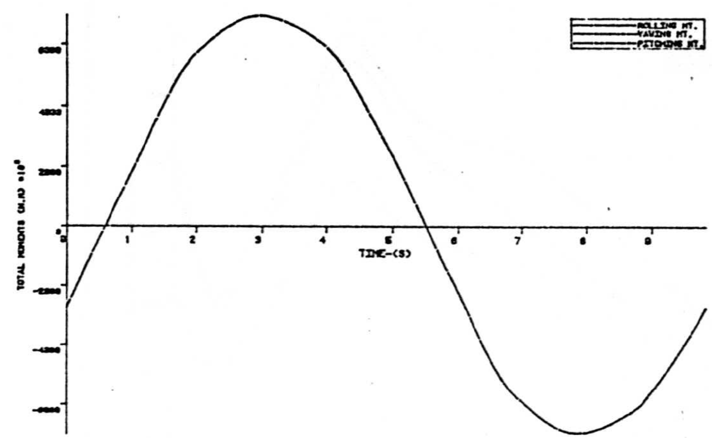

COEFFICIENTS FROM: BV , ω = 0.64, $\beta = \frac{\pi}{4}$
FIG.(31) TOTAL MOMENTS Vs. TIME FOR OSS

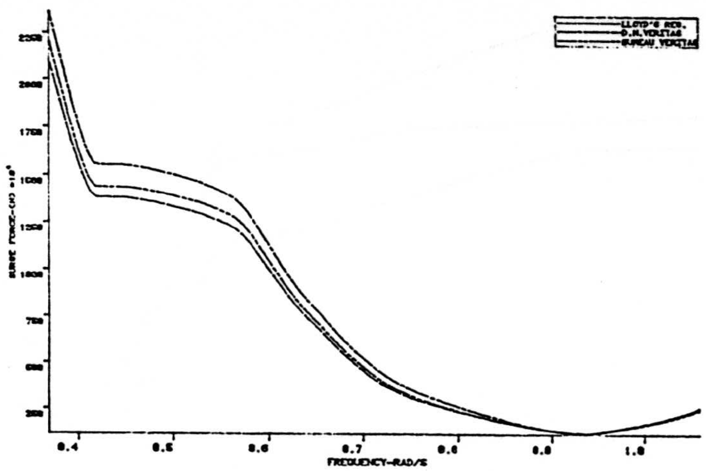

PROGRAM: OSS , β = 0.0
FIG.(32) MAX: SURGE FORCES Vs. FREQUENCY FOR L.R,Dn.V&B.V

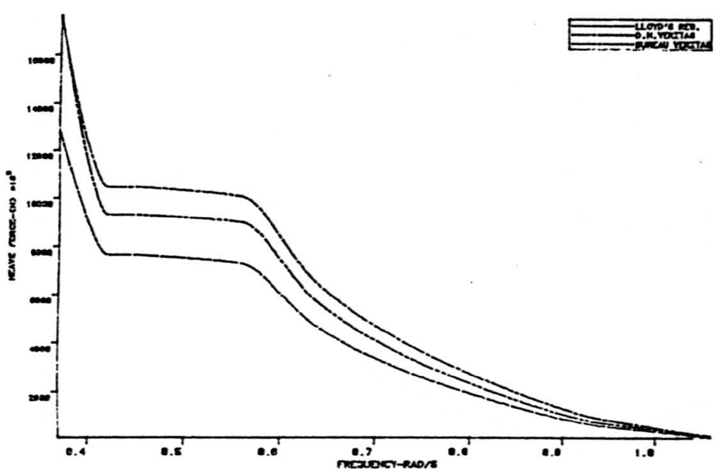

PROGRAM: OSS , β = 0.0
FIG.(33) MAX. HEAVE FORCES Vs. FREQUENCY FOR L.R,Dn.V&B.V

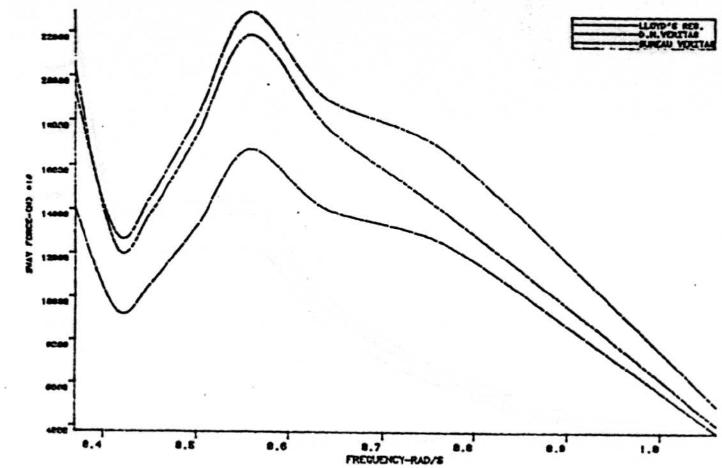

PROGRAM: OSS , β = 0.0
FIG.(34) MAX. SWAY FORCES Vs. FREQUENCY FOR L.R,Dn.V&B.V

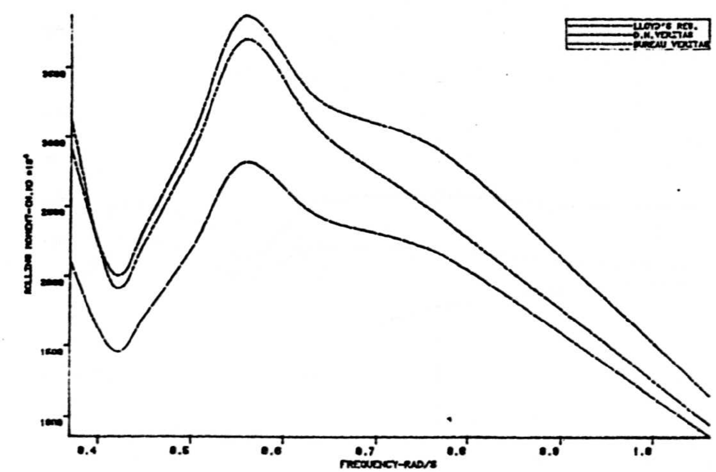

PROGRAM: OSS , β = 0.0
FIG.(35) MAX. ROLLING MOMENTS Vs. FREQUENCY FOR L.R,Dn.V&B.V

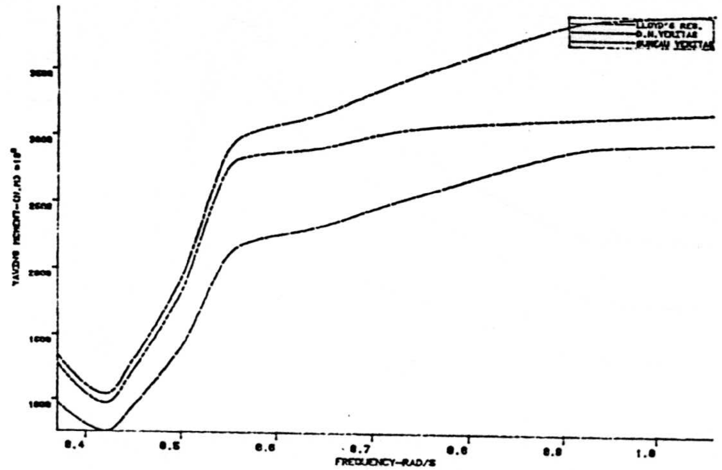

PROGRAM: OSS , β = 0.0
FIG.(36) MAX. YAWING MOMENTS Vs. FREQUENCY FOR L.R,Dn.V&B.V

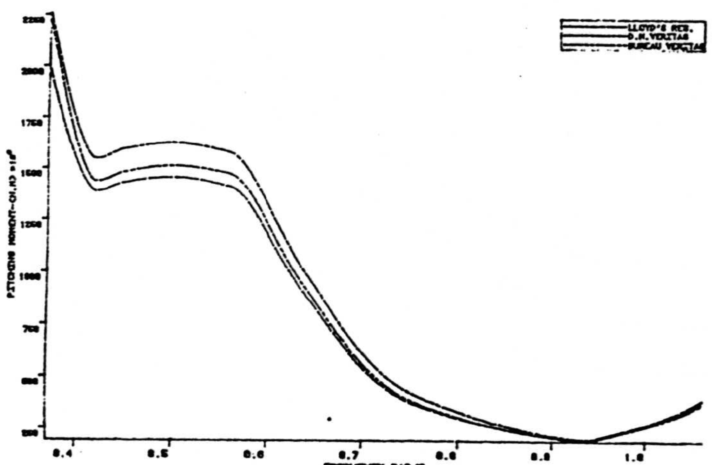

PROGRAM: OSS , β = 0.0
FIG.(37) MAX. PITCHING MOMENTS Vs. FREQUENCY FOR L.R,Dn.V&B.V

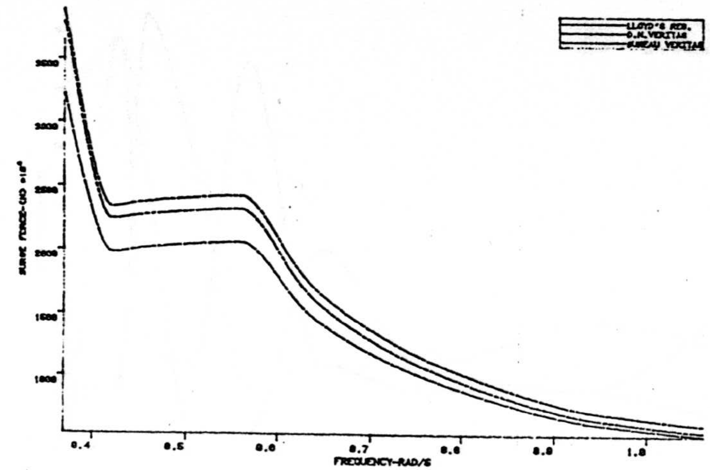

PROGRAM: MRSEQ , β = 0.0
FIG.(38) MAX. SURGE FORCES Vs. FREQUENCY FOR L.R,Dn.V&B.V

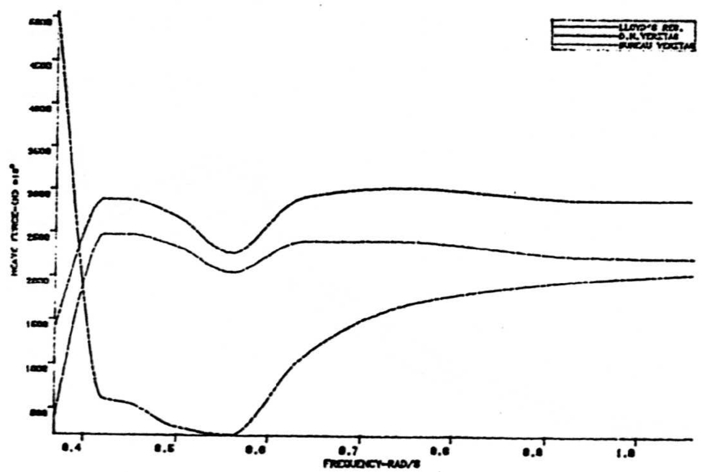

PROGRAM: MRSEQ , β = 0.0
FIG.(39) MAX. HEAVE FORCES Vs. FREQUENCY FOR L.R,Dn.V&B.V

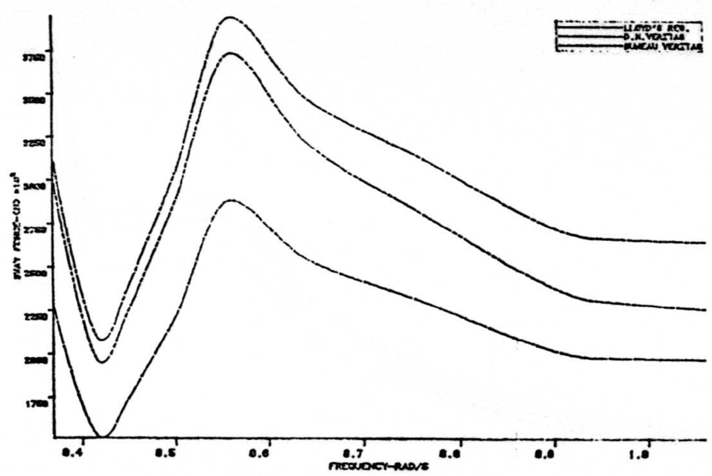

PROGRAM: MRSEQ , β = 0.0
FIG.(40) MAX. SWAY FORCES Vs. FREQUENCY FOR L.R,Dn.V&B.V

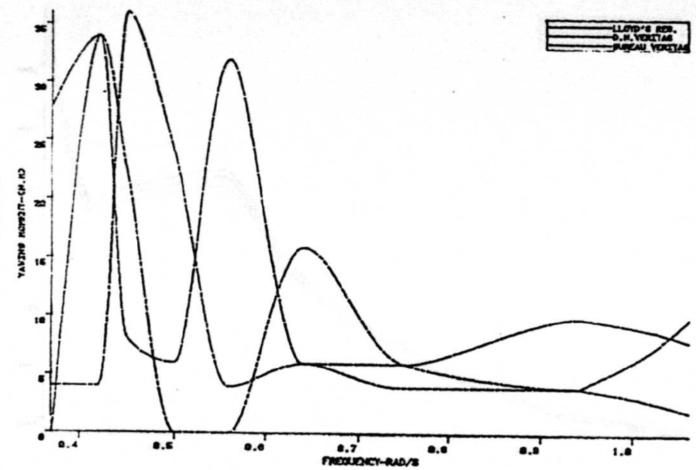

PROGRAM: MRSEQ , β = 0.0
FIG.(42) MAX. YAWING MOMENTS Vs. FREQUENCY FOR L.R,Dn.V&B.V

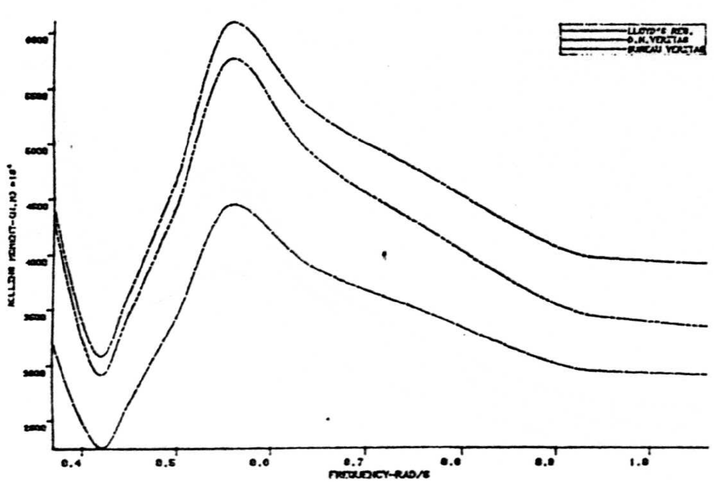

PROGRAM: MRSEQ , β = 0.0
FIG.(41) MAX. ROLLING MOMENTS Vs. FREQUENCY FOR L.R,Dn.V&B.V

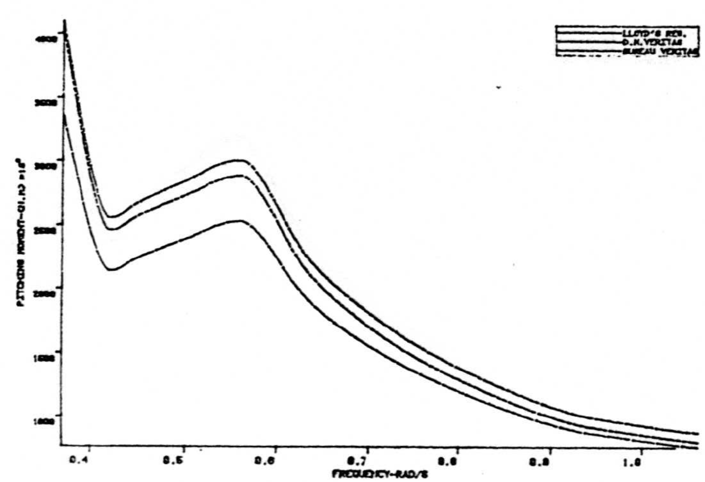

PROGRAM: MRSEQ , β = 0.0
FIG.(43) MAX. PITCHING MOMENTS Vs. FREQUENCY FOR L.R,Dn.V&B.V

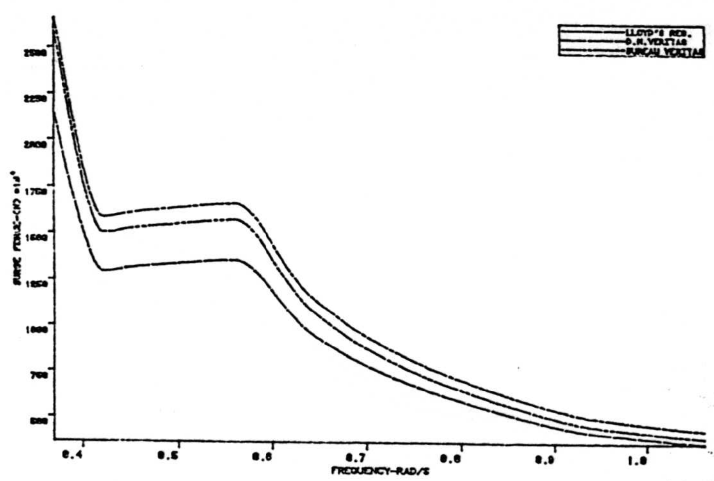

PROGRAM: MRSEQ2 ,β = 0.0
FIG.(44) MAX. SURGE FORCES Vs. FREQUENCY FOR L.R,Dn.V&B.V

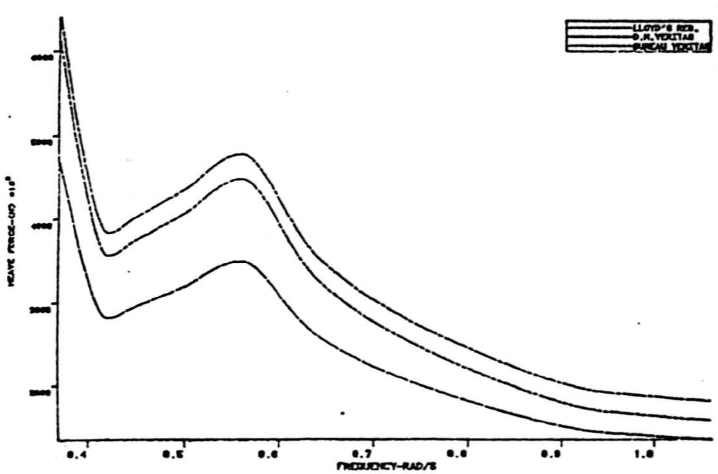

PROGRAM: MRSEQ2 ,β = 0.0
FIG.(45) MAX. HEAVE FORCES Vs. FREQUENCY FOR L.R,Dn.V&B.V

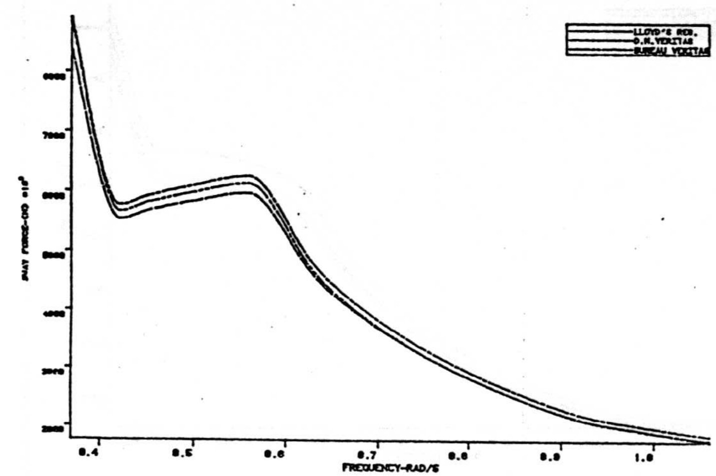

PROGRAM: MRSEQ2 ,β = 0.0
FIG.(46) MAX. SWAY FORCES Vs. FREQUENCY FOR L.R,Dn.V&B.V

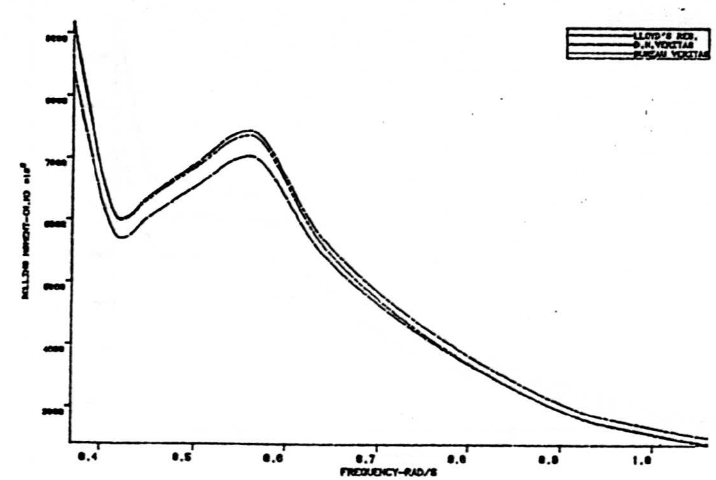

PROGRAM: MRSEQ2 ,β = 0.0
FIG.(47) MAX. ROLLING MOMENTS Vs. FREQUENCY FOR L.R,Dn.V&B.V

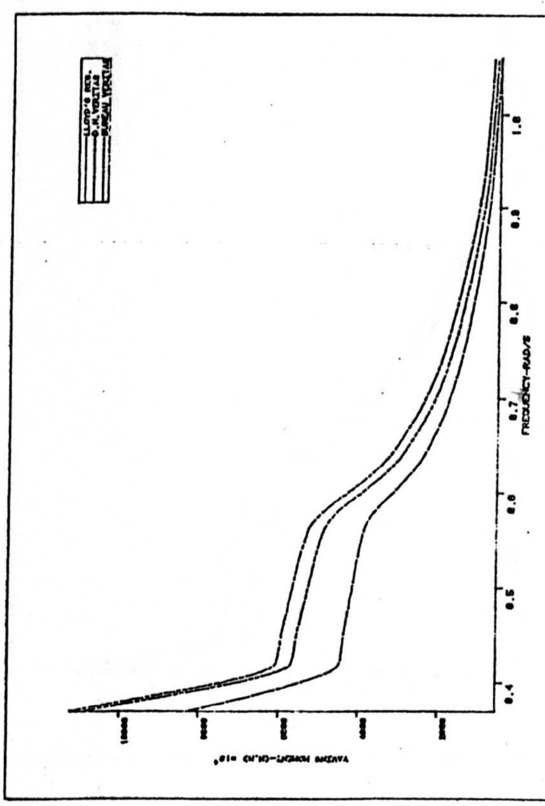

PROGRAM: MSSD2
FIG.(48) MAX. YAWING MOMENTS Vs. FREQUENCY FOR L.R,Dn.V&B.V , β = 0.0

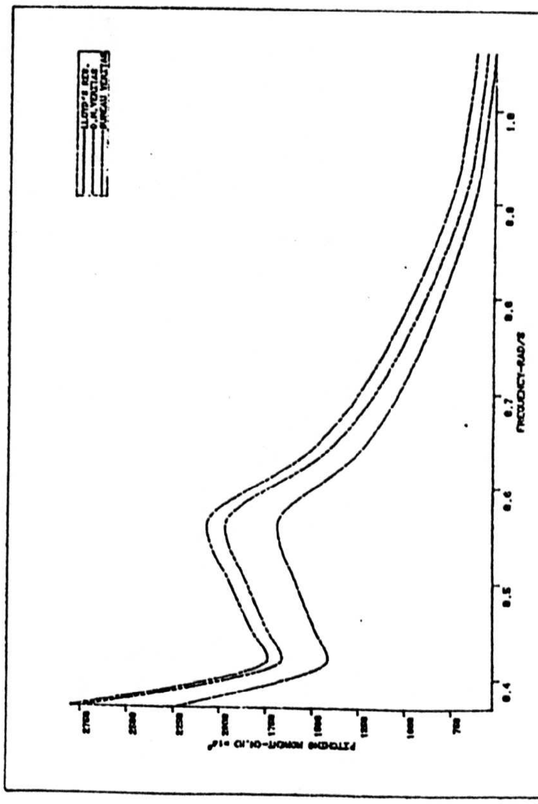

PROGRAM: MSSD2
FIG.(49) MAX. PITCHING MOMENTS Vs. FREQUENCY FOR L.R,Dn.V&B.V , β = 0.0

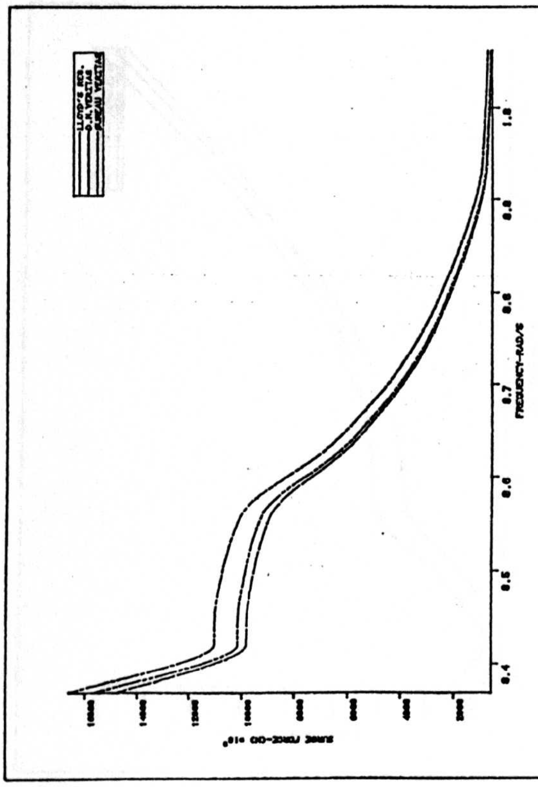

PROGRAM: OSS
FIG.(50) MAX. SURGE FORCES Vs. FREQUENCY FOR L.R,Dn.V&B.V , $\beta = \frac{\pi}{4}$

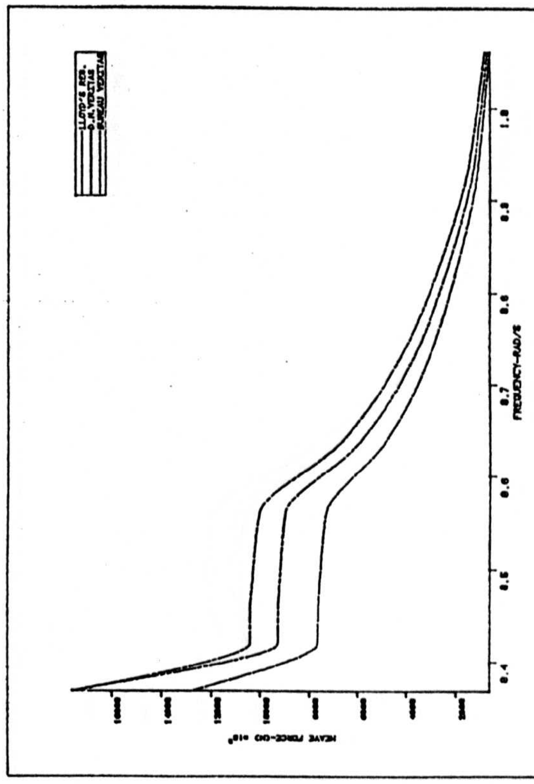

PROGRAM: OSS
FIG.(51) MAX. HEAVE FORCES Vs. FREQUENCY FOR L.R,Dn.V&B.V , $\beta = \frac{\pi}{4}$

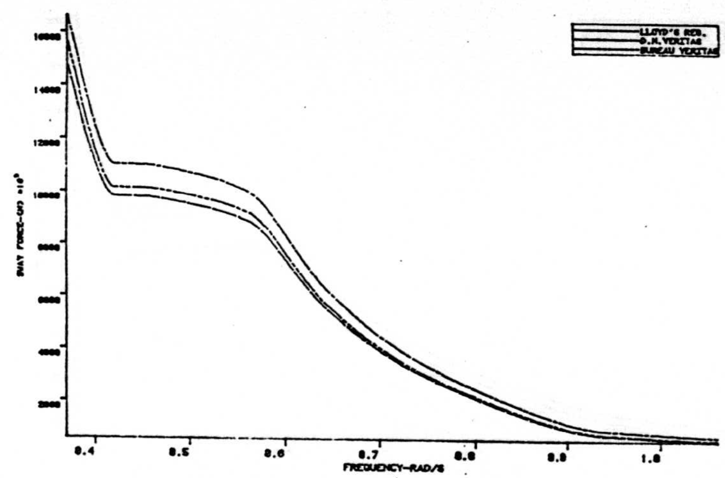

PROGRAM: OSS $\beta = \frac{\pi}{4}$
FIG.(52) MAX. SWAY FORCES Vs. FREQUENCY FOR L.R,Dn.V&B.V

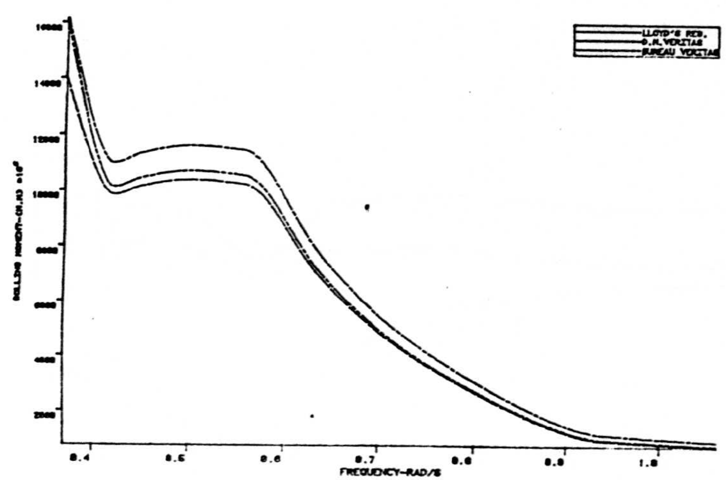

PROGRAM: OSS $\beta = \frac{\pi}{4}$
FIG.(53) MAX. ROLLING MOMENTS Vs. FREQUENCY FOR L.R,Dn.V&B.V

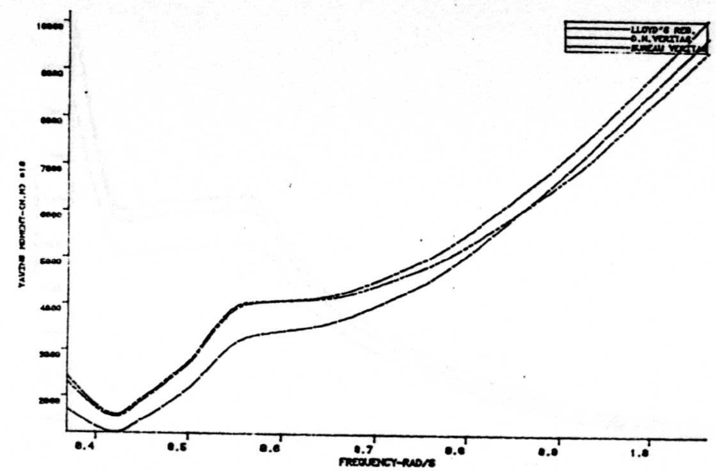

PROGRAM: OSS $\beta = \frac{\pi}{4}$
FIG.(54) MAX. YAWING MOMENTS Vs. FREQUENCY FOR L.R,Dn.V&B.V

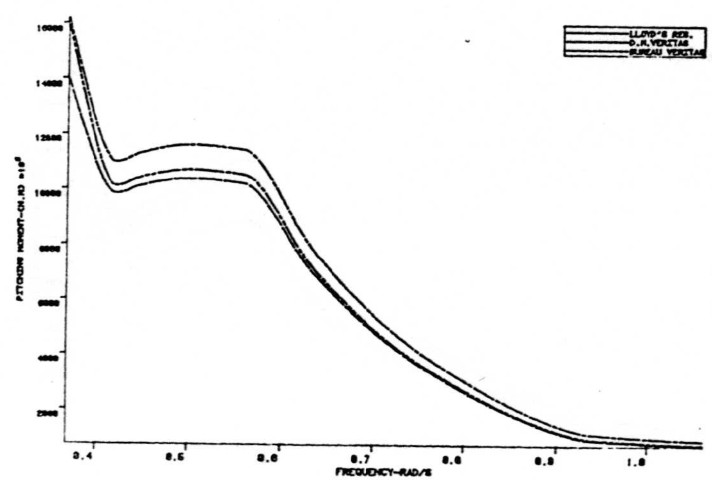

PROGRAM: OSS $\beta = \frac{\pi}{4}$
FIG.(55) MAX. PITCHING MOMENTS Vs. FREQUENCY FOR L.R,Dn.V&B.V

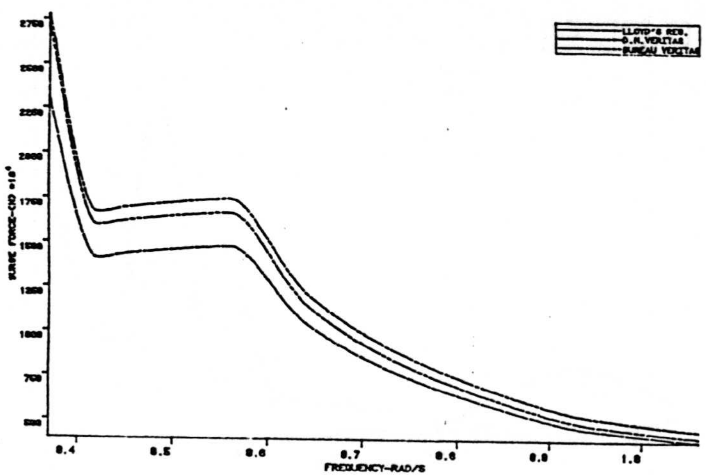

PROGRAM: MRSEQ $, \beta = \frac{\pi}{4}$

FIG.(56) MAX. SURGE FORCES Vs. FREQUENCY FOR L.R,Dn.V&B.V

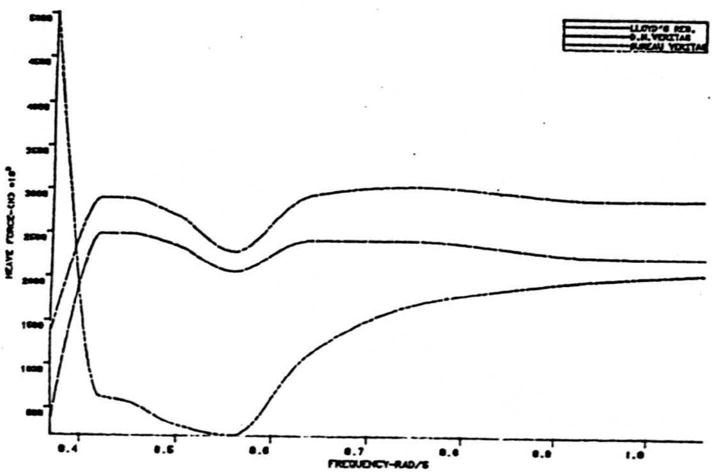

PROGRAM: MRSEQ $, \beta = \frac{\pi}{4}$

FIG.(57) MAX. HEAVE FORCES Vs. FREQUENCY FOR L.R,Dn.V&B.V

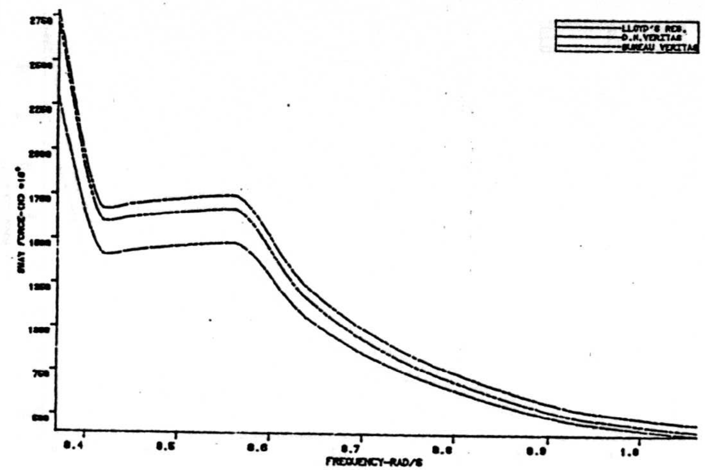

PROGRAM: MRSEQ $, \beta = \frac{\pi}{4}$

FIG.(58) MAX. SWAY FORCES Vs. FREQUENCY FOR L.R,Dn.V&B.V

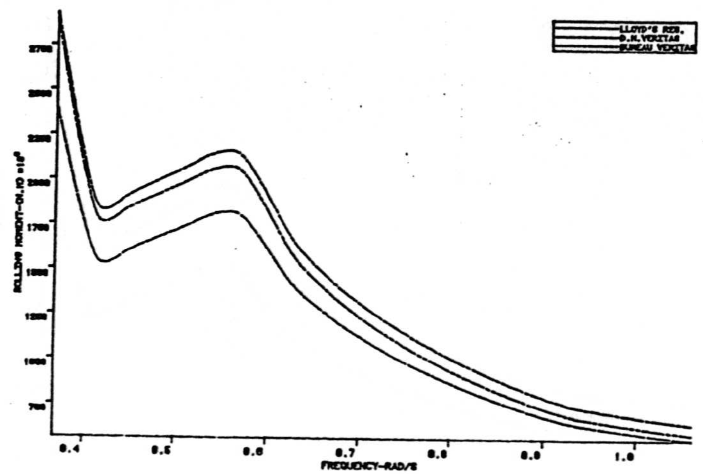

PROGRAM: MRSEQ $, \beta = \frac{\pi}{4}$

FIG.(59) MAX. ROLLING MOMENTS Vs. FREQUENCY FOR L.R,Dn.V&B.V

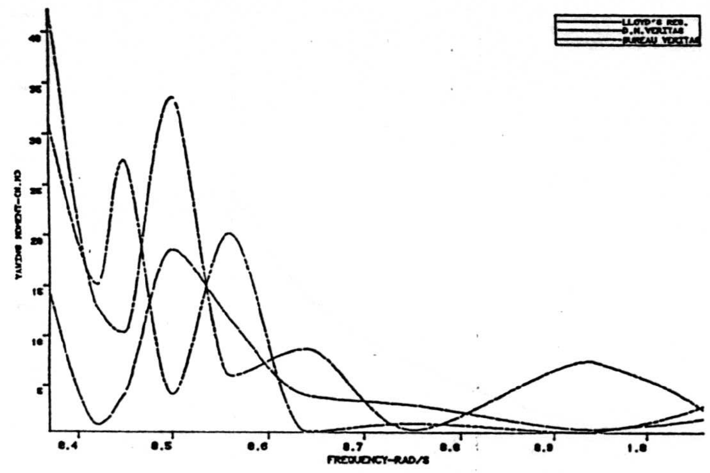

PROGRAM: MRSEQ , $\beta = \frac{\pi}{4}$
FIG.(60) MAX. YAWING MOMENTS Vs. FREQUENCY FOR L.R,Dn.V&B.V

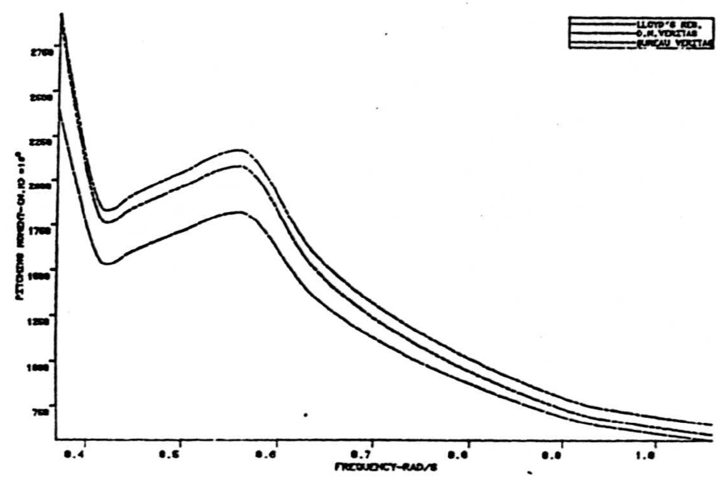

PROGRAM: MRSEQ , $\beta = \frac{\pi}{4}$
FIG.(61) MAX. PITCHING MOMENTS Vs. FREQUENCY FOR L.R,Dn.V&B.V

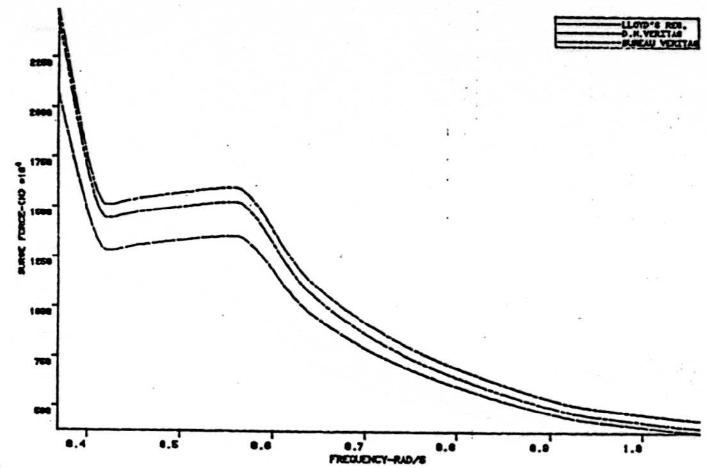

PROGRAM: MRSEQ2 , $\beta = \frac{\pi}{4}$
FIG.(62) MAX. SURGE FORCES Vs. FREQUENCY FOR L.R,Dn.V&B.V

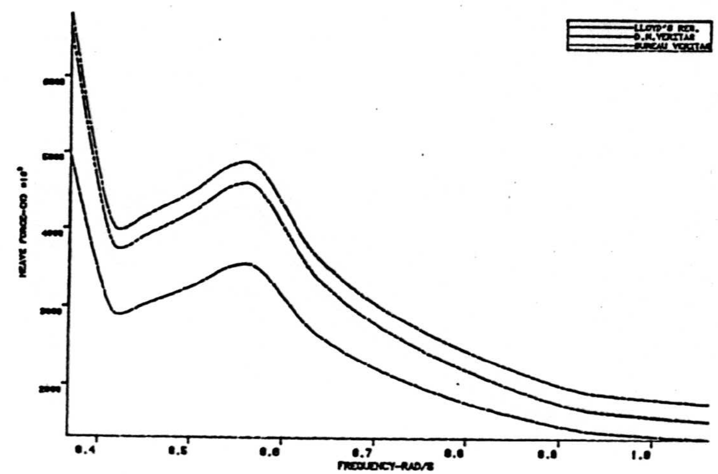

PROGRAM: MRSEQ , $\beta = \frac{\pi}{4}$
FIG.(63) MAX. HEAVE FORCES Vs. FREQUENCY FOR L.R,Dn.V&B.V

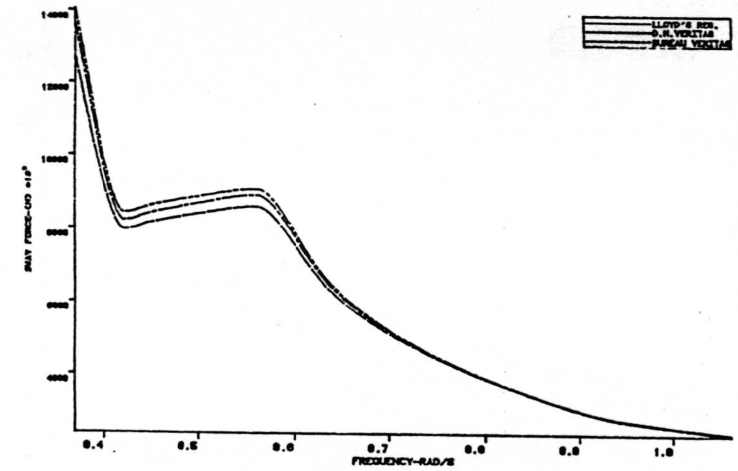

PROGRAM: MRSEQ2 , $\beta = \frac{\pi}{4}$
FIG.(64) MAX. SWAY FORCES Vs. FREQUENCY FOR L.R,Dn.V&B.V

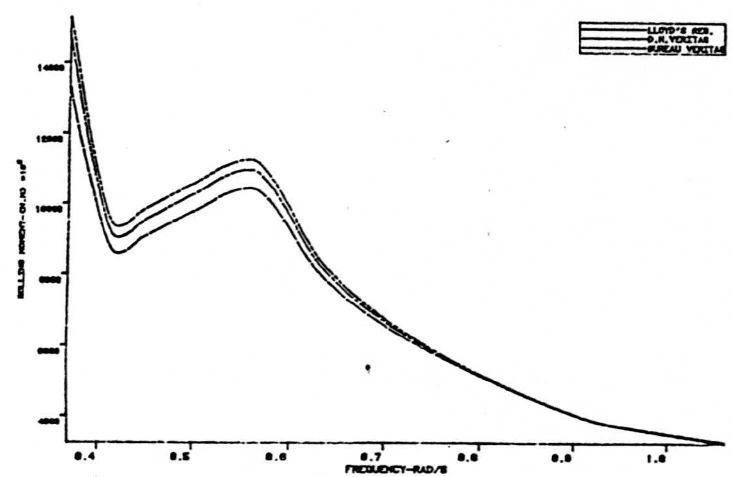

PROGRAM: MRSEQ2 , $\beta = \frac{\pi}{4}$
FIG.(65) MAX. ROLLING MOMENTS Vs. FREQUENCY FOR L.R,Dn.V&B.V

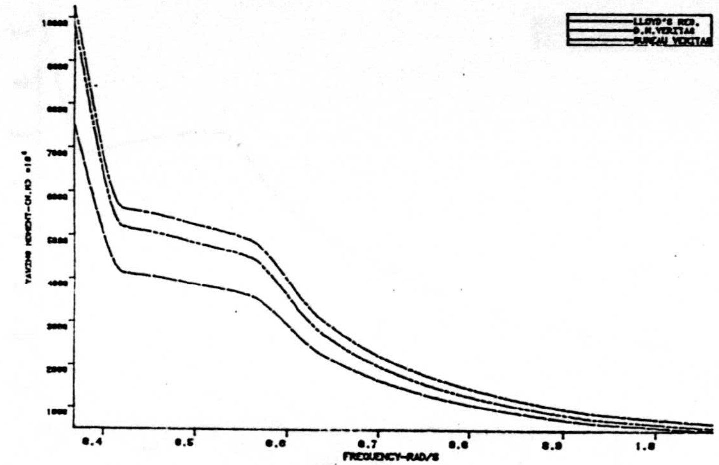

PROGRAM: MRSEQ2 , $\beta = \frac{\pi}{4}$
FIG.(66) MAX. YAWING MOMENTS Vs. FREQUENCY FOR L.R,Dn.V&B.V

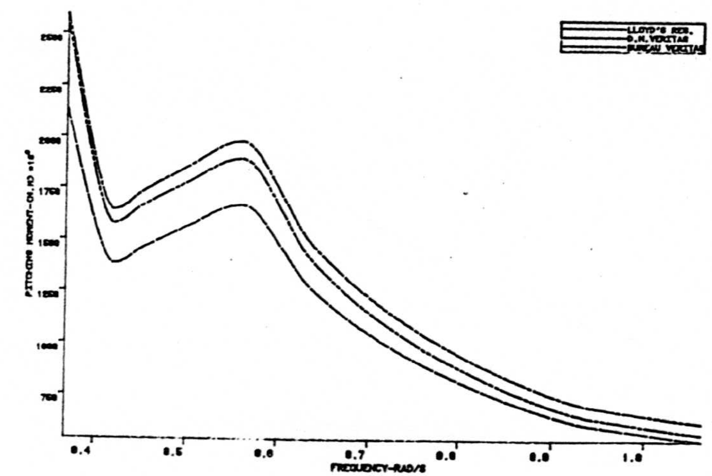

PROGRAM: MRSEQ2 , $\beta = \frac{\pi}{4}$
FIG.(67) MAX. PITCHING MOMENTS Vs. FREQUENCY FOR L.R,Dn.V&B.V

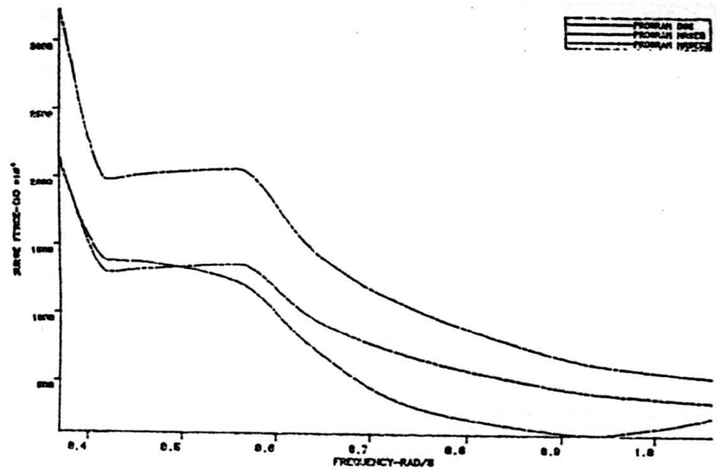

-COEFFICIENTS: LR ,β = 0.0
FIG.(68) MAX. SURGE FORCES Vs. FREQUENCY FOR THREE PROGRAMS

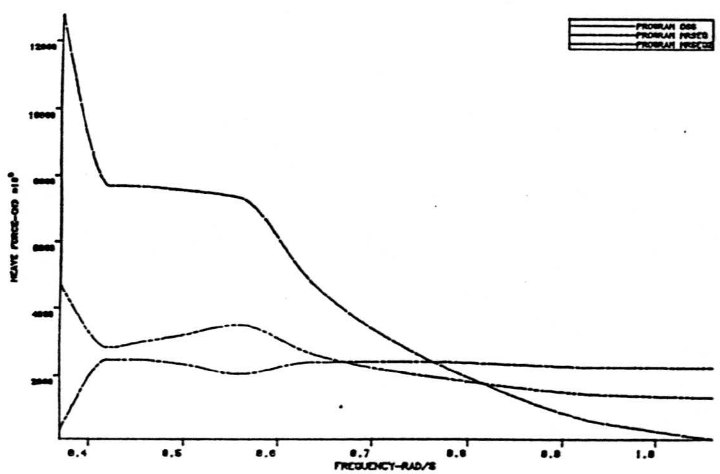

COEFFICIENTS: LR ,β = 0.0
FIG.(69) MAX. HEAVE FORCES Vs. FREQUENCY FOR THREE PROGRAMS

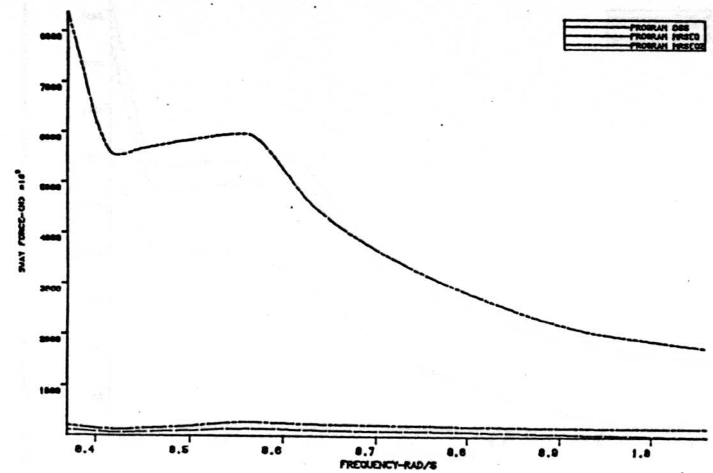

COEFFICIENTS: LR ,β = 0.0
FIG.(70) MAX. SWAY FORCES Vs. FREQUENCY FOR THREE PROGRAMS

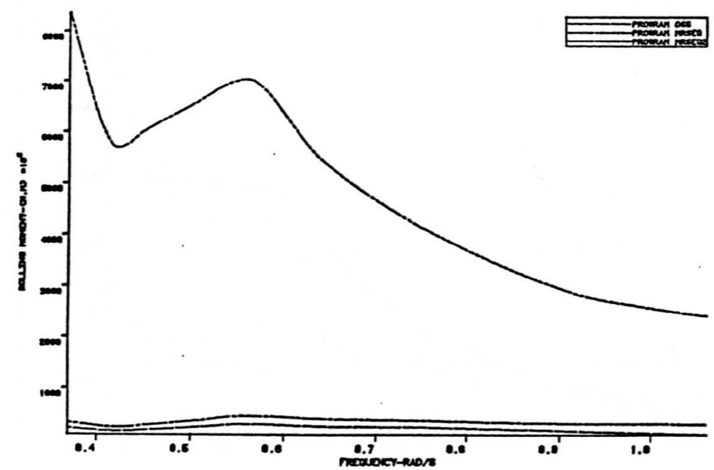

COEFFICIENTS: LR ,β = 0.0
FIG.(71) MAX. ROLLING MOMENTS Vs. FREQUENCY FOR THREE PROGRAMS

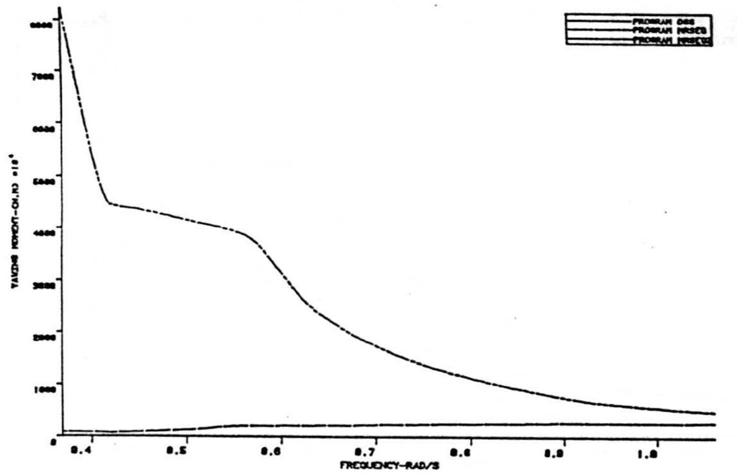

COEFFICIENTS: LR , $\beta = 0.0$
FIG.(72) MAX. YAWING MOMENTS Vs. FREQUENCY FOR THREE PROGRAMS

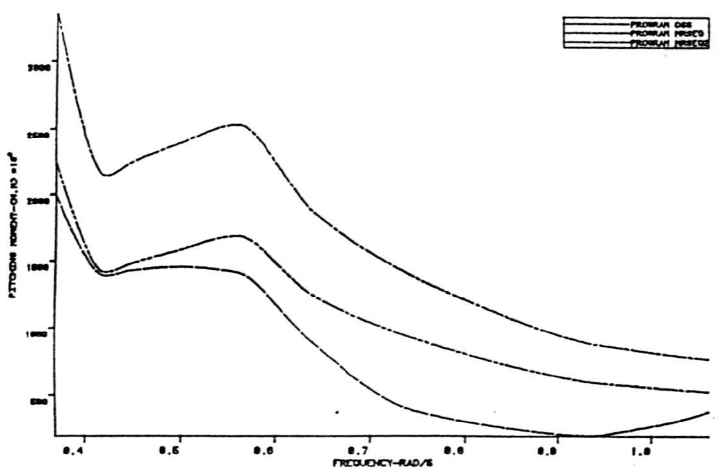

COEFFICIENTS: LR , $\beta = 0.0$
FIG.(73) MAX. PITCHING MOMENTS Vs. FREQUENCY FOR THREE PROGRAMS

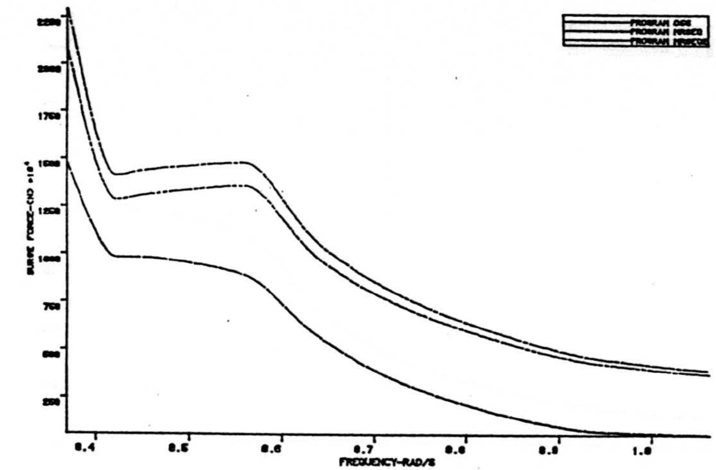

COEFFICIENTS: LR , $\beta = \frac{\pi}{4}$
FIG.(74) MAX. SURGE FORCES Vs. FREQUENCY FOR THREE PROGRAMS

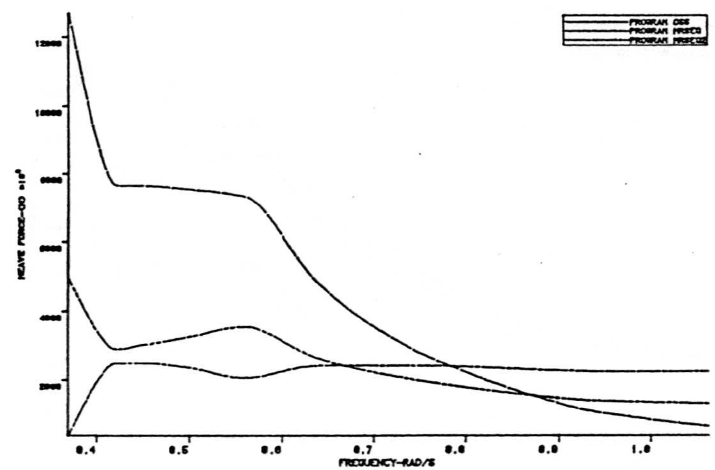

COEFFICIENTS: LR , $\beta = \frac{\pi}{4}$
FIG.(75) MAX. HEAVE FORCES Vs. FREQUENCY FOR THREE PROGRAMS

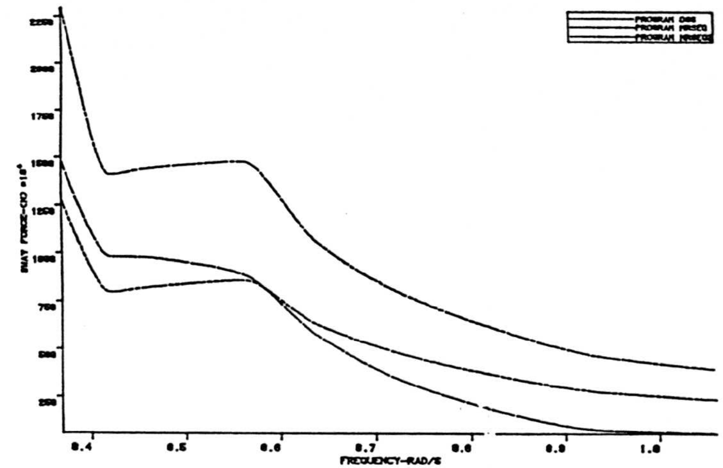

COEFFICIENTS: LR , $\beta = \frac{\pi}{4}$
FIG.(76) MAX. SWAY FORCES Vs. FREQUENCY FOR THREE PROGRAMS

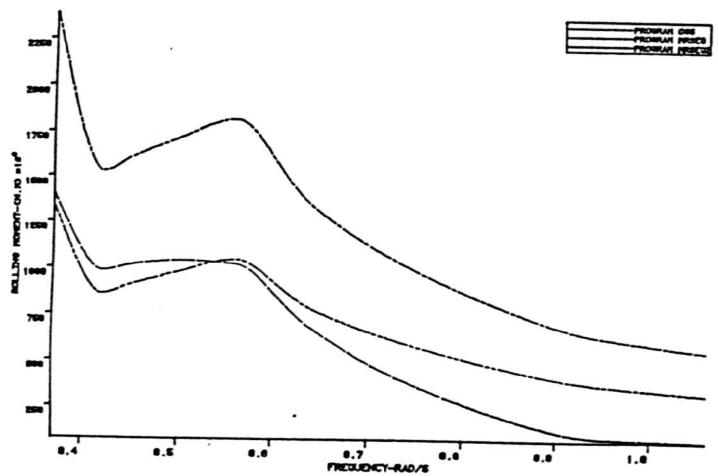

COEFFICIENTS: LR , $\beta = \frac{\pi}{4}$
FIG.(77) MAX. ROLLING MOMENTS Vs. FREQUENCY FOR THREE PROGRAMS

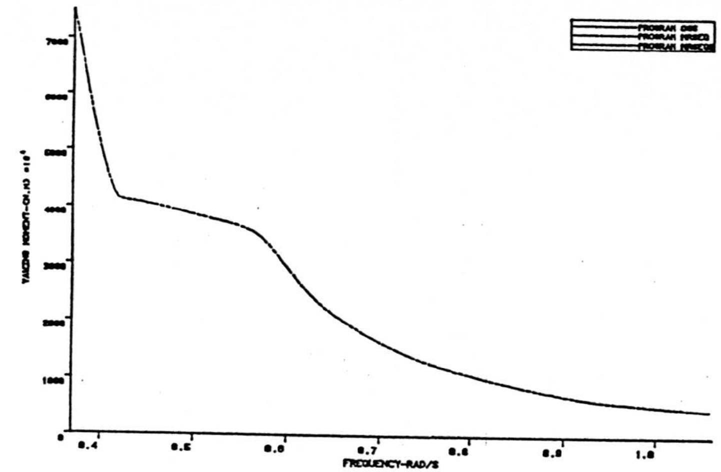

COEFFICIENTS: LR , $\beta = \frac{\pi}{4}$
FIG.(78) MAX. YAWING MOMENTS Vs. FREQUENCY FOR THREE PROGRAMS

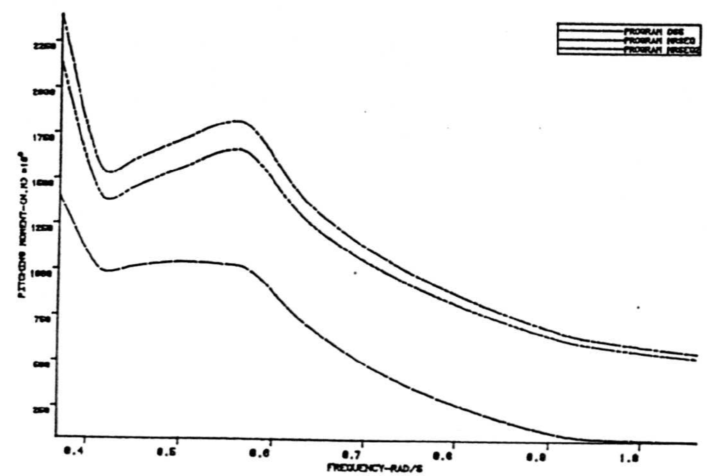

COEFFICIENTS: LR , $\beta = \frac{\pi}{4}$
FIG.(79) MAX. PITCHING MOMENTS Vs. FREQUENCY FOR THREE PROGRAMS

CHAPTER 5

CHAPTER 5

THE EFFECTS OF LIFT FORCES AND SURFACE ROUGHNESS ON WAVE LOADING

1. INTRODUCTION

Chapter 4 analysed the results of calculations performed on a typical platform to show the significant effects of the hydrodynamic coefficients C_D and C_M on the loading estimation. The drag and inertia coefficients used in the calculations were constant values as recommended by three classification societies (Lloyd's Register, Det Norske Veritas and Bureau Veritas) for smooth cylinders, i.e., the variations of the coefficients with Reynolds number (R_e), Keulegan-Carpenter number (K) and the surface roughness were not taken into account.

Marine roughness on offshore structures can be broadly classified into two types: (a) rigid, such as rust, scales, barnacles and mussels, (b) flexible, such as seaweeds and anemones. The type and amount of marine fouling varies with the location under consideration, water temperature, salinity, pressure, and depth below sea surface (amount of sunlight).

The effects of surface roughness on the hydrodynamic coefficients and wave forces for circular cylinders have been investigated and reported in a number of papers (see Chapter 2). Most of the published work was mainly related to either steady flow or to oscillatory (harmonic) flow about cylinders, with few tests carried out to study roughness effects in waves.

Heaf (1) found that marine fouling influences the loading of an offshore structure in at least five ways:-

a. Increased tube diameters, leading to increased projected area and displaced volume and, hence, to increased hydrodynamic loading.

b. Increased drag coefficient, leading to increased hydrodynamic loading.

c. Increased mass and hydrodynamic added mass, leading to reduced natural frequency and, hence, to an increased dynamic amplification factor.

d. Increased structural weight both in the water and above the water level in air.

e. Effect on hydrodynamic instabilities such as vortex shedding.

The purpose of this Chapter is to explore the effects of surface roughness on the wave loading calculations for jacket structures and the importance of taking the transverse (lift) forces into consideration when estimating the wave forces.

The experimental results of Sarpkaya (Refs. 3 - 10) are the most comprehensive data covering a wide range of R_e and K numbers and take into consideration the effect of surface roughness on the hydrodynamic coefficients.

In order to use Sarpkaya's results in the computer program (OSS), the data were curve fitted by the method of least squares and put into a subroutine (CDCMCL) which is connected to the main wave loading program. The method of curve fitting used and different subroutines associated with subroutine CDCMCL are described in sections 2 and 3 below.

2. CURVE FITTING PROCEDURE

The curve-fitting of the data was performed by a computer program using the least squares method where the curves are represented by polynomials. Each curve was treated separately, by dividing it into two or more parts according to its complexity of shape, while the curves of fair shape and without sharp curvatures were fitted by a single expression.

The data points were read by means of an electronic digitiser and as many points as possible were obtained to get better definition.

For each individual part, the curve fitting program was tried with polynomials of different orders and the suitable order which gave the best fit was selected. The linear parts of the curves were represented by equations of straight lines. This gave at the end, for each curve, a number of equations covering the whole range of the horizontal axis, which is Reynolds number R_e. The complete set of equations are given in Appendix (B).

To make sure that the equations represent the intended curves as accurately as possible, numerical calculations were carried out for each curve and the results were compared with those obtained directly from the original curve. The comparison showed that the curve fitting was generally accurate to within 3%.

3. DESCRIPTION OF SUBROUTINE CDCMCL

This subroutine is used to determine the hydrodynamic coefficients C_D, C_M and C_L at any point in the structure when the Reynolds number R_e, Keulegan-Carpenter number K and the surface roughness SR are known. To obtain C_D and C_M, subroutine CDCMCL calls another five subroutines F1, F2, F3, F4 and F5, each of which is concerned with a particular value of K and linear interpolation is used for intermediate values of K. Subroutines F1 to F5 in turn call a series of other subroutines depending on the value of SR. To obtain C_L subroutine CDCMCL calls another subroutine LIFT which, for smooth cylinders, calls another seven subroutines (TVS1 to TVS7) according to the value of K. For rough cylinders C_L is calculated as a function of K, see Fig. (1).

3.1 Subroutine F1

This subroutine calculates the C_D and C_M coefficients for K = 20 and interpolates for any value of the surface roughness SR between 0.0 (smooth cylinders) and 1/50. Subroutine F1 calls another six subroutines F11,F12,F13,F14,F15 and F16, each of which determines the coefficients at a particular value of surface roughness.

3.2 Subroutine F2

Subroutine F2 calculates C_D and C_M coefficients for K = 30 and interpolates for any value of the surface roughness SR between 0.0 and 1/50. It calls another six subroutines F21, F22, F23, F24, F25 and F26, each of which determines the coefficients at a particular value of surface roughness.

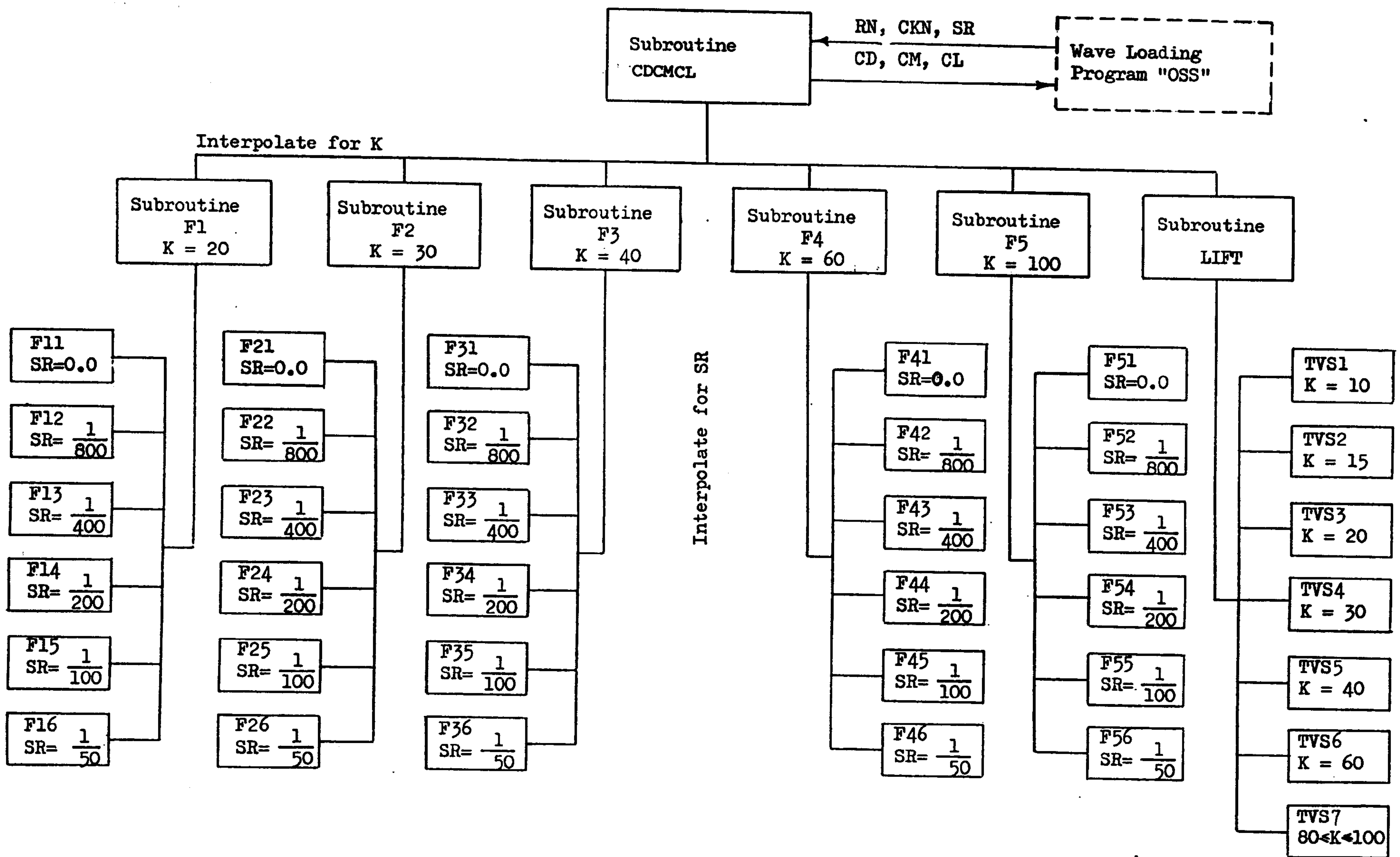

Fig. (1) Arrangement of Subroutine CDCMCL

3.3 Subroutine F3

Subroutine F3 calculates C_D and C_M coefficients for K = 40 and interpolates for any value of the surface roughness SR between 0.0 and 1/50. It calls another six subroutines F31, F32, F33, F34, F35 and F36, each of which determines the coefficients at a particular value of surface roughness.

3.4 Subroutine F4

Subroutine F4 calculates C_D and C_M coefficients for K = 60 and interpolates for any value of the surface roughness SR between 0.0 and 1/50. It calls another six subroutines F41, F42, F43, F44, F45 and F46, each of which determines the coefficients at a particular value of surface roughness.

3.5 Subroutine F5

Subroutine F5 calculates C_D and C_M coefficients for K = 100 and interpolates for any value of the surface roughness SR between 0.0 and 1/50. It calls another six subroutines F51, F52, F53, F54, F55, and F56, each of which determines the coefficients at a particular value of surface roughness.

3.6 Subroutine LIFT

This subroutine calculates the C_L coefficient for smooth and rough cylinders. In the case of rough cylinders, C_L is calculated as a function of K only. For smooth cylinders, subroutine LIFT calls another seven subroutines, TVS1 to TVS7 according to the value of K and linear interpolation is used.

4. WAVE LOADING ESTIMATION USING SARPKAYA'S RESULTS FOR C_D, C_M AND C_L

4.1 General Procedure

The results of calculations using Sarpkaya's coefficients (C_D, C_M and C_L) were compared with the calculations using the recommended C_D and C_M coefficients by Lloyd's Register of Shipping (LR). According to LR (2), for smooth cylinders, $C_D = 0.5$ and $C_M = 1.5$ if the diameter of the cylinder is less than 3.5m, otherwise, $C_M = 2.0$.

The calculations were carried out for the same jacket structure of 119 members used in Chapter 4.

The calculations were carried out for nine wave frequencies varying from 0.37 rad/s (L = 450.01m) to 1.06 rad/s (L = 54.83m), see Table (1), Chapter 4.

Since the structure is square in planform, two values for the incident angle of wave (β) were considered, namely 0° and 45°.

The wave heights were chosen near to the maximum for each wave length since the viscous forces depend on the square of the wave height and, therefore, are most significant at the maximum height.

When using Sarpkaya's results, the calculations were performed considering both smooth and rough cylinders. The values of the relative roughness (k/d) were assumed to be 1/800 (or 0.00125) and 1/200 (or 0.005).

4.2 Comparison between LR and Sarpkaya's Coefficients

In order to compare LR recommended coefficients with those obtained from Sarpkaya's results and to show the differences in the resulting wave forces on the individual members at the different frequencies, 21 representative members were chosen from the jacket structure, Fig. (2). The first 7 of these members are horizontal members at different levels below the water surface. The second set consists of 7 inclined bracing members and the third set consists of 7 members constituting one of the main columns of the structure.

For the 7 horizontal members, which represent the different levels of the structure under the surface, C_D, C_M and C_L were calculated from Sarpkaya's results for the smooth and rough cylinders at two values of the relative roughness (SR = 1/800 and SR = 1/200). LR recommended coefficients (C_D and C_M) for smooth cylinders were also calculated for the same members. The data were represented in the form of graphs and tables as follows:-

a. Figure (3) shows the variation of C_D, C_M and C_L for the 7 horizontal members, with wave frequency for the case of smooth cylinders.

b. Figures (4.1) to (4.3) show the variation of C_D, C_M and C_L with depth below water surface, R_e and K for the 7 horizontal members at three different frequencies for smooth cylinders.

c. Figures (5.1) to (5.3) show the variation of C_D, C_M and C_L

with R_e and K for three individual members for smooth cylinders.

d. Figures (6), (7) and (8) are similar to Figs. (3), (4) and (5) but for rough cylinders where SR = 1/800.

e. Figures (9), (10) and (11) are similar to Figs. (3), (4) and (5) but for rough cylinders where SR = 1/200.

f. Tables (1.1) to (1.3) compares C_D and C_M coefficients for LR and Sarpkaya for the 7 horizontal members at the different frequencies for smooth cylinders (SR = 0.0).

g. Tables (2.1) to (2.3) compare Sarpkaya's C_D and C_M for smooth (SR = 0.0) and rough cylinders (SR = 1/800 and SR = 1/200).

From the above mentioned graphs and tables, the following was noted:-

1. For the case of smooth bracing members (SR = 0.0), LR recommended C_D and C_M are 0.5 and 1.5, respectively, for the seven members. According to Sarpkaya, the values of C_D and C_M are approximately 0.7 and 1.75 up to ω = 0.64 rad/s. For the higher frequencies, the drag and inertia coefficients may have values up to 2.0 and 1.0, respectively. According to Sarpkaya, C_L for smooth cylinders is about 0.2, while LR does not recommend any value for the lift coefficient. Thus, for the lower frequencies one would expect a substantial increase in wave forces as both C_D and C_M are increased but at the higher frequencies the reduction in C_M makes the position uncertain.

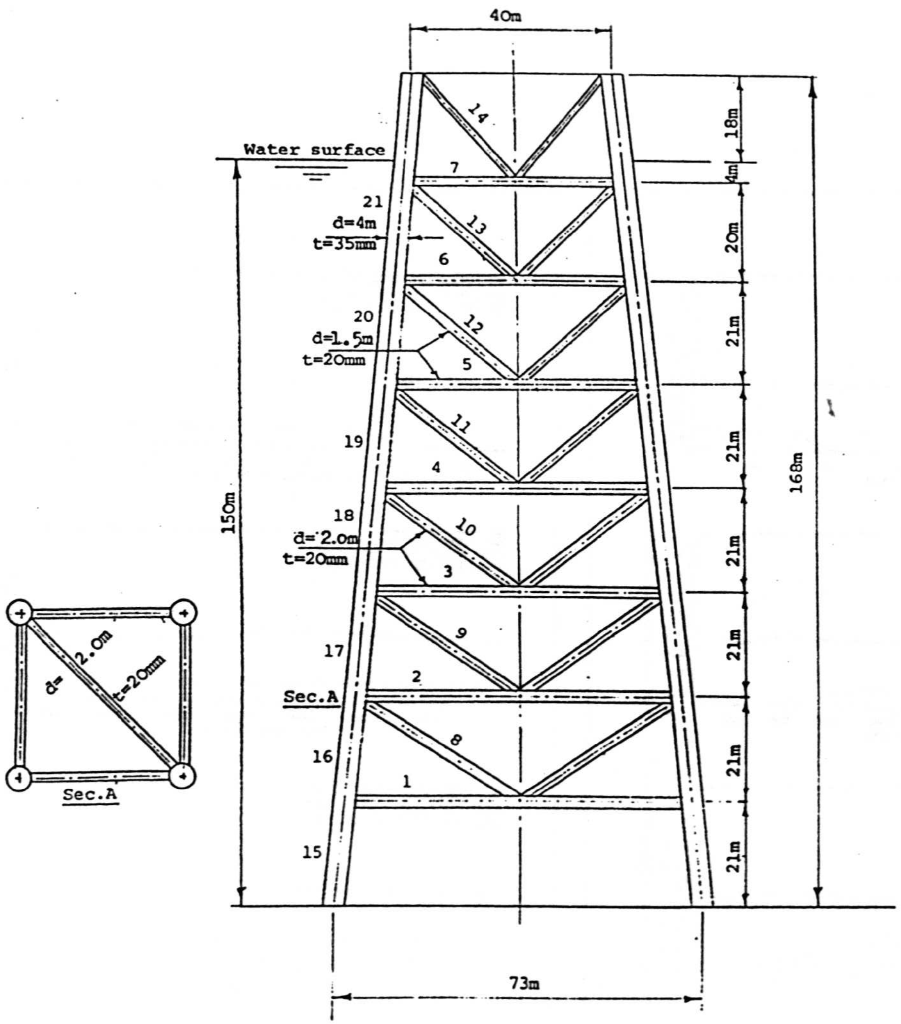

Fig. (2) Locations of the 21 Members of the Structure

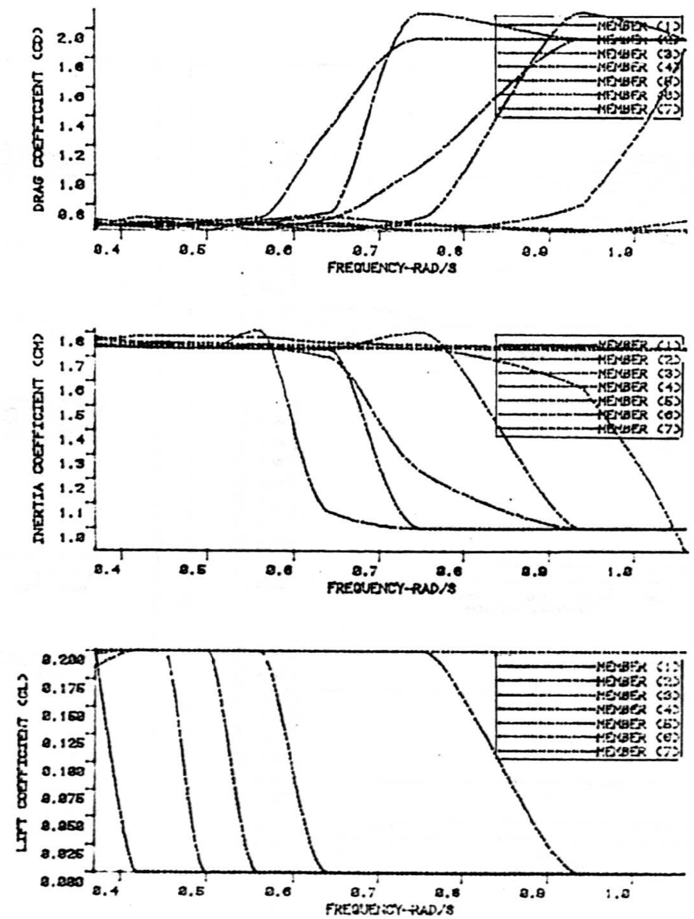

SR = 0.0

FIG.(3) HYDRODYNAMIC COEFFICIENTS Vs. FREQUENCY

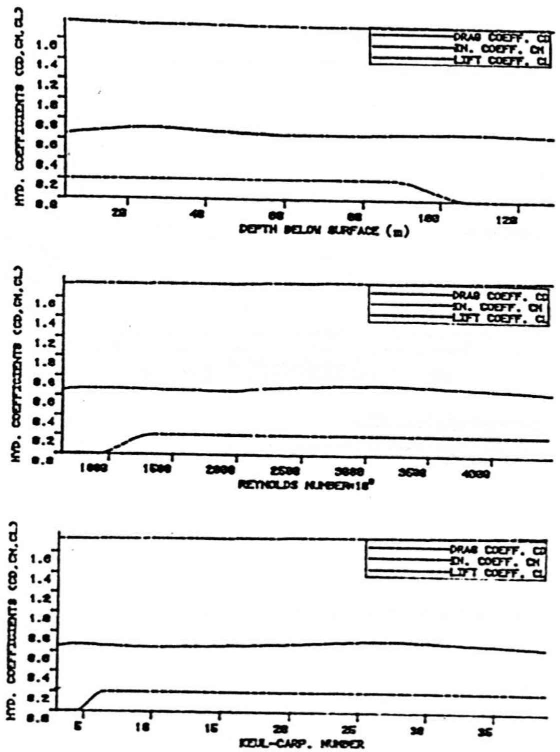

SR = 0.0

FIG. (4.1) DRAG, INERTIA AND LIFT COEFFICIENTS ω = 0.42 R/S

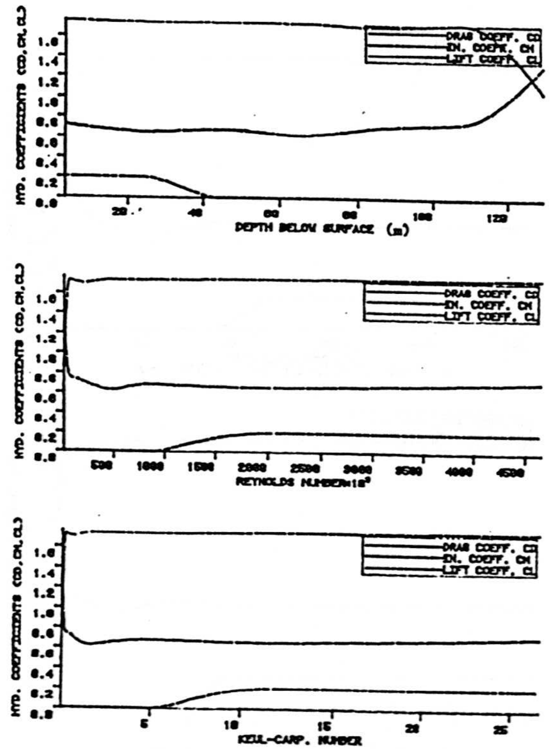

SR = 0.0

FIG. (4.2) DRAG, INERTIA AND LIFT COEFFICIENTS ω = 0.64 R/S

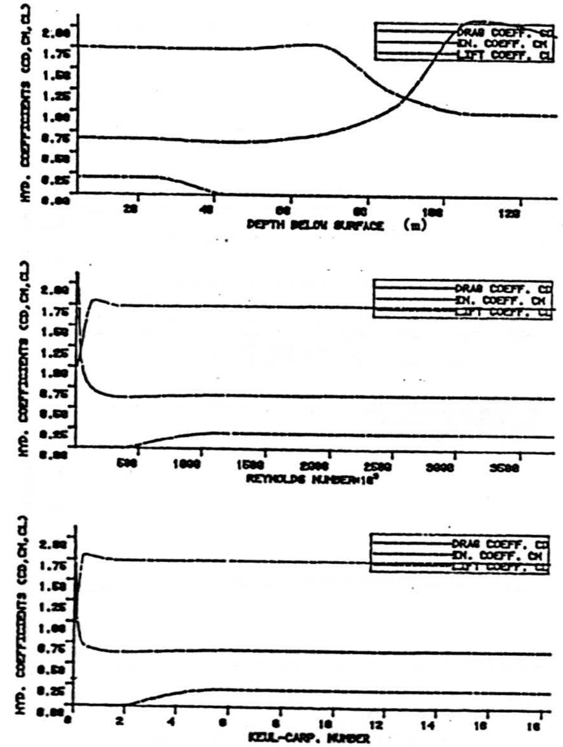

SR = 0.0

FIG. (4.3) DRAG, INERTIA AND LIFT COEFFICIENTS ω = 0.75 R/S

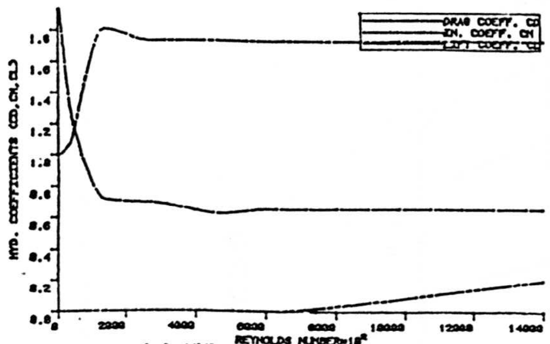

(a) HYD. COEFFICIENTS Vs. Re

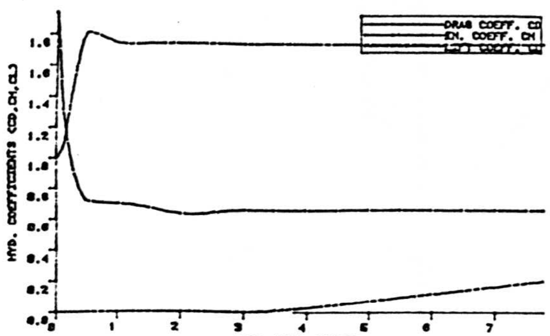

(b) HYD. COEFFICIENTS Vs. KC

SR = 0.0

FIG. (5.1) DRAG,INERTIA AND LIFT COEFFICIENTS FOR MEMBER(1)

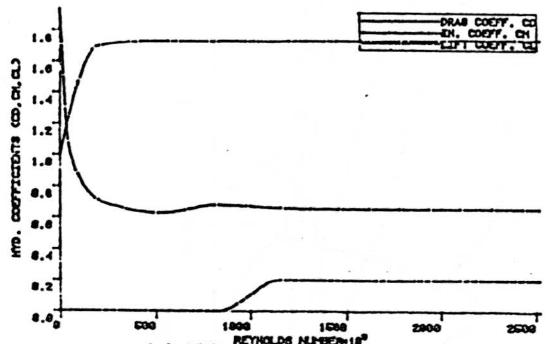

(a) HYD. COEFFICIENTS Vs. Re

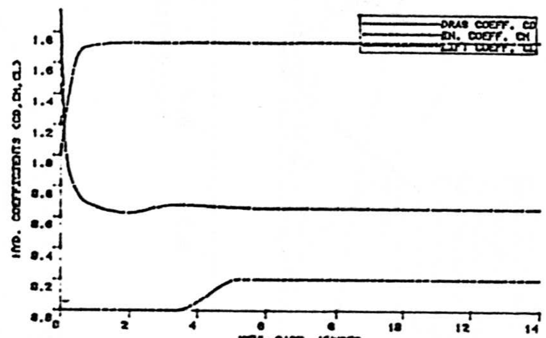

(b) HYD. COEFFICIENTS Vs. KC

SR = 0.0

FIG. (5.2) DRAG,INERTIA AND LIFT COEFFICIENTS FOR MEMBER(3)

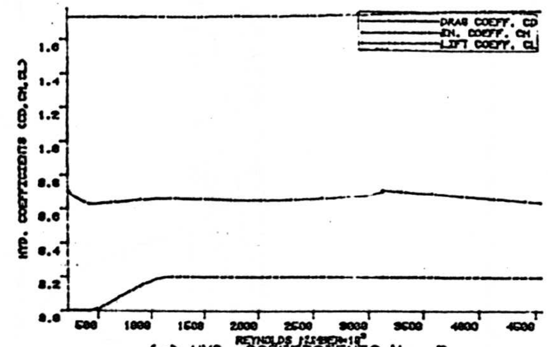

(a) HYD. COEFFICIENTS Vs. Re

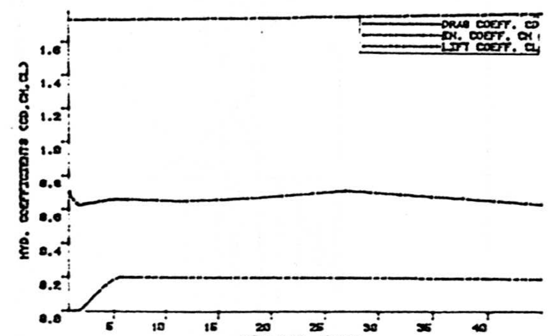

(b) HYD. COEFFICIENTS Vs. KC

SR = 0.0

FIG. (5.3) DRAG,INERTIA AND LIFT COEFFICIENTS FOR MEMBER(6)

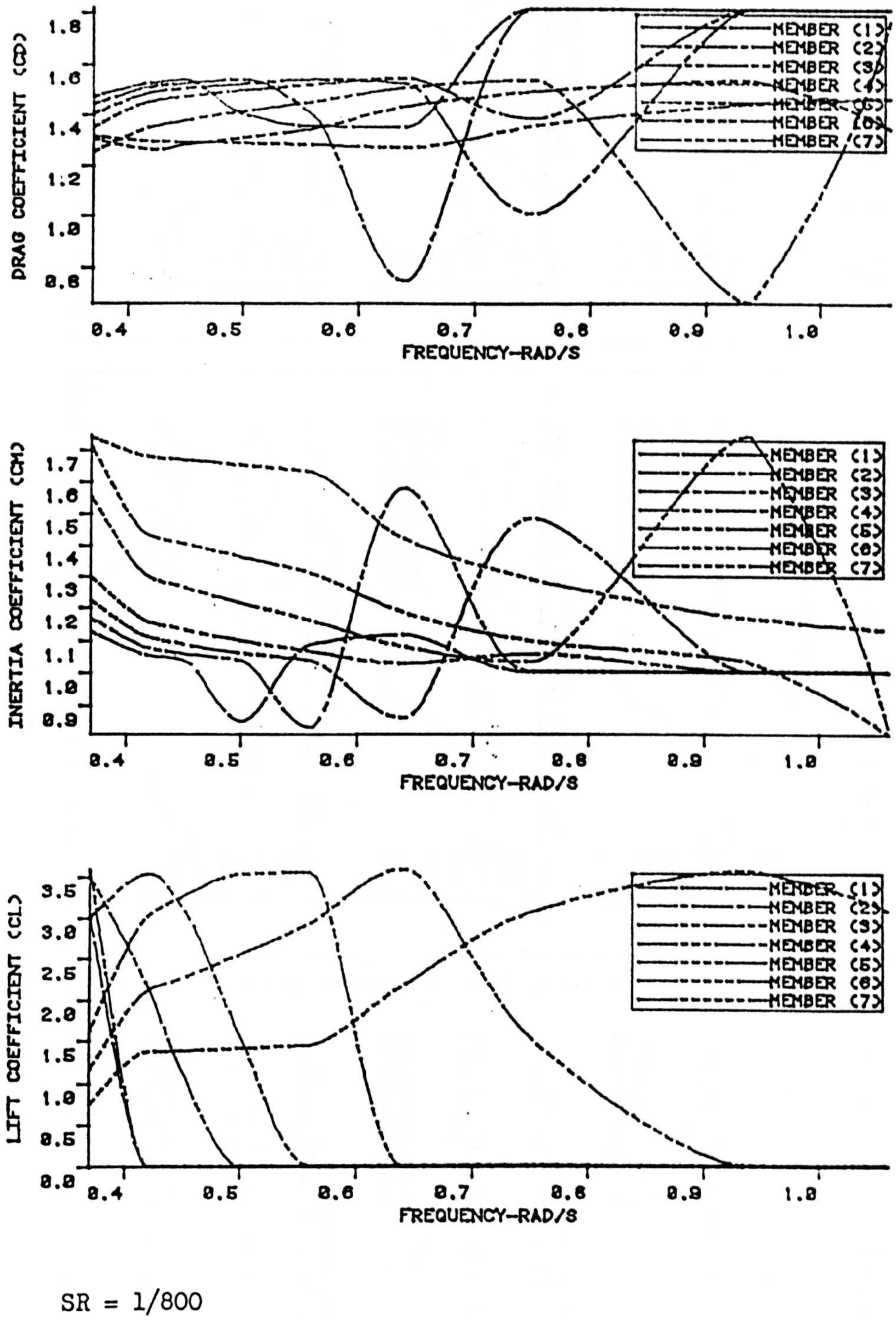

SR = 1/800

FIG. (6) HYDRODYNAMIC COEFFICIENTS Vs. FREQUENCY

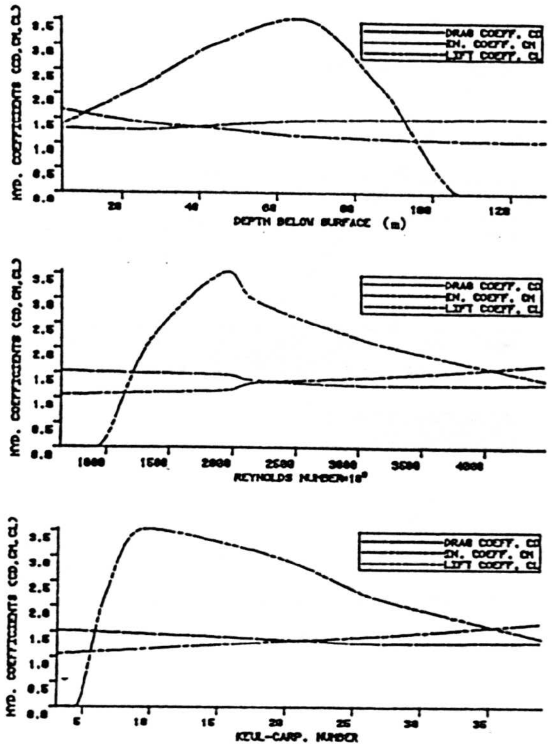

SR = 1/800

FIG. (7.1) DRAG, INERTIA AND LIFT COEFFICIENTS ω = 0.42 R/S

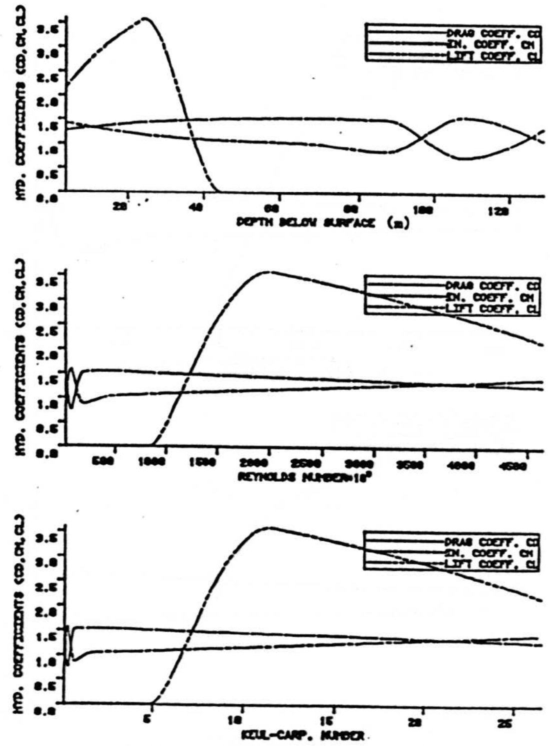

SR = 1/800

FIG. (7.2) DRAG, INERTIA AND LIFT COEFFICIENTS ω = 0.64 R/S

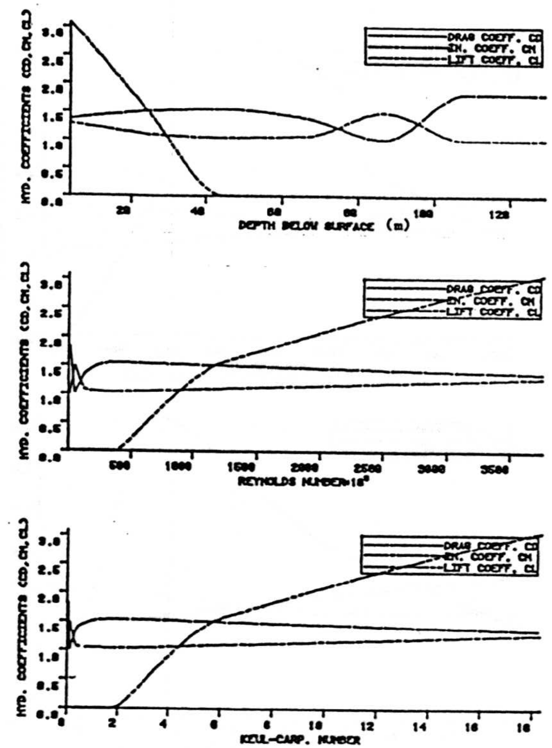

SR = 1/800

FIG. (7.3) DRAG, INERTIA AND LIFT COEFFICIENTS ω = 0.75 R/S

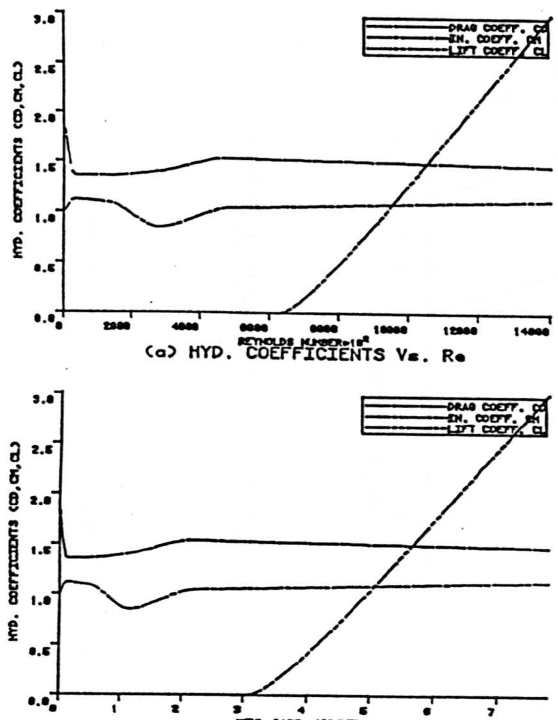

(a) HYD. COEFFICIENTS Vs. Re

(b) HYD. COEFFICIENTS Vs. KC

SR = 1/800

FIG. (8.1) DRAG,INERTIA AND LIFT COEFFICIENTS FOR MEMBER(1)

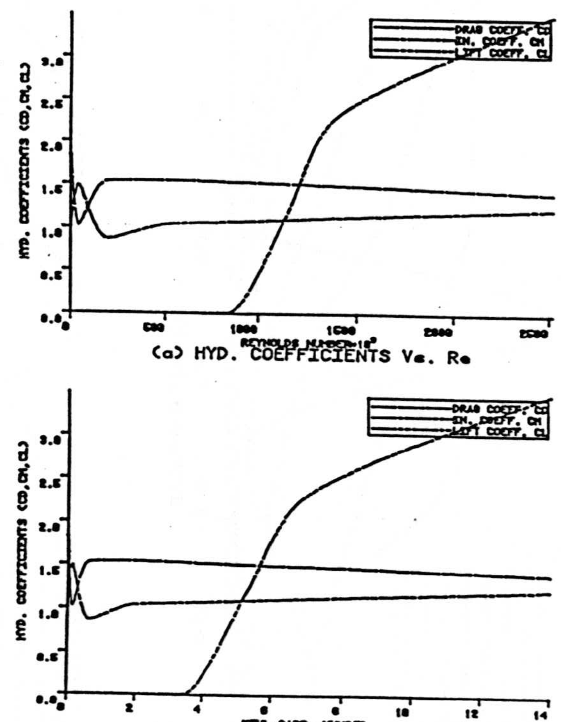

(a) HYD. COEFFICIENTS Vs. Re

(b) HYD. COEFFICIENTS Vs. KC

SR = 1/800

FIG. (8.2) DRAG,INERTIA AND LIFT COEFFICIENTS FOR MEMBER(3)

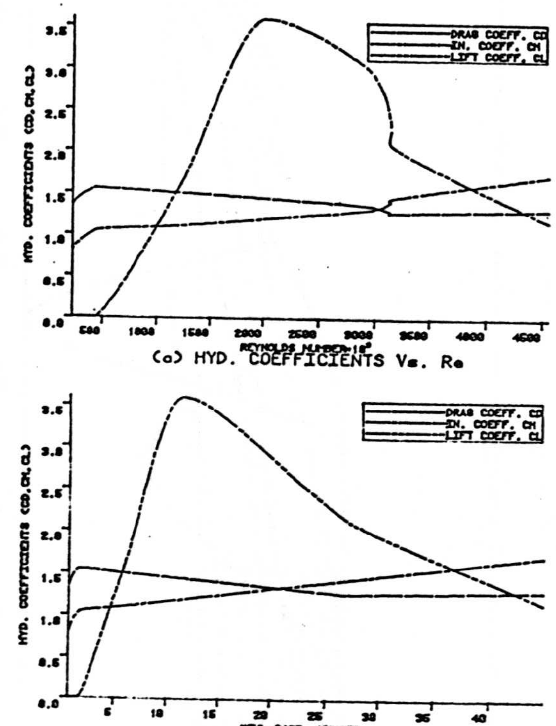

(a) HYD. COEFFICIENTS Vs. Re

(b) HYD. COEFFICIENTS Vs. KC

SR = 1/800

FIG. (8.3) DRAG,INERTIA AND LIFT COEFFICIENTS FOR MEMBER(6)

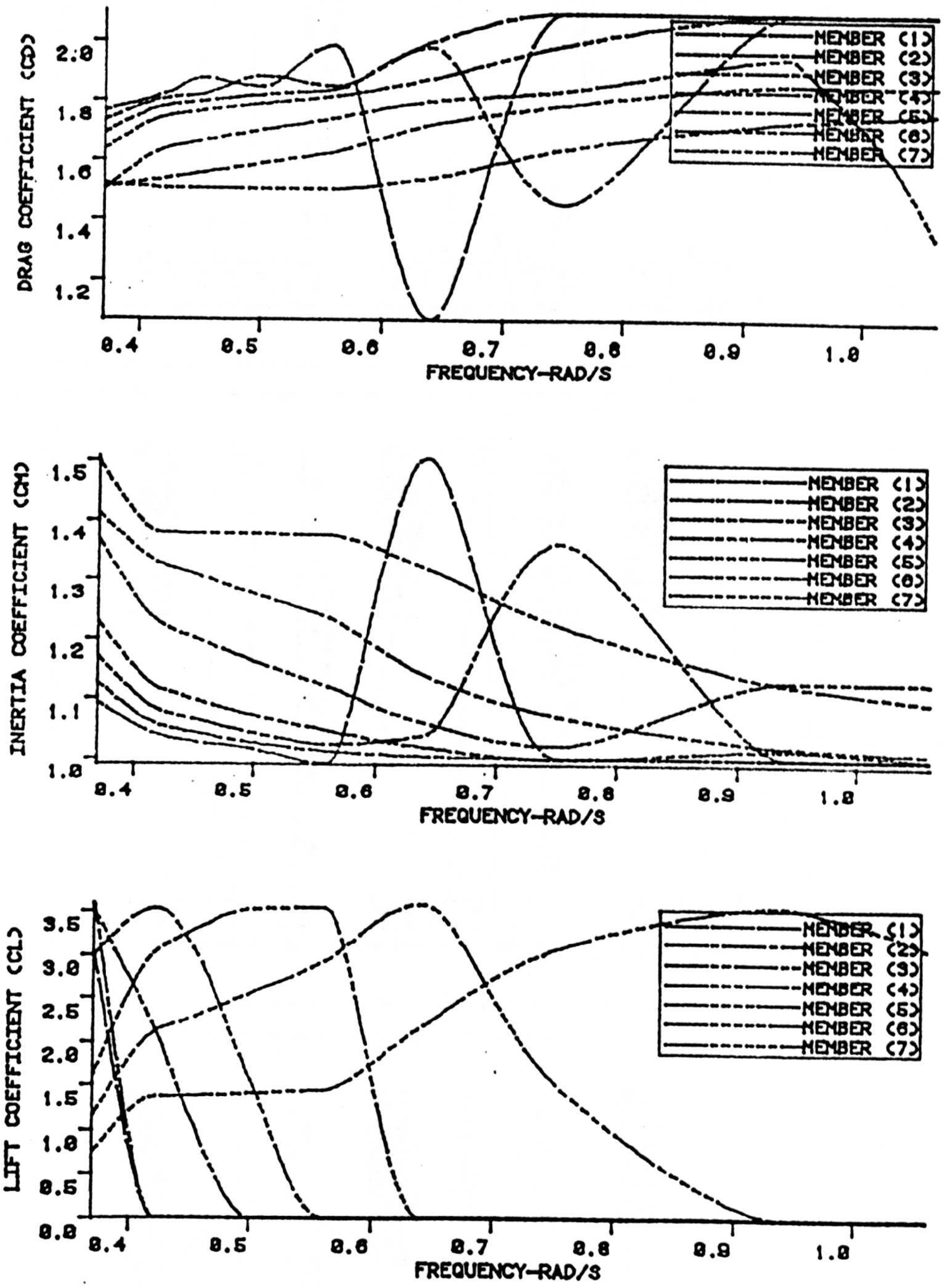

SR = 1/200

FIG. (9) HYDRODYNAMIC COEFFICIENTS Vs. FREQUENCY

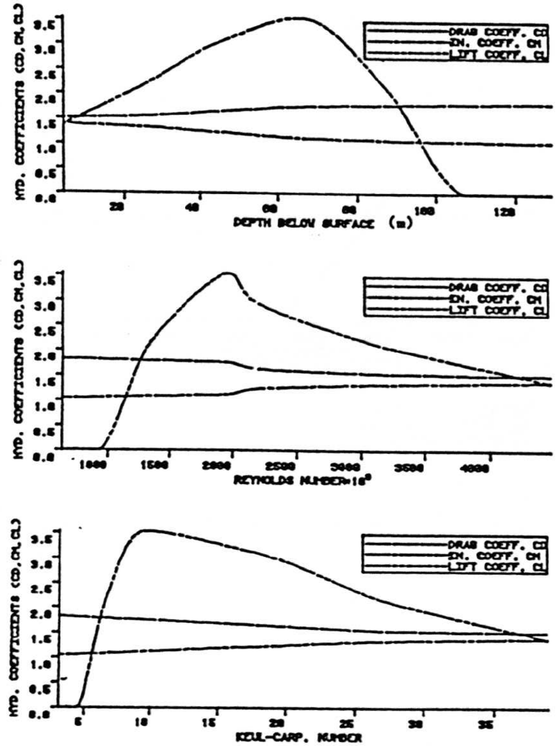

SH = 1/200

FIG. (10.1) DRAG, INERTIA AND LIFT COEFFICIENTS ω = 0.42 R/S

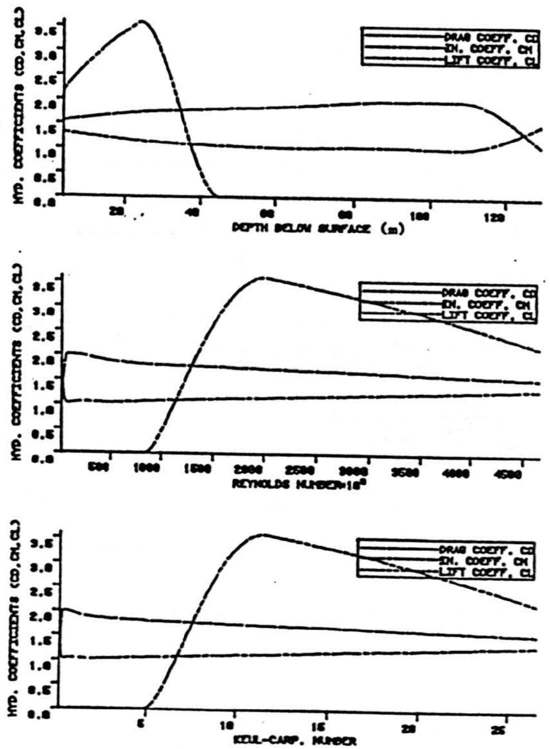

SR = 1/200

FIG. (10.2) DRAG, INERTIA AND LIFT COEFFICIENTS ω = 0.64R/S

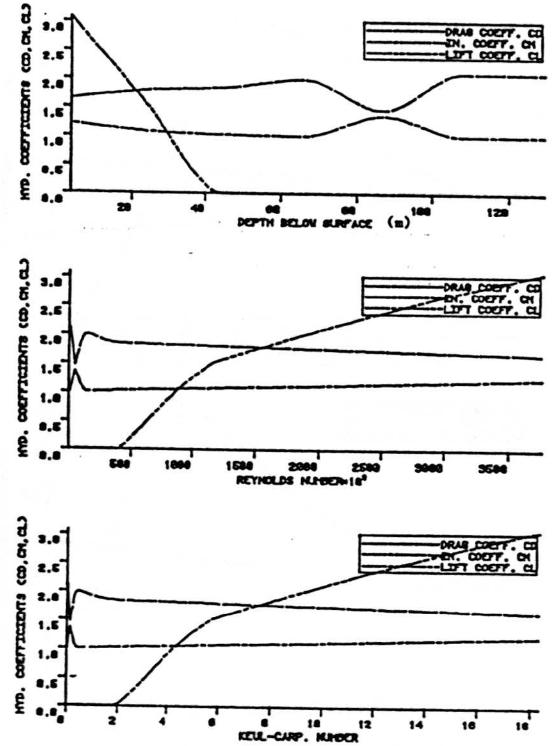

SR = 1/200

FIG. (10.3) DRAG, INERTIA AND LIFT COEFFICIENTS ω = 0.75 R/S

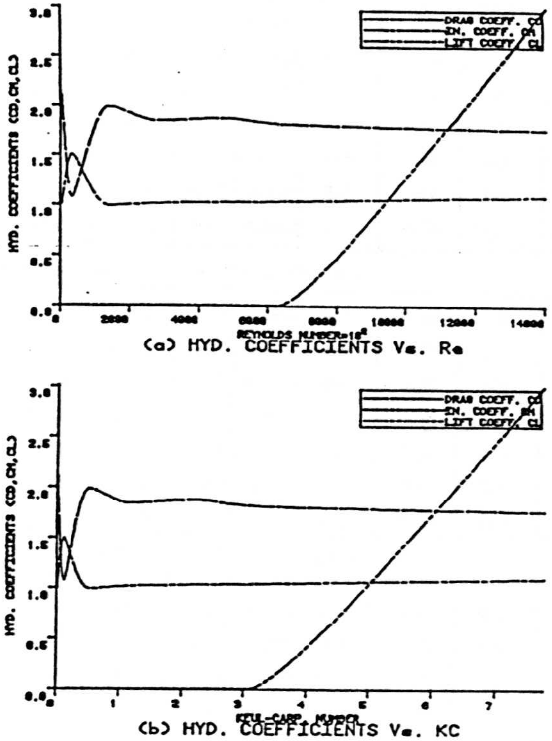

SR = 1/200

FIG. (11.1) DRAG, INERTIA AND LIFT COEFFICIENTS FOR MEMBER(1)

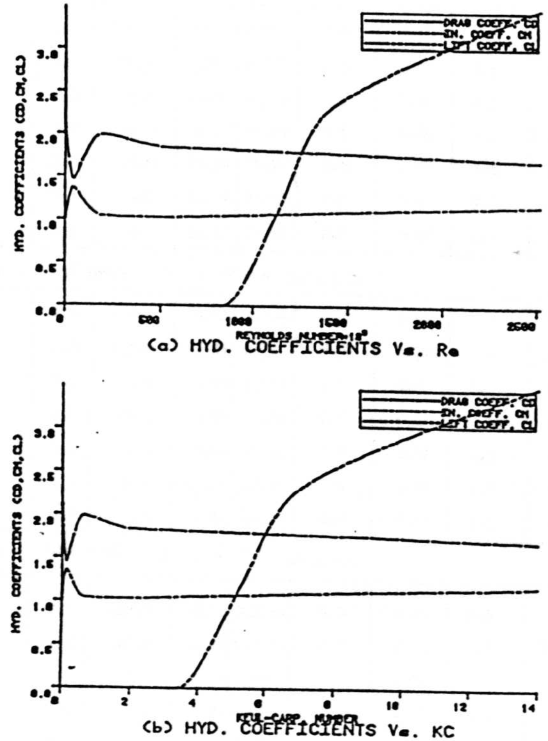

SR = 1/200

FIG. (11.2) DRAG, INERTIA AND LIFT COEFFICIENTS FOR MEMBER(3)

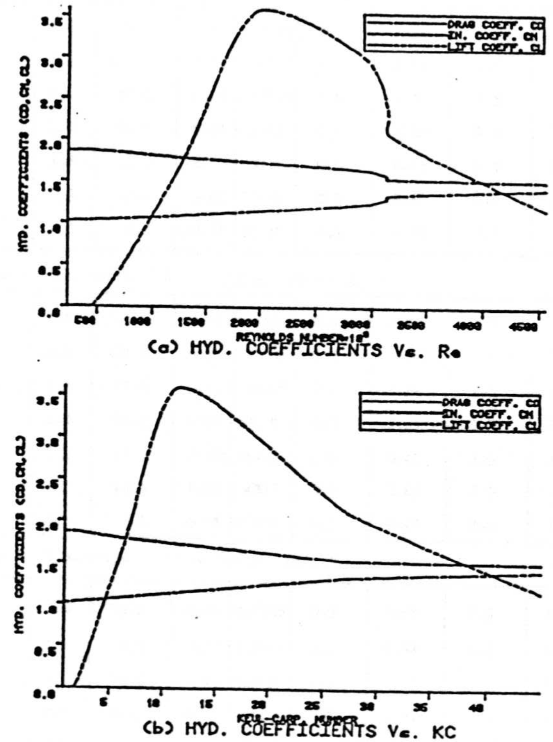

SR = 1/200

FIG. (11.3) DRAG, INERTIA AND LIFT COEFFICIENTS FOR MEMBER(6)

Member No.	Diam. (m)	Depth Below Surface (m)	K	R_e x10^{-7}	Drag Coeff. C_D LR	Drag Coeff. C_D SARPKAYA	Inertia Coeff. C_M LR	Inertia Coeff. C_M SARPKAYA
ω = 0.37 rad/s H = 30.0 m SR = 0.0								
1	2.0	129.0	7.78	0.1400	0.5	0.66	1.5	1.74
2	2.0	108.0	10.43	0.1877	0.5	0.65	1.5	1.74
3	2.0	87.0	13.99	0.2516	0.5	0.66	1.5	1.74
4	2.0	66.0	18.75	0.3373	0.5	0.67	1.5	1.75
5	1.5	45.0	33.51	0.3391	0.5	0.69	1.5	1.77
6	1.5	24.0	44.93	0.4546	0.5	0.64	1.5	1.78
7	1.5	4.0	59.39	0.6010	0.5	0.66	1.5	1.76
ω = 0.42 rad/s H = 20.0 m SR = 0.0								
1	2.0	129.0	3.09	0.0630	0.5	0.66	1.5	1.73
2	2.0	108.0	4.50	0.0920	0.5	0.67	1.5	1.74
3	2.0	87.0	6.57	0.1342	0.5	0.66	1.5	1.74
4	2.0	66.0	9.58	0.1957	0.5	0.65	1.5	1.74
5	1.5	45.0	18.64	0.2141	0.5	0.68	1.5	1.75
6	1.5	24.0	27.19	0.3124	0.5	0.71	1.5	1.75
7	1.5	4.0	38.96	0.4475	0.5	0.65	1.5	1.78
ω = 0.45 rad/s H = 20.0 m SR = 0.0								
1	2.0	129.0	2.19	0.0479	0.5	0.63	1.5	1.73
2	2.0	108.0	3.38	0.0739	0.5	0.69	1.5	1.73
3	2.0	87.0	5.21	0.1140	0.5	0.66	1.5	1.74
4	2.0	66.0	8.04	0.1759	0.5	0.65	1.5	1.74
5	1.5	45.0	16.54	0.2035	0.5	0.67	1.5	1.75
6	1.5	24.0	25.51	0.3140	0.5	0.71	1.5	1.76
7	1.5	4.0	38.55	0.4744	0.5	0.65	1.5	1.78

Table (1.1) Drag and Inertia Coefficients for LR & SARPKAYA for Bracing Members.

Member No.	Diam. (m)	Depth Below Surface (m)	K	R_e x10^{-5}	Drag Coeff. C_D LR	Drag Coeff. C_D SARPKAYA	Inertia Coeff. C_M LR	Inertia Coeff. C_M SARPKAYA
ω = 0.5 rad/s H = 20.0 m SR = 0.0								
1	2.0	129.0	1.17	2.851	0.5	0.69	1.5	1.73
2	2.0	108.0	2.00	4.869	0.5	0.62	1.5	1.73
3	2.0	87.0	3.42	8.315	0.5	0.68	1.5	1.73
4	2.0	66.0	5.84	14.20	0.5	0.65	1.5	1.74
5	1.5	45.0	13.30	18.19	0.5	0.66	1.5	1.74
6	1.5	24.0	22.71	31.06	0.5	0.69	1.5	1.75
7	1.5	4.0	37.81	51.70	0.5	0.66	1.5	1.78
ω = 0.56 rad/s H = 20.0 m SR = 0.0								
1	2.0	129.0	0.51	1.384	0.5	0.72	1.5	1.81
2	2.0	108.0	0.99	2.707	0.5	0.70	1.5	1.73
3	2.0	87.0	1.95	5.298	0.5	0.63	1.5	1.73
4	2.0	66.0	3.81	10.37	0.5	0.67	1.5	1.73
5	1.5	45.0	9.93	15.21	0.5	0.66	1.5	1.74
6	1.5	24.0	19.44	29.77	0.5	0.68	1.5	1.75
7	1.5	4.0	36.84	56.43	0.5	0.67	1.5	1.78
ω = 0.64 rad/s H = 15.0 m SR = 0.0								
1	2.0	129.0	0.11	0.3356	0.5	1.32	1.5	1.07
2	2.0	108.0	0.26	0.8065	0.5	0.75	1.5	1.73
3	2.0	87.0	0.62	1.938	0.5	0.71	1.5	1.70
4	2.0	66.0	1.50	4.658	0.5	0.62	1.5	1.73
5	1.5	45.0	4.80	8.396	0.5	0.68	1.5	1.74
6	1.5	24.0	11.53	20.18	0.5	0.65	1.5	1.74
7	1.5	4.0	26.57	46.51	0.5	0.72	1.5	1.76

Table (1.2) Drag and Inertia Coefficients for LR & SARPKAYA for Bracing Members.

Member No.	Diam. (m)	Depth Below Surface (m)	K	R_e x10^{-2}	Drag Coeff. C_D LR	Drag Coeff. C_D SARPKAYA	Inertia Coeff. C_M LR	Inertia Coeff. C_M SARPKAYA
ω = 0.75 rad/s H = 11.0 m SR = 0.0								
1	2.0	129.0	0.01	38.62	0.5	1.94	1.5	1.00
2	2.0	108.0	0.04	128.7	0.5	2.12	1.5	1.00
3	2.0	87.0	0.12	429.2	0.5	1.07	1.5	1.23
4	2.0	66.0	0.39	1431	0.5	0.72	1.5	1.80
5	1.5	45.0	1.74	3578	0.5	0.63	1.5	1.73
6	1.5	24.0	5.82	11930	0.5	0.66	1.5	1.74
7	1.5	4.0	18.31	37550	0.5	0.67	1.5	1.75
ω = 0.94 rad/s H = 7.0 m SR = 0.0								
1	2.0	129.0	0.00	0.4516	0.5	1.94	1.5	1.00
2	2.0	108.0	0.00	2.994	0.5	1.94	1.5	1.00
3	2.0	87.0	0.00	19.85	0.5	1.94	1.5	1.00
4	2.0	66.0	0.03	131.6	0.5	2.13	1.5	1.00
5	1.5	45.0	0.254	654.2	0.5	0.81	1.5	1.57
6	1.5	24.0	1.69	4337	0.5	0.63	1.5	1.73
7	1.5	4.0	10.22	26280	0.5	0.64	1.5	1.74
ω = 1.06 rad/s H = 6.0 m SR = 0.0								
1	2.0	129.0	0.00	0.0186	0.5	1.94	1.5	1.00
2	2.0	108.0	0.00	0.2061	0.5	1.94	1.5	1.00
3	2.0	87.0	0.00	2.283	0.5	1.94	1.5	1.00
4	2.0	66.0	0.01	25.30	0.5	1.94	1.5	1.00
5	1.5	45.0	0.07	210.3	0.5	1.87	1.5	0.91
6	1.5	24.0	0.80	2330	0.5	0.70	1.5	1.73
7	1.5	4.0	7.94	23030	0.5	0.64	1.5	1.74

Table (1.3) Drag and Inertia Coefficients for LR & SARPKAYA for Bracing Members.

Member No.	Diam. (m)	R_e $\times10^{-7}$	Drag Coeff. C_D SR = 0.0	SR = $\frac{1}{800}$	SR = $\frac{1}{200}$	Inertia Coeff. C_M SR = 0.0	SR = $\frac{1}{800}$	SR = $\frac{1}{200}$
ω = 0.37 rad/s				H = 30.0 m				
1	2.0	0.1400	0.66	1.47	1.77	1.74	1.13	1.09
2	2.0	0.1877	0.65	1.45	1.74	1.74	1.17	1.13
3	2.0	0.2516	0.66	1.41	1.69	1.74	1.22	1.17
4	2.0	0.3373	0.67	1.35	1.64	1.75	1.30	1.23
5	1.5	0.3391	0.69	1.26	1.50	1.77	1.55	1.37
6	1.5	0.4546	0.64	1.30	1.51	1.78	1.71	1.41
7	1.5	0.6010	0.66	1.32	1.52	1.76	1.74	1.50
ω = 0.42 rad/s				H = 20.0 m				
1	2.0	0.0630	0.66	1.53	1.82	1.73	1.05	1.04
2	2.0	0.0920	0.67	1.51	1.81	1.74	1.08	1.05
3	2.0	0.1342	0.66	1.49	1.78	1.74	1.11	1.08
4	2.0	0.1957	0.65	1.46	1.75	1.74	1.15	1.12
5	1.5	0.2141	0.68	1.36	1.64	1.75	1.29	1.22
6	1.5	0.3124	0.71	1.26	1.53	1.76	1.43	1.33
7	1.5	0.4475	0.65	1.29	1.50	1.78	1.68	1.38
ω = 0.45 rad/s				H = 20.0 m				
1	2.0	0.0479	0.63	1.54	1.88	1.73	1.04	1.03
2	2.0	0.0739	0.69	1.52	1.82	1.73	1.06	1.04
3	2.0	0.1140	0.66	1.50	1.80	1.74	1.09	1.06
4	2.0	0.1759	0.65	1.47	1.76	1.74	1.13	1.10
5	1.5	0.2035	0.67	1.38	1.66	1.75	1.26	1.20
6	1.5	0.3140	0.71	1.28	1.55	1.76	1.40	1.31
7	1.5	0.4744	0.65	1.29	1.50	1.78	1.67	1.38

Table (2.1) Drag and Inertia Coefficients for Smooth & Rough Cylinders for Bracing Members.

Member No.	Diam. (m)	R_e $\times10^{-5}$	Drag Coeff. C_D SR = 0.0	SR = $\frac{1}{800}$	SR = $\frac{1}{200}$	Inertia Coeff. C_M SR = 0.0	SR = $\frac{1}{800}$	SR = $\frac{1}{200}$
ω = 0.5 rad/s				H = 20.0 m				
1	2.0	2.851	0.69	1.40	1.85	1.73	0.85	1.01
2	2.0	4.869	0.62	1.54	1.88	1.73	1.04	1.02
3	2.0	8.135	0.68	1.52	1.82	1.73	1.06	1.04
4	2.0	14.200	0.65	1.50	1.79	1.74	1.10	1.07
5	1.5	18.19	0.66	1.41	1.70	1.74	1.21	1.16
6	1.5	31.06	0.69	1.31	1.59	1.75	1.36	1.27
7	1.5	51.70	0.66	1.29	1.50	1.78	1.65	1.38
ω = 0.56 rad/s				H = 20.0 m				
1	2.0	1.384	0.72	1.35	1.99	1.81	1.09	0.99
2	2.0	2.707	0.70	1.40	1.85	1.73	0.83	1.01
3	2.0	5.298	0.63	1.54	1.84	1.73	1.04	1.02
4	2.0	10.37	0.67	1.52	1.81	1.73	1.06	1.05
5	1.5	15.21	0.66	1.45	1.74	1.74	1.16	1.12
6	1.5	29.77	0.68	1.35	1.63	1.75	1.31	1.23
7	1.5	56.43	0.67	1.28	1.50	1.78	1.63	1.37
ω = 0.64 rad/s				H = 15.0 m				
1	2.0	0.3356	1.32	1.35	1.07	1.07	1.12	1.50
2	2.0	0.8065	0.75	0.75	2.00	1.73	1.58	1.00
3	2.0	1.938	0.71	1.52	1.98	1.70	0.86	1.04
4	2.0	4.658	0.62	1.54	1.88	1.73	1.03	1.02
5	1.5	8.396	0.68	1.51	1.80	1.74	1.08	1.06
6	1.5	20.18	0.65	1.43	1.72	1.74	1.18	1.14
7	1.5	46.51	0.72	1.27	1.54	1.76	1.42	1.32

Table (2.2) Drag and Inertia Coefficients for Smooth & Rough Cylinders for Bracing Members.

Member No.	Diam. (m)	R_e $\times10^{-2}$	Drag Coeff. C_D SR = 0.0	SR = $\frac{1}{800}$	SR = $\frac{1}{200}$	Inertia Coeff. C_M SR = 0.0	SR = $\frac{1}{800}$	SR = $\frac{1}{200}$
ω = 0.75 rad/s				H = 11.0 m				
1	2.0	38.62	1.94	1.82	2.10	1.00	1.00	1.00
2	2.0	128.7	2.12	1.82	2.10	1.00	1.00	1.00
3	2.0	429.2	1.07	1.01	1.45	1.23	1.48	1.36
4	2.0	1431	0.72	1.39	1.99	1.80	1.06	1.00
5	1.5	3578	0.63	1.54	1.84	1.73	1.03	1.02
6	1.5	11930	0.66	1.50	1.79	1.74	1.10	1.07
7	1.5	37550	0.67	1.36	1.64	1.75	1.29	1.22
ω = 0.94 rad/s				H = 7.0 m				
1	2.0	0.4516	1.94	1.82	2.10	1.00	1.00	1.00
2	2.0	2.994	1.94	1.82	2.10	1.00	1.00	1.00
3	2.0	19.85	1.94	1.82	2.10	1.00	1.00	1.00
4	2.0	131.6	2.13	1.82	2.10	1.00	1.00	1.02
5	1.5	654.2	0.81	0.66	1.95	1.57	1.75	1.13
6	1.5	4337	0.63	1.54	1.86	1.73	1.03	1.02
7	1.5	26280	0.64	1.45	1.74	1.74	1.16	1.12
ω = 1.06 rad/s				H = 6.0 m				
1	2.0	0.0186	1.94	1.82	2.10	1.00	1.00	1.00
2	2.0	0.2061	1.94	1.82	2.10	1.00	1.00	1.00
3	2.0	2.283	1.94	1.82	2.10	1.00	1.00	1.00
4	2.0	25.30	1.94	1.82	2.10	1.00	1.00	1.00
5	1.5	210.3	1.87	1.77	1.34	0.91	0.83	1.13
6	1.5	2330	0.70	1.35	1.86	1.73	0.81	1.01
7	1.5	23030	0.64	1.47	1.77	1.74	1.13	1.10

Table (2.3) Drag and Inertia Coefficients for Smooth & Rough Cylinders for Bracing Members.

2. According to Sarpkaya, the maximum values of C_D, C_M and C_L for rough cylinders are 2, 1.7 and 3.5, respectively. LR does not recommend specific coefficients for rough cylinders.

5. THE EFFECT OF VARIABLE COEFFICIENTS

In this section, the results of calculations using both LR and Sarpkaya's coefficients assuming smooth and rough cylinders will be discussed to show the influence of using the variable coefficients which depend on R_e and K (Sarpkaya) against fixed values throughout the whole structure (LR). The first part deals with the wave forces on the individual members, Fig.(2), while the second part analyses the results of the total forces (surge, heave and sway) and moments (rolling, yawing and pitching) on the complete structure.

5.1. Forces on the Individual Members, LR vs. Sarpkaya

For the particulars of waves (frequency, height, length, etc) used in the calculations, see Table (1), Chapter 4, and for the position and numbering of the members, see Fig. (2).

5.1.1 Maximum Forces on the Members in 'v' and 'w' Directions

The maximum forces in 'v' and 'w' directions (F_{T_w} and F_{T_v}) were calculated at the different frequencies for six members (Nos. 1, 4, 7, 15, 18 and 21), (3 horizontal, 3 inclined at various depths). The results are shown in the form of Tables, Nos.(3) to (12), and graphs, Figs (12) to (21). The differences in the force estimation between Sarpkaya and LR are as follows:-

a. Smooth Cylinders

(1) For member No (1), F_{T_w} according to Sarpkaya was increased relative to LR by 15.4% (ω = 0.5 rad/s) to 20.5% (ω = 0.56 rad/s). At the higher frequencies, the magnitude of F_{T_w} becomes very small and the values according to Sarpkaya were reduced (relative to LR) by a maximum of 33.4% (ω = 0.94 rad/s). According to LR, F_{T_v} has no value (there is no lift force), and the same applies to Sarpkaya except when ω = 0.37 rad/s.

(2) For member No (4), F_{T_w} was increased up to ω = 0.75 rad/s. The differences ranged from 15.5% (ω = 0.64 rad/s) to 20.7% (ω = 0.37 rad/s). At the higher frequences, F_{T_w} is very small and the value according to Sarpkaya is reduced by 33.4% (ω = 0.94 rad/s). According to LR, F_{T_v} has no value and the same is valid for Sarpkaya when ω is larger than 0.5 rad/s.

(3) For member No (7), which is the nearest to the water surface, the differences in F_{T_w} ranged from 15.9% (ω = 1.06 rad/s) to 31% (ω = 0.56 rad/s). According to Sarpkaya, F_{T_v} had values (lift forces) throughout the whole range of frequencies.

(4) For member No (15), the differences between Sarpkaya and LR in F_{T_w} ranged from -9.8% (ω = 0.56 rad/s) to -50.2% (ω = 0.64 rad/s) and the differences in F_{T_v} ranged from -11% (ω = 0.56 rad/s) to -50% (ω = 0.75 rad/s).

Wave Frequency ω (rad/s)	Wave Height H (m)	w Direction					v Direction				
		$F_{TW} \times 10^{-2}$ (N)		Diff.%	Relative Time "tr"		F_{TV} (N)		Diff.%	Relative Time "tr"	
		LR	SARPKAYA		LR	SARPKAYA	LR	SARPKAYA		LR	SARPKAYA
0.37	30.0	1086	1258	15.8%	0.0	0.0	0.0	0.1005×10^{5}			0.8
0.42	20.0	540.5	624.5	15.5%	0.0	0.0	0.0	0.0			
0.45	20.0	431.1	497.8	15.5%	0.0	0.0	0.0	0.0			
0.50	20.0	272.1	314.1	15.4%	0.0	0.0	0.0	0.0			
0.56	20.0	136.7	164.7	20.5%	0.0	0.0	0.0	0.0			
0.64	15.0	32.25	22.91	-29%	0.0	0.0	0.0	0.0			
0.75	11.0	2.938	1.959	-33.3%	0.0	0.0	0.0	0.0			
0.94	7.0	0.1185×10^{-2}	0.7897×10^{-3}	-33.4%	0.0	0.0	0.0	0.0			
1.06	6.0	0.7847×10^{-3}	0.5231×10^{-3}	-33.3%	0.0	0.0	0.0	0.0			

Table (3) Maximum Forces in "v" and "w" Directions on Member No. 1

Wave Frequency ω (rad/s)	Wave Height H (m)	w Direction					v Direction				
		$F_{TW} \times 10^{-2}$ (N)		Diff.%	Relative Time "tr"		F_{TV} (N)		Diff.%	Relative Time "tr"	
		LR	SARPKAYA		LR	SARPKAYA	LR	SARPKAYA		LR	SARPKAYA
0.37	30.0	2268	2737	20.7%	0.6	0.1	0.0	0.4892×10^{5}			0.8
0.42	20.0	1406	1631	16%	0.0	0.0	0.0	0.1589×10^{5}			0.8
0.45	20.0	1335	1547	15.9%	0.0	0.0	0.0	0.1261×10^{5}			0.8
0.50	20.0	1162	1344	15.7%	0.0	0.0	0.0	0.781×10^{4}			0.8
0.56	20.0	901.9	1042	15.5%	0.0	0.0	0.0	0.0			
0.64	15.0	417.4	481.9	15.5%	0.0	0.0	0.0	0.0			
0.75	11.0	118.2	141.9	20.1%	0.0	0.0	0.0	0.0			
0.94	7.0	4.885	3.256	-33.4%	0.0	0.0	0.0	0.0			
1.06	6.0	0.1392	0.09282	-33.3%	0.0	0.0	0.0	0.0			

Table (4) Maximum Forces in "v" and "w" Directions on Member No. 4

Wave Frequency ω (rad/s)	Wave Height H (m)	w Direction					v Direction				
		$F_{TW} \times 10^{-6}$ (N)		Diff.%	Relative Time "tr"		$F_{TV} \times 10^{-2}$ (N)		Diff.%	Relative Time "tr"	
		LR	SARPKAYA		LR	SARPKAYA	LR	SARPKAYA		LR	SARPKAYA
0.37	30.0	0.4837	0.6236	28.9%	0.2	0.2	0.0	1533			0.8
0.42	20.0	0.2842	0.3603	26.8%	0.7	0.7	0.0	899.8			0.8
0.45	20.0	0.3158	0.4032	27.7%	0.7	0.7	0.0	996.4			0.8
0.50	20.0	0.3659	0.4726	29.2%	0.7	0.7	0.0	1146			0.8
0.56	20.0	0.4181	0.5476	31%	0.7	0.7	0.0	1296			0.8
0.64	15.0	0.3340	0.4220	26.4%	0.1	0.1	0.0	799.2			0.8
0.75	11.0	0.2536	0.3086	21.7%	0.6	0.6	0.0	432.6			0.8
0.94	7.0	0.1185	0.1386	17%	0.0	0.6	0.0	130.3			0.8
1.06	6.0	0.05738	0.06649	15.9	0.0	0.0	0.0	53.57			0.8

Table (5) Maximum Forces in "v" and "w" Directions on Member No. 7

Wave Frequency ω (rad/s)	Wave Height H (m)	w Direction					v Direction				
		$F_{TW} \times 10^{-2}$ (N)		Diff.%	Relative Time "tr"		$F_{TV} \times 10^{-2}$ (N)		Diff.%	Relative Time "tr"	
		LR	SARPKAYA		LR	SARPKAYA	LR	SARPKAYA		LR	SARPKAYA
0.37	30.0	1146	992.4	-13.4%	0.2	0.2	1120	970.7	-13.3%	0.7	0.7
0.42	20.0	558.5	483.4	-13.5%	0.7	0.7	530.4	459.7	-13.3%	0.7	0.7
0.45	20.0	436.1	377.5	-13.4%	0.7	0.7	432.1	373.8	-13.5%	0.1	0.1
0.50	20.0	273.8	236.4	-13.7%	0.1	0.1	278.8	241.4	-13.4%	0.1	0.1
0.56	20.0	144.0	129.9	- 9.8%	0.1	0.1	140.2	124.8	-11%	0.6	0.6
0.64	15.0	34.97	17.40	-50.2%	0.0	0.0	35.98	19.39	-46.1%	0.0	0.0
0.75	11.0	4.157	2.079	-50%	1.0	1.0	4.188	2.094	-50%	0.4	0.4
0.94	7.0	0.04809	0.02404	-50%	0.8	0.8	0.04613	0.02306	-50%	0.2	0.2
1.06	6.0	0.1836×10^{-2}	0.0918×10^{-2}	-50%	0.1	0.1	0.1878×10^{-2}	0.09389×10^{-2}	-50%	0.1	0.1

Table (6) Maximum Forces in "v" and "w" Directions on Member No. 15

Wave Frequency ω (rad/s)	Wave Height H (m)	w Direction					v Direction				
		$F_{TW} \times 10^{-2}$ (N)		Diff.%	Relative Time "tr"		$F_{TV} \times 10^{-2}$ (N)		Diff.%	Relative Time "tr"	
		LR	SARPKAYA		LR	SARPKAYA	LR	SARPKAYA		LR	SARPKAYA
0.37	30.0	2743	2379	-13.3%	0.2	0.2	2727	2367	-13.2%	0.7	0.7
0.42	20.0	1747	1513	-13.4%	0.7	0.7	1698	1474	-13.2%	0.7	0.7
0.45	20.0	1633	1414	-13.4%	0.7	0.7	1565	1359	-13.2%	0.7	0.7
0.50	20.0	1368	1186	-13.3%	0.7	0.7	1360	1177	-13.5%	0.1	0.1
0.56	20.0	1055	912.7	-13.5%	0.1	0.1	1069	925.1	-13.5%	0.1	0.1
0.64	15.0	505	437.3	-13.4%	0.6	0.6	483.7	418.7	-13.5%	0.6	0.6
0.75	11.0	158.4	136.8	-13.6%	0.0	0.0	157	137.9	-12.2%	1.0	1.0
0.94	7.0	13.83	6.917	-50%	0.9	0.9	13.69	6.821	-50.2%	0.3	0.3
1.06	6.0	2.479	1.240	-50%	0.8	0.8	2.533	1.267	-50%	0.2	0.2

Table (7) Maximum Forces in "v" and "w" Directions on Member No. 18

Wave Frequency ω (rad/s)	Wave Height H (m)	w Direction					v Direction				
		$F_{TW} \times 10^{-6}$ (N)		Diff.%	Relative Time "tr"		$F_{TV} \times 10^{-6}$ (N)		Diff.%	Relative Time "tr"	
		LR	SARPKAYA		LR	SARPKAYA	LR	SARPKAYA		LR	SARPKAYA
0.37	30.0	0.7547	0.7139	-5.4%	0.8	0.3	0.7698	0.6846	-11.1%	0.2	0.3
0.42	20.0	0.6334	0.5503	-13.1%	0.2	0.2	0.6304	0.5480	-13.1%	0.7	0.7
0.45	20.0	0.7103	0.6184	-12.9%	0.2	0.2	0.6997	0.6094	-12.9%	0.7	0.7
0.50	20.0	0.8315	0.7272	-12.5%	0.7	0.2	0.8081	0.7066	-12.6%	0.7	0.7
0.56	20.0	0.9609	0.8496	-11.6%	0.7	0.7	0.9343	0.8087	-13.4%	0.1	0.7
0.64	15.0	0.8439	0.7305	-13.4%	0.1	0.1	0.8556	0.7415	-13.3%	0.6	0.1
0.75	11.0	0.7396	0.6425	-13.1%	0.6	0.6	0.7083	0.6124	-13.5%	0.0	0.0
0.94	7.0	0.5453	0.4727	-13.3%	1.0	1.0	0.5485	0.4747	-13.5%	0.4	0.4
1.06	6.0	0.5026	0.4353	-13.4%	0.9	0.9	0.4870	0.4212	-13.5%	0.3	0.3

Table (8) Maximum Forces in "v" and "w" Directions on Member No. 21

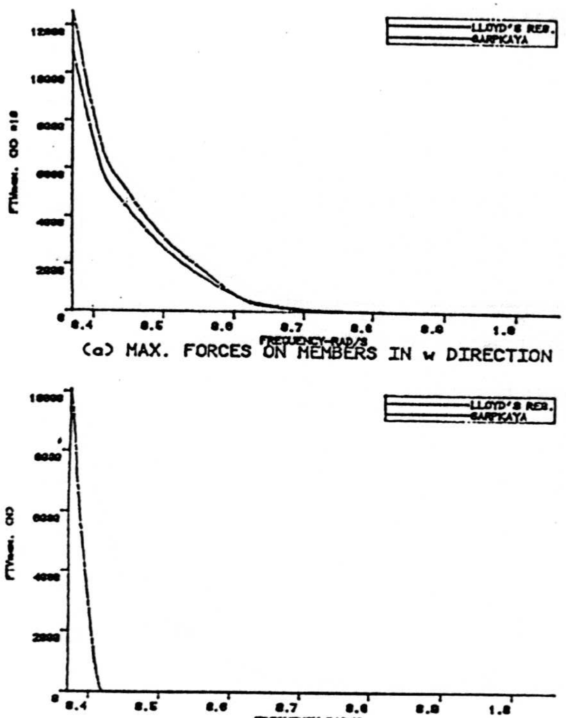

(a) MAX. FORCES ON MEMBERS IN w DIRECTION

(b) MAX. FORCES ON MEMBERS IN v DIRECTION

SR = 0.0 PROGRAM: OSS ,COEFFICIENTS: LR & S , β = 0.0
FIG. (12) MAX. FORCES ON MEMBER (1) Vs. FREQUENCY

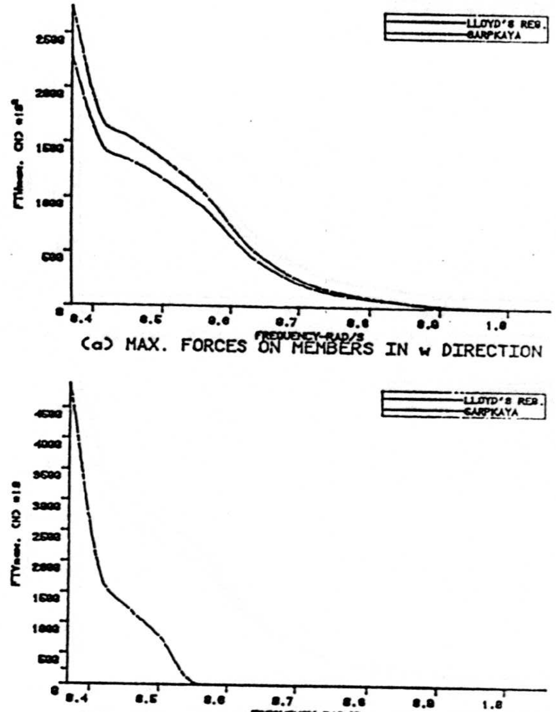

(a) MAX. FORCES ON MEMBERS IN w DIRECTION

(b) MAX. FORCES ON MEMBERS IN v DIRECTION

SR = 0.0 PROGRAM: OSS ,COEFFICIENTS: LR & S β = 0.0
FIG. (13) MAX. FORCES ON MEMBER (4) Vs. FREQUENCY

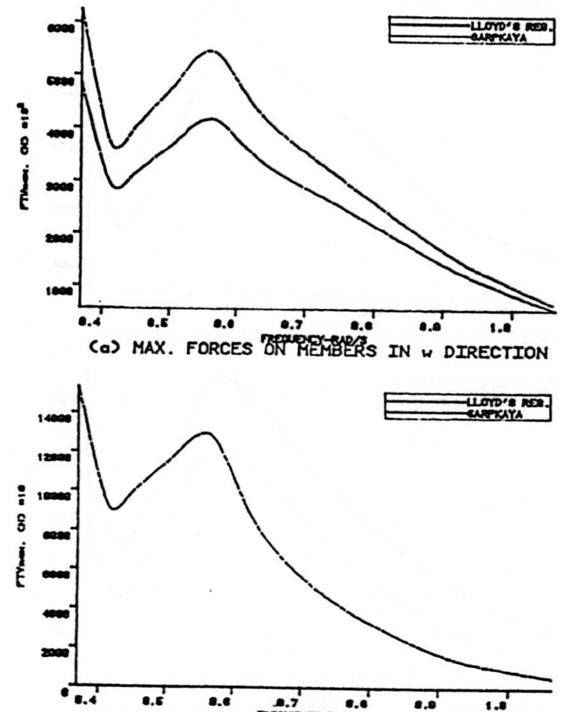

(a) MAX. FORCES ON MEMBERS IN w DIRECTION

(b) MAX. FORCES ON MEMBERS IN v DIRECTION

SR = 0.0 PROGRAM: OSS ,COEFFICIENTS: LR & S β = 0.0
FIG. (14) MAX. FORCES ON MEMBER (7) Vs. FREQUENCY

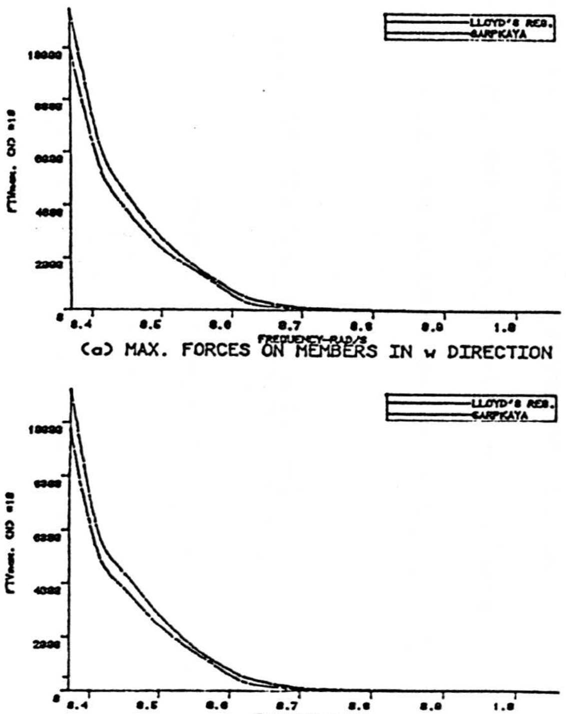

(a) MAX. FORCES ON MEMBERS IN w DIRECTION

(b) MAX. FORCES ON MEMBERS IN v DIRECTION

SR = 0.0 PROGRAM: OSS ,COEFFICIENTS: LR & S, β = 0.0
FIG. (15) MAX. FORCES ON MEMBER (15) Vs. FREQUENCY

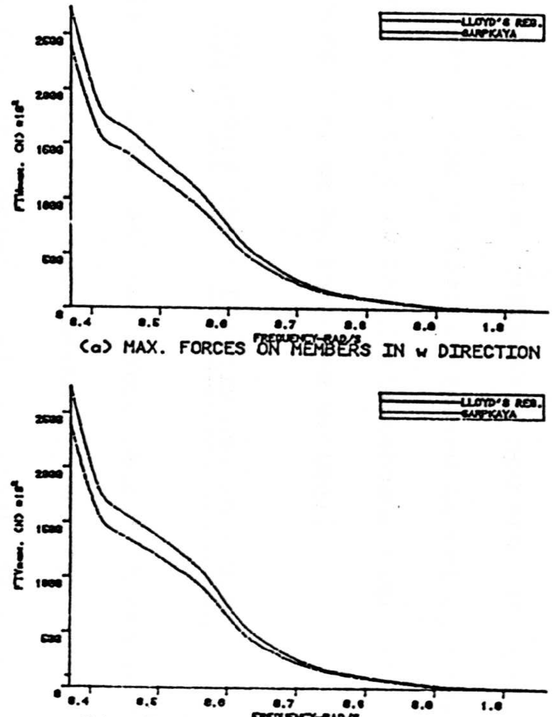

(a) MAX. FORCES ON MEMBERS IN w DIRECTION

(b) MAX. FORCES ON MEMBERS IN v DIRECTION

SR = 0.0 PROGRAM: OSS ,COEFFICIENTS: LR & S β = 0.0
FIG. (16) MAX. FORCES ON MEMBER (18) Vs. FREQUENCY

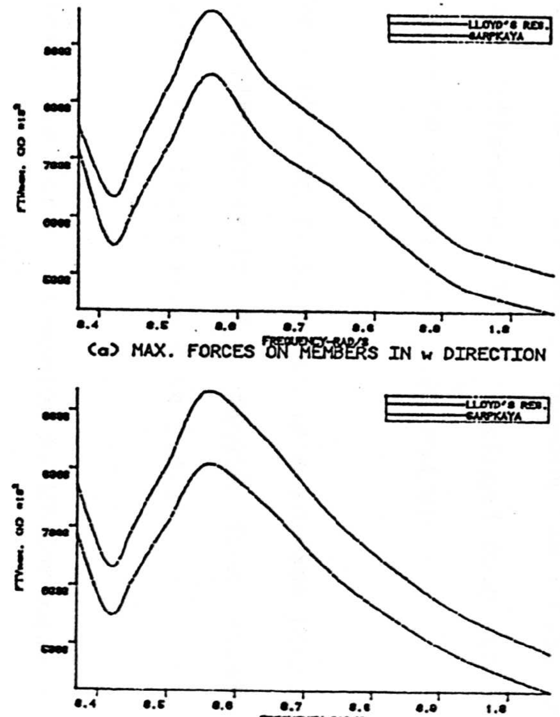

(a) MAX. FORCES ON MEMBERS IN w DIRECTION

(b) MAX. FORCES ON MEMBERS IN v DIRECTION

SR = 0.0 PROGRAM: OSS ,COEFFICIENTS: LR & S β = 0.0
FIG. (17) MAX. FORCES ON MEMBER (21) Vs. FREQUENCY

(5) For member No (18), the differences in F_{T_w} ranged from -13.3% (ω = 0.37 rad/s) to -50% (ω = 0.94 rad/s) and the differences in F_{T_v} ranged from -12.2% (ω = 0.75 rad/s) to -50.2% (ω = 0.94 rad/s).

(6) For member No (21), which is a surface piercing member, the differences in F_{T_w} ranged from -5.4% (ω = 0.37 rad/s) to -13.4% (ω = 0.64 rad/s).

The increase in force estimation by LR for members No 15, 18 and 21 is mainly due to the higher value of the inertia force where C_M = 2.0 for these members of 4.0m diameter. It was also noted that the 'relative time' for the different members at the different frequencies was the same as that estimated according to both LR and Sarpkaya. (The relative time is the instantaneous time at which the maximum force occurs divided by the wave period).

b. Rough Cylinders (SR = 0.00125 and SR = 0.005)

The results and the percentage differences between LR and Sarpkaya for two members, Nos (4) and (21), are summarised in Tables (9) to (12). In this case it was noted that the relative time at the different frequencies is not the same as estimated by LR and Sarpkaya. This suggests that the surface roughness affects the values of the maximum forces as well as the relative time.

5.1.2 Forces on the Members per Unit Wave Height

To examine the effect of frequency on the maximum force per unit wave height for the 21 members of the structure, Fig. (2), the maximum forces in 'v' and 'w' directions were calculated at the

Wave Frequency ω (rad/s)	Wave Height H (m)	w Direction					v Direction				
		$F_{TW} \times 10^{-2}$ (N)		Diff.%	Relative Time "tr"		$F_{TV} \times 10^{-6}$ (N)		Diff.%	Relative Time "tr"	
		LR SR = 0.0	SARPKAYA SR=0.00125		LR	SARPKAYA	LR SR = 0.0	SARPKAYA SR= 0.00125		LR	SARPKAYA
0.37	30.0	2268	3886	71.3%	0.6	0.2	0.0	0.7368			0.8
0.42	20.0	1406	1495	6.3%	0.0	0.7	0.0	0.2820			0.8
0.45	20.0	1335	1241	-7%	0.0	0.1	0.0	0.1965			0.8
0.50	20.0	1162	980.9	-15.6%	0.0	0.1	0.0	0.0605			0.8
0.56	20.0	901.9	683.8	-24.2%	0.0	0.6	0.0	0.0			
0.64	15.0	417.4	286.1	-31.5%	0.0	0.0	0.0	0.0			
0.75	11.0	118.2	83.32	-29.5%	0.0	0.0	0.0	0.0			
0.94	7.0	4.885	3.256	-33.4%	0.0	0.0	0.0	0.0			
1.06	6.0	0.1392	0.09282	-33.3%	0.0	0.0	0.0	0.0			

Table(9) Maximum Forces in "v" and "w" Directions on Member No. 4

Wave Frequency ω (rad/s)	Wave Height H (m)	w Direction					v Direction				
		$F_{TW} \times 10^{-6}$ (N)		Diff.%	Relative Time "tr"		$F_{TV} \times 10^{-6}$ (N)		Diff.%	Relative Time "tr"	
		LR SR = 0.0	SARPKAYA SR=0.00125		LR	SARPKAYA	LR SR=0.0	SARPKAYA SR=0.00125		LR	SARPKAYA
0.37	30.0	0.7547	2.582	242%	0.8	0.4	0.7698	2.556	232%	0.2	1.0
0.42	20.0	0.6334	1.456	130%	0.2	0.4	0.6304	1.155	83.2%	0.7	0.4
0.45	20.0	0.7103	1.589	124%	0.2	0.4	0.6997	1.250	78.7%	0.7	0.4
0.50	20.0	0.8315	1.751	111%	0.7	0.9	0.8081	1.363	68.7%	0.7	0.4
0.56	20.0	0.9609	1.827	90.1%	0.7	0.9	0.9343	1.387	48.5%	0.1	0.9
0.64	15.0	0.8439	0.896	6.2%	0.1	0.3	0.8556	0.6098	-28.7%	0.6	0.8
0.75	11.0	0.7396	0.4362	-41%	0.6	0.2	0.7083	0.3944	-44.3%	0.0	0.1
0.94	7.0	0.5453	0.286	-47.6%	1.0	1.0	0.5485	0.2818	-48.6%	0.4	0.4
1.06	6.0	0.5026	0.2594	-48.4%	0.9	0.9	0.4870	0.251	-48.5%	0.3	0.9

Table (10) Maximum Forces in "v" and "w" Directions on Member No. 21

Wave Frequency ω (rad/s)	Wave Height Hw (m)	w Direction $F_{TW} \times 10^{-2}$ (N) LR SR = 0.0	SARPKAYA SR=0.005	Diff.%	Relative Time "tr" LR	SARPKAYA	v Direction $F_{TV} \times 10^{-6}$ (N) LR SR = 0.0	SARPKAYA SR= 0.005	Diff.%	Relative Time "tr" LR	SARPKAYA
0.37	30.0	2268	4541	100%	0.6	0.2	0.0	0.7368			0.8
0.42	20.0	1406	1716	22.1%	0.0	0.7	0.0	0.282			0.8
0.45	20.0	1335	1413	5.8%	0.0	0.7	0.0	0.1965			0.8
0.50	20.0	1162	1023	-12%	0.0	0.1	0.0	0.0605			0.8
0.56	20.0	901.9	707.2	-21.6%	0.0	0.6	0.0	0.0			
0.64	15.0	417.4	283.3	-32.1%	0.0	0.0	0.0	0.0			
0.75	11.0	118.2	78.77	-33.4%	0.0	0.0	0.0	0.0			
0.94	7.0	4.885	3.31	-32.2%	0.0	0.0	0.0	0.0			
1.06	6.0	0.1392	0.09282	-33.3%	0.0	0.0	0.0	0.0			

Table (11) Maximum Forces in "v" and "w" Directions on Member No. 4

Wave Frequency ω (rad/s)	Wave Height Hw (m)	w Direction $F_{TW} \times 10^{-6}$ (N) LR SR = 0.0	SARPKAYA SR = 0.005	Diff.%	Relative Time "tr" LR	SARPKAYA	v Direction $F_{TV} \times 10^{-6}$ (N) LR SR = 0.0	SARPKAYA SR = 0.005	Diff.%	Relative Time "tr" LR	SARPKAYA
0.37	30.0	0.7547	2.699	258%	0.8	0.4	0.7698	2.706	252%	0.2	1.0
0.42	20.0	0.6334	1.525	141%	0.2	0.4	0.6304	1.233	95.6%	0.7	0.4
0.45	20.0	0.7103	1.669	135%	0.2	0.4	0.6997	1.339	91.4%	0.7	0.4
0.50	20.0	0.8315	1.849	122%	0.7	0.9	0.8081	1.466	81.4%	0.7	0.4
0.56	20.0	0.9609	1.943	102%	0.7	0.9	0.9343	1.503	60.9%	0.1	0.9
0.64	15.0	0.8439	0.9483	12.4%	0.1	0.3	0.8556	0.672	-21.5%	0.6	0.8
0.75	11.0	0.7396	0.4536	-38.7%	0.6	0.2	0.7083	0.393	-44.5%	0.0	0.1
0.94	7.0	0.5453	0.2840	-47.9%	1.0	1.0	0.5485	0.2776	-49.4%	0.4	0.4
1.06	6.0	0.5026	0.2573	-48.8%	0.9	0.9	0.4870	0.2499	-48.7%	0.3	0.9

Table (12) Maximum Forces in "v" and "w" Directions on Member No. 21

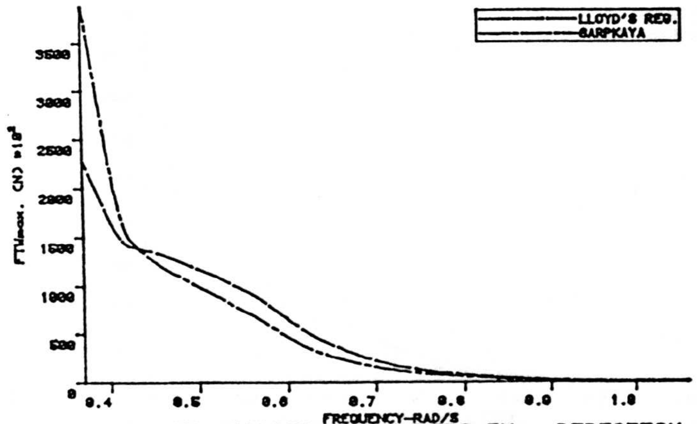

(a) MAX. FORCES ON MEMBERS IN w DIRECTION

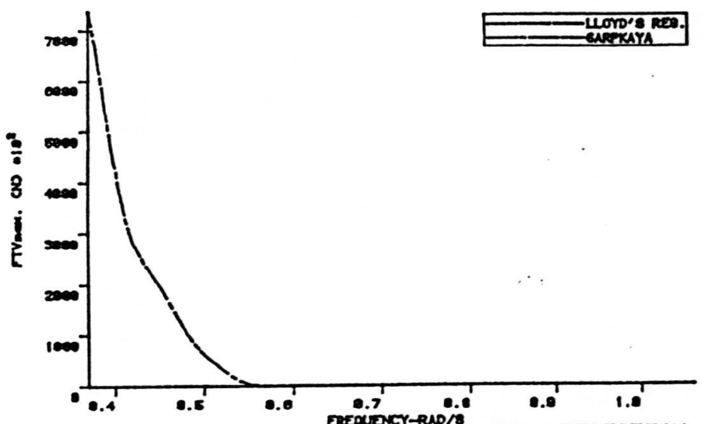

(b) MAX. FORCES ON MEMBERS IN v DIRECTION

SR = 1/800 PROGRAM: OSS ,COEFFICIENTS: LR & S, β = 0.0
FIG. (18) MAX. FORCES ON MEMBER (4) Vs. FREQUENCY

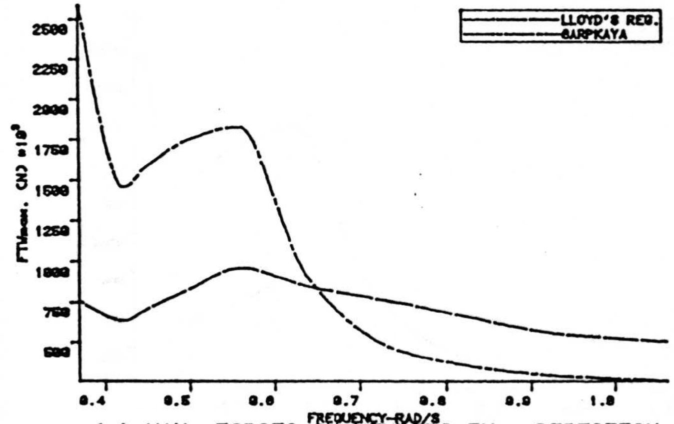

(a) MAX. FORCES ON MEMBERS IN w DIRECTION

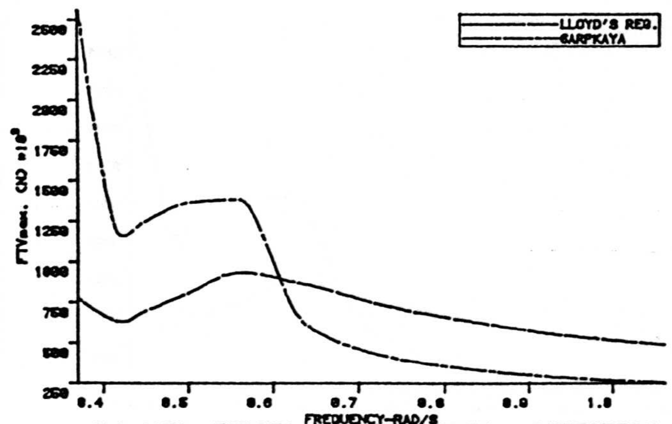

(b) MAX. FORCES ON MEMBERS IN v DIRECTION

SR = 1/800 PROGRAM: OSS ,COEFFICIENTS: LR & S, β = 0.0
FIG. (19) MAX. FORCES ON MEMBER (21) Vs. FREQUENCY

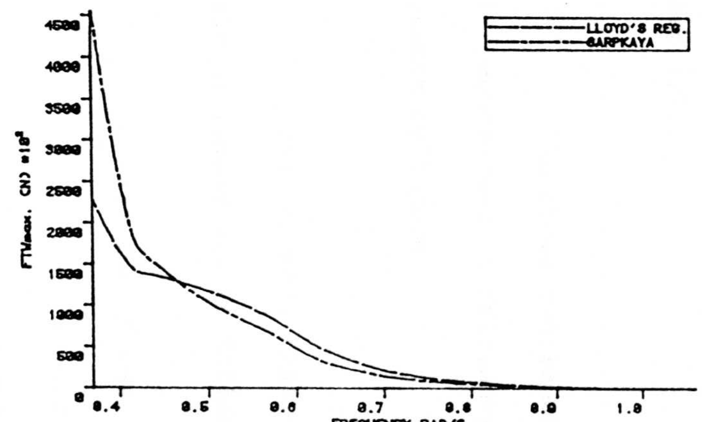

(a) MAX. FORCES ON MEMBERS IN w DIRECTION

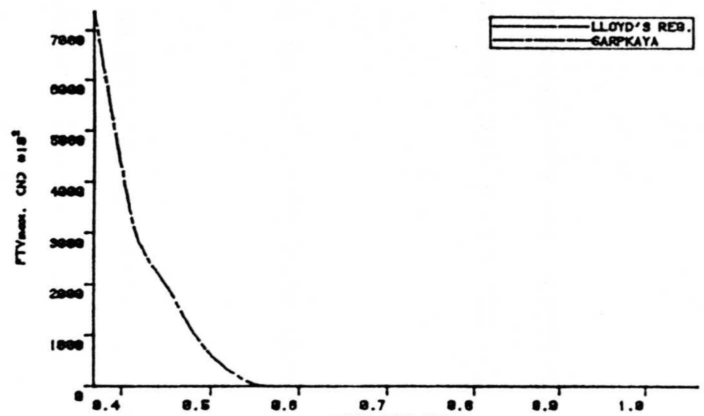

(b) MAX. FORCES ON MEMBERS IN v DIRECTION

SR = 1/200 PROGRAM: OSS , COEFFICIENTS: LR & S β = 0.0
FIG. (20) MAX. FORCES ON MEMBER (4) Vs. FREQUENCY

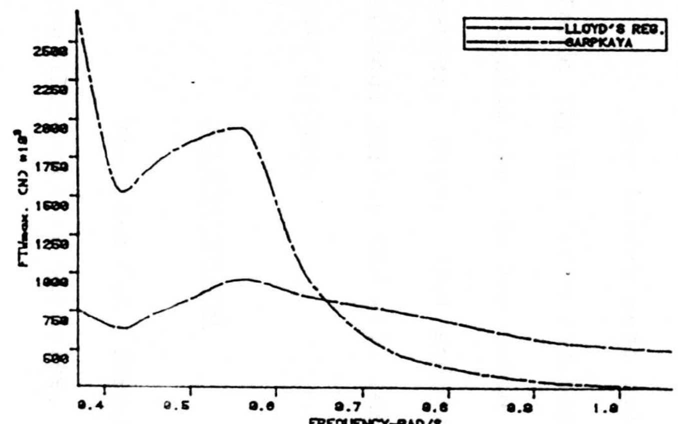

(a) MAX. FORCES ON MEMBERS IN w DIRECTION

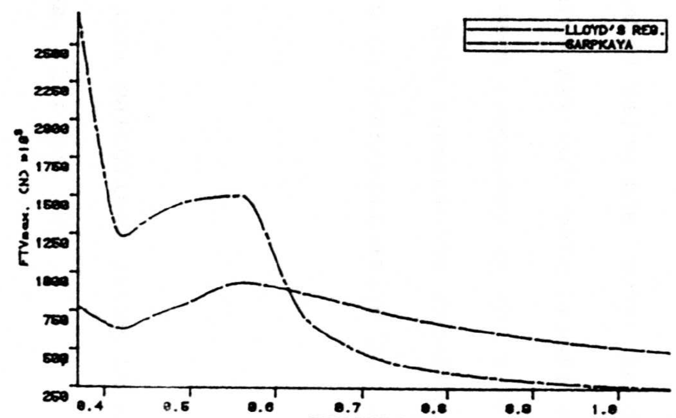

(b) MAX. FORCES ON MEMBERS IN v DIRECTION

SR = 1/200 PROGRAM: OSS , COEFFICIENTS: LR & S β = 0.0
FIG. (21) MAX. FORCES ON MEMBER (21) Vs. FREQUENCY

different frequencies, for each group of members, by three different methods as given below.

First Method

The forces were calculated using the wave heights given in Table (1) Chapter 4 and the force per unit wave height was obtained by dividing the maximum force at each frequency by the corresponding wave height, Figs. (22) and (23). This ignores the non-linear term in the viscous forces and will lead to an over-estimation of the force per unit height.

Second Method

The maximum forces were calculated using 1m wave height for the different frequencies, Figs. (24) and (25).

Third Method

The forces were calculated as in the first method but using waves of constant steepness of 1/15, Table (6), Chapter 4, Figs. (26) and (27).

The above mentioned calculations were carried out using both LR recommended coefficients and Sarpkaya's results (C_D, C_M and C_L) for smooth cylinders.

The graphs, Figs. (22) to (27), show some general trends which may be summarised as follows:-

a. (1) The forces on the horizontal members, Nos (1) to (6), in 'w' direction are largely inversely proportional to the frequency. Member No (7) shows an unsteady relation between the force and the frequency with a maximum value at $\omega = 0.6 - 0.8$ rad/s. The forces in 'v' direction (lift forces) showed similar behaviour when using Sarpkaya's lift coefficient. For member No (7), the maximum force occurred when $\omega = 0.56$ rad/s. According to LR, there are no forces in 'v' direction because $C_L = 0.0$ in this case. The graph may also be regarded as reflecting the effect of depth below surface with the highest force being experienced by member No (7) which is the nearest to the surface.

(2) The forces on the inclined members in 'w' direction, Nos (8) to (12), tend to be inversely proportional to the frequency. Members No (13) and (14) which are the nearest to the surface have different trends. In the range of $\omega = 0.56$ to 1.06 rad/s, the force on member No (13) is almost constant, while for member No (14), the force is directly proportional to the frequency.

In 'v' direction, the forces per unit wave height are almost constant in magnitude for all members except member No (14) where the force is directly proportional to the wave frequency.

(3) The forces on the third group of members, Nos (15) to (21), have the same trend in both 'v' and 'w' directions. The forces per unit wave height slightly decrease with frequency for all members except No (21) which is a surface piercing member, for which the force is directly proportional to the frequency.

b. As far as the differences in force estimation by LR and

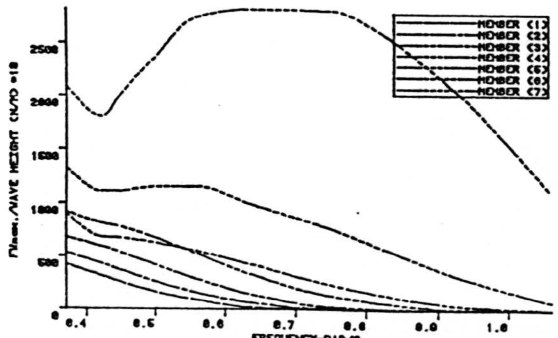

(a) MAX. FORCES ON MEMBERS IN w DIRECTION

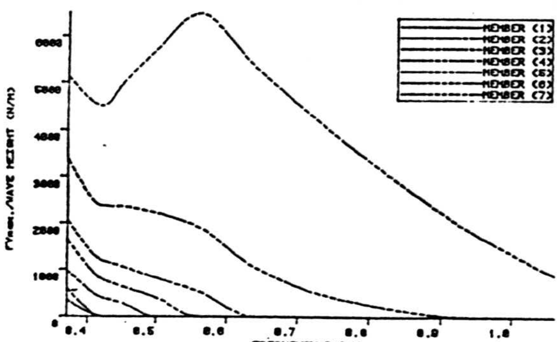

(b) MAX. FORCES ON MEMBERS IN v DIRECTION

PROGRAM: OSS , COEFFICIENTS: SARP , $\beta = 0.0$
FIG.(22.1) MAX. FORCES/UNIT WAVE HEIGHT Vs. FREQUENCY

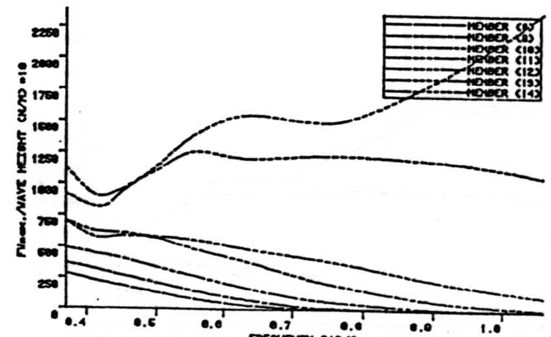

(a) MAX. FORCES ON MEMBERS IN w DIRECTION

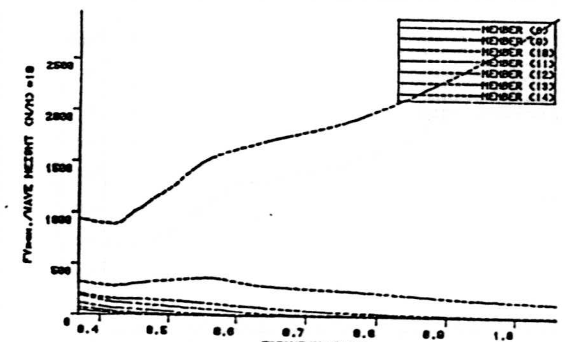

(b) MAX. FORCES ON MEMBERS IN v DIRECTION

PROGRAM: OSS , COEFFICIENTS: SARP , $\beta = 0.0$
FIG.(22.2) MAX. FORCES/UNIT WAVE HEIGHT Vs. FREQUENCY

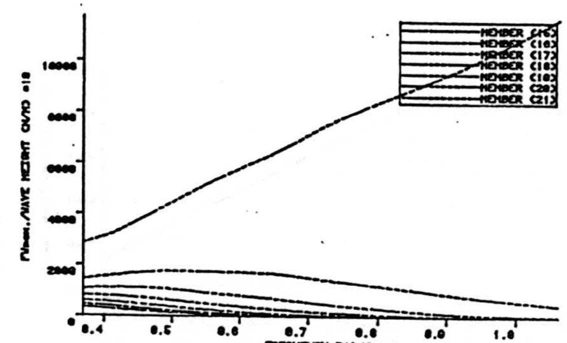

(a) MAX. FORCES ON MEMBERS IN w DIRECTION

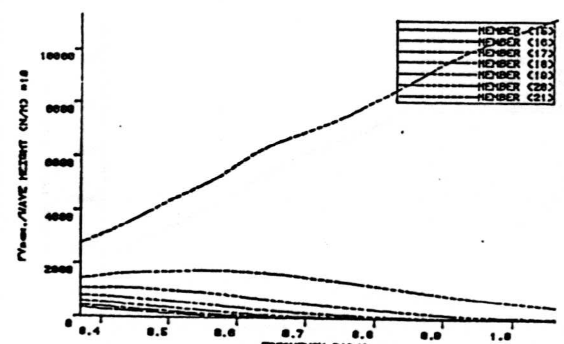

(b) MAX. FORCES ON MEMBERS IN v DIRECTION

PROGRAM: OSS , COEFFICIENTS: SARP , $\beta = 0.0$
FIG.(22.3) MAX. FORCES/UNIT WAVE HEIGHT Vs. FREQUENCY

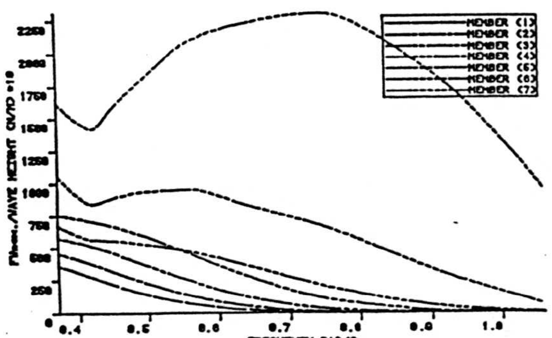

(a) MAX. FORCES ON MEMBERS IN w DIRECTION

PROGRAM: OSS ,COEFFICIENTS: LR ,β = 0.0
FIG. (23.1) MAX. FORCES/UNIT WAVE HEIGHT Vs. FREQUENCY

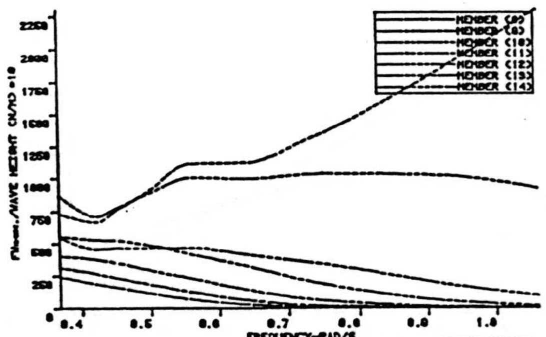

(a) MAX. FORCES ON MEMBERS IN w DIRECTION

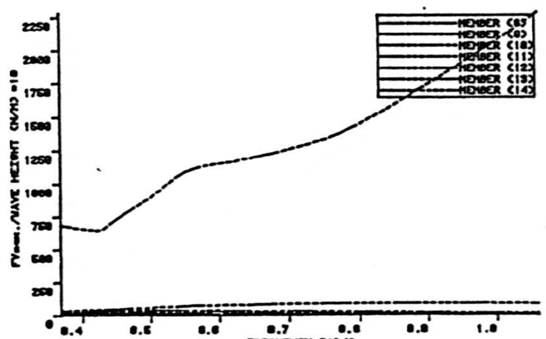

(b) MAX. FORCES ON MEMBERS IN v DIRECTION

PROGRAM: OSS ,COEFFICIENTS: LR ,β = 0.0
FIG. (23.2) MAX. FORCES/UNIT WAVE HEIGHT Vs. FREQUENCY

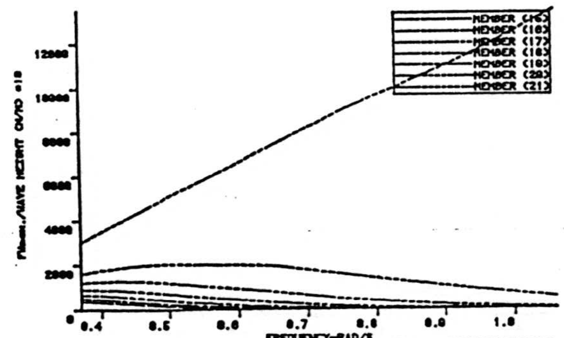

(a) MAX. FORCES ON MEMBERS IN w DIRECTION

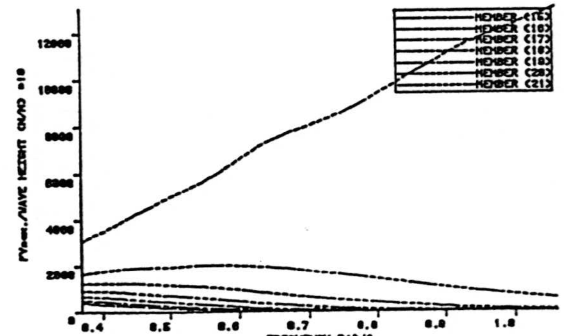

(b) MAX. FORCES ON MEMBERS IN v DIRECTION

PROGRAM: OSS ,COEFFICIENTS: LR ,β = 0.0
FIG. (23.3) MAX. FORCES/UNIT WAVE HEIGHT Vs. FREQUENCY

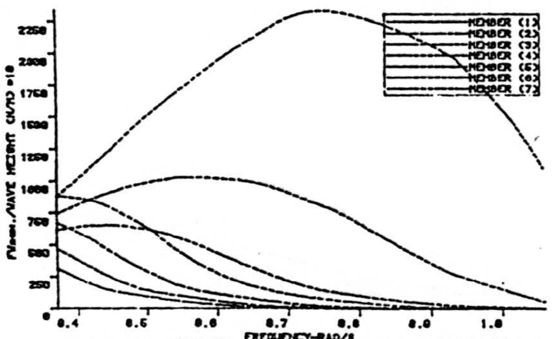

(a) MAX. FORCES ON MEMBERS IN w DIRECTION

H = 1.0 m PROGRAM: OSS , COEFFICIENTS: SARP , β = 0.0
FIG. (24.1) MAX. FORCES/UNIT WAVE HEIGHT Vs. FREQUENCY

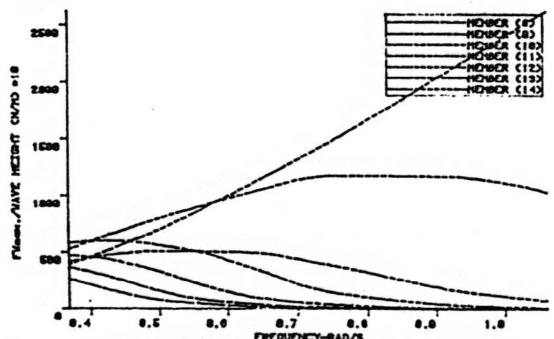

(a) MAX. FORCES ON MEMBERS IN w DIRECTION

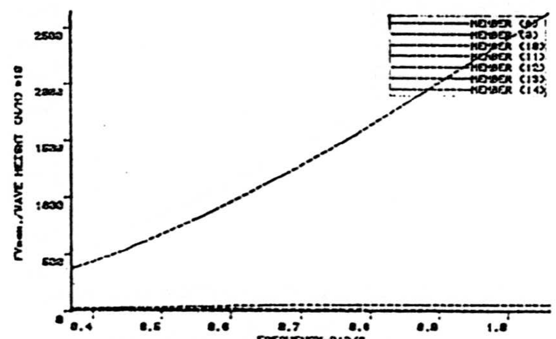

(b) MAX. FORCES ON MEMBERS IN v DIRECTION

H = 1.0 m PROGRAM: OSS , COEFFICIENTS: SARP , β = 0.0
FIG. (24.2) MAX. FORCES/UNIT WAVE HEIGHT Vs. FREQUENCY

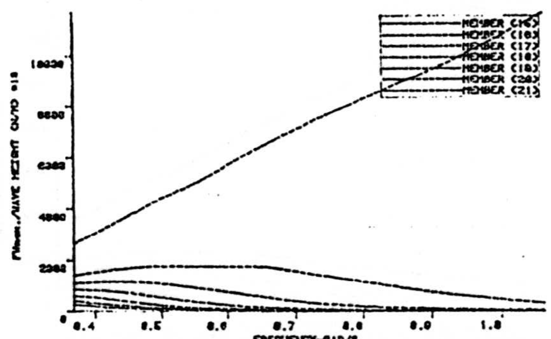

(a) MAX. FORCES ON MEMBERS IN w DIRECTION

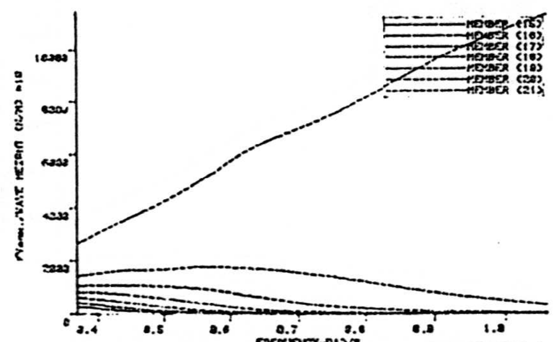

(b) MAX. FORCES ON MEMBERS IN v DIRECTION

H = 1.0 m PROGRAM: OSS , COEFFICIENTS: SARP , β = 0.0
FIG. (24.3) MAX. FORCES/UNIT WAVE HEIGHT Vs. FREQUENCY

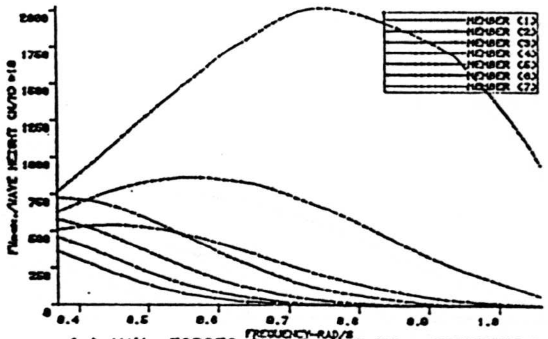

(a) MAX. FORCES ON MEMBERS IN w DIRECTION

PROGRAM: OSS ,COEFFICIENTS: LR , β = 0.0
FIG.(25.1) MAX. FORCES/UNIT WAVE HEIGHT Vs. FREQUENCY

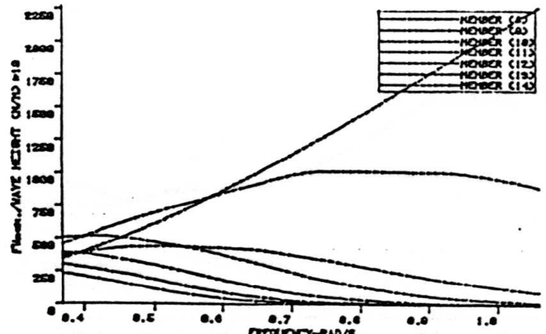

(a) MAX. FORCES ON MEMBERS IN w DIRECTION

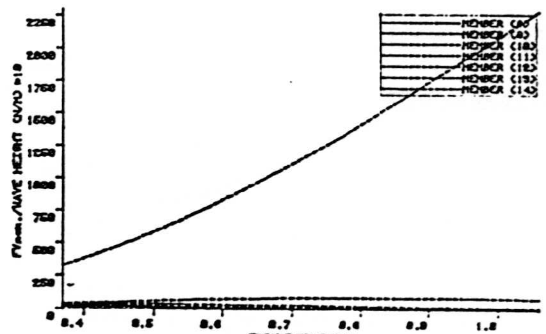

(b) MAX. FORCES ON MEMBERS IN v DIRECTION

PROGRAM: OSS ,COEFFICIENTS: LR , β = 0.0
FIG.(25.2) MAX. FORCES/UNIT WAVE HEIGHT Vs. FREQUENCY

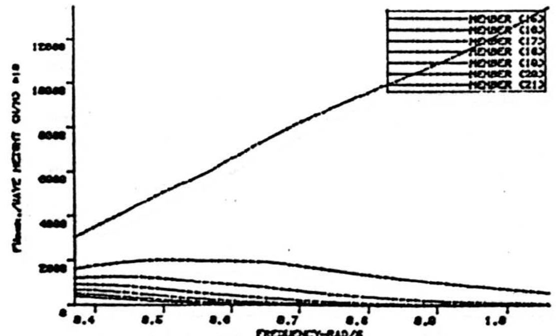

(a) MAX. FORCES ON MEMBERS IN w DIRECTION

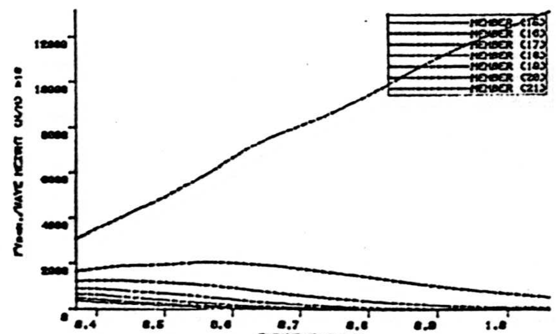

(b) MAX. FORCES ON MEMBERS IN v DIRECTION

PROGRAM: OSS ,COEFFICIENTS: LR , β = 0.0
FIG.(25.3) MAX. FORCES/UNIT WAVE HEIGHT Vs. FREQUENCY

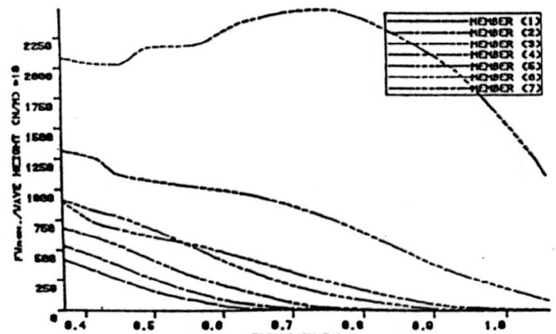

(a) MAX. FORCES ON MEMBERS IN w DIRECTION

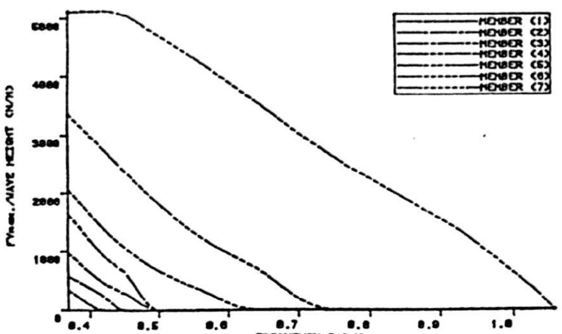

(b) MAX. FORCES ON MEMBERS IN v DIRECTION

H/λ = 1/15 PROGRAM: OSS , COEFFICIENTS: SARP, β = 0.0
FIG. (26.1) MAX. FORCES/UNIT WAVE HEIGHT Vs. FREQUENCY

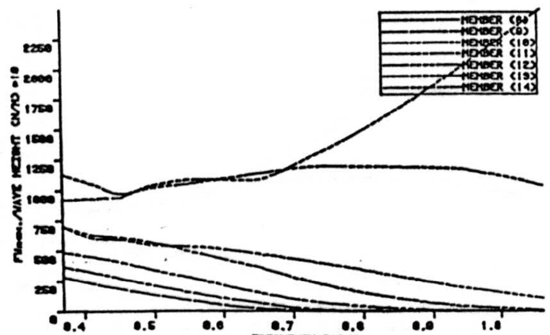

(a) MAX. FORCES ON MEMBERS IN w DIRECTION

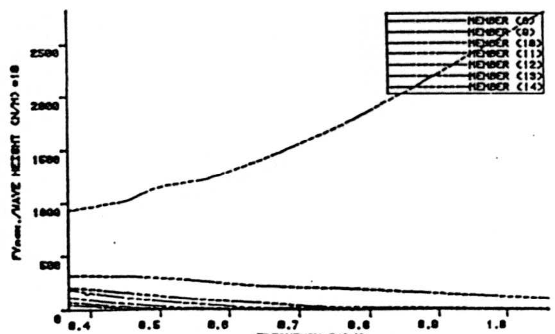

(b) MAX. FORCES ON MEMBERS IN v DIRECTION

H/λ = 1/15 PROGRAM: OSS , COEFFICIENTS: SARP, β = 0.0
FIG. (26.2) MAX. FORCES/UNIT WAVE HEIGHT Vs. FREQUENCY

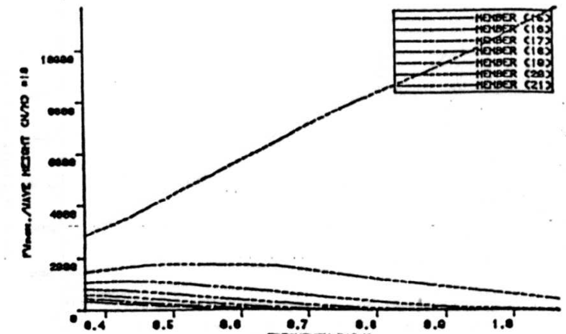

(a) MAX. FORCES ON MEMBERS IN w DIRECTION

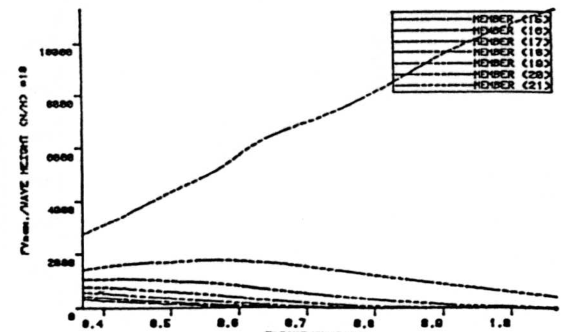

(b) MAX. FORCES ON MEMBERS IN v DIRECTION

H/λ = 1/15 PROGRAM: OSS , COEFFICIENTS: SARP, β = 0.0
FIG. (26.3) MAX. FORCES/UNIT WAVE HEIGHT Vs. FREQUENCY

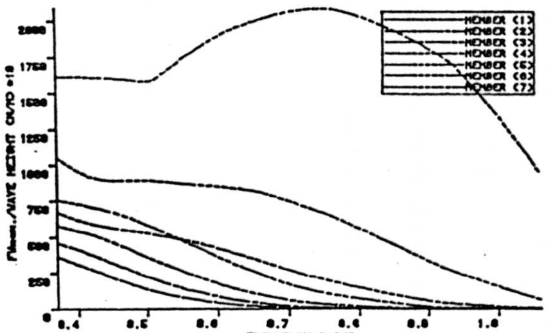

(a) MAX. FORCES ON MEMBERS IN w DIRECTION

PROGRAM: OSS ,COEFFICIENTS: LR , β = 0.0
FIG.(27.1) MAX. FORCES/UNIT WAVE HEIGHT Vs. FREQUENCY

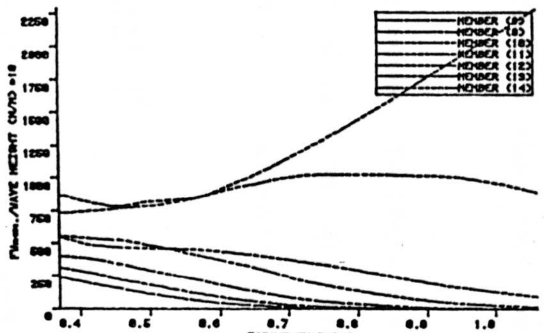

(a) MAX. FORCES ON MEMBERS IN w DIRECTION

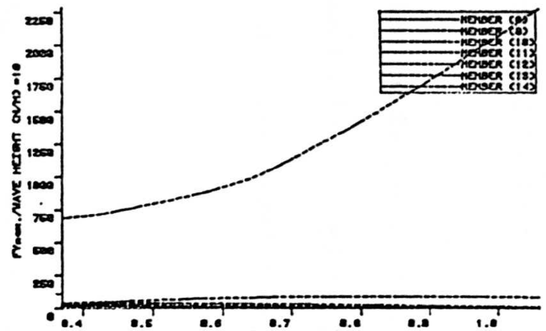

(b) MAX. FORCES ON MEMBERS IN v DIRECTION

PROGRAM: OSS ,COEFFICIENTS: LR , β = 0.0
FIG.(27.2) MAX. FORCES/UNIT WAVE HEIGHT Vs. FREQUENCY

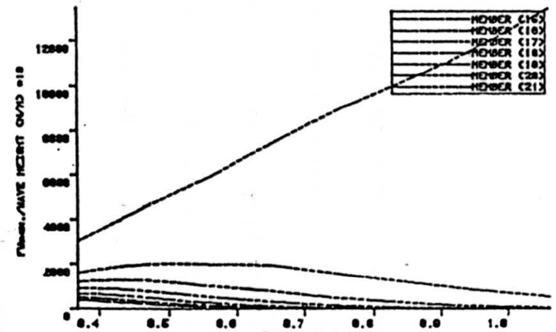

(a) MAX. FORCES ON MEMBERS IN w DIRECTION

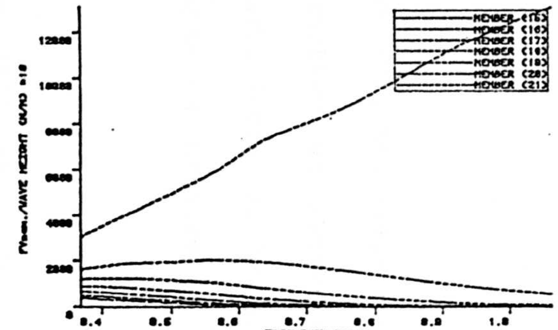

(b) MAX. FORCES ON MEMBERS IN v DIRECTION

PROGRAM: OSS ,COEFFICIENTS: LR , β = 0.0
FIG.(27.3) MAX. FORCES/UNIT WAVE HEIGHT Vs. FREQUENCY

Sarpkaya, the results for the members near the water surface (which had the largest forces) show that:-

First Method

(1) For the horizontal member No (7), the maximum force per unit wave height in 'w' direction was increased by 22% when using Sarpkaya's coefficients. In 'w' direction, there is no force according to LR because C_L is not considered.

(2) For the inclined member No (14), the maximum force in 'w' direction was increased by 3.4% and in 'v' direction the force was increased by 29.4%.

(3) For member No (21), according to Sarpkaya, the force in 'w' direction was reduced by 13.3% (relative to LR), and in 'v' direction, the force was reduced by 13.5%.

Second Method

(1) For the horizontal member No (7), the maximum force in 'w' direction was increased by 15.5% according to Sarpkaya. In 'v' direction, there are no forces in both cases of LR and Sarpkaya. Since the value of Keulegan-Carpenter number K in this case is small (less than 5), according to Sarpkaya's results, $C_L = 0.0$.

(2) For member No (14), the forces in both 'w' and 'v' directions were increased by 15.5%.

(3) For member No (21), according to Sarpkaya, the forces in 'w' and 'v' directions were reduced by 13.3% and 13.5% respectively.

Third Method

(1) For member No (7), the force in 'w' direction according to Sarpkaya was increased by 19.1%. In 'w' direction there is no force according to LR.

(2) For member No (14), the force in 'w' direction according to Sarpkaya was increased by 8.9% and in 'v' direction the force was increased by 23.7%.

(3) For member No (21), the forces in 'w' and 'v' directions were reduced (relative to LR) by 13.4% and 13.5% respectively.

5.2 Total Forces and Moments on the Structure

Tables (13) to (16) summarise the results of calculations using both LR recommended coefficients and Sarpkaya's data for C_D, C_M and C_L. The results correspond to the case of smooth cylinders (SR = 0.0). The second row in the tables shows the results when the lift (transverse) forces are neglected, ie $C_L = 0.0$, while the third row shows the results when the lift forces are taken into account. For the case of $C_L = 0.0$ (second row), the results are analysed as shown below.

5.2.1 Maximum Surge, Heave and Sway Forces ($\beta = 0.0$)

From Table (13), the following was noted:-

a. The differencess between LR and Sarpkaya's results are smallest for the surge forces. From $\omega = 0.42$ rad/s to $\omega = 0.64$ rad/s, the values are the same for both LR and Sarpkaya. At $\omega = 0.37$ rad/s and $\omega = 0.75$ rad/s, the surge forces were decreased by 15.6% and 11% respectively.

b. The differences in the heave forces varied from 22.1% ($\omega = 0.42$ rad/s) to 31% ($\omega = 0.94$ rad/s) (Sarpkaya's being larger).

c. The differences in the sway forces varied from 16% ($\omega = 1.06$ rad/s) to a maximum of 35% ($\omega = 0.45$ rad/s).

5.2.2 Maximum Rolling, Yawing and Pitching Moments ($\beta = 0.0$)

From Table (14), the following was noted:-

a. The differences in the rolling moments ranged from 16.1% ($\omega = 1.06$ rad/s) to 33.8% ($\omega = 0.42$ rad/s). Except when $\omega = 0.37$ rad/s, the differences are decreasing with the increase of frequency.

b. The yawing moments had differences similar to those of the rolling moments ranging from 15.1% ($\omega = 1.06$ rad/s) to 34.9% ($\omega = 0.45$ rad/s).

c. The differences in the pitching moments are negligible in the range of frequencies from $\omega = 0.42$ rad/s to $\omega = 0.75$ rad/s. For the other frequencies, the differences ranged from -10.4% ($\omega = 0.94$ rad/s) to 2.8% ($\omega = 0.37$ rad/s).

β = 0.0	Surge Force x 10^{-8} (N)					Heave Force x 10^{-7} (N)					Sway Force x 10^{-6} (N)				
Coefficients	ω (rad/s)					ω (rad/s)					ω (rad/s)				
	0.37	0.42	0.45	0.50	0.56	0.37	0.42	0.45	0.50	0.56	0.37	0.42	0.45	0.50	0.56
LR	0.2087	0.1382	0.1377	0.1332	0.1229	1.274	0.7665	0.7649	0.7533	0.7303	0.1392	0.09205	0.1058	0.1320	0.1673
SARPKAYA CL = 0.0 SR = 0.0	0.2105 0.9%	0.1376	0.1372	0.1330	0.1233	1.609 26.3%	0.9361 22.1%	0.9376 22.6%	0.9310 23.6%	0.9139 25.1%	0.1647 18.3%	0.1238 34.5%	0.1428 35%	0.1776 34.5%	0.2243 34.1%
SARPKAYA SR = 0.0	0.2241 7.4%	0.1434 3.8%	0.1428 3.7%	0.1382 3.8%	0.1280 4.1%	1.575 23.6%	0.8883 15.9%	0.8906 16.4%	0.8854 17.5%	0.8707 19.2%	1.931 1287%	0.9025 880%	0.9155 765%	0.9292 604%	0.9495 468%
Coefficients	ω (rad/s)				ω (rad/s)				ω (rad/s)						
	0.64	0.75	0.94	1.06	0.64	0.75	0.94	1.06	0.64	0.75	0.94	1.06			
LR	0.07423	0.03105	0.01225	0.02558	0.4669	0.2594	0.05904	0.01125	0.1404	0.1277	0.07461	0.03751			
SARPKAYA CL = 0.0 SR = 0.0	0.07439	0.03145 1.3%	0.01034 -15.6%	0.02277 -11%	0.5914 26.7%	0.3256 25.5%	0.07737 31%	0.01451 29%	0.1756 25.1%	0.1498 17.3%	0.08686 16.4%	0.0435 16%			
SARPKAYA SR = 0.0	0.07651 3.1%	0.03223 3.8%	0.01037 -15.3%	0.02309 -9.7%	0.5692 21.9%	0.3173 22.3%	0.07968 35%	0.01616 43.6%	0.5901 320%	0.3634 185%	0.1412 89.3%	0.06952 85.3%			

Table (13) Maximum Surge, Heave and Sway Forces (LR & SARPKAYA, β = 0.0)

β = 0.0	Rolling Moment x 10^{-8} (NM)					Yawing Moment x 10^{-7} (NM)					Pitching Moment x 10^{-9} (NM)				
Coefficients	ω (rad/s)					ω (rad/s)					ω (rad/s)				
	0.37	0.42	0.45	0.50	0.56	0.37	0.42	0.45	0.50	0.56	0.37	0.42	0.45	0.50	0.56
LR	0.2091	0.1457	0.1717	0.2197	0.2824	0.09685	0.07592	0.09567	0.1407	0.2172	1.981	1.386	1.428	1.454	1.411
SARPKAYA CL = 0.0 SR = 0.0	0.2502 19.7%	0.1950 33.8%	0.2298 33.8%	0.2932 33.5%	0.3755 33%	0.1138 17.5%	0.1014 33.6%	0.1291 34.9%	0.1896 34.8%	0.2927 34.8%	2.036 2.8%	1.375 -0.8%	1.417 -0.8%	1.445 -0.6%	1.407
SARPKAYA SR = 0.0	2.225 964%	1.150 689%	1.205 602%	1.283 484%	1.363 383%	0.4221 336%	0.2291 202%	0.3168 231%	0.4553 224%	0.6018 177%	2.161 9.1%	1.454 4.9%	1.496 4.8%	1.522 4.7%	1.481 5%
Coefficients	ω (rad/s)				ω (rad/s)				ω (rad/s)						
	0.64	0.75	0.94	1.06	0.64	0.75	0.94	1.06	0.64	0.75	0.94	1.06			
LR	0.2418	0.2217	0.1412	0.08591	0.2318	0.2577	0.2939	0.2976	0.8910	0.3758	0.1950	0.3777			
SARPKAYA CL = 0.0 SR = 0.0	0.3009 24.4%	0.2616 18%	0.1647 16.6%	0.09974 16.1%	0.2911 25.6%	0.3054 18.5%	0.3385 15.2%	0.3424 15.1%	0.8857 -0.6%	0.3738 -0.5%	0.1748 -10.4%	0.3432 -9.1%			
SARPKAYA SR = 0.0	0.8839 266%	0.5665 156%	0.2430 72.1%	0.1374 59.9%	0.3668 58.2%	0.4624 79.4%	0.4824 64.1%	0.4437 49.1%	0.9227 3.6%	0.3889 3.8%	0.1736 -11%	0.3472 -8.1%			

Table (14) Maximum Rolling, Yawing and Pitching Moments (LR & SARPKAYA, β = 0.0)

5.2.3 Maximum Surge, Heave and Sway Forces ($\beta = \pi/4$)

From the second row of Table (15), the following was noted:-

a. Due to the symmetry of the jacket structure, the surge forces and sway forces are identical. Up to ω = 0.64 rad/s, the differences in the forces as calculated by LR and Sarpkaya's coefficients are negligible. Otherwise, the differences ranged from 1.4% (ω = 0.75 rad/s) to 11.3% (ω = 1.06 rad/s).

b. The differences in the heave forces are larger than those of the surge or sway forces. The variations ranged from 14.7% (ω = 1.06 rad/s) to 27.1% (ω = 0.37 rad/s).

5.2.4 Maximum Rolling, Yawing and Pitching Moments ($\beta = \pi/4$)

From Table (16), the following was noted:-

a. Due to the symmetry of the structure, the values of the rolling moments are identical to the values of the pitching moments. The percentage differences between LR and Sarpkaya's results are relatively small, ranging from -1.1% (ω = 0.42 rad/s) to 10.6% (ω = 0.94 rad/s).

b. The differences in the yawing moments are much larger compared with the rolling or pitching moments. Up to ω = 0.75 rad/s, the moments were increased by 19.9% (ω = 0.75 rad/s) to 122% (ω = 0.37 rad/s). For ω = 0.94 rad/s and ω = 1.06 rad/s, the moments were decreased by 6.5% and 12.5% respectively.

$\beta = \frac{\pi}{4}$	Surge Force x 10^{-7} (N)					Heave Force x 10^{-7} (N)					Sway Force x 10^{-7} (N)				
Coefficients	ω (rad/s)					ω (rad/s)					ω (rad/s)				
	0.37	0.42	0.45	0.50	0.56	0.37	0.42	0.45	0.50	0.56	0.37	0.42	0.45	0.50	0.56
LR	1.472	0.9807	0.9788	0.9518	0.8890	1.268	0.7641	0.7626	0.7514	0.7305	1.470	0.9799	0.9781	0.9511	0.8883
SARPKAYA CL = 0.0 SR = 0.0	1.481 0.6%	0.9744 -0.6%	0.9732 -0.6%	0.9481	0.8892	1.611 27.1%	0.9333 22.1%	0.9345 22.5%	0.9273 23.4%	0.9123 24.9%	1.480 0.7%	0.9737 -0.6%	0.9725 -0.6%	0.9474	0.8885
SARPKAYA SR = 0.0	1.642 11.5%	1.045 6.6%	1.045 6.8%	1.02 7.2%	0.9602 8%	1.577 24.4%	0.8715 14.1%	0.8721 14.4%	0.8657 15.2%	0.8488 16.2%	1.622 13.1%	1.050 7.2%	1.048 7.1%	1.02 7.2%	0.9574 7.8%

Coefficients	ω (rad/s)				ω (rad/s)				ω (rad/s)			
	0.64	0.75	0.94	1.06	0.64	0.75	0.94	1.06	0.64	0.75	0.94	1.06
LR	0.5631	0.292	0.07335	0.05711	0.4754	0.2804	0.1070	0.06487	0.5627	0.2918	0.07332	0.05708
SARPKAYA CL = 0.0 SR = 0.0	0.5628	0.2691 1.4%	0.08269 12.7%	0.0636 11.4%	0.5973 25.6%	0.3466 23.6%	0.1283 19.9%	0.07443 14.7%	0.5624	0.2959 1.4%	0.08262 12.7%	0.06355 11.3%
SARPKAYA SR = 0.0	0.5981 6.2%	0.3111 6.5%	0.08651 17.9%	0.06494 13.7%	0.5620 18.2%	0.3295 17.5%	0.1233 15.2%	0.07167 10.5%	0.5994 6.5%	0.3148 7.9%	0.08681 18.4%	0.0649 13.7%

Table (15) Maximum Surge, Heave and Sway Forces (LR & SARPKAYA, $\beta = \frac{\pi}{4}$)

$\beta = \frac{\pi}{4}$	Rolling Moment x 10^{-9} (NM)					Yawing Moment x 10^{-5} (NM)					Pitching Moment x 10^{-9} (NM)				
Coefficients	ω (rad/s)					ω (rad/s)					ω (rad/s)				
	0.37	0.42	0.45	0.50	0.56	0.37	0.42	0.45	0.50	0.56	0.37	0.42	0.45	0.50	0.56
LR	1.395	0.9828	1.014	1.038	1.021	0.1705	0.1211	0.1515	0.2174	0.3267	1.396	0.9836	1.015	1.039	1.022
SARPKAYA CL = 0.0 SR = 0.0	1.474 5.7%	0.9723 -1.1%	1.003 -1.1%	1.028 -1.0%	1.014 -0.7%	0.3792 122%	0.2679 121%	0.3176 110%	0.1409 89%	0.5479 67.7%	1.475 5.7%	0.9729 -1.1%	1.004 -1.1%	1.029 -1.0%	1.015 -0.7%
SARPKAYA SR = 0.0	1.613 15.6%	1.070 8.9%	1.103 8.8%	1.128 8.7%	1.113 9%	105.9 very large differences	50.09	55.50	59.35	71.77	1.594 14.2%	1.066 8.4%	1.101 8.5%	1.130 8.8%	1.118 9.4%

Coefficients	ω (rad/s)				ω (rad/s)				ω (rad/s)			
	0.64	0.75	0.94	1.06	0.64	0.75	0.94	1.06	0.64	0.75	0.94	1.06
LR	0.6802	0.366	0.08996	0.07345	0.3572	0.4458	0.7476	0.9791	0.6807	0.3662	0.08998	0.07347
SARPKAYA CL = 0.0 SR = 0.0	0.6741 -0.9%	0.3666	0.0995 10.6%	0.08051 9.6%	0.5188 45.2%	0.5345 19.9%	0.6992 -6.5%	0.8564 -12.5%	0.6746 -0.9%	0.3668	0.09955 10.6%	0.08055 9.6%
SARPKAYA SR = 0.0	0.7296 7.3%	0.3958 8.1%	0.1063 18.2%	0.08290 12.9%	45.78 very large differences	21.01	1.598 114%	1.832 87.1%	0.7285 7%	0.3906 6.7%	0.1058 17.6%	0.08293 12.9%

Table (16) Maximum Rolling, Yawing and Pitching Moments (LR & SARPKAYA, $\beta = \frac{\pi}{4}$)

6. THE EFFECT OF TRANSVERSE FORCE (LIFT) ON WAVE LOADING

Tables (13) to (16) (third row) show the differences in the total forces and moments between LR and Sarpkaya due to the effect of the lift forces. Since the values of the Reynolds number (R_e) were relatively high, Table (1), the lift coefficient C_L was in the range of 0.2 (smooth cylinders). However, despite the small value of C_L, its effect on the total forces and moments is quite noticeable as indicated below.

6.1 Maximum Surge, Heave and Sway Forces (β = 0.0)

Table (13) shows that:-

a. The surge forces gave the lowest differences compared with the heave or sway forces ranging from -15.3% (ω = 0.94 rad/s) to 7.4% (ω = 0.37 rad/s).

b. The heave forces came in the second place and gave differences ranging from 15.9% (ω = 0.42 rad/s) to 43.6% (ω = 1.06 rad/s).

c. As might be expected, the introduction of the transverse (lift) forces had considerable effect on the magnitude of the sway forces. The differences decrease with the increase of frequency ranging from 85.3% (ω = 1.06 rad/s) to a maximum of over 1000% (ω = 0.37 rad/s). However, these forces are still much less than the surge forces although the gap between the two has been gradually reduced.

6.2 Maximum Rolling, Yawing and Pitching Moments ($\beta = 0.0$)

Similar to the sway forces, both the rolling and yawing moments, Table (14), were largely affected by the lift forces, while the pitching moments were slightly affected as shown below:-

a. The differences in the rolling moments ranged from 59.9% ($\omega = 1.06$ rad/s) to a maximum of 964% ($\omega = 0.37$ rad/s).

b. The differences in the yawing moments ranged from 49.1% ($\omega = 1.06$ rad/s) to a maximum of 336% ($\omega = 0.37$ rad/s).

c. Up to $\omega = 0.75$ rad/s, the pitching moments were increased by 3.8% ($\omega = 0.75$ rad/s) to 9.1% ($\omega = 0.37$ rad/s). For the higher frequencies, $\omega = 0.94$ rad/s, $\omega = 1.06$ rad/s, the pitching moments were reduced by 11% and 8.1%, respectively.

6.3 Maximum Surge, Heave and Sway Forces ($\beta = \pi/4$)

Due to the symmetry of the structure, the values of the surge and sway forces and the percentage differences, Table (15), are approximately the same:-

a. The differences in the surge forces ranged from 6.2% ($\omega = 0.64$ rad/s) to 17.9% ($\omega = 0.94$ rad/s).

b. The differences in the heave forces ranged from 10.5% ($\omega = 1.06$ rad/s) to 24.4% ($\omega = 0.37$ rad/s).

c. The differences in the sway forces ranged from 6.5% ($\omega = 0.64$ rad/s) to 18.4% ($\omega = 0.94$ rad/s).

6.4 Maximum Rolling, Yawing and Pitching Moments ($\beta = \pi/4$)

Table (16) shows that the values of the rolling moments and the pitching moments are almost the same. This applies also to the percentage differences from LR results.

a. The differences in the rolling moments ranged from 7.3% ($\omega = 0.64$ rad/s) to 18.2% ($\omega = 0.94$ rad/s).

b. In the range of frequency from $\omega = 0.37$ rad/s to $\omega = 0.75$ rad/s, the differences in the yawing moments are extremely large. At $\omega = 0.94$ rad/s and $\omega = 1.06$ rad/s, the differences are 114% and 87.1%, respectively.

c. The differences in the pitching moments ranged from 6.7% ($\omega = 0.75$ rad/s) to 17.6% ($\omega = 0.94$ rad/s).

7. THE EFFECT OF SURFACE ROUGHNESS ON WAVE LOADING

To investigate the effect of roughness on wave loading, the calculations were carried out using Sarpkaya's coefficients (C_D, C_M and C_L) for two assumed values of the relative roughness, namely SR = 1/800 (or 0.00125), and SR = 1/200 (or 0.005). The results were compared with those of the smooth cylinders (SR = 0.0) as shown in Tables (17) to (20).

7.1 Maximum Surge, Heave and Sway Forces ($\beta = 0.0$)

Table (17) shows that:-

a. When SR = 1/800, the differences in the surge forces (relative to the smooth cylinders) ranged from -27.6%

(ω = 0.94 rad/s) to 43.1% (ω = 0.37 rad/s). When SR = 1/200, the differences ranged from -23.4% (ω = 0.94 rad/s) to 55.8% (ω = 0.37 rad/s).

b. When SR = 1/800, the differences in the heave forces ranged widely from -4.1% (ω = 0.75 rad/s) to 324% (ω = 1.06 rad/s). When SR = 1/200, the differences ranged from 17.5% (ω = 0.75 rad/s) to 305% (ω = 1.06 rad/s).

c. The sway forces were largely affected by the surface roughness. For the two values of the surface roughness, the percentage differences are almost the same. When SR = 1/800, the differences ranged from 568% (ω = 1.06 rad/s) to 800% (ω = 0.42 rad/s) and when SR = 1/200, the differences ranged from 566% (ω = 1.06 rad/s) to 800% (ω = 0.42 rad/s). This may be explained by the fact that the sway forces are dominated by the lift forces especially for rough cylinders where the lift coefficient C_L may have values up to 3, see Fig.(6), and since C_L is assumed to be the same irrespective of the relative roughness, the absolute values of the sway forces and also the percentage differences (relative to the smooth cylinders) for the two cases of the surface roughness are the same.

7.2 Maximum Rolling, Yawing and Pitching Moments (β = 0.0)

Table (18) shows that:-

a. The rolling moments were largely affected by the surface roughness. Similar to the sway forces, the values of the rolling moments and also the percentage differences, relative to the smooth cylinders are the same for the two

β = 0.0	Surge Force x 10^{-8} (N)					Heave Force x 10^{-7} (N)					Sway Force x 10^{-6} (N)				
Coefficients	ω (rad/s)					ω (rad/s)					ω (rad/s)				
	0.37	0.42	0.45	0.50	0.56	0.37	0.42	0.45	0.50	0.56	0.37	0.42	0.45	0.50	0.56
SARPKAYA SR = 0.0	0.2241	0.1434	0.1428	0.1382	0.1280	1.575	0.8883	0.8906	0.8854	0.8707	1.931	0.9025	0.9155	0.9292	0.9495
SARPKAYA SR = 0.00125	0.3206 43.1%	0.1704 18.8%	0.1674 17.2%	0.1609 16.4%	0.1550 21.1%	2.513 59.6%	1.120 26.1%	1.124 26.2%	1.136 28.3%	1.139 30.8%	14.58 655.%	8.126 800%	7.924 766%	7.623 720%	7.476 687%
SARPKAYA SR = 0.005	0.3491 55.8%	0.1773 23.6%	0.1758 23.1%	0.1726 24.9%	0.1671 30.5%	2.964 88.2%	1.331 49.8%	1.338 50.2%	1.348 52.2%	1.349 54.9%	14.56 654%	8.126 800%	7.925 766%	7.627 721%	7.477 688%

Coefficients	ω (rad/s)				ω (rad/s)				ω (rad/s)			
	0.64	0.75	0.94	1.06	0.64	0.75	0.94	1.06	0.64	0.75	0.94	1.06
SARPKAYA SR = 0.0	0.07651	0.03223	0.01037	0.02309	0.5692	0.3173	0.07968	0.01616	0.5901	0.3634	0.1412	0.06952
SARPKAYA SR = 0.00125	0.09121 19.2%	0.04193 30.1%	0.007506 -27.6%	0.01927 -16.5%	0.6300 10.7%	0.3044 -4.1%	0.1322 65.9%	0.06847 324%	5.196 781%	3.170 772%	1.084 668%	0.4647 568%
SARPKAYA SR = 0.005	0.09842 28.6%	0.04488 39.2%	0.007948 -23.4%	0.01951 -15.5%	0.7601 33.5%	0.3728 17.5%	0.1491 87.1%	0.06536 305%	5.205 782%	3.181 775%	1.079 664%	0.4631 566%

Table (17) Maximum Surge, Heave and Sway Forces (Smooth & Rough Cylinders, β = 0.0)

β = 0.0	Rolling Moment x 10^{-8} (NM)					Yawing Moment x 10^{-7} (NM)					Pitching Moment x 10^{-9} (NM)				
Coefficients	ω (rad/s)					ω (rad/s)					ω (rad/s)				
	0.37	0.42	0.45	0.50	0.56	0.37	0.42	0.45	0.50	0.56	0.37	0.42	0.45	0.50	0.56
SARPKAYA SR = 0.0	2.225	1.150	1.205	1.283	1.363	0.4221	0.2291	0.3168	0.4553	0.6016	2.161	1.454	1.496	1.522	1.481
SARPKAYA SR = 0.00125	13.96 527%	9.519 728%	9.678 703%	9.815 665%	9.981 632%	6.372 very large diff.	2.534	3.102 879%	4.883 973%	6.907	3.485 61.3%	1.918 31.9%	1.957 30.8%	2.005 31.7%	2.015 36.1%
SARPKAYA SR = 0.005	13.94 527%	9.519 728%	9.680 703%	9.821 666%	9.989 633%	6.346 very large diff.	2.537	3.07 869%	4.833 963%	6.821	3.792 75.5%	2.066 42.1%	2.112 41.2%	2.159 41.9%	2.116 46.3%

Coefficients	ω (rad/s)				ω (rad/s)				ω (rad/s)			
	0.64	0.75	0.94	1.06	0.64	0.75	0.94	1.06	0.64	0.75	0.94	1.06
SARPKAYA SR = 0.0	0.8839	0.5665	0.2430	0.1374	0.3668	0.4624	0.4824	0.4437	0.9227	0.3899	0.1736	0.3472
SARPKAYA SR = 0.00125	7.278 723%	4.578 708%	1.586 553%	0.7028 412%	3.613 885%	3.199 592%	2.787 478%	1.784 302%	1.227 33%	0.5687 45.9%	0.1015 -41.5%	0.2840 -18.2%
SARPKAYA SR = 0.005	7.294 725%	4.593 711%	1.576 549%	0.6981 408%	3.552 868%	3.208 594%	2.778 476%	1.776 300%	1.319 43%	0.6041 54.9%	0.1088 -37.3%	0.2885 -16.9%

Table (18) Maximum Rolling, Yawing and Pitching Moments (Smooth & Rough Cylinders, β = 0.0) roughness values. When SR = 1/800, the differences ranged from 412% (ω = 1.06 rad/s) to 728% (ω = 0.42 rad/s) and when SR = 1/200, the differences are 408% and 728% at ω = 1.06 rad/s and ω = 0.42 rad/s respectively.

b. At ω = 0.37, 0.42 and 0.56 rad/s, the differences in the yawing moments (relative to the smooth cylinders) are extremely large at both values of the surface roughness. For the other frequencies, the differences ranged from 302% (ω = 1.06 rad/s) to 973% (ω = 0.5 rad/s) when SR = 1/800 and from 300% (ω = 1.06 rad/s) to 963% (ω = 0.5 rad/s) when SR = 1/200.

The explanation previously mentioned regarding the sway forces is applicable also to the cases of the rolling and yawing moments.

c. The effects due to roughness are lowest on the pitching moments compared with the rolling or yawing moments. The pitching moments were decreased at the highest two frequencies (0.94 and 1.06). When SR = 1/800, the differences ranged from -41.5% (ω = 0.94 rad/s) to 61.3% (ω = 0.37 rad/s) and when SR = 1/200, the differences ranged from -37.3% (ω = 0.94 rad/s) to 75.5% (ω = 0.37 rad/s).

7.3 Maximum Surge, Heave and Sway Forces ($\beta = \pi/4$)

Table (19) shows that:-

a. The values of the surge forces and the percentage differences are almost the same for the two cases of surface roughness. In the case of 1/800 surface roughness, the differences ranged from 2.7% (ω = 1.06 rad/s) to 65.7% (ω = 0.37 rad/s) and in the case of 1/200 roughness, the differences ranged from 10.4% (ω = 1.06 rad/s) to 65.7% (ω = 0.37 rad/s).

b. The heave forces gave the smallest differences compared with the surge and sway forces. When SR = 1/800, the heave forces were reduced (relative to the smooth cylinders) for the three highest frequencies by 2% (ω = 0.75 rad/s) to 24.8% (ω = 1.06 rad/s). For the other frequencies, the heave forces were increased by 12.5% (ω = 0.64 rad/s) to 60.6% (ω = 0.37 rad/s). When SR = 1/200, the heave forces were increased by 18.1% (ω = 0.75 rad/s) to 89.3% (ω = 0.37 rad/s) and at the two highest frequencies (0.94 and 1.06 rad/s), the heave forces were reduced by 1.6% and 10.9% respectively.

c. The differences in the sway forces ranged from 4.3% (ω = 1.06 rad/s) to 71.4% (ω = 0.37 rad/s) in the case of 1/800 roughness, the differences ranged from 12.3% (ω = 1.06 rad/s) to 73.4% (ω = 0.37 rad/s) in the case of 1/200 roughness. At some frequencies, the values of the sway forces are slightly different from the corresponding surge forces.

7.4 Maximum Rolling, Yawing and Pitching Moments ($\beta = \pi/4$)

Table (20) shows that the values of the moments and the percentage differences are the same for the two cases of surface roughness for most of the frequencies.

$\beta = \frac{\pi}{4}$ Coefficients	Surge Force x 10^{-7} (N) ω (rad/s) 0.37	0.42	0.45	0.50	0.56	Heave Force x 10^{-7} (N) ω (rad/s) 0.37	0.42	0.45	0.50	0.56	Sway Force x 10^{-7} (N) ω (rad/s) 0.37	0.42	0.45	0.50	0.56
SARPKAYA SR = 0.0	1.642	1.045	1.045	1.02	0.9602	1.577	0.8715	0.8721	0.8657	0.8488	1.662	1.050	1.048	1.02	0.9574
SARPKAYA SR = 0.00125	2.720 65.7%	1.504 43.9%	1.503 43.8%	1.484 45.5%	1.430 48.9%	2.532 60.6%	1.118 28.3%	1.118 28.2%	1.131 30.6%	1.138 34.1%	2.849 71.4%	1.550 47.6%	1.518 44.8%	1.459 43%	1.413 47.6%
SARPKAYA SR = 0.005	2.720 65.7%	1.510 44.5%	1.511 44.6%	1.495 46.6%	1.441 50.1%	2.986 89.3%	1.326 52.2%	1.332 52.7%	1.341 54.9%	1.345 58.5%	2.882 73.4%	1.556 48.2%	1.525 45.5%	1.511 48.1%	1.510 57.7%

Coefficients	Surge ω (rad/s) 0.64	0.75	0.94	1.06	Heave ω (rad/s) 0.64	0.75	0.94	1.06	Sway ω (rad/s) 0.64	0.75	0.94	1.06
SARPKAYA SR = 0.0	0.5981	0.3111	0.08651	0.06494	0.5620	0.3295	0.1233	0.07167	0.5994	0.3148	0.08681	0.0649
SARPKAYA SR =0.00125	0.8425 40.9%	0.4422 42.1%	0.1303 50.6%	0.06672 2.7%	0.6321 12.5%	0.3230 -2%	0.1010 -18.1%	0.05389 -24.8%	0.8885 48.2%	0.5041 60.1%	0.1335 53.8%	0.06767 4.3%
SARPKAYA SR = 0.005	0.8509 42.3%	0.4441 42.8%	0.1304 50.7%	0.07171 10.4%	0.7581 34.9%	0.3891 18.1%	0.1213 -1.6%	0.06384 -10.9%	0.9321 55.5%	0.5061 60.8%	0.1336 53.9%	0.07286 12.3%

Table (19) Maximum Surge, Heave and Sway Forces (Smooth & Rough Cylinders, $\beta = \frac{\pi}{4}$)

$\beta = \frac{\pi}{4}$ Coefficients	Rolling Moment x 10^{-9} (NM) ω (rad/s) 0.37	0.42	0.45	0.50	0.56	Yawing Moment x 10^{-5} (NM) ω (rad/s) 0.37	0.42	0.45	0.50	0.56	Pitching Moment x 10^{-9} (NM) ω (rad/s) 0.37	0.42	0.45	0.50	0.56
SARPKAYA SR = 0.0	1.613	1.070	1.103	1.128	1.113	105.9	50.09	55.50	59.35	71.77	1.594	1.066	1.101	1.130	1.118
SARPKAYA SR=0.00125	2.849 76.6%	1.743 62.9%	1.768 60.3%	1.787 58.4%	1.825 64%	1671	758.3 very large differences	838.2	911.7	1121	2.792 75.2%	1.720 61.4%	1.782 61.9%	1.847 63.5%	1.860 66.4%
SARPKAYA SR = 0.005	3.032 88%	1.746 63.2%	1.797 62.9%	1.878 66.5%	1.948 75%	1670	758.3 very large differences	838.1	911.6	1121	2.931 83.9%	1.723 61.6%	1.787 62.3%	1.856 64.2%	1.871 67.4%

Coefficients	Rolling ω (rad/s) 0.64	0.75	0.94	1.06	Yawing ω (rad/s) 0.64	0.75	0.94	1.06	Pitching ω (rad/s) 0.64	0.75	0.94	1.06
SARPKAYA SR = 0.0	0.7296	0.3958	0.1063	0.0829	45.78	21.01	1.598	1.832	0.7285	0.3906	0.1058	0.08293
SARPKAYA SR=0.00125	1.205 65.2%	0.7156 80.8%	0.1882 77%	0.09293 12.1%	680.3 very large	258.6 diff.	10.33 546%	6.384 249%	1.152 58.1%	0.6269 60.5%	0.1835 73.4%	0.09281 11.9%
SARPKAYA SR = 0.005	1.248 71.1%	0.7179 81.4%	0.1882 77%	0.09776 17.9%	680.3 very large	258.5 diff.	10.29 544%	6.379 248%	1.161 59.4%	0.6292 61.1%	0.1835 73.4%	0.09604 15.8%

Table (20) Maximum Rolling, Yawing and Pitching Moments (Smooth & Rough Cylinders, $\beta = \frac{\pi}{4}$)

a. When SR 1/800, the differences in the rolling moments ranged from 12.1% (ω = 1.06 rad/s) to 80.8% (ω = 0.75 rad/s) and when SR = 1/200, the differences ranged from 17.9% (ω = 1.06 rad/s) to 88% (ω = 0.37 rad/s).

b. The yawing moments for the rough cylinders (SR = 1/800 and 1/200) are extremely large compared with the smooth cylinders (SR = 0.0). The minimum **differences** at ω = 1.06 rad/s are 249% (SR = 1/800) and 248% (SR = 1/200).

c. The differences in the pitching moments ranged from 11.9% (ω = 1.06 rad/s) to 75.2% (ω = 0.37 rad/s) for the case of 1/800 roughness and from 15.8% (ω = 1.06 rad/s) to 83.9% (ω = 0.37 rad/s) for the case of 1/200 roughness.

8. THE EFFECT OF WAVE HEIGHT

To examine the effect of wave height on loading estimation, the calculations were carried out using both LR and Sarpkaya's coefficients for smooth cylinders. The frequency was kept constant at 0.37 rad/s and 5 different wave heights were chosen, namely, 1.0, 5.0, 10.0, 15.0 and 25.0m. The results are summarised in Tables (21) and (22) and were analysed as shown below.

8.1 Maximum Surge, Heave and Sway Forces (β = 0.0)

From Table (21) the following was noted:-

a. At wave heights 1.0 and 5.0m, the surge forces according to Sarpkaya were reduced by 5.6% and 7.8% (relative to LR) and at 10m wave height there is no difference. When H = 15m and 25m, the surge forces were increased by 2.3% and 5.8% respectively.

b. The differences in the heave forces ranged from 10.2% (H = 1.0m) to 16.1% (H = 25.0m).

c. The sway forces had the largest differences compared with the surge and heave forces. When H = 1.0m, the sway force according to Sarpkaya was reduced by 12.8% (relative to LR) but for the other wave heights the surge forces according to Sarpkaya were largely increased. The differences ranged from 295% (H = 5.0m) to 1230% (H = 25.0m). This is mainly because when H = 1.0m, the lift coefficient C_L = 0.0, while for larger wave heights, the combined effect of the lift forces and the drag forces increases the sway forces dramatically.

8.2 Maximum Rolling, Yawing and Pitching Moments (β = 0.0)

From Table (21) the following was noted:-

a. The differences in the rolling moments are the largest relative to the yawing and pitching moments and they increase with the increase of the wave height ranging from 8.5% (H = 1.0m) to a maximum of 934% (H = 25.0m).

b. When H = 1.0 and 5.0m, the yawing moments according to Sarpkaya were reduced by 35.8% and 75.1%, respectively, but for the higher waves the yawing moments were increased (relative to LR) by 204% (H = 10.0m) to 330% (H = 25.0m).

c. Similar to the surge forces, the pitching moments were first reduced by 5.2% (H = 1.0m) and 2% (H = 5.0m) and then increased by 0.7% (H = 10.0m) to 7.3% (H = 25.0m).

$\beta = 0.0$, $\omega = 0.37$	Surge Force x 10^{-7} (N)					Heave Force x 10^{-7} (N)					Sway Force x 10^{-5} (N)				
	Wave Height (m)					Wave Height (m)					Wave Height (m)				
Coefficients	1.0	5.0	10.0	15.0	25.0	1.0	5.0	10.0	15.0	25.0	1.0	5.0	10.0	15.0	25.0
LR	0.06304	0.3197	0.6506	0.9928	1.711	0.03474	0.1737	0.3474	0.5295	1.002	0.02725	0.1399	0.2888	0.4736	1.036
SARPKAYA SR = 0.0	0.05949	0.3139	0.6521	1.016	1.811	0.03828	0.1990	0.3896	0.6147	1.147	0.02375	0.5525	2.191	5.148	13.78
Diff.%	-5.6%	-1.8%		2.3%	5.8%	10.2%	14.6%	12.2%	16.1%	14.5%	-12.8%	295%	659%	987%	1230%
Coefficients	Rolling Moment x 10^{-7} (NM)					Yawing Moment x 10^{-6} (NM)					Pitching Moment x 10^{-9} (NM)				
	1.0	5.0	10.0	15.0	25.0	1.0	5.0	10.0	15.0	25.0	1.0	5.0	10.0	15.0	25.0
LR	0.03555	0.1843	0.3850	0.6861	1.543	0.01733	0.8665	0.2012	0.3474	0.7310	0.05939	0.3016	0.6146	0.9390	1.622
SARPKAYA SR = 0.0	0.03856	0.7219	2.731	6.105	15.96	0.01113	0.2157	0.6125	1.314	3.143	0.05629	0.2955	0.6186	0.9683	1.741
Diff.%	8.5%	292%	609%	790%	934%	-35.8%	-75.1%	204%	278%	330%	-5.2%	-2%	0.7%	3.1%	7.3%

Table (21) Maximum Forces and Moments at Different Wave Heights (LR & SARPKAYA, $\beta = 0.0$)

$\beta = \frac{\pi}{4}$, $\omega = 0.37$	Surge Force x 10^{-7} (N)					Heave Force x 10^{-7} (N)					Sway Force x 10^{-7}				
	Wave Height (m)					Wave Height (m)					Wave Height (m)				
Coefficients	1.0	5.0	10.0	15.0	25.0	1.0	5.0	10.0	15.0	25.0	1.0	5.0	10.0	15.0	25.0
LR	0.04506	0.2281	0.4630	0.7048	1.209	0.03477	0.1738	0.3477	0.5283	0.9981	0.04503	0.2279	0.4626	0.7043	1.208
SARPKAYA SR = 0.0	0.0424	0.2254	0.4691	0.7347	1.321	0.03783	0.1987	0.3863	0.6056	1.148	0.04237	0.2258	0.4717	0.7405	1.336
Diff.%	-5.9%	-1.2%	1.3%	4.2%	9.3%	8.8%	14.3%	11.1%	14.6%	15%	-5.9%	-0.9%	2%	5.1%	10.6%
Coefficients	Rolling Moment x 10^{-9} (NM)					Yawing Moment x 10^{-5} (NM)					Pitching Moment x 10^{-9} (NM)				
	1.0	5.0	10.0	15.0	25.0	1.0	5.0	10.0	15.0	25.0	1.0	5.0	10.0	15.0	25.0
LR	0.04247	0.2151	0.4372	0.6662	1.145	0.001236	0.008901	0.02562	0.05013	0.1225	0.0425	0.2153	0.4375	0.6667	1.146
SARPKAYA SR = 0.0	0.04044	0.2132	0.4492	0.7089	1.291	0.008031	0.2529	6.567	19.38	70.12	0.04046	0.2127	0.4463	0.7034	1.277
Diff.%	-4.8%	-0.9%	2.7%	6.4%	12.8%	550%	very large differences				-4.8%	-1.2%	2%	5.5%	11.4%

Table (22) Maximum Forces and Moments at Different Wave Heights (LR & SARPKAYA, $\beta = \frac{\pi}{4}$)

8.3 Maximum Surge, Heave and Sway Forces ($\beta = \pi/4$)

From Table (22) the following was noted:-

a. When H = 1.0 and 5.0m, the surge forces according to Sarpkaya were reduced by 5.9% and 1.2%, respectively, (relative to LR). For the higher waves, the differences are positive ranging from 1.3% (H = 10.0m) to 9.3% (H = 25.0m).

b. The differences in the heave forces ranged from 8.8% (H = 1.0m) to 15% (H = 25.0m).

c. The sway forces and their percentage differences are approximately the same as the surge forces. When H = 1.0 and 5.0m, the sway forces according to Sarpkaya were reduced by 5.9% and 0.9%, respectively, while for the higher waves, the sway forces were increased from 2% (H = 10,0m) to 10.6% (H = 25.0m).

8.4 Maximum Rolling, Yawing and Pitching Moments ($\beta = \pi/4$)

From Table (22) the following was noted:-

a. At the first two wave heights, 1.0 and 5.0m, the rolling moments according to Sarpkaya were reduced by 4.8% and 0.9%, respectively, (relative to LR), but for the higher waves the differences ranged positively from 2.7% (H = 10.0m) to 12.8% (H = 25.0m).

b. The yawing moments according to Sarpkaya are extremely large compared with the values of LR. The differences increased with the increase of wave height with a minimum difference of 550% (H = 1.0m).

c. The values of the pitching moments and the percentage differences between Sarpkaya and LR are approximately the same as the rolling moments. When H = 1.0 and 5.0m, the pitching moments according to Sarpkaya were reduced by 4.8% and 1.2% respectively, but for the higher waves, the differences ranged positively from 2% (H = 10.0m) to 11.4% (H = 25.0m).

9. THE USE OF APPROXIMATE LENGTHS vs EXACT LENGTHS

All the calculations mentioned in the previous sections were performed assuming that the starting and end points of the bracing members (horizontal or inclined) are the nodes resulting from the intersection of the centre line of the member with the other members at each end. Therefore, the length of the bracing member (the approximate length) is, in fact, larger than the actual or exact length by about 8%. However, for the main columns (4.0m diameter members, Fig.(2), the exact lengths were used.

To find out the effect of this approximation on the results of wave loading, the calculations were repeated for the case of SR = 1/200 using the exact lengths and compared with those with the approximate lengths as shown in Tables (23) to (26).

9.1 Maximum Forces and Moments (β = 0.0)

Tables (23) and (24) show that:-

a. The differences between the actual surge forces (ie when using the exact lengths) and the approximate forces, ranged from -3.3% (ω = 0.75 rad/s) to -19.7% (ω = 0.94 rad/s).

b. In the range from $\omega = 0.37$ rad/s to $\omega = 0.75$ rad/s, the actual heave forces were reduced relative to the approximate forces, the reduction ranged from 4.9% ($\omega = 0.75$ rad/s) to 7.8% ($\omega = 0.37$ rad/s). At $\omega = 0.94$ rad/s, the difference is negligible, while at $\omega = 1.06$ rad/s, the heave force was increased by 8.2%.

c. From $\omega = 0.37$ rad/s, the reduction in the sway forces (exact values relative to approximate values) ranged from 3.6% ($\omega = 0.75$ rad/s) to 7.4% ($\omega = 0.42$ rad/s). At $\omega = 0.94$ rad/s and $\omega = 1.06$ rad/s, the sway forces were increased by 0.7% and 12.7%, respectively.

d. From $\omega = 0.37$ rad/s to $\omega = 0.75$ rad/s, the reduction in the rolling moments ranged from 3.4% ($\omega = 0.75$ rad/s) to 7.4% ($\omega = 0.42$ rad/s). At $\omega = 0.94$ rad/s and $\omega = 1.06$ rad/s, the rolling moments were increased by 0.9% and 14.4%, respectively.

e. At $\omega = 0.42$ rad/s, the yawing moment was increased by 9.3% and at $\omega = 0.45$ rad/s the difference between the exact and approximate moments is negligible. For the other frequencies, the yawing moments were reduced by 6.7% ($\omega = 0.37$ rad/s) to 23.9% ($\omega = 0.75$ rad/s).

f. The reductions in the pitching moments ranged from 2.8% ($\omega = 0.75$ rad/s) to 26.8% ($\omega = 0.94$ rad/s).

β = 0.0	Surge Force x 10^{-8} (N)					Heave Force x 10^{-7} (N)					Sway Force x 10^{-6} (N)				
SARPKAYA SR = 0.005	ω (rad/s)					ω (rad/s)					ω (rad/s)				
	0.37	0.42	0.45	0.5	0.56	0.37	0.42	0.45	0.50	0.56	0.37	0.42	0.45	0.50	0.56
Approx. lengths	0.3491	0.1773	0.1758	0.1726	0.1671	2.964	1.331	1.338	1.348	1.349	14.56	8.126	7.925	7.627	7.477
Exact lengths	0.3278	0.1667	0.1655	0.1627	0.1578	2.733	1.227	1.235	1.247	1.253	13.53	7.523	7.346	7.092	6.994
Diff.%	-6.1%	-6. %	-5.9%	-5.7%	-5.6%	-7.8%	-7.8%	-7.7%	-7.5%	-7.1%	-7.1%	-7.4%	-7.3%	-7%	-6.5%

SARPKAYA SR = 0.005	ω (rad/s)				ω (rad/s)				ω (rad/s)			
	0.64	0.75	0.94	1.06	0.64	0.75	0.94	1.06	0.64	0.75	0.94	1.06
Approx. lengths	0.09842	0.04488	0.007948	0.01951	0.7601	0.3728	0.1491	0.06536	5.205	3.181	1.079	0.4631
Exact lengths	0.09328	0.0434	0.006386	0.01748	0.7097	0.3544	0.1486	0.07074	4.922	3.068	1.087	0.5219
Diff.%	-5.2%	-3.3%	-19.7%	-10.4%	-6.6%	-4.9%		8.2%	-5.4%	-3.6%	0.7%	12.7%

Table (23) Maximum Surge, Heave and Sway Forces for the Exact and Approximate lengths (β = 0.0)

β = 0.0	Rolling Moment x 10^{-8} (NM)					Yawing Moment x 10^{-7} (NM)					Pitching Moment x 10^{-9} (NM)				
SARPKAYA SR = 0.005	ω (rad/s)					ω (rad/s)					ω (rad/s)				
	0.37	0.42	0.45	0.50	0.56	0.37	0.42	0.45	0.50	0.56	0.37	0.42	0.45	0.50	0.56
Approx. lengths	13.94	9.519	9.680	9.821	9.989	6.346	2.537	3.07	4.838	6.821	3.792	2.066	2.112	2.159	2.166
Exact lengths	12.92	8.813	8.975	9.134	9.345	5.919	2.773	3.065	4.416	6.282	3.561	1.942	1.987	2.036	2.047
Diff.%	-7.3%	-7.4%	-7.3%	-7%	-6.5%	-6.7%	9.3%		-8.7%	-7.9%	-6.5%	-6.4%	-6.3%	-6%	-5.8%

SARPKAYA SR = 0.005	ω (rad/s)				ω (rad/s)				ω (rad/s)			
	0.64	0.75	0.94	1.06	0.64	0.75	0.94	1.06	0.64	0.75	0.94	1.06
Approx. lengths	7.294	4.593	1.576	0.6981	3.552	3.208	2.778	1.776	1.319	0.6041	0.1088	0.2885
Exact lengths	6.902	4.436	1.590	0.7983	3.045	2.442	2.276	1.552	1.253	0.5879	0.08584	0.2573
Diff.%	-5.4%	-3.4%	0.9%	14.4%	-14.3%	-23.9%	-18.1%	-12.6%	-5.3%	-2.8%	-26.8%	-12.1%

Table (24) Maximum Rolling, Yawing and Pitching Moments for the Exact and Approximate lengths (β = 0.0)

$\beta = \frac{\pi}{4}$ SARPKAYA SR = 0.005	Surge Force x 10^{-7} (N)					Heave Force x 10^{-7} (N)					Sway Force x 10^{-7} (N)				
	ω (rad/s)					ω (rad/s)					ω (rad/s)				
	0.37	0.42	0.45	0.50	0.56	0.37	0.42	0.45	0.50	0.56	0.37	0.42	0.45	0.50	0.56
Approx. lengths	2.720	1.510	1.511	1.495	1.441	2.986	1.326	1.332	1.341	1.345	2.882	1.556	1.525	1.511	1.510
Exact lenghts	2.536	1.408	1.411	1.397	1.348	2.751	1.221	1.228	1.241	1.250	2.717	1.447	1.426	1.427	1.428
Diff.%	-6.8%	-6.8%	-6.6%	-6.6%	-6.5%	-7.9%	-7.9%	-7.8%	-7.5%	-7.1%	-5.7%	-7%	-6.5%	-5.6%	-5.4%

SARPKAYA	ω (ard/s)				ω (rad/s)				ω (rad/s)			
SR = 0.005	0.64	0.75	0.94	1.06	0.64	0.75	0.94	1.06	0.64	0.75	0.94	1.06
Approx. lenghts	0.8509	0.4441	0.1304	0.07171	0.7581	0.3891	0.1213	0.06384	0.9321	0.5061	0.1336	0.07286
Exact lengths	0.7951	0.4155	0.1248	0.06789	0.7099	0.3712	0.1185	0.06237	0.8852	0.4774	0.1280	0.06904
Diff.%	-6.6%	-6.4%	-4.3%	-5.3%	-6.4%	-4.6%	-2.3%	-2.3%	-5%	-5.7%	-4.2%	-5.2%

Table (25) Maximum Surge, Heave and Sway Forces for the Exact and Approximate length, ($\beta = \frac{\pi}{4}$)

$\beta = \frac{\pi}{4}$ SARPKAYA SR = 0.005	Rolling Moment x 10^{-9} (NM)					Yawing Moment x 10^{-5} (NM)					Pitching Moment x 10^{-9} (NM)				
	ω (rad/s)					ω (rad/s)					ω (rad/s)				
	0.37	0.42	0.45	0.50	0.56	0.37	0.42	0.45	0.50	0.56	0.37	0.42	0.45	0.50	0.56
Approx. lenghts	3.032	1.746	1.797	1.878	1.948	1670	758.3	838.1	911.6	1121	2.931	1.723	1.787	1.856	1.871
Exact lenghts	2.854	1.637	1.692	1.771	1.841	1649	747	826.6	900.5	1116	2.761	1.603	1.664	1.730	1.745
Diff.%	-5.9%	-6.2%	-5.8%	-5.7%	-5.5%	-1.3%	-1.5%	-1.4%	-1.2%	-0.5%	-6.2%	-7.5%	-7.4%	-7.3%	-7.2%

SARPKAYA SR = 0.005	ω (rad/s)				ω (rad/s)				ω (rad/s)			
	0.64	0.75	0.94	1.06	0.64	0.75	0.94	1.06	0.64	0.75	0.94	1.06
Approx. lengths	1.248	0.7179	0.1882	0.09776	680.3	258.5	10.24	6.379	1.161	0.6292	0.1835	0.09604
Exact lenghts	1.186	0.6754	0.1808	0.09200	681.9	258.4	10.22	6.332	1.082	0.5868	0.1761	0.09028
Diff.%	-5%	-5.9%	-3.9%	-5.9%.			-0.7%	-0.7%	-7.3%	-7.2%	-4.2%	-6.4%

Table (26) Maximum Rolling, Yawing and Pitvhing Moments for the Exact and Approximate lengths,$\beta = \frac{\pi}{4}$.)

9.2 Maximum Forces and Moments ($\beta = \pi/4$)

Tables (25) and (26) show that:-

a. The reduction in the surge forces ranged from 4.3% (ω = 0.94 rad/s) to 6.8% (ω = 0.37 rad/s).

b. The reduction in the heave forces ranged from 2.3% (ω = 0.94 rad/s) to 7.9% (ω = 0.37 rad/s).

c. The reduction in the sway forces ranged from 4.2% (ω = 0.94 rad/s) to 7% (ω = 0.42 rad/s).

d. The reduction in the rolling moments ranged from 3.9% (ω = 0.94 rad/s) to 6.2% (ω = 0.42 rad/s).

e. The reduction in the yawing moments ranged from 0.5% (ω = 0.56 rad/s) to 1.5% (ω = 0.42 rad/s).

f. The reduction in the pitching moments ranged from 4.2% (ω = 0.94 rad/s) to 7.5% (ω = 0.42 rad/s).

From the previous results it may be concluded that the differences in load estimation between the exact lengths and the approximate ones are not large. However, estimating every aspect of the loading problem as accurately as possible, by using the exact dimensions, would lead to better accuracy and more reliable results in the final solution.

10. CONCLUSIONS

a. The effect of roughness on the hydrodynamic coefficients C_D, C_M and C_L is quite significant. Tables (2.1) to (2.3) show the large differences between the smooth and rough cylinders. Even for small relative roughness (1/800), the differences are large.

b. The lift or transverse forces represent a significant percentage of the total wave load especially the total sway forces, rolling and yawing moments at the base of the structure and must be taken into consideration in design.

c. For jacket platforms and other deep water structures, where a large number of members with different diameters are used, it is essential to estimate the hydrodynamic coefficients in relation to the position of the member under water surface and the particulars of the wave (ie R_e and K). Choosing constant coefficients throughout the whole structure adds another dimension to the uncertainty in load estimation for the complete structure and also for the individual members.

d. The total forces (surge, heave and sway) and total moments (rolling, yawing and pitching) are greatly increased due to roughness compared with the case of smooth cylinders. Estimating the relative roughness accurately is not so important, the vital thing is to take the roughness into account by a reasonable or average value. The results of Tables (17) to (20) show that the differences between the smooth cylinders (SR = 0.0) and rough cylinders of 1/800 are much larger than the differences between the two roughnesses of 1/800 and 1/200, although the difference in the relative roughness in the second case is three times the first case.

REFERENCES

1. HEAF, N J, 'The Effect of Marine Growth on the Performance of Fixed Offshore Platforms in the North Sea', OTC Paper No 3386, Houston, Texas, 1979.

2. LLOYD'S REGISTER OF SHIPPING, 'Rules for the Construction and Classification of Mobile Offshore Units', 1972.

3. SARPKAYA, T, 'In-Line and Transverse Forces on Smooth and Sand-Roughened Cylinders in Oscillatory Flow at High Reynolds Numbers', Naval Postgraduate School, Technical Report No NPS-69SL76062, Monterey, CA, Jun 76.

4. SARPKAYA, T, 'Vortex Shedding and Resistance in Harmonic Flow about Smooth and Rough Circular Cylinders at High Reynolds Numbers', Naval Postgraduate School, Technical Report No NPS-59SL76021, Moneterey, CA, Feb 76.

5. SARPKAYA, T, 'In-Line and Transverse Forces on Cylinders in Oscillatory Flow at High Reynolds Numbers', OTC Paper No 2533, Houston, Texas, May 76.

6. SARPKAYA, T, 'Vortex Shedding and Resistance in Harmonic Flow about Smooth and Rough Circular Cylinders', BOSS '76, Trondheim, Vol I, 1976, pp220-235.

7. SARPKAYA, T, 'In-Line and Transverse Forces on Cylinders in Oscillatory Flow at High Reynolds Numbers', Jour of Ship Research, Vol 24, No 4, Dec 77, pp200-216.

8. SARPKAYA, T, 'The Hydrodynamic Resistance of Roughened Cylinders in Harmonic Flow', Trans RINA, Vol 120, 1978, pp41-55.

9. SARPKAYA, T, COLLINS, N J, and EVANS, S R, 'Wave Forces on Rough-Walled Cylinders at High Reynolds Numbers', OTC Paper No 2901, Houston, Texas, 1977.

10. SARPKAYA, T, and ISAACSON, M, 'Mechanics of Wave Forces on Offshore Structures', Van Nostrand Reinhold, New York, 1981.

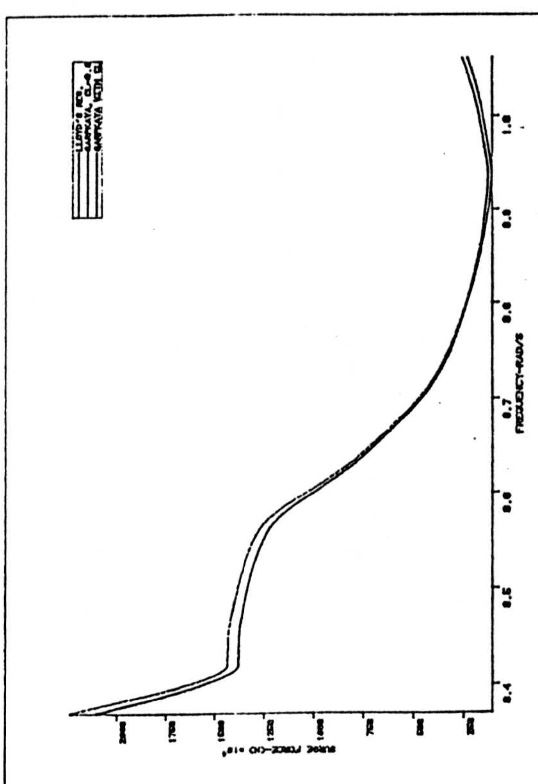

COEFFICIENTS: LR & SARPK , β =0.0 ,SR= 0.0
FIG. (28) MAX. SURGE FORCES Vs. FREQUENCY

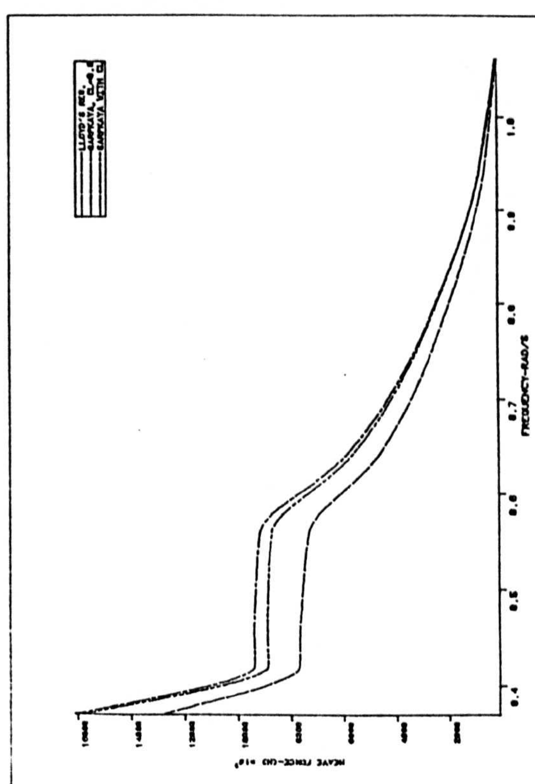

COEFFICIENTS: LR & SARPK , β = 0.0 ,SR= 0.0
FIG. (29) MAX. HEAVE FORCES Vs. FREQUENCY

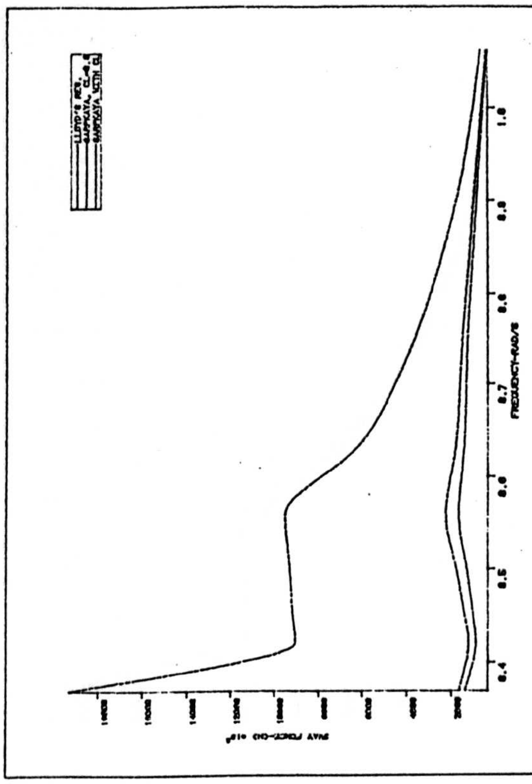

COEFFICIENTS: LR & SARPK , β =0.0 ,SR= 0.0
FIG. (30) MAX. SWAY FORCES Vs. FREQUENCY

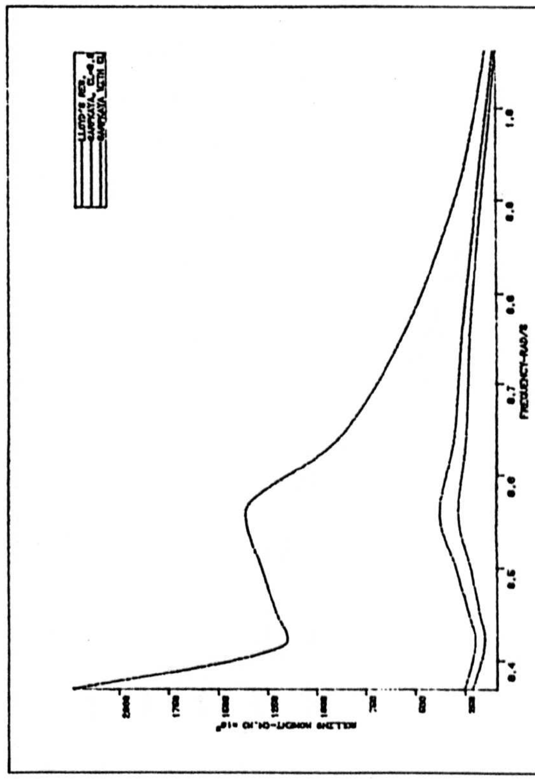

COEFFICIENTS: LR & SARPK , β =0.0 ,SR= 0.0
FIG. (31) MAX. ROLLING MOMENTS Vs. FREQUENCY

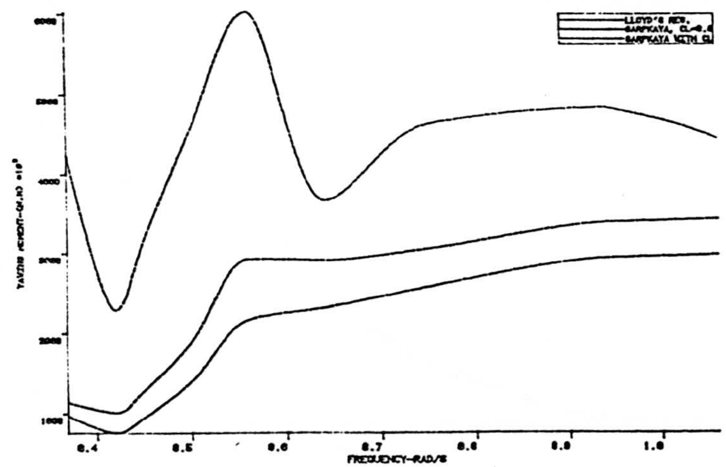

COEFFICIENTS: LR & SARPK , β =0.0 , SR= 0.0
FIG. (32) MAX. YAWING MOMENTS Vs. FREQUENCY

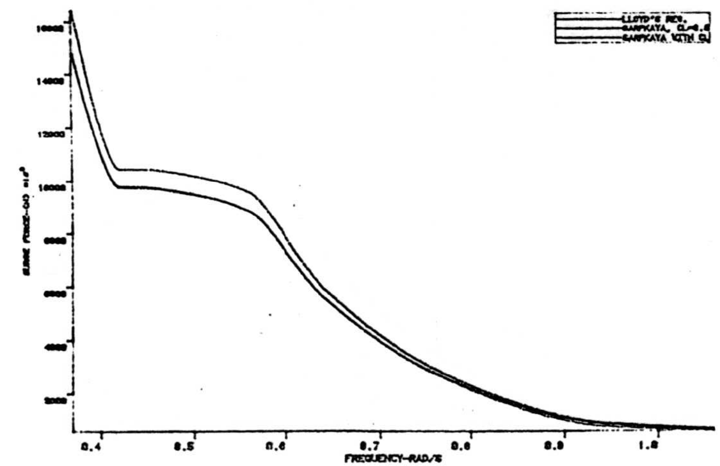

COEFFICIENTS: LR & SARPK , $\beta = \frac{\pi}{4}$, SR= 0.0
FIG. (34) MAX. SURGE FORCES Vs. FREQUENCY

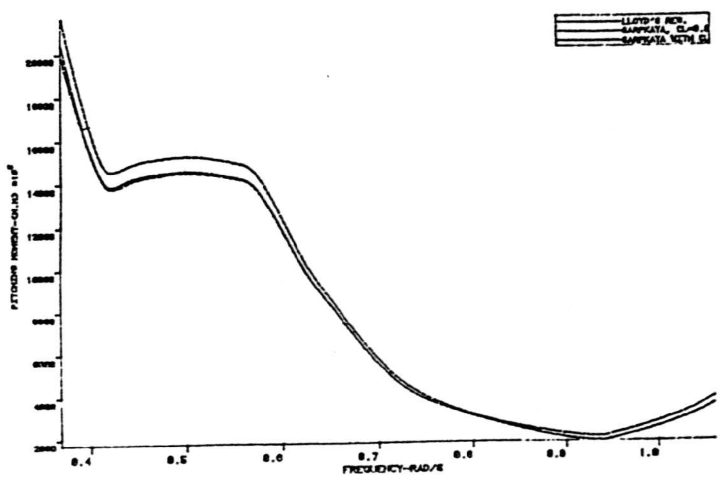

COEFFICIENTS: LR & SARPK , β =0.0 , SR= 0.0
FIG. (33) MAX. PITCHING MOMENTS Vs. FREQUENCY

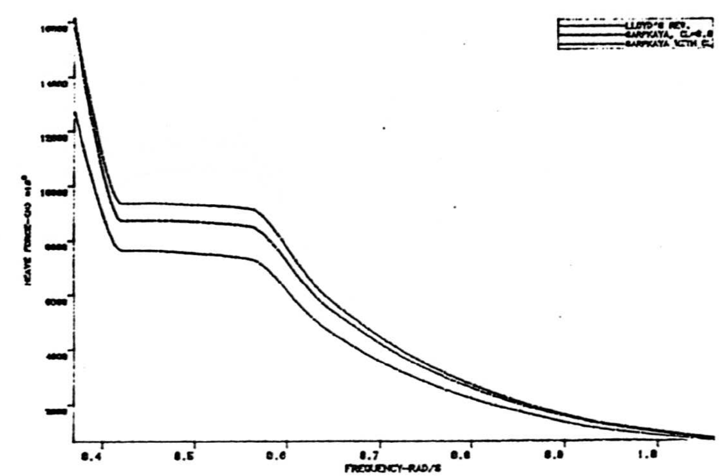

COEFFICIENTS: LR & SARPK , $\beta = \frac{\pi}{4}$, SR=0.0
FIG. (35) MAX. HEAVE FORCES Vs. FREQUENCY

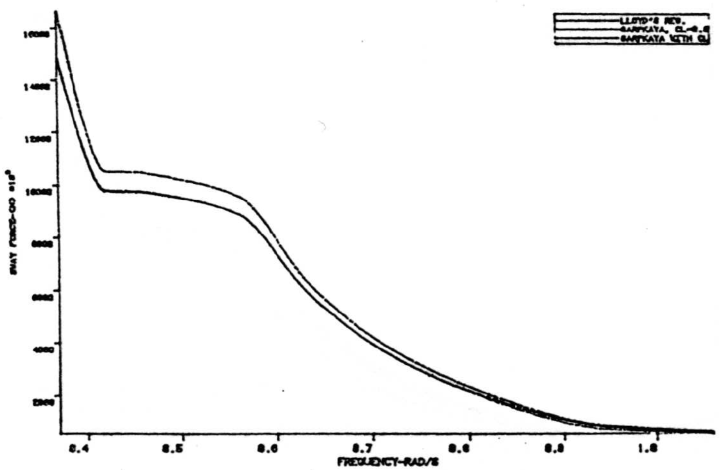

COEFFICIENTS: LR & SARPK , $\beta = \frac{\pi}{4}$, SR= 0.0
FIG. (36) MAX. SWAY FORCES Vs. FREQUENCY

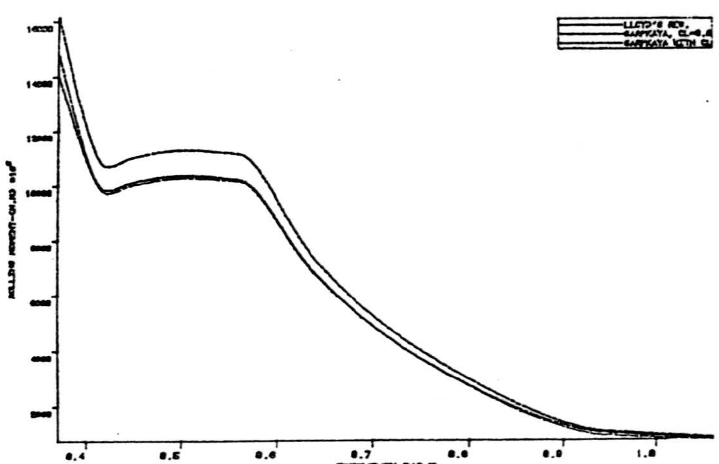

COEFFICIENTS: LR & SARPK , $\beta = \frac{\pi}{4}$, SR= 0.0
FIG. (37) MAX. ROLLING MOMENTS Vs. FREQUENCY

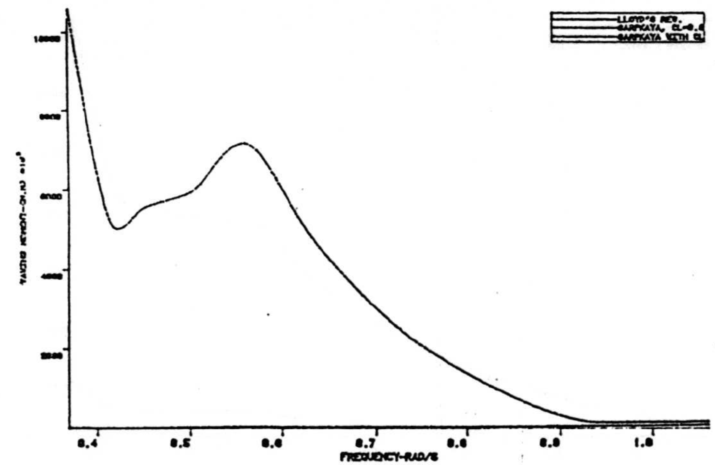

COEFFICIENTS: LR & SARPK , $\beta = \frac{\pi}{4}$, SR= 0.0
FIG. (38) MAX. YAWING MOMENTS Vs. FREQUENCY

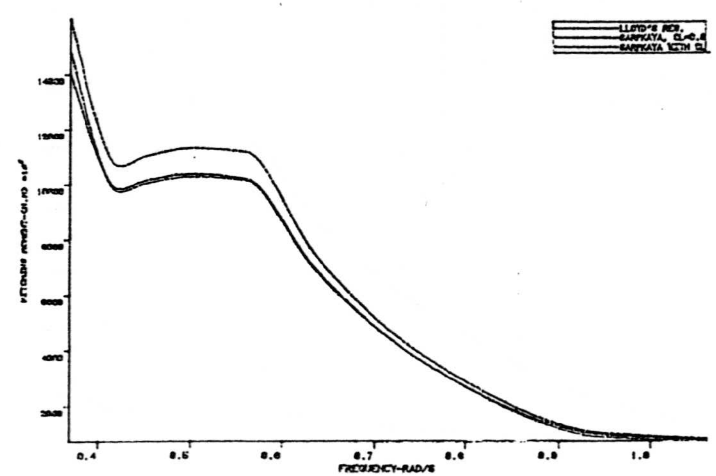

COEFFICIENTS: LR & SARPK , $\beta = \frac{\pi}{4}$, SR= 0.0
FIG. (39) MAX. PITCHING MOMENTS Vs. FREQUENCY

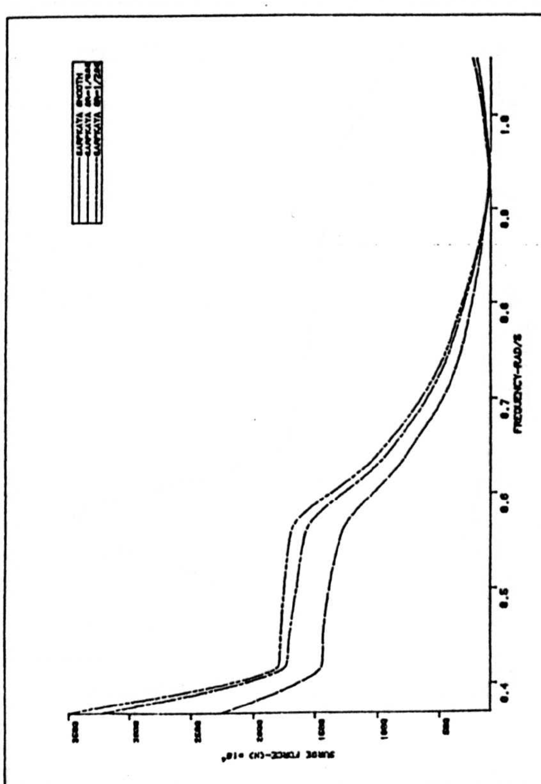

COEFFICIENTS: SARPKAYA , β = 0.0, SR= 0.0, 1/800, 1/200
FIG. (40) MAX. SURGE FORCES Vs. FREQUENCY

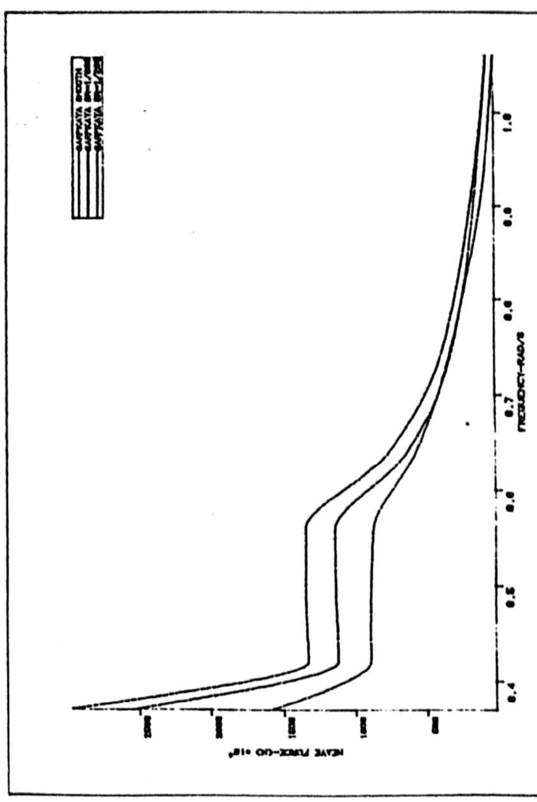

COEFFICIENTS: SARPKAYA , β = 0.0, SR= 0.0, 1/800, 1/200
FIG. (41) MAX. HEAVE FORCES Vs. FREQUENCY

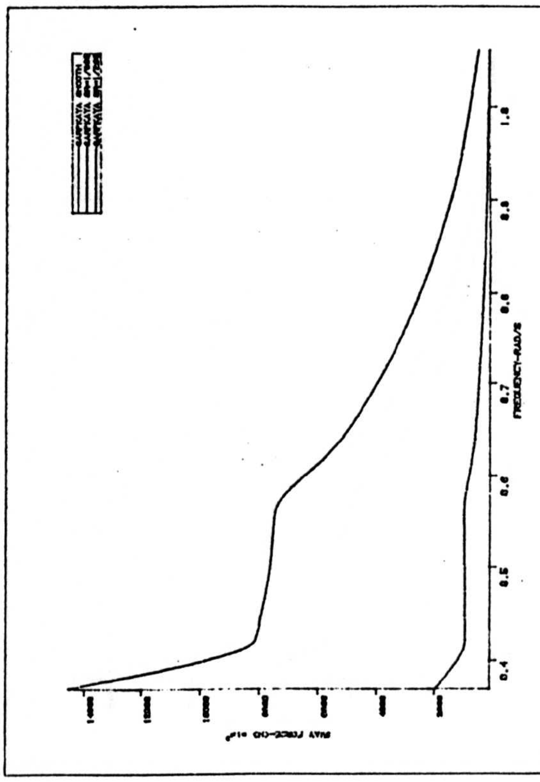

COEFFICIENTS: SARPKAYA , β = 0.0, SR= 0.0, 1/800, 1/200
FIG. (42) MAX. SWAY FORCES Vs. FREQUENCY

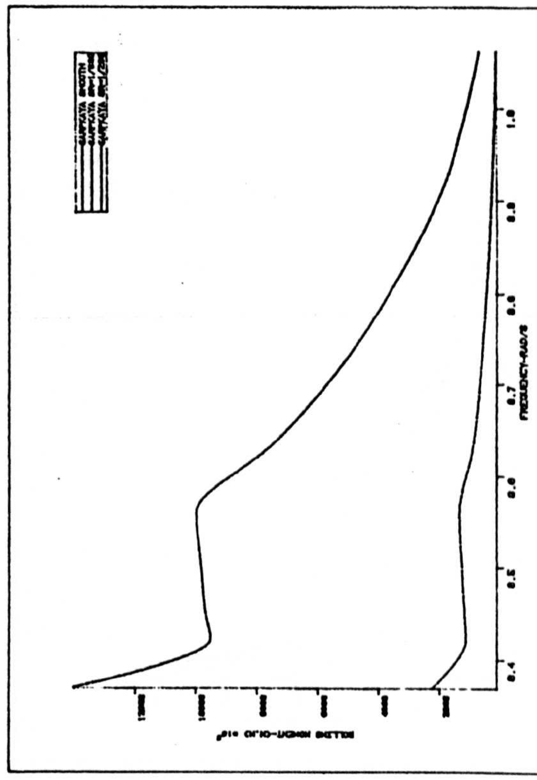

COEFFICIENTS: SARPKAYA , β = 0.0, SR= 0.0, 1/800, 1/200
FIG. (43) MAX. ROLLING MOMENTS Vs. FREQUENCY

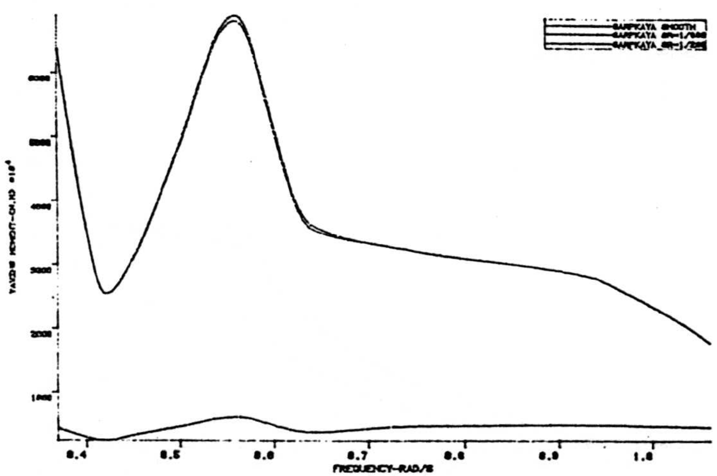

COEFFICIENTS: SARPKAYA , $\beta = 0.0$, SR= 0.0, 1/800, 1/200
FIG. (44) MAX. YAWING MOMENTS Vs. FREQUENCY

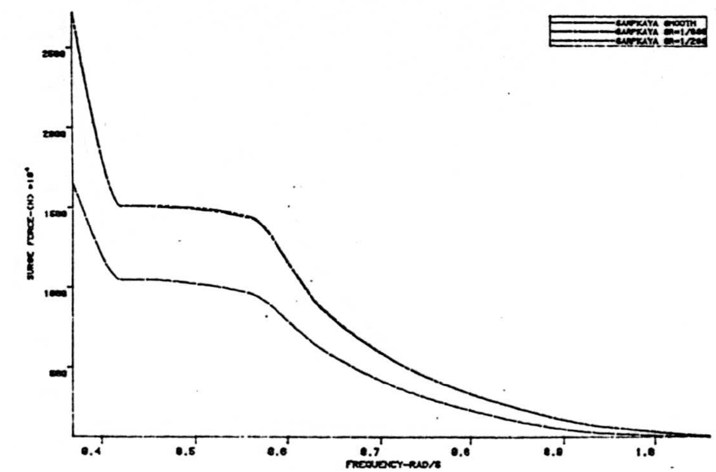

COEFFICIENTS: SARPKAYA , $\beta = \frac{\pi}{4}$, SR= 0.0, 1/800, 1/200
FIG. (46) MAX. SURGE FORCES Vs. FREQUENCY

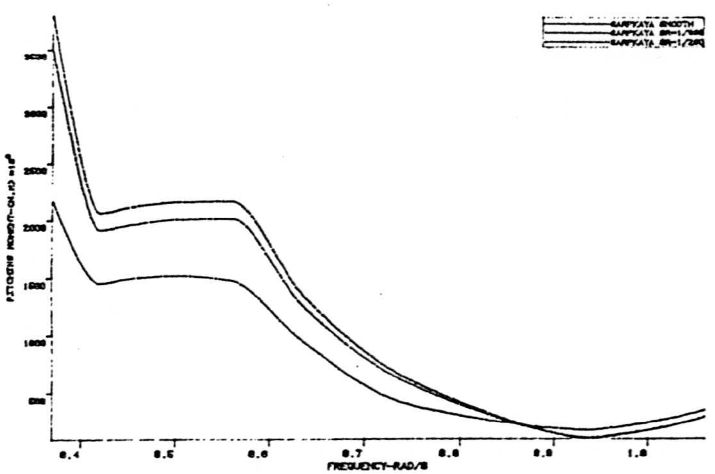

COEFFICIENTS: SARPKAYA , $\beta = 0.0$, SR= 0.0, 1/800, 1/200
FIG. (45) MAX. PITCHING MOMENTS Vs. FREQUENCY

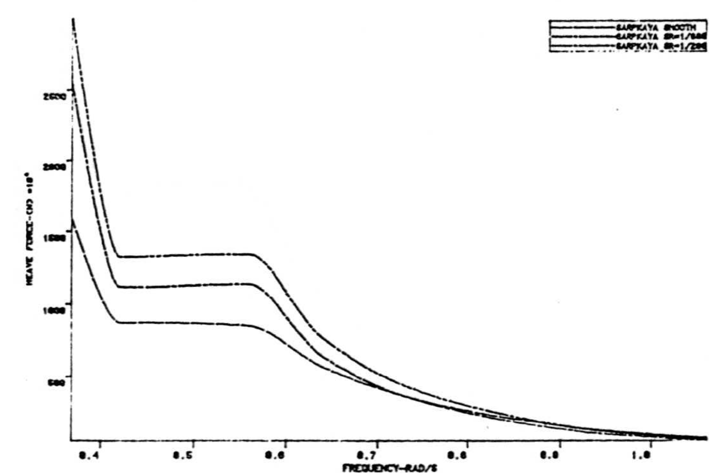

COEFFICIENTS: SARPKAYA , $\beta = \frac{\pi}{4}$, SR= 0.0, 1/800, 1/200
FIG. (47) MAX. HEAVE FORCES Vs. FREQUENCY

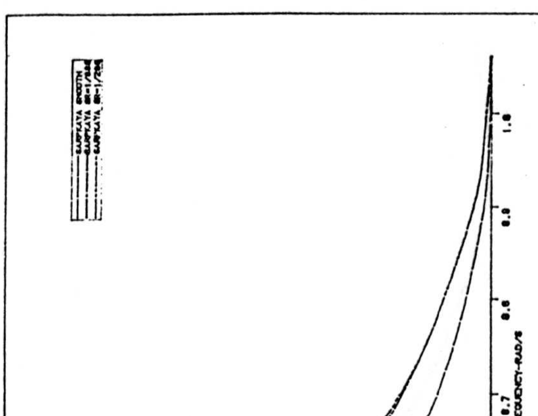

COEFFICIENTS: SARPKAYA , $\beta = \frac{1}{4}$,SR= 0.0, 1/800, 1/200
FIG. (48) MAX. SWAY FORCES Vs. FREQUENCY

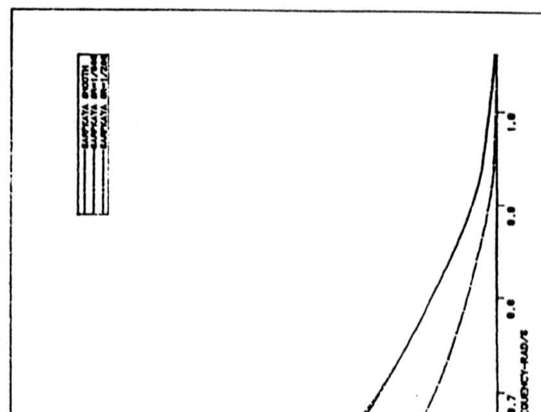

COEFFICIENTS: SARPKAYA , $\beta = \frac{1}{4}$,SR= 0.0, 1/800, 1/200
FIG. (49) MAX. ROLLING MOMENTS Vs. FREQUENCY

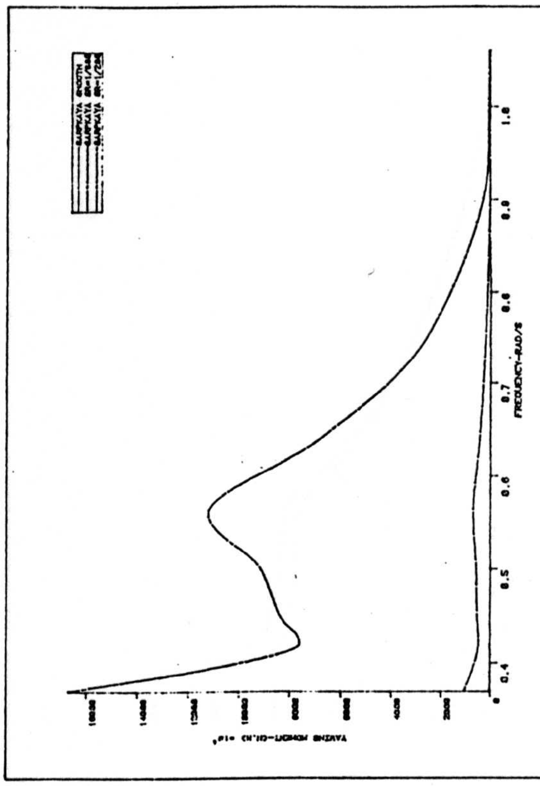

COEFFICIENTS: SARPKAYA , $\beta = \frac{1}{4}$,SR= 0.0, 1/800, 1/200
FIG. (50) MAX. YAWING MOMENTS Vs. FREQUENCY

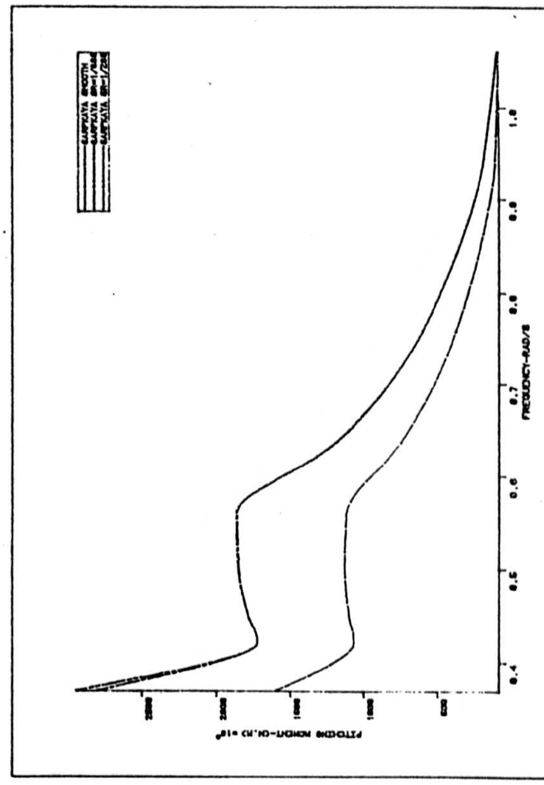

COEFFICIENTS: SARPKAYA , $\beta = \frac{1}{4}$,SR= 0.0, 1/800, 1/200
FIG. (51) MAX. PITCHING MOMENTS Vs. FREQUENCY

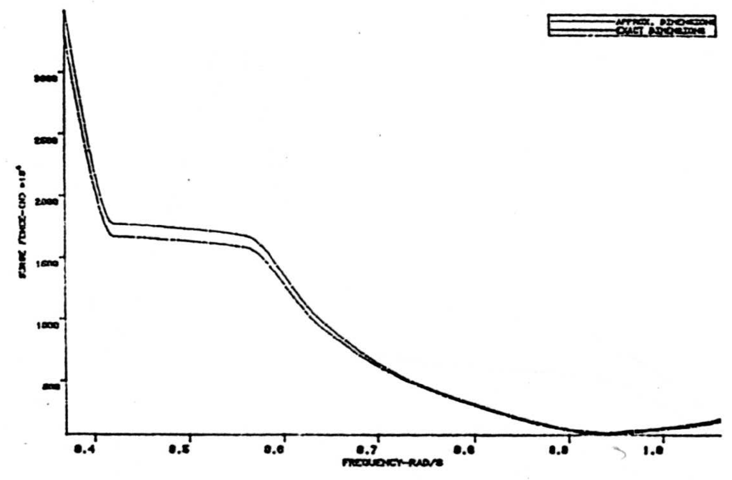

COEFFICIENTS: SARPKAYA , β =0.0 , SR= 1/200
FIG. (52) MAX. SURGE FORCES Vs. FREQUENCY

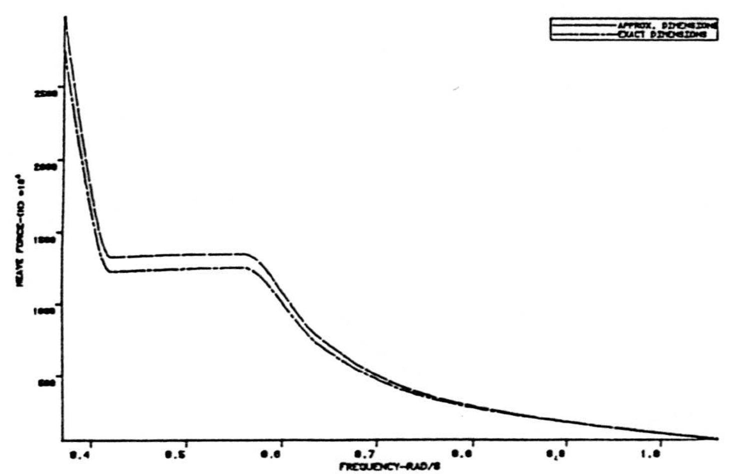

COEFFICIENTS: SARPKAYA , β = 0.0, SR= 1/200
FIG. (53) MAX. HEAVE FORCES Vs. FREQUENCY

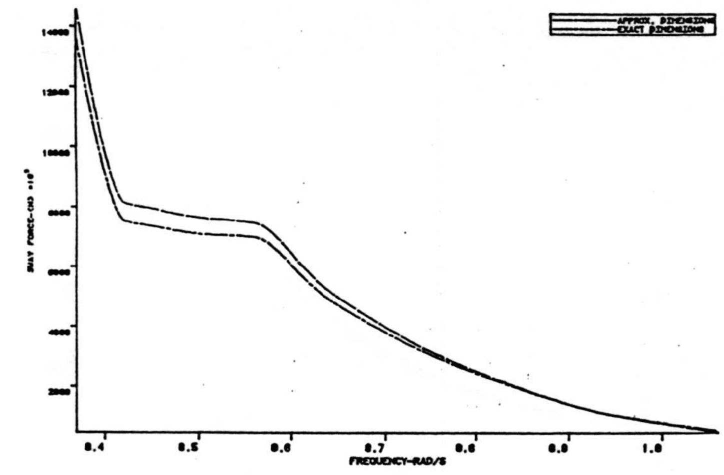

COEFFICIENTS: SARPKAYA , β = 0.0, SR= 0.005
FIG. (54) MAX. SWAY FORCES Vs. FREQUENCY

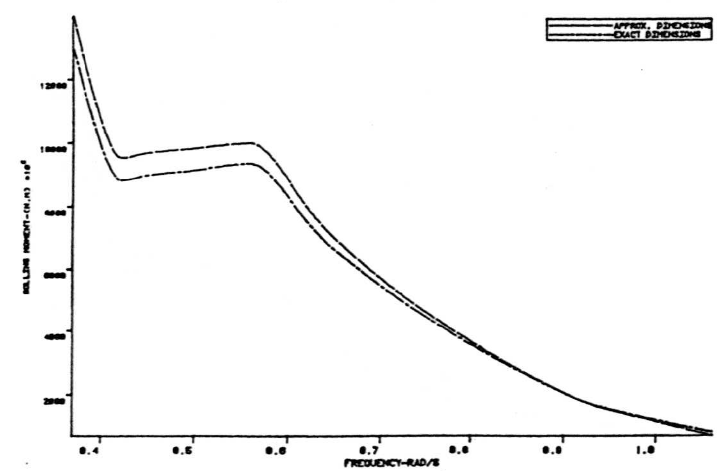

COEFFICIENTS: SARPKAYA , β = 0.0, SR= 1/200
FIG. (55) MAX. ROLLING MOMENTS Vs. FREQUENCY

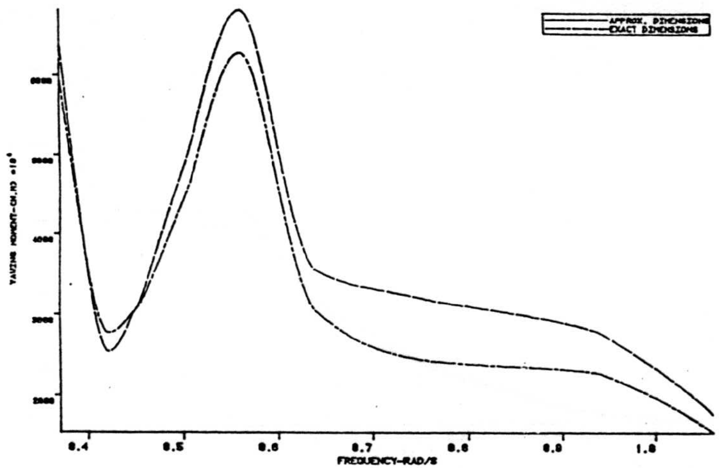

COEFFICIENTS: SARPKAYA , $\beta = 0.0$, SR= 1/200
FIG. (56) MAX. YAWING MOMENTS Vs. FREQUENCY

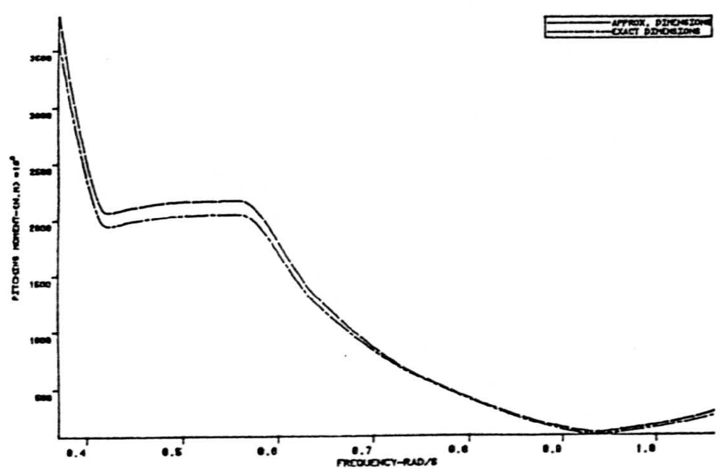

COEFFICIENTS: SARPKAYA , $\beta = 0.0$, SR= 1/200
FIG. (57) MAX. PITCHING MOMENTS VS. FREQUENCY

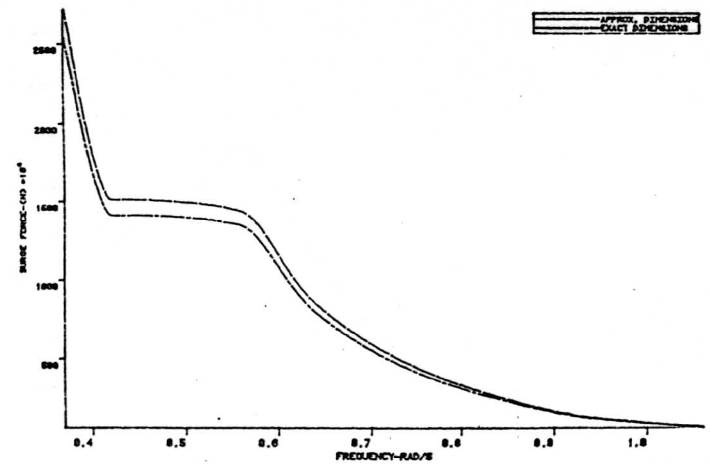

COEFFICIENTS: SARPKAYA , $\beta = \frac{\pi}{4}$, SR= 1/200
FIG. (58) MAX. SURGE FORCES Vs. FREQUENCY

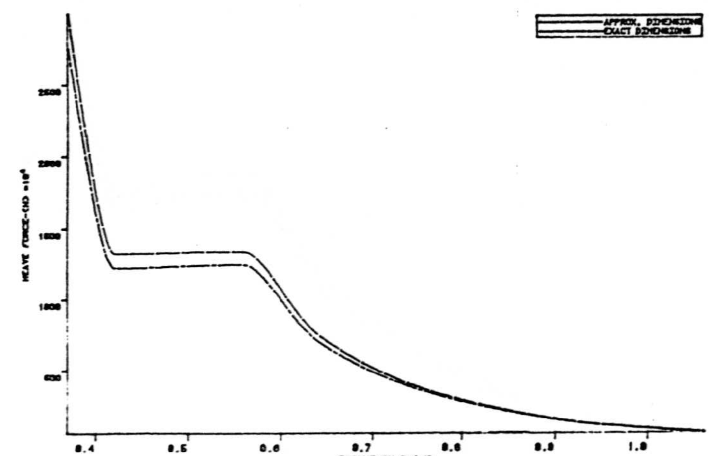

COEFFICIENTS: SARPKAYA , $\beta = \frac{\pi}{4}$, SR= 1/200
FIG. (59) MAX. HEAVE FORCES Vs. FREQUENCY

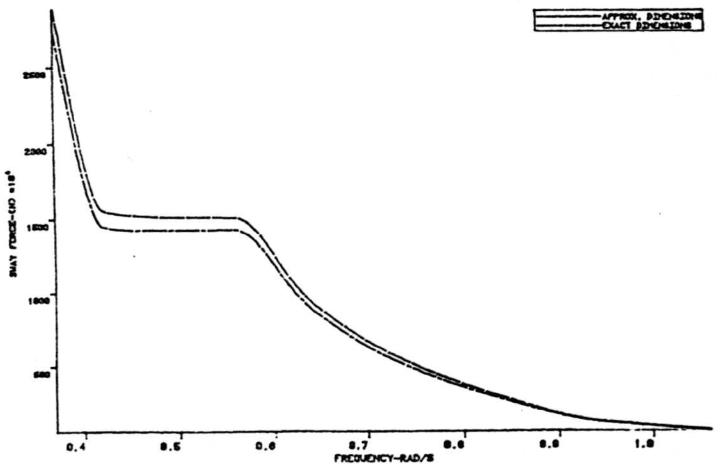

COEFFICIENTS: SARPKAYA , $\beta = \frac{\pi}{4}$,SR= 1/200
FIG.-(60) MAX. SWAY FORCES Vs. FREQUENCY

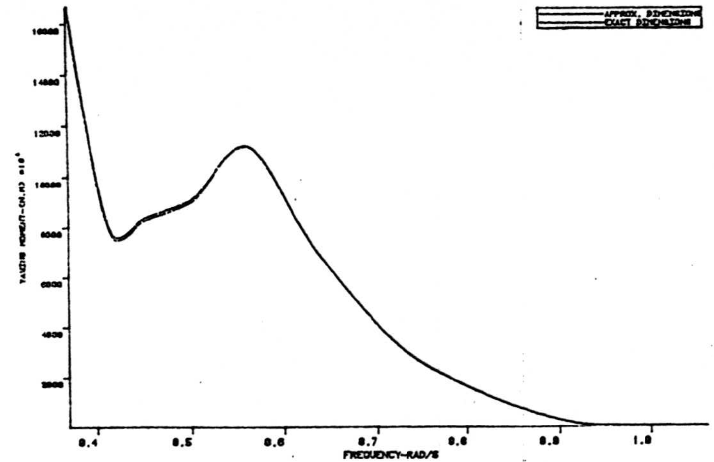

COEFFICIENTS: SARPKAYA , $\beta = \frac{\pi}{4}$,SR= 1/200
FIG. (62) MAX. YAWING MOMENTS Vs. FREQUENCY

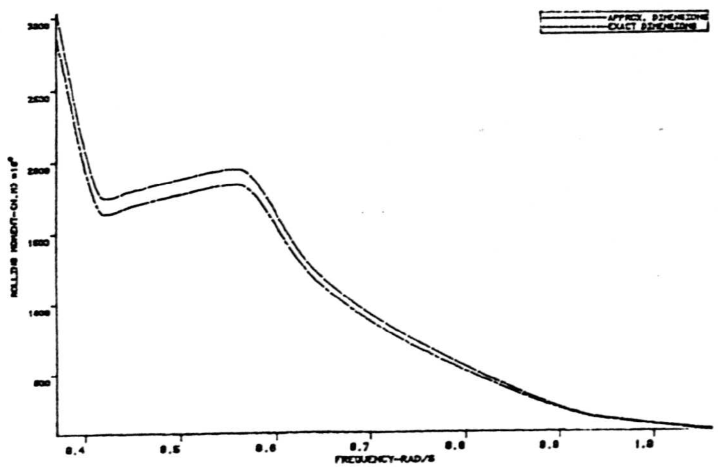

COEFFICIENTS: SARPKAYA , $\beta = \frac{\pi}{4}$,SR= 1/200
FIG. (61) MAX. ROLLING MOMENTS Vs. FREQUENCY

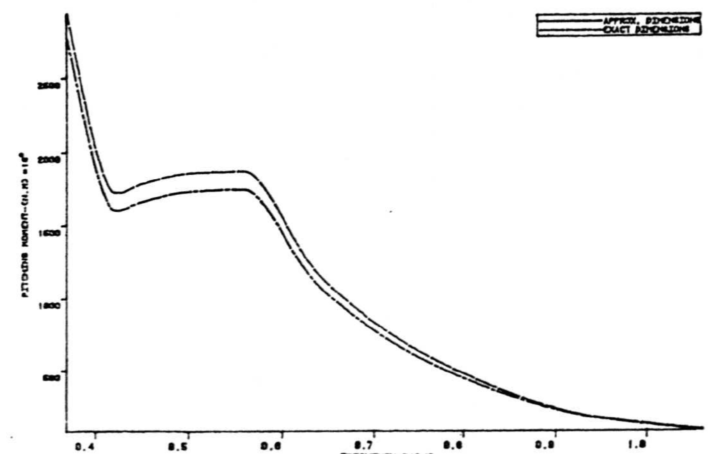

COEFFICIENTS: SARPKAYA , $\beta = \frac{\pi}{4}$,SR= 1/200
FIG. (63) MAX. PITCHING MOMENTS VS. FREQUENCY

CHAPTER 6

CHAPTER 6

WAVE LOADING CALCULATIONS BY AIRY AND STOKES' HIGHER ORDER WAVE THEORIES

1. INTRODUCTION

The rapid build up in offshore activities and the tendency to construct fixed offshore structures in deeper waters require the development of safe and economical designs capable of withstanding the severe environmental conditions. This, in turn, necessitates the ability to calculate the design wave(s) kinematics as accurately as possible and, hence, improve the accuracy of the calculated wave forces and moments.

However, the problem of selecting, from a large number of wave theories, the most suitable one for a particular design environment is difficult.

The majority of the available studies comparing different wave theories are mainly concerned with examining the ability of the different theories to fit the boundary conditions and they recommend one theory or another to be used in a certain situation (eg deep or shallow waters). This, however, will not guarantee that the chosen wave theory will predict the actual forces and the moments on the structure more accurately.

The errors in fitting the boundary conditions and the differences in the velocities and accelerations as predicted by the various theories may not be a true reflection of the final differences in the forces and moments. Besides accuracy, the availability and simplicity of using a wave theory is also one of the important factors to be considered in making the choice.

The first part of the present chapter compares three of the wave theories (Airy, Stokes' 2nd order and Stokes' 5th order) in terms of wave profile, horizontal and vertical velocities and accelerations. The second part compares the results of wave loading calculations for a typical jacket platform by Airy wave and Stokes' 5th order wave theories.

2 WAVE THEORIES AND THEIR VALIDITIES

Dean (3) compared the various wave theories by calculating the fits to the two non-linear (kinematic and dynamic) free surface boundary conditions as indicators of the relative validities of the different theories. The results of Dean's paper are shown in Fig. (1). Dean found that Stokes' fifth order wave provides the best fit for $d/T^2 > 0.2$ in the case of the dynamic free surface boundary condition. For $d/T^2 < 0.2$, the fit to the boundary condition for Airy theory is better than that for either the third or fifth order Stokes' theories. In other words, the Stokes' fifth order theory provides the best fit for deep water waves whereas Airy theory provides the best fit for shallower water waves. However, Dean emphasised that the better agreement with the specified boundary conditions does not necessarily imply the best overall theory.

For intermediate water depths, Dean's calculations (3) showed that the maximum drag force according to the Airy wave theory is 59% and 69% of the values calculated according to Stokes' third and

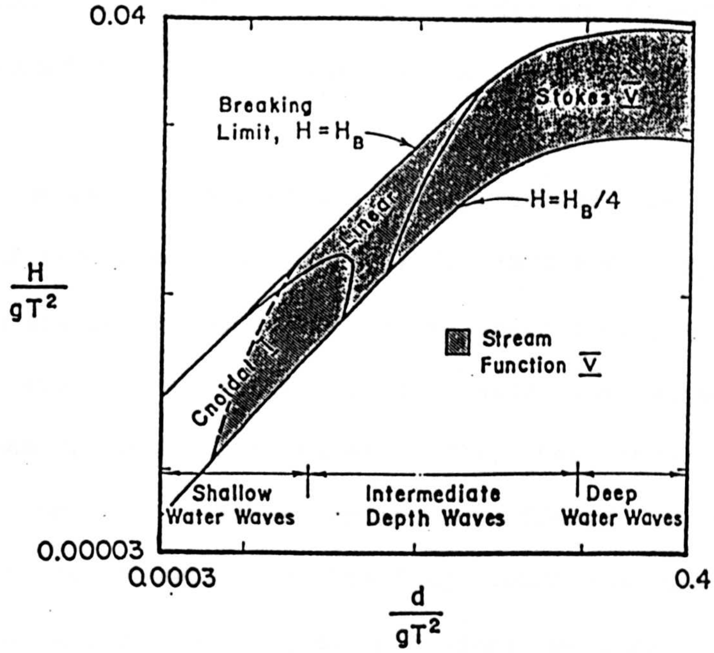

FIG. (1) Ranges of Validity of Various Wave Theories (Dean 1970), Ref 13

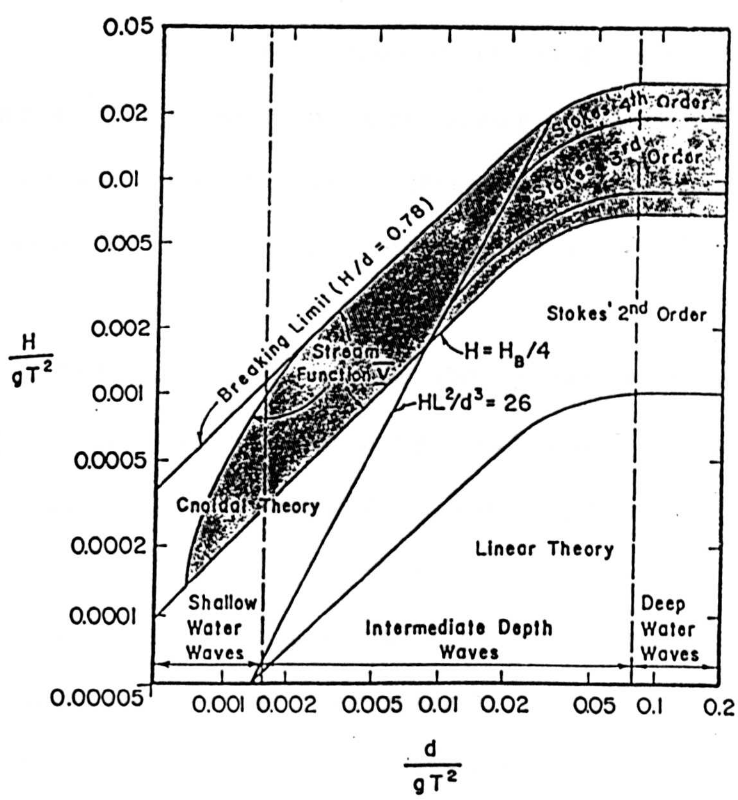

FIG. (2) Ranges of Validity of Various Wave Theories (Le Mehaute 1976), Ref 13 fifth orders, respectively.

Le Mehaute (9) presented a graph similar to that of Dean showing the approximate limits of validity for the different wave theories. It shows that Stokes' third and fourth order theories are recommended for the deep water range, Fig. (2).

Hogben and Standing (7) compared Airy and Stokes' fifth order waves of the same height and period. (H/d = 0.2, H/g.T = 0.015, 0.01). For the steeper wave, Stokes' fifth order theory gave a wave length 7% longer than that given by the Airy theory. When integration was performed up to the mean water level, the total inertia and drag forces on a slender cylinder differed by about 7% and 13% respectively. Hogben and Standing concluded that Airy theory is adequate except for drag dominated members (eg conductor tubes) especially near the free surface of the wave.

In deep water, Hogben et al (8) suggested that the prediction of the wave loading using Airy theory but integrating the forces up to the actual wave surface, gives results which do not differ greatly from those of Stokes' fifth order theory.

The suitability of one theory over another from a theoretical viewpoint is not necessarily reflected in better agreement with experimental data from the laboratory or the field (13).

Tsuchiya and Yamaguchi (15) compared theoretical predictions with measurements of wave celerity, horizontal and vertical particle velocities at various depths in phase with a wave crest and trough and temporal variations of the wave profile and the horizontal and vertical velocity components. The study included Airy wave theory, Stokes' fourth and fifth order theories and the second and third approximations to cnoidal wave theory. They found that finite amplitude wave theories predict velocities well but they did not recommend any one theory as being the most suitable over any particular range.

Grace (6) measured wave particle velocities and accelerations in the ocean environment and found a favourable comparison between the observed maximum horizontal velocity and the predictions of Airy wave theory.

Ohmart and Gratz (12) compared water surface profiles and horizontal particle velocities and accelerations measured in the Gulf of Mexico with the predictions of Airy, Stokes' fifth and stream function wave theories. They found that, except for the higher waves, the Airy theory predictions were close to those of the Stokes' fifth order theory.

Dean et al (4) analysed the data of up to 178 of the higher waves measured during three separate storms/storm seasons (1976-1978) on the Ocean Test Structure (OTS). The wave height ranged from 9ft to 24ft and the wave period ranged from 6 to 12 sec.

It was found that Stokes' fifth order theory generally yielded kinematics and forces that were of the order of 10% to 30% larger than those obtained from measured velocities.

Bishop et al (1) found that the measured particle velocities and accelerations from the Christchurch Bay Tower were larger than the values calculated in the design phase, which were based on shallow water wave theories. The measured kinematics tended to agree better with Airy wave theory. Bishop et al also pointed out that shallow water wave theories can grossly overpredict the kinematics of sea waves which are depth limited.

Chakrabarti (2) mentioned that recent test results in a wave tank have established that the stream function theory (5) predicts the wave motion in the tank more accurately over its whole range of development than the Airy theory.

McNamee et al (10) reported measurements of wave profiles and horizontal and vertical components of water particle velocity to investigate the properties of intermediate depth waves generated in the laboratory. The wave period ranged from 1.1 to 2.5 sec. The wave steepness (H/L) varied from 0.008 to 0.049 while the depth to wave length ratio (d/L) varied from 0.15 to 0.50. The experimental data were compared with Airy wave theory. It was found that the Airy theory predicted the attenuation of the velocity field with depth successfully but it overestimated both components of the velocity slightly.

3. CALCULATION OF THE WAVE KINEMATICS BY THE VARIOUS THEORIES

A brief description for the calculaton of the wave velocities and accelerations by each wave theory is given below. The complete set of equations for each theory is presented in Appendix (C).

The method of transferring the particle velocities and accelerations from the wave reference system (x, y, z) to the structure reference system (X, Y, Z) or to the member reference system (u, v, w) has been described in Chapter 3 for the case of Airy theory. The same method has been used also for Stokes' second order and fifth order wave theories.

3.1 Airy (Linear) Wave Theory

The wave properties were calculated from the expressions given in Table (C.1), Appendix (C), for deep water (13). The calculations of the wave loading were done by program OSS.

3.2 Stokes' 2nd Order Wave Theory

The wave properties were calculated from the expressions given in Table (C.3), Appendix (C). The calculations of the wave loading were done by Program SNDOR.

3.3. Stokes' 5th Order Wave Theory

The wave properties were calculated according to the theory of Skjelbreia and Hendrickson (14) as follows.

For a given design wave, described by the height (H) and length (L), the two coefficients k and λ are related by the following pair of equations (14):-

$$\frac{\pi . H}{d} = \frac{1}{(d/L)} \{\lambda + \lambda^3 . B_{33} + \lambda^5 (B_{35} + B_{55})\} \tag{1}$$

$$\frac{d}{L_o} = (\frac{d}{L}) \text{ Tanh } (kd) \{1 + \lambda^2 C_1 + \lambda^4 C_2\} \tag{2}$$

where: d = water depth (m)

k = wave number, $2\pi/L$

$L_o = \frac{g.T^2}{2\pi}$ (m)

T = wave period (sec)

g = acceleration due to gravity (m/s^2)

From equation (1), $\frac{d}{L} = \frac{d}{\pi.H} \{\lambda + \lambda^3.B_{33} + \lambda^5 (B_{35} + B_{55})\}$

or $\frac{d}{L} = \frac{d}{\pi.H} (\lambda + \lambda^3.B_{33} + \lambda^5.B_t)$ (3)

where: $B_t = B_{35} + B_{55}$

Substituting for $(\frac{d}{L})$ in equation (2) and arranging, we get:

$$\frac{\pi.H}{L_o} = \{\lambda + \lambda^3 (B_{33} + C_1) + \lambda^5 (B_t + C_1.B_{33} + C_2)$$

$$+ \lambda^7(B_t.C_1 + B_{33}.C_2) + \lambda^9.B_t.C_2\}\text{Tanh}\,\frac{2d}{H} (\lambda + \lambda^3.B_{33} + \lambda^5.B_t) \quad (4)$$

Since the coefficients B_{33}, B_{35}, B_{55}, C_1 and C_2 are known functions of d/L only, Appendix (C), the solution may be started by approximating d/L to d/L_o and the coefficients can be calculated from the expressions given in Table (C.5), Appendix (C).

A computer program was used to solve equation (4) by an iterative procedure so that λ can be determined. From equation (3) the correct value of d/L can be determined and, hence, the wave length (L) can be calculated.

The correct values of the coefficients (A, B, C ...) can now be estimated, Table (C.5), Appendix (C), and the wave profile, velocities and accelerations can be calculated from the expressions given in Table (C.4), Appendix (C). The calculations of the wave loading were performed by program STKFS.

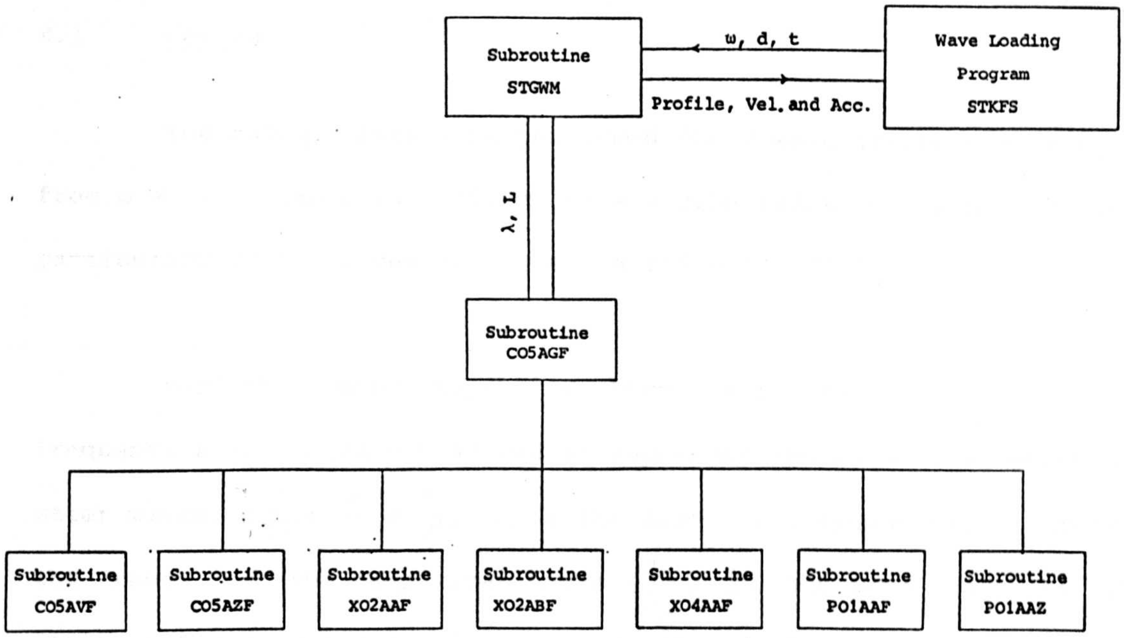

Fig. (3) Arrangement of Program STKFS

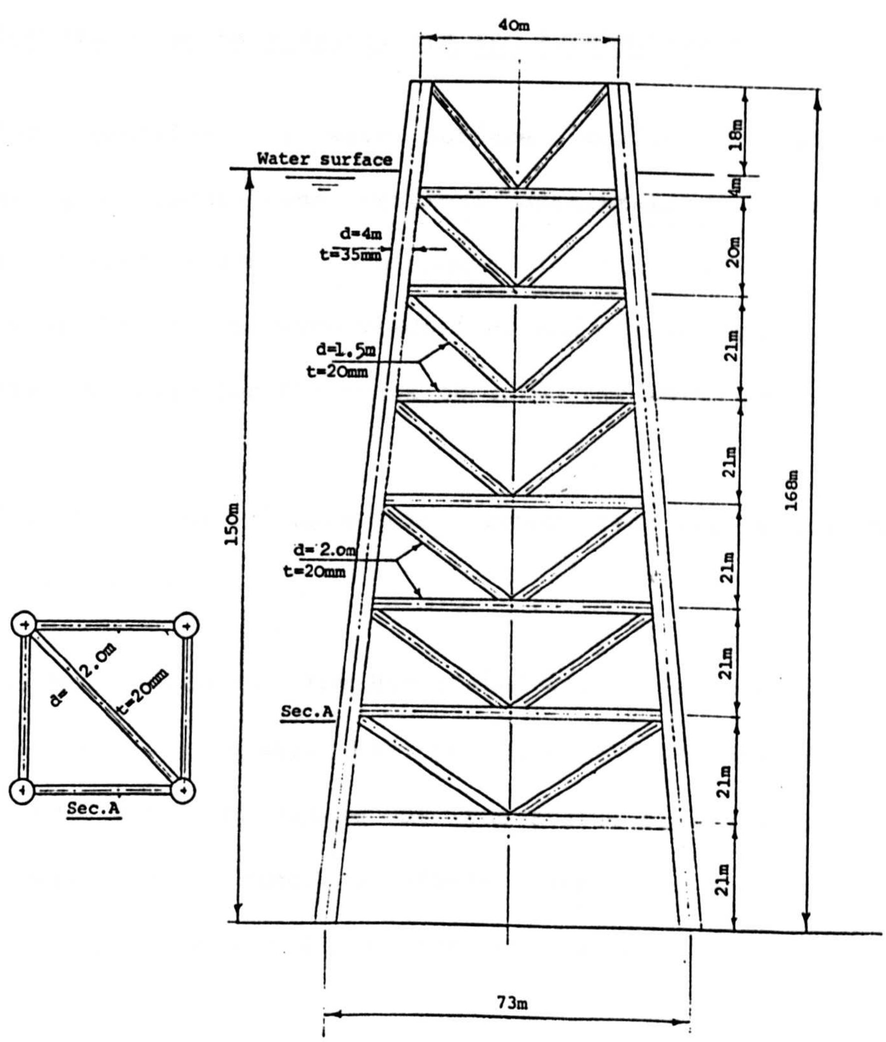

Fig. (4) Main Particulars of the Jacket Structure

4 WAVE PROFILE, VELOCITY AND ACCELERATION CALCULATIONS

4.1 General

The calculations were performed for 7 wave frequencies ranging from ω = 0.32 rad/s (H = 30.0m) to ω = 0.56 rad/s (H = 20m). The full particulars of the waves are given in Table (1).

For the water depth of 150m, Fig. (4), the first four frequencies (ω = 0.32 - 0.42 rad/s) represent the case of intermediate water waves, ($\frac{1}{20} \leqslant \frac{d}{L_o} \leqslant \frac{1}{2}$), while the last three frequencies represent the range of the deep water waves ($\frac{d}{L_o} \geqslant \frac{1}{2}$). The wave steepness ($\frac{H}{L_o}$) varies between $\frac{1}{20}$ for the longest wave (L_o = 601m) to a maximum of $\frac{1}{10}$ for the shortest one (L_o = 196.45m).

4.2 Comparison of Wave Velocities and Accelerations

The profiles of wave surface, horizontal and vertical velocities and horizontal and vertical accelerations calculated by Airy and Stokes' theories are shown in Figs. (5) to (7). The variations of the maximum wave velocities and accelerations with the depth below surface for the three theories are shown in Figs. (8) to (14).

Figures (5) to (7) show some common features which may be summarised as follows:-

a. The profiles of the horizontal velocities and the vertical accelerations show that, for Airy wave (sinusoidal wave), the absolute values at the start, middle and end of the wave are the same. For Stokes' waves, the absolute value of the horizontal velocity (or vertical acceleration) at the

Wave Frequency ω (rad/s)	Height H (m)	Length Lo (m)	Period T (s)	H/Lo	$\frac{d}{Lo}$	Condition
0.32	30.0	601	19.6	0.05 $(\frac{1}{20})$	0.25	Intermediate
0.34	30.0	532	18.47	0.06 $(\frac{1}{16})$	0.28	Intermediate
0.37	30.0	450.01	16.97	0.07 $(\frac{1}{15})$	0.33	Intermediate
0.42	25.0	349.24	14.95	0.07 $(\frac{1}{15})$	0.43	Intermediate
0.45	20.0	304.23	13.96	0.07 $(\frac{1}{15})$	0.49	Deep Water
0.50	20.0	246.43	12.56	0.08 $(\frac{1}{12})$	0.60	Deep Water
0.56	20.0	196.45	11.21	0.10 $(\frac{1}{10})$	0.76	Deep Water

TABLE (1) Particulars of Waves

middle of the wave length is smaller than the values at the ends.

b. The profiles of the vertical velocities and horizontal accelerations show a phase difference between Airy wave, Stokes' second order and Stokes' fifth order waves. This may affect the timing of occurrence of the maximum forces and moments on the members of the structure.

c. For the shorter waves (ω = 0.42 - 0.56 rad/s), the profiles of velocities and accelerations according to both Airy theory and Stokes' second order theory are almost the same. This may be explained by the fact that the velocities and accelerations of the Airy theory were calculated by the expressions approximated for the case of deep water, Table (C.2), Appendix (C), and, therefore, the accuracy is better than the range of intermediate depth waves (ω = 0.32 - 0.37 rad/s).

The graphs of the variations of the maximum velocities and accelerations with the depth below the water surface, Figs.(8) to (14), show also some features:-

a. For the longer waves (ω = 0.37 rad/s), the deviations between the curves for the different theories are relatively large. However, unlike Stokes' fifth order and second order theories, the curves of Airy theory do not tend to converge with the corresponding curves for the Stokes' theories when the depth below surface is larger than about 60m. This may be due to the reduced accuracy of the approximate expressions for velocities and accelerations when used for intermediate depth rather than deep water.

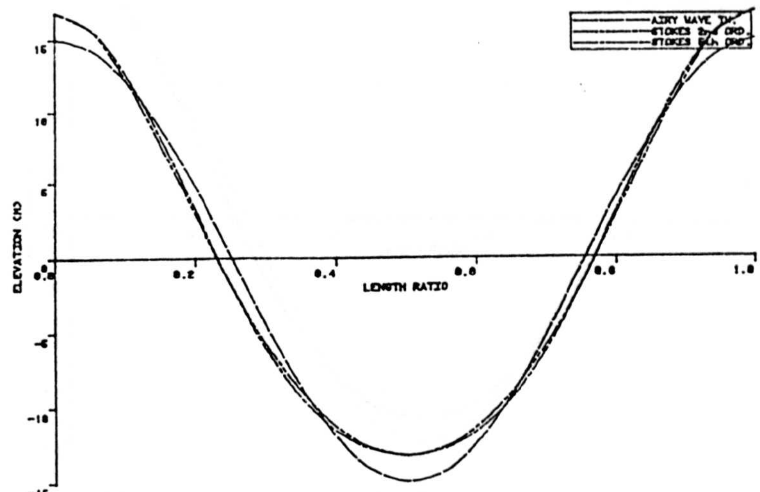

FREQUENCY(ω)= 0.37 R/S HEIGHT(H)=30.0 M LENGTH(Lo)=450.0 M
FIG.(5.1) WAVE PROFILE BY DIFFERENT WAVE THEORIES

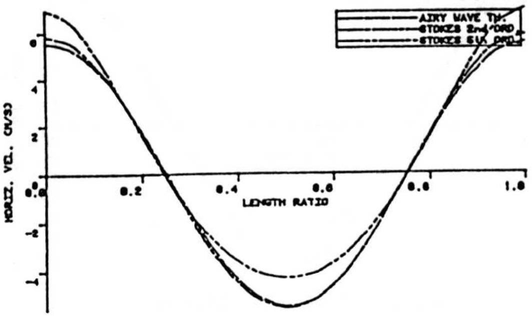

(a) HORIZONTAL VELOCITY(Ux)

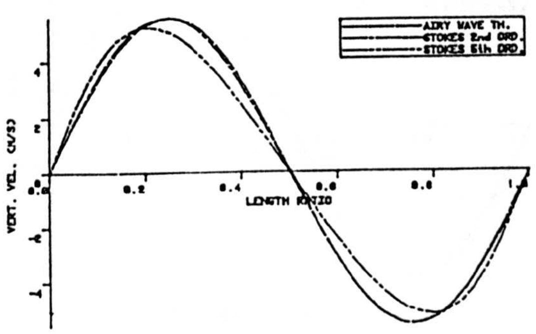

(b) VERTICAL VELOCITY(Uy)

ω = 0.37 R/S

FIG.(5.2) WAVE VELOCITY BY DIFFERENT WAVE THEORIES

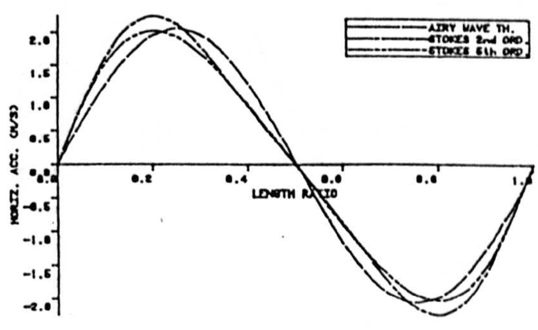

(a) HORIZONTAL ACCELERATION(Ax)

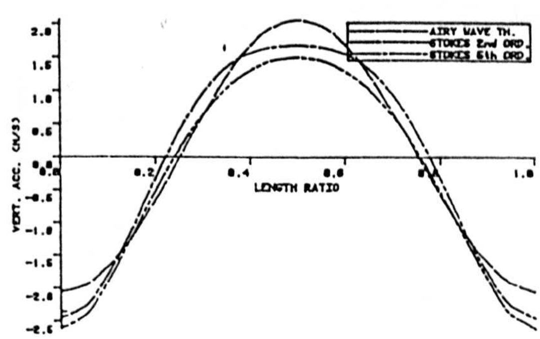

(b) VERTICAL ACCELERATION(Ay)

ω = 0.37 R/S

FIG.(5.3) WAVE ACCELERATION BY DIFFERENT WAVE THEORIES

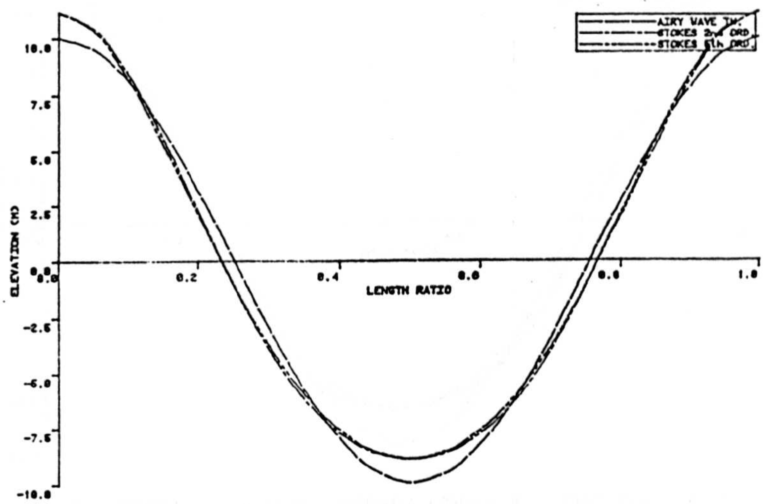

FREQUENCY(ω)=0.45 R/S HEIGHT(H)=20.0 M LENGTH(Lo)=304.2M
FIG.(6.1) WAVE PROFILE BY DIFFERENT WAVE THEORIES

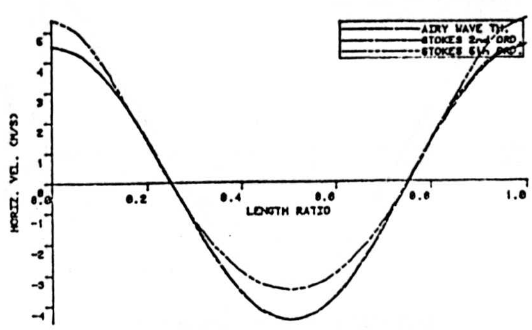

(a) HORIZONTAL VELOCITY(Ux)

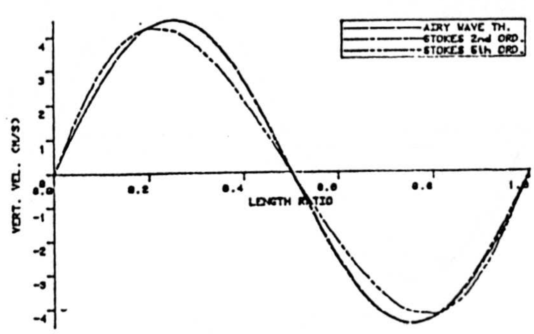

(b) VERTICAL VELOCITY(Uy)

ω = 0.45 R/S

FIG.(6.2) WAVE VELOCITY BY DIFFERENT WAVE THEORIES

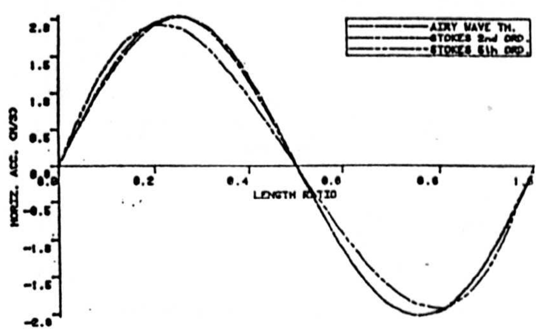

(a) HORIZONTAL ACCELERATION(Ax)

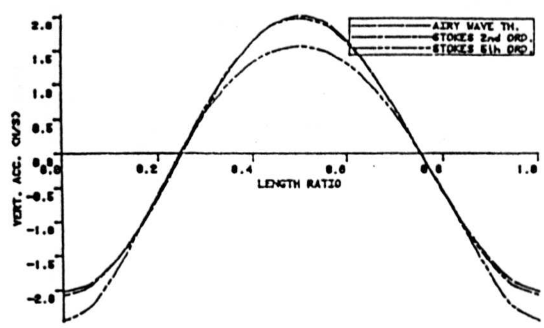

(b) VERTICAL ACCELERATION(Ay)

ω = 0.45 R/S

FIG.(6.3) WAVE ACCELERATION BY DIFFERENT WAVE THEORIES

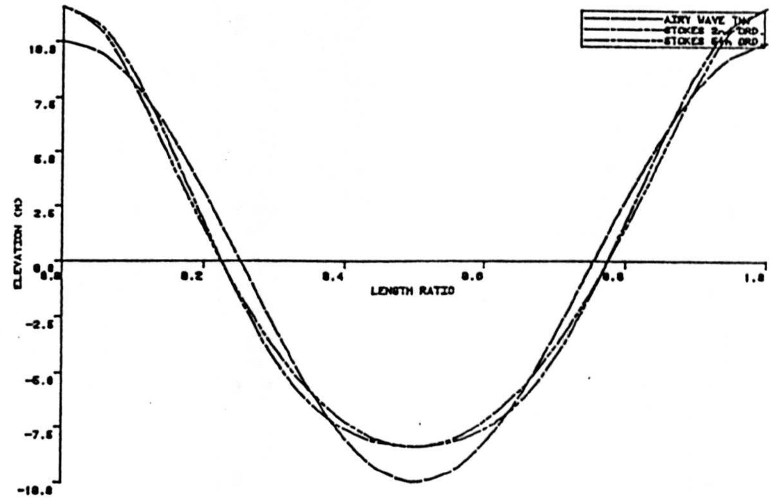

FREQUENCY(ω)= 0.56R/S HEIGHT(H)=20.0 M LENGTH(L_0)= 196.5M

FIG.(7.1) WAVE PROFILE BY DIFFERENT WAVE THEORIES

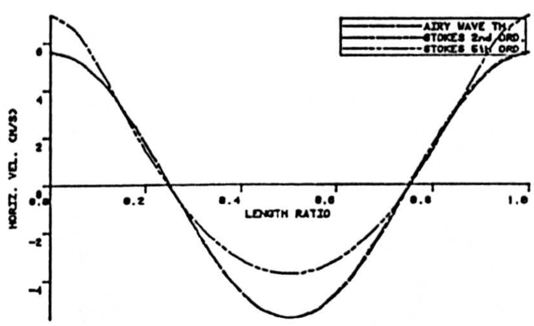

(a) HORIZONTAL VELOCITY(Ux)

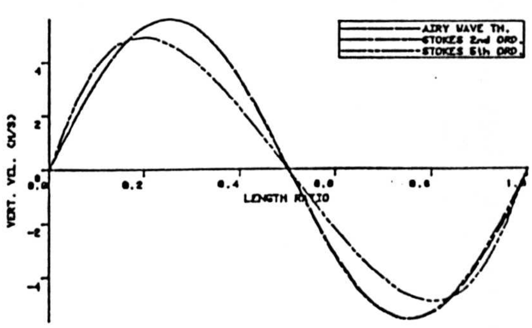

(b) VERTICAL VELOCITY(Uy)

ω = 0.56 R/S

FIG.(7.2) WAVE VELOCITY BY DIFFERENT WAVE THEORIES

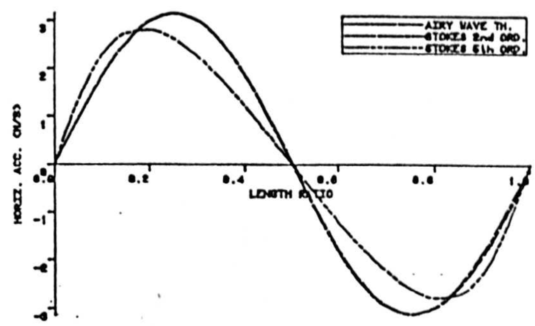

(a) HORIZONTAL ACCELERATION(Ax)

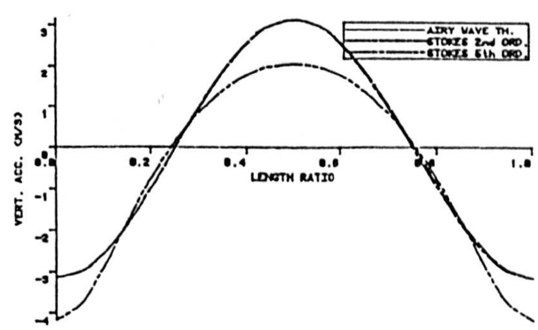

(b) VERTICAL ACCELERATION(Ay)

ω = 0.56 R/S

FIG.(7.3) WAVE ACCELERATION BY DIFFERENT WAVE THEORIES

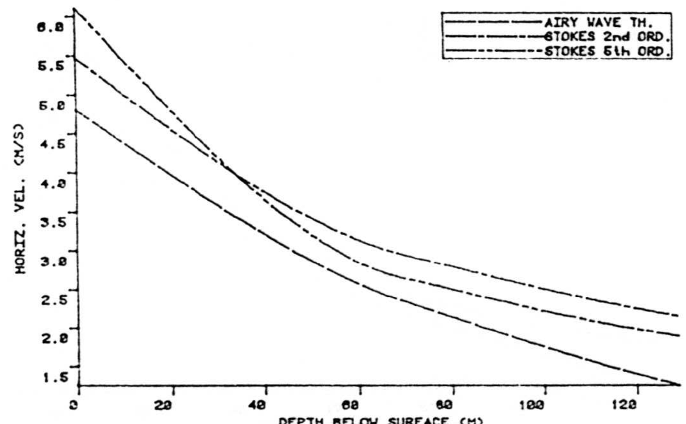

(a) MAX. HORIZONTAL VELOCITY(Uxm)

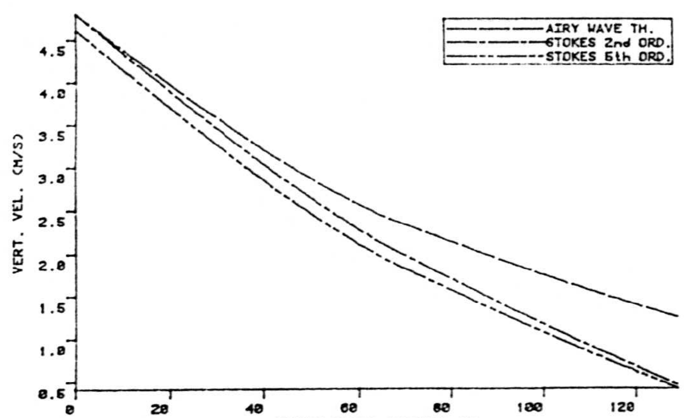

(b) MAX. VERTICAL VELOCITY(Uym)

$\omega = 0.32$ R/S

FIG.(8.1) MAX. VELOCITIES Vs. DEPTH BY DIFFERENT THEORIES

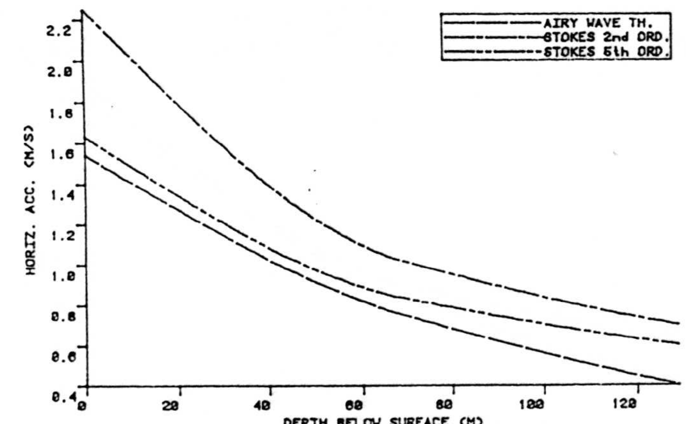

(a) MAX. HORIZONTAL ACCELERATION(Axm)

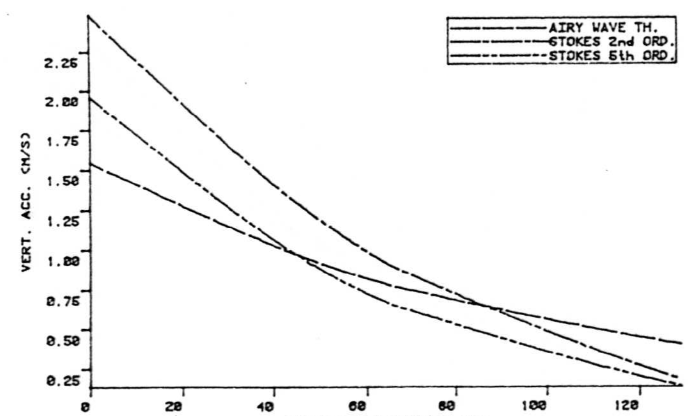

(b) MAX. VERTICAL ACCELERATION(Aym)

$\omega = 0.32$ R/S

FIG.(8.2) MAX. ACCEL. Vs. DEPTH BY DIFFERENT THEORIES

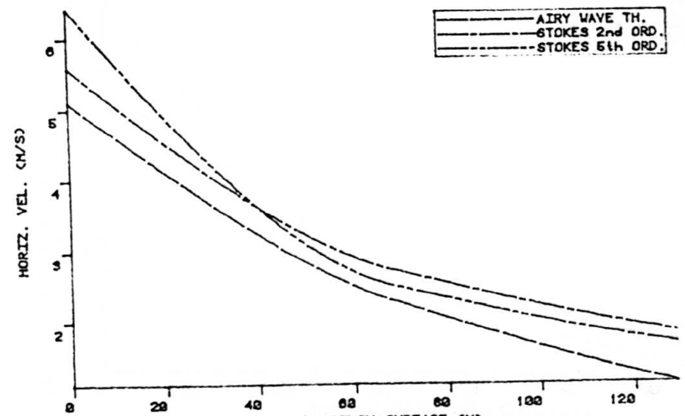

(a) MAX. HORIZONTAL VELOCITY(Uxm)

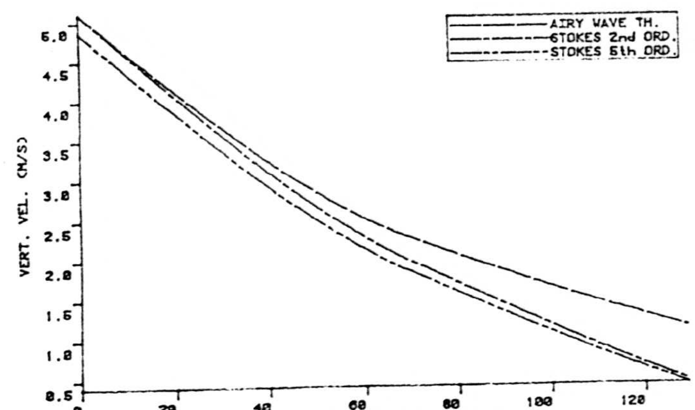

(b) MAX. VERTICAL VELOCITY(Uym)

ω = 0.34 R/S

FIG. (9.1) MAX. VELOCITIES Vs. DEPTH BY DIFFERENT THEORIES

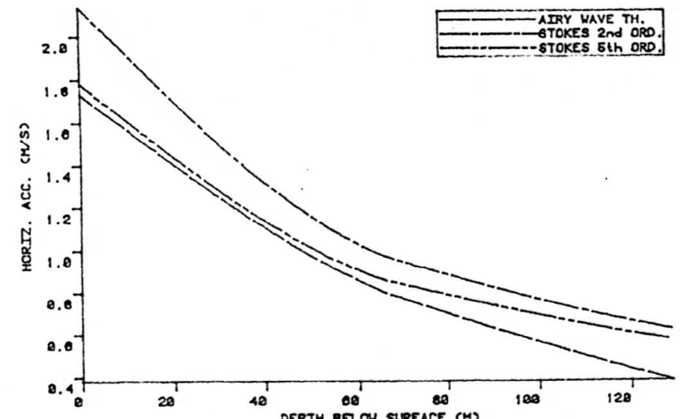

(a) MAX. HORIZONTAL ACCELERATION(Axm)

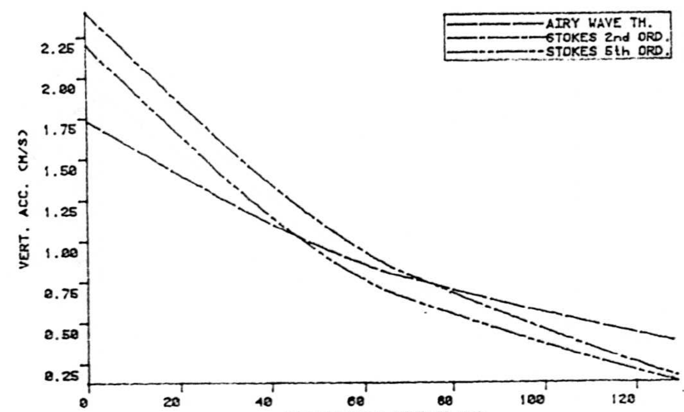

(b) MAX. VERTICAL ACCELERATION(Aym)

ω = 0.34 R/S

FIG. (9.2) MAX. ACCEL. Vs. DEPTH BY DIFFERENT THEORIES

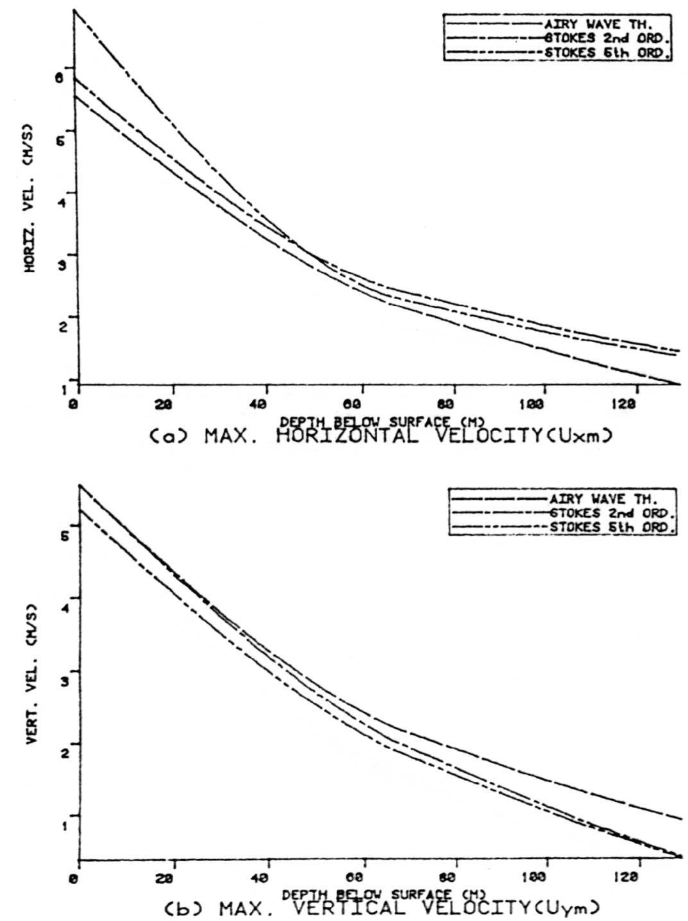

(a) MAX. HORIZONTAL VELOCITY(Uxm)

(b) MAX. VERTICAL VELOCITY(Uym)

ω = 0.37 R/S

FIG. (10.1) MAX. VELOCITIES Vs. DEPTH BY DIFFERENT THEORIES

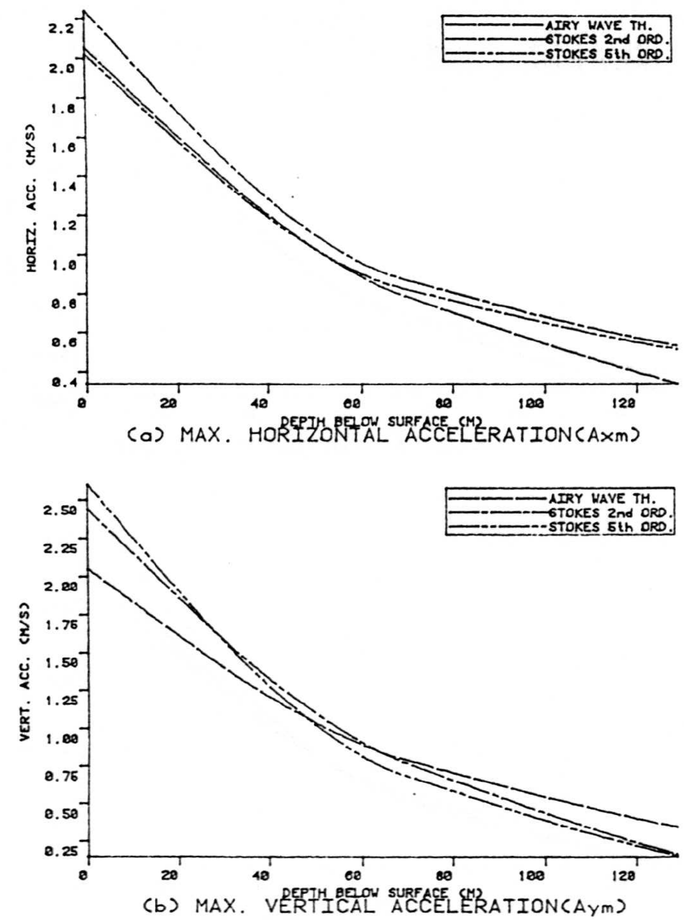

(a) MAX. HORIZONTAL ACCELERATION(Axm)

(b) MAX. VERTICAL ACCELERATION(Aym)

ω = 0.37 R/S

FIG. (10.2) MAX. ACCEL. Vs. DEPTH BY DIFFERENT THEORIES

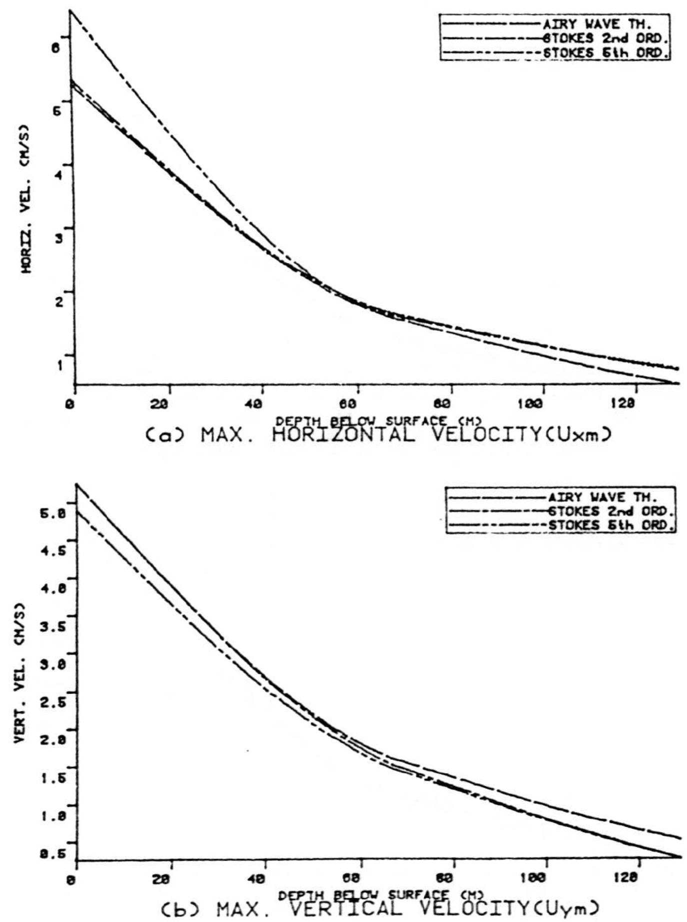

ω = 0.42 R/S

FIG. (11.1) MAX. VELOCITIES Vs. DEPTH BY DIFFERENT THEORIES

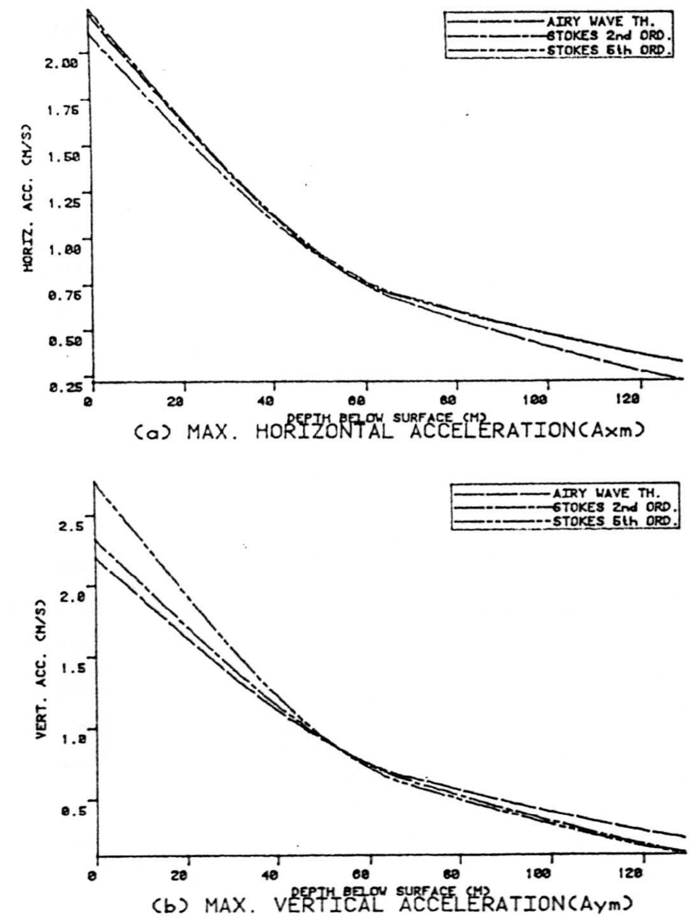

ω = 0.42 R/S

FIG. (11.2) MAX. ACCEL. Vs. DEPTH BY DIFFERENT THEORIES

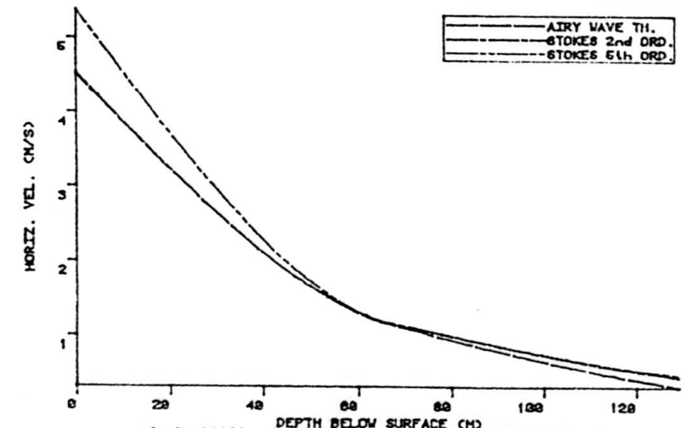

(a) MAX. HORIZONTAL VELOCITY(Uxm)

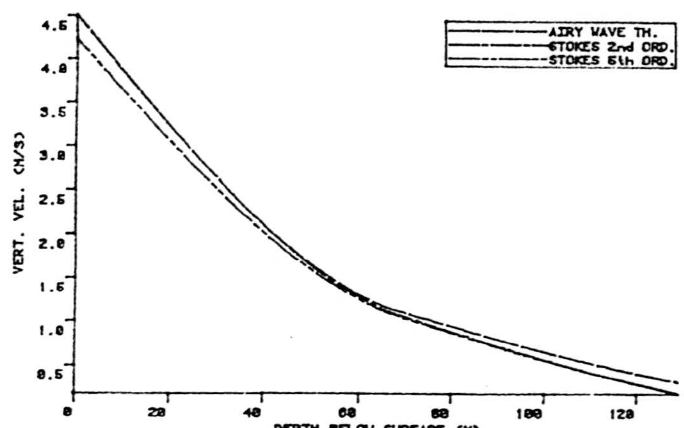

(b) MAX. VERTICAL VELOCITY(Uym)

ω = 0.45 R/S

FIG. (12.1) MAX. VELOCITIES Vs. DEPTH BY DIFFERENT THEORIES

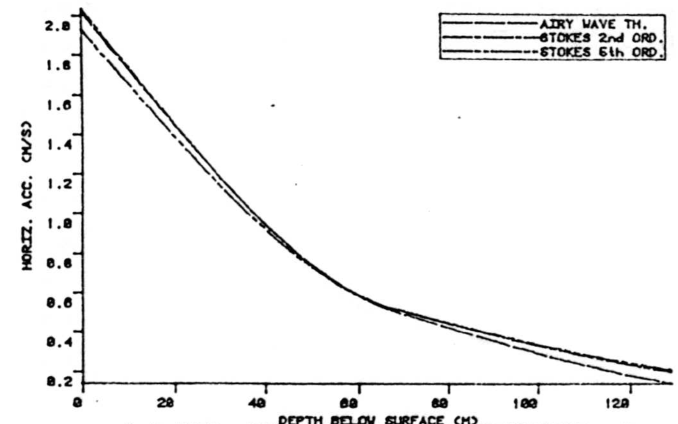

(a) MAX. HORIZONTAL ACCELERATION(Axm)

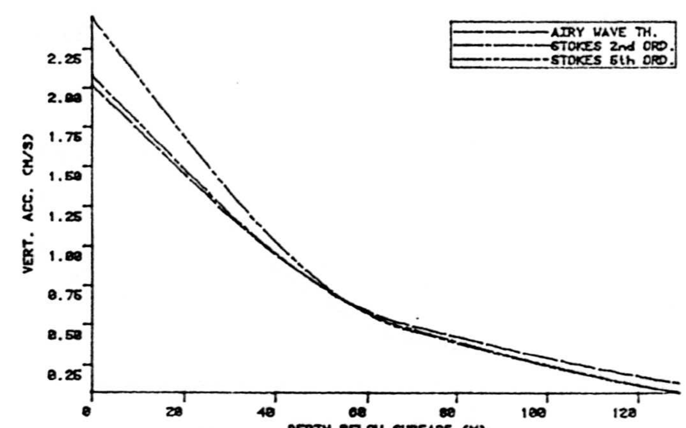

(b) MAX. VERTICAL ACCELERATION(Aym)

ω = 0.45 R/S

FIG. (12.2) MAX. ACCEL. Vs. DEPTH BY DIFFERENT THEORIES

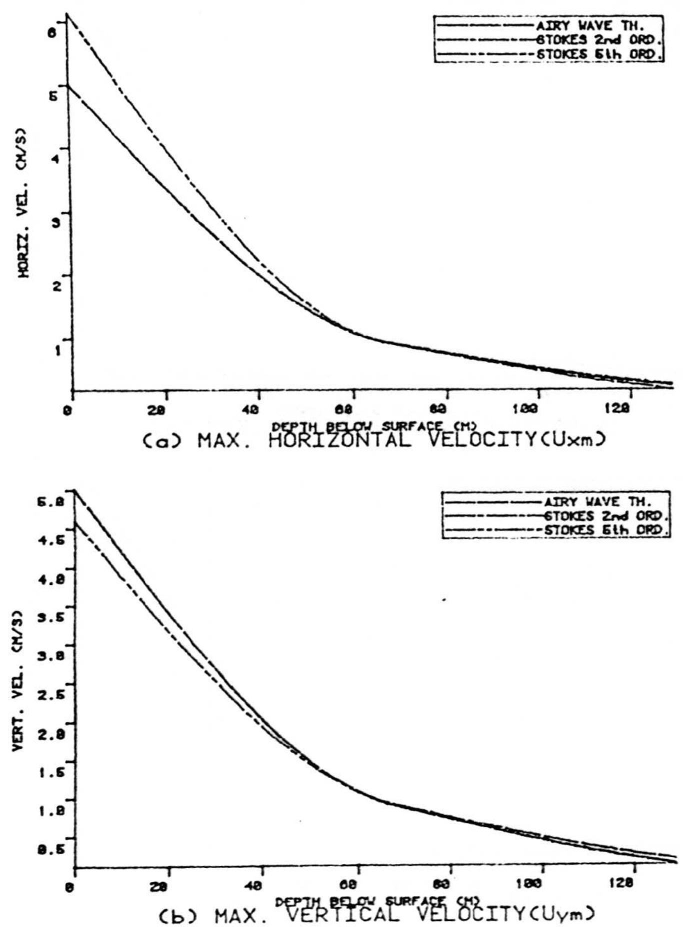

ω = 0.5 R/S

FIG. (13.1) MAX. VELOCITIES Vs. DEPTH BY DIFFERENT THEORIES

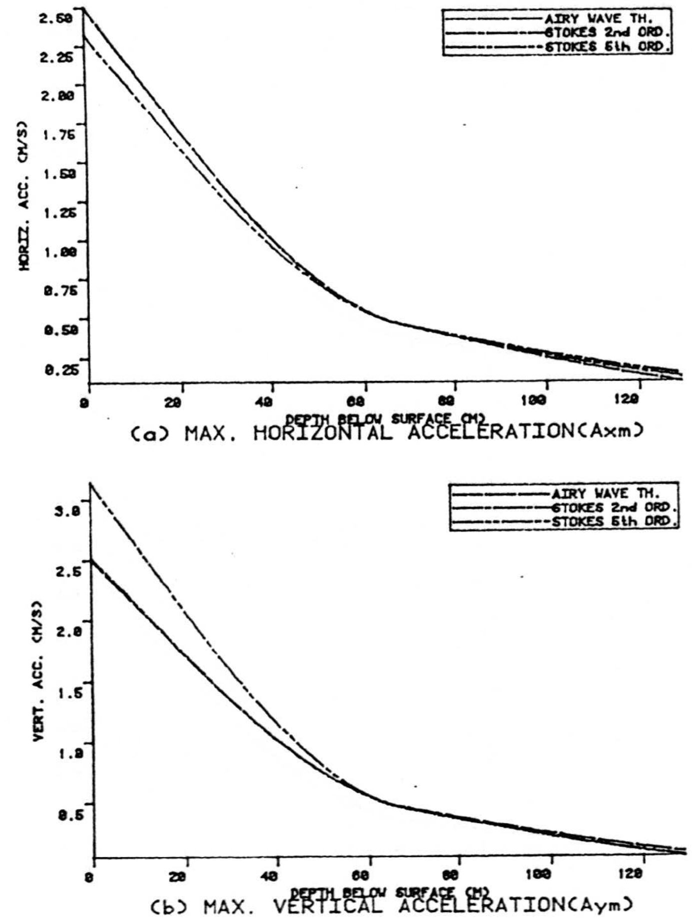

ω = 0.5 R/S

FIG. (13.2) MAX. ACCEL. Vs. DEPTH BY DIFFERENT THEORIES

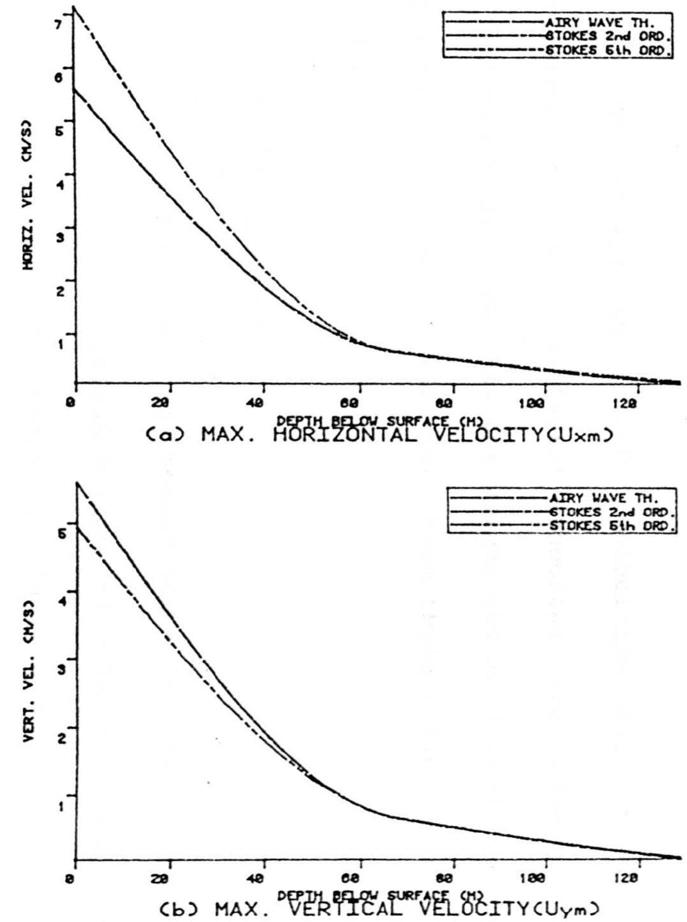

ω = 0.56 R/S

FIG. (14.1) MAX. VELOCITIES Vs. DEPTH BY DIFFERENT THEORIES

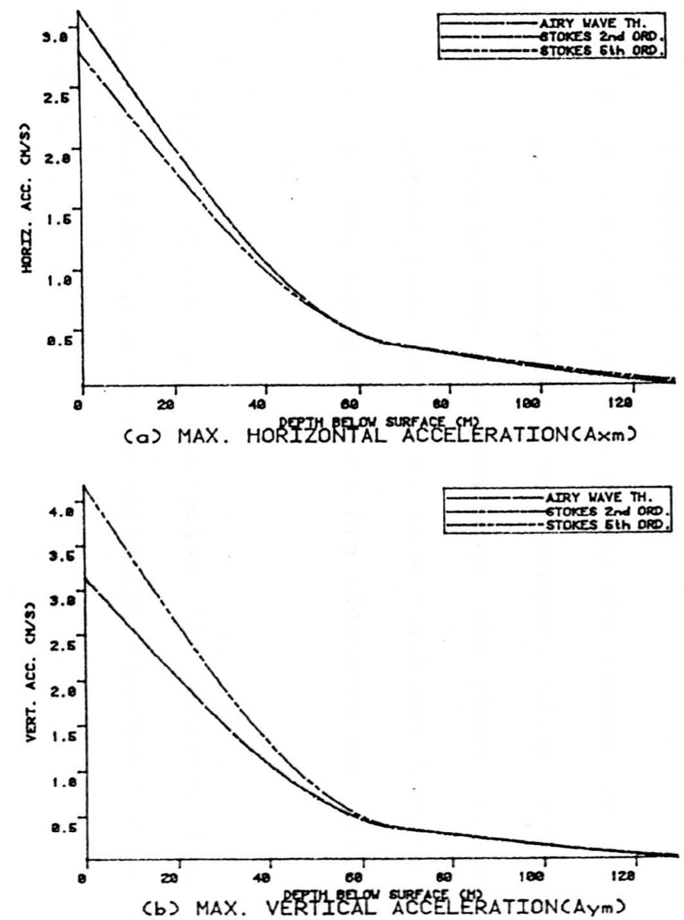

ω = 0.56 R/S

FIG. (14.2) MAX. ACCEL. Vs. DEPTH BY DIFFERENT THEORIES

b. For the two frequencies ω = 0.42 and 0.45 rad/s the curves for Airy theory and Stokes' second order theory are very close and at ω = 0.5 and 0.56 rad/s the curves are identical.

c. At ω = 0.42 and 0.45 rad/s, the curves of the velocities and accelerations for Stokes' fifth and second order theories are identical when the depth below surface is larger than about 60m. At ω = 0.5 and 0.56 rad/s the curves of the three theories are identical for depths larger than 60m.

Tables (2) to (5) summarise the maximum velocities and accelerations calculated by the different theories for all frequencies at three levels:-

1. The free surface, (the mean water level)is 150m above sea bed.
2. 66.0m below surface (84.0m above sea bed).
3. 129m below surface (21.0m above sea bed).

The variations in the velocities and accelerations as estimated by the different theories are shown as percentage differences with respect to the values obtained from Airy theory, the (-)ve sign indicates a reduction. From these tables, the following was noted:-

a. <u>Free Surface</u>

(1) According to Stokes' 5th order theory, the differences in the maximum horizontal velocity ranged from 19.6% (ω = 0.45 rad/s) to 27% (ω = 0.56 rad/s). According to Stokes' 2nd order theory, the differences ranged from 0.7% (ω = 0.45 rad/s) to 13.8% (ω = 0.32 rad/s).

(2) The differences in the maximum vertical velocity ranged from -8.2% (ω = 0.50 rad/s) to -12% (ω = 0.56 rad/s) for Stokes' 5th order theory. For Stokes' 2nd order theory the values are the same as Airy theory.

(3) The differences in the maximum horizontal acceleration ranged from -10.8% (ω = 0.56 rad/s) to 5.84% (ω = 0.32 rad/s) for the 5th order theory and from 1% (ω = 0.45 rad/s) to 46.1% (ω = 0.32 rad/s) for the 2nd order theory.

(4) The differences in the maximum vertical acceleration ranged from 21.3% (ω = 0.45 rad/s) to 32.8% (ω = 0.56 rad/s) for the 5th order theory and from 0.8% (ω = 0.50 rad/s) to 61% (ω = 0.32 rad/s) for the 2nd order theory.

(5) For the 5th order theory the maximum increase in the wave length is 8.2% (ω = 0.56 rad/s). The 2nd order theory gives the same wave length as the Airy theory.

b. <u>66.0m Below Surface</u>

(1) The differences in the maximum horizontal velocity ranged from 1.7% (ω = 0.50 rad/s) to 12% (ω = 0.32 rad/s) in the case of Stokes 5th order theory and from -1.5% (ω = 0.56 rad/s) to 24.5% (ω = 0.32 rad/s) in the case of Stokes 2nd order theory.

(2) The differences in the maximum vertical velocity ranged from -20.3% (ω = 0.32 rad/s) to 1.5 (ω = 0.56 rad/s) for the 5th order theory and from -1.5% (ω = 0.56 rad/s) to -13.7% (ω = 0.32 rad/s) for the 2nd order theory.

(3) The differences in the maximum horizontal acceleration ranged from 1.9% (ω = 0.45 rad/s) to 10.4% (ω = 0.32 rad/s) for the 5th order theory and from 1.9% (ω = 0.45 rad/s) to 35.1% (ω = 0.32 rad/s) for the 2nd order theory.

(4) The differences in the maximum vertical acceleration ranged from -15.6% (ω = 0.32 rad/s) to 2.6% (ω = 0.56 rad/s) in the case of 5th order theory and from -3.9% (ω = 0.45 rad/s) to 15.6% (ω = 0.32 rad/s) in the case of 2nd order theory.

c. <u>129.0m Below Surface</u>

In this case, the percentage differences in the maximum velocities and accelerations are much larger compared with cases (a) and (b). However, the actual magnitudes of the maximum velocities and maximum accelerations are much smaller than those of case (a) or case (b), especially at the higher frequencies.

(1) The differences in the maximum horizontal velocity ranged from 42.1% (ω = 0.50 rad/s) to 55.6% (ω = 0.56 rad/s) for the 5th order theory and from 22.2% (ω = 0.56 rad/s) to 72% (ω = 0.32 rad/s) for the 2nd order theory.

(2) The differences in the maximum vertical velocity ranged from -11.1% (ω = 0.56 rad/s) to -66.4% (ω = 0.32 rad/s) for the 5th order theory and from -22.2% (ω = 0.56 rad/s) to -63.2% (ω = 0.32 rad/s) for the 2nd order theory.

(3) The differences in the maximum horizontal acceleration ranged from 45.5% (ω = 0.42 rad/s) to 60%

Water Level	Free Surface					84m Above Sea Bed (66m Below Surface)					21m Above Sea Bed (129m Below Surface)				
Wave Theory	Airy	Stokes' 2nd Ord	Stokes' 5th Ord	Diff % 2nd	Diff % 5th	Airy	Stokes' 2nd Ord	Stokes' 5th Ord	Diff % 2nd	Diff % 5th	Airy	Stokes' 2nd Ord	Stokes' 5th Ord	Diff % 2nd	Diff % 5th
Wave Frequency (ω) = 0.32 rad/s									Wave Height (H) = 30.0m						
Uxm (m/s)	4.8	5.46	6.11	13.8	27.3	2.41	3.0	2.7	24.5	12.0	1.25	2.15	1.89	72	51.2
Uym (m/s)	4.8	4.8	4.61	-	-4	2.41	2.08	1.92	-13.7	-20.3	1.25	0.46	0.42	-63.2	-66.4
Axm (m/s²)	1.54	2.25	1.63	46.1	5.84	0.77	1.04	0.85	35.1	10.4	0.40	0.7	0.60	75	50
Aym (m/s²)	1.54	2.48	1.96	61	27.3	0.77	0.89	0.65	15.6	-15.6	0.40	0.18	0.14	-55	-65
L (m)															
Wave Frequency (ω) = 0.34 rad/s									Wave Height (H) = 30.0m						
Uxm (m/s)	5.1	5.58	6.41	9.4	25.7	2.34	2.77	2.55	18.4	9	1.12	1.84	1.68	64.3	50
Uym (m/s)	5.1	5.10	4.86	-	-4.7	2.34	2.07	1.93	-11.5	-17.5	1.12	0.45	0.41	-59.8	-63.4
Axm (m/s²)	1.73	2.14	1.78	25.9	4.7	0.80	0.97	0.86	21.3	7.5	0.38	0.62	0.57	63.2	50
Aym (m/s²)	1.73	2.40	2.20	41.2	29.4	0.80	0.84	0.68	5	-15	0.38	0.17	0.14	-55.3	-63.2
L (m)															

TABLE (2) Maximum Velocities and Accelerations by Different Wave Theories

Water Level	Free Surface					84m Above Sea Bed (66m Below Surface)					21m Above Sea Bed (129m Below Surface)				
Wave Theory	Airy	Stokes' 2nd Ord	Stokes' 5th Ord	Diff % 2nd	Diff % 5th	Airy	Stokes' 2nd Ord	Stokes' 5th Ord	Diff % 2nd	Diff % 5th	Airy	Stokes' 2nd Ord	Stokes' 5th Ord	Diff % 2nd	Diff % 5th
Wave Frequency (ω) = 0.37 rad/s									Wave Height (H) = 30.0m						
Uxm (m/s)	5.55	5.83	6.93	5.1	24.9	2.21	2.46	2.33	11.3	5.4	0.92	1.44	1.37	56.5	48.9
Uym (m/s)	5.55	5.55	5.21	-	-6.1	2.21	2.02	1.89	-8.6	-14.5	0.92	0.41	0.39	-55.4	-57.6
Axm (m/s²)	2.05	2.24	2.02	9.3	-1.5	0.82	0.9	0.85	9.8	3.7	0.34	0.53	0.51	55.9	50
Aym (m/s²)	2.05	2.44	2.60	19	26.8	0.82	0.81	0.72	-1.2	-12.2	0.34	0.16	0.15	-52.9	-55.9
L (m)	450.01	450.01	453.58	-	0.8										
Wave Frequency (ω) = 0.42 rad/s									Wave Height (H) = 25.0m						
Uxm (m/s)	5.25	5.33	6.42	1.5	22.3	1.60	1.68	1.64	5	2.5	0.52	0.75	0.77	44.2	48.1
Uym (m/s)	5.25	5.25	4.89	-	-6.9	1.60	1.52	1.47	-5	-8.1	0.52	0.27	0.27	-48.1	-48.1
Axm (m/s²)	2.20	2.23	2.10	1.4	-4.6	0.67	0.70	0.69	4.5	3	0.22	0.32	0.32	45.5	45.5
Aym (m/s²)	2.20	2.33	2.74	5.9	24.6	0.67	0.65	0.62	-3	-7.5	0.22	0.12	0.11	-45.4	-50
L (m)	349.24	349.24	360.23	-	3.1										

TABLE (3) Maximum Velocities and Accelerations by Different Wave Theories

Water Level	Free Surface					84m Above Sea Bed (66m Below Surface)					21m Above Sea Bed (129m Below Surface)				
Wave Theory	Airy	Stokes' 2nd Ord	Stokes' 5th Ord	Diff % 2nd	Diff % 5th	Airy	Stokes' 2nd Ord	Stokes' 5th Ord	Diff % 2nd	Diff % 5th	Airy	Stokes' 2nd Ord	Stokes' 5th Ord	Diff % 2nd	Diff % 5th
Wave Frequency (ω) = 0.45 rad/s						Wave Height (H) = 20.0m									
Uxm (m/s)	4.50	4.53	5.38	0.7	19.6	1.15	1.18	1.17	2.6	1.7	0.31	0.44	0.46	41.9	48.4
Uym (m/s)	4.50	4.51	4.23	-	-6	1.15	1.11	1.09	-3.5	-5.2	0.31	0.18	0.18	-41.9	-41.9
Axm (m/s^2)	2.02	2.04	1.93	1	-4.5	0.52	0.53	0.53	1.9	1.9	0.14	0.20	0.21	42.9	50
Aym (m/s^2)	2.02	2.08	2.45	3	21.3	o.52	0.50	0.49	-3.9	5.8	0.14	0.08	0.08	-42.9	-42.9
L (m)	304.23	304.23	313.22		3										
Wave Frequency (ω) = 0.50 rad/s						Wave Height (H) = 20.0m									
Uxm (m/s)	5.0	5.01	6.14	-	22.8	0.93	0.93	0.94	-	1.1	0.19	0.25	0.27	31.6	42.6
Uym (m/s)	5.0	5.01	4.59	-	-8.2	0.93	0.91	0.91	-2.2	-2.2	0.19	0.12	0.13	-36.8	-31.6
Axm (m/s^2)	2.50	2.50	2.32	-	-7.2	0.47	0.47	0.47	-	-	0.09	0.12	0.14	33.3	55.6
Aym (m/s^2)	2.50	2.52	3.14	0.8	25.6	0.47	0.46	0.46	-2.1	-2.1	0.09	0.06	0.06	-33.3	-33.3
L (m)															

TABLE (4) Maximum Velocities and Accelerations by Different Wave Theories

Water Level	Free Surface					84m Above Sea Bed (66m Below Surface)					21m Above Sea Bed (129m Below Surface)				
Wave Theory	Airy	Stokes' 2nd Ord	Stokes' 5th Ord	Diff % 2nd	Diff % 5th	Airy	Stokes' 2nd Ord	Stokes' 5th Ord	Diff % 2nd	Diff % 5th	Airy	Stokes' 2nd Ord	Stokes' 5th Ord	Diff % 2nd	Diff % 5th
Wave Frequency (ω) = 0.56 rad/s						Wave Height (H) = 20.0m									
Uxm (m/s)	5.6	5.6	7.15	-	27.7	0.68	0.67	0.70	-1.5	2.9	0.09	0.11	0.14	22.2	55.6
Uym (m/s)	5.6	5.6	4.93	-	-12	0.68	0.67	0.69	-1.5	1.5	0.09	0.07	0.08	-22.2	-11.1
Axm (m/s^2)	3.14	3.14	2.80	-	-10.8	0.38	0.38	0.39	-	2.6	0.05	0.06	0.08	20	60
Aym (m/s^2)	3.14	3.14	4.17	-	32.8	0.38	0.37	0.39	-2.6	2.6	0.05	0.04	0.04	-20	-20
L (m)	196.45	196.45	212.49	-	8.2										
Wave Frequency (ω) = rad/s						Wave Height (H) =									
Uxm (m/s)															
Uym (m/s)															
Axm (m/s^2)															
Aym (m/s^2)															
L (m)															

TABLE (5) Maximum Velocities and Accelerations by Different Wave Theories

(ω = 0.56 rad/s) for the 5th order theory and from 20% (ω = 0.56 rad/s) to 75% (ω = 0.32 rad/s) for the 2nd order theory.

(4) The differences in the maximum vertical acceleration ranged from -20% (ω = 0.56 rad/s) to -65% (ω = 0.32 rad/s) for the 5th order theory and from -20% (ω = 0.56 rad/s) to -55.3% (ω = 0.34 rad/s) for the 2nd order theory.

5. WAVE LOADING CALCULATIONS

5.1 General

From the previous analysis of the results of the variations of the velocities and the accelerations at the free surface and at the different levels below surface, it is evident that the differences in predicting the maximum wave velocities and accelerations by the Airy, Stokes' 2nd order and Stokes' 5th order theories are large in magnitude and may be positive (increase) or negative (decrease) relative to the values of the Airy theory.

Also, taking into consideration the fact that the forces and moments on the individual members of the structure are calculated taking into account the relative position, the instantaneous time and the variable hydrodynamic coefficients (C_D, C_M and C_L), it is difficult to anticipate the possible variations or differences in the forces and moments on the individual members and in the total forces (surge, heave, sway) and total moments (rolling, yawing, pitching) for the complete structure without carrying out the wave loading calculations.

The calculations were performed for the same jacket structure used before in chapters 4 and 5. Seven wave frequencies were used, ranging from $\omega = 0.32$ rad/s (H = 30.0m) to $\omega = 0.56$ rad/s (H = 20.0m), Table (1).

The comparison was made considering the following three cases:-

a. Airy wave theory and using LR coefficients (C_D, C_M).

b. Airy wave theory and using Sarpkaya's coefficients (C_D, C_M and C_L) for smooth cylinders.

c. Stokes' fifth order theory and using Sarpkaya's coefficients for smooth cylinders.

Parts of the data presented in this Chapter for cases a and b have been presented previously in Chapter 5.

5.2 Description of the Computer Programs

5.2.1 Program OSS

This program which was used with the Airy theory has been described in Chapter 3.

5.2.2 Program SNDOR

This program is similar to OSS as far as the general procedure of calculations but the wave velocities and accelerations are estimated according to Stokes' 2nd order theory from the expressions given in Table (C.3), Appendix (C), by calling subroutine SECMX. Unlike program OSS, the integration for the forces and moments for the surface-piercing members is done up to the free surface of the wave taking into account the changing of the wave position relative to the structure with time.

Subroutine SECMX

This subroutine is used to calculate the wave particulars according to Stokes' 2nd order wave theory.

5.2.3 Program STKFS

This program is also similar to OSS except that the wave profile, velocities and accelerations are estimated according to Stokes 5th order theory (14). The integration for the forces and moments for the surface-piercing members is carried out up to the temporal wave surface.

Solving equation (4) and determining the wave properties is done by calling subroutine STGWM which in turn calls eight other subroutines, Fig. (3).

Subroutine STGWM

This subroutine contains all the expressions for the coefficients A, B, C...etc and the equations of the wave profile, velocities and accelerations listed in Tables (C.4) and (C.5), Appendix (C). Subroutine STGWM calls subroutine CO5AGF.

Subroutine CO5AGF

This subroutine is used to solve equation (4) to determine the value of the coefficient λ and the wave length L.

Subroutine CO5AGF calls seven subroutines: CO5AVF, CO5AZF, XO2AAF, XO2ABF, XO4AAF, PO1AAF and POIAAZ, Fig. (3).

The detailed description of these subroutines is given in Ref. (11).

6. ANALYSIS OF THE RESULTS

6.1 Forces on the Individual Members

The maximum forces in (v,w) directions (F_{T_v} and F_{T_w}) were calculated at the different frequencies for five members (Nos 8,11,15,18 and 21) Fig.(15). The results are shown in Tables (6) to (10) and Figs. (16) to (19). The differences in the forces are given by Sarpkaya (5th order theory) relative to LR (Airy), Tables (6) to (10) and are as follows:-

a. For member No (8), the percentage differences in F_{T_v} ranged from -8% (ω = 0.56 rad/s) to 200% (ω = 0.32 rad/s). The differences in F_{T_w} are much smaller, ranging from 0.7% (ω = 0.34 rad/s) to 28.8% (ω = 0.56 rad/s).

b. For member No (11), the percentage differences in F_{T_v} ranged from 106% (ω = 0.56 rad/s) to 405% (ω = 0.32 rad/s). The differences in F_{T_w} are much smaller, ranging from 15.4% (ω = 0.42 rad/s) to 22.7% (ω = 0.32 rad/s).

c. For member No (15), the percentage differences in F_{T_v} ranged from 45.3% (ω = 0.32 rad/s) to 71.2% (ω = 0.56 rad/s). The differences in F_{T_w} are of the same order, ranging from 44.1% (ω = 0.32 rad/s) to 67.2% (ω = 0.56 rad/s).

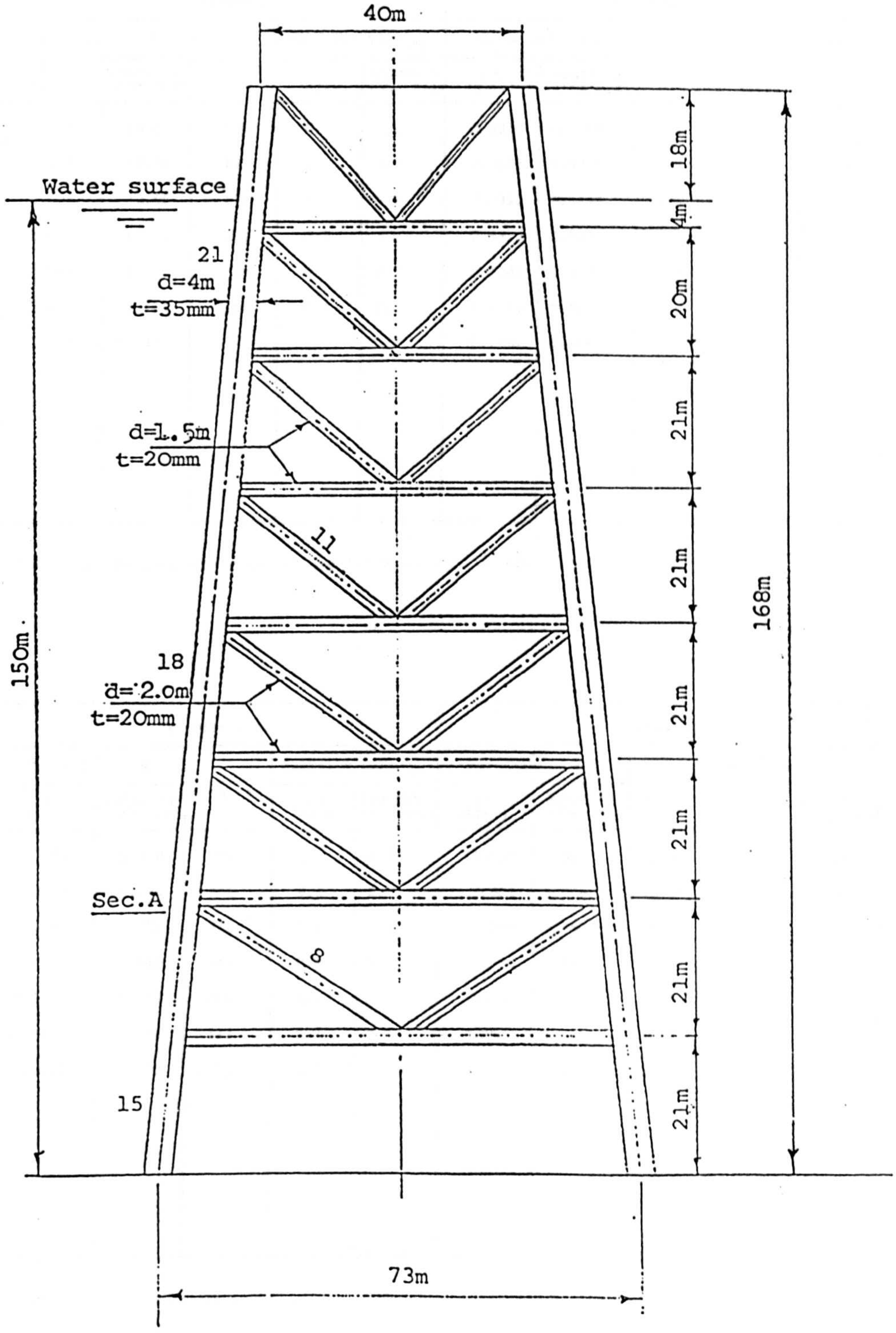

Fig. (15) Positions and Numbering of the Five Members

Wave Frequency ω (rad/s)	Wave Height H (m)	'v' Direction $F_{T_v} \times 10^{-3}$ (N) LR (Airy)	SARPKAYA (5th Ord)	Diff %	Relative Time t_r LR (Airy)	SARPKAYA (5th Ord)	'w' Direction $F_{T_v} \times 10^{-5}$ (N) LR (Airy)	SARPKAYA (5th Ord)	Diff %	Relative Time t_r LR (Airy)	SARPKAYA (5th Ord)
0.32	30.0	5.220	15.67	200	0.2	0.8	0.8317	0.8389	0.9	0.6	0.7
0.34	30.0	5.037	14.55	189	0.2	0.8	0.7965	0.8023	0.7	0.6	0.7
0.37	30.0	4.623	12.55	171	0.2	0.8	0.7216	0.7349	1.8	0.6	0.7
0.42	25.0	3.081	6.431	109	0.2	0.8	0.4652	0.5187	11.5	0.6	0.1
0.45	20.0	2.058	2.429	18	0.7	0.7	0.3141	0.3507	11.7	0.0	0.1
0.50	20.0	1.412	1.312	-7.11	0.7	0.2	0.2216	0.2527	14	0.0	0.1
0.56	20.0	0.7939	0.7301	-8	0.7	0.2	0.1291	0.1663	28.8	0.0	1.0

Table (6) Maximum Forces in 'v' and 'w' Directions on Member No 8 SR = 0.0

Wave Frequency ω (rad/s)	Wave Height H (m)	'v' Direction $F_{T_v} \times 10^{-4}$ (N) LR (Airy)	SARPKAYA (5th Ord)	Diff %	Relative Time t_r LR (Airy)	SARPKAYA (5th Ord)	'w' Direction $F_{T_v} \times 10^{-5}$ (N) LR (Airy)	SARPKAYA (5th Ord)	Diff %	Relative Time t_r LR (Airy)	SARPKAYA (5th Ord)
0.32	30.0	1.077	5.434	405	0.2	0.8	1.602	1.965	22.7	0.2	0.8
0.34	30.0	1.132	5.448	381	0.2	0.8	1.643	1.966	19.7	0.2	0.8
0.37	30.0	1.193	5.319	346	0.2	0.8	1.664	1.983	19.2	0.2	0.7
0.42	25.0	1.030	3.515	241	0.2	0.8	1.328	1.533	15.4	0.1	0.1
0.45	20.0	0.8169	2.199	169	0.2	0.8	1.041	1.208	16	0.6	0.1
0.50	20.0	0.7690	1.794	133	0.7	0.8	0.9682	1.143	18.1	0.6	0.1
0.56	20.0	0.6645	1.370	106	0.7	0.7	0.8244	1.004	21.8	0.0	1.0

Table (7) Maximum Forces in 'v' and 'w' directions on Member No 11 SR = 0.0

Wave Frequency ω (rad/s)	Wave Height H (m)	'v' Direction $F_{T_v} \times 10^{-5}$ (N) LR (Airy)	SARPKAYA (5th Ord)	Diff %	Relative Time t_r LR (Airy)	SARPKAYA (5th Ord)	'w' Direction $F_{T_v} \times 10^{-5}$ (N) LR (Airy)	SARPKAYA (5th Ord)	Diff %	Relative Time t_r LR (Airy)	SARPKAYA (5th Ord)
0.32	30.0	1.383	2.009	45.3	0.7	0.7	1.382	1.991	44.1	0.2	0.7
0.34	30.0	1.291	1.893	46.6	0.7	0.7	1.303	1.878	44.1	0.2	0.7
0.37	30.0	1.120	1.671	49.2	0.7	0.7	1.146	1.661	44.9	0.2	0.7
0.42	25.0	0.6634	1.011	52.4	0.7	0.7	0.6982	1.011	44.8	0.7	0.7
0.45	20.0	0.4321	0.6449	49.3	0.1	0.6	0.4361	0.6321	44.9	0.7	0.6
0.50	20.0	0.2788	0.4319	54.9	0.1	0.6	0.2738	0.4259	55.6	0.1	0.6
0.56	20.0	0.1402	0.2400	71.2	0.6	0.1	0.1440	0.2407	67.2	0.1	0.1

Table (8) Maximum Forces in 'v' and 'w' Directions on Member No 15 SR = 0.0

Wave Frequency ω (rad/s)	Wave Height H (m)	'v' Direction $F_{T_v} \times 10^{-6}$ (N) LR (Airy)	SARPKAYA (5th Ord)	Diff %	Relative Time t_r LR (Airy)	SARPKAYA (5th Ord)	'w' Direction $F_{T_v} \times 10^{-5}$ (N) LR (Airy)	SARPKAYA (5th Ord)	Diff %	Relative Time t_r LR (Airy)	SARPKAYA (5th Ord)
0.32	30.0	0.2673	0.2678	-	0.2	0.7	2.621	2.700	3	0.2	0.8
0.34	30.0	0.2724	0.2675	-1.8	0.7	0.7	2.700	2.662	-1.4	0.2	0.2
0.37	30.0	0.2727	0.2618	-4	0.7	0.7	2.743	2.617	-4.6	0.2	0.7
0.42	25.0	0.2125	0.1989	-6.4	0.7	0.7	2.184	2.025	-7.3	0.7	0.7
0.45	20.0	0.1565	0.1445	-7.7	0.7	0.7	1.163	1.494	-8.5	0.7	0.7
0.50	20.0	0.1360	0.1245	-8.5	0.1	0.1	1.368	1.266	-7.5	0.7	0.7
0.56	20.0	0.1069	0.1022	-4.4	0.1	0.1	1.055	0.9946	-5.7	0.1	0.1

Table (9) Maximum Forces in 'v' and 'w' Directions on Member No 18 SR = 0.0

Wave Frequency ω (rad/s)	Wave Height H (m)	'v' Direction $F_{T_v} \times 10^{-6}$ (N) LR (Airy)	'v' Direction $F_{T_v} \times 10^{-6}$ (N) SARPKAYA (5th Ord)	'v' Direction Diff %	'v' Direction Relative Time t_r LR (Airy)	'v' Direction Relative Time t_r SARPKAYA (5th Ord)	'w' Direction $F_{T_v} \times 10^{-6}$ (N) LR (Airy)	'w' Direction $F_{T_v} \times 10^{-6}$ (N) SARPKAYA (5th Ord)	'w' Direction Diff %	'w' Direction Relative Time t_r LR (Airy)	'w' Direction Relative Time t_r SARPKAYA (5th Ord)
0.32	30.0	0.5963	1.121	88	0.2	0.9	0.5948	1.204	102	0.8	0.9
0.34	30.0	0.6651	1.189	78.8	0.2	0.9	0.6585	1.290	95.9	0.8	0.9
0.37	30.0	0.7698	1.304	69.4	0.2	0.9	0.7547	1.436	90.3	0.8	0.9
0.42	25.0	0.7885	0.9721	23.3	0.7	0.9	0.7913	1.143	44.5	0.2	0.9
0.45	20.0	0.6997	0.7563	8.1	0.7	0.8	0.7103	0.8268	16.4	0.2	0.8
0.50	20.0	0.8081	0.8874	9.8	0.7	0.8	0.8315	0.9872	18.7	0.7	0.8
0.56	20.0	0.9343	1.045	11.9	0.1	0.8	0.9609	1.195	24.4	0.7	0.8

Table (10) Maximum Forces in 'v' and 'w' Directions on Member No 21 SR = 0.0

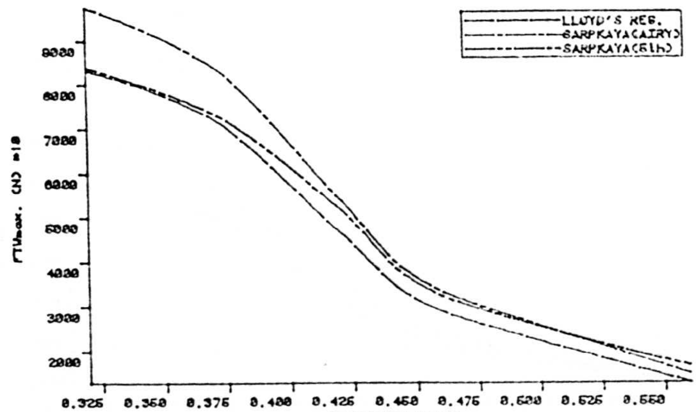

(a) MAX. FORCES ON MEMBERS IN w DIRECTION

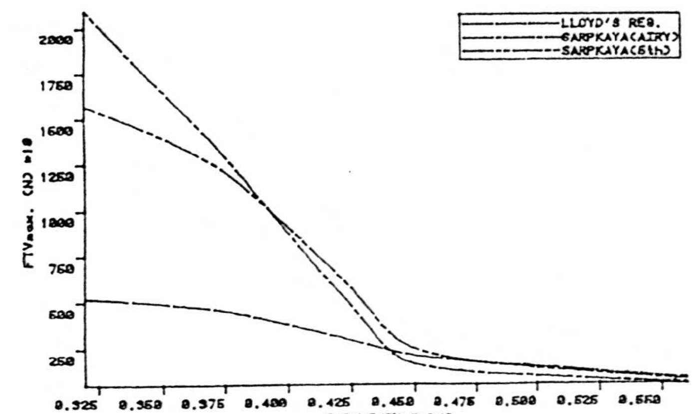

(b) MAX. FORCES ON MEMBERS IN v DIRECTION

PROGRAM: ,COEFFICIENTS:LR&S , $\beta = 0^{o}$
FIG.(16) MAX. FORCES ON MEMBER (8) Vs. FREQUENCY

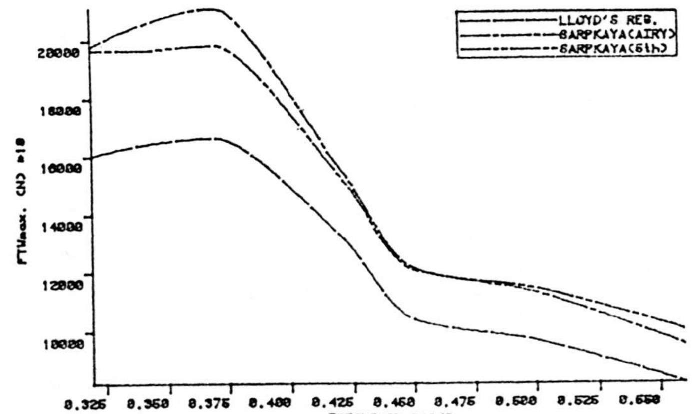

(a) MAX. FORCES ON MEMBERS IN w DIRECTION

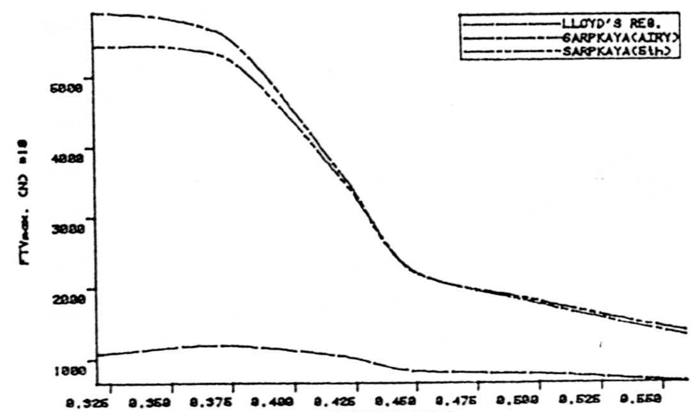

(b) MAX. FORCES ON MEMBERS IN v DIRECTION

PROGRAM: ,COEFFICIENTS:LR&S , $\beta = 0^{o}$
FIG.(17) MAX. FORCES ON MEMBER (11) Vs. FREQUENCY

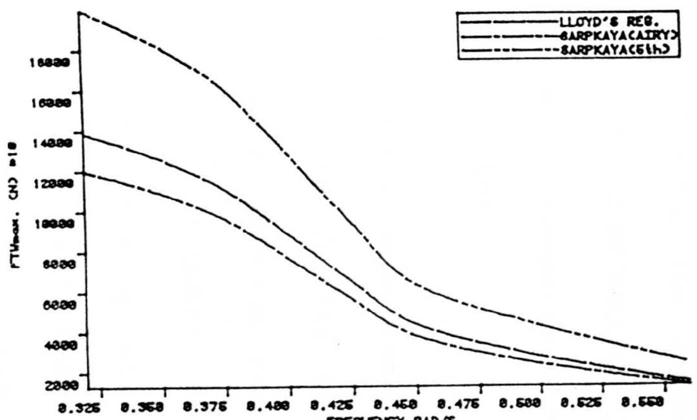

(a) MAX. FORCES ON MEMBERS IN w DIRECTION

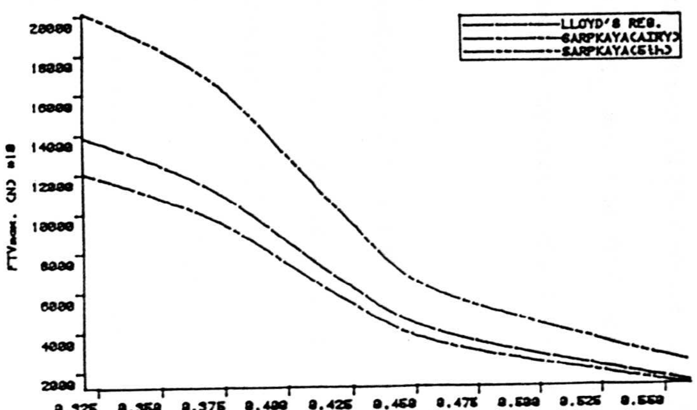

(b) MAX. FORCES ON MEMBERS IN v DIRECTION

PROGRAM: ,COEFFICIENTS: LR&S , $\beta = 0^o$

FIG.(18) MAX. FORCES ON MEMBER (15) Vs. FREQUENCY

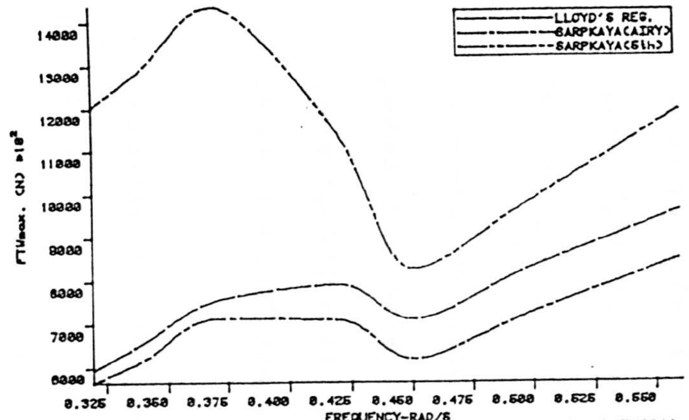

(a) MAX. FORCES ON MEMBERS IN w DIRECTION

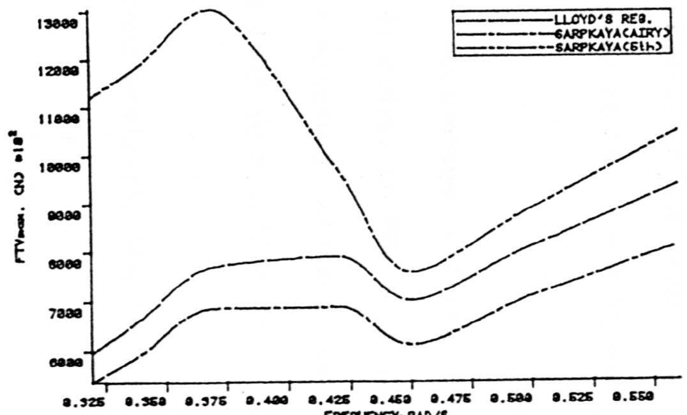

(b) MAX. FORCES ON MEMBERS IN v DIRECTION

PROGRAM: ,COEFFICIENTS: LR&S , $\beta = 0^o$

FIG.(19) MAX. FORCES ON MEMBER (21) Vs. FREQUENCY

d. For member No (18), the percentage differences in the forces are relatively small ranging from -8.5% (ω = 0.5 rad/s) to -1.8% (ω = 0.34 rad/s) in the case of F_{T_v} and from -8.5% (ω = 0.45 rad/s) to 3% (ω = 0.32 rad/s) in the case of F_{T_w}.

e. For member No (21), the percentage differences in F_{T_v} ranged from 8.1% (ω = 0.45 rad/s) to 88% (ω = 0.32 rad/s). The differences in F_{T_w} are slightly higher, ranging from 16.4% (ω = 0.45 rad/s) to 102% (ω = 0.32 rad/s).

In addition to the previous analysis, the following points should be noted:-

a. The large percentage differences, eg larger than 100%, are usually associated with the forces of relatively small absolute magnitudes.

b. For the small diameter members, Nos. (8) and (11), where d = 2.0m, the large percentage differences are due to the combined effects of C_D, C_M, C_L and the differences in the wave kinematics estimation by Airy and Stokes' 5th order theories.

c. For the large diameter members (d = 4.0m), the large value of the inertia coefficient recommended by LR (C_M = 2.0m) may balance the other effects, as in the case of member No. (18). For member No. (15), the differences are mainly influenced by the large value of C_D and/or C_L due to the small Reynolds number (R_e) at that level. In the case of the surface piercing member No.(21), the biggest contribution to the differences comes from the integration of the forces up to the wave surface when using the 5th order theory.

d. The relative time (t_r) was not largely affected.

6.2 Total Forces and Moments on the Structure

Tables (11) to (14) summarise the results of calculations for the three cases: a. LR (Airy); b. Sarpkaya (Airy); and c. Sarpkaya (5th order). Since the comparison between LR (Airy) and Sarpkaya (Airy) has been discussed in Chapter 5 in detail, the discussion in the present chapter will be confined to cases a. and c.

6.2.1 Maximum Surge, Heave and Sway Forces (β = 0.0)

Table (11) shows that:-

a. The percentage differences in the surge forces ranged from 11% (ω = 0.5 rad/s) to 43.3% (ω = 0.32 rad/s).

b. The percentage differences in the heave forces ranged from 2.5% (ω = 0.32 rad/s) to 14.6% (ω = 0.56 rad/s).

c. The percentage differences in the sway forces are extremely large, in fact the values of sway forces according to LR are negligible compared with the values of the 5th order theory. This is mainly due to the effect of the lift coefficient (C_L).

However, the absolute values of the sway forces are small compared with either the surge or heave forces.

β = 0.0	Surge Force x 10^{-8} (N)					Heave Force x 10^{-7} (N)					Sway Force x 10^{-6} (N)				
Coefficients	ω (rad/s)					ω (rad/s)					ω (rad/s)				
	0.32	0.34	0.37	0.42	0.45	0.32	0.34	0.37	0.42	0.45	0.32	0.34	0.37	0.42	0.45
LR (Airy)	0.1927	0.2003	0.2087	0.1759	0.1377	1.221	1.241	1.274	1.02	0.7649	0.1102	0.1208	0.1392	0.1313	0.1058
SARPKAYA (Airy)	0.2084	0.2159	0.2241	0.1854	0.1428	1.538	1.558	1.575	1.171	0.8906	1.893	1.912	1.931	1.385	0.9155
Diff %	8.2	7.8	7.4	5.4	3.7	2.6	25.5	23.6	14.8	16.4	1618	1483	1287	955	965
SARPKAYA (5th Ord)	0.2762	0.2730	0.2695	0.2021	0.1533	1.251	1.303	1.372	1.068	0.8414	1.447	1.506	1.575	1.249	0.8364
Diff %	43.3	36.3	29.1	14.9	11.3	2.5	5	7.7	4.7	10	1213		1031	851	691
Coefficients	ω (rad/s)					ω (rad/s)					ω (rad/s)				
	0.50	0.56				0.50	0.56				0.50	0.56			
LR (Airy)	0.1332	0.1229				0.7533	0.7303				0.1320	0.1673			
SARPKAYA ((Airy)	0.1382	0.1280				0.8854	0.8707				0.9292	0.9495			
Diff %	3.8	4.2				17.5	19.2				604	468			
SARPKAYA (5th Ord)	0.1479	0.1399				0.8513	0.8366				0.8471	0.8391			
Diff %	11	13.8				13	14.6				542	402			

Table (11) Maximum Surge, Heave and Sway Forces (LR & SARPKAYA)

β = 0.0	Rolling Moment x 10^{-8} (NM)					Yawing Moment x 10^{-7} (NM)					Pitching Moment x 10^{-9} (NM)				
Coefficients	ω (rad/s)					ω (rad/s)					ω (rad/s)				
	0.32	0.34	0.37	0.42	0.45	0.32	0.34	0.37	0.42	0.45	0.32	0.34	0.37	0.42	0.45
LR (Airy)	0.1494	0.1714	0.2091	0.2089	0.1717	0.0664	0.0771	0.09685	0.1074	0.09567	1.729	1.837	1.981	1.767	1.428
SARPKAYA (Airy)	1.997	2.092	2.225	1.737	1.205	0.4350	0.4378	0.4221	0.4617	0.3168	1.924	2.013	2.161	1.888	1.496
Diff %	1237	1120	964	732	602	555	468	336	330	231	11.3	9.6	9.1	6.9	4.8
SARPKAYA (5th Ord)	1.577	1.676	1.810	1.555	1.092	0.5386	0.6618	0.6252	0.7446	0.528	2.807	2.850	2.921	2.198	1.602
Diff %	956	878	766	644	536	711	758	546	593	452	62.4	55.1	47.5	24.4	12.2
Coefficients	ω (rad/s)					ω (rad/s)					ω (rad/s)				
	0.50	0.56				0.50	0.56				0.50	0.56			
LR (Airy)	0.2197	0.2824				0.1407	0.2172				1.454	1.411			
SARPKAYA (Airy)	1.283	1.363				0.4553	0.6018				1.522	1.481			
Diff %	484	383				224	177				4.7	5			
SARPKAYA (5th Ord)	1.151	1.189				0.7830	1.04				1.633	1.630			
Diff %	424	321				457	379				12.3	15.5			

Table (12) Maximum Rolling, Yawing and Pitching Moments (LR & SARPKAYA)

6.2.2 Maximum Rolling, Yawing and Pitching Moments ($\beta = 0.0$)

Similarly to the sway forces, Table (12) shows that the percentage differences in both the rolling and yawing moments are very large, as given below:-

a. The differences in the rolling moments ranged from 321% ($\omega = 0.56$ rad/s) to 956% ($\omega = 0.32$ rad/s).

b. The differences in the yawing moments ranged from 379% ($\omega = 0.56$ rad/s) to 758% ($\omega = 0.34$ rad/s).

c. The differences in the pitching moments ranged from 12.2% ($\omega = 0.45$ rad/s) to 62.4% ($\omega = 0.32$ rad/s).

It is also to be noted that the absolute values of both the rolling and yawing moments are small compared with the pitching moments.

6.2.3 Maximum Surge, Heave, and Sway Forces ($\beta = \pi/4$)

Table (13) shows that:-

a. The percentage differences in the surge forces ranged from 11.4% ($\omega = 0.5$ rad/s) to 52.3% ($\omega = 0.32$ rad/s).

b. The differences in the heave forces ranged from -7.4% ($\omega = 0.32$ rad/s) to 3.9% ($\omega = 0.5$ rad/s).

c. The differences in the sway forces ranged from 2.8% ($\omega = 0.56$ rad/s) to 47.6% ($\omega = 0.32$ rad/s).

6.2.4 Maximum Rolling, Yawing and Pitching Moments ($\beta = \pi/4$)

Table (14) shows that:-

$\beta = \pi/4$	Surge Force x 10^{-7} (N)					Heave Force x 10^{-7} (N)					Sway Force x 10^{-7} (N)				
Coefficients	ω (rad/s)					ω (rad/s)					ω (rad/s)				
	0.32	0.34	0.37	0.42	0.45	0.32	0.34	0.37	0.42	0.45	0.32	0.34	0.37	0.42	0.45
LR (Airy)	1.360	1.413	1.472	1.245	0.9788	1.219	1.239	1.268	1.016	0.7626	1.359	1.412	1.470	1.244	0.9781
SARPKAYA (Airy)	1.529	1.583	1.642	1.357	1.045	1.538	1.559	1.577	1.153	0.8721	1.556	1.608	1.622	1.365	1.048
Diff %	12.4	12	11.5	9.0	6.8	26.2	25.8	24.4	13.5	14.4	14.5	13.9	10.3	9.7	7.1
SARPKAYA (5th Ord)	2.071	2.062	2.086	1.539	1.106	1.129	1.197	1.273	0.9931	0.7914	2.006	1.980	1.981	1.429	1.065
Diff %	52.3	45.9	41.7	23.6	13	-7.4	-3.4	-	-2.3	3.8	47.6	40.2	34.8	14.9	8.9
Coefficients	ω (rad/s)					ω (rad/s)					ω (rad/s)				
	0.50	0.56				0.50	0.56				0.50	0.56			
LR (Airy)	0.9518	0.8890				0.7514	0.7305				0.9511	0.8883			
SARPKAYA ((Airy)	1.02	0.9602				0.8657	0.8488				1.02	0.9574			
Diff %	7.2	8				15.2	16.2				7.2	7.8			
SARPKAYA (5th Ord)	1.06	1.016				0.7807	0.7275				1.006	0.9129			
Diff %	11.4	14.3				3.9	-				5.8	2.8			

Table (13) Maximum Surge, Heave and Sway Forces (LR & SARPKAYA)

$\beta = \pi/4$	Rolling Moment x 10^{-9} (NM)					Yawing Moment x 10^{-5} (NM)					Pitching Moment x 10^{-9} (NM)				
Coefficients	ω (rad/s)					ω (rad/s)					ω (rad/s)				
	0.32	0.34	0.37	0.42	0.45	0.32	0.34	0.37	0.42	0.45	0.32	0.34	0.37	0.42	0.45
LR (Airy)	1.218	1.294	1.395	1.249	1.014	0.1175	0.1367	0.1705	0.1769	0.1515	1.219	1.295	1.396	1.250	1.015
SARPKAYA (Airy)	1.426	1.508	1.613	1.397	1.103	81.23	90.50	105.9	85.23	55.50	1.416	1.484	1.594	1.391	1.101
Diff %	17.1	16.5	15.6	11.8	8.8		Very large differences				16.2	14.6	14.2	11.3	8.5
SARPKAYA (5th Ord)	2.079	2.107	2.211	1.658	1.158	155.7	172.7	186.5	131.0	78.15	2.134	2.174	2.299	1.743	1.226
Diff %	70.7	62.8	58.5	32.7	14.2		Very large differences				75.1	67.9	64.7	39.4	20.8
Coefficients	ω (rad/s)					ω (rad/s)					ω (rad/s)				
	0.50	0.56				0.50	0.56				0.50	0.56			
LR (Airy)	1.038	1.021				0.2174	0.3267				1.039	1.022			
SARPKAYA (Airy)	1.128	1.113				59.35	71.77				1.130	1.118			
Diff %	8.7	9					Very large differences				8.8	9.4			
SARPKAYA (5th Ord)	1.166	1.128				75.09	117.3				1.258	1.258			
Diff %	12.3	10.5									21.1	23.1			

Table (14) Maximum Rolling, Yawing and Pitching Moments (LR & SARPKAYA)

a. The percentage differences in the rolling moments ranged from 10.5% (ω = 0.56 rad/s) to 70.7% (ω = 0.32 rad/s).

b. The values of the yawing moments according to LR are negligible compared with the values when using the 5th order theory together with Sarpkaya's coefficients. However, the yawing moments both by LR and the 5th order theory are negligible compared with the rolling or pitching moments.

c. The differences in the pitching moments ranged from 20.8% (ω = 0.45 rad/s) to 75.1% (ω = 0.32 rad/s).

6.3 Effect of the Wave Height

To examine the effect of wave height on loading estimation, the calculations were carried out at a constant frequency of 0.37 rad/s and 5 different wave heights, namely 5.0, 10.0, 15.0, 20.0 and 25.0m. The results are summarised in Tables (15) and (16). The variations of the total forces and moments per unit wave height against the increasing wave height from 5.0 to 25.0m are shown in Figs. (28) to (37).

6.3.1 Maximum Forces and Moments (β = 0.0)

Table (15) shows the following:-

a. The percentage differences in the surge forces ranged from 6.8% (H = 5.0m) to 19.1% (H = 25.0m).

b. The differences in the heave forces ranged from -2.8% (H = 5.0m) to 1.8% (H = 15.0m).

$\beta = 0.0$ $\omega = 0.37r/s$ Coefficients	Surge Force x 10^{-7} (N)					Heave Force x 10^{-7} (N)					Sway Force x 10^{-5} (N)				
	H (m)					H (m)					H (m)				
	5.0	10.0	15.0	20.0	25.0	5.0	10.0	15.0	20.0	25.0	5.0	10.0	15.0	20.0	25.0
LR (Airy)	0.3197	0.6506	0.9928	1.346	1.711	0.1737	0.3474	0.5295	0.7536	1.002	0.1399	0.2888	0.4736	0.7303	1.036
SARPKAYA (Airy) Diff. %	0.3139 -1.8	0.6521 -	1.016 2.3	1.402 4.2	1.811 5.8	0.1990 14.6	0.3896 12.2	0.6147 16.1	0.8658 14.9	1.147 14.5	0.5525 295	2.191 659	5.148 987	9.071 1142	13.78 1230
SARPKAYA (5th Ord) Diff %	0.3413 6.8	0.7236 11.3	1.139 14.7	1.574 16.9	2.037 19.1	0.1688 -2.8	0.3400 -2.1	0.5388 1.8	0.7446 -1.2	1.013 1.1	0.5805 315	2.126 636	4.643 280	8.003 996	12.10 1068
Coefficients	Rolling Moment x 10^{-7} (NM)					Yawing Moment x 10^{-6} (NM)					Pitching Moment x 10^{-9} (NM)				
	5.0	10.0	15.0	20.0	25.0	5.0	10.0	15.0	20.0	25.0	5.0	10.0	15.0	20.0	25.0
LR (Airy)	0.1843	0.3850	0.6861	1.074	1.543	0.8665	0.2012	0.3474	0.5240	0.7310	0.3016	0.6146	0.9390	1.275	1.622
SARPKAYA ((Airy) Diff %	0.7219 292	2.731 609	6.105 790	10.57 884	15.96 934	0.2157 -75.1	0.6125 204	1.314 278	2.190 318	3.143 330	0.2955 -2	0.6186 0.7	0.9683 3.1	1.342 5.3	1.741 7.3
SARPKAYA (5th Ord) Diff %	0.7136 287	2.571 568	5.516 704	9.495 784	14.19 820	0.2748 -68.3	0.7077 252	1.154 232	2.185 317	4.598 529	0.3123 3.6	0.6365 3.6	1.072 14.2	1.490 16.9	2.105 29.8

Table (15) Maximum Forces and Moments at Different Wave Heights (SR=0.0)

$\beta = \pi/4$ $\omega = 0.37r/s$ Coefficients	Surge Force x 10^{-7} (N)					Heave Force x 10^{-7} (N)					Sway Force x 10^{-7} (N)				
	H (m)					H (m)					H (m)				
	5.0	10.0	15.0	20.0	25.0	5.0	10.0	15.0	20.0	25.0	5.0	10.0	15.0	20.0	25.0
LR (Airy)	0.2281	0.4630	0.7048	0.9535	1.209	0.1738	0.3477	0.5283	0.7513	0.9981	0.2279	0.4626	0.7403	0.9528	1.208
SARPKAYA (Airy) Diff. %	0.2254 -1.3	0.4691 1.3	0.7347 4.2	1.018 6.8	1.321 9.3	0.1987 14.3	0.3863 11.1	0.6056 14.6	0.8517 13.4	1.148 15	0.2258 -0.9	0.4717 2	0.7405 5.1	1.028 7.9	1.336 10.6
SARPKAYA (5th Ord) Diff %	0.2486 9	0.5244 13.3	0.8191 16.2	1.139 19.5	1.546 27.9	0.1639 -5.7	0.3338 -4	0.5134 -2.8	0.7079 -5.2	0.9481 -5	0.2423 6.3	0.5134 11	0.8012 13.8	1.117 17.2	1.463 21.1
Coefficients	Rolling Moment x 10^{-9} (NM)					Yawing Moment x 10^{-5} (NM)					Pitching Moment x 10^{-9} (NM)				
	5.0	10.0	15.0	20.0	25.0	5.0	10.0	15.0	20.0	25.0	5.0	10.0	15.0	20.0	25.0
LR (Airy)	0.2151	0.4372	0.6662	0.9022	1.145	0.0089	0.0256	0.0501	0.0824	0.1225	0.2153	0.4375	0.6667	0.9029	1.146
SARPKAYA ((Airy) Diff %	0.2132 -0.9	0.4492 2.7	0.7089 6.41	0.9892 9.61	1.291 12.8	0.2529	6.567 Large	19.38 Differences	41.50	70.12	0.2127 -1.2	0.4463 2	0.7034 5.5	0.9801 8.6	1.277 11.4
SARPKAYA (5th Ord) Diff %	0.2265 5.3	0.4873 11.5	0.7635 14.6	1.098 21.7	1.597 39.5	12.35	19.15 Large	38.40 Differences	71.93	117.9	0.2293 6.5	0.4939 12.9	0.7789 16.8	1.139 26.2	1.656 44.5

Table (16) Maximum Forces and Moments at Different Wave Heights (SR=0.0)

c. The differences in the sway forces are very large due to the effect of the lift forces, ranging from 315% (H = 5.0m) to 1068% (H = 25.0m). However, the sway forces are smaller than both the surge and heave forces.

d. The differences in the rolling moments are also very large due to the effect of the lift forces, ranging from 287% (H = 5.0m) to 820% (H = 25.0m).

e. The differences in the yawing moments come next to the differences in the surge forces, ranging from -68.3% (H = 5.0m) to 529% (H = 25.0m). However, both the rolling and yawing moments are smaller than the values of the pitching moments.

f. The percentage differences in the pitching moments ranged from 3.6% (H = 5.0m) to 29.8% (H = 25.0m).

6.3.2 Maximum Forces and Moments ($\beta = \pi/4$)

Table (16) shows the following:-

a. The percentage differences in the surge forces ranged from 9% (H = 5.0m) to 27.9% (H = 25.0m).

b. The differences in the heave forces ranged from -5.8% (H = 20.0m) to -2.8% (H = 15.0m).

c. The differences in the sway forces ranged from 6.3% (H = 5.0m) to 21.1% (H = 25.0m).

d. The differences in the rolling moments ranged from 5.3% (H = 5.0m) to 39.5% (H = 25.0m).

e. The absolute values of the yawing moments, according to LR,

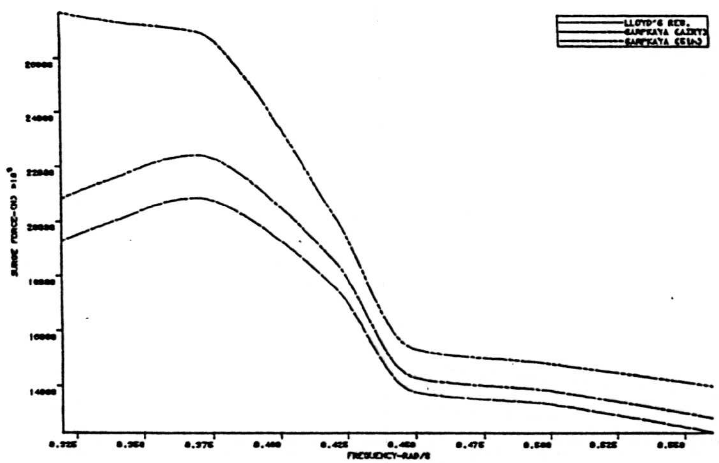

COEFFICIENTS: LR & SARPK , $\beta = 0.0$, SR= 0.0
FIG.(20) MAX. SURGE FORCES Vs. FREQUENCY

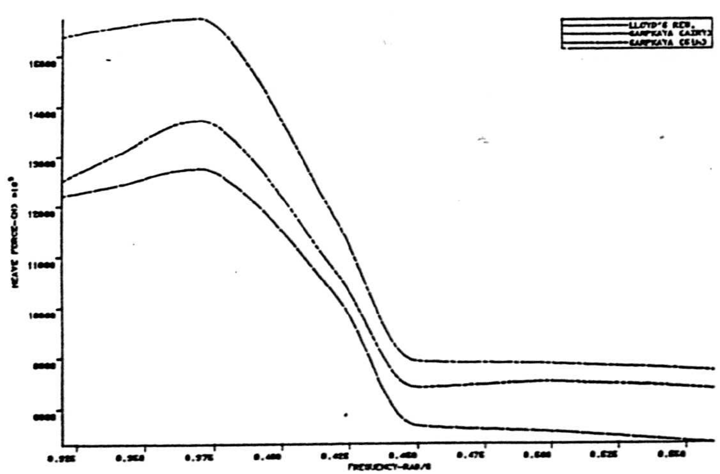

COEFFICIENTS: LR & SARPK , $\beta = 0.0$, SR= 0.0
FIG.(21) MAX. HEAVE FORCES Vs. FREQUENCY

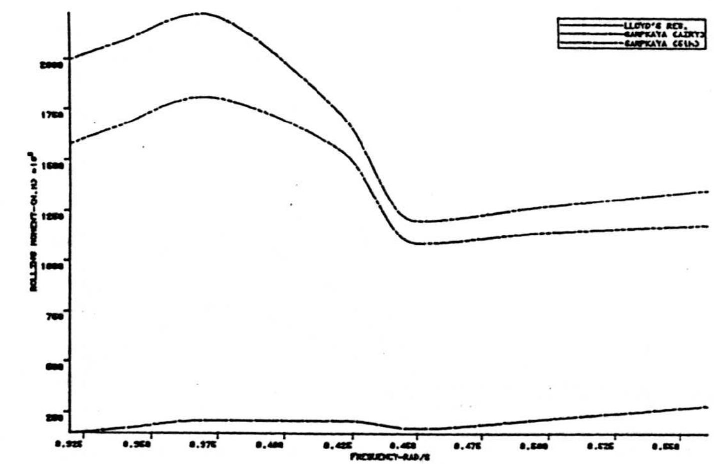

COEFFICIENTS: LR & SARPK , $\beta = 0.0$, SR= 0.0
FIG.(22) MAX. ROLLING MOMENTS Vs. FREQUENCY

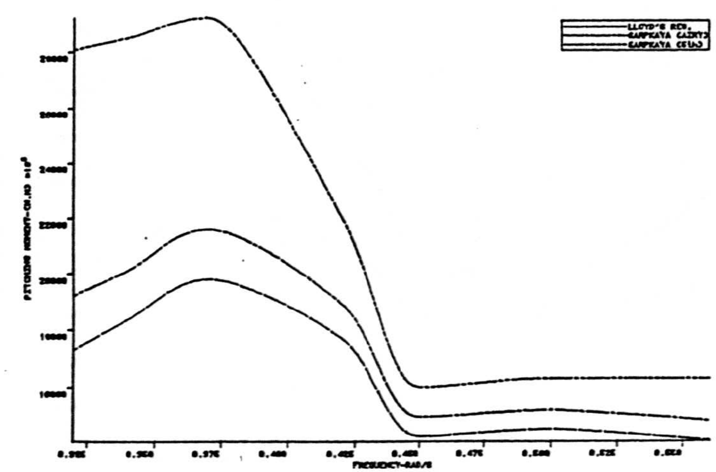

COEFFICIENTS: LR & SARPK , $\beta = 0.0$, SR= 0.0
FIG.(23) MAX. PITCHING MOMENTS Vs. FREQUENCY

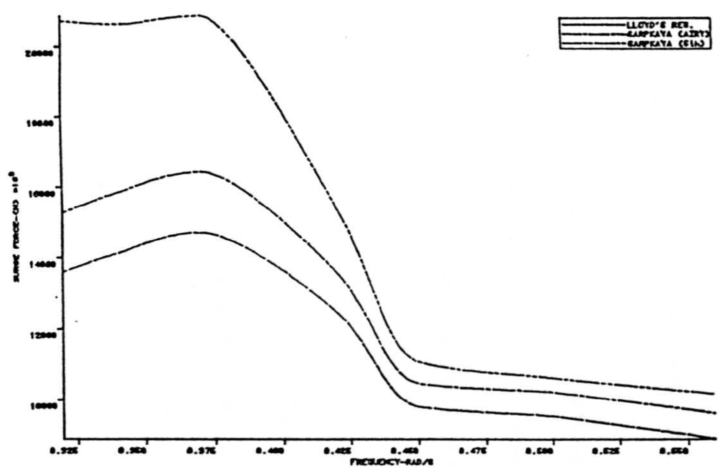

COEFFICIENTS: LR & SARPK , $\beta = \pi/4$, SR= 0.0
FIG.(24) MAX. SURGE FORCES Vs. FREQUENCY

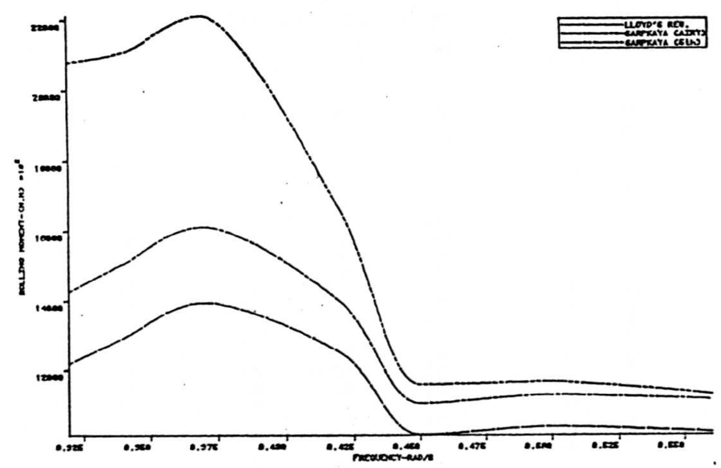

COEFFICIENTS: LR & SARPK , $\beta = \pi/4$, SR= 0.0
FIG.(26) MAX. ROLLING MOMENTS Vs. FREQUENCY

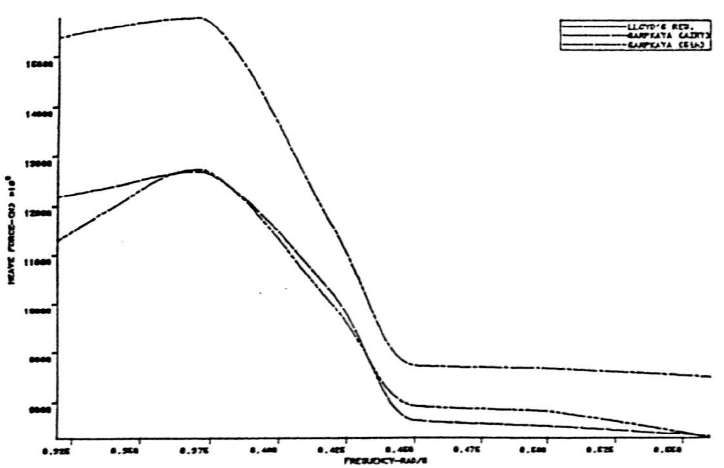

COEFFICIENTS: LR & SARPK , $\beta = \pi/4$, SR= 0.0
FIG.(25) MAX. HEAVE FORCES Vs. FREQUENCY

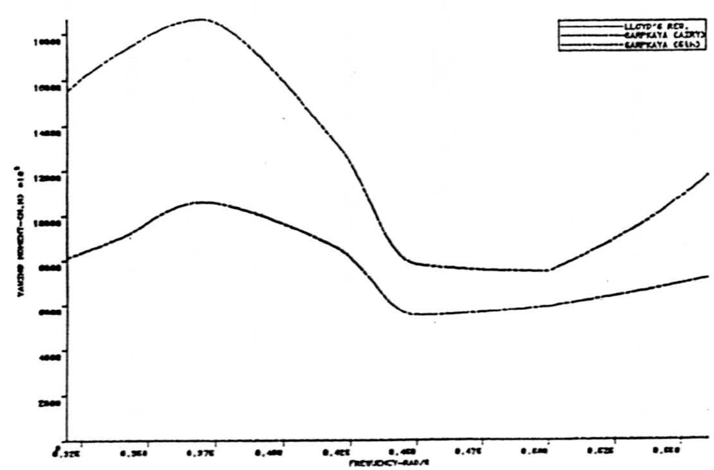

COEFFICIENTS: LR & SARPK , $\beta = \pi/4$, SR= 0.0
FIG.(27) MAX. YAWING MOMENTS Vs. FREQUENCY

are negligible compared with the values by the 5th order theory.

f. The differences in the pitching moments ranged from 6.5% (H = 5.0m) to 44.5% (H = 25.0m).

6.3.3 Maximum Forces and Moments per Unit Wave Height

Figures (28) to (37) exhibit the following features:-

a. In general, the force (or moment) per unit wave height is not constant, it increases with the increase of wave height (H). This is mainly the effect of the drag and lift forces which are proportional to $(H)^2$.

b. The relation between the (surge force/wave height) and (H) is linear for Airy theory and non-linear for the 5th order theory. For the Airy theory, the slope of the straight line (rate of change) is larger when using Sarpkaya's coefficients than LR coefficients. The differences between LR and the 5th order theory increase with increasing (H).

c. The relation between the (heave force/wave height) and (H) is non-linear for both Airy and the 5th order theory. The differences between LR and the 5th order theory are very small.

d. The relation between the (sway force/wave height) and (H) is linear for Airy (Sarpkaya) and non-linear for the 5th order theory. For LR the values are negligible when $\beta = 0.0$.

e. The (rolling moment/wave height) is approximately constant

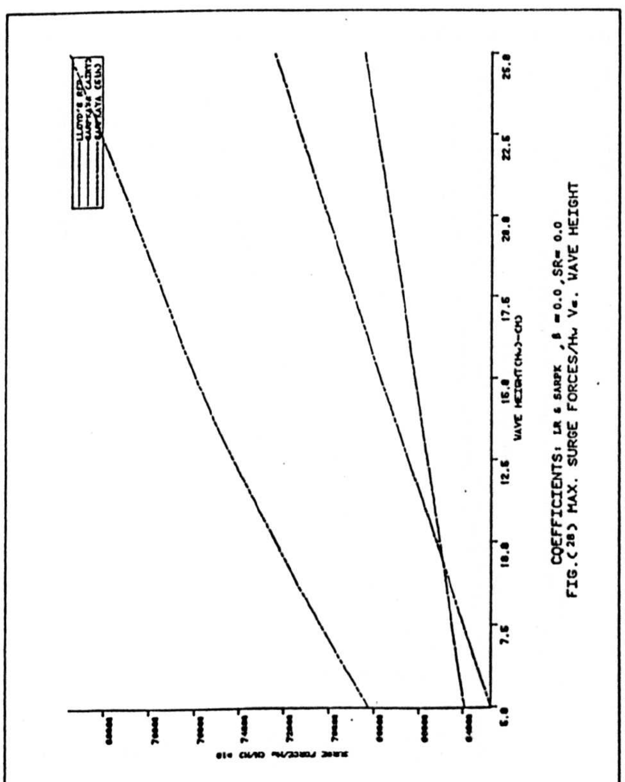

COEFFICIENTS: LR & SARPK , β = 0.0 ,SR= 0.0
FIG.(28) MAX. SURGE FORCES/Hw Vs. WAVE HEIGHT

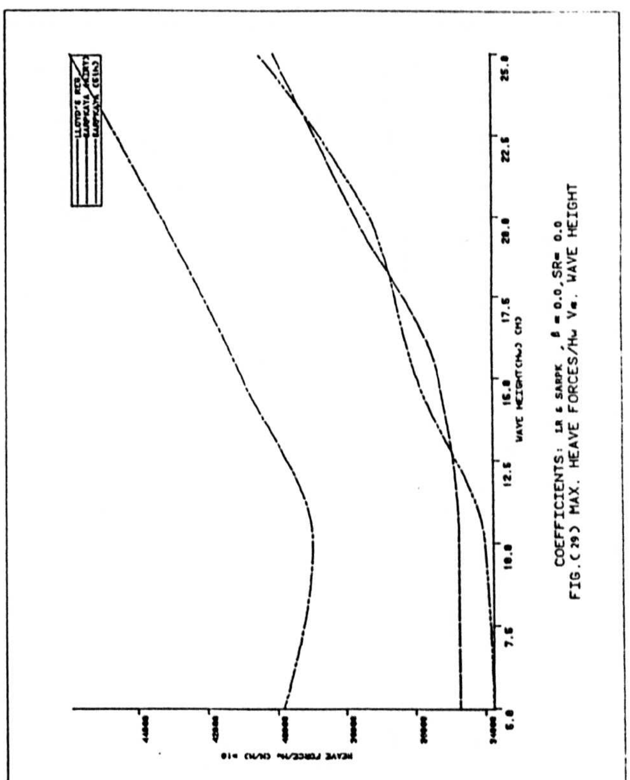

COEFFICIENTS: LR & SARPK , β = 0.0 ,SR= 0.0
FIG.(29) MAX. HEAVE FORCES/Hw Vs. WAVE HEIGHT

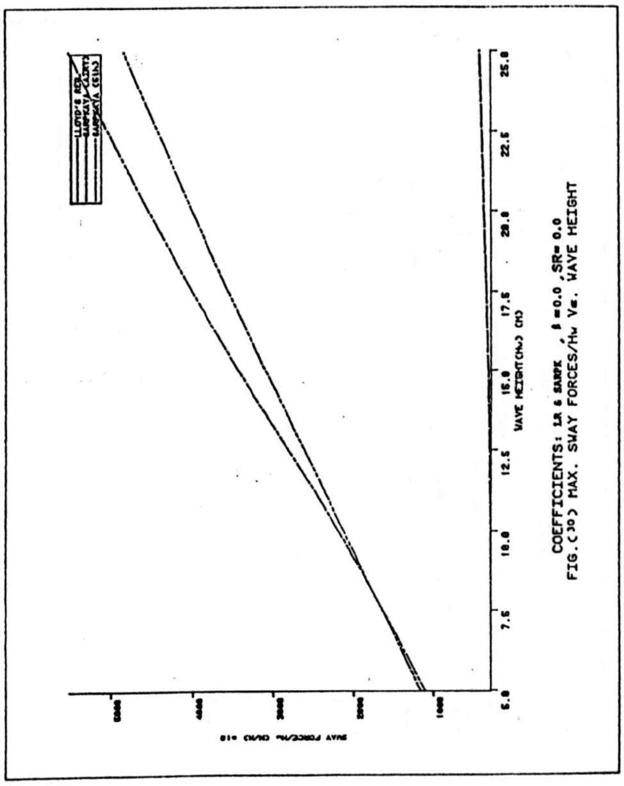

COEFFICIENTS: LR & SARPK , β = 0.0 ,SR= 0.0
FIG.(30) MAX. SWAY FORCES/Hw Vs. WAVE HEIGHT

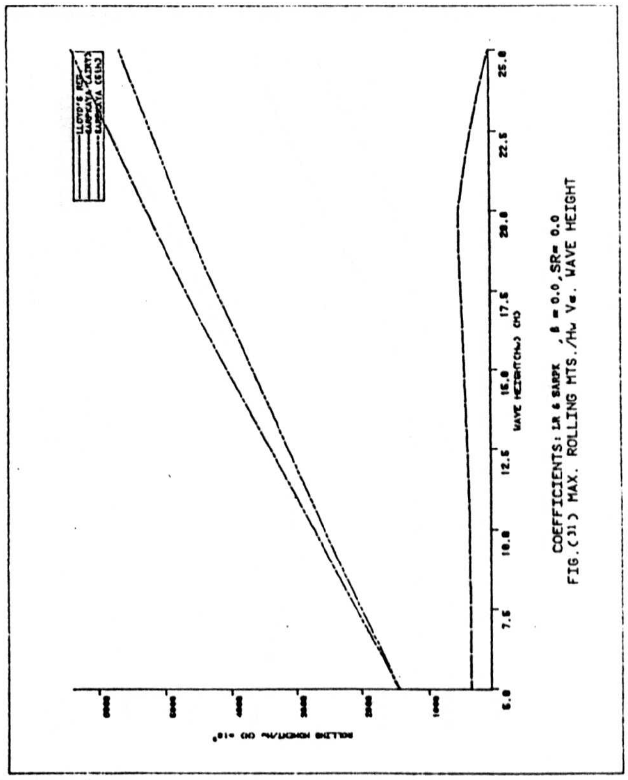

COEFFICIENTS: LR & SARPK , β = 0.0 ,SR= 0.0
FIG.(31) MAX. ROLLING MTS./Hw Vs. WAVE HEIGHT

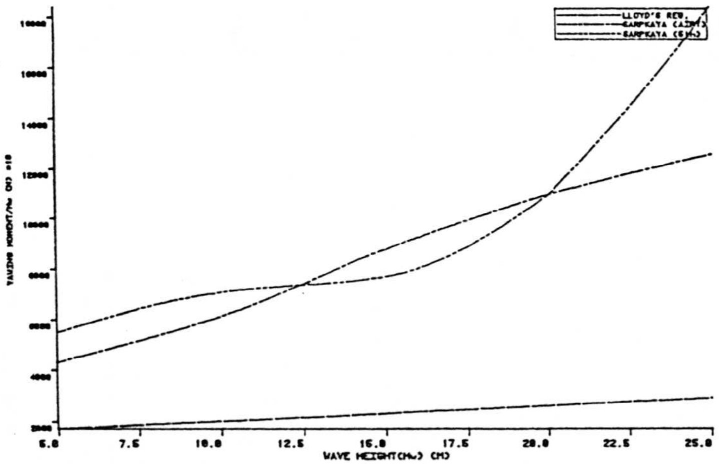

COEFFICIENTS: LR & SARPK , β = 0.0, SR= 0.0
FIG.(32) MAX. YAWING MTS./Hw Vs. WAVE HEIGHT

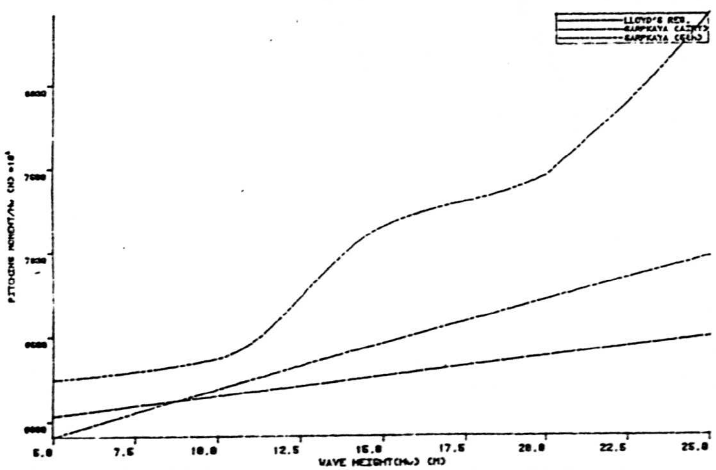

COEFFICIENTS: LR & SARPK , β = 0.0, SR= 0.0
FIG.(33) MAX. PITCHING MTS./Hw Vs. WAVE HEIGHT

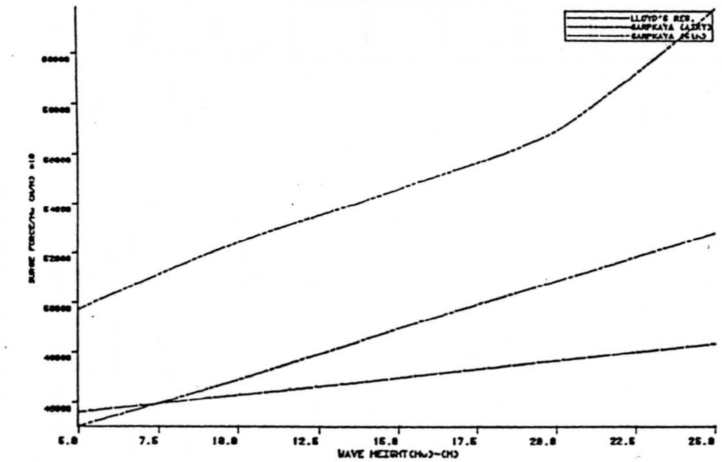

COEFFICIENTS: LR & SARPK , $\beta = \pi/4$, SR= 0.0
FIG.(34) MAX. SURGE FORCES/Hw Vs. WAVE HEIGHT

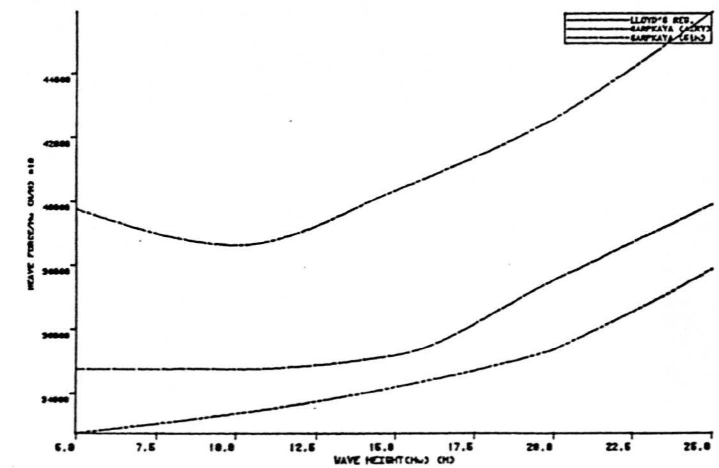

COEFFICIENTS: LR & SARPK , $\beta = \pi/4$, SR= 0.0
FIG.(35) MAX. HEAVE FORCES/Hw Vs. WAVE HEIGHT

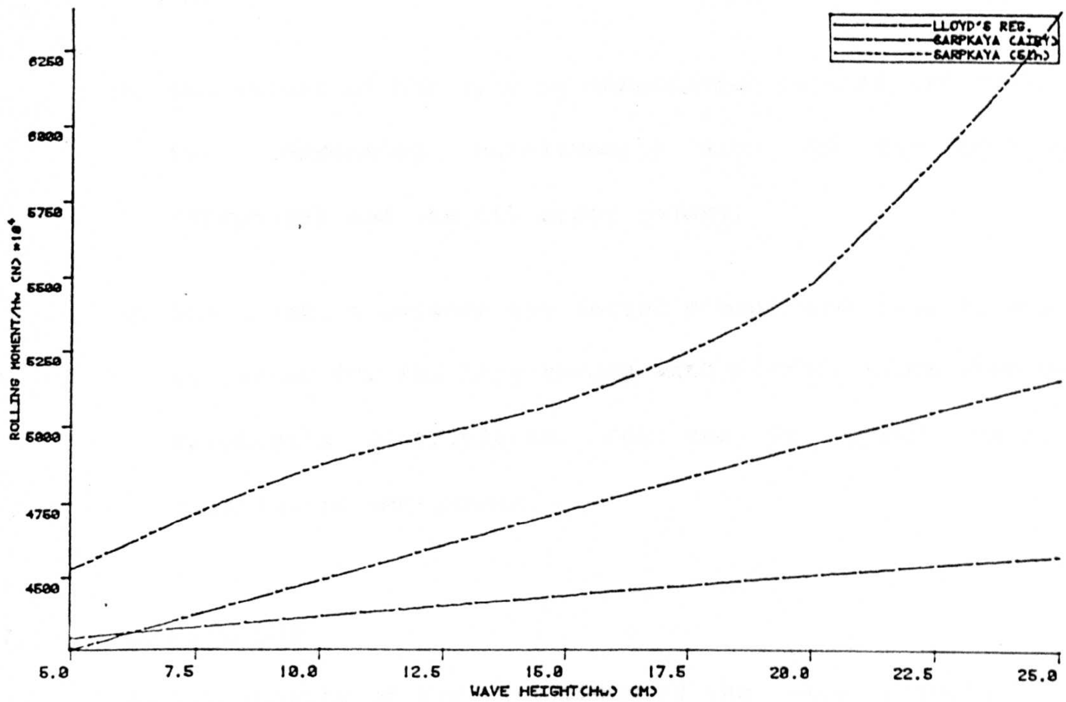

COEFFICIENTS: LR & SARPK , $\beta = \pi/4$, SR= 0.0
FIG.(36) MAX. ROLLING MTS./Hw Vs. WAVE HEIGHT

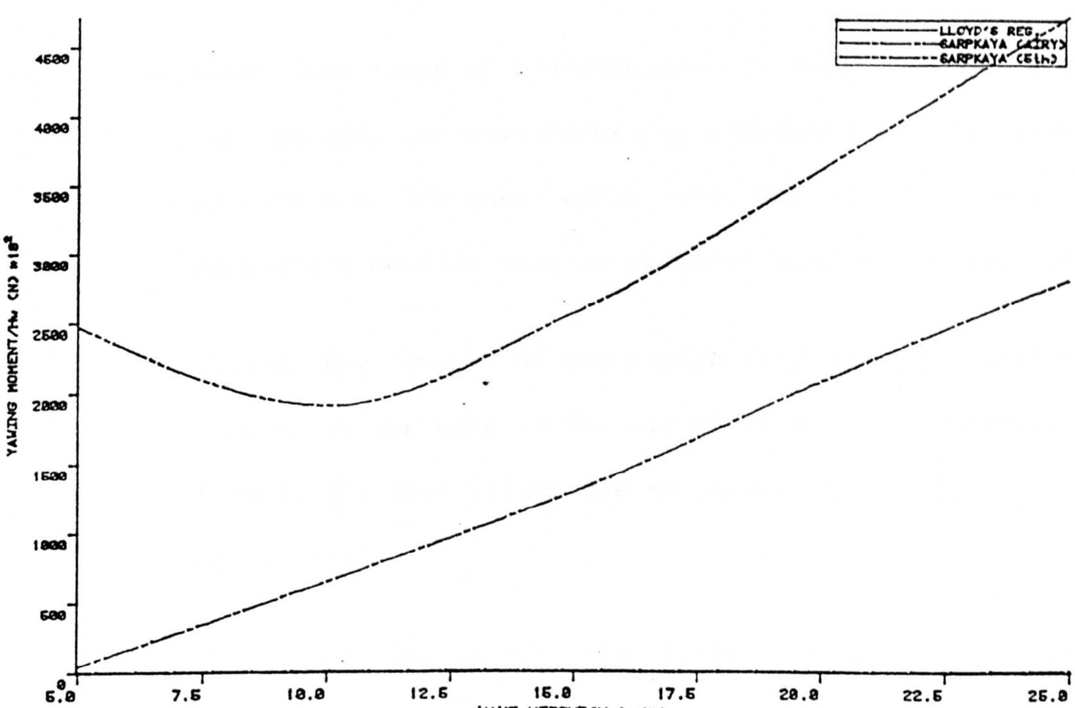

COEFFICIENTS: LR & SARPK , $\beta = \pi/4$, SR= 0.0
FIG.(37) MAX. YAWING MTS./Hw Vs. WAVE HEIGHT

for LR, especially when $\beta = 0.0$, increasing linearly with (H) for Airy (Sarpkaya) and non-linearly for the 5th order theory.

f. The values of the (yawing moment/wave height) are small for LR, increasing non-linearly with (H) for both Airy (Sarpkaya) and the 5th order theory.

g. The relation between the (pitch moment/wave height) and (H) is linear for the Airy theory, with a larger slope when using Sarpkaya's coefficients. For the 5th order theory the relation is non-linear.

7. CONCLUSIONS

a. The results of the variations of the wave velocities and accelerations at the mean water line and below it showed that the differences in predicting the maximum velocities and accelerations by the Airy, Stokes' 2nd order and Stokes' 5th order theories can be large.

b. Within the range of a design wave of 30.0m height and 17 sec period, the wave forces on a member could be increased by more than 50% when using the 5th order theory with Sarpkaya's coefficients as compared with the LR results.

c. Within the range of the design wave the total forces and moments at the base of the structure could be increased by from 30-60% when using the 5th order theory compared with LR results.

d. The differences in the total forces and moments between the results of the 5th order theory and LR increase with the wave height (H).

e. For jacket structures installed in deep water, Stokes' 5th order theory should be used to evaluate the flow kinematics. Since some field experiments indicated differences between the measured flow kinematics and those predicted by the 5th order theory, some differences must be expected between the calculated and the actual forces and moments.

REFERENCES

1. BISHOP, J R, TICKELL, R G, and GALLAGHER, K A, 'The UK Christchurch Bay Project; A Review of Results', NMI Report NMI-R87, Jun 80.

2. CHAKRABARTI, S K, 'Inline Forces on Fixed Vertical Cylinder in Waves', Jour of the Waterway, Port, Coastal and Ocean Div, ASCE, Vol 106, No WW2, May 80.

3. DEAN, R G, 'Relative Validities of Water Wave Theories', Jour of the Waterways, Harbors and Coastal Engineering Div, ASCE, Vol 96, No WW1, 1970, pp105-119.

4. DEAN, R G, LO, J-M, and JOHANSSON, P I, 'Rare Wave Kinematics Vs Design Practice', Civil Engineering in the Oceans IV, ASCE, 1979, pp1030-1049.

5. DEAN, R G,'Stream Function Representation of Nonlinear Ocean Waves', Jour of Geophysical Research, Vol 70, No 18, 1965, pp4561-4572.

6. GRACE, R A, 'Near-Bottom Water Motion Under Ocean Waves', Proc 15th Coastal Engineering Conf, Honolulu, Vol III, 1976, pp2371-2386.

7. HOGBEN, N and STANDING, R D, 'Experience in Computing Wave Loads on Large Bodies', OTC Paper No 2189, Houston, Texas, 1975.

8. HOGBEN, N, MILLER, B L, SEARLE, J W and WARD, G, 'Estimation of Fluid Loading on Offshore Structures', NMI Report NMI-R11, Apr 77.

9. Le MEAHAUTE, B, 'An Introduction to Hydrodynamics and Water Waves', Springer-Verlag, Dusseldorf, 1976.

10. McNAMEE, B P, SHARP, B B, and STEVENS, L K, 'Measurement of Water Particle Velocities in Waves', Applied Ocean Research, Vol 5, No 1, 1983.

11. NAG FORTRAN Library Manual, Mark 9, Vol 1, 1982, Numerical Algorithms Group Limited.

12. OHMART, R D, and GRATZ, R L, 'A Comparison of Measured and Predicted Ocean Wave Kinematics', OTC Paper No 3276, Houston, Texas, 1978.

13. SARPKAYA, T, and ISAACSON, M, 'Mechanics of Wave Forces on Offshore Structures', Van Nostrand Reinhold, New York, 1981.

14. SKJELBREIA, L, and HENDRICKSON, J A, 'Fifth Order Gravity Wave Theory', Proc 7th Coastal Engineering Conf, The Hague, 1961, pp184-196.

15. TSUCHIYA, Y, and YAMAGUCHI, M, 'Some Considerations on Water Particle Velocities of Finite Amplitude Wave Theories', Coastal Engineering in Japan, Vol 15, 1976, pp43-57.

CHAPTER 7

CHAPTER 7

DRAG INTERFERENCE EFFECTS BETWEEN JACKET MEMBERS

1. INTRODUCTION

Many offshore structures have multiple cylinders in proximity to one another. Riser configurations usually consist of smaller diameter cylinders in a circular array. Deep water articulated towers are often designed as circular or square sections towers composed of vertical cylinders with horizontal or diagonal braces. The conductors in a fixed drilling platform are sometimes arranged in a linear array along one side of the platform. Jacket platforms and many semi-submersibles have tubular members that will experience interaction among one another. Therefore, it is important to assess the effect of the neighbouring members on the forces on each cylinder in an array.

When two or more cylinders are in close proximity, not only the flow about the downstream cylinder but also the flow about the upstream cylinder may be affected. For large cylinders where drag effects are negligible, the wave forces on a group of cylinders can be determined analytically by linear diffraction theory. The methods of calculation and other information are presented in Refs. (4,5,12,14,16,17,19,21,22,28 and 29). However, no analytical method is available for the determination of forces on a group of cylinders when drag and inertia forces are both important. Designers have to rely on the experimental results which have been reported by several investigators.

2. A REVIEW OF EXPERIMENTAL DATA

Zdravkovich (30) has presented an extensive review of flow interference between two circular cylinders in various arrangements including an extensive list of references, see also Ref. (28).

Experiments have shown that there is strong interference between two cylinders in tandem, one cylinder behind the other, for spacing ratios (S/d) smaller than about 3.5. At (S/d) of about 3.5 there is a sudden change of the flow pattern in the gap between the two cylinders. The critical spacing ratio (S/d) is below 3.5 at $R_e = 5.8 \times 10^4$, equal to 3.5 for $R_e = 8.3 \times 10^4$ and slightly larger than 3.5 at $R_e = 1.1 \times 10^5$.

At the critical spacing, the discontinuous changes of the flow patterns cause the following: a jump in drag coefficient of the upstream cylinder, the commencement of vortex shedding and a drop in the base pressure. For the downstream cylinder, the base and side pressure coefficients drop, vortex shedding frequency jumps and the gap pressure and drag coefficient increase suddenly (28).

For Reynolds numbers (R_e) less than 2×10^5, the downstream cylinder has no effect on the upstream one when the spacing is larger than the critical. At high subcritical Reynolds numbers, the wake turbulence from the upstream cylinder induces a supercritical flow around the downstream cylinder and hence the drag remains small even at large spacing (28).

Pearcey et al (23) reported the wind-tunnel tests on two cylinders in tandem ($R_e = 1.2 \times 10^5 - 8.3 \times 10^6$) and on arrays of cylinders ($R_e = 4 \times 10^4 - 8 \times 10^4$) having different numbers of rows and columns. At $R_e = 7 \times 10^6 - 8 \times 10^6$, for two cylinders in tandem at S/d = 5, the reduction in drag was found to be 36%. A smaller and decreasing reduction occurs for each successive stage for a column of members in an array. For any individual member that lies to the side of the wake of an upstream one, the maximum increment in drag was found to be 27.5% when the line of centres, of the two cylinders, makes an angle of 18^o to the direction of the undisturbed flow. Similarly, smaller increments occur at successive stages in the columns of an array.

Because the significant reductions in drag occur only when the columns of the array are lined up to within $\pm 10^o$ of the undisturbed flow direction, Pearcey et al suggested that it would be unwise to assume in design that the total drag force would be less than the drag of the same number of members all in isolation.

Instead it would be safer to assume that the drag would be 10-20% higher than that value. They pointed out that the static drag forces on individual members could be up to 30% greater than that for an isolated cylinder with higher percentages for dynamic loads.

At lower Reynolds numbers, the interference effect on the drag of the downstream cylinder of a tandem pair was observed to vary from a decrease in the drag coefficient (C_D) from 1.2 to 0.25 at R_e of about 10^5 to an increase from 0.2 to 0.5 at $R_e = 7 \times 10^5$.

Side-by-side as well as staggered arrangements have also been investigated and reported. For S/d = 1.1-2.2, the wakes of the two cylinders interfere and are alternatingly entrained by each other.

This gives rise to changes in the base pressures of both cylinders so that when the flow is biased to one cylinder it produces a resultant force inclined to the free stream direction and having a component perpendicular to the free flow direction, ie a lift force. The results for the staggered arrangement show that the upstream and downstream cylinders may experience negligible or strong lift forces and reduced or increased drag forces, depending on their relative positions in the array.

Experiments by Biermann and Herrnstein (2) have shown that the difference between the drag coefficient measured on the second cylinder of a tandem pair and the drag coefficient of the single cylinder at the same R_e may be negative (-0.6) for S/d from 1.2 to 2.0.

Ross (25) tested a side-by-side arrangement of 3 cylinders in a wave tank in the range of critical Reynolds numbers. The results indicated that the wave forces increase significantly only when S/d is less than 2.0.

Hoerner (15) suggested that the interaction effects in steady subcritical flow are negligible for the side-by-side arrangement if S/d > 4.0, and for the tandem arrangement if S/d > 5.0.

Dalton and Szabo (10) reported the experiments in a wind tunnel to investigate the effects of spacing, orientation and Reynolds number on the drag of each cylinder in a group of two and three cylinders. They have found that the middle and downstream cylinder drag coefficients are smaller and noticeably more dependent on orientation than is the upstream cylinder. The drag coefficient for the upstream cylinder remained nearly constant.

Laird and Warren (18) oscillated a group of 24 tubes arranged in a circular fashion in still water. The inline and transverse forces were measured during the test. The spacing ratio (S/d) varied from 9 to 1. At S/d = 9, there was no interference effect. At S/d = 5, the total inline force on the cylinder group was reduced by about 10%. When the cylinders touched one another (S/d = 1.0), the inline force was reduced by about 67% while the transverse force was found to increase by a factor of 1.7.

Arita et al (1) considered a six-pile arrangement (S/d = 2.18, 4.74) and carried out extensive measurements in a calm sea. At subcritical Reynolds numbers, the middle cylinders experienced the least resistance (C_D = 0.2). At supercritical Reynolds numbers, the drag coefficienmt of the cylinders in the front row was reduced from 1.0 to 0.7. All other cylinders experienced the same low drag coefficient of about 0.07.

Bushnell (3) studied the interference effects between cylinders in an array in a pulsating water tunnel. Two cylinders, as well as a 3 x 3 array of cylinders of equal diameter, were tested. In all cases, the spacing ratio (S/d) was 3.0. The oscillating flow was at 0^o, 20^o and 40^o to the centre line. The interference effect increased with increased obliqueness of the flow. On a shielded cylinder, the maximum drag force was reduced relative to an exposed cylinder by up to 50%, while the lift force increased significantly by a factor of three to four.

Loken et al (20) presented results for five basic multitube riser configurations tested in steady and oscillatory flow. The geometries consisted of a large centre pipe and varying number of outer pipes arranged at varying pitch circle diameters (d_p).

For the steady flow the Reynolds number (R_e) ranged from 3.5×10^4 to 1.58×10^6. For the oscillatory flow, R_e ranged from 1.3×10^3 to 1.26×10^6 and the Keulegan-Carpenter (K) ranged from 20 to 100. The tests were carried out for smooth and rough cylinders ($k/d = 0.01$, 0.02 and 0.05).

The inline and transverse forces on the riser systems were measured during the oscillatory flow and the drag, inertia and lift coefficients (C_D, C_M, C_L) were presented as functions of K, R_e and k/d.

A drag interference coefficient was defined as:-

$$I_D = \frac{C_D d_p}{\Sigma C_{D_i} . d_i}$$

where C_D and d_p are the drag coefficient and pitch circle diameter of the multiple riser and C_{D_i} and d_i are the drag coefficient and diameter for the individual cylinders in isolation.

The density of packing of the cylinders in the array was expressed by 'length solidification' defined as:-

$$S_L = \frac{\Sigma d_i}{d_p}$$

Over the range tested, the results showed that I_D decreases with the increase of S_L. Sarpkaya (26) determined the drag and inertia coefficients for various multiple-tube riser configurations (15 outer pipes and one central pipe). The arrays were subjected to harmonically oscillating flow in a U-shaped water tunnel.

For one particular array, the drag coefficient decreased gradually from 1.3 to 0.75 with increasing K from 12 to 150 and reached an almost constant value for K larger than about 90 ($K=\frac{U_m.T}{d_e}$, d_e = equivalent diameter = Σd_i^2).

The inertia coefficient, (based on d),increased from 2.5 with increasing K and reached a terminal value of about 6.0. The total drag force acting on the array was 10% smaller than the sum of the drag forces acting on each cylinder in isolation.

Sarpkaya et al (27) determined the lift, drag and inertia coefficients for a pair of cylinders subjected to harmonic flow. The line joining the centres of the cylinders was rotated at suitable steps relative to the flow direction. The spacing ratio (S/d) was varied from 1.5 to 3.5. For the tandem arrangement, the results show that the drag and inertia coeficients depend on both K and (S/d). As the amplitude of flow oscillation becomes comparable or smaller than the gap between the two cylinders, C_D and C_M gradually approach those values corresponding to an isolated cylinder. For the side-by-side arrangement, when (S/d) is larger than 2.5, the cylinders behave as if they were independent.

Rains and Chakrabarti (24) tested an offshore drilling tower model pivoted near the bottom and consisting of 60 tubes. The tower was mechanically excited with a known oscillatory forcing function in still water. The mean added mass coefficient for the group at a spacing ratio S/d = 3.0 was found to be 2.8 while the mean drag coefficient was 2.4.

Chakrabarti (6-9) reported the results of extensive tests carried out with a vertical array of smooth tubes (d = 76mm) in a wave tank of 1.52 m water depth. The wave period ranged from 1.5 to 8.0 sec and the maximum wave height was 0.61 m. The wave kinematics were calculated from the measured profiles by stream function theory (11).

The array consisted of 2, 3 and 5 tubes and was tested at 90^o, 45^o and 0^o relative to the wave direction. The spacing ratio (S/d) was varied from 1.1 to 5.0. The inline and transverse forces on the tubes as well as on small instrumented sections (0.30 m) of the tubes were measured. The Keulegan-Carpenter number (K) ranged from 0.0 to 65.0 while the Reynolds number ranged from 10^4 to 5×10^4.

The drag, inertia and lift coefficients were determined from the forces on the instrumented sections and the mean values were presented graphically as functions of K and (S/d).

The main conclusions can be summarised as follows:-

a. At 90^o to the waves (side-by-side arrangement), the array experienced an increase in the inline force as the spacing ratio decreased. The centre tube in the array experienced the maximum force. The interaction among the tubes virtually disappeared at S/d = 5.0. In the 45^o and 0^o arrays, the forces on the different tubes in the array were similar at S/d > 1.1. At S/d = 1.1 the centre tube showed a decrease in the force compared to the outer tubes.

b. For the side-by-side arrangement, C_D and C_M were found to increase steadily with the decrease of (S/d) at all K values. The results have shown that C_D and C_M increase dramatically for (S/d) smaller than 1.3. A change in (S/d) from 1.3 to 1.1 for the 5-tube arrangement can double C_D and increase C_M by a factor of about three. For (S/d) larger than about 2.0, C_D and C_M do not significantly differ from those of a single cylinder at the corresponding K and R_e values. It has been shown that the vortex shedding from a tube surface is suppressed by the presence of neighbouring tubes. At the smallest spacings, the centre tube experiences only a small lift force. The outer sections experience asymmetric lift forces, since they are higher on the open side than on the closed side.

c. For the tandem arrangement, it was found that the drag and inertia coefficients generally decrease with decreased spacings due to shielding while the lift coefficient increases.

The main experimental data reviewed in this section are summarised in Table (1).

3. METHOD OF CALCULATION

The interference effects were determined using the drag interference curves for a pair of circular cylinders given in Refs. (2, 13). These curves give the drag coefficient ratios for the test cylinder as a function of spacing ratio (S/d) for the two cases of tandem arrangement (one cylinder behind the other) and the side-by-side arrangement. The curves were reproduced from Ref. (13) and are shown in Fig. (3).

Reference	Flow Particulars	No of Cylinders	d	S/d	R_e	K	$C_{in}=C_{D_i}/C_D$	Other Effects
SIDE-BY-SIDE ARRANGEMENT								
ARITA(1)	Calm Sea	6			Subcritical		<1.0 middle cylinders	
					Supercritical		<1.0 all cylinders	
BIERMAN et al(2)	Steady Flow (Wind Tunnel)	2		1.2-2.0	$6.5 \times 10^4 - 1.63 \times 10^5$		$1.0-(0.6/C_D)$	
				2.25	$6.5 \times 10^4 - 1.63 \times 10^5$		$1.0+(0.3/C_D)$	
				>5.0	$6.5 \times 10^4 - 1.63 \times 10^5$		1.0	
CHAKRABARTI (6-9)	Wave Flow (Wave Tank) T=1.5-8.0sec H_{max}=0.61m	2, 3, 5	7.6cm	1.1-5.0	$10^4 - 5 \times 10^4$	0.0-65		
		5		1.1				100% Increase in C_D 30% Increase in C_M
				>2.0				No interference effect
HOERNER(15)	Steady Flow	2		>4.0	Subcritical			No interference effect
LAIRD et al(18)	Still Water	24		1.0				67% reduction in inline force
				5.0				10% reduction in inline force
								170% increase in lift force
				9.0			1.0	No effect
LOKEN et al(20)	Oscillatory Flow	Variable	4.45-13.65cm	Variable	$1.3 \times 10^3 - 1.2 \times 10^6$	20-100		I_D decreases with increase of S_L $I_D = \frac{C_D . d_p}{\Sigma C_{D_i} . d_i}$ $S_L = \frac{\Sigma d_i}{d_p}$

Table (1.1) Summary of Experimental Data on Interference Effect

Reference	Flow Particulars	No of Cylinders	d	S/d	R_e	K	$C_{in}=C_{D_i}/C_D$	Other Effects
SIDE-BY-SIDE ARRANGEMENT								
Raines(24)	Still Water	60 (Oscillatory)		3				For the group mean $C_M = 2.8$ mean $C_D = 2.4$
ROSS(25)	Wave Flow (Wave Tank)	3		<2.0	Critical			Significant increase in wave force
SARPKAYA et al(27)	Oscillatory Flow (U-Tube)	2		>2.5			1.0	No interference effect
TANDEM ARRANGEMENT								
BIERMAN et al(2)	Steady Flow (Wind Tunnel)	2	2.54-6.35cm	3.0	$0.65x10^5-1.63x10^5$		$\{1.0-0.4/C_D\}$ to $\{1.0-1.2/C_D\}$	
BUSHNELL(3)	Harmonic Flow (Pulsating water tunnel)	2 at 0^o, 20^o, 40^o to the flow	7.62cm	3.0	$2.0x10^4-8.6x10^4$		0.5 (at 0^o)	270% increase in lift force at 20^o
		3 x 3	7.62cm	3.0	$2.0x10^4-8.6x10^4$		0.5 (at 0^o)	300-400% increase in lift force at 20^o
Chakrabarti (6-9)	Wave Flow (Wave Tank) T=1.5-8secs H_{max}=0.61m	2, 3, 5	7.6cm	1.1-5	10^4-5x10^4	0.0-65		C_D and C_M decrease with the decrease of S/d but C_L increases
HOERNER(15)	Steady Flow	2		>5.0	Subcritical			No interference effect
PEARCEY et al(23)	Steady Flow (Wind Tunnel)	2		5.0	$1.2x10^5-8.3x10^6$ $4x10^4-8x10^4$		0.64 1.28 at 18^o for downstream cylinder	
SARPKAYA et al (27)	Oscillatory Flow (U-tube)	2	1.5-3.5					C_{D_i} and C_{M_i} depend on K and S/d
ZDRAKOVICH (30)		2		<3.5 3.5 >3.5	$5.8x10^4$ $8.3x10^4$ $1.1x10^5$		>1.0 >1.0 >1.0	

Table (1.2) Summary of Experimental Data on Interference Effect

The results presented in Ref. (16) for the wave forces on two circular cylinders in tandem and side-by-side arrangement shows that the interference effects on the inertia coefficient (C_M) are negligible when S/d is larger than about 2.25. For the jacket structure under consideration, S/d for the main legs is larger than 10 and, therefore, the inertia coefficient will not be affected.

In order to use the interference data in calculations by the wave loading computer program (OSS) the two curves (Fig. 3) were curve-fitted by the least squares method and represented by polynomial equations, (See Appendix D). To determine the drag interference effect on the wave loading for the jacket structure, Fig. (2), the following procedure was used to estimate the 'interference coefficients' C_{in} for the individual members of the structure:-

a. For each individual member, the nearest neighbouring members which are most likely to have the largest interference effect were determined. These members may establish a tandem or side-by-side arrangement with the member under consideration.

b. For the tandem or side-by-side arrangement, the length of the member is divided into 10 equal sections and the different spacing ratios (S/d) along the length were calculated and the interference coefficients C_{in} (or correction factor) were determined from the appropriate curve.

c. If the member under consideration is affected by two members at the same time (one side-by-side and the other in tandem arrangement), the interference coefficient is taken as the product of the two individual effects ie $C_{in} = C_s \times C_t$ where:-

C_{in} = interference coefficient

C_s = interference coefficient due to the side-by-side member.

C_t = interference coefficient due to the member of tandem arrangement.

d. The drag coefficient due to interference C_{D_i} is calculated by the relation,

$$C_{D_i} = C_D.C_{in}$$

where C_D is the drag coefficient for the member in isolation, ie without interference effect.

In the above mentioned procedure, the effect of the members lying in the horizontal plane (the horizontal bracing and diagonal members) was not taken into account since there is no available information dealing with interference between horizontal members.

The calculations were carried out for the jacket structure shown in Fig. (2), which has been used in the previous chapters.

The calculations were performed for 9 wave frequencies ranging from $\omega = 0.37$ rad/s (H = 30.0m), L = 450.01m) to $\omega = 1.06$ rad/s (H = 6.0m, L = 54.83m). The full particulars of the waves are given in Table (2).

Wave Length L(m)	Wave Height H(m)	Wave Period T(s)	Frequency ω(rad/s)
54.83	6	5.92	1.06
69.72	7	6.68	0.94
109.52	11	8.37	0.75
150.40	15	9.81	0.64
196.45	20	11.21	0.56
246.43	20	12.56	0.50
304.23	20	13.96	0.45
349.24	20	14.95	0.42
450.01	30	16.97	0.37

Table (2) Particulars of Waves

The drag, inertia and lift coefficients (C_D, C_M, C_L) were determined from Sarpkaya's experimental results (See chapter 5).

Since no data are available showing the interference effect between roughened cylinders, the same interference coefficients which were estimated in the case of smooth cylinders, were also applied to the case of rough cylinders. In the case of rough cylinders, two values for the relative roughness were assumed, namely, SR = 1/800 (or 0.00125) and SR = 1/200 (or 0.005).

4. DESCRIPTION OF PROGRAM IBCM (Interference Between Cylindrical Members)

This program is used to calculate the interference coefficients C_{in} for the different members of the jacket structure. It is to be run before running the main wave loading program (OSS). IBCM is arranged in such a way that its output, ie the interference coefficients, are stored in a data file which can be used afterwards by the wave loading program for different runs (eg using different coefficients, relative roughness ...etc) without the need to run IBCM again.

Program IBCM calls two subroutines, AHDCY and SIDECY.

a. Subroutine AHDCY

This subroutine is used to calculate the interference coefficients when the two members are in tandem arrangement, ie one member behind the other.

b. Subroutine SIDECY

This subroutine is used to calculate the interference coefficients when the two members are side-by-side. (See Appendix (D)).

5. ANALYSIS OF THE RESULTS

5.1 Forces on the Individual Members

The maximum forces in (v, w) directions (F_{T_v}, F_{T_w}) were calculated at the different frequencies for six members (Nos. 11, 12, 13, 19, 20 and 21), Fig. (2). Smooth and rough cylinders were considered (SR = 0.005). The results are shown in Tables (3) to (14) and Figs. (4) to (12) and are analysed below.

5.1.1 Maximum Forces in (v, w) Directions (Smooth Cylinders, SR = 0.0)

Tables (3) to (8) show that:-

a. For member No. 11, the differences in F_{T_v} due to interference are negligible. The differences in F_{T_w} ranged from -0.6% (ω = 0.75 rad/s) to -14.9% (ω = 0.37 rad/s).

b. For member No. 12, the differences in F_{T_v} are very small ranging from -0.6% (ω = 0.5 rad/s) to -0.7% (ω = 0.56 rad/s). The differences in F_{T_w} are large, ranging from -1.4% (ω = 0.75 rad/s) to -38% (ω = 0.37 rad/s), with some variations in the relative time at the higher frequencies.

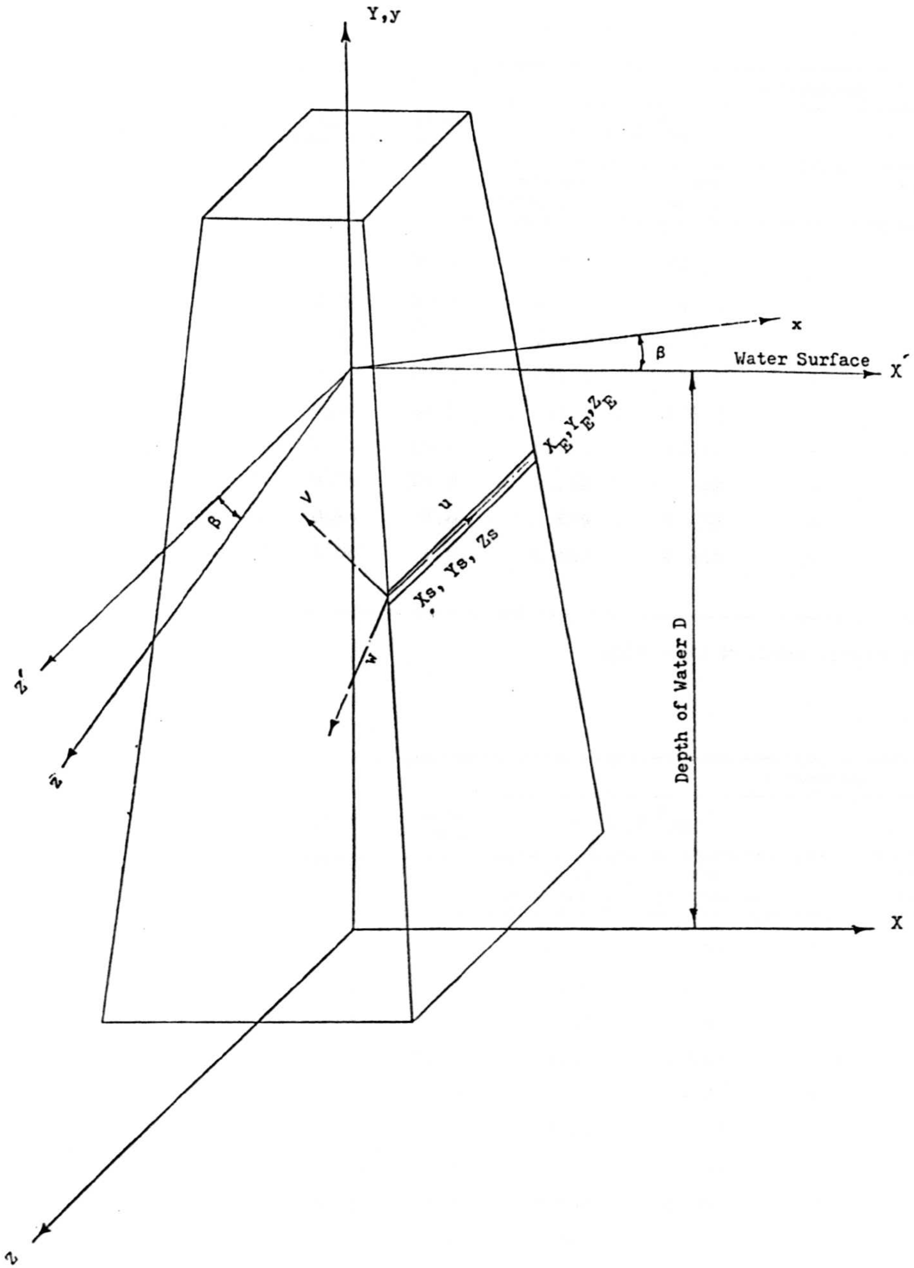

Fig. (1) Reference Systems

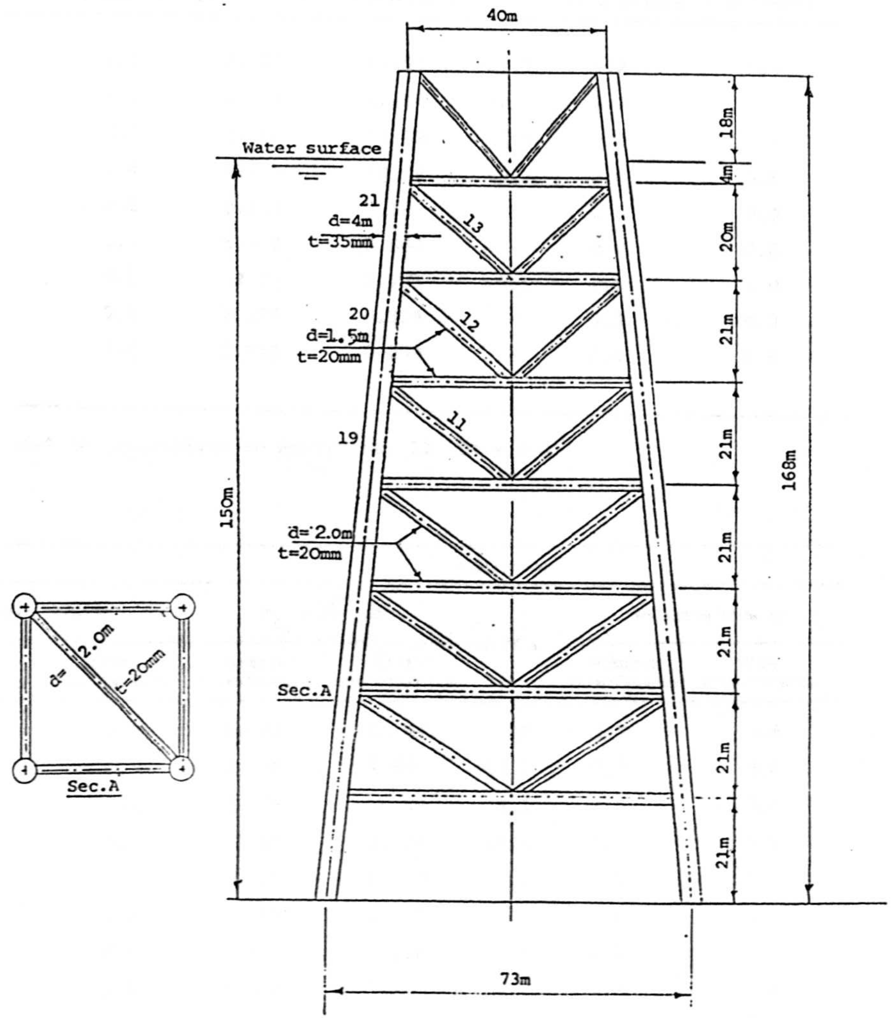

Fig. (2) Positions and Numbering of the Six Members

Wave Frequency ω(rad/s)	Wave Height H(m)	v Direction: $F_{T_V} \times 10^{-2}$ (N) Without Interference	v Direction: $F_{T_V} \times 10^{-2}$ (N) With Interference	v Direction: Diff %	v Direction: Relative Time tr Without Interference	v Direction: Relative Time tr With Interference	w Direction: $F_{T_W} \times 10^{-4}$ (N) Without Interference	w Direction: $F_{T_W} \times 10^{-4}$ (N) With Interference	w Direction: Diff %	w Direction: Relative Time tr Without Interference	w Direction: Relative Time tr With Interference
0.37	30.0	564.3	562.7	-	0.3	0.3	-21.08	17.93	-14.9	0.2	0.6
0.42	20.0	246.2	245.4	-	0.8	0.8	12.34	12.06	-2.3	0.6	0.6
0.45	20.0	221.2	220.4	-	0.8	0.8	12.16	11.82	-2.8	0.6	0.6
0.50	20.0	175.2	174.5	-	0.8	0.8	11.29	10.90	-3.5	0.6	0.6
0.56	20.0	130.8	130.7	-	0.2	0.2	9.537	9.587	-	0.0	0.0
0.64	15.0	37.38	37.40	-	0.1	0.1	5.572	5.563	-	0.0	0.0
0.75	11.0	10.48	10.48	-	0.1	0.1	2.29	2.277	-0.6	1.0	1.0
0.94	7.0	1.679	1.678	-	0.0	0.0	0.326	0.326	-	0.3	0.3
1.06	6.0	0.467	0.467	-	0.4	0.4	0.058	0.058	-	0.8	0.8

Table (3) Maximum Forces in 'v' and 'w' Directions on Member No. 11 SR = 0.0

Wave Frequency ω(rad/s)	Wave Height H(m)	v Direction: $F_{T_V} \times 10^{-3}$ (N) Without Interference	v Direction: $F_{T_V} \times 10^{-3}$ (N) With Interference	v Direction: Diff %	v Direction: Relative Time tr Without Interference	v Direction: Relative Time tr With Interference	w Direction: $F_{T_W} \times 10^{-4}$ (N) Without Interference	w Direction: $F_{T_W} \times 10^{-4}$ (N) With Interference	w Direction: Diff %	w Direction: Relative Time tr Without Interference	w Direction: Relative Time tr With Interference
0.37	30.0	62.13	61.90	-	0.3	0.3	20.93	12.98	-38	0.8	0.6
0.42	20.0	31.78	31.65	-	0.3	0.3	11.39	9.649	-15.3	0.2	0.6
0.45	20.0	31.18	31.03	-	0.3	0.3	11.69	10.04	-14.1	0.2	0.6
0.50	20.0	28.81	28.64	-0.6	0.8	0.8	11.56	10.34	-10.6	0.7	0.6
0.56	20.0	24.23	24.05	-0.7	0.8	0.8	11.00	10.10	-8.2	0.1	0.6
0.64	15.0	12.04	12.01	-	0.2	0.2	7.161	7.137	-	0.6	0.0
0.75	11.0	4.24	4.24	-	0.1	0.1	4.277	4.216	-1.4	1.0	1.0
0.94	7.0	0.654	0.654	-	0.0	0.0	1.362	1.355	-	0.9	0.9
1.06	6.0	0.302	0.302	-	0.4	0.4	0.65	0.65	-	0.3	0.8

Table (4) Maximum Forces in 'v' and 'w' Directions on Member No. 12 SR = 0.0

Wave Frequency ω(rad/s)	Wave Height H(m)	v Direction $F_{T_V} \times 10^{-5}$ (N) Without Interference	With Interference	Diff %	Relative Time tr Without Interference	With Interference	w Direction $F_{T_W} \times 10^{-5}$ (N) Without Interference	With Interference	Diff %	Relative Time tr Without Interference	With Interference
0.37	30.0	0.9566	0.9528	-	0.3	0.3	-3.374	1.627	-51.8	0.8	0.7
0.42	20.0	0.5632	0.5607	-	0.3	0.3	1.801	1.315	-27	0.8	0.6
0.45	20.0	0.6123	0.6093	-	0.3	0.3	1.915	1.452	-24.2	0.8	0.6
0.50	20.0	0.6799	0.6759	-0.6	0.3	0.3	2.212	1.666	-24.7	0.2	0.6
0.56	20.0	0.7298	0.7243	-0.8	0.8	0.8	2.521	1.884	-25.3	0.2	0.6
0.64	15.0	0.4356	0.4312	-1	0.8	0.8	1.805	1.540	-14.7	0.1	0.0
0.75	11.0	0.2760	0.2746	-	0.2	0.2	1.356	1.298	-4.3	0.6	0.0
0.94	7.0	0.1202	0.1197	-	0.6	0.6	0.821	0.813	-1	0.4	0.4
1.06	6.0	0.0842	0.084	-	1.0	1.0	0.641	0.617	-3.7	0.9	0.3

Table (5) Maximum Forces in 'v' and 'w' Directions on Member No. 13 SR = 0.0

Wave Frequency ω(rad/s)	Wave Height H(m)	v Direction $F_{T_V} \times 10^{-4}$ (N) Without Interference	With Interference	Diff %	Relative Time tr Without Interference	With Interference	w Direction $F_{T_W} \times 10^{-4}$ (N) Without Interference	With Interference	Diff %	Relative Time tr Without Interference	With Interference
0.37	30.0	31.78	31.78	-	0.7	0.7	31.72	31.71	-	0.2	0.2
0.42	20.0	21.66	21.67	-	0.7	0.7	22.08	22.08	-	0.2	0.2
0.45	20.0	21.23	21.24	-	0.7	0.7	21.89	21.89	-	0.7	0.7
0.50	20.0	19.79	19.78	-	0.1	0.1	20.48	20.48	-	0.7	0.7
0.56	20.0	18.05	18.05	-	0.1	0.1	17.52	17.51	-	0.1	0.1
0.64	15.0	10.27	10.27	-	0.6	0.6	10.53	10.53	-	0.1	0.1
0.75	11.0	4.548	4.548	-	0.0	0.0	4.48	4.48	-	0.0	0.0
0.94	7.0	0.6906	0.6906	-	0.9	0.9	0.657	0.657	-	0.9	0.9
1.06	6.0	0.1381	0.1381	-	0.8	0.8	0.1397	0.1397	-	0.8	0.8

Table (6) Maximum Forces in 'v' and 'w' Directions on Member No. 19 SR = 0.0

Wave Frequency ω(rad/s)	Wave Height H(m)	v Direction $F_{T_v} \times 10^{-5}$ (N) Without Interference	With Interference	Diff %	Relative Time tr Without Interference	With Interference	w Direction $F_{T_w} \times 10^{-5}$ (N) Without Interference	With Interference	Diff %	Relative Time tr Without Interference	With Interference
0.37	30.0	4.263	4.263	-	0.2	0.2	4.366	4.387	-	0.8	0.8
0.42	20.0	3.180	3.180	-	0.7	0.7	3.221	3.221	-	0.2	0.2
0.45	20.0	3.311	3.313	-	0.7	0.7	3.389	3.389	-	0.2	0.2
0.50	20.0	3.392	3.396	-	0.7	0.7	3.536	4.537	-	0.7	0.7
0.56	20.0	3.502	3.501	-	0.1	0.1	3.472	3.475	-	0.7	0.7
0.64	15.0	2.499	2.499	-	0.6	0.6	2.520	2.520	-	0.1	0.1
0.75	11.0	1.501	1.500	-	0.0	0.0	1.471	1.471	-	0.6	0.6
0.94	7.0	0.5339	0.5339	-	0.9	0.9	0.5348	0.5347	-	0.4	0.4
1.06	6.0	0.2700	0.2700	-	0.8	0.8	0.2648	0.2648	-	0.3	0.3

Table (7) Maximum Forces in 'v' and 'w' Directions on Member No. 20 SR = 0.0

Wave Frequency ω(rad/s)	Wave Height H(m)	v Direction $F_{T_v} \times 10^{-6}$ (N) Without Interference	With Interference	Diff %	Relative Time tr Without Interference	With Interference	w Direction $F_{T_w} \times 10^{-6}$ (N) Without Interference	With Interference	Diff %	Relative Time tr Without Interference	With Interference
0.37	30.0	0.6846	0.6842	-	0.3	0.3	0.7139	0.7137	-	0.3	0.3
0.42	20.0	0.5480	0.5480	-	0.7	0.7	0.5503	0.5503	-	0.2	0.2
0.45	20.0	0.6094	0.6904	-	0.7	0.7	0.6184	0.6184	-	0.2	0.2
0.50	20.0	0.7066	0.7065	-	0.7	0.7	0.7272	0.7272	-	0.2	0.2
0.56	20.0	0.8087	0.8086	-	0.7	0.7	0.8496	0.8495	-	0.7	0.7
0.64	15.0	0.7415	0.7415	-	0.1	0.1	0.7305	0.7305	-	0.1	0.1
0.75	11.0	0.6124	0.6125	-	0.0	0.0	0.6425	0.6425	-	0.6	0.6
0.94	7.0	0.4747	0.4747	-	0.4	0.4	0.4727	0.4727	-	1.0	1.0
1.06	6.0	0.4212	0.4212	-	0.3	0.3	0.4353	0.4353	-	0.9	0.9

Table (8) Maximum Forces in 'v' and 'w' Directions on Member No. 21 SR = 0.0

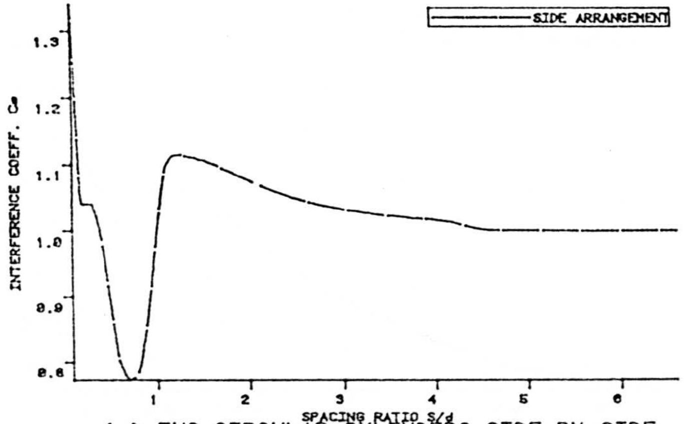

(a) TWO CIRCULAR CYLINDERS SIDE-BY-SIDE

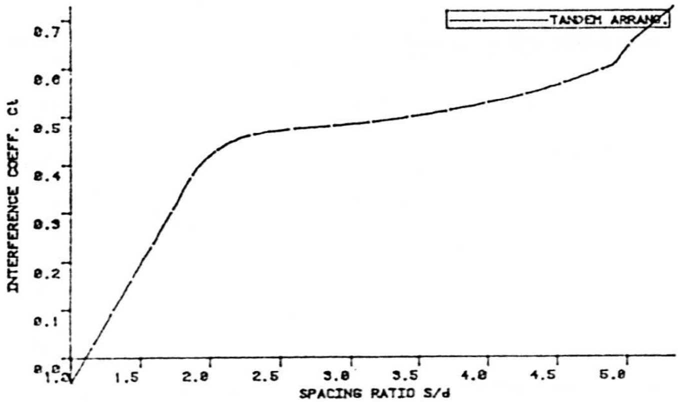

(b) TWO CIRCULAR CYLINDERS IN TANDEM

FIG.(3) INTERFERENCE COEFFICIENT Vs. SPACING RATIO (Ref.13)

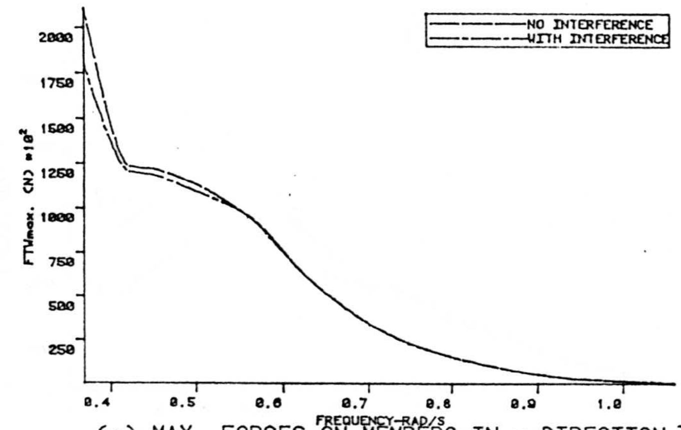

(a) MAX. FORCES ON MEMBERS IN w DIRECTION

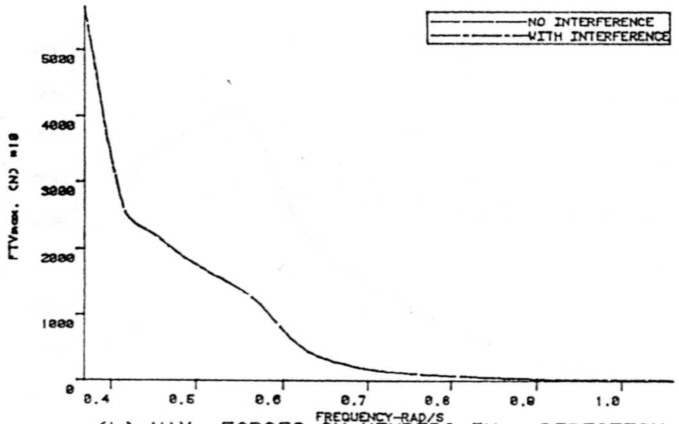

(b) MAX. FORCES ON MEMBERS IN v DIRECTION

PROGRAM: OSS ,COEFFICIENTS:SARPK ,SR = 0.0
FIG.(4) MAX. FORCES ON MEMBER (11) Vs. FREQUENCY

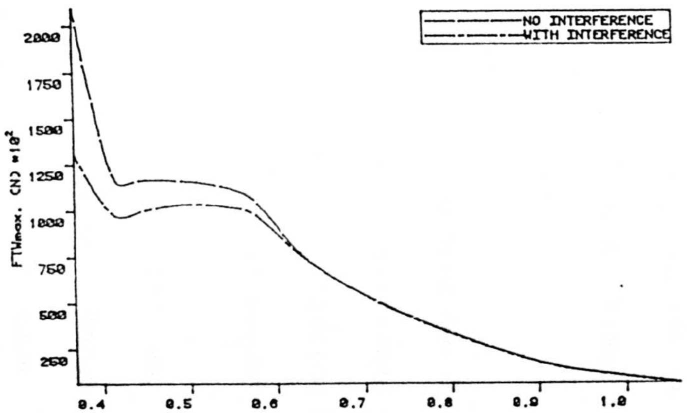

(a) MAX. FORCES ON MEMBERS IN w DIRECTION

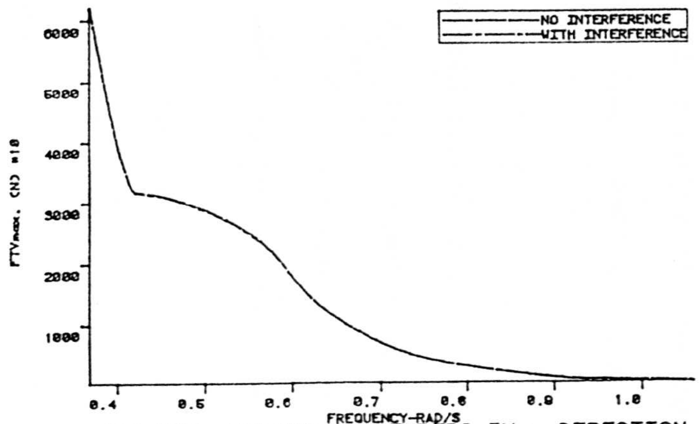

(b) MAX. FORCES ON MEMBERS IN v DIRECTION

PROGRAM: OSS ,COEFFICIENTS: SARPK, SR = 0.0
FIG.(5) MAX. FORCES ON MEMBER (12) Vs. FREQUENCY

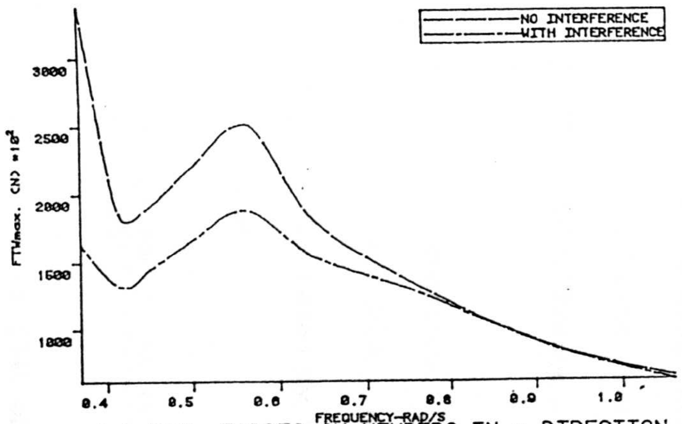

(a) MAX. FORCES ON MEMBERS IN w DIRECTION

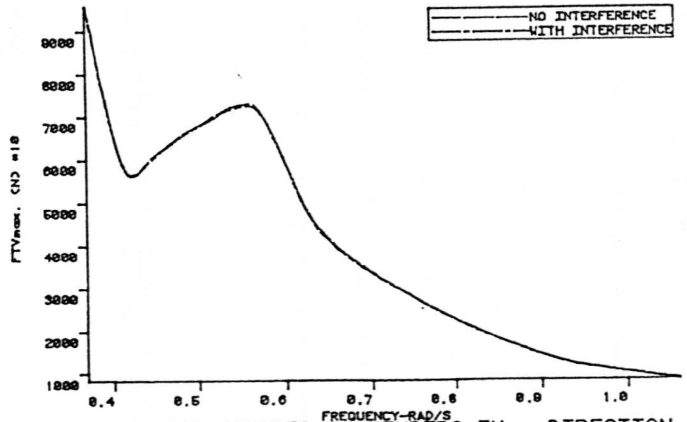

(b) MAX. FORCES ON MEMBERS IN v DIRECTION

PROGRAM: OSS ,COEFFICIENTS: SARPK , SR = 0.0
FIG.(6) MAX. FORCES ON MEMBER (13) Vs. FREQUENCY

c. For member No. 13, the differences in F_{T_v} ranged from -0.6% (ω = 0.50 rad/s) to -1.0% (ω = 0.64 rad/s), without any change in the relative time. The differences in F_{T_w} are large ranging from -1% (ω = 0.94 rad/s) to -51.8% (ω = 0.37 rad/s) with variation in the relative time for the whole range of frequencies.

d. For members No. (19), (20) and (21), both F_{T_v} and F_{T_w} were not affected. This is because the forces on these members are dominated by the inertia forces rather than the drag forces.

5.1.2 <u>Maximum Forces in (v, w) Directions (Rough Cylinders, SR = 0.005)</u>

Tables (9) to (14) show that:-

a. For member No. 11, the differences in F_{T_v} are negligible. The differences in F_{T_w} are larger than the corresponding values for smooth cylinders, ranging from -2.7% (ω = 0.75 rad/s) to -56.1% (ω = 0.37 rad/s) with some changes in the relative time in the range from ω = 0.37 rad/s to 0.64 rad/s.

b. For member No. 12, the differences in F_{T_v} are negligible. The differences in F_{T_w} are larger than that for smooth cyinders ranging from -0.8% (ω = 1.06 rad/s) to -62.1% (ω = 0.37 rad/s) with some changes in the relative time.

c. For member No. 13, the differences in F_{T_v} are negligible. F_{T_w} gave large differences compared with the smooth cylinders case ranging from -22.4% (ω = 1.06 rad/s) to -64.7% (ω = 0.37 rad/s) with some variations in the relative time.

Wave Frequency ω(rad/s)	Wave Height H(m)	v Direction $F_{T_V} \times 10^{-4}$ (N) Without Interference	With Interference	Diff %	Relative Time tr Without Interference	With Interference	w Direction $F_{T_W} \times 10^{-3}$ (N) Without Interference	With Interference	Diff %	Relative Time tr Without Interference	With Interference
0.37	30.0	40.63	40.58	-	0.3	0.3	-355.0	155.8	-56.1	0.8	0.2
0.42	20.0	26.96	26.93	-	0.3	0.3	145.4	84.00	-42.2	0.8	0.6
0.45	20.0	24.65	24.63	-	0.3	0.3	125.5	81.02	-35.4	0.2	0.6
0.50	20.0	18.55	18.53	-	0.8	0.8	104.7	72.91	-30.4	0.2	0.6
0.56	20.0	9.347	9.33	-	0.8	0.8	75.62	59.69	-21.1	0.7	0.6
0.64	15.0	0.3491	0.3474	-	0.7	0.7	34.30	33.24	-3.1	0.6	0.0
0.75	11.0	0.1336	0.1336	-	0.6	0.6	13.76	13.39	-2.7	1.0	1.0
0.94	7.0	0.0168	0.0168	-	0.0	0.0	2.39	2.377	-	0.9	0.9
1.06	6.0	0.0047	0.0047	-	0.4	0.4	0.702	0.701	-	0.8	0.8

Table (9) Maximum Forces in 'v' and 'w' Directions on Member No. 11 SR = 0.005

Wave Frequency ω(rad/s)	Wave Height H(m)	v Direction $F_{T_V} \times 10^{-3}$ (N) Without Interference	With Interference	Diff %	Relative Time tr Without Interference	With Interference	w Direction $F_{T_W} \times 10^{-4}$ (N) Without Interference	With Interference	Diff %	Relative Time tr Without Interference	With Interference
0.37	30.0	240.9	240.2	-	0.3	0.3	44.37	16.84	-62.1	0.3	0.8
0.42	20.0	215.0	214.7	-	0.3	0.3	19.82	8.192	-58.7	0.8	0.2
0.45	20.0	230.8	230.4	-	0.3	0.3	19.14	8.217	-57.1	0.8	0.2
0.50	20.0	246.9	246.5	-	0.3	0.3	17.14	7.874	-54.1	0.8	0.6
0.56	20.0	241.0	240.5	-	0.8	0.8	14.39	7.51	-47.8	0.2	0.6
0.64	15.0	110.4	110.1	-	0.8	0.8	7.037	4.548	-35.4	0.7	0.6
0.75	11.0	17.33	17.28	-	0.7	0.7	2.932	2.600	-11.3	0.6	1.0
0.94	7.0	0.8097	0.8099	-	0.0	0.0	0.8185	0.7976	-2.6	0.4	0.9
1.06	6.0	0.2917	0.2918	-	0.4	0.4	0.376	0.373	-0.8	0.3	0.3

Table (10) Maximum Forces in 'v' and 'w' Directions on Member No. 12 SR = 0.005

Wave Frequency ω(rad/s)	Wave Height H(m)	v Direction $F_{T_v} \times 10^{-5}$ (N) Without Interference	v Direction $F_{T_v} \times 10^{-5}$ (N) With Interference	v Direction Diff %	v Direction Relative Time tr Without Interference	v Direction Relative Time tr With Interference	w Direction $F_{T_w} \times 10^{-5}$ (N) Without Interference	w Direction $F_{T_w} \times 10^{-5}$ (N) With Interference	w Direction Diff %	w Direction Relative Time tr Without Interference	w Direction Relative Time tr With Interference
0.37	30.0	2.586	2.575	-	0.3	0.3	7.124	2.516	-64.7	0.3	0.8
0.42	20.0	2.656	2.649	-	0.3	0.3	3.792	1.315	-65.3	0.3	0.8
0.45	20.0	2.994	2.986	-	0.3	0.3	4.068	1.367	-66.4	0.3	0.8
0.50	20.0	3.554	3.532	-	0.3	0.3	4.411	1.520	-65.5	0.8	0.2
0.56	20.0	4.150	4.133	-	0.3	0.3	4.581	1.650	-64	0.8	0.2
0.64	15.0	3.634	3.622	-	0.8	0.8	2.752	1.221	-55.6	0.2	0.6
0.75	11.0	2.542	2.538	-	0.2	0.2	1.626	0.8894	-45.3	0.7	0.0
0.94	7.0	0.9286	0.9272	-	0.1	0.1	0.7199	0.5164	-28.3	0.0	0.4
1.06	6.0	0.4961	0.4955	-	0.0	0.0	0.5112	0.3967	-22.4	0.4	0.9

Table (11) Maximum Forces in 'v' and 'w' Directions on Member No. 13 SR = 0.005

Wave Frequency ω(rad/s)	Wave Height H(m)	v Direction $F_{T_v} \times 10^{-4}$ (N) Without Interference	v Direction $F_{T_v} \times 10^{-4}$ (N) With Interference	v Direction Diff %	v Direction Relative Time tr Without Interference	v Direction Relative Time tr With Interference	w Direction $F_{T_w} \times 10^{-4}$ (N) Without Interference	w Direction $F_{T_w} \times 10^{-4}$ (N) With Interference	w Direction Diff %	w Direction Relative Time tr Without Interference	w Direction Relative Time tr With Interference
0.37	30.0	51.24	52.95	3.3	0.4	0.4	69.92	71.44	2.2	0.4	0.4
0.42	20.0	14.19	14.56	2.6	0.3	0.3	14.09	14.33	1.7	0.3	0.3
0.45	20.0	13.28	13.66	2.9	0.8	0.8	13.53	13.79	1.9	0.3	0.3
0.50	20.0	12.23	12.29	-	0.7	0.2	12.30	12.31	-	0.7	0.2
0.56	20.0	10.65	10.65	-	0.1	0.1	10.56	10.59	-	0.7	0.7
0.64	15.0	6.023	6.026	-	0.6	0.6	6.138	6.138	-	0.1	0.1
0.75	11.0	2.637	2.637	-	0.0	0.0	2.598	2.597	-	0.0	0.0
0.94	7.0	0.5106	0.5106	-	0.9	0.9	0.5492	0.5492	-	0.9	0.9
1.06	6.0	0.1664	0.1664	-	0.8	0.8	0.1622	0.1622	-	0.8	0.8

Table (12) Maximum Forces in 'v' and 'w' Directions on Member No. 19 SR = 0.005

Wave Frequency ω(rad/s)	Wave Height H(m)	v Direction					w Direction				
		$F_{T_v} \times 10^{-5}$ (N)		Diff %	Relative Time tr		$F_{T_w} \times 10^{-5}$ (N)		Diff %	Relative Time tr	
		Without Interference	With Interference		Without Interference	With Interference	Without Interference	With Interference		Without Interference	With Interference
0.37	30.0	11.57	11.84	2.3	0.4	0.4	-13.44	13.68	1.8	0.4	0.4
0.42	20.0	2.875	3.014	4.8	0.9	0.9	4.503	4.631	2.8	0.4	0.4
0.45	20.0	2.553	2.630	3	0.3	0.3	3.769	3.902	3.5	0.9	0.9
0.50	20.0	2.413	2.502	3.7	0.8	0.3	2.823	2.924	3.6	0.3	0.9
0.56	20.0	2.210	2.235	1.1	0.2	0.2	2.285	2.363	3.4	0.8	0.8
0.64	15.0	1.485	1.485	-	0.6	0.6	1.480	1.480	-	0.1	0.1
0.75	11.0	0.8743	0.8737	-	0.0	0.0	0.8682	0.8694	-	0.6	0.6
0.94	7.0	0.3092	0.3092	-	0.9	0.9	0.3069	0.3069	-	0.4	0.4
1.06	6.0	0.1595	0.1595	-	0.8	0.8	0.1608	0.1607	-	0.3	0.3

Table (13) Maximum Forces in 'v' and 'w' Directions on Member No. 20 SR = 0.005

Wave Frequency ω(rad/s)	Wave Height H(m)	v Direction					w Direction				
		$F_{T_v} \times 10^{-6}$ (N)		Diff %	Relative Time tr		$F_{T_w} \times 10^{-6}$ (N)		Diff %	Relative Time tr	
		Without Interference	With Interference		Without Interference	With Interference	Without Interference	With Interference		Without Interference	With Interference
0.37	30.0	2.706	2.704	-	1.0	1.0	2.699	2.697	-	0.4	0.4
0.42	20.0	1.233	1.232	-	0.4	0.4	1.525	1.524	-	0.4	0.4
0.45	20.0	1.339	1.337	-	0.4	0.4	1.669	1.667	-	0.4	0.4
0.50	20.0	1.466	1.464	-	0.4	0.4	1.849	1.847	-	0.9	0.9
0.56	20.0	1.503	1.500	-	0.9	0.9	1.943	1.939	-	0.9	0.9
0.64	15.0	0.6720	0.6694	-	0.8	0.8	0.9483	0.9460	-	0.3	0.3
0.75	11.0	0.3930	0.3928	-	0.1	0.1	0.4536	0.4524	-	0.2	0.2
0.94	7.0	0.2776	0.2777	-	0.4	0.4	0.2840	0.2840	-	1.0	1.0
1.06	6.0	0.2499	0.2498	-	0.9	0.9	0.2573	0.2573	-	0.9	0.9

Table (14) Maximum Forces in 'v' and 'w' Directions on Member No 21 SR = 0.005

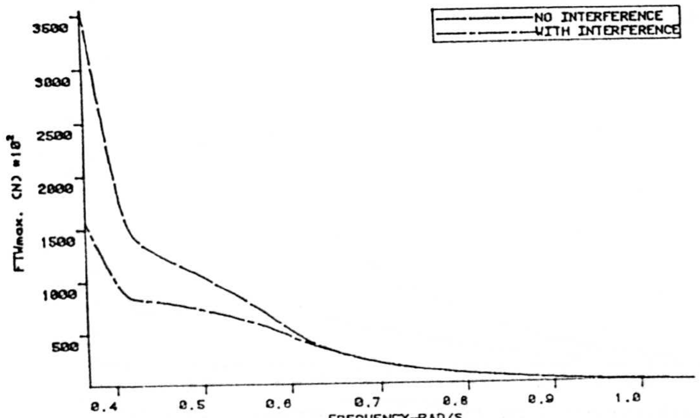

(a) MAX. FORCES ON MEMBERS IN w DIRECTION

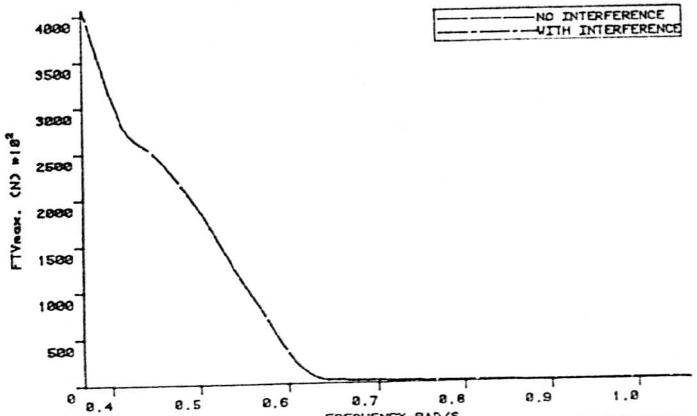

(b) MAX. FORCES ON MEMBERS IN v DIRECTION

PROGRAM: oss ,COEFFICIENTS: SARPK, SR = 0.005
FIG.(7) MAX. FORCES ON MEMBER (11) Vs. FREQUENCY

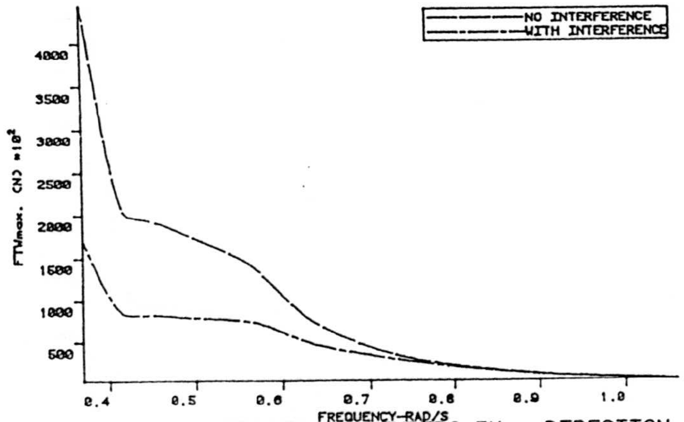

(a) MAX. FORCES ON MEMBERS IN w DIRECTION

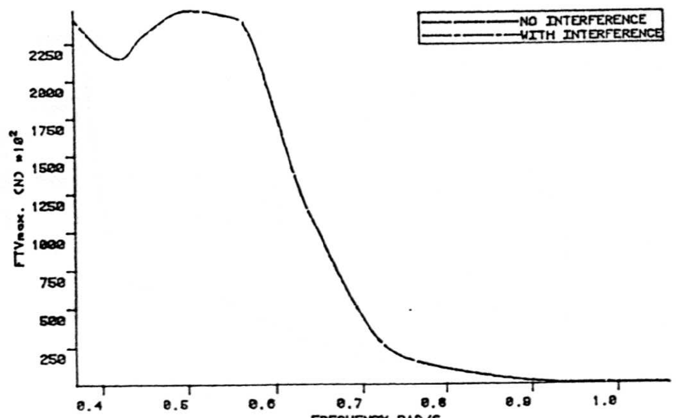

(b) MAX. FORCES ON MEMBERS IN v DIRECTION

PROGRAM: oss ,COEFFICIENTS: SARPK, SR = 0.005
FIG.(8) MAX. FORCES ON MEMBER (12) Vs. FREQUENCY

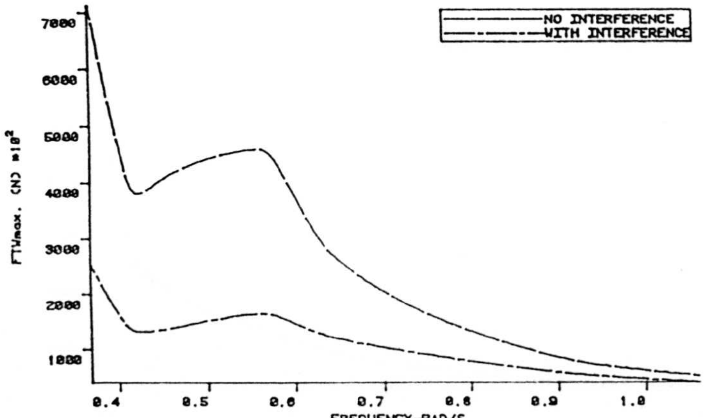

(a) MAX. FORCES ON MEMBERS IN w DIRECTION

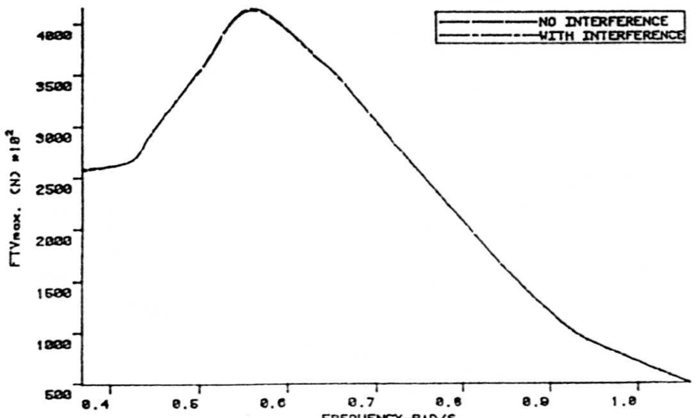

(b) MAX. FORCES ON MEMBERS IN v DIRECTION

PROGRAM: OSS ,COEFFICIENTS: SARPK , SR = 0.005
FIG.(9) MAX. FORCES ON MEMBER (13) Vs. FREQUENCY

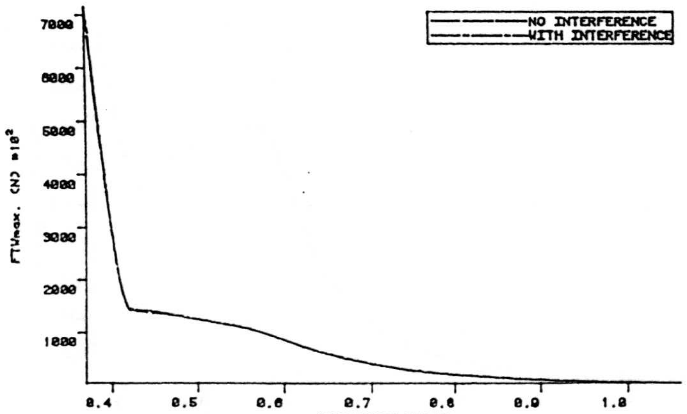

(a) MAX. FORCES ON MEMBERS IN w DIRECTION

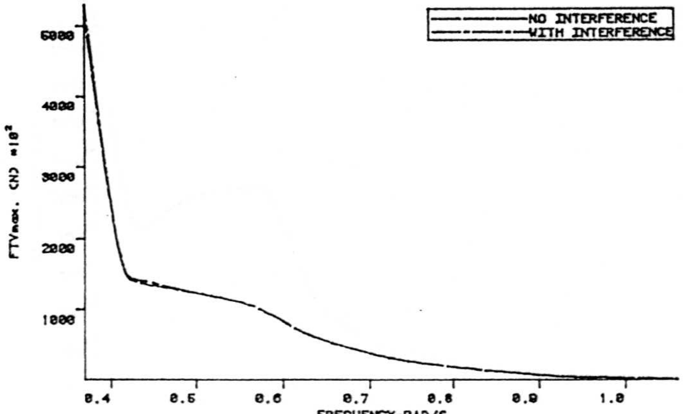

(b) MAX. FORCES ON MEMBERS IN v DIRECTION

PROGRAM: OSS ,COEFFICIENTS: SARPK, SR = 0.005
FIG.(10) MAX. FORCES ON MEMBER (19) Vs. FREQUENCY

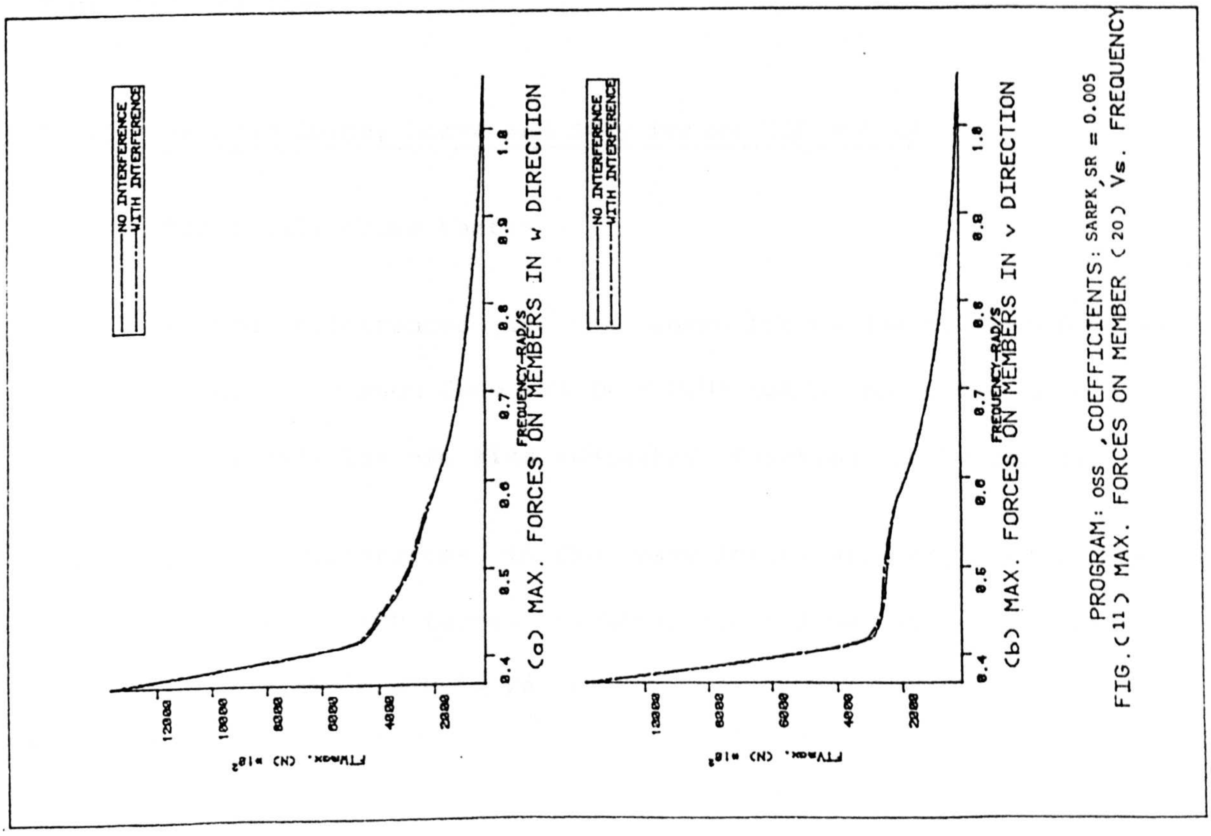

PROGRAM: OSS ,COEFFICIENTS: SARPK ,SR = 0.005
FIG.(11) MAX. FORCES ON MEMBER (20) Vs. FREQUENCY

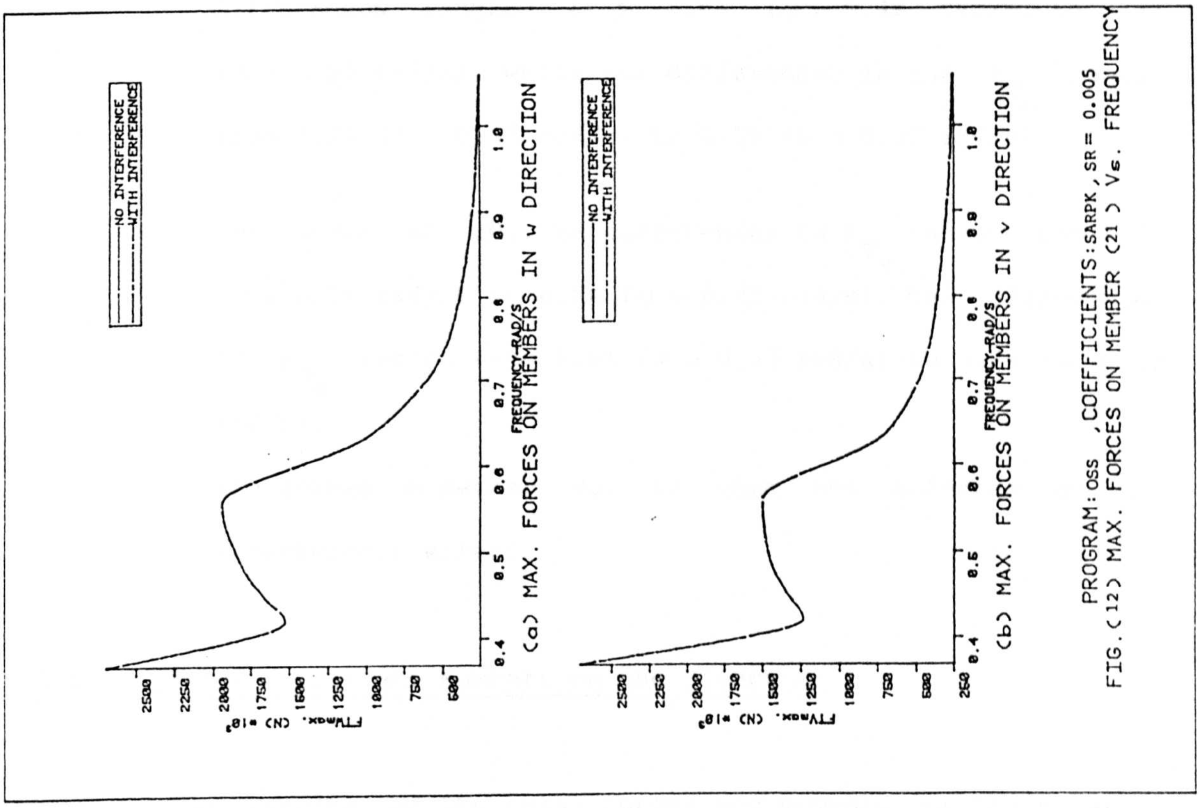

PROGRAM: OSS ,COEFFICIENTS: SARPK ,SR = 0.005
FIG.(12) MAX. FORCES ON MEMBER (21) Vs. FREQUENCY

d. For member No. 19, the differences in the forces were obtained at the first three frequencies only. F_{T_v} gave differences ranging from 2.6% (ω = 0.42 rad/s) to 3.3% (ω = 0.37 rad/s), while the differences in the F_{T_w} ranged from 1.7% (ω = 0.42 rad/s) to 2.2% (ω = 0.37 rad/s).

e. For member No. 20, the differences in F_{T_v} ranged from 1.1% (ω = 0.56 rad/s) to 4.8% (ω = 0.42 rad/s). The differences in F_{T_w} ranged from 1.8% (ω = 0.37 rad/s) to 3.6% (ω = 0.5 rad/s).

f. The forces on member No. 21 were not affected by the interference effect.

5.2 Total Forces and Moments on the Structure

The results of the total forces and moments for the cases of smooth and rough structures are summarised in Tables (15) to (20), Figs. (13) to (24).

5.2.1 Maximum Surge, Heave and Sway Forces (SR = 0.0)

Table (15) shows that:-

a. The differences in the surge forces due to interference effect ranged from -5% (ω = 0.94 rad/s) to 0.6% (ω = 0.75 rad/s). The -ve sign indicates reduction in the forces.

b. The differences in the heave forces are larger than those of the surge forces, ranging from -41.9% (ω = 1.06 rad/s) to 2.9% (ω = 0.75 rad/s).

β = 0.0	Surge Force x 10^{-7} (N)					Heave Force x 10^{-7} (N)					Sway Force x 10^{-6} (N)				
Program	ω(rad/s)					ω(rad/s)					ω(rad/s)				
	0.37	0.42	0.45	0.50	0.56	0.37	0.42	0.45	0.50	0.56	0.37	0.42	0.45	0.50	0.56
Without Interference	2.241	1.434	1.428	1.382	1.280	1.575	0.8883	0.8906	0.8854	0.8707	1.931	0.9025	0.9155	0.9292	0.9495
With Interference	2.18	1.408	1.403	1.358	1.259	1.496	0.8785	0.8797	0.8723	0.8543	1.931	0.9025	0.9155	0.9292	0.9495
Diff %	-2.7	-1.8	-1.8	-1.7	-1.6	-5	-1.1	-1.2	-1.5	-1.9	-	-	-	-	-
Program	ω(Rad/s)					ω(Rad/s)					ω(Rad/s)				
	0.64	0.75	0.94	1.06		0.64	0.75	0.94	1.06		0.64	0.75	0.94	1.06	
Without Interference	0.7651	0.3223	0.1037	0.2309		0.5692	0.3173	0.07978	0.0162		0.5901	0.3634	0.1412	0.0695	
With Interference	0.7574	0.3243	0.0985	0.2276		0.5561	0.3080	0.0751	0.0094		0.5901	0.3634	0.1412	0.0695	
Diff %	-1	0.6	-5	-1.4		-2.3	2.9	-5.8	-41.9		-	-	-	-	

Table (15) Maximum Surge, Heave and Sway Forces for Smooth Cylinders (SR = 0.0)

β = 0.0	Rolling Moment x 10^{-8} (NM)					Yawing Moment x 10^{-7} (NM)					Pitching Moment x 10^{-9} (NM)				
Program	ω(rad/s)					ω(rad/s)					ω(rad/s)				
	0.37	0.42	0.45	0.50	0.56	0.37	0.42	0.45	0.50	0.56	0.37	0.42	0.45	0.50	0.56
Without Interference	2.225	1.150	1.205	1.283	1.363	0.4221	0.2291	0.3168	0.4553	0.6018	2.161	1.454	1.496	1.522	1.481
With Interference	2.225	1.150	1.205	1.283	1.363	0.4221	0.2291	0.3168	0.4553	0.6018	2.077	1.417	1.459	1.486	1.449
Diff %	-	-	-	-	-	-	-	-	-	-	-4	-2.6	-2.5	-2.4	-2.2
Program	ω(rad/s)					ω(rad/s)					ω(rad/s)				
	0.64	0.75	0.94	1.06		0.64	0.75	0.94	1.06		0.64	0.75	0.94	1.06	
Without Interference	0.8839	0.5665	0.2430	0.1374		0.3668	0.4624	0.4824	0.4437		0.9227	0.3899	0.1736	0.3472	
With Interference	0.8839	0.5665	0.2430	0.1374		0.3668	0.4624	0.4824	0.4437		0.9100	0.3923	0.1660	0.3422	
Diff %	-	-	-	-		-	-	-	-		-1.4	0.6	-4.6	-1.5	

Table (16) Maximum Rolling, Yawing and Pitching Moments for Smooth Cylinders (SR = 0.0)

c. The sway forces were not changed due to interference effect. The values of the forces, with and without interference, are the same.

5.2.2 Maximum Rolling, Yawing and Pitching Moments (SR = 0.0)

Table (16) shows that both the rolling and yawing moments were not affected due to interference. The differences in the pitching moments are similar to those of the surge forces, ranging from -4.6% (ω = 0.94 rad/s) to 0.6% (ω = 0.75 rad/s).

5.2.3 Maximum Surge, Heave and Sway Forces (SR = 0.00125)

Table (17) shows that:-

a. The reductions in the surge forces due to the interference ranged from 2.9% (ω = 0.5 rad/s) to 18.7% (ω = 0.94 rad/s).

b. The reductions in the heave forces ranged from 4.1% (ω = 1.06 rad/s) to 14.7% (ω = 0.75 rad/s).

c. The sway forces were not affected.

5.2.4 Maximum Rolling, Yawing and Pitching Moments (SR = 0.00125)

Table (18) shows that both the rolling and yawing moments were not affected. The pitching moments were reduced by from 0.9% (ω = 0.75 rad/s) to 8% (ω = 0.37 rad/s).

5.2.5 Maximum Surge, Heave and Sway Forces (SR = 0.005)

Table (19) shows that:-

β = 0.0	Surge Force x 10^{-7} (N)					Heave Force x 10^{-6} (N)					Sway Force x 10^{-6} (N)				
Program	ω(rad/s)					ω(rad/s)					ω(rad/s)				
	0.37	0.42	0.45	0.50	0.56	0.37	0.42	0.45	0.50	0.56	0.37	0.42	0.45	0.50	0.56
Without Interference	3.206	1.704	1.674	1.609	1.550	25.13	11.20	11.24	11.36	11.39	14.58	8.126	7.924	7.623	7.476
With Interference	3.022	1.652	1.624	1.562	1.476	23.55	10.40	10.18	10.19	10.14	14.58	8.126	7.924	7.623	7.476
Diff %	-5.7	-3.1	-3	-2.9	-4.8	-6.3	-7.1	-9.4	-10.3	-11	-	-	-	-	-
Program	ω(rad/s)					ω(rad/s)					ω(rad/s)				
	0.64	0.75	0.94	1.06		0.64	0.75	0.94	1.06		0.64	0.75	0.94	1.06	
Without Interference	0.9121	0.4193	0.0751	0.1927		6.30	3.044	1.322	0.6847		5.196	3.17	1.084	0.4647	
With Interference	0.8735	0.3986	0.0611	0.1838		5.555	2.596	1.136	0.6564		5.196	3.170	1.084	0.4647	
Diff %	-4.2	-4.9	-18.7	-4.6		-11.8	-14.7	-14.1	-4.1		-	-	-	-	

Table (17) Maximum Surge, Heave and Sway Forces for Rough Cylinders (SR = 0.00125)

β = 0.0	Rolling Moment x 10^{-8} (NM)					Yawing Moment x 10^{-7} (NM)					Pitching Moment x 10^{-9} (NM)				
Program	ω(rad/s)					ω(rad/s)					ω(rad/s)				
	0.37	0.42	0.45	0.50	0.56	0.37	0.42	0.45	0.50	0.56	0.37	0.42	0.45	0.50	0.56
Without Interference	13.96	9.519	9.678	9.815	9.981	6.372	2.534	3.102	4.883	6.907	3.485	1.918	1.957	2.005	2.015
With Interference	13.96	9.519	9.678	8.815	9.981	6.372	2.534	3.102	4.883	6.907	3.227	1.844	1.877	1.897	1.904
Diff %	-	-	-	-	-	-	-	-	-	-	-8	-4	-4.3	-5.7	-5.8
Program	ω(rad/s)					ω(rad/s)					ω(rad/s)				
	0.64	0.75	0.94	1.06		0.64	0.75	0.94	1.06		0.64	0.75	0.94	1.06	
Without Interference	7.278	4.578	1.586	0.7028		3.613	3.199	2.787	1.784		1.227	0.5687	0.1015	0.2840	
With Interference	7.278	4.578	1.586	0.7028		3.613	3.199	2.787	1.784		1.169	0.5638	0.0969	0.2709	
Diff %	-	-	-	-		-	-	-	-		-5	-0.9	-4.7	-4.8	

Table (18) Maximum Rolling, Yawing and Pitching Moments for Rough Cylinders (SR = 0.00125)

a. The reductions in the surge forces ranged from 4.8% (ω = 0.64 rad/s) to a maximum of 21.1% (ω = 0.94 rad/s).

b. The reductions in the heave forces ranged from 5.2% (ω = 1.06 rad/s) to 16.7% (ω = 0.94 rad/s).

c. The sway forces were not affected.

5.2.6 Maximum Rolling, Yawing and Pitching Moments (SR = 0.005)

Table (20) shows that both the rolling and yawing moments were not affected, while the pitching moments were reduced by from 5.6% (ω = 0.64 rad/s) to 8.7% (ω = 0.37 rad/s).

The results of the sway forces, rolling and yawing moments, Tables (15) to (20) may be justified by the following considerations:-

a. The sway forces, rolling and yawing moments are largely dominated by the lift or transverse forces. In the calculations of the forces and moments, the lift coefficient (C_L) was assumed to be unaffected by the interference effect between the members.

b. The horizontal bracing members of the structure were assumed to be unaffected due to the interference.

c. The structure is symmetrical with respect to both X and Z axes, Fig. (1) and the calculations were carried out for a wave angle, β = 0.0 .

β = 0.0	Surge Force x 10^{-7} (N)					Heave Force x 10^{-6} (N)					Sway Force x 10^{-6} (N)				
	ω(rad/s)					ω(rad/s)					ω(rad/s)				
Program	0.37	0.42	0.45	0.50	0.56	0.37	0.42	0.45	0.50	0.56	0.37	0.42	0.45	0.50	0.56
Without Interference	3.491	1.773	1.758	1.726	1.671	29.64	13.31	13.38	13.48	13.49	14.56	8.126	7.925	7.627	7.477
With Interference	3.275	1.677	1.663	1.634	1.585	27.34	12.18	12.09	12.10	12.02	14.56	8.126	7.925	7.627	7.477
Diff %	-6.2	-5.4	-5.4	-5.3	-5.2	-7.8	-8.5	-9.6	-10.2	-10.9	-	-	-	-	-

	ω(rad/s)				ω(rad/s)				ω(rad/s)			
Program	0.64	0.75	0.94	1.06	0.64	0.75	0.94	1.06	0.64	0.75	0.94	1.06
Without Interference	0.9842	0.4488	0.0795	0.1951	7.601	3.728	1.491	0.6536	5.205	3.181	1.079	0.4631
With Interference	0.9373	0.4237	0.0627	0.1846	6.695	3.186	1.242	0.6197	5.205	3.181	1.079	0.4631
Diff %	-4.8	-5.6	-21.1	-5.4	-11.9	-14.5	-16.7	-5.2	-	-	-	-

Table (19) Maximum Surge, Heave and Sway Forces for Rough Cylinders (SR = 0.005)

β = 0.0	Rolling Moment x 10^{-8} (NM)					Yawing Moment x 10^{-7} (NM)					Pitching Moment x 10^{-9} (NM)				
	ω(rad/s)					ω(rad/s)					ω(rad/s)				
Program	0.37	0.42	0.45	0.50	0.56	0.37	0.42	0.45	0.50	0.56	0.37	0.42	0.45	0.50	0.56
Without Interference	13.94	9.519	9.680	9.821	9.989	6.346	2.537	3.07	4.838	6.821	3.792	2.066	2.112	2.159	2.166
With Interference	13.94	9.519	9.680	9.821	9.989	6.346	2.537	3.07	4.838	6.821	3.490	1.927	1.973	2.024	2.036
Diff %	-	-	-	-	-	-	-	-	-	-	-8.7	-7.2	-7.1	-6.7	-6.4

	ω(rad/s)				ω(rad/s)				ω(rad/s)			
Program	0.64	0.75	0.94	1.06	0.64	0.75	0.94	1.06	0.64	0.75	0.94	1.06
Without Interference	7.294	4.593	1.576	0.6981	3.552	3.208	2.778	1.776	1.319	0.6041	0.1088	0.2885
With Interference	7.294	4.593	1.576	0.6981	3.552	3.208	2.778	1.776	1.249	0.5712	0.1022	0.2729
Diff %	-	-	-	-	-	-	-	-	-5.6	-5.8	-6.5	-5.7

Table (20) Maximum Rolling, Yawing and Pitching Moments for Rough Cylinders (SR = 0.005)

5.3 Effect of Wave Height

The maximum forces (surge, heave and sway) and maximum moments (rolling, yawing and pitching) were calculated for a constant frequency of 0.37 rad/s and five wave heights, namely 1.0, 5.0, 10.0, 15.0 and 25.0m. The results are given in Tables (21) and (22).

5.3.1 Maximum Forces and Moments for Smooth Cylinders (SR = 0.0)

In general, the percentage differences, Table (21), are small and can be summarised as follows:-

a. The percentage differences in the surge forces ranged from 0.5% (H = 5.0m) to -2.3% (H = 25.0m).

b. The differences in the heave forces ranged from 0.6% (H = 10.0m) to -1.7% (H = 25.0m).

c. The sway forces, rolling and yawing moments were not affected.

d. The differences in the sway forces ranged from -0.8% (H = 5.0m) to -3.3% (H = 25.0m).

5.3.2 Maximum Forces and Moments for Rough Cylinders (SR = 0.005)

The differences in Table (22) are larger than those of the smooth cylinders, Table (20), and may be summarised as follows:-

a. The percentage differences in the surge forces ranged from -0.5% (H = 1.0m) to -5.9% (H = 25.0m).

b. The differences in the heave forces ranged from -4.8% (H = 5.0m) to -7.4% (H = 25.0m).

β = 0.0	Surge Force x 10^{-6} (N)					Heave Force x 10^{-6} (N)					Sway Force x 10^{-4} (N)				
ω = 0.37r/s	Wave Height (m)					Wave Height (m)					Wave Height (m)				
Coefficients	1.0	5.0	10.0	15.0	25.0	1.0	5.0	10.0	15.0	25.0	1.0	5.0	10.0	15.0	25.0
Without Interference	0.5949	3.139	6.521	10.16	18.11	0.3828	1.99	3.896	6.147	11.47	0.2375	5.525	21.91	51.48	137.8
With Interference	0.5946	3.122	6.453	10.01	17.69	0.3830	1.996	3.919	6.096	11.28	0.2375	5.525	21.91	51.48	137.8
Diff %	-	0.5	-1	-1.5	-2.3	-	-	0.6	-0.8	-1.7	-	-	-	-	-
	Rolling Moment x 10^{-6} (NM)					Yawing Moment x 10^{-5} (NM)					Pitching Moment x 10^{-8} (NM)				
Coefficients	1.0	5.0	10.0	15.0	25.0	1.0	5.0	10.0	15.0	25.0	1.0	5.0	10.0	15.0	25.0
Without Interference	0.3856	7.219	27.31	61.05	159.6	0.1113	2.157	6.125	13.14	31.43	0.5629	2.955	6.186	9.683	17.41
With Interference	0.3856	7.219	27.31	61.05	159.6	0.1113	2.157	6.125	13.14	31.43	0.5630	2.932	6.091	9.474	16.83
Diff %	-	-	-	-	-	-	-	-	-	-	-	-0.8	-1.5	-2.2	-3.3

Table (21) Maximum Forces and Moments at Different Wave Heights (SR = 0.0)

β = 0.0	Surge Force x 10^{-6} (N)					Heave Force x 10^{-6} (N)					Sway Force x 10^{-4} (N)				
ω = 0.37r/s	Wave Height (m)					Wave Height (m)					Wave Height (m)				
Coefficients	1.0	5.0	10.0	15.0	25.0	1.0	5.0	10.0	15.0	25.0	1.0	5.0	10.0	15.0	25.0
Without Interference	0.3683	2.400	6.492	11.66	25.80	0.2412	1.226	3.888	7.842	20.64	0.2657	59.24	272.7	560.2	1166
With Interference	0.3664	2.357	6.330	11.31	24.29	0.2419	1.167	3.666	7.370	19.12	0.2657	59.24	272.7	560.2	1166
Diff %	-0.5	-1.8	-2.5	-3	-5.9	-	-4.8	-5.7	-6.0	-7.4	-	-	-	-	-
	Rolling Moment x 10^{-6} (NM)					Yawing Moment x 10^{-5} (NM)					Pitching Moment x 10^{-8} (NM)				
Coefficients	1.0	5.0	10.0	15.0	25.0	1.0	5.0	10.0	15.0	25.0	1.0	5.0	10.0	15.0	25.0
Without Interference	0.2925	79.74	337.2	630.6	1164	0.1932	18.09	83.56	229.9	285.8	0.3401	2.469	7.004	12.43	28.14
With Interference	0.2925	79.74	337.2	630.6	1164	0.1932	18.09	83.56	229.9	285.8	0.3374	2.409	6.781	11.95	26.02
Diff %	-	-	-	-	-	-	-	-	-	-	-0.8	-2.4	-3.2	-3.9	-7.5

Table (22) Maximum Forces and Moments at Different Wave Heights (SR = 0.005)

c. Similarly to the case of smooth cylinders, the sway forces, rolling moments and yawing moments were not changed due to the interference effect.

d. The differences in the pitching moments ranged from -0.8% (H = 1.0m) to -7.5% (H = 25.0m).

6. DISCUSSION

The above results show that the interference effect is significant and should be considered in wave loading calculations. The procedure described represents one way to deal with the problem by using interference coefficients in the calculation. However, the accuracy of the results will depend on the quality and reliability of the experimental data used to derive the interference coefficients. The available experimental data are not sufficient and do not give clear guides to the designers to make proper judgement on the possible effects on the wave loading. This is due to the following shortcomings:-

a. The tests in wave tanks (eg Chakrabarti) although covering a wide range of arrangements and Keulegan-Carpenter number (K) are limited in the range of R_e. The tests in steady flow are not confidently applicable to wavy flows.

b. The tests carried out with special configuration (eg Sarpkaya) may be useful when applied to similar geometries but may not be applicable to other configurations.

c. All the tests with cylinder arrays of two or more tubes assumed the same diameter for all cylinders. The interference between cylinders with different diameters was not investigated.

d. The interference between two (or more) cylinders inclined to each other, which is the case of jacket members, was not investigated at all.

e. The effect of roughness (except Ref. (20)) was neglected. All the tests were carried out for smooth cylinders only.

Thus, it is clear that a lot of work has yet to be done to improve knowledge in this area. More reliable tests seem to be the only solution. The best one can hope to achieve is to calculate the interference effect on the forces for each member and, hence, for the whole jacket. This is the ideal solution but it could be very difficult. At the other extreme end there is the very approximate way suggested by Pearcey et al (23) by allowing 10-20% increase in the total drag force. The practical solution may be something in between these two extremes.

This may be achieved by testing (preferably in a wave tank) different groups of members, each with a particular configuration, which represent the actual geometries used in practice (K, X, diagonal, horizontal bracing, etc). From the tests results an overall 'correction factor' for each geometry can be estimated which can be applied in design.

7. CONCLUSIONS

a. For the bracing members (d = 1.5, 2.0m) where the drag forces are significant, the reduction in the total forces (F_{T_w}) due to a design wave (H = 30.0m, T = 17 sec) could be 15 -52% for smooth cylinders. For rough cylinders the reduction in the forces could be 56-65%.

b. Within the range of a design wave (H = 30.0m, T = 17 sec) the reductions in the total force and moments on the structure are 3-5% for smooth cylinders. For rough cylinders the differences are 6 - 9%. This conclusion is based on calculations which ignore interference on the horizontal members and this probably underestimates the correction.

c. The above conclusions correspond to the drag interference data obtained from Ref. (13). Using other experimental data may change the percentage differences positively or negatively.

d. More experimental tests are needed in order to account for the interference effect properly in the design of jackets.

REFERENCES

1. ARITA, Y, FUJITA, H, and TAGAYA, K, 'A Study on the Forces of Current Acting on a Multitubular Column Structure', OTC Paper No 1815, Houston, Texas, 1973.

2. BIERMAN, D, and HERRNSTEIN, W H, 'The Interference Between Struts in Various Combinations', NACA Tech Report 468, 1933.

3. BUSHNELL, M J, 'Forces on Cylinder Arrays in Oscillatory Flow', OTC Paper No 2903, Houston, Texas, 1977.

4. CHAKRABARTI, S K, 'Wave Forces on Multiple Vertical Cylinders', Jour of the Waterway, Port, Coastal and Ocean Div, ASCE, Vol 104, No WW2, May 78.

5. CHAKRABARTI, S K, 'Wave Interaction with Multiple Horizontal Cylinders', Applied Ocean Research, Vol 1, No 4, 1979, pp213-216.

6. CHAKRABARTI, S K, 'Wave Forces on Vertical Array of Tubes', Proc of Civil Engineering in the Ocean, ASCE, 1979, pp241-259.

7. CHAKRABARTI, S K, 'Hydrodynamic Coefficients for a Vertical Tube in an Array', Applied Ocean Research, Vol 3, No 1, 1981, pp2-12.

8. CHAKRABARTI, S K, 'Inline and Transverse Forces on a Tube Array in Tandem with Waves', Applied Ocean Research, Vol 4, No 1, 1982, pp25-32.

9. CHAKRABARTI, S K, 'Transverse Forces on Vertical Tube Array in Waves', Jour of the Waterway, Port, Coastal and Ocean Div, ASCE, Vol 108, No WW1, Feb 82.

10. DALTON, C, and SZABO, J M, 'Drag on a Group of Cylinders', Jour of Pressure Vessel Technology, ASME, Paper No 76-Pet-42, 1977, pp152-156.

11. DEAN, R G, 'Stream Function Representation of Nonlinear Ocean Waves', Jour of Geophysical Research, Vol 70, No 18, 1965, pp4561-4572.

12. GIBSON, R J, and WANG, H, 'Added Mass of Pile Group', Jour of the Waterway, Port, Coastal and Ocean Div, ASCE, Vol 103, No WW2, May 77.

13. GREKOUSSIS, C, and MILLER, N S, 'Interference Drag Effects between Cylinders with Particular Reference to Semi-Submersible Design', Dept of Naval Architecture and Ocean Engineering, University of Glasgow, Report No NAOE-HL-09-76, 1976.

14. HOGBEN, N, and STANDING, R G, 'Wave Loads on Large Bodies', Proc, Intl Symp on the Dynamics of Marine Vehicles and Structures in Waves, University College, London, Apr 74.

15. HOERNER, S F, 'Fluid-Dynamic Drag', 3rd Ed, New Jersey, 1965.

16. INCECIK, A, 'Wave Loading on Circular Cylindrical Members of Offshore Structures in Different Regimes', Dept of Naval Architecture and Ocean Engineering, Report No NAOE-HL-80-16, University of Glasgow, 1981.

17. ISAACSON, M, 'Interference Effects Between Large Cylinders in Waves', OTC Paper No 3067, Houston, Texas, 1978.

18. LAIRD, A D K, and WARREN, R P, 'Groups of Vertical Cylinders Oscillating in Water', Jour of the Engineering Mechanics Div, ASCE, Vol 89, No EM1, Feb 63, pp25-35.

19. LEONARD, J W, HUANG, M C, and HUDSPETH, R T, 'Hydrodynamic Interference between Floating Cylinders in Oblique Seas', Applied Ocean Research, Vol 5, No 3, 1983.

20. LOKEN, A E, TORSET, O P, MATHIASSEN, S, and ARNESON, T, 'Aspects of Hydrodynamic Loading in Design of Production Risers', OTC Paper No 3538, 1979, pp1591-1601.

21. OHKUSU, M, 'Hydrodynamic Forces on Multiple Cylinders in Waves', Proc Intl Symp on the Dynamics of Marine Vehicles and Structures, University College, London, 1974.

22. OORTMERSSEN, G V, 'Hydrodynamic Interaction between Two Structures, Floating in Waves', BOSS '79, London, 1979.

23. PEARCEY, H H, CASH, R F, SALTER, I J, and BORIBOND, A, 'Interference Effects on the Drag Loading for Groups of Cylinders in Uni-Directional Flow', NMI, Report NMI-R 130, Sep, 82.

24. RAINES, C P, and CHAKRABARTI, S K, 'Mechanical Excitation of Offshore Tower Model', Jour Waterways, Harbors and Coastal Engineering Div, ASCE, 98, WW1, 1972.

25. ROSS, C W, 'Large-Scale Tests of Wave Forces on Piling (Preliminary Report)', US Corps of Engineers Beach Erosion Board, Tech Memo 111, 1959.

26. SARPKAYA, T, 'Hydrodynamic Forces on Various Multiple-Tube Riser Configurations', OTC Paper No 3539, Houston, Texas, 1979, p1603.

27. SARPKAYA, T, CINAR, M, and OZKAYNAK, S, 'Hydrodynamic Interference of Two Cylinders in Harmonic Flow', OTC Paper 3775, Houston, Texas, 1980.

28. SARPKAYA, T, and ISAACSON, M, 'Mechanics of Wave Forces on Offshore Structures', Van Nostrand Reinhold, New York, 1981.

29. YAMAMOTO, T, and NATH, J H, 'Hydrodynamic Forces on Groups of Cylinders', OTC Paper No 2499, Houston, Texas, 1976.

30. ZDRAKOVICH, M M, 'Review of Flow Interference Between Two Circular Cylinders in Various Arrangements', Jour of Fluids Engineering, ASME, Dec 77.

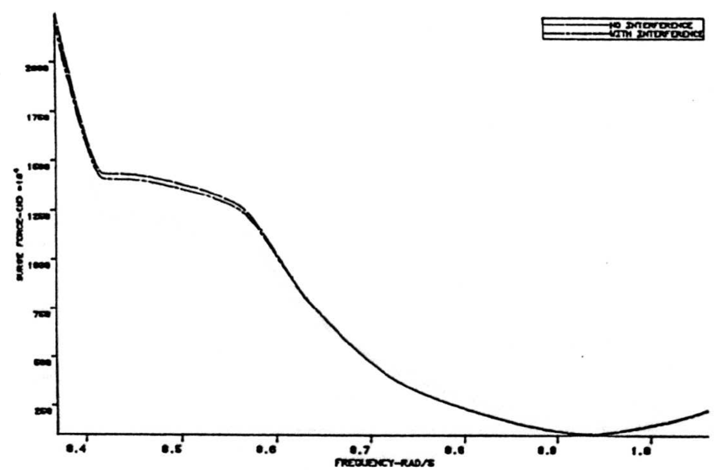

COEFFICIENTS: SARPKAYA , β = 0.0, SR= 0.0
FIG.(13) MAX. SURGE FORCES Vs. FREQUENCY

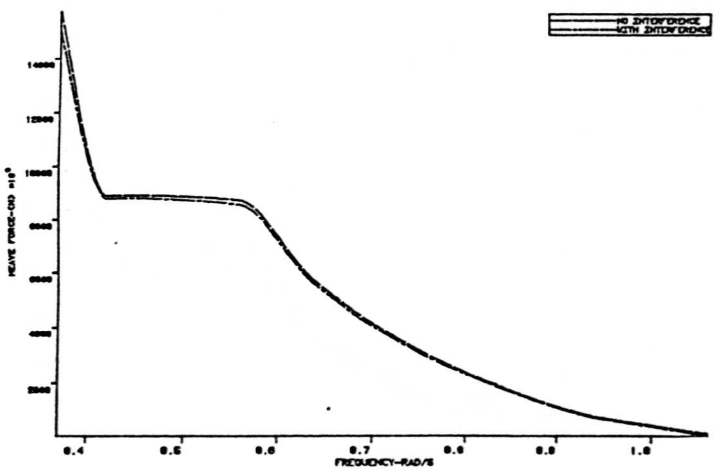

COEFFICIENTS: SARPKAYA , β = 0.0, SR= 0.0
FIG.(14) MAX. HEAVE FORCES Vs. FREQUENCY

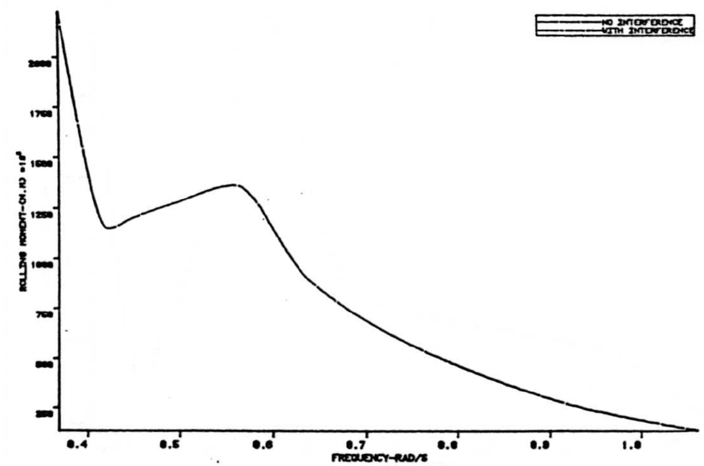

COEFFICIENTS: SARPKAYA , β = 0.0, SR= 0.0
FIG.(15) MAX. ROLLING MOMENTS Vs. FREQUENCY

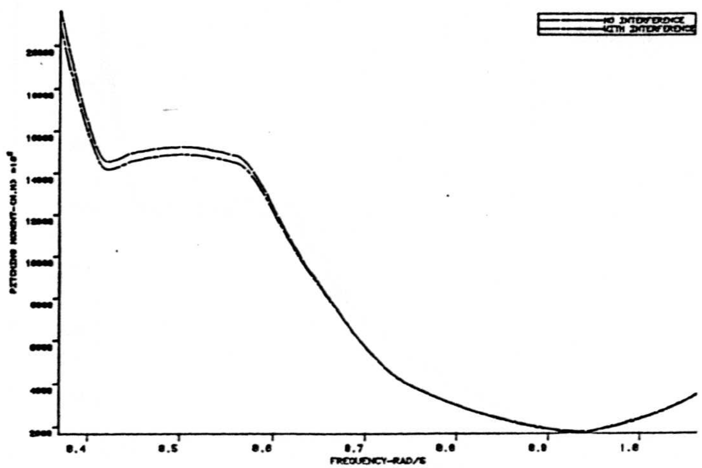

COEFFICIENTS: SARPKAYA , β = 0.0, SR= 0.0
FIG.(16) MAX. PITCHING MOMENTS VS. FREQUENCY

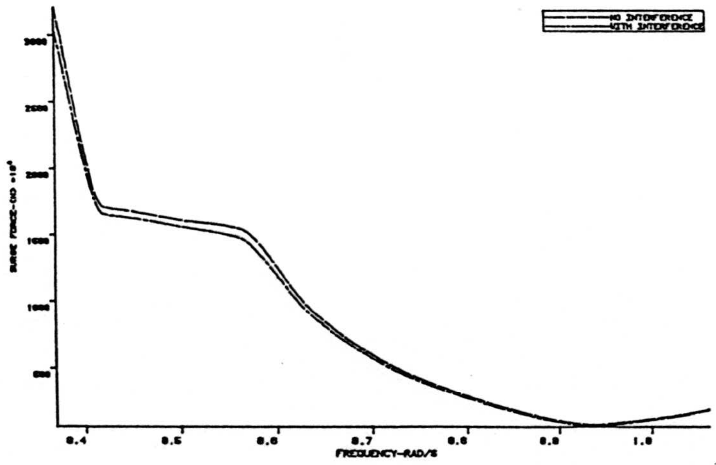

COEFFICIENTS: SARPKAYA , β =0.0 ,SR= 0.00125
FIG.(17) MAX. SURGE FORCES Vs. FREQUENCY

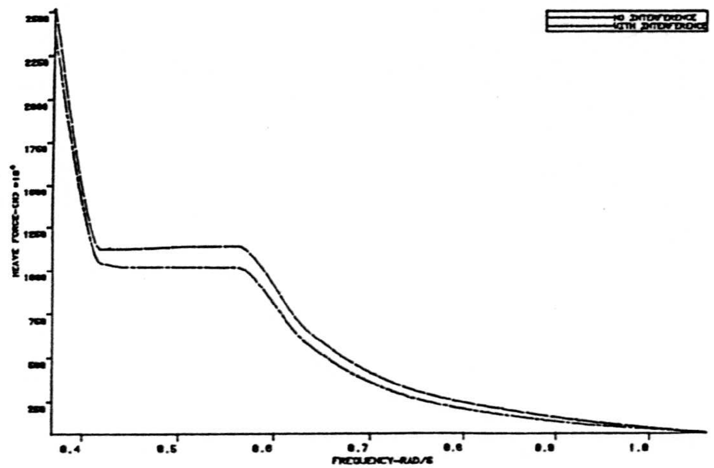

COEFFICIENTS: SARPKAYA , β = 0.0, SR= 0.00125
FIG.(18) MAX. HEAVE FORCES Vs. FREQUENCY

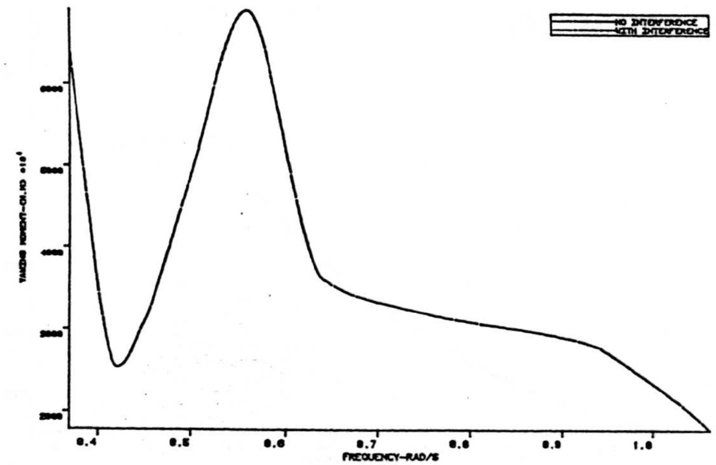

COEFFICIENTS: SARPKAYA , β = 0.0, SR= 0.00125
FIG.(19) MAX. YAWING MOMENTS Vs. FREQUENCY

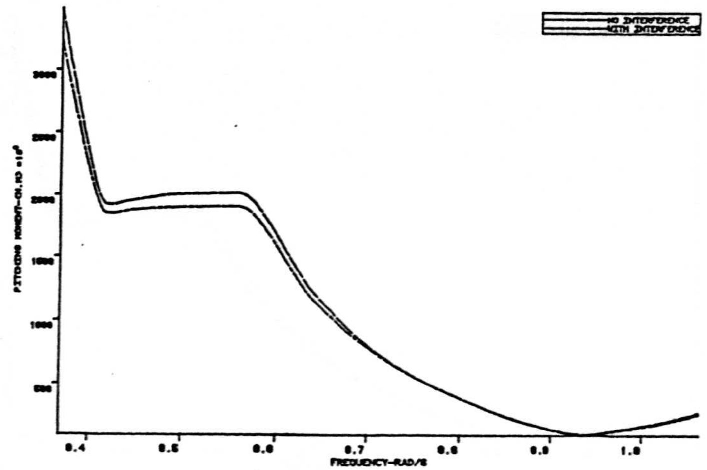

COEFFICIENTS: SARPKAYA , β = 0.0, SR= 0.00125
FIG.(20) MAX. PITCHING MOMENTS VS. FREQUENCY

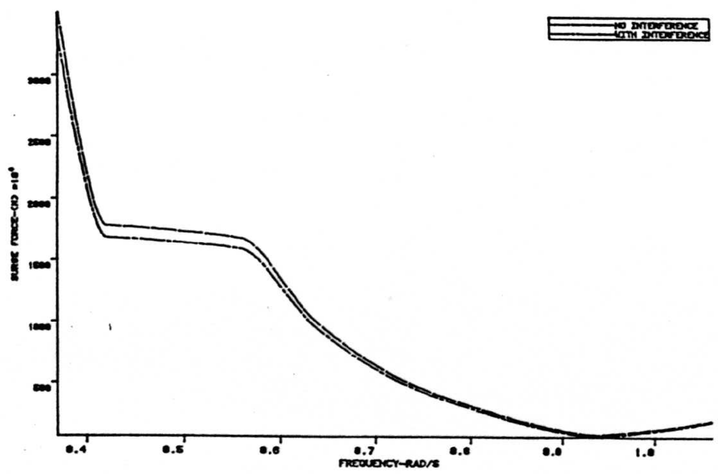

COEFFICIENTS: SARPKAYA , β = 0.0, SR= 0.005
FIG.(21) MAX. SURGE FORCES Vs. FREQUENCY

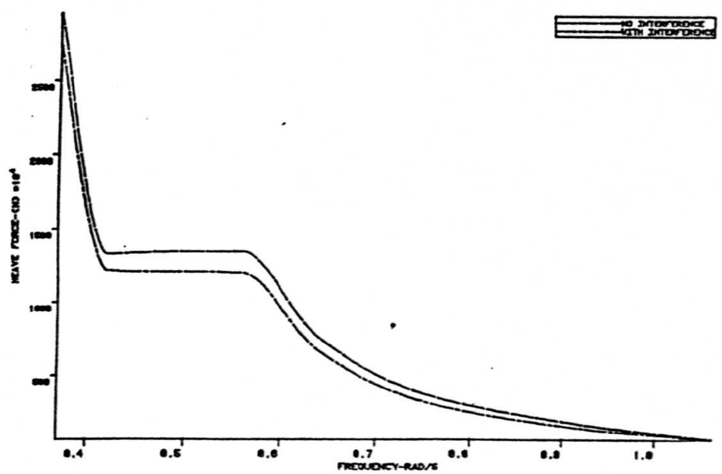

COEFFICIENTS: SARPKAYA , β = 0.0, SR= 0.005
FIG.(22) MAX. HEAVE FORCES Vs. FREQUENCY

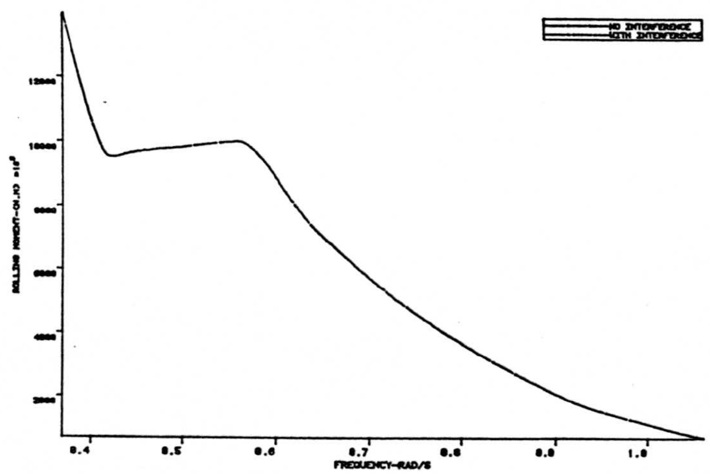

COEFFICIENTS: SARPKAYA , β = 0.0, SR= 0.005
FIG.(23) MAX. ROLLING MOMENTS Vs. FREQUENCY

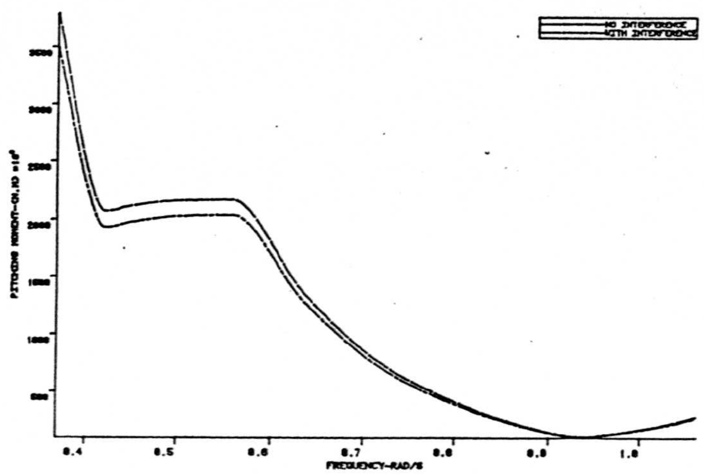

COEFFICIENTS: SARPKAYA , β = 0.0, SR= 0.005
FIG.(24) MAX. PITCHING MOMENTS VS. FREQUENCY

CHAPTER 8

CHAPTER 8

EFFECT OF CURRENT ON WAVE LOADING

1. INTRODUCTION

When estimating the fluid loading on jacket structures, sited in areas of strong currents, it is necessary to compute the total water particle velocities of the combined wave-current flow field. The drag and lift forces are proportional to the square of this total fluid velocity.

A common practice which has been used by the offshore industry to include current effect in wave loading calculations is to add current velocity vectorially to the wave particle velocities when calculating the drag (or lift) forces. This method is applied in this chapter to assess the effect of current velocity and direction on the fluid loading of a jacket platform using the drag and inertia coefficients recommended by Lloyds Register of Shipping (LR), Reference (4).

A comparison was also made between the results based on LR coefficients and those by Det norske Veritas (DnV), References (1-3), with and without current effect.

2. CALCULATION PROCEDURE

The calculations were carried out by Program OSS, for the same jacket structure used in the previous chapters. Nine wave frequencies ranging from ω = 0.37 rad/s (H = 30.0m, L = 450.01m) to ω = 1.06 rad/s (H = 6.0m, L = 54.83m) were used.

Since the main objective was to assess only the effect of current on wave loading estimation, constant drag and inertia coefficients (C_D, C_M) as recommended by Lloyds Register of Shipping (LR) and Det norske Veritas (DnV) for smooth cylinders were used in the calculations.

The waves were assumed to pass through the jacket in the direction of X-axis, ie $\beta = 0.0$. Two directions for the current were assumed (in the horizontal plane) one coinciding with the wave direction ($\theta = 0.0$), the other at $\theta = 45^{o}$ relative to the wave propagation.

The current was assumed to be mainly tidal. Wind generated current was neglected. The variation of current velocity with water depth was calculated by the following relation:-

$$V_h = V_s (h/D)^{1/7}$$

where, V_h is the current velocity at a distance h above sea bottom (m/s)

V_s is the current velocity at the still water level (m/s)

h is the distance above bottom (m)

D is the water depth (150.0m).

At each current direction ($\theta = 0^{o}, 45^{o}$) two current velocities (V_s) were assumed, namely 0.5m/s and 1.0m/s. The current velocity was added vectorially to the velocities of the wave particles.

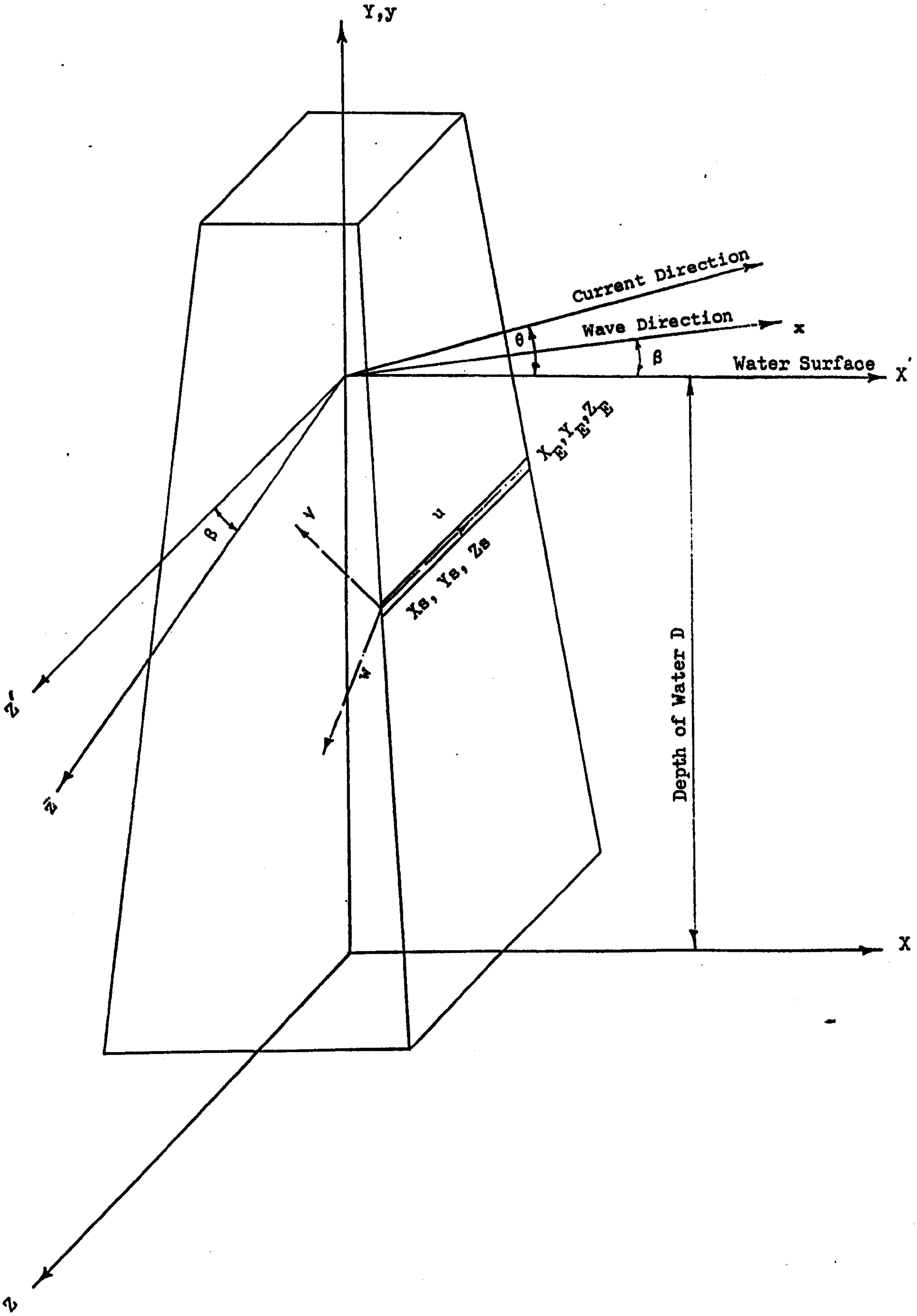

Fig. (1) Positions of the current and wave relative to the structure

3. ANALYSIS OF THE RESULTS

The results of calculations are summarised in Tables (1) to (12) and are presented graphically in Figs. (2) to (13).

3.1 Effect of Current Speed (LR, $\theta = 0^{o}$)

Tables (1) and (2) compare the results when the effect of current is considered (V_s = 0.5, 1.0m/s) with the case when the current speed is zero (V_s = 0.0). The differences are given as percentage increases in the forces and moments relative to the case when V_s = 0.0 as follows:-

a. The percentage differences in the surge forces ranged from 6.7% (ω = 0.37 rad/s) to 39.2% (ω = 0.94 rad/s) when V_s = 0.5 m/s and from 15.9% (ω = 0.37 rad/s) to 116% (ω = 0.94 rad/s).

b. The differences in the heave forces are small because the current velocity has no vertical component. When V_s = 0.5 m/s, the percentage differences ranged from 0.5% (ω = 0.64 rad/s) to 1.4% (ω = 0.42 rad/s) and when V_s = 1.0 m/s, the differences ranged from 0.9% (ω = 0.75 rad/s) to 4.3% (ω = 1.06 rad/s).

c. The differences in the sway forces ranged from 9.8% (ω = 0.75 rad/s) to 31.4% (ω = 1.06 rad/s) when V_s = 0.5 m/s and from 21.5% (ω = 0.75 rad/s) to 64.1% (ω = 1.06 rad/s) when V_s = 1.0 m/s.

d. The differences in the rolling moments ranged from 7.9% (ω = 0.75 rad/s) to 18.6% (ω = 1.06 rad/s) when

$\beta = 0.0$	Surge Force $\times 10^{-7}$ (N)					Heave Force $\times 10^{-7}$ (N)					Sway Force $\times 10^{-6}$ (N)				
$\theta = 0.0$	ω (rad/s)					ω (rad/s)					ω (rad/s)				
Coefficients	0.37	0.42	0.45	0.50	0.56	0.37	0.42	0.45	0.50	0.56	0.37	0.42	0.45	0.50	0.56
LR $V_s = 0.0$	2.087	1.382	1.377	1.332	1.229	1.274	0.7665	0.7649	0.7533	0.7303	0.1392	0.09205	0.1058	0.1320	0.1673
LR $V_s = 0.5$ m/s	2.226	1.482	1.478	1.437	1.339	1.291	0.7769	0.7744	0.7609	0.7358	0.1610	0.1084	0.1229	0.1507	0.1881
Diff. %	6.7	7.2	7.3	7.9	9	1.3	1.4	1.2	1.0	0.8	15.7	17.8	16.2	14.2	12.4
LR $V_s = 1.0$ m/s	2.419	1.628	1.620	1.577	1.482	1.311	0.7897	0.7862	0.7708	0.7435	0.1911	0.1282	0.1436	0.1730	0.2124
Diff %	15.9	17.8	17.6	18.4	20.6	2.9	3	2.8	2.3	1.8	37.3	39.3	35.7	31.1	27
Coefficients	ω (rad/s)					ω (rad/s)					ω (rad/s)				
	0.64	0.75	0.94	1.06		0.64	0.75	0.94	1.06		0.64	0.75	0.94	1.06	
LR $V_s = 0.0$	0.7423	0.3105	0.1225	0.2558		0.4669	0.2594	0.05904	0.01125		0.1404	0.1277	0.07461	0.03751	
LR $V_s = 0.5$ m/s	0.8327	0.3830	0.1705	0.2943		0.4693	0.2603	0.05942	0.01140		0.1570	0.1402	0.08733	0.04928	
Diff %	12.2	23.4	39.2	15.1		0.5	-	0.6	1.3		11.8	9.8	17.1	31.4	
LR $V_s = 1.0$ m/s	0.9594	0.4966	0.2650	0.3836		0.4733	0.2618	0.05996	0.01173		0.1784	0.1551	0.1011	0.06154	
Diff %	29.2	59.9	116	50		1.4	0.9	1.6	4.3		27.1	21.5	35.5	64.1	

Table (1) Maximum Surge, Heave and Sway Forces at Different Current Speeds.

$\beta = 0.0$	Rolling Moment $\times 10^{-8}$ (NM)					Yawing Moment $\times 10^{-7}$ (NM)					Pitching Moment $\times 10^{-9}$ (NM)				
$\theta = 0.0$	ω (rad/s)					ω (rad/s)					ω (rad/s)				
Coefficients	0.37	0.42	0.45	0.50	0.56	0.37	0.42	0.45	0.50	0.56	0.37	0.42	0.45	0.50	0.56
LR $V_s = 0.0$	0.2091	0.1457	0.1717	0.2197	0.2824	0.09685	0.07592	0.09567	0.1407	0.2172	1.981	1.386	1.428	1.454	1.411
LR $V_s = 0.5$m/s	0.2425	0.1683	0.1962	0.2471	0.3130	0.1046	0.08244	0.1032	0.1506	0.2311	2.121	1.489	1.535	1.569	1.538
Diff%	16.0	15.5	14.3	12.5	10.8	8.0	8.6	7.9	7.0	6.4	7.1	7.4	7.5	7.9	9.0
LR $V_s = 1.0$m/s	0.2805	0.1936	0.2233	0.2773	0.3466	0.1123	0.08895	0.1108	0.1605	0.2449	2.423	1.629	1.673	1.709	1.685
Diff %	34.1	32.9	30.1	26.2	22.7	16	17.2	15.8	14.1	12.8	22.3	17.5	17.2	17.5	19.4
Coefficients	ω (rad/s)					ω (rad/s)					ω (rad/s)				
	0.64	0.75	0.94	1.06		0.64	0.75	0.94	1.06		0.64	0.75	0.94	1.06	
LR $V_s = 0.0$	0.2418	0.2217	0.1412	0.08591		0.2318	0.2577	0.2939	0.2976		0.8910	0.3758	0.1950	0.3777	
LR $V_s = 0.5$ m/s	0.2634	0.2393	0.1587	0.1019		0.2475	0.2741	0.2939	0.2976		0.9974	0.4612	0.2472	0.4164	
Diff %	8.9	7.9	12.4	18.6		6.8	6.4	-	-		11.9	22.7	26.8	10.3	
LR $V_s = 1.0$ m/s	0.2921	0.2576	0.1751	0.1161		0.2632	0.2916	0.2939	0.2976		1.127	0.5746	0.3335	0.4952	
Diff %	20.8	16.2	24	35.1		13.5	13.2	-	-		26.5	52.9	71	31.1	

Table (2) Maximum Rolling, Yawing and Pitching Moments at Different Current Speeds.

V_s = 0.5 m/s and from 16.2% (ω = 0.75 rad/s) to 35.1% (ω = 1.06 rad/s) when V_s = 1.0 m/s.

e. The differences in the yawing moments ranged from 6.4% (ω = 0.75 rad/s) to 8.6% (ω = 0.42 rad/s) when V_s = 0.5 m/s and from 12.8% (ω = 0.56 rad/s) to 17.2% (ω = 0.42 rad/s) when V_s = 1.0 m/s.

f. The differences in the pitching moments ranged from 7.1% (ω = 0.37 rad/s) to 26.8% (ω = 0.94 rad/s) when V_s = 0.5 m/s and from 17.2% (ω = 0.45 rad/s) to 71% (ω = 0.94 rad/s) when V_s = 1.0 m/s.

3.2 Effect of Current Direction (LR, V_s = 1.0 m/s)

Tables (3) and (4) compare the results with current speed of 1.0 m/s in two directions (θ = 0°, 45°) against the results without current (V_s = 0.0). The differences in the forces and moments are as follows:-

a. The differences in the surge forces ranged from 15.9% (ω = 0.37 rad/s) to 116% (ω = 0.94 rad/s) in the case of θ = 0° and from 11.2% (ω = 0.37 rad/s) to 82.5% (ω = 0.94 rad/s) at θ = 45°.

b. The differences in the heave forces are small because there is no vertical component for the current velocity. At θ = 0° the differences ranged from 0.9% (ω = 0.75 rad/s) to 4.3% (ω = 1.06 rad/s) and at θ = 45° the differences ranged from 0.9% (ω = 0.64 rad/s) to -5.2% (ω = 1.06 rad/s).

c. At θ = 0° the differences in the sway forces ranged from 21.5% (ω = 0.75 rad/s) to 64.1% (ω = 1.06 rad/s). At

β = 0.0	Surge Force x 10^{-7} (N)					Heave Force x 10^{-7} (N)					Sway Force x 10^{-6} (N)				
V_s = 1.0 m/s	ω (rad/s)					ω (rad/s)					ω (rad/s)				
Coefficients	0.37	0.42	0.45	0.50	0.56	0.37	0.42	0.45	0.50	0.56	0.37	0.42	0.45	0.50	0.56
LR	2.087	1.382	1.377	1.332	1.229	1.274	0.7665	0.7649	0.7533	0.7303	0.1392	0.09205	0.1058	0.1320	0.1673
LR θ = 0.0 Diff %	2.419 15.9	1.628 17.8	1.620 17.6	1.577 18.4	1.482 20.6	1.311 2.9	0.7897 3	0.7862 2.8	0.7708 2.3	0.7435 1.8	0.1911 37.3	0.1282 39.3	0.1436 35.7	0.1730 31.1	0.2124 27
LR θ = π/4 Diff %	2.320 11.2	1.558 12.7	1.552 12.7	1.509 13.3	1.411 14.8	1.304 2.4	0.7850 2.4	0.7813 2.1	0.7659 1.7	0.7393 1.2	2.669	1.942 Very Large Differences	1.905	1.833	1.736
Coefficients	ω (rad/s)					ω (rad/s)					ω (rad/s)				
	0.64	0.75	0.94	1.06		0.64	0.75	0.94	1.06		0.64	0.75	0.94	1.06	
LR V_s = 0.0	0.7423	0.3105	0.1225	0.2558		0.4669	0.2594	0.05904	0.01125		0.1404	0.1277	0.07461	0.03751	
LR θ = 0.0 Diff %	0.9594 29.2	0.4966 59.9	0.2650 116	0.3836 50		0.4733 1.4	0.2618 0.9	0.05996 1.6	0.01173 4.3		0.1784 27.1	0.1551 21.5	0.1011 35.5	0.06154 64.1	
LR θ = π/4 Diff %	0.8976 20.9	0.4432 42.7	0.2236 82.5	0.3460 35.3		0.4711 0.9	0.2605 -	0.05930 -	0.01066 -5.2		1.350	1.104 Very Large Differences	0.9481	0.8841	

Table (3) Maximum Surge, Heave and Sway Forces at Different Current Directions

β = 0.0	Rolling Moment x 10^{-8} (NM)					Yawing Moment x 10^{-7} (NM)					Pitching Moment x 10^{-9} (NM)				
V_s = 1.0 m/s	ω (rad/s)					ω (rad/s)					ω (rad/s)				
Coefficients	0.37	0.42	0.45	0.50	0.56	0.37	0.42	0.45	0.50	0.56	0.37	0.42	0.45	0.50	0.56
LR V_s = 0.0	0.2091	0.1457	0.1717	0.2197	0.2824	0.09685	0.07592	0.09567	0.1407	0.2172	1.981	1.386	1.428	1.454	1.411
LR θ = 0.0 Diff %	0.2825 34.1	0.1936 32.9	0.2233 30.1	0.2773 26.2	0.3466 22.7	0.1123 16	0.08895 17.2	0.1108 15.8	0.1605 14.1	0.2449 12.8	2.423 22.3	1.629 17.5	1.673 17.2	1.709 17.5	1.685 19.4
LR θ = π/4 Diff %	2.671	1.960 Very Large Differences	1.963	1.948	1.897	1.314	0.9893 Very Large Differences	1.036	1.072	1.051	2.259 14	1.560 12.6	1.604 12.3	1.639 12.7	1.608 14
Coefficients	ω (rad/s)					ω (rad/s)					ω (rad/s)				
	0.64	0.75	0.94	1.06		0.64	0.75	0.94	1.06		0.64	0.75	0.94	1.06	
LR V_s = 0.0	0.2418	0.2217	0.1412	0.08591		0.2318	0.2577	0.2939	0.2976		0.8910	0.3758	0.1950	0.3777	
LR θ = 0.0 Diff %	0.2921 20.8	0.2576 16.2	0.1751 24	0.1161 35.1		0.2632 13.5	0.2916 13.2	0.2939 -	0.2976 -		1.127 26.5	0.5746 52.9	0.3335 71	0.4952 31.1	
LR θ = π/4 Diff %	1.438	1.147 Very Large Differences	0.9314	0.8225		0.8188 253	0.6620 157	0.4503 53.2	0.3761 26.4		1.060 19	0.5177 37.8	0.2937 50.6	0.4607 22	

Table (4) Maximum Rolling, Yawing and Pitching Moments at Different Current Directions

$\theta = 45^{\circ}$ the differences are very large due to the component of current velocity normal to the direction of wave propagation, ie in Z-direction.

d. At $\theta = 0^{\circ}$ the differences in the rolling moments ranged from 16.2% (ω = 0.75 rad/s) to 35.1% (ω = 1.06 rad/s). Similarly to the sway forces, the differences in the rolling moments at $\theta = 45^{\circ}$ are very large.

e. The differences in the yawing moments ranged from 12.8% (ω = 0.56 rad/s) to 17.2% (ω = 0.42 rad/s) at $\theta = 0^{\circ}$. At $\theta = 45^{\circ}$ the differences ranged from 26.4% to 253% in the range of frequencies between ω = 1.06 rad/s to ω = 0.64 rad/s. At the smaller frequencies less than 0.64 rad/s, the differences are very large.

f. At $\theta = 0^{\circ}$ the differences in the pitching moments ranged from 17.2% (ω = 0.45 rad/s) to 71% (ω = 0.94 rad/s) and at $\theta = 45^{\circ}$ the differences ranged from 12.6% (ω = 0.42 rad/s) to 50.6% (ω = 0.94 rad/s).

3.3 Comparison Between LR and DnV

Tables (5) to (12) compare the results of LR with those of DnV at the two current velocities (V_s = 0.5, 1.0 m/s) and two directions ($\theta = 0^{\circ}, 45^{\circ}$). The percentage differences are given relative to LR values. The third row in each table (V_s = 0.0) gives the percentage differences between LR and DnV results when the current is not included. These results were discussed in detail in Chapter 4 and are presented here for comparison.

3.3.1 Maximum Forces and Moments ($\theta = 0$, $V_s = 0.5$ m/s)

Tables (5) and (6) show that:-

a. The percentage differences in the surge forces ranged from 6.8% (ω = 1.06 rad/s) to 19.7% (ω = 0.75 rad/s) with current included and from -3.3% (ω = 0.94 rad/s) to 14.9% (ω = 0.75 rad/s) without current

b. The differences in the heave forces are identical for the two cases (with and without current), ranging from 36.1% (ω = 0.42 rad/s) to 50.9% (ω = 0,94 rad/s).

c. The differences in the sway forces are almost the same for the two cases, ranging from 34.8% (ω = 0.75 rad/s) to 39.9% (ω = 0.37 rad/s), with current and from 33.4% (ω = 1.06 rad/s) to 37.6% (ω = 0.37 rad/s) without current.

d. The differences in the rolling moments are similar for the two cases, ranging from 34.5% (ω = 0.94 rad/s) to 40% (ω = 0.37 rad/s) with current and from 33.6% (ω = 1.06 rad/s) to 38.7% (ω = 0.37 rad/s) without current.

e. The differences in the yawing moments are the same for the two cases ranging from 33.3% (ω = 0.94 rad/s) to 37.3% (ω = 0.37 rad/s).

f. The differences in the pitching moments ranged from 6.7% (ω = 1.06 rad/s) to 19.2% (ω = 0.37 rad/s) with current and from 2.5% (ω = 0.94 rad/s) to 13.8% (ω = 0.37 rad/s) without current.

The relatively small effect of current on the percentage differences in the forces and moments indicate that the inertia

θ = 0.0 V_s=0.5 m/s	Surge Force x 10^{-7} (N)					Heave Force x 10^{-7} (N)					Sway Force x 10^{-6} (N)				
	ω (rad/s)					ω (rad/s)					ω (rad/s)				
Coefficients	0.37	0.42	0.45	0.50	0.56	0.37	0.42	0.45	0.50	0.56	0.37	0.42	0.45	0.50	0.56
LR	2.226	1.482	1.478	1.437	1.339	1.291	0.7769	0.7744	0.7609	0.7358	0.1610	0.1084	0.1229	0.1507	0.1881
DnV	2.598	1.691	1.688	1.646	1.542	1.758	1.057	1.056	1.042	1.013	0.2253	0.1490	0.1691	0.2073	0.2585
Diff %	16.7	14.1	14.2	14.5	15.2	36.2	36.1	36.4	36.9	37.7	39.9	37.5	37.6	37.6	37.4
Diff % V_s = 0.0	13.2	12.3	12.4	12.5	12.9	36.7	36.1	36.4	36.9	37.6	37.6	37.1	37.2	37.2	37.1
	ω (rad/s)					ω (rad/s)					ω (rad/s)				
Coefficients	0.64	0.75	0.94	1.06		0.64	0.75	0.94	1.06		0.64	0.75	0.94	1.06	
LR	0.8327	0.3830	0.1705	0.2943		0.4693	0.2603	0.05942	0.01140		0.1570	0.1402	0.08733	0.04928	
DnV	0.9644	0.4583	0.1857	0.3143		0.6509	0.3663	0.08961	0.01647		0.2150	0.1890	0.1177	0.06658	
Diff %	15.8	19.7	8.9	6.8		38.7	40.7	50.8	44.5		36.9	34.8	34.8	35.1	
Diff % V_s = 0.0	12.9	14.9	-3.3	1.8		38.7	40.7	50.9	44.4		35.4	34.3	33.8	33.4	

Table (5) Maximum Surge, Heave and Sway Forces by LR and DnV

θ = 0.0 V_s = 0.5m/s	Rolling Moment x 10^{-8} (NM)					Yawing Moment x 10^{-7} (NM)					Pitching Moment x 10^{-9} (NM)				
	ω (rad/s)					ω (rad/s)					ω (rad/s)				
Coefficients	0.37	0.42	0.45	0.50	0.56	0.37	0.42	0.45	0.50	0.56	0.37	0.42	0.45	0.50	0.56
LR	0.2425	0.1683	0.1962	0.2471	0.3130	0.1046	0.08244	0.1032	0.1506	0.2311	2.121	1.489	1.535	1.569	1.538
DnV	0.3395	0.2316	0.2699	0.3398	0.4303	0.1436	0.1130	0.1417	0.2068	0.3172	2.624	1.692	1.744	1.787	1.759
Diff %	40	37.6	37.6	37.5	37.4	37.3	37.1	37.3	37.3	37.3	19.2	12	12	12.2	12.6
Diff % V_s = 0.0	38.7	37.3	37.3	37.2	37.2	37.1	36.9	37	37.1	37.1	13.8	11.7	11.7	11.8	12.1
	ω (rad/s)					ω (rad/s)					ω (rad/s)				
Coefficients	0.64	0.75	0.94	1.06		0.64	0.75	0.94	1.06		0.64	0.75	0.94	1.06	
LR	0.2634	0.2393	0.1587	0.1019		0.2475	0.2741	0.2939	0.2976		0.9974	0.4612	0.2472	0.4164	
DnV	0.3606	0.3225	0.2135	0.1372		0.3379	0.3715	0.3918	0.3969		1.145	0.5432	0.2729	0.4462	
Diff %	36.9	34.8	34.5	34.6		36.5	35.5	33.3	33.4		12.9	15.1	9.4	6.7	
Diff % V_s = 0.0	34.6	34.3	33.9	33.6		36.3	35.2	33.3	33.4		11.8	12.8	2.5	3.8	

Table (6) Maximum Rolling, Yawing and Pitching Moments by LR and DnV

forces, rather than the drag, are dominant.

3.3.2 Maximum Forces and Moments ($\theta = 0^o$, $V_s = 1.0$ m/s)

Tables (7) and (8) show that:-

a. The differences in the surge forces ranged from 14.5% (ω = 1.06 rad/s) to 25.6% (ω = 0.37 rad/s) with current and from -3.3% (ω = 0.94 rad/s) to 14.9% (ω = 0.75 rad/s) without current.

b. The differences in the heave forces are the same for the two cases, ranging from 36.1% (ω = 0.42 rad/s) to 50.9% (ω = 0.75 rad/s).

c. The differences in the sway forces ranged from 35.3% (ω = 0.75 rad/s) to 40% (ω = 0.37 rad/s) with current and from 33.4% (ω = 1.06 rad/s) to 37.6% (ω = 0.37 rad/s) without current.

d. The differences in the rolling moments ranged from 35.1% (ω = 0.94 rad/s) to 40% (ω = 0.37 rad/s) with current and from 33.6% (ω = 1.06 rad/s) to 38.7% (ω = 0.37 rad/s) without current.

e. The differences in the yawing moments are similar for the two cases, ranging from 33.3% (ω = 0.94 rad/s) to 37.5% (ω = 0.37 rad/s) with current and from 33.3% (ω = 0.94 rad/s) to 37.1% (ω = 0.37 rad/s) without current.

f. The differences in the pitching moments ranged from 11% (ω = 1.06 rad/s) to 20.7% (ω = 0.37 rad/s) with current and from 2.5% (ω = 0.94 rad/s) to 13.8% (ω = 0.37 rad/s) without current.

$\theta = 0.0$, $V_s = 1.0m/s$	Surge Force x 10^{-7} (N)					Heave Force x 10^{-7} (N)					Sway Force x 10^{-6} (N)				
	ω (rad/s)					ω (rad/s)					ω (rad/s)				
Coefficients	0.37	0.42	0.45	0.50	0.56	0.37	0.42	0.45	0.50	0.56	0.37	0.42	0.45	0.50	0.56
LR	2.419	1.628	1.620	1.577	1.482	1.311	0.7897	0.7862	0.7708	0.7435	0.1911	0.1282	0.1436	0.1730	0.2124
DnV	3.039	1.896	1.888	1.841	1.741	1.786	1.075	1.072	1.056	1.024	0.2676	0.1769	0.1981	0.2385	0.2926
Diff %	25.6	16.5	16.5	16.7	17.5	36.2	36.1	36.4	37	37.7	40	38	38	37.9	37.8
$V_s = 0.0$ Diff %	13.2	12.3	12.4	12.5	12.9	36.7	36.1	36.4	36.9	37.6	37.6	37.1	37.2	37.2	37.1
	ω (rad/s)					ω (rad/s)					ω (rad/s)				
Coefficients	0.64	0.75	0.94	1.06		0.64	0.75	0.94	1.06		0.64	0.75	0.94	1.06	
LR	0.9594	0.4966	0.2650	0.3826		0.4733	0.2618	0.05996	0.01173		0.1784	0.1551	0.1011	0.06154	
DnV	1.142	0.6173	0.3180	0.4393		0.6565	0.3683	0.09037	0.01692		0.2449	0.2098	0.1369	0.08374	
Diff %	19.1	24.3	20	14.5		38.7	40.7	50.7	44.3		37.3	35.3	35.4	36.1	
$V_s = 0.0$ Diff %	12.9	14.9	-3.3	1.8		38.7	40.7	50.9	44.4		35.4	34.3	33.8	33.4	

Table (7) Maximum Surge, Heave and Sway Forces by LR and DnV

$\theta = 0.0$, $V_s = 1.0m/s$	Rolling Moment x 10^{-8} (NM)					Yawing Moment x 10^{-7} (NM)					Pitching Moment x 10^{-9} (NM)				
	ω (rad/s)					ω (rad/s)					ω (rad/s)				
Coefficients	0.37	0.42	0.45	0.50	0.56	0.37	0.42	0.45	0.50	0.56	0.37	0.42	0.45	0.50	0.56
LR	0.2805	0.1936	0.2233	0.2773	0.3466	0.1123	0.08895	0.1108	0.1605	0.2449	2.423	1.629	1.673	1.709	1.685
DnV	0.3927	0.2671	0.3079	0.3820	0.4771	0.1544	0.1221	0.1523	0.2207	0.3365	3.057	1.911	1.938	1.982	1.964
Diff %	40	38	37.9	37.8	37.7	37.5	37.3	37.5	37.5	37.4	20.7	14.8	13.7	13.8	14.2
$V_s = 0.0$ Diff %	38.7	37.3	37.3	37.2	37.2	37.1	36.9	37	37.1	37.1	13.8	11.7	11.7	11.8	12.1
	ω (rad/s)					ω (rad/s)					ω (rad/s)				
Coefficients	0.64	0.75	0.94	1.06		0.64	0.75	0.94	1.06		0.64	0.75	0.94	1.06	
LR	0.2921	0.2576	0.1751	0.1161		0.2632	0.2916	0.2939	0.2976		1.127	0.5746	0.3335	0.4952	
DnV	0.4008	0.3481	0.2365	0.1570		0.3598	0.3960	0.3918	0.3969		1.326	0.7020	0.3938	0.5565	
Diff %	37.2	35.1	35.1	35.2		36.7	35.8	33.3	33.4		15	18.2	15.3	11	
$V_s = 0.0$ Diff %	34.6	34.3	33.9	33.6		36.3	35.2	33.3	33.4		11.8	12.8	2.5	3.8	

Table (8) Maximum Rolling, Yawing and Pitching Moments by LR and DnV

3.3.3 Maximum Forces and Moments ($\theta = 45^{o}$, $V_s = 0.5$ m/s)

Tables (9) and (10) show that:-

a. The differences in the surge forces ranged from 5.6% (ω = 1.06 rad/s) to 18.5% (ω = 0.75 rad/s) with current and from -3.3% (ω = 0.94 rad/s) to 14.9% (ω = 0.75 rad/s) without current.

b. The differences in the heave forces are similar for the two cases, ranging from 36.1% (ω = 0.37 rad/s) to 50.8% (ω = 0.94 rad/s) with current and from 36.1% (ω = 0.42 rad/s) to 50.9% (ω = 0.94 rad/s) without current.

c. The differences in the sway forces ranged from 38.4% (ω = 0.75 rad/s) to 40.1% (ω = 0.37 rad/s) with current and from 33.4% (ω = 1.06 rad/s) to 37.6% (ω = 0.37 rad/s) without current.

d. The differences in the rolling moments ranged from 37.8% (ω = 0.94 rad/s) to 40% (ω = 0.37 - 0.56 rad/s) with current and from 33.6% (ω = 1.06 rad/s) to 38.7% (ω = 0.37 rad/s) without current.

e. The differences in the yawing moments ranged from 34.9% (ω = 1.06 rad/s) to 39.9% (ω = 0.37 rad/s) with current and from 33.3% (ω = 0.94 rad/s) to 37.1% (ω = 0.37 rad/s) without current.

f. The differences in the pitching moments ranged from 5.9% (ω = 1.06 rad/s) to 17.4% (ω = 0.37 rad/s) with current and from 2.5% (ω = 0.94 rad/s) to 13.8% (ω = 0.37 rad/s) without current.

$\theta = \pi/4$	Surge Force x 10^{-7} (N)					Heave Force x 10^{-7} (N)					Sway Force x 10^{-6} (N)				
V_s = 0.5m/s	ω (rad/s)					ω (rad/s)					ω (rad/s)				
Coefficients	0.37	0.42	0.45	0.50	0.56	0.37	0.42	0.45	0.50	0.56	0.37	0.42	0.45	0.50	0.56
LR	2.186	1.454	1.45	1.408	1.308	1.287	0.7744	0.7718	0.7584	0.7340	1.226	0.8305	0.8176	0.7914	0.7536
DnV	2.501	1.653	1.649	1.605	1.498	1.752	1.054	1.052	1.038	1.011	1.717	1.163	1.145	1.108	1.055
Diff %	14.4	13.7	13.7	14	14.5	36.1	36.1	36.3	36.9	37.7	40.1	40	40	40	40
Diff %	13.2	12.3	12.4	12.5	12.9	36.7	36.1	36.4	36.9	37.6	37.6	37.1	37.2	37.2	37.1
Coefficients	ω (rad/s)					ω (rad/s)					ω (rad/s)				
	0.64	0.75	0.94	1.06		0.64	0.75	0.94	1.06		0.64	0.75	0.94	1.06	
LR	0.8071	0.3625	0.1570	0.2834		0.4684	0.2598	0.05917	0.01103		0.5378	0.4504	0.3379	0.2747	
DnV	0.9286	0.4295	0.1668	0.2992		0.6496	0.3656	0.00925	0.01595		0.7491	0.6232	0.4685	0.3822	
Diff %	15.1	18.5	6.2	5.6		38.7	40.7	50.8	44.6		39.3	38.4	38.7	39.1	
Diff %	12.9	14.9	-3.3	1.8		38.7	40.7	50.9	44.4		35.4	34.3	33.8	33.4	

Table (9) Maximum Surge, Heave and Sway Forces by LR and DnV

$\theta = \pi/4$	Rolling Moment x 10^{-8} (NM)					Yawing Moment x 10^{-7} (NM)					Pitching Moment x 10^{-9} (NM)				
V_s = 0.5m/s	ω (rad/s)					ω (rad/s)					ω (rad/s)				
Coefficients	0.37	0.42	0.45	0.50	0.56	0.37	0.42	0.45	0.50	0.56	0.37	0.42	0.45	0.50	0.56
LR	1.298	0.8952	0.9064	0.9148	0.9084	0.6770	0.4983	0.5109	0.5059	0.5575	2.081	1.460	1.505	1.537	1.502
DnV	1.817	1.253	1.269	1.281	1.272	0.9468	0.6968	0.7142	0.7067	0.7741	2.519	1.652	1.703	1.742	1.709
Diff %	40	40	40	40	40	39.9	39.8	39.8	39.7	38.9	17.4	11.6	11.6	11.8	12.1
Diff %	38.7	37.3	37.3	37.2	37.2	37.1	36.9	37	37.1	37.1	13.8	11.7	11.7	11.8	12.1
Coefficients	ω (rad/s)					ω (rad/s)					ω (rad/s)				
	0.64	0.75	0.94	1.06		0.64	0.75	0.94	1.06		0.64	0.75	0.94	1.06	
LR	0.6694	0.5603	0.4025	0.3082		0.5230	0.4333	0.3490	0.3183		0.9674	0.4371	0.2328	0.4057	
DnV	0.9291	0.7719	0.5548	0.4260		0.7236	0.5944	0.4728	0.4295		1.103	0.5095	0.2527	0.4313	
Diff %	38.8	37.8	37.8	38.2		38.4	37.2	35.5	34.9		12.3	14.2	7.9	5.9	
Diff %	34.6	34.3	33.9	33.6		36.3	35.2	33.3	33.4		11.8	12.8	2.5	3.8	

Table (10) Maximum Rolling, Yawing and Pitching Moments by LR and DnV

3.3.4 Maximum Forces and Moments ($\theta = 45^{o}$, $V_s = 1.0$ m/s)

Tables (11) and (12) show that:-

a. The differences in the surge forces ranged from 11.8% (ω = 1.06 rad/s) to 22.4% (ω = 0.75 rad/s) with current and from -3.3% (ω = 0.94 rad/s) to 14.9% (ω = 0.75 rad/s) without current.

b. The differences in the heave forces are similar for the two cases, ranging from 36.2% (ω = 0.37 rad/s) to 50.8% (ω = 0.94 rad/s) with current and from 36.1% (ω = 0.42 rad/s) to 50.9% (ω = 0.94 rad/s) without current.

c. The differences in the sway forces are constant at about 40% for the whole range of frequencies when current is included. Without current, the differences ranged from 33.4% (ω = 1.06 rad/s) to 37.6% (ω = 0.37 rad/s).

d. Similarly to the sway forces, the rolling moments had average difference of 40%, with current. Without current, the differences ranged from 33.6% (ω = 1.06 rad/s) to 38.7% (ω = 0.37 rad/s).

e. The differences in the yawing moments ranged from 35.7% (ω = 1.06 rad/s) to 39.9% (ω = 0.37 - 0.45 rad/s) with curent and from 33.3% (ω = 0.94 rad/s) to 37.1% (ω = 0.37 rad/s) without current.

f. The differences in the pitching moments ranged from 9.4% (ω = 1.06 rad/s) to 20.1% (ω = 0.37 rad/s) with current and from 2.5% (ω = 0.94 rad/s) to 13.8% (ω = 0.37 rad/s) without current.

$\theta = \pi/4$ $V_s = 1.0m/s$	Surge Force x 10^{-7} (N)					Heave Force x 10^{-7} (N)					Sway Force x 10^{-6} (N)				
	ω (rad/s)					ω (rad/s)					ω (rad/s)				
Coefficients	0.37	0.42	0.45	0.50	0.56	0.37	0.42	0.45	0.50	0.56	0.37	0.42	0.45	0.50	0.56
LR	2.320	1.558	1.552	1.509	1.411	1.304	0.7850	0.7813	0.7659	0.7393	2.669	1.942	1.905	1.833	1.736
DnV Diff %	2.807 21	1.798 15.4	1.792 15.5	1.746 15.7	1.642 16.4	1.776 36.2	1.069 36.2	1.066 36.4	1.049 37	1.018 37.7	3.736 40	2.719 40	2.667 40	2.560 40	2.431 40
Diff %	13.2	12.3	12.4	12.5	12.9	36.7	36.1	36.4	36.9	37.6	37.6	37.1	37.2	37.2	37.1
Coefficients	ω (rad/s)					ω (rad/s)					ω (rad/s)				
	0.64	0.75	0.94	1.06		0.64	0.75	0.94	1.06		0.64	0.75	0.94	1.06	
LR Diff %	0.8976	0.4432	0.2236	0.3460		0.4711	0.2605	0.05930	0.01066		1.350	1.104	0.9481	0.8841	
DnV Diff %	1.055 17.5	0.5425 22.4	0.2601 16.3	0.3868 11.8		0.6534 38.7	0.3665 40.7	0.08944 50.8	0.01543 44.8		1.890 40	1.538 39.3	1.323 39.5	1.236 39.8	
Diff %	12.9	14.9	-3.3	1.8		38.7	40.7	50.9	44.4		35.4	34.3	33.8	33.4	

Table (11) Maximum Surge, Heave and Sway Forces by LR and DnV

$\theta = \pi/4$ $V_s = 1.0m/s$	Rolling Moment x 10^{-8} (NM)					Yawing Moment x 10^{-7} (NM)					Pitching Moment x 10^{-9} (NM)				
	ω (rad/s)					ω (rad/s)					ω (rad/s)				
Coefficients	0.37	0.42	0.45	0.50	0.56	0.37	0.42	0.45	0.50	0.56	0.37	0.42	0.45	0.50	0.56
LR	2.671	1.960	1.963	1.948	1.897	1.314	0.9893	1.036	1.072	1.051	2.259	1.560	1.604	1.639	1.608
DnV %	3.739 40	2.744 40	2.749 40	2.727 40	2.656 40	1.838 39.9	1.384 39.9	1.449 39.9	1.499 39.8	1.468 39.7	2.827 20.1	1.792 13	1.842 12.9	1.884 13	1.857 13.4
Diff %	38.7	37.3	37.3	37.2	37.2	37.1	36.9	37	37.1	37.1	13.8	11.7	11.7	11.8	12.1
Coefficients	ω (rad/s)					ω (rad/s)					ω (rad/s)				
	0.64	0.75	0.94	1.06		0.64	0.75	0.94	1.06		0.64	0.75	0.94	1.06	
LR	1.438	1.147	0.9314	0.8225		0.8188	0.6620	0.4503	0.3761		1.060	0.5177	0.2937	0.4607	
DnV Diff %	2.014 40.1	1.594 39	1.295 39	1.146 39.3		1.138 39	0.9145 38.1	0.6145 36.5	0.5105 35.7		1.232 14	0.6223 16.8	0.3380 13.1	0.5083 9.4	
Diff %	34.6	34.3	33.9	33.6		36.3	35.2	33.3	33.4		11.8	12.8	2.5	3.8	

Table (12) Maximum Rolling, Yawing and Pitching Moments by LR and DnV

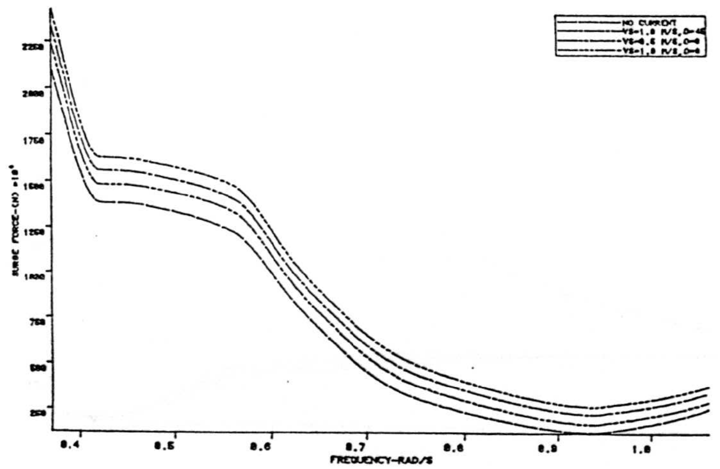

COEFFICIENTS: LR , $\beta = 0^{o}$,SR= 0.0
FIG.(2) MAX. SURGE FORCES VS. FREQUENCY

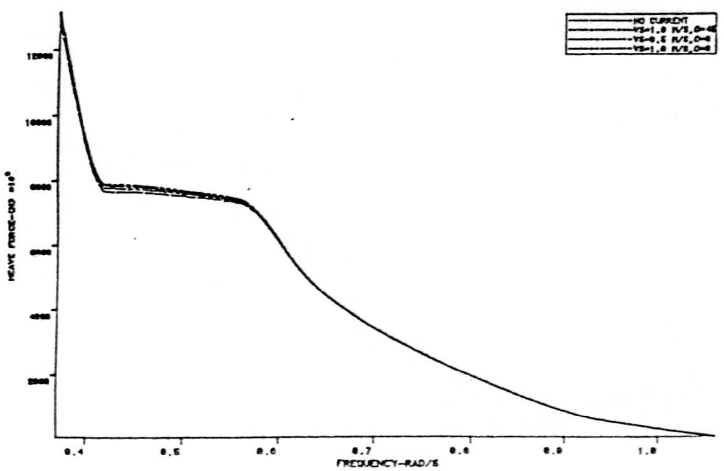

COEFFICIENTS: LR , $\beta = 0^{o}$,SR= 0.0
FIG.(3) MAX. HEAVE FORCES VS. FREQUENCY

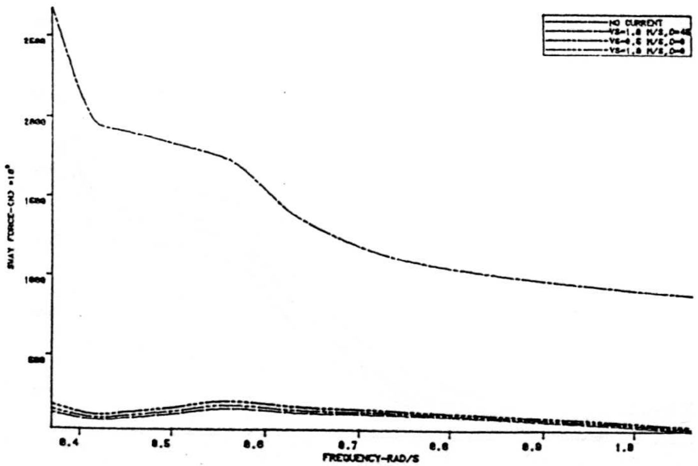

COEFFICIENTS: LR , $\beta = 0^{o}$,SR= 0.0
FIG.(4) MAX. SWAY FORCES VS. FREQUENCY

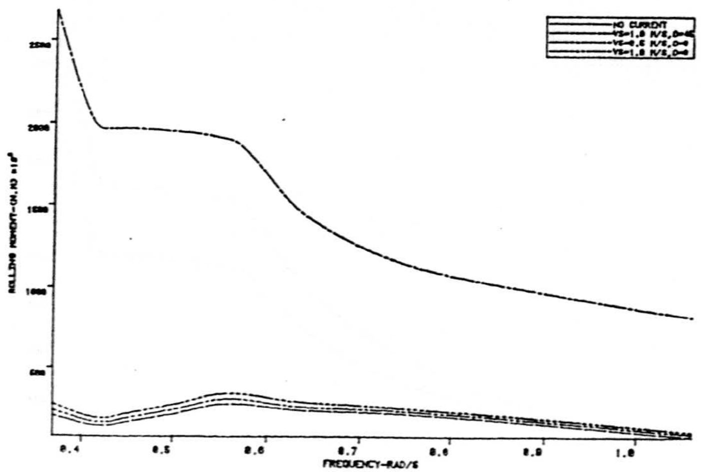

COEFFICIENTS: LR , $\beta = 0^{o}$,SR= 0.0
FIG.(5) MAX. ROLLING MOMENTS VS. FREQUENCY

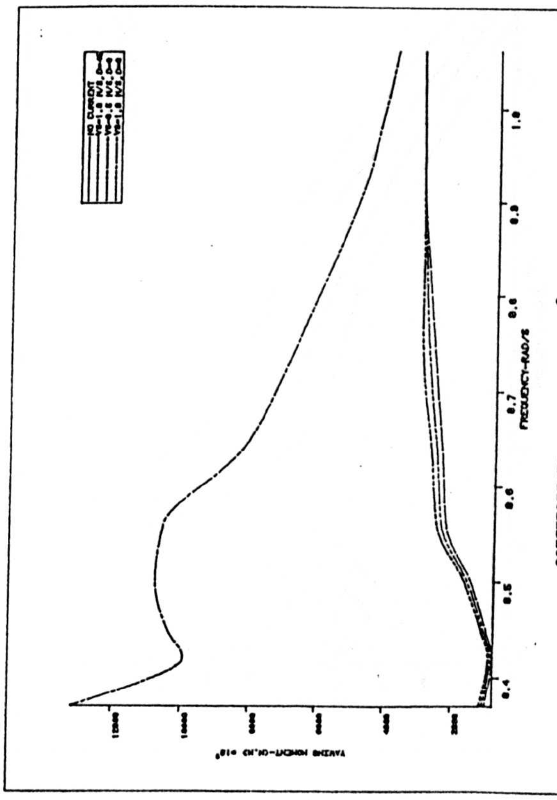

COEFFICIENTS: LR, β = 0°, SR= 0.0
FIG.(6) MAX. YAWING MOMENTS VS. FREQUENCY

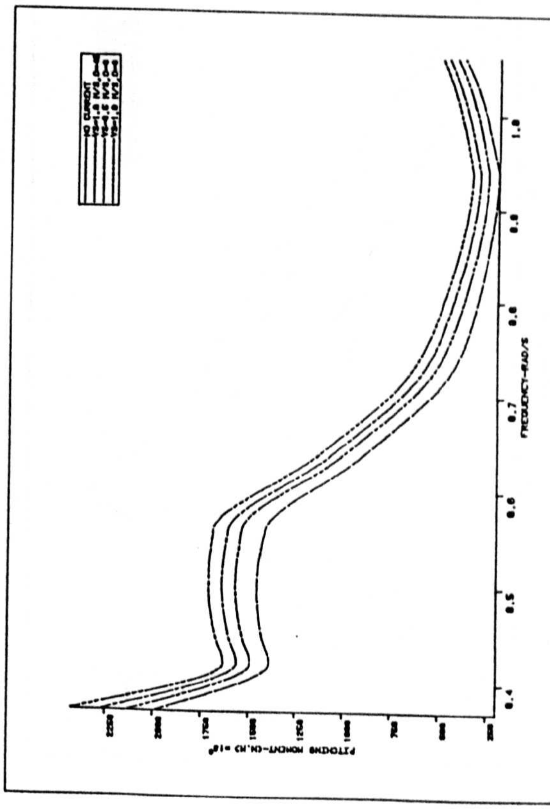

COEFFICIENTS: LR, β = 0°, SR= 0.0
FIG.(7) MAX. PITCHING MOMENTS VS. FREQUENCY

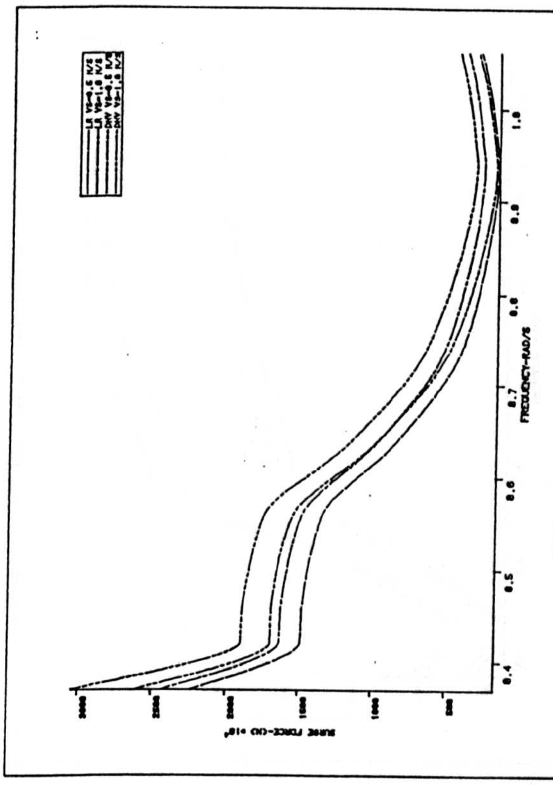

COEFFICIENTS: LR & DnV, β = 0°, SR= 0.0
FIG.(8) MAX. SURGE FORCES VS. FREQUENCY

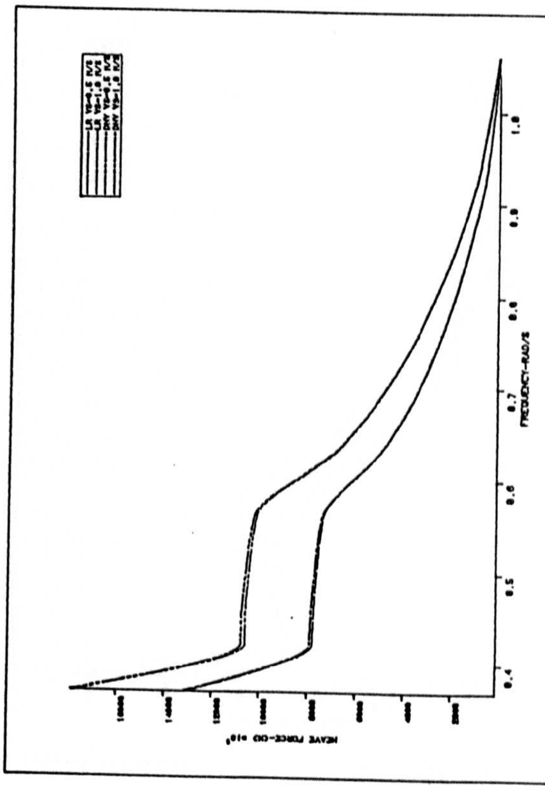

COEFFICIENTS: LR & DnV, β = 0°, SR= 0.0
FIG.(9) MAX. HEAVE FORCES VS. FREQUENCY

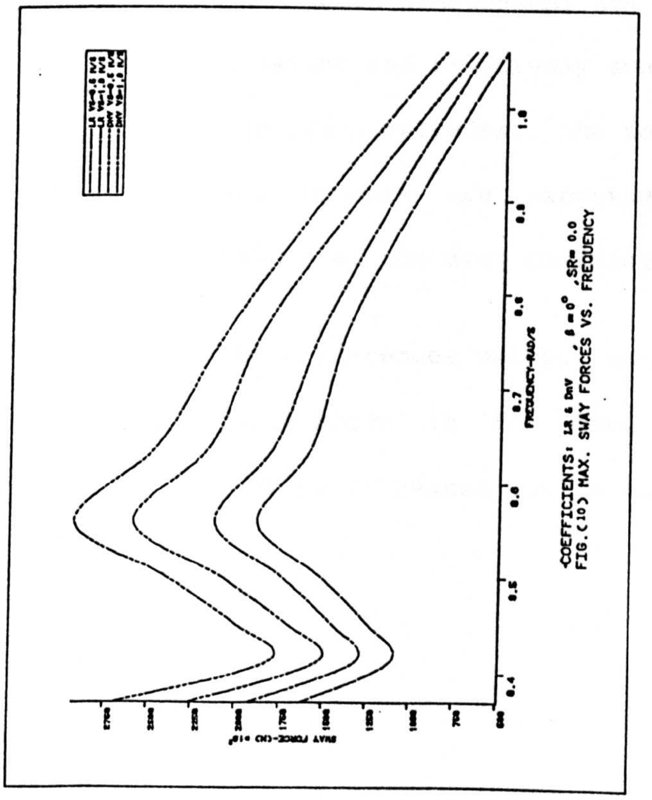

COEFFICIENTS: LR & DnV , $\beta = 0^{o}$,SR= 0.0
FIG.(10) MAX. SWAY FORCES VS. FREQUENCY

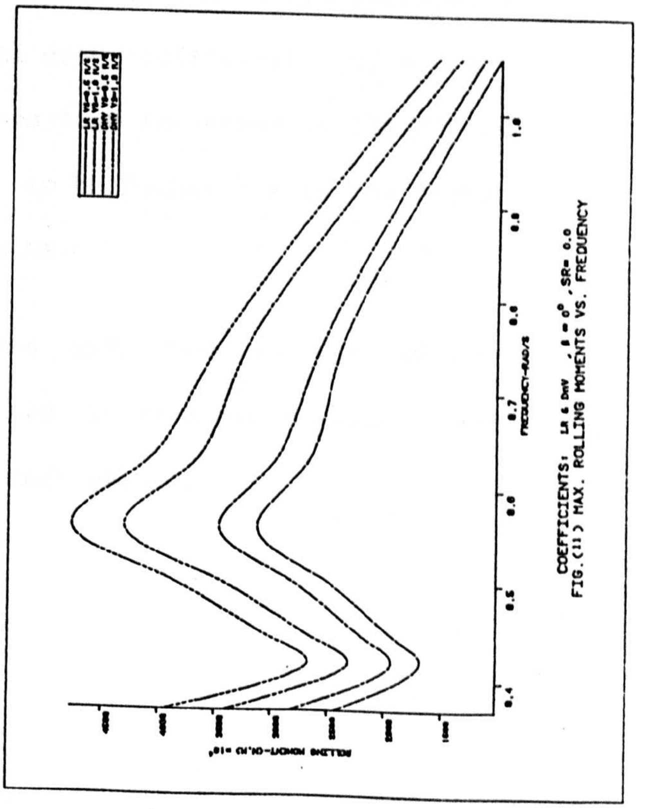

COEFFICIENTS: LR & DnV , $\beta = 0^{o}$,SR= 0.0
FIG.(11) MAX. ROLLING MOMENTS VS. FREQUENCY

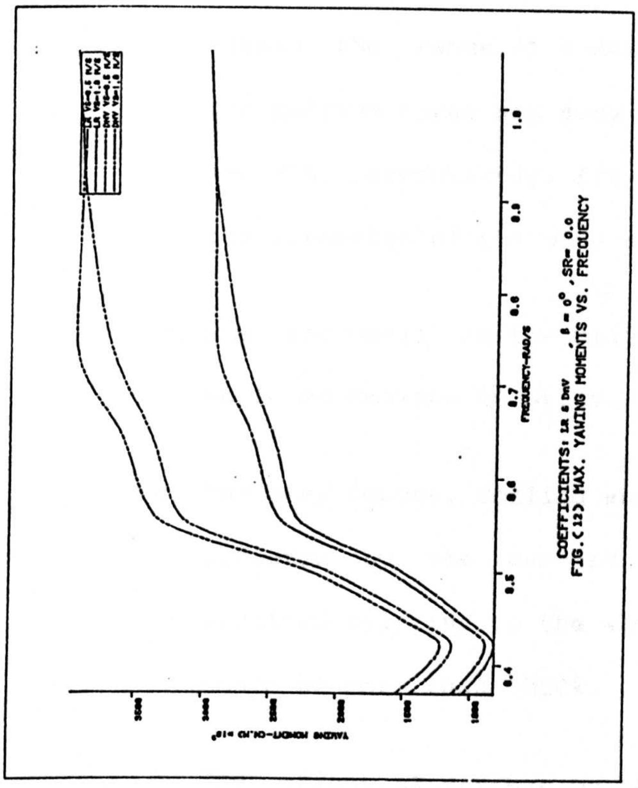

COEFFICIENTS: LR & DnV , $\beta = 0^{o}$,SR= 0.0
FIG.(12) MAX. YAWING MOMENTS VS. FREQUENCY

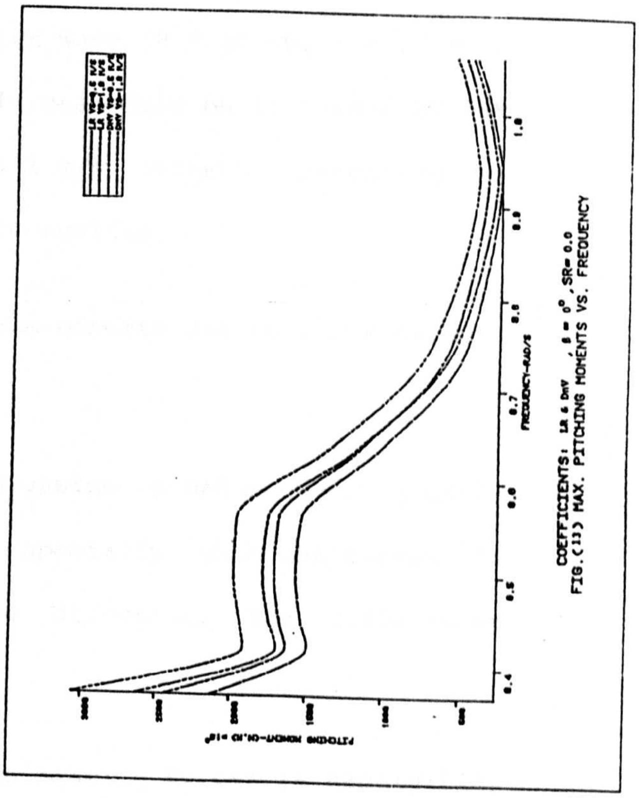

COEFFICIENTS: LR & DnV , $\beta = 0^{o}$,SR= 0.0
FIG.(13) MAX. PITCHING MOMENTS VS. FREQUENCY

4. CONCLUSIONS

a. Within the range of a design wave (H = 30.0m, T = 17 sec) the maximum surge and sway forces could be increased by 16% and 37%, respectively, for a 1 m/s current travelling in the direction of the wave propagation.

b. The increases in the maximum moments due to 1 m/s current could be between 16 to 34%.

c. The sway forces, rolling and yawing moments were greatly affected by the current especially when the current is inclined relative to the wave direction. The differences could be more than 1000%.

d. The effect of current on the heaving forces is negligible, since the current velocity was assumed to have no vertical component.

e. The above conclusions are related to smooth cylinders with constant and relatively small drag coefficient (C_D = 0.5). For rough cylinders, the percentage increases in the forces and moments are expected to be higher due to the higher values of the drag coefficients.

f. The differences between LR and DnV results, due to the differences in the drag and inertia coefficients, were further increased due to current effect.

REFERENCES

1. DET NORSKE VERITAS, 'Rules for the Design, Construction and Inspection of Mobile Offshore Units', 1974.

2. DET NORSKE VERITAS, 'Rules for the Construction and Classification of Mobile Offshore Units', 1975.

3. DET NORSKE VERITAS, 'Rules for the Design, Construction and Inspection of Offshore Structures', Appendix B, 1977.

4. LLOYD'S REGISTER OF SHIPPING, 'Rules for the Construction and Classification of Mobile Offshore Units', 1972.

CHAPTER 9

CHAPTER 9

STATIC ANALYSIS OF JACKET STRUCTURES

1. INTRODUCTION

During the course of the wave loading investigation in the previous chapters, large differences in the wave loading estimation were found, for example, when using different hydrodynamic coefficients, or when applying different wave theories.

In the present chapter, the purpose is to examine the results of the static analysis of a typical jacket structure when different patterns of wave loadings are used. The first part of this chapter compares the results of maximum forces, moments and stresses on the members after the analysis of the indeterminate structure has been made using the wave loads determined, from the recommended coefficients by LR, DnV and BV, Tables (2) and (3). The second part compares the results according to LR with those of Sarpkaya, (7)-(14) both in the cases of Airy and Stokes' fifth order theories (15). This was necessary as it is possible that the distribution of the loads throughout the jacket might alter the proportion of load carried by a particular member. As before the comparison is based on the recommended coefficients of LR.

2. STATIC ANALYSIS OF THE STRUCTURE

The analysis was carried out for the jacket structure of 119 members, which has been used throughout the investigation, of the wave loading.

The main particulars of the structures are shown in Fig. (2) and a three-dimensional representation of the jacket with member numbering is shown in Figs. (3) and (4). The calculations were performed for two wave frequencies, $\omega = 0.37$ rad/s and $\omega = 0.56$ rad/s, the first of which may represent the design wave. The full particulars of the waves are given in Table (1). The two waves were assumed to pass through the structure in the direction of the X-axis, ie $\beta = 0^{\circ}$, Fig. (1).

It is to be noted that the static analysis was based on the wave loading only. The other environmental loads (wind, current, etc) and functional loads (deck loads, dynamic loads, etc) were not taken into account.

This is because the main objective was to investigate the effects of the variations in the wave loading calculations, when using different hydrodynamic coefficients and different wave theories, on the final structural loading and stresses experienced by the individual members of the structure. However, for actual design calculations, all types of loads (environmental and functional) should be taken into consideration.

2.1 Description of the Computer Programs

The various steps in the static analysis of the jacket structure were carried out by a set of computer programs: OSS, STKFS, JNS, SAP IV, STRESS and PERDIF. Programs OSS and STKFS were described in Chapter 3 and Chapter 6, respectively.

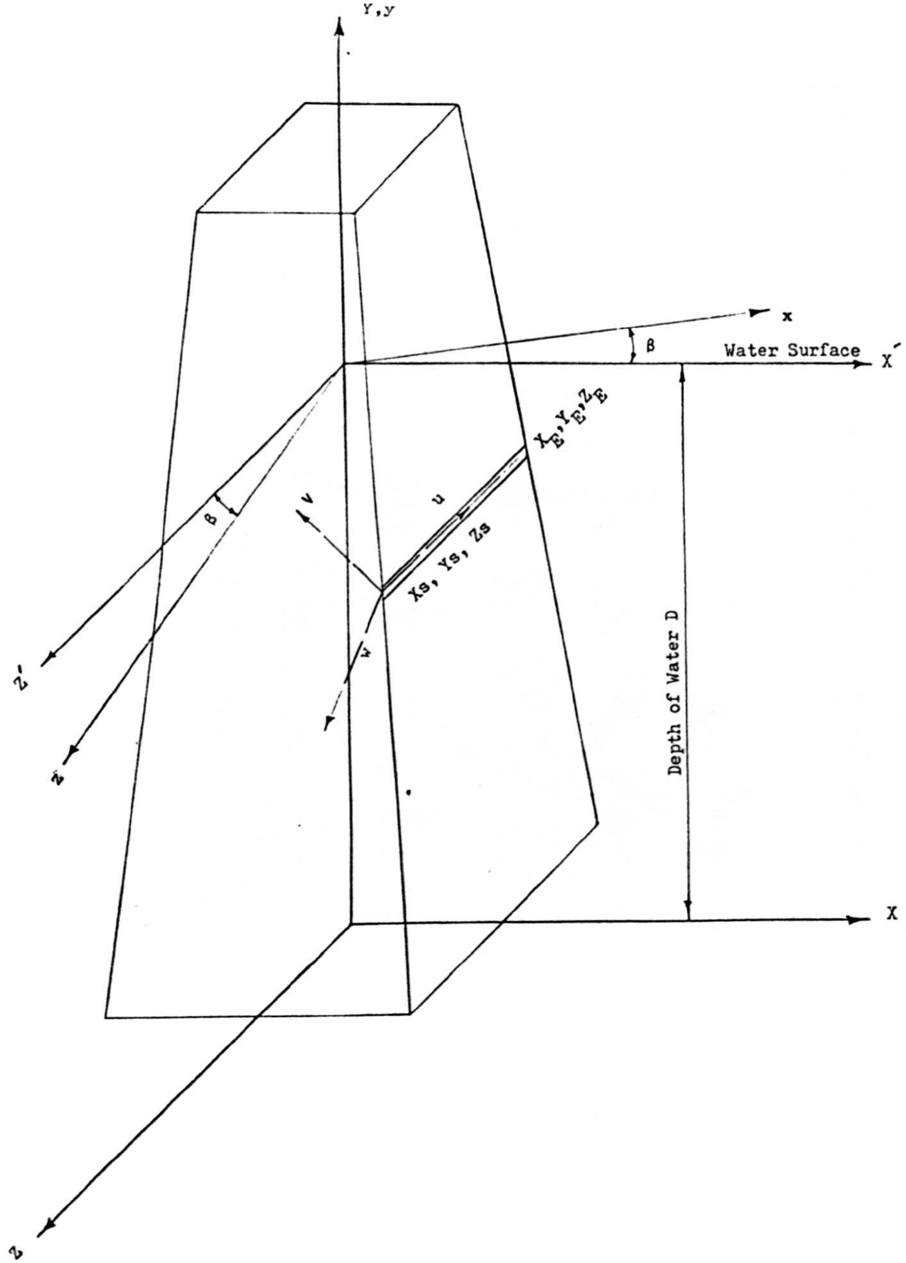

Fig. (1) Reference Systems

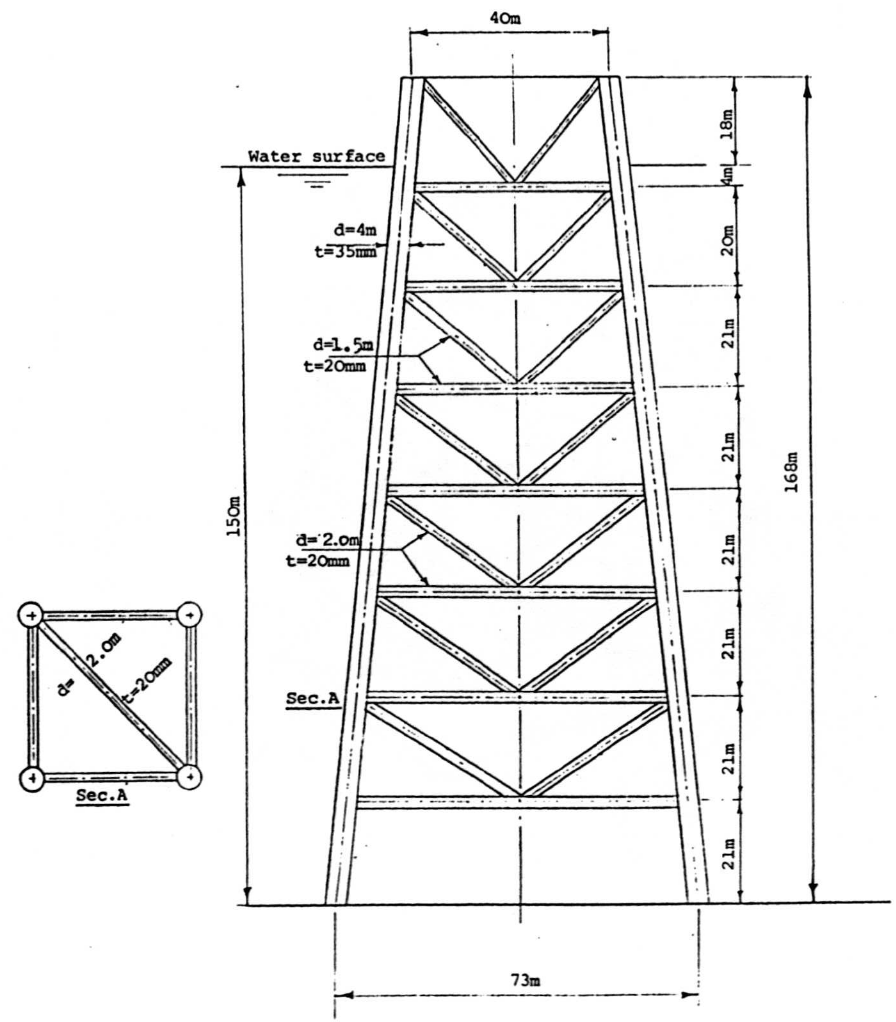

Fig. (2) Main Particulars of the Jacket Structure

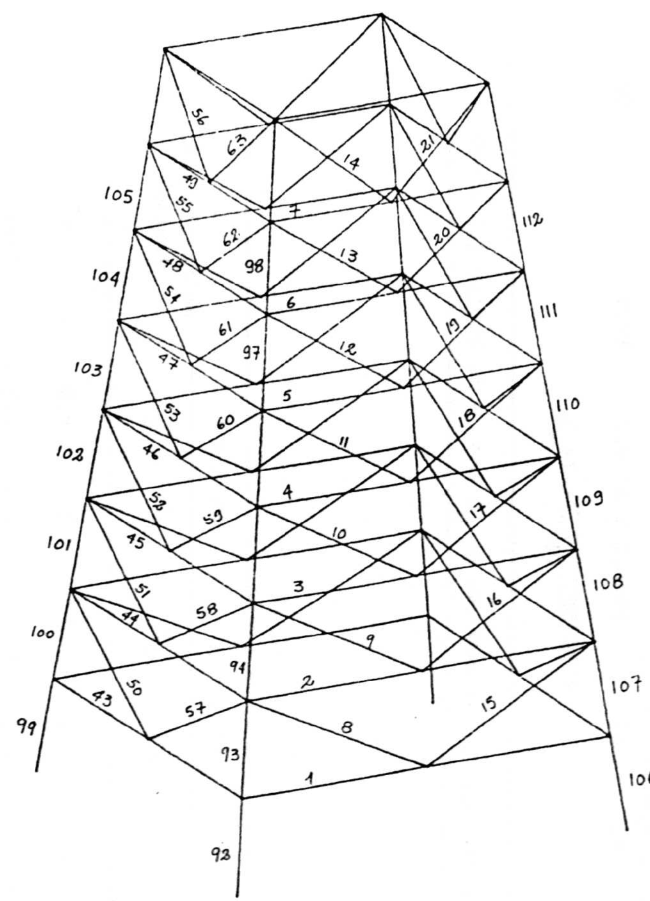

BASE DIMENSIONS=73X73 m TOP DIMENSIONS=40X40 m
HEIGHT=168 m NUMBER OF MEMBERS=119
FIG.(3) 3-DIM. REPRESENTATION OF THE JACKET STRUCTURE

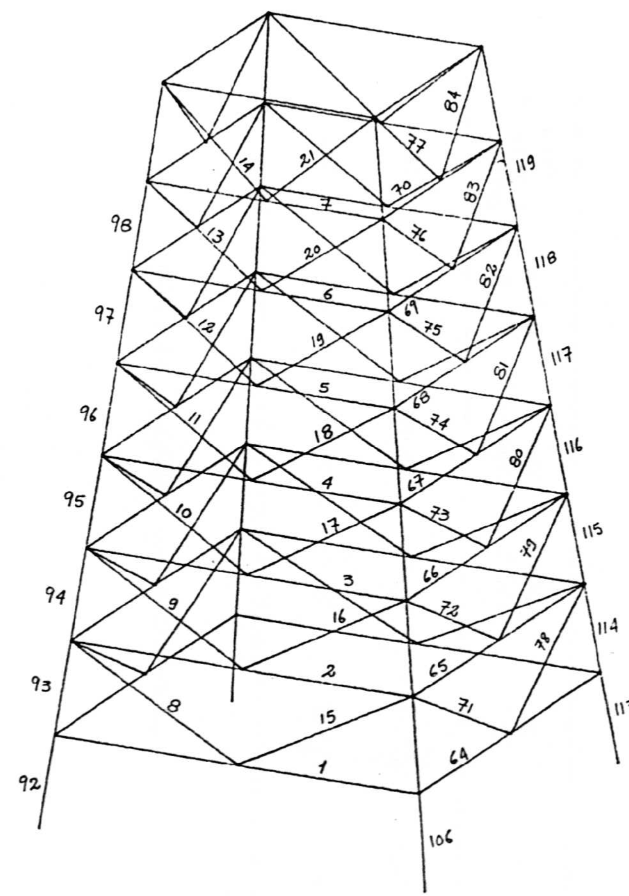

BASE DIMENSIONS=73X73 m TOP DIMENSIONS=40X40 m
HEIGHT=168 m NUMBER OF MEMBERS=119
FIG.(4) 3-DIM. REPRESENTATION OF THE JACKET STRUCTURE

Wave Frequency ω (rad/s)	Height H (m)	Length L (m)	Period T (s)	$\frac{H}{L}$	$\frac{D}{L}$
0.37	30.0	450.01	16.97	$0.07(\frac{1}{15})$	0.33
0.56	20.0	196.45	11.21	$0.10(\frac{1}{10})$	0.76

Table (1) Particulars of the Waves

Classi-cation Society	Drag Co-efficient C_D	Inertia Coefficient C_M	Notes
LR	0.5	1.5 (d $\leq$ 3.5m) 2.0 (d $\geq$ 3.5m)	smooth cylinders d=dia of cylinder
DnV	$\geq$ 0.7	1.5 (d/ℓ = 1.0) 2.0 ($d/\ell \leq$ 0.1)	$R_e > 3 \times 10^6$ ℓ=length of cylinder if $0.1 < d/\ell < 1$ interpolate for C_M
BV	0.75	1.6 (d $\leq$ 1.45m) $C_M=1+\sqrt{\log_{10}(10d)-0.8}$	(d > 1.45m)

Table (2) Values of C_D and C_M as recommended by LR, DnV and BV

Classification Society	d = 1.5m		d = 2.0m		d = 4.0m	
	C_D	C_M	C_D	C_M	C_D	C_M
LR	0.5	1.5	0.5	1.5	0.5	2.0
DnV	0.7	2.0	0.7	2.0	0.7	2.0
BV	0.75	1.613	0.75	1.708	0.75	1.896

Table (3) Recommended Values of C_D and C_M for the Jacket Structure

2.1.1 Program JNS

This program (16) reads the data stored in the files generated by program OSS or program STKFS, (one file each time) and calculates the 'equivalent loads' (concentrated forces and moments) for each member of the structure at the positions specified by the user. The program reads also the input data required to run program SAP IV such as:-

a. The total number of members, the total number of nodes, the numbering and co-ordinates (X, Y, Z) of each node, ..etc.

b. The outside diameter and wall thickness of the different members.

c. The material(s) specifications (modulus of elasticity, Possion's ratio, ..etc).

The output data of program JNS are stored in files which are used by program SAP IV as input.

2.1.2 Program SAP IV

This is an advanced, large size, finite element computer program for the static and dynamic analysis of linear structural systems. The full description of the program is presented in Ref.(1).

For each member of the structure, the distributions of the axial force (N), shearing forces (F_y and F_z), torsion (Q) and bending moments (M_y and M_z)along the length of the member are stored in a file for stress analysis by program STRESS.

2.1.3 Program STRESS

This program is used to calculate the maximum combined stresses for 24 selected members representing the whole jacket structure. The positions and numbering of these members are shown in Fig. (5).

The program starts by picking up the maximum values of the forces (N, F_y and F_z) and moments (Q, M_y and M_z) for each member and then calculates the maximum stresses by the method given in Appendix (E).

The method is based on determining, from basic principles, the maximum combined stresses on the member surface due to:-

a. The direct stresses (tension or compression) due to the axial force (N).

b. The bending stresses due to the moments M_y and M_z.

c. The shearing stresses due to the forces F_y and F_z.

d. The shearing stresses due to torsion (Q).

The maximum values of the forces, moments and stresses for the 24 members are stored in one file corresponding to a certain wave frequency and a particular interval of time (t) and can be used for further analysis.

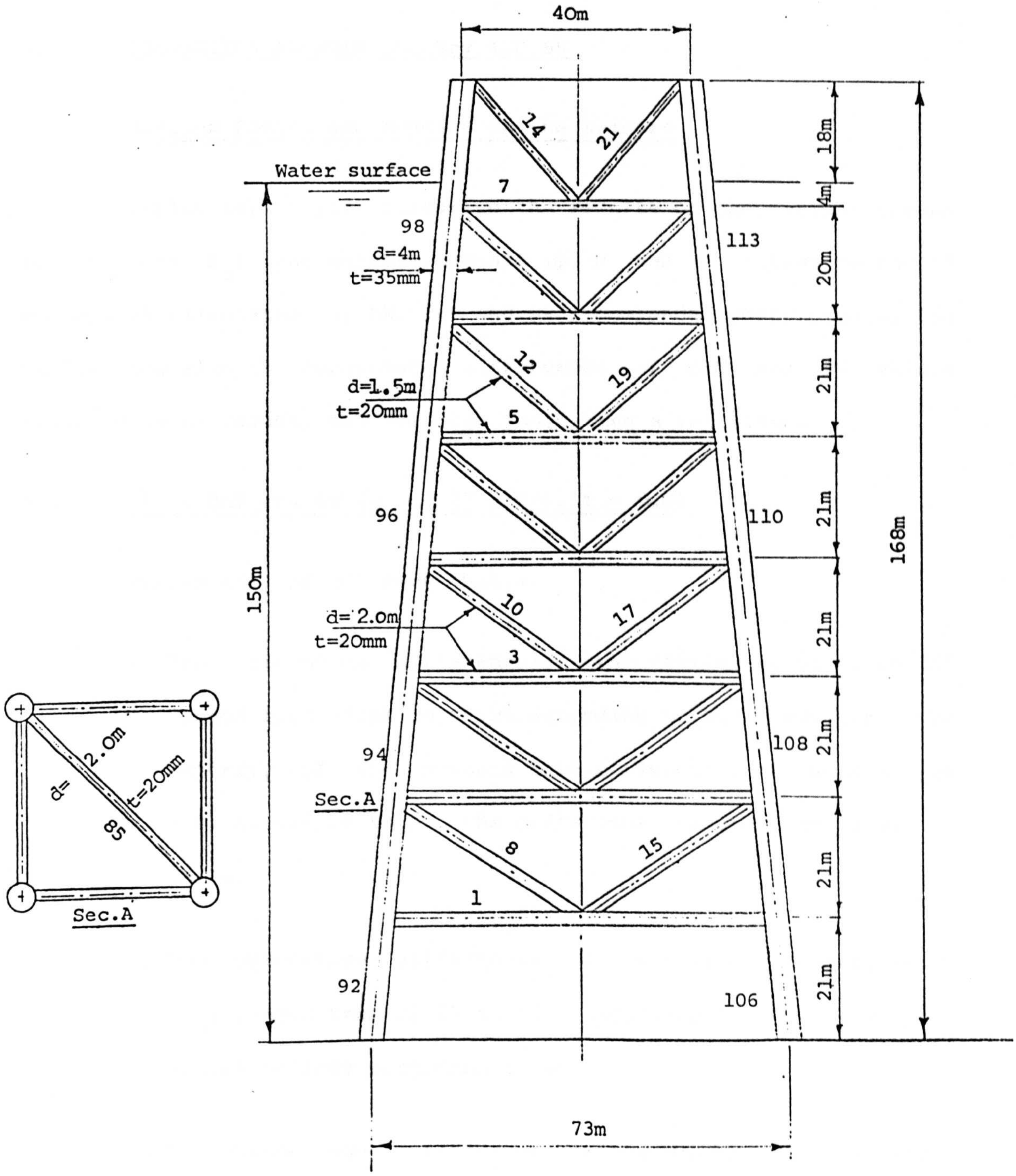

Fig. (5) Members for Static Analysis

2.1.4 Program PERDIF

This program reads the files of data created by program STRESS according to LR, DnV, BV and Sarpkaya's coefficients and calculates the percentage differences in the forces, moments and stresses for the individual members, taking LR values as a basis for comparison.

3. COMPARISON BETWEEN LR, DnV AND BV

3.1 Maximum Forces and Moments on the Members

Tables (4) to (15) summarise the results of the maximum forces (N, F_y and F_z) and maximum moments (Q, M_y and M_z) acting on the 24 members as calculated by LR, DnV and BV recommended coefficients. The tables show also the percentage differences of DnV and BV values relative to LR values, the -ve sign indicating a reduction.

3.1.1 LR vs DnV and BV (ω = 0.37 rad/s, t = 0.0)

Tables (4) and (5) show that:-

a. The percentage differences in the maximum axial force (N) ranged from -0.6% to 48.0% according to DnV. However, the majority of the members have differences of the order of 40%. According to BV, the differences ranged from 3.2% to 88.7%.

b. The percentage differences in the maximum shearing force (F_y) ranged from 22.2% to 102% according to DnV and from -18.2% to 169% according to BV.

c. The percentage differences in the maximum shearing force (F_z) ranged from 10.7% to 142% according to DnV and from -9.4% to 177% according to BV.

Member No	Max Axial Force N (N) x 10^{-6} LR	DnV	BV	Diff % DnV	Diff % BV	Max Shearing Force F_y (N) x 10^{-6} LR	DnV	BV	Diff % DnV	Diff % BV	Max Shearing Force F_z (N) x 10^{-6} LR	DnV	BV	Diff % DnV	Diff % BV
1	2.0238	2.8110	3.0026	38.9	48.4	0.0551	0.0759	0.0745	37.7	35.2	-0.0099	-0.0135	-0.0134	37.1	36.3
3	1.5964	2.1930	2.3341	37.4	46.2	0.0491	0.0667	0.0603	35.9	22.9	-0.0201	-0.0276	-0.0279	37.8	39.4
5	1.2579	1.6986	1.7959	35.0	42.8	0.0403	0.0539	0.0472	33.9	17.2	-0.0227	-0.0313	-0.0316	38.1	39.2
7	0.2186	0.2510	0.2715	14.8	24.2	-0.0584	-0.0784	-0.0654	34.3	12.0	-0.0372	-0.0518	-0.0545	39.2	46.4
8	2.2198	-3.1157	-3.3725	40.4	51.9	-0.0382	-0.0514	-0.0454	34.4	18.7	-0.0114	-0.0160	-0.0163	40.0	42.9
10	1.7224	-2.4180	-2.6276	40.4	52.6	-0.0473	-0.0627	-0.0517	32.5	9.3	-0.0225	-0.0312	-0.0321	38.8	42.7
12	1.3608	1.9097	-2.0741	40.3	52.4	-0.0287	-0.0372	-0.0234	29.9	-18.2	-0.0181	-0.0248	-0.0260	36.8	43.7
14	-0.0663	-0.0981	-0.1250	48.0	88.7	0.0055	-0.0078	-0.0103	40.7	86.3	-0.0128	-0.0180	-0.0194	40.4	51.8
15	2.4133	3.3726	3.5924	39.8	48.9	-0.0359	-0.0482	-0.0433	34.4	20.7	-0.0096	-0.0134	-0.0144	40.4	50.5
17	1.9958	2.7821	2.9385	39.4	47.2	0.0589	0.0791	0.0695	34.3	18.0	-0.0185	-0.0260	-0.0281	40.7	52.0
19	1.5746	2.1935	2.3034	39.3	46.3	0.0642	0.0869	0.0768	35.5	19.7	-0.0162	-0.0228	-0.0250	41.0	54.4
21	0.2329	0.3199	0.3114	37.4	33.7	-0.0350	-0.0472	-0.0474	35.0	35.6	-0.0115	-0.0163	-0.0180	41.5	56.6
85	0.0549	0.0676	0.0605	23.2	10.2	-0.0754	-0.1009	-0.0884	33.7	17.2	-0.0193	-0.0264	-0.0252	36.4	30.3
87	0.0374	0.0410	0.0405	9.5	8.2	0.1116	-0.1491	-0.1227	33.7	14.4	-0.438	-0.0601	-0.0591	37.1	34.8
89	0.0354	0.0352	0.0366	-0.6	3.2	0.0991	-0.1322	0.1072	33.4	8.1	-0.0676	-0.0939	-0.0939	38.9	41.6
91	-0.0447	-0.0644	-0.0572	44.2	28.1	0.1523	0.2034	0.1662	33.5	9.1	-0.1628	-0.2269	-0.2371	39.4	45.7
92	5.6889	7.9890	8.8471	40.4	55.5	-1.2904	-1.7933	-1.8708	39.0	45.0	0.8423	1.1858	1.3307	40.8	58.0
94	4.2529	5.9901	6.6758	40.8	57.0	-0.0782	-0.1066	-0.1180	36.4	51.0	0.0556	0.0615	0.0679	10.7	22.1
96	2.2871	3.2293	3.6503	41.2	59.6	-0.0206	-0.0416	-0.0554	102	169	-0.0651	-0.0649	-0.0590	-	9.4
98	0.4545	0.6564	0.7916	44.4	74.2	0.0970	0.1476	0.1346	52.2	38.7	-0.0251	-0.0606	-0.0694	142	177
106	-6.7743	-9.4786	-9.9853	39.9	47.4	0.9307	1.3108	1.4608	40.9	57.0	1.2281	1.6961	1.7741	38.1	44.5
108	-5.3918	-7.5333	-7.8742	39.7	46.0	0.0601	0.0827	0.0966	37.6	60.7	0.1182	0.1483	0.1492	25.5	26.2
110	-3.1407	-4.3826	-4.5255	39.5	44.1	-0.0780	-0.0953	-0.0914	22.2	17.2	0.1165	0.1358	0.1338	16.6	14.8
112	-1.8714	-1.2151	-1.2146	39.4	39.4	0.1941	0.2535	0.2575	30.6	32.7	0.2227	0.2762	0.2823	24.0	26.8

Table (4) Maximum Axial and Shearing Forces by LR, DnV & BV (ω = 0.37 rad/s, t = 0.0)

Member No	Max Torsion Q (NM) x 10^{-6} LR	DnV	BV	Diff % DnV	Diff % BV	Max Bending Moment M_y (NM) x 10^{-6} LR	DnV	BV	Diff % DnV	Diff % BV	Max Bending Moment M_z (NM) x 10^{-6} LR	DnV	BV	Diff % DnV	Diff % BV
1	0.0279	0.0372	0.0336	33.5	20.4	0.2193	0.3042	0.3173	38.7	44.7	-1.0487	-1.4601	-1.5108	39.2	44.1
3	0.0241	0.0323	0.0303	33.9	25.5	0.4280	0.5963	0.6315	39.3	47.5	-0.5478	-0.7569	-0.7319	38.2	33.6
5	0.0179	0.0241	0.00225	24.2	25.6	0.4335	0.6036	0.6311	39.2	45.6	-0.2988	-0.4110	-0.3738	37.5	25.1
7	0.0226	0.0312	0.0324	38.3	43.3	0.6300	0.8882	0.9788	41.0	55.4	-0.3066	-0.4147	-0.3511	35.2	14.5
8	-0.0245	-0.0343	-0.0383	40.0	56.1	0.2100	0.2920	0.3046	39.1	45.1	0.2417	0.3325	0.3266	37.6	35.1
10	-0.0601	-0.0856	-0.0981	42.4	63.3	0.4805	0.6699	0.7020	39.4	46.1	0.2342	0.3181	0.2911	35.8	24.3
12	-0.0610	-0.0862	-0.00969	41.4	58.9	0.3637	0.5085	0.5353	39.8	47.2	-0.1543	0.2001	-0.1214	29.7	-21.3
14	-0.0629	-0.0903	-0.1065	43.6	69.2	0.2996	0.4208	0.4593	40.4	53.3	0.0829	0.1144	0.1071	38.1	29.2
15	-0.0497	-0.0682	-0.0691	37.2	39.1	-0.2464	-0.3442	-0.3614	39.7	46.7	-0.4608	-0.6288	-0.6143	36.5	33.3
17	-0.1408	-0.1941	-0.1981	37.9	40.7	-0.5206	-0.7299	-0.7783	40.2	49.5	-0.4310	-0.5837	-0.5341	35.4	23.9
19	-0.1162	-0.1614	-0.1687	38.9	45.2	-0.3809	-0.5370	-0.5866	41.0	54.0	-0.3705	-0.5038	-0.4477	36.0	20.8
21	-0.1511	-0.2110	-0.2219	39.7	46.9	-0.3399	-0.4790	-0.5250	40.9	54.5	0.0877	0.1180	0.1094	34.6	24.7
85	0.0109	0.0149	0.0137	36.0	25.8	-0.3271	-0.4430	-0.4106	35.4	25.5	1.5649	2.1084	1.9169	34.7	22.5
87	0.0144	0.0191	0.0167	32.6	16.0	-0.7492	-1.0171	-0.9543	35.8	27.4	1.8511	2.4804	2.1570	34.0	16.5
89	0.0082	0.0109	0.0094	32.7	14.6	-0.9159	-1.2630	-1.2556	37.9	37.1	1.3619	1.8183	1.4810	33.5	8.7
91	0.0104	0.0137	0.0119	31.5	14.0	-1.8203	-2.5266	-2.5961	38.8	42.6	1.7165	2.2890	1.8537	33.4	8.0
92	-0.1769	-0.2733	-0.4043	54.5	129	-11.8838	-16.9224	-19.0452	42.4	60.3	-18.2431	-25.4396	-26.5214	39.4	45.4
94	-0.1448	-0.2355	-0.3931	62.6	171	-0.3962	-0.6064	-0.7621	53.1	92.4	-1.0341	-1.4596	-1.5942	41.1	54.2
96	-0.5441	-0.7916	-0.9850	45.5	81.2	0.4203	0.4887	-0.4486	16.3	6.7	-0.3626	-0.5330	-0.6485	47.0	78.8
98	0.4372	0.5785	0.4432	32.3	1.4	0.7474	1.0075	1.0862	34.8	45.3	-0.7561	-1.0133	-0.5916	34.0	-21.8
106	-1.4184	-1.9495	-1.9411	37.4	36.8	-17.5444	-24.3522	-25.4927	38.8	45.3	13.1745	18.5764	20.6555	41.0	56.8
108	-1.0071	-1.4093	-1.4875	39.9	47.7	-1.2153	-1.6657	-1.6977	37.1	39.7	0.9831	1.3452	1.4384	36.8	46.3
110	-1.4134	-1.9951	-2.1939	41.2	55.2	-0.5169	-0.6671	-0.6319	29.1	22.3	0.8894	1.1090	0.9729	24.7	9.4
112	-0.5393	-0.7799	-0.9402	44.4	74.3	1.6148	2.1190	2.2166	31.2	37.3	-2.1413	-2.9206	-2.5250	36.4	17.9

Table (5) Maximum Torsion and Bending Moments by LR, DnV & BV (ω=0.37 rad/s, t=0.0)

d. The percentage differences in the maximum torsion (Q) ranged from 31.5% to 62.6% according to DnV and from 1.4% to 171% according to BV.

e. The percentage differences in the maximum bending moment (M_y) ranged from 16.3% to 53.1% according to DnV and from 6.7% to 92.4% according to BV.

f. The percentage differences in the maximum bending moment (M_z) ranged from 24.7% to 47.0% according to DnV and from -21.8% to 78.8% according to BV.

3.1.2 LR vs DnV and BV (ω = 0.37 rad/s, t = 0.3T)

Tables (6) and (7) show that the percentage differences are generally smaller than those of Tables (4) and (5) for the majority of members.

a. The percentage differences in the maximum axial force (N) ranged from -16.9% to 35.0% according to DnV. In the case of BV, the differences ranged from -33.1% to 292%.

b. The percentage differences in the maximum shearing force (F_y) ranged from 1.9% to 52.7% according to DnV. In the case of BV, the differences ranged from -23.8% to 90.9%.

c. The differences in the maximum shearing force (F_z) ranged from 0.5% to 36.4% according to DnV. In the case of BV, the differences ranged from -5.4% to 26.6%.

d. The percentage differences in the maximum torsion (Q) ranged from -89.7% to 52.7% according to DnV. In the case of BV, the differences ranged from -90.3% to 131%.

Member No	Max Axial Force N (N) x 10^{-6}					Max Shearing Force F_y (N) x 10^{-6}					Max Shearing Force F_z (N) x 10^{-6}				
				Diff %					Diff %					Diff %	
	LR	DnV	BV	DnV	BV	LR	DnV	BV	DnV	BV	LR	DnV	BV	DnV	BV
1	-4.74	-5.33	-4.97	12.4	4.9	-0.0881	-0.100	0.0919	13.5	4.3	0.0163	0.0202	0.0178	23.9	9.2
3	-3.07	-3.44	-3.21	12.1	4.6	-0.0389	-0.0475	-0.0474	22.1	21.9	0.0261	0.0344	0.0303	31.8	16.1
5	-1.83	-2.03	1.89	10.9	3.3	-0.0426	-0.0569	-0.0600	33.6	40.8	0.0234	0.0315	0.0292	34.6	24.8
7	-0.205	-0.254	-0.25	23.9	22.0	0.0983	0.1390	0.152	41.4	54.6	0.0376	0.0513	0.0476	36.4	26.6
8	5.62	6.33	.5.91	12.6	5.2	0.0278	0.0333	0.0319	19.8	14.7	0.0205	0.0257	0.0226	25.4	10.2
10	3.80	4.27	4.00	12.4	5.3	-0.0414	-0.0557	-0.0584	34.5	41.1	0.0272	0.0349	0.0301	28.3	10.7
12	2.44	2.74	2.59	12.3	6.1	-0.0849	-0.117	-0.122	37.8	43.7	0.0187	0.0237	0.0197	26.7	5.3
14	0.206	0.269	0.272	30.6	32.0	-0.0406	-0.0560	-0.0583	37.9	43.6	0.0118	0.0158	0.0136	33.9	15.3
15	-5.63	-6.34	-5.91	12.6	5.0	0.0331	0.0396	0.0343	19.6	3.6	0.0228	0.0290	0.0258	27.2	13.2
17	-3.77	-4.22	-3.93	11.9	4.2	-0.0228	-0.0274	-0.0182	20.2	-20.2	0.0309	0.0402	0.0356	30.1	15.2
19	-2.30	-2.53	-2.35	10.0	2.2	0.0130	0.0157	-0.0099	20.8	-23.8	0.0247	0.0323	0.0289	30.8	17.0
21	-0.0112	0.0093	0.0439	-16.9	292	0.0157	0.0194	0.0153	23.6	-2.53	0.0130	0.0177	0.0161	36.2	23.8
85	-0.0161	-0.0197	-0.0123	22.4	-23.6	0.0247	0.0289	0.0263	17.0	6.5	0.0498	0.0665	0.0566	33.5	13.7
87	-0.0339	-0.0431	-0.0362	27.1	6.8	-0.0243	-0.0371	-0.0464	52.7	90.9	0.0795	.0.106	-0.0905	33.3	13.8
89	-0.0423	-0.0539	-0.0474	27.4	12.1	-0.0844	-0.120	-0.136	42.2	61.1	-0.0746	-0.101	-0.0859	35.4	15.1
91	-0.0626	-0.0845	-0.0901	35.0	43.9	-0250	-0.353	-0.388	41.2	55.2	-0.124	-0.167	-0.146	34.7	17.7
92	-13.10	-14.9	-14.10	13.7	7.6	2.78	3.13	2.89	12.6	4.0	-2.66	-2.99	-2.82	12.4	6.0
94	-9.63	-11.0	-10.50	14.2	9.0	0.265	0.303	0.282	14.3	6.4	-0.175	-0.188	-0.182	7.4	4.0
96	-5.09	-5.90	-5.69	15.9	11.8	0.231	0.262	0.249	13.4	7.8	0.168	0.175	0.168	4.2	-
98	-1.27	-1.55	-1.54	22.0	21.3	0.365	0.418	0.421	14.5	15.3	-0.275	-0.294	-0.293	6.9	6.5
106	12.0	13.4	12.40	11.7	3.3	-2.87	-3.26	-3.06	13.6	6.6	-2.63	-2.92	-2.71	11.0	3.0
108	8.43	9.33	8.59	10.7	1.9	-0.225	-0.249	-0.238	10.7	5.8	-0.221	-0.237	-0.221	7.2	-
110	3.83	4.15	3.75	8.4	-2.1	-0.173	-0.180	-0.180	4.0	4.0	-0.186	-0.187	-0.176	0.5	-5.4
112	0.453	0.421	0.303	-7.1	-33.1	0.313	0.319	0.319	1.9	1.9	-0.294	-0.305	-0.287	3.7	-2.4

Table (6) Maximum Axial and Shearing Forces by LR, DnV & BV (ω =0.37 rad/s, t = 0.3T)

Member No	Maximum Torsion Q (NM) x 10^{-6}					Max Bending Moment M_Y (NM) x 10^{-6}					Max Bending Moment M_Z (NM) x 10^{-6}				
				Diff %					Diff %					Diff %	
	LR	DnV	BV	DnV	BV	LR	DnV	BV	DnV	BV	LR	DnV	BV	DnV	BV
1	-0.0218	-0.0295	-0.0278	35.3	27.5	0.480	0.600	0.538	25.0	12.1	-2.130	-2.40	-2.25	12.7	5.6
3	-0.0229	-0.0299	-0.0269	30.6	17.5	0.814	1.08	0.952	32.7	17.0	-0.651	-0.731	-0.717	12.3	10.1
5	-0.0193	-0.0249	-0.0236	29.0	22.3	0.579	0.777	0.699	34.2	20.7	-0.333	-0.414	-0.422	24.3	26.7
7	-0.0173	-0.0226	-0.0187	30.6	8.1	0.782	1.06	0.961	35.5	22.9	-0.521	-0.744	-0.813	42.8	56.0
8	0.0515	0.0695	0.0597	35.0	15.9	-0.370	-0.490	-0.424	32.4	14.6	-0.662	-0.768	-0.726	16.0	9.7
10	0.0994	0.135	0.118	35.8	18.7	-0.568	-0.752	-0.642	32.4	13.0	-0.429	-0.523	-0.534	21.9	24.5
12	0.0608	0.0837	0.0729	37.7	19.9	-0.298	-0.391	-0.321	31.2	7.7	-0.520	-0.700	-0.726	34.6	39.6
14	0.0785	0.107	0.0986	36.3	25.6	-0.254	-0.342	-0.295	34.6	16.1	-0.0793	-0.113	-0.131	42.5	65.2
15	0.0839	0.112	0.0967	33.5	15.3	0.485	0.645	0.560	33.0	15.5	0.673	0.774	0.700	15.0	4.0
17	0.169	0.224	0.192	32.5	13.6	0.752	1.01	0.879	34.3	16.9	0.337	0.376	0.314	11.6	-6.8
19	0.114	0.152	0.131	33.3	14.9	0.476	0.642	0.572	34.9	20.2	0.0947	0.0947	0.0545	-	-42.4
21	0.124	0.166	0.142	33.9	14.5	0.396	0.538	0.486	35.9	22.7	0.104	0.140	0.140	34.6	34.6
85	-0.0125	-0.0164	-0.0141	31.2	12.8	0.751	1.01	0.844	34.5	12.4	-0.943	-1.04	0.895	10.3	-5.1
87	-0.0052	-0.0059	-0.004	12.4	-24.5	1.01	1.34	1.19	32.7	17.8	0.353	0.453	0.632	28.3	79.0
89	-0.0015	-0.0010	0.0001	-30.6	-90.3	0.871	1.17	1.00	34.3	14.8	0.964	1.41	1.63	46.3	69.1
91	-0.0016	-0.0002	0.0013	-89.7	-18.9	1.21	1.64	1.44	35.5	19.0	2.70	3.82	4.25	41.5	57.4
92	1.30	1.73	1.54	33.1	18.5	38.1	42.9	40.5	12.6	6.3	39.0	43.9	40.5	12.6	3.8
94	0.569	0.776	0.720	36.4	26.5	2.00	2.21	2.13	10.5	6.5	2.69	3.15	2.88	17.1	7.1
96	0.387	0.534	0.509	38.0	31.5	0.745	0.819	0.776	9.9	4.2	1.17	1.52	1.37	29.9	17.1
98	0.205	0.313	0.473	52.7	131	-1.86	-2.07	-1.97	11.3	5.9	-2.74	-3.20	-3.38	16.8	23.4
106	2.49	3.320	2.85	33.3	14.5	37.3	41.6	38.5	11.5	3.2	-40.1	-45.60	-42.9	13.7	7.0
108	1.29	1.73	1.50	34.1	16.3	1.99	2.24	2.05	12.6	3.0	2.25	-2.53	-2.38	12.4	5.8
110	1.11	1.51	1.33	36.0	19.8	-1.08	-1.08	-1.04	-	13.7	0.702	0.827	0.868	17.8	23.6
112	0.533	0.736	0.757	38.1	42.0	-2.61	-2.79	-2.66	6.9	1.9	-2.40	-3.39	-3.87	41.3	61.3

Table (7) Maximum Torsion and Bening Moments by LR, DnV & BV (ω=0.37 rad/s, t=0.3T)

e. The differences in the maximum bending moment (M_y) ranged from 6.9% to 35.9% according to DnV, while in the case of BV the differences ranged from -3.7% to 22.9%.

f. The differences in the maximum bending moment (M_z) ranged from 10.3% to 46.4% according to DnV. In the case of BV, the differences ranged from -42.4% to 79.0%.

3.1.3 LR vs DnV and BV (ω = 0.37 rad/s, t = 0.6T)

Tables (8) and (9) show that:-

a. The percentage differences in the maximum axial force (N) ranged from -87.3% to 413% according to DnV, and from -81.3% to 585% according to BV.

b. The differences in the shearing force (F_y) ranged from -41.2% to 39.7% according to DnV, and from -78.1% to 50.9% according to BV.

c. The differences in the shearing force (F_z) ranged from -64.8% to 92.1% according to DnV, and from -83.9% to 244% according to BV.

d. The differences in the maximum torsion (Q) ranged from 19.8% to 275% according to DnV, and from -52.9% to a large value of 1445% according to BV. However, it is to be noted that the absolute values of the torsional moments are negligible in this case.

e. The differences in the maximum bending moment (M_y) ranged from -38.2% to 58.8% according to DnV, and from -72.7% and 226% according to BV.

Member No	Max Axial Force N (N) x 10^{-6}					Max Shearing Force F_y (N) x 10^{-6}					Max Shearing Force F_z (N) x 10^{-6}				
				Diff %					Diff %					Diff %	
	LR	DnV	BV	DnV	BV	LR	DnV	BV	DnV	BV	LR	DnV	BV	DnV	BV
1	-1.3134	-1.02	-0.619	-22.1	-52.7	0.0410	0.0427	0.0330	4.1	-19.5	-0.0095	-0.0115	-0.0094	20.9	-0.9
3	-0.7088	-0.439	-0.173	-38.1	-75.6	0.0401	0.0502	-0.0447	25.2	11.5	-0.0141	-0.0181	-0.0137	28.4	-2.8
5	-0.3406	-0.294	-0.466	-13.8	36.7	0.0406	-0.0551	-0.0530	35.7	30.5	0.0098	0.0142	0.0170	45.0	73.6
7	-0.1822	-0.220	-0.250	20.9	37.4	0.0928	0.1270	0.124	36.9	33.6	0.0147	0.0213	0.0271	44.9	84.4
8	-1.5540	-1.22	-0.735	-21.3	-52.6	-0.0352	-0.0451	-0.0380	28.1	8.0	-0.0044	-0.0044	0.0032	1.1	-27.1
10	-0.8788	-0.571	-0.226	-35.0	-74.3	0.0584	0.0768	0.066	31.5	13.0	0.0064	0.0085	0.0103	33.9	61.7
12	-0.3639	-0.0887	0.148	-75.6	-59.3	0.0531	0.0703	0.0566	32.4	6.6	0.0084	0.0115	0.0123	36.3	45.7
14	-0.0730	-0.0850	-0.0615	16.4	-15.8	0.0218	0.0281	0.0245	28.9	12.4	0.0021	0.0033	0.0054	54.7	155
15	1.3762	0.982	0.525	-28.8	-62.0	-0.0315	-0.0406	-0.0359	28.9	14.0	-0.0049	-0.0051	-0.0021	2.0	-56.8
17	0.5998	0.197	-0.122	-67.2	-81.3	-0.0512	-0.0712	-0.0679	39.1	32.6	-0.0021	0.0029	0.0071	37.0	242
19	0.0786	-0.299	-0.502	280	539	-0.0806	-0.122	-0.113	39.0	40.2	0.0019	0.0033	0.0064	76.5	244
21	-0.1807	-0.261	-0.270	44.2	49.2	0.0411	0.0574	0.0620	39.7	50.9	-0.0010	-0.0009	0.0026	-10.0	162
85	-0.0447	-0.0548	-0.0522	22.6	16.8	-0.0656	0.0851	-0.0747	29.7	13.9	0.0336	0.0445	0.0370	32.7	10.1
87	-0.0314	-0.0354	-0.0402	12.7	28.0	0.1096	0.148	-0.131	34.5	19.1	0.0507	0.0668	0.0540	31.8	6.5
89	-0.0487	-0.0572	-0.0663	17.5	36.1	-0.1248	-0.169	-0.156	35.2	24.8	0.0252	0.0319	0.0384	26.6	52.4
91	0.0136	0.0203	0.0095	49.3	-30.2	-0.2433	-0.332	-0.318	36.6	30.9	0.0714	0.103	0.127	44.3	77.9
92	3.2416	2.39	1.13	-26.2	-65.1	-0.5796	-0.341	-0.127	-41.2	-78.1	0.9976	0.918	0.683	-8.0	-31.6
94	2.3678	1.76	0.812	-25.7	-65.7	-0.1257	-0.124	-0.105	-1.6	-16.7	0.1206	0.117	0.104	-3.3	-14.0
96	1.2587	0.986	0.476	-21.7	-62.2	-0.1545	-0.159	-0.142	2.6	-8.4	0.1375	0.138	0.134	-	-2.9
98	0.4637	0.486	0.362	4.7	-22.0	-0.2478	-0.271	-0.243	9.3	-2.0	-0.2008	-0.184	-0.177	-8.5	-11.9
106	-1.6533	-0.210	0.821	-87.3	-50.2	0.9451	0.845	0.591	-10.6	-37.5	0.5735	0.361	0.167	-37.1	-70.9
108	-0.6670	0.573	1.29	-14.1	93.4	0.0934	0.0959	0.0798	2.7	-14.6	0.0264	0.0093	-0.0043	-64.8	-83.9
110	0.1968	1.01	1.35	413	585	0.0751	0.0765	0.0683	1.9	-9.1	-0.0220	-0.0222	-0.0266	-3.5	15.7
112	0.3491	0.614	0.664	75.9	90.3	0.1249	0.1520	0.138	21.6	10.4	-0.0557	-0.107	-0.1260	92.1	126

Table (8) Maximum Axial and Shearing Forces by LR, DnV & BV (ω=0.37 rad/s, t=0.6T)

Member No	Maximum Torsion Q (NM) x 10^{-6}					Max Bending Moment M_y (NM) x 10^{-6}					Max Bending Moment M_z (NM) x 10^{-6}				
				Diff %					Diff %					Diff %	
	LR	DnV	BV	DnV	BV	LR	DnV	BV	DnV	BV	LR	DnV	BV	DnV	BV
1	-0.0190	-0.0252	-0.0249	32.6	31.1	-0.1889	-0.217	0.172	14.8	-9.0	0.7283	0.647	0.444	-11.1	5.7
3	-0.0106	-0.0131	-0.0137	23.6	29.2	0.2517	0.343	0.338	36.1	34.1	0.3470	0.368	0.294	6.1	17.4
5	-0.0128	-0.0166	-0.0169	29.7	32.0	0.2097	0.287	0.280	36.7	33.3	0.2209	0.300	0.306	35.7	22.2
7	-0.0133	-0.0193	-0.0230	45.1	72.9	0.2347	0.327	0.351	39.1	49.4	0.4502	0.614	0.599	36.4	29.3
8	-0.0229	-0.0303	-0.0217	32.3	-5.2	0.0960	0.118	0.105	22.9	9.4	0.3744	0.401	0.320	9.6	-83.9
10	-0.0450	-0.0593	-0.0402	31.8	-10.7	0.1477	0.203	0.210	37.2	41.9	0.3908	0.476	0.399	21.7	-26.5
12	-0.0166	-0.0213	-0.0078	28.3	-52.9	0.1250	0.172	0.176	37.6	40.8	0.3077	0.402	0.336	30.5	-1.7
14	-0.0477	-0.0626	-0.0475	31.2	-	0.0434	0.0617	-0.0869	42.2	100	0.0771	0.105	0.102	36.2	20.3
15	0.0009	0.0033	0.0135	275	1445	0.0417	0.0649	0.0604	55.3	44.5	0.1774	0.248	0.223	40.1	-36.9
17	0.0445	0.0668	0.0911	50.1	105	0.0741	0.118	0.242	58.8	226	0.2823	0.405	0.396	43.6	8.7
19	0.0499	0.0733	0.0938	46.9	88	0.0754	0.113	0.200	49.9	165	0.4357	0.618	0.621	41.7	25.0
21	0.0661	0.0959	0.1220	45.1	84.6	0.0647	0.0921	0.152	42.3	135	-0.0977	-0.134	-0.134	37.2	29.6
85	-0.0091	-0.0130	-0.0140	42.7	53.7	-0.5807	-0.778	-0.659	33.9	13.4	-1.4042	-1.74	-1.48	24.3	5.7
87	-0.0165	-0.0230	-0.0223	39.4	35.2	-0.8698	-1.16	-0.991	33.3	13.9	-1.7752	-2.34	-2.09	31.5	17.4
89	-0.0111	-0.0156	-0.0152	40.5	36.9	-0.4084	0.548	0.6860	34.3	68.1	-1.6724	-2.26	-2.04	35.3	22.2
91	-0.0139	-0.0197	-0.0193	41.7	38.8	0.9833	1.40	1.630	42.4	65.8	-2.7010	-3.68	-3.49	36.3	29.3
92	-0.9779	-1.290	-1.05	31.9	7.4	-13.8774	-12.7	-9.31	-8.6	-33.0	-7.6502	-4.24	-1.23	-44.6	-83.9
94	-0.6134	-0.813	-0.661	32.6	7.8	-0.9547	-0.909	-0.713	-4.8	-25.3	-0.8068	-0.741	0.593	-8.2	-26.5
96	-0.3350	-0.435	-0.292	29.9	-12.8	-0.5746	-0.630	-0.599	9.6	4.2	0.8326	0.884	0.819	6.1	-1.7
98	-0.7008	-0.965	-0.947	37.7	35.1	-0.7268	-0.977	-1.110	34.4	52.7	2.1731	2.83	2.61	30.4	20.3
106	0.0441	0.2340	0.517	62.5	259	-8.1110	-5.01	-2.21	-38.2	-72.7	13.0305	11.60	7.940	-10.8	-38.9
108	0.3466	0.5260	0.759	51.6	118.7	0.2413	0.194	0.205	-19.5	-14.9	-0.9754	-1.22	-1.06	25.1	8.7
110	0.7488	1.090	1.400	45.5	86.9	0.3885	0.508	0.515	30.6	32.4	0.8244	-1.13	-1.030	37.1	25.0
112	0.0718	0.0860	0.1310	19.8	82.5	0.6477	-0.716	-0.902	10.5	39.2	2.5271	3.47	3.280	37.2	29.6

Table (9) Maximum Torsion and Bending Moments by LR, DnV & BV (ω = 0.37 rad/s, t=0.6T)

f. The differences in the maximum bending moment (M_z) ranged from -44.6% to 43.6% according to DnV, and from -83.9% to 29.6% according to BV.

3.1.4 <u>LR vs DnV and BV (ω = 0.56 rad/s, t = 0.0)</u>

Tables (10) and (11) show that:-

a. The differences in the maximum axial force (N) ranged from -11.4% to 47.2% according to DnV, while BV gave differences ranging from -34.7% to 166%.

b. The differences in the maximum shearing force (F_y) ranged from -3.2% to 38.1% in the case of DnV, while BV gave differences ranging from -7.3% to 60.9%.

c. The differences in the maximum shearing force (F_z) ranged from -8.1% to 48.6% in the case of DnV, while BV gave differences ranging from -10.0% to 79.3%.

d. The differences in the maximum torsion (Q) ranged from 20.2% to 42.7% in the case of DnV, while BV gave differences ranging from -90.5% to 71.2%.

e. The differences in the maximum bending moment (M_y) ranged from 6.2% to 46.1% according to DnV, and from 5.9% to 83.3% according to BV.

f. The differences in the maximum bending moment (M_z) ranged from 12.9% to 44.4% in the case of DnV, while BV gave differences ranging from 4.6% to 49.6%.

Member No	Max Axial Force N (N) $\times 10^{-6}$ LR	DnV	BV	Diff % DnV	Diff % BV	Max Shearing Force F_y (N) $\times 10^{-6}$ LR	DnV	BV	Diff % DnV	Diff % BV	Max Shearing Force F_z (N) $\times 10^{-6}$ LR	DnV	BV	Diff % DnV	Diff % BV
1	0.533	0.738	0.797	38.5	49.5	0.0113	0.0155	0.0161	37.2	42.5	-0.0030	-0.0040	-0.0038	35.7	27.6
3	0.549	0.737	0.778	34.2	41.7	0.0146	0.0192	0.0178	31.5	21.9	-0.0071	-0.0096	-0.0090	35.1	26.4
5	0.766	0.962	0.985	25.6	28.6	0.0250	0.0326	0.0280	30.4	12.0	-0.0109	-0.0148	-0.0140	35.8	28.4
7	0.595	0.626	0.611	5.2	2.7	-0.0844	-0.114	-0.0989	35.1	17.2	-0.0223	-0.0306	-0.0308	37.2	38.1
8	-0.587	-0.823	-0.900	40.2	53.3	-0.0076	-0.0103	-0.0092	35.0	20.8	-0.0011	-0.0016	-0.0018	44.0	68.8
10	-0.514	-0.721	-0.792	40.3	54.1	-0.0220	-0.0293	-0.0248	33.2	12.7	-0.0048	-0.0068	-0.0071	39.9	47.5
12	-0.549	-0.766	-0.849	39.5	54.6	-0.0424	-0.0567	-0.0450	33.7	6.1	-0.0074	-0.0103	-0.0104	39.6	40.9
14	0.0202	0.0179	-0.0132	-11.4	-34.7	-0.0050	-0.0049	-0.0049	-3.2	-3.4	-0.0045	-0.0063	-0.0069	41.0	55.2
15	0.619	0.865	0.936	39.7	51.2	-0.0069	-0.0093	-0.0086	35.0	25.8	-0.0036	-0.0050	-0.0048	37.2	32.2
17	0.612	0.849	0.903	38.7	47.5	0.0230	0.0307	0.0264	33.5	14.8	-0.0082	-0.0114	-0.0112	39.0	36.6
19	0.714	0.982	1.02	37.5	42.9	0.0455	0.0610	0.0498	34.1	9.5	-0.0088	-0.0124	-0.0128	40.6	45.1
21	0.215	0.293	0.272	36.3	26.5	-0.0400	-0.0529	-0.0514	32.3	28.5	-0.0029	-0.0043	-0.0052	48.6	79.3
85	0.0215	0.0253	0.0217	17.7	0.9	-0.0107	-0.0143	-0.0129	33.6	20.6	-0.0041	-0.0055	-0.0047	33.6	13.5
87	0.0471	0.0533	0.0488	13.2	3.6	-0.0321	-0.0429	-0.0368	33.6	14.6	-0.0149	-0.0199	-0.0172	33.6	15.4
89	0.123	0.134	0.126	8.9	2.4	0.0636	0.0849	0.0694	33.5	9.1	-0.0286	-0.0387	-0.0350	35.3	22.4
91	0.114	0.123	0.119	7.9	4.4	0.223	0.299	0.251	34.1	12.6	-0.161	-0.222	-0.222	37.9	37.9
92	1.93	2.67	3.03	38.3	57.0	-0.402	-0.555	-0.572	38.1	42.3	0.146	0.210	0.261	43.8	78.8
94	1.42	1.97	2.29	38.7	61.3	-0.0252	-0.0326	-0.0361	29.4	43.3	0.0295	0.0312	0.0329	5.8	11.5
96	0.689	0.965	1.22	40.1	77.1	0.0860	0.0892	0.0835	3.7	-2.9	-0.0709	-0.0699	-0.0682	-1.4	-3.8
98	-0.0375	-0.0380	0.0997	1.3	166	0.234	0.251	0.217	7.3	-7.3	0.211	0.194	0.190	-8.1	-10.0
106	-2.33	-3.16	-3.29	41.7	47.5	0.233	0.328	0.375	40.8	60.9	0.319	0.440	0.463	37.9	45.1
108	-1.89	-2.69	-2.76	42.3	46.0	-0.0263	-0.0258	0.0252	-1.9	-4.2	0.0361	0.0416	0.0416	15.2	15.2
110	-1.27	-1.81	-1.81	42.5	42.5	-0.0950	-0.0987	-0.0930	3.9	-2.1	0.0802	0.0806	0.0760	0.5	-5.2
112	-0.394	-0.580	-0.536	47.2	36.0	-0.231	-0.244	-0.249	5.6	7.8	0.296	0.330	0.325	11.5	9.8

Table (10) Maximum Axial and Shearing Forces by LR, DnV & BV (ω=0.56 rad/s, t=0.0)

Member No	Maximum Torsion Q (NM) $\times 10^{-6}$ LR	DnV	BV	Diff % DnV	Diff % BV	Max Bending Moment M_y (NM) $\times 10^{-6}$ LR	DnV	BV	Diff % DnV	Diff % BV	Max Bending Moment M_z (NM) $\times 10^{-5}$ LR	DnV	BV	Diff % DnV	Diff % BV
1	0.0094	0.0125	0.0117	33.1	24.6	-0.0698	-0.0934	-0.0819	33.8	17.3	-0.244	-0.343	-0.365	40.6	49.6
3	0.0123	0.0161	0.0150	30.9	22.0	-0.179	-0.240	-0.210	34.1	17.3	-0.139	-0.199	-0.195	43.2	40.3
5	0.0089	0.0112	0.0118	26.6	33.3	-0.169	-0.225	-0.194	33.1	14.8	-0.139	-0.176	-0.155	26.6	11.5
7	0.0234	0.0319	0.0320	36.3	36.8	-0.295	-0.416	-0.461	41.0	56.3	-0.391	-0.536	-0.458	37.1	17.1
8	0.0070	0.0092	0.0067	31.8	-4.3	-0.0302	-0.040	-0.0336	32.5	11.3	0.0612	0.0848	0.0853	38.6	39.4
10	0.0212	0.0278	0.0184	31.1	-13.2	-0.103	-0.139	-0.126	35.0	22.3	0.105	0.144	0.132	37.1	25.7
12	0.0077	0.0093	-0.0007	20.2	-90.5	-0.104	-0.141	-0.128	35.6	23.1	-0.218	-0.290	-0.228	33.0	4.6
14	0.0379	0.0483	0.0323	27.4	-14.8	0.0739	0.105	0.130	42.1	75.9	0.0727	0.105	0.0963	44.4	32.5
15	-0.0191	-0.0257	-0.0232	34.6	21.5	-0.118	-0.160	-0.147	35.6	24.6	-0.104	-0.142	-0.142	36.5	36.5
17	-0.0754	-0.102	-0.0938	35.3	24.4	-0.273	-0.375	-0.358	37.4	31.1	-0.153	-0.204	-0.183	33.3	19.6
19	-0.0769	-0.105	-0.101	36.5	31.3	-0.220	-0.308	-0.316	40.0	43.6	-0.249	-0.328	-0.277	31.7	11.2
21	-0.104	-0.143	-0.140	37.5	34.6	-0.162	-0.228	-0.247	40.7	52.5	0.0901	0.121	0.108	34.3	19.9
85	0.0099	0.0133	0.0122	34.6	23.5	0.104	0.139	0.120	33.7	15.4	0.248	0.337	0.320	35.9	29.0
87	0.0128	0.0170	0.0148	32.8	15.6	-0.349	-0.465	-0.392	33.2	12.3	0.544	0.728	0.634	33.8	16.5
89	0.0103	0.0138	0.0119	34.0	15.5	-0.461	-0.620	-0.548	34.5	18.9	0.850	1.13	0.913	32.9	7.4
91	0.0166	0.0221	0.0191	33.1	15.1	-1.91	-2.63	-2.61	37.7	36.6	2.46	3.29	2.71	33.7	10.2
92	0.357	0.473	0.379	32.5	6.2	-2.04	-2.98	-3.74	46.1	83.3	-5.66	-7.85	-8.08	38.7	42.8
94	0.357	0.469	0.353	31.4	-1.1	0.109	-0.134	-0.172	22.9	57.8	-0.322	-0.429	-0.453	33.2	40.7
96	0.290	0.360	0.172	24.1	-40.7	0.322	0.342	0.303	6.2	-5.9	-0.598	-0.675	-0.647	12.9	8.2
98	0.528	0.694	0.511	31.4	-3.2	1.00	1.21	1.26	21.0	26.0	-1.82	-2.43	-2.06	33.5	13.2
106	-0.721	-0.971	-0.869	34.7	20.5	-4.63	-6.43	-6.75	38.9	45.8	3.24	4.58	5.25	41.4	62.0
108	-0.698	-0.949	-0.880	36.0	26.1	-0.351	-0.476	-0.488	35.6	39.0	0.312	0.366	0.375	17.3	20.2
110	-1.11	-1.54	-0.0154	38.7	38.7	-0.322	-0.382	-0.355	18.6	10.2	0.939	1.10	1.01	17.1	7.6
112	-0.736	-1.05	-0.0126	42.7	71.2	1.85	2.17	2.20	17.3	18.9	-1.65	-2.29	-1.82	38.8	10.3

Table (11) Maximum Torsion and Bending Moments by LR, DnV & BV (ω = 0.56 rad/s, t = 0.0)

3.1.5 LR vs DnV and BV ($\omega = 0.56$ rad/s, $t = 0.3T$)

Tables (12) and (13) show that the percentage differences are smaller than the corresponding values of tables (10) and (11) as follows:-

a. The percentage differences in the maximum axial force (N) ranged from -3.3% to 29.7% according to DnV, and from -67.3% to 31.4% according to BV.

b. The differences in the maximum shearing force (F_y) ranged from -3.6% to 40.7% accoruing to DnV, and from -16.6% to 54.3% according to BV.

c. The differences in the maximum shearing force (F_z) ranged from -3.1% to 36.6% according to DnV and from -6.2% to 27.4% according to BV.

d. The differences in the maximum torsion (Q) ranged from -5.1% to 50.5% according to DnV and from -56.8% to 113% according to BV.

e. The differences in the maximum bending moment (M_y) ranged from -6.4% to 35.6% according to DnV, and from -11.8% to 21.4% according to BV.

f. The differences in the maximum bending moment (M_z) ranged from 1.4% to 43.0% according to DnV and from -20.5% to 58.7% according to BV.

3.1.6 LR vs DnV and BV ($\omega = 0.56$ rad/s, $t = 0.6T$)

Tables (14) and (15) show that:-

Member No	Max Axial Force N (N) x 10^{-6} LR	DnV	BV	Diff % DnV	Diff % BV	Max Shearing Force F_y (N) x 10^{-6} LR	DnV	BV	Diff % DnV	Diff % BV	Max Shearing Force F_z (N) x 10^{-6} LR	DnV	BV	Diff % DnV	Diff % BV
1	-2.62	-2.92	-2.73	11.5	4.2	-0.0459	-0.0514	-0.048	12.0	4.6	0.0062	0.0074	0.0066	18.6	5.8
3	-2.11	-2.35	-2.2	11.4	4.3	-0.0250	-0.0291	-0.0266	16.4	6.4	0.0108	0.0142	0.0120	31.5	11.1
5	-1.75	-1.94	-1.81	10.9	3.4	-0.0192	-0.0229	-0.0210	19.3	9.4	0.0127	0.0160	0.0143	32.3	12.6
7	-0.198	-0.194	-0.162	-2.0	-18.2	0.0947	0.133	0.140	40.4	47.8	0.0328	0.0448	0.0418	36.6	27.4
8	3.12	3.46	3.25	10.9	4.2	0.0110	0.0123	0.0116	11.8	5.5	0.0763	0.0093	0.0085	21.6	11.0
10	2.60	2.88	2.71	10.8	4.2	-0.0047	-0.0050	-0.0047	6.3	-1.7	0.0154	0.0196	0.0175	27.3	13.6
12	2.26	2.51	2.38	11.1	5.3	-0.0210	-0.0286	-0.0324	36.2	54.3	0.0173	0.0221	0.0194	27.7	12.1
14	0.229	0.297	0.301	29.7	31.4	-0.0395	-0.0540	-0.0555	36.7	40.5	0.0096	0.0127	0.0108	32.7	12.9
15	-3.13	-3.48	-3.26	11.2	4.2	0.0132	0.0152	0.0140	15.2	6.1	0.009	0.0110	0.0097	22.8	8.3
17	-2.62	-2.91	-2.73	11.1	4.2	-0.0092	-0.0108	-0.0091	17.9	-0.5	0.0174	0.0223	0.0192	28.2	10.3
19	-2.25	-2.51	-2.35	11.6	4.4	0.0163	0.0211	0.0136	29.4	-16.6	0.0202	0.0261	0.0228	29.2	12.9
21	-0.0881	-0.0918	-0.0544	4.2	-38.3	0.0225	0.0276	0.0216	22.7	-4.0	0.0098	0.0133	0.0119	36.0	21.7
85	-0.0030	-0.0029	-0.0099	-3.3	-67.3	0.0124	0.0142	0.0132	14.5	6.5	0.0071	0.0094	0.0079	32.9	11.6
87	-0.0235	-0.0287	-0.0232	22.1	-1.3	-0.0139	-0.0195	-0.0158	40.3	13.7	0.0250	0.0333	0.0279	33.2	11.6
89	-0.0602	-0.0711	-0.0585	18.1	-2.8	-0.0186	-0.0246	-0.0256	32.3	37.6	0.0461	0.0613	0.0488	33.0	5.9
91	-0.0596	-0.0665	-0.0517	11.6	-13.3	-0.226	-0.318	-0.345	40.7	52.7	-0.163	-0.220	-0.195	35.0	19.6
92	-9.24	-10.40	-9.80	12.6	6.1	1.530	1.710	1.59	11.8	3.9	-1.33	-1.460	-1.390	9.8	4.5
94	-7.21	-8.11	-7.70	12.5	6.8	0.119	0.134	0.125	12.6	5.0	-0.0617	-0.0663	-0.0634	7.5	2.8
96	-4.19	-4.75	-4.56	13.4	8.8	0.0907	0.101	0.0960	11.4	5.8	0.0713	0.0786	0.0754	10.2	5.8
98	-1.11	-1.30	-1.30	17.1	17.1	-0.259	0.283	0.294	9.3	13.5	-0.251	-0.284	-0.282	13.1	12.4
106	8.38	9.48	8.86	10.5	3.3	-1.510	-1.68	-1.580	11.3	4.6	-1.37	-1.510	-1.420	10.2	3.6
108	6.57	7.24	6.75	10.2	2.7	-0.108	-0.118	-0.111	9.3	2.8	-0.0828	-0.0886	-0.0838	7.0	1.2
110	3.53	3.850	3.57	9.1	1.1	0.0933	0.0899	0.0846	-3.6	-9.3	-0.0834	-0.0808	-0.0782	-3.1	-6.2
112	0.537	0.530	0.456	-1.3	-15.1	0.379	0.3820	0.368	0.8	-2.9	-0.338	-0.3550	-0.330	5.0	-2.4

Table (12) Maximum Axial and Shearing Forces by LR,DnV & BV (ω = 0.56 rad/s, t = 0.3T)

Member No	Max Torsion Q (NM) x 10^{-6} LR	DnV	BV	Diff % DnV	Diff % BV	Max Bending Moment M_Y (NM) x 10^{-6} LR	DnV	BV	Diff % DnV	Diff % BV	Max Bending Moment M_Z (NM) x 10^{-6} LR	DnV	BV	Diff % DnV	Diff % BV
1	-0.0118	-0.0161	-0.0135	36.4	14.4	-0.162	-0.193	-0.175	19.1	8.0	-1.16	-1.29	-1.21	11.2	4.3
3	-0.0123	-0.-163	-0.0129	32.5	4.9	0.302	0.397	0.342	31.5	13.2	0.402	0.439	0.413	9.2	2.7
5	-0.0126	-0.0159	-0.0135	26.2	7.1	0.333	0.444	0.385	33.3	15.6	-0.163	-0.179	-0.171	9.8	4.9
7	-0.0247	-0.0340	-0.0303	37.7	22.7	0.676	0.914	0.815	35.2	20.6	-0.449	-0.642	-0.685	43.0	52.6
8	0.0125	0.0169	0.0155	35.2	24.0	-0.103	-0.137	-0.125	33.0	21.4	-0.321	-0.357	-0.335	11.2	4.4
10	0.0422	0.0580	0.0542	37.4	28.4	-0.293	-0.392	-0.354	33.8	20.8	-0.157	-0.167	-0.158	6.4	0.6
12	0.0459	0.0638	0.0599	39.0	30.5	-0.274	-0.364	-0.325	32.8	18.6	-0.160	-0.202	-0.220	26.3	37.5
14	0.0520	0.0722	0.0741	38.8	42.5	-0.208	-0.282	-0.251	35.6	20.7	-0.0768	0.103	0.0978	34.1	27.3
15	0.0239	0.0319	0.0264	33.5	10.5	0.168	0.221	0.184	31.5	9.5	0.341	0.384	0.357	12.6	4.7
17	0.0834	0.111	0.0906	33.1	8.6	0.403	0.536	0.446	33.0	10.7	0.207	0.225	0.211	8.7	1.9
19	0.0862	0.114	0.0943	32.3	9.4	0.366	0.488	0.415	33.3	13.4	0.111	0.131	0.0882	18.0	-20.5
21	0.0980	0.131	0.105	33.7	7.1	0.326	0.441	0.390	35.3	19.6	0.118	0.154	0.145	30.5	22.9
85	-0.0121	-0.0162	-0.0135	33.9	11.6	-0.105	-0.136	-0.118	29.5	12.4	-0.535	-0.602	-0.562	12.5	5.0
87	-0.0067	-0.0086	-0.0065	28.4	-3.0	0.343	0.453	0.360	32.1	5.0	-0.241	-0.275	-0.245	14.1	1.7
89	-0.0038	-0.0046	-0.003	19.6	-22.2	0.552	0.729	0.554	32.1	-	0.128	0.160	-0.157	25.0	22.7
91	-0.0050	-0.0047	-0.0021	-5.1	-56.8	1.66	2.250	1.98	35.5	19.3	2.23	3.17	3.54	42.2	58.7
92	0.3100	0.421	0.402	35.8	29.7	19.40	21.30	20.2	9.8	4.1	21.6	24.2	22.50	12.0	4.2
94	0.3450	0.476	0.466	38.0	35.1	1.12	1.22	1.16	8.9	3.6	1.470	1.66	1.54	12.9	4.8
96	0.676	0.932	0.922	37.9	36.4	0.685	0.799	0.767	16.6	12.0	0.697	0.847	0.768	21.5	10.2
98	0.216	0.325	0.460	50.5	113	-2.12	-2.520	-2.41	18.9	13.7	-1.660	-1.72	-1.91	3.6	15.1
106	0.791	1.050	0.861	32.7	8.8	20.000	22.00	20.6	10.0	3.0	-21.20	-23.7	-22.3	11.8	5.2
108	0.833	1.110	0.903	33.3	8.4	1.190	1.320	1.24	10.9	4.2	-1.29	-1.430	-1.35	10.9	4.7
110	1.380	1.850	1.50	34.1	8.7	-0.330	0.309	-0.291	-6.4	-11.8	-0.642	-0.651	-0.580	1.4	-9.7
112	1.290	1.750	1.58	35.7	22.5	-2.94	-3.22	-3.00	9.5	2.0	1.65	-2.250	-2.580	36.4	56.4

Table (13) Maximum Torsion and Bending Moments by LR, DnV & BV (ω = 0.56 rad/s, t = 0.3T)

Member No	Max Axial Force N (N) x 10^{-6}					Max Shearing Force F_y (N) x 10^{-6}					Max Shearing Force F_z (N) x 10^{-6}				
				Diff %					Diff %					Diff %	
	LR	DnV	BV	DnV	BV	LR	DnV	BV	DnV	BV	LR	DnV	BV	DnV	BV
1	-1.01	-0.944	-0.756	-6.5	-25.1	0.0191	0.0188	0.0152	-1.6	-20.4	-0.0040	-0.0047	-0.0040	18.1	1.3
3	-0.822	-0.756	-0.601	-8.0	-26.9	0.0169	0.0194	0.0162	14.8	-4.1	-0.0075	-0.0098	-0.0082	30.5	9.6
5	-0.750	-0.673	-0.530	-10.3	-29.3	0.0246	0.0306	0.0249	24.4	1.2	-0.0090	-0.0117	-0.0092	30.3	2.3
7	-0.600	-0.684	-0.700	14.0	16.7	0.102	0.141	0.139	38.2	36.3	-0.0170	-0.0223	-0.0223	31.2	-2.4
8	-1.19	-1.11	-0.885	-6.7	-25.6	-0.0077	-0.0093	-0.0078	20.9	1.6	-0.0039	-0.0045	-0.0036	16.0	-6.5
10	-0.959	-0.876	-0.685	-8.7	-28.6	0.0206	0.0267	0.0231	29.6	12.1	-0.0057	-0.0067	-0.0049	18.5	-14.2
12	-0.714	-0.604	-0.426	-15.4	-40.3	0.0464	0.0617	0.0516	33.0	11.2	-0.0058	-0.0067	-0.0042	15.3	-27.6
14	-0.139	-0.170	-0.139	22.3	-	0.0288	0.0371	0.0318	28.8	10.4	-0.0025	-0.0030	-0.0013	22.2	-46.4
15	1.16	1.07	0.856	-7.8	-26.2	-0.0082	-0.0099	-0.0083	21.5	1.7	0.0017	0.0017	0.0018	-0.6	4.8
17	0.877	0.767	0.591	-12.5	-32.6	-0.0170	-0.0236	-0.0203	38.8	19.4	-0.0015	0.0017	0.0030	15.4	103
19	0.554	0.392	0.243	-29.2	-56.1	-0.0417	-0.0572	-0.0506	37.2	21.3	-0.0025	-0.0022	0.0025	-12.3	-2.8
21	-0.168	-0.247	-0.250	47.0	48.8	0.0433	0.0598	0.0637	38.1	47.1	-0.0046	-0.0060	-0.0044	30.0	-5.4
85	-0.0195	-0.0231	-0.0208	18.5	6.7	-0.0098	-0.0115	-0.0096	17.5	-1.5	0.0073	0.0097	0.0083	33.3	14.7
87	-0.0330	-0.0360	-0.0347	9.1	5.2	0.0306	0.0415	0.0356	35.6	16.3	0.0249	0.0332	0.0286	33.3	14.9
89	-0.0925	-0.0999	-0.101	8.0	9.2	0.0631	0.0850	0.0702	34.7	11.3	0.0379	0.0504	0.0401	33.0	5.0
91	-0.0990	0.113	-0.121	14.1	22.2	-0.283	-0.387	-0.368	36.7	30.0	0.0669	0.0954	0.119	42.6	77.9
92	3.28	3.04	2.29	-7.3	-30.2	-0.467	-0.396	-0.295	-15.2	-36.8	0.635	0.632	0.530	-0.5	-16.5
94	2.65	2.51	1.90	-5.3	-28.3	-0.0621	-0.0606	-0.0506	-2.4	-18.5	0.0470	0.0461	0.0412	-1.9	-12.3
96	1.70	1.69	1.30	-0.6	-23.5	-0.130	-0.137	-0.129	5.4	-0.8	-0.114	-0.111	-0.107	-2.6	-6.1
98	0.716	0.817	0.701	14.1	-2.1	-0.423	-0.468	-0.444	10.6	5.0	-0.365	-0.367	-0.367	0.5	0.5
106	-2.69	-2.17	-1.62	-19.3	-39.8	0.628	0.615	0.498	-2.1	-20.7	0.471	0.411	0.324	-12.7	-31.2
108	-1.88	-1.39	-1.00	-26.1	-46.8	0.0511	0.0503	0.0417	-1.6	-18.4	0.0307	0.0274	0.0239	-10.7	-22.1
110	-0.788	-0.397	-0.218	-49.6	-72.3	0.0399	0.0470	0.0443	17.8	11.0	-0.0298	-0.0321	-0.0292	7.7	-2.0
112	0.185	0.267	0.258	44.3	39.5	0.0993	0.143	0.127	44.0	27.9	0.101	-0.126	-0.138	24.8	36.6

Table (14) Maximum Axial and Shearing Forces by LR, DnV & BV (ω= 0.56 rad/s, t = 0,6T)

Member No	Max Torsion Q (NM) x 10^{-6}					Max Bending Moment M_y (NM) x 10^{-6}					Max Bending Moment M_z (NM) x 10^{-6}				
				Diff %					Diff %					Diff %	
	LR	DnV	BV	DnV	BV	LR	DnV	BV	DnV	BV	LR	DnV	BV	DnV	BV
1	-0.0035	-0.0046	-0.0055	30.5	55.9	0.0698	0.0854	0.0782	22.3	12.0	0.454	0.427	0.341	-5.9	-24.9
3	-0.0070	-0.0092	-0.0104	31.0	48.6	0.155	0.210	0.198	35.5	27.7	0.178	0.175	0.139	-1.7	-21.9
5	-0.0034	-0.0043	-0.0066	25.6	91.0	0.169	0.228	0.215	34.9	27.2	0.134	0.162	0.129	20.9	-3.7
7	-0.0096	-0.0138	-0.0174	43.5	80.9	0.270	0.368	0.374	36.3	38.5	0.466	0.643	0.628	38.0	34.8
8	-0.0154	-0.0206	-0.0173	33.8	12.3	0.0943	0.124	0.104	31.5	10.3	0.159	0.162	0.132	1.9	-17.0
10	-0.0510	-0.0687	-0.0574	34.7	12.5	0.171	0.222	0.175	29.8	2.3	0.166	0.196	0.164	18.1	-1.2
12	-0.0412	-0.0561	-0.0447	36.2	8.5	0.111	0.139	0.106	25.2	-4.5	0.258	0.333	0.276	29.1	7.0
14	-0.0899	-0.121	-0.108	34.6	20.1	0.0779	0.102	0.0684	30.9	-12.2	0.0590	0.0823	0.0756	39.5	28.1
15	0.0058	0.0079	0.0895	35.3	53.5	0.0308	0.0435	0.0517	41.2	67.9	-0.0971	-0.0937	-0.0764	-3.5	-21.3
17	0.0312	0.0435	0.0487	39.4	56.1	0.0605	0.0903	0.133	49.3	120	-0.115	-0.1290	-0.110	12.2	-4.3
19	0.0328	0.0466	0.0562	42.1	71.3	0.0635	0.0850	0.107	33.9	68.5	0.194	0.277	0.244	42.8	25.8
21	0.0496	0.0708	0.0845	42.7	70.4	0.0844	0.1150	0.120	36.3	42.2	-0.0793	-0.108	0.129	36.2	62.7
85	-0.0042	-0.0059	-0.0066	40.2	57.2	-0.143	-0.195	-0.171	36.4	19.6	-0.334	-0.369	-0.306	10.5	-8.4
87	-0.0100	-0.0136	-0.0128	36.0	28.0	-0.468	-0.630	-0.559	34.6	19.4	-0.463	-0.558	-0.504	27.0	8.9
89	-0.0093	-0.0128	-0.0121	37.3	29.8	-0.567	-0.758	-0.631	33.7	11.3	-0.809	-1.10	-0.920	36.0	13.7
91	-0.0129	-0.0182	-0.0168	41.1	30.2	0.882	1.18	1.42	43.6	72.7	-3.16	-4.31	-4.01	36.4	26.9
92	-0.554	-0.740	-0.631	33.6	13.9	-9.18	-9.13	-7.64	-0.5	-16.8	-6.50	-5.47	-4.05	-15.8	-37.7
94	-0.612	-0.823	-0.704	34.5	15.0	-0.597	-0.590	-0.498	-1.2	-16.6	-0.544	-0.508	-0.391	-6.6	-28.1
96	-0.850	-1.140	-0.960	34.1	12.9	-0.639	-0.638	-0.576	-	-9.9	0.651	0.718	0.699	10.3	7.4
98	-0.903	-1.230	-1.16	36.2	28.5	1.08	-1.320	-1.55	22.2	43.5	2.86	3.39	3.25	18.5	13.6
106	0.339	0.451	0.467	33.0	37.8	-6.77	-5.87	-4.60	-13.3	-32.1	8.83	8.66	7.01	-1.9	-20.6
108	0.277	0.392	0.461	41.5	66.4	-0.331	-0.261	-0.194	-21.1	-41.4	0.489	0.467	0.372	-4.5	-23.9
110	0.457	0.673	0.913	47.3	99.8	0.155	0.205	0.192	32.3	23.9	-0.579	-0.749	-0.706	29.4	21.9
112	0.191	0.254	0.239	33.0	25.1	0.822	0.901	0.626	9.6	-23.8	2.23	3.18	2.84	42.6	27.4

Table (15) Maximum Torsion and Bending Moments by LR, DnV & BV (ω = 0.56 rad/s, t = 0.6T)

a. The percentage differences in the maximum axial force (N) ranged from -49.6% to 47.0% in the case of DnV and from -72.3% to 48.8% in the case of BV.

b. The percentage differences in the maximum shearing force (F_y) ranged from -15.2% to 44.0% in the case of DnV and from -36.8% to 47.1% in the case of BV.

c. The differences in the maximum shearing force (F_z) ranged from -12.7% to 42.6% in the case of DnV and from -46.4% to 103% according to BV.

d. The differences in the maximum torsion (Q) ranged from 25.6% to 47.3% in the case of DnV and from 8.5% to 99.8% in the case of BV.

e. The differences in the maximum bending moment (M_y) ranged from -21.1% to 49.3% in the case of DnV and from -41.4% to 120% in the case of BV.

f. The differences in the maximum benuing moment (M_z) ranged from -15.8% to 42.8% in the case of DnV and from -37.7% to 62.7% in the case of BV.

3.2 Maximum Stresses on the Members

The above analysis of the forces and moments for the results of LR, DnV and BV showed large percentage differences, either positive or negative, relative to the values of LR. However, for a certain member of the structure, the effect of an increase in the force in one or more directions may be counteracted by the increase, or even decrease, in the torsion or bending moments. Therefore, it is difficult to anticipate the final effect on a certain member without calculating the stresses due to the system of forces and moments acting on it. Since the scantlings of the members (diameter and wall thickness) are controlled by the maximum stresses, the analysis of the results of the stresses on the different members, as calculated by LR, DnV and BV, is more important. This is summarised below.

3.2.1 LR vs DnV and BV (ω = 0.37 rad/s)

Tables (16) to (18) show that:-

a. When t = 0.0, the percentage differences in the maximum tensile or compressive stress (σ max) ranged from 33.8% to 41.5% according to DnV and from 17.8% to 57.7% according to BV. The differences in the maximum shearing stress (τ max) are almost the same as those of σ max, ranging from 33.1% to 41.3% in the case of DnV and from 17.5% to 58.6% in the case of BV.

b. When t = 0.3T, the differences in σ max ranged from 8.3% to 41.0% according to DnV ana from 2.0% to 51.0% according to BV. The differences in τ max are almost the same as those of σ max ranging from 8.9% to 40.5% in the case of DnV and from 2.3% to 50.9% in the case of BV.

c. When t = 0.6T, the differences in σ max ranged from -24.5% to 87.3% according to DnV and from -46.8% to 112% according to BV. The differences in τ max ranged from -24.2% to 76.5% in the case of DnV and -46.5% to 103% in the case of BV.

3.2.2 LR vs DnV and BV (ω = 0.56 rad/s)

Tables (19) to (21) show that:-

Member No	Max Tensile (Compr) Stress (N/m^2) x 10^{-8} LR	DnV	BV	Diff % DnV	Diff % BV	Max Shearing Stress (N/m^2) x 10^{-8} LR	DnV	BV	Diff % DnV	Diff % BV
1	0.388	0.471	0.495	39.3	46.4	0.169	0.235	0.247	39.1	46.2
3	0.243	0.335	0.347	37.9	42.8	0.122	0.168	0.173	37.7	41.8
5	0.291	0.398	0.410	36.8	40.9	0.146	0.200	0.205	37.0	40.4
7	0.231	0.317	0.337	37.2	45.9	0.116	0.160	0.169	37.9	45.7
8	0.231	-0.323	-0.344	39.8	48.9	0.116	0.162	0.172	39.7	48.3
10	0.227	-0.317	-0.336	39.6	48.0	0.114	0.159	0.168	39.5	47.4
12	0.263	0.366	-0.385	39.2	46.4	0.131	0.183	0.193	39.7	47.3
14	-0.0996	-0.140	-0.154	40.6	54.6	0.0503	0.0703	0.178	39.8	55.1
15	0.280	0.389	0.406	38.9	45.0	0.140	0.195	0.203	39.3	45.0
17	0.271	0.377	0.391	39.1	44.3	0.136	0.189	0.196	39.0	44.1
19	0.326	0.453	0.465	39.0	42.6	0.163	0.227	0.233	39.3	42.9
21	0.135	0.188	0.200	39.3	48.1	0.0703	0.0983	0.104	39.8	47.9
85	0.267	0.359	0.326	34.5	22.1	0.133	0.179	0.163	34.6	22.6
87	0.331	0.443	0.390	33.8	17.8	0.166	0.221	0.195	33.1	17.5
89	0.488	0.657	0.577	34.6	18.2	0.245	0.329	0.289	34.3	18.0
91	-0.744	-1.01	-0.949	35.8	27.6	0.373	0.509	0.476	36.5	27.6
92	0.639	0.896	0.965	40.2	51.0	0.319	0.448	0.482	40.4	51.1
94	0.123	0.174	0.194	41.5	57.7	0.0617	0.0872	0.0973	41.3	57.7
96	0.0663	0.0921	0.104	38.9	56.9	0.0336	0.0466	0.0533	38.7	58.6
98	0.0374	0.0519	0.0499	38.8	33.4	0.0198	0.0277	0.0264	39.9	33.3
106	-0.668	-0.933	-0.995	39.7	49.0	0.334	0.467	0.498	39.8	49.1
108	-0.161	-0.224	-0.234	39.1	45.3	0.0811	0.113	0.118	39.3	45.5
110	-0.101	-0.138	-0.139	36.6	37.6	0.0532	0.0722	0.0732	35.7	37.6
112	-0.0827	-0.112	-0.107	35.4	29.4	0.0414	0.0563	0.0539	36.0	30.2

Table (16) Maximum Stresses on the Members by LR, DnV & BV (ω = 0.37 rad/s, t=0.0)

Member No	Max Tensile (Compr) Stress (N/m^2) x 10^{-8} LR	DnV	BV	Diff % DnV	Diff % BV	Max Shearing Stress (N/m^2) x 10^{-8} LR	DnV	BV	Diff % DnV	Diff % BV
1	-0.739	-0.834	-0.779	12.9	5.4	0.370	0.417	0.390	12.7	5.4
3	-0.418	-0.490	-0.453	17.2	8.4	0.209	0.245	0.227	17.2	8.6
5	-0.393	-0.478	0.444	21.6	13.0	0.197	0.239	0.222	21.3	12.7
7	-0.299	-0.410	-0.399	37.1	33.4	0.150	0.205	0.200	36.7	33.3
8	0.576	0.658	0.613	14.2	6.4	0.288	0.329	0.306	14.2	6.3
10	0.422	0.494	0.459	17.1	8.8	0.211	0.247	0.230	17.1	9.0
12	0.439	0.532	0.513	21.2	16.9	0.220	0.266	0.257	20.9	16.8
14	0.104	0.140	0.129	34.6	24.0	0.0537	0.0723	0.0668	34.6	24.4
15	-0.589	-0.676	-0.622	14.8	5.6	0.295	0.338	0.311	14.6	5.4
17	-0.439	-0.516	-0.469	17.5	6.8	0.220	0.258	0.235	17.3	6.8
19	-0.391	-0.465	-0.422	18.9	7.9	0.196	0.233	0.211	18.9	7.7
21	0.126	0.170	0.157	34.9	24.6	0.0648	0.0873	0.087	34.7	24.5
85	-0.199	-0.24	-0.203	20.6	2.0	0.0995	0.120	0.102	20.6	2.5
87	-0.178	-0.236	-0.224	32.6	25.8	0.0892	0.118	0.113	32.3	26.7
89	-0.388	-0.547	-0.571	41.0	47.2	0.195	0.274	0.286	40.5	46.6
91	-0.881	-1.24	-1.33	40.7	51.0	0.442	0.620	0.667	40.3	50.9
92	-1.57	-1.77	-1.66	12.7	5.7	0.786	0.887	0.830	12.8	5.6
94	-0.299	-0.343	-0.324	14.7	8.4	0.150	0.172	0.162	14.7	8.0
96	-0.151	-0.178	-0.169	17.9	11.9	0.0763	0.0898	0.0856	17.7	12.2
98	-0.106	-0.124	-0.127	17.0	19.8	0.0533	0.0623	0.0637	16.9	19.5
106	1.56	1.75	1.63	12.2	4.5	0.786	0.875	0.815	12.5	4.8
108	0.264	0.194	0.271	11.4	2.7	0.133	0.148	0.136	11.3	2.3
110	0.120	0.130	0.12	8.3	-	0.0609	0.0663	0.0611	8.9	-
112	0.0934	0.113	0.118	21.0	26.3	0.0468	0.0570	0.0593	21.8	26.7

Table (17) Maximum Stresses on the Members by LR, DnV & BV (ω = 0.37 rad/s, t=0.3T)

Member No	Max Tensile (Compr) Stress $(N/m^2) \times 10^{-8}$					Max Shearing Stress $(N/m^2) \times 10^{-8}$				
				Diff %					Diff %	
	LR	DnV	BV	DnV	BV	LR	DnV	BV	DnV	BV
1	-0.229	-0.194	-0.128	-15.3	-44.1	0.114	0.0970	-14.9	-43.9	
3	-0.127	-0.118	-0.0877	-7.1	-30.9	0.0637	0.0590	0.044	-7.4	-30.9
5	-0.127	-0.154	-0.172	21.3	35.4	0.0638	0.0770	0.0861	20.7	35.0
7	-0.170	-0.230	-0.233	35.3	37.1	0.0856	0.116	0.118	35.5	37.9
8	-0.188	-0.168	-0.114	-10.6	-39.4	0.0941	0.084	0.0572	-10.7	-39.2
10	-0.140	-0.132	-0.0931	-5.7	-33.5	0.070	0.0663	0.0470	-5.3	-32.9
12	-0.137	-0.139	0.128	1.5	-6.6	0.0690	0.0701	0.0645	1.6	-6.5
14	-0.0365	-0.0483	-0.0466	32.3	27.7	0.0195	0.0258	0.0235	32.3	20.5
15	0.141	0.121	0.0802	-14.2	-43.1	0.0703	0.0605	0.0401	-13.9	-43.0
17	0.0961	0.0851	-0.0852	-11.4	-11.3	0.0480	0.0426	0.0427	-11.4	-11.2
19	0.139	-0.217	-0.0246	56.1	77.0	0.0695	0.109	0.123	56.8	77.0
21	-0.0577	-0.0814	-0.0964	41.1	67.1	0.0307	0.0434	0.0521	41.4	69.7
85	-0.253	-0.317	-0.270	25.3	6.7	0.126	0.158	0.135	25.4	7.1
87	-0.327	-0.432	-0.383	32.1	17.1	0.164	0.217	0.191	32.3	16.5
89	-0.512	-0.690	-0.642	34.8	25.4	0.256	0.345	0.321	34.8	25.4
91	0.849	1.16	1.14	36.6	34.3	0.425	0.583	0.569	37.2	33.9
92	0.444	0.368	0.246	-17.1	-44.6	0.222	0.185	0.123	-16.7	-44.6
94	0.0842	0.0693	0.0448	-17.7	-46.8	0.0425	0.0354	0.0247	-16.7	-41.9
96	0.0555	0.0519	0.0384	-6.5	-30.8	0.0293	0.0279	0.0211	-4.8	-28.0
98	0.0643	0.0816	0.0753	26.9	17.1	0.0322	0.0411	0.0381	27.6	18.3
106	-0.396	-0.299	0.211	-24.5	-46.7	0.198	0.150	0.106	-24.2	-46.5
108	-0.0391	0.0429	0.0565	9.7	44.5	0.0198	0.0219	0.0291	10.6	47.0
110	0.0299	0.0560	0.0635	87.3	112	0.0170	0.0300	0.0345	76.5	103
112	0.0689	0.0971	0.0949	40.9	37.7	0.0344	0.0487	0.0476	41.6	38.4

Table (18) Maximum Stresses on the Members by LR, DnV & BV (ω =0.37 rad/s, t=0.6T)

Member No	Max Tensile (Compr) Stress $(N/m^2) \times 10^{-8}$					Max Shearing Stress $(N/m^2) \times 10^{-8}$				
				Diff %					Diff %	
	LR	DnV	BV	DnV	BV	LR	DnV	BV	DnV	BV
1	0.0845	0.118	0.125	39.6	47.9	0.0423	0.0588	0.0627	39.0	48.2
3	0.0813	0.110	0.109	35.3	34.1	0.0407	0.0552	0.0547	35.6	34.4
5	0.147	0.188	0.179	27.9	21.8	0.0734	0.0938	0.0896	27.8	22.1
7	0.210	0.269	0.259	28.1	23.3	0.106	0.136	0.131	28.3	23.6
8	-0.0584	-0.0816	-0.0874	39.7	49.7	0.0292	0.0408	0.0437	39.7	49.7
10	-0.0656	-0.0909	-0.0937	38.6	42.8	0.0329	0.0456	0.0469	38.6	42.6
12	-0.130	-0.178	-0.168	36.9	29.2	0.0653	0.0891	0.0844	36.4	29.2
14	0.0341	0.0469	-0.0493	37.5	44.6	0.0178	0.0243	0.0247	36.5	38.8
15	0.0756	0.105	0.109	38.9	44.2	0.0379	0.0525	0.0545	38.5	43.8
17	0.101	0.138	0.139	36.6	37.6	0.0504	0.0693	0.0694	37.5	37.7
19	0.175	0.239	0.234	36.6	33.7	0.0876	0.119	0.117	35.8	33.6
21	0.0836	0.115	0.116	37.6	38.8	0.0448	0.0618	0.0620	37.9	38.4
85	0.0458	0.0618	0.0578	34.9	26.2	0.0229	0.0309	0.0289	34.9	26.2
87	0.110	0.146	0.126	32.7	14.5	0.0549	0.0730	0.0631	33.0	14.9
89	0.298	0.395	0.328	32.6	10.1	0.149	0.198	0.164	32.9	10.1
91	0.932	1.26	1.12	35.2	20.2	0.467	0.631	0.564	35.1	20.8
92	0.185	0.257	0.277	38.9	49.7	0.0924	0.129	0.139	39.6	50.4
94	0.0408	0.056	0.0641	37.3	57.1	0.0208	0.0282	0.0321	35.6	54.3
96	0.0318	0.0417	0.0456	31.1	43.4	0.0160	0.0218	0.0232	36.3	45.0
98	-0.0496	0.0646	0.0588	30.2	18.5	0.0249	0.0325	0.0295	30.5	18.5
106	-0.183	-0.257	-0.275	40.4	50.3	0.0919	0.129	0.138	40.4	50.2
108	-0.0562	-0.0778	-0.0791	38.4	40.7	0.0290	0.0400	0.0403	37.9	39.0
110	-0.0578	-0.0755	-0.0734	30.6	27.0	0.0316	0.0412	0.0402	30.4	27.2
112	-0.0746	-0.0963	-0.0896	29.1	20.1	0.0417	0.0530	0.0510	27.1	22.3

Table (19) Maximum Stresses on the Members by LR, DnV & BV (ω =0.56 rad/s, t=0.0)

Member No	Max Tensile (Compr) Stress $(N/m^2) \times 10^{-8}$					Max Shearing Stress $(N/m^2) \times 10^{-8}$				
				Diff %					Diff %	
	LR	DnV	BV	DnV	BV	LR	DnV	BV	DnV	BV
1	-0.403	-0.448	-0.420	11.2	4.2	0.202	0.224	0.210	10.9	4.0
3	-0.253	-0.286	-0.265	13.0	4.7	0.126	0.143	0.132	13.5	4.8
5	-0.298	-0.349	-0.319	17.1	7.0	0.149	0.175	0.160	17.4	7.4
7	-0.261	-0.351	-0.332	34.5	27.2	0.131	0.176	0.167	34.4	27.5
8	0.306	0.341	0.320	11.4	4.6	0.153	0.171	0.160	11.8	4.6
10	0.263	0.302	0.281	14.8	6.8	0.132	0.151	0.141	14.4	6.8
12	0.336	0.393	0.371	17.0	10.4	0.168	0.197	0.186	17.3	10.7
14	0.0923	0.124	0.116	34.3	25.7	0.0473	0.0641	0.0603	35.5	27.5
15	-0.314	-0.352	-0.328	12.1	4.5	0.157	0.176	0.164	12.1	4.5
17	-0.285	-0.330	-0.301	15.8	5.6	0.143	0.165	0.150	15.4	4.9
19	-0.356	-0.420	-0.379	18.0	6.5	0.178	0.210	0.190	18.0	6.7
21	-0.115	-0.152	-0.131	32.2	13.9	0.0592	0.0781	0.0673	31.9	13.7
85	-0.0896	-0.101	-0.0943	12.7	5.2	0.0448	0.0507	0.0472	13.2	5.4
87	-0.0708	-0.0895	-0.0735	26.4	3.8	0.0355	0.0449	0.0369	26.5	3.9
89	-0.173	-0.227	-0.176	31.2	1.7	0.0866	0.114	0.0882	31.6	1.8
91	-0.830	-1.16	-1.2	39.8	44.6	0.417	0.580	0.604	39.1	44.8
92	-0.889	-0.991	-0.930	11.5	4.6	0.445	0.496	0.465	11.5	4.5
94	-0.209	-0.234	-0.222	12.0	6.2	0.104	0.117	0.111	12.5	6.7
96	-0.120	-0.138	-0.132	15.0	10.0	0.0609	0.070	0.067	14.9	10.0
98	-0.0921	-0.101	-0.102	9.7	10.7	0.0479	0.0506	0.0509	5.6	6.3
106	0.876	0.973	0.911	11.1	4.0	0.438	0.487	0.456	11.2	4.1
108	0.1[illegible]2	0.212	0.198	10.4	3.1	0.0963	0.106	0.0993	10.1	3.1
110	0.101	0.112	0.101	10.9	-	0.0520	0.0589	0.0521	13.3	-
112	0.103	0.106	0.105	2.9	1.9	0.0585	0.0541	0.0537	-7.5	-8.2

Table (20) Maximum Stresses on the Members by LR, DnV & BV (ω =0.56 rad/s, t=0.3T)

Member No	Max Tensile (Compr) Stress $(N/m^2) \times 10^{-8}$					Max Shearing Stress $(N/m^2) \times 10^{-8}$				
				Diff %					Diff %	
	LR	DnV	BV	DnV	BV	LR	DnV	BV	DnV	BV
1	-0.157	-0.147	-0.118	-6.4	-24.8	0.0783	0.0736	0.0591	-6.0	-24.5
3	-0.105	-0.106	-0.0880	1.0	-16.2	0.0524	0.0528	0.0441	0.8	-15.8
5	-0.144	-0.155	-0.131	7.6	-9.0	0.0721	0.0775	0.0655	7.5	-9.2
7	-0.223	-0.292	-0.291	30.9	30.5	0.112	0.146	0.146	30.4	30.4
8	-0.126	-0.123	-0.0986	-2.4	-21.7	0.0629	0.0613	0.0493	-2.5	-21.6
10	-0.116	-0.119	-0.0949	2.6	-18.2	0.0583	0.0600	0.0477	2.9	-18.2
12	-0.160	-0.172	-0.134	7.5	-16.3	0.0802	0.0865	0.0671	7.9	-16.3
14	-0.050	-0.0653	-0.0527	30.6	5.4	0.0282	0.0369	0.0302	30.9	7.1
15	0.110	0.103	0.0839	-6.4	-23.7	0.0551	0.0516	0.0420	-6.4	-33.8
17	0.0917	0.0875	0.0758	-4.6	-17.3	0.0459	0.0438	0.0379	-4.6	-17.4
19	0.120	0.127	0.105	5.8	-12.5	0.0598	0.0638	0.0525	6.7	-12.2
21	-0.0560	-0.0784	-0.0841	40.0	50.2	0.0299	0.0419	0.0446	40.1	49.2
85	-0.0612	-0.0703	-0.0592	14.9	-3.3	0.0306	0.0351	0.0296	14.7	-3.3
87	-1.111	-0.145	-0.127	30.6	14.4	0.0556	0.0725	0.0635	30.4	14.2
89	-0.301	-0.405	-0.340	34.6	13.0	0.151	0.203	0.170	34.4	12.6
91	-0.973	-1.33	-1.27	36.7	30.5	0.487	0.665	0.635	36.6	30.4
92	0.338	0.318	0.255	-5.9	-24.6	0.169	0.159	0.127	-5.9	-24.9
94	0.0805	0.077	0.0596	-4.3	-26.0	0.0406	0.0392	0.0305	-3.4	-24.9
96	0.0620	0.064	0.0533	3.2	-14.0	0.0318	0.0335	0.0278	5.3	-12.6
98	0.0930	0.104	0.101	11.8	8.6	0.0534	0.0522	0.0506	-2.2	-5.2
106	-0.321	-0.294	-0.233	-8.4	-27.4	0.161	0.147	0.117	-8.7	-27.3
108	-0.0572	-0.0449	-0.0336	-21.5	-41.3	0.0287	0.0227	0.0172	-20.9	-40.1
110	-0.0336	-0.0304	-0.0277	-9.5	-17.6	0.0175	0.0168	0.0166	-4.0	-5.1
112	0.0608	0.0833	0.0738	37.0	21.4	0.0309	0.0417	0.0369	35.0	19.4

Table (21) Maximum Stresses on the Members by LR, DnV & BV (ω =0.56 rad/s, t=0.6T)

a. When $t = 0.0$, the percentage differences in σ max ranged from 27.9% to 40.4% according to DnV and from 10.1% to 57.1% according to BV. The differences in τ max ranged from 27.1% to 40.4% in the case of DnV and from 10.1% to 54.3% in the case of BV.

b. When $t = 0.3T$, the percentage differences in σ max ranged from 2.9% to 39.8% according to DnV and from 1.7% to 44.6% according to BV. The differences in τ max ranged from -7.5% to 39.1% in the case of DnV and from -8.2% to 44.8% in the case of BV.

c. When $t = 0.6T$, the percentage differences in σ max ranged from -21.5% to 40.0% according to DnV and from -41.3% to 50.2% according to BV. The differences in τ max ranged from -20.9% to 40.1% in the case of DnV and from -40.1% to 49.2% in the case of BV.

3.3 Average Differences

Tables (22) and (23) summarise the average percentage differences in the forces, moments and stresses (DnV and BV relative to LR) at the two frequencies, $\omega = 0.37$ rad/s and $\omega = 0.56$ rad/s. The average percentage difference is calculated by adding the percentage differences for the 24 members together and then dividing the sum by 24.

These data are intended to give a quick and general idea about the amount of differences in the forces, moments and stresses and its relation to the change in time and frequency. However, these results should not be taken for granted, in isolation from the detailed

Forces Moment or Stress	DnV Min Diff %	DnV Member No	DnV Max Diff %	DnV Member No	DnV Av Diff %	BV Min Diff %	BV Member No	BV Max Diff %	BV Member No	BV Av Diff %
t = 0.0										
N	-0.6	89	48.0	14	35.5	3.2	89	88.7	14	44.0
F_Y	22.2	110	102	96	38.1	-18.2	12	169	96	33.2
F_Z	10.7	94	142	98	38.4	-9.4	96	177	98	44.5
Q	31.5	91	62.6	94	39.7	1.4	98	171	94	50.0
M_Y	16.3	96	53.1	94	37.9	16.3	96	53.1	94	44.6
M_Z	24.7	110	47	96	36.2	-21.8	98	78.8	96	26.3
σ max	33.8	87	41.5	94	38.2	17.8	87	57.7	94	41.7
τ max	33.1	87	41.3	94	38.2	17.5	87	58.6	96	41.7
t = 0.3T										
N	-16.9	21	35	91	14.4	-33.1	112	292	21	18.6
F_Y	1.9	112	52.7	87	23.5	-23.8	19	90.9	87	20.3
F_Z	0.5	110	36.4	7	23.2	-5.4	110	26.6	7	10.8
Q	-89.7	91	52.7	98	26.2	-90.3	89	131	98	16.4
M_Y	6.9	112	35.9	21	25.4	-3.7	110	22.9	7	12.1
M_Z	10.3	85	46.3	89	23.2	-42.4	19	79	87	24.0
σ max	8.3	110	41.0	89	21.3	2.0	85	51	91	15.3
τ max	8.9	110	40.5	89	21.3	2.3	108	50.9	91	15.3
t = 0.6T										
N	-87.3	106	413	110	20.0	-81.3	17	585	110	30.9
F_Y	-41.2	92	39.7	21	20.4	-78.1	92	50.9	21	6.9
F_Z	-64.8	108	92.1	112	19.7	-83.9	108	244	19	43.9
Q	19.8	112	275	15	47.8	-52.9	12	1445	15	107
M_Y	-38.2	106	58.8	17	26.3	-72.7	106	226	17	42.3
M_Z	-44.6	92	43.6	17	22.0	-83.9	8	29.6	21	8.3
σ max	-24.5	106	87.3	110	14.6	-46.8	94	112	110	6.7
τ max	-24.2	106	76.5	110	14.5	-46.5	106	103	110	6.7

Table (22) Percentage Differences of DnV & BV Relative to LR (ω=0.37 rad/s)

Forces Moment or Stress	DnV Min Diff %	DnV Member No	DnV Max Diff %	DnV Member No	DnV Av Diff %	BV Min Diff %	BV Member No	BV Max Diff %	BV Member No	BV Av Diff %
t = 0.0										
N	-11.4	14	47.2	112	29.3	-34.7	14	166	98	40.1
F_Y	-3.2	14	38.1	92	26.2	-7.3	98	60.9	106	16.8
F_Z	-8.1	98	48.6	21	30.0	-10.0	98	79.3	21	31.5
Q	20.2	12	42.7	112	32.8	-90.5	12	71.2	112	12.2
M_Y	6.2	96	46.1	92	32.8	-5.9	96	83.3	92	31.2
M_Z	12.9	96	44.4	14	33.6	4.6	12	49.6	1	24.0
σ max	27.9	5	40.4	106	35.2	10.1	89	57.1	94	34.4
τ max	27.1	112	40.4	106	35.2	10.1	89	54.3	94	34.2
t = 0.3T										
N	-3.3	85	29.7	14	11.0	-67.3	85	31.4	14	-1.7
F_Y	-3.6	110	40.7	91	18.9	-16.6	19	54.3	12	11.9
F_Z	-3.1	110	36.6	7	22.4	-6.2	110	27.4	7	9.6
Q	-5.1	91	50.5	98	32.9	-56.8	91	113	98	16.8
M_Y	-6.4	110	35.6	14	24.8	-11.8	110	21.4	8	10.8
M_Z	1.4	103	43.0	7	17.7	-20.5	19	58.7	91	13.4
σ max	2.9	112	39.8	91	17.7	1.7	89	44.6	91	9.0
τ max	-7.5	112	39.1	91	17.3	-8.2	112	44.8	91	8.6
t = 0.6T										
N	-49.6	110	47	21	-0.9	-72.3	110	48.8	21	-16.1
F_Y	-15.2	92	44.0	112	21.0	-36.8	92	47.1	21	5.9
F_Z	-12.7	99	42.6	91	15.1	-46.4	14	103	17	3.2
Q	25.6	5	47.3	110	36.5	8.5	12	99.8	110	42.7
M_Y	-21.1	108	49.3	17	24.3	-41.4	108	120	17	18.7
M_Z	-15.8	92	42.8	19	17.0	-37.7	92	62.7	21	2.7
σ max	-21.5	108	40.0	21	9.4	-41.3	108	50.2	21	-5.8
τ max	-20.9	108	40.1	21	9.1	-40.1	108	49.2	21	-5.8

Table (23) Percentage Differences of DnV & BV Relative to LR (ω=0.56 rad/s) information given in Tables (4) to (21) which reflect the true picture for the whole situation.

From Tables (22) and (23) it is noted that the average percentage differences for the stresses decrease with the increase of time from t = 0.0 to t = 0.6T, this trend is valid for the two frequencies (ω = 0.37 and 0.56 rad/s). It is also noted that the average percentage differences at ω = 0.37 rad/s are larger than the corresponding values at ω = 0.56 rad/s, ie the differences decrease for the higher frequencies.

4. COMPARISON BETWEEN LR AND SARPKAYA

4.1 Maximum Forces and Moments on the Members

Tables (24) to (35) summarise the results of the maximum forces (N, F_y and F_z) and maximum moments (Q, M_y and M_z) acting on the 24 members as calculated by LR and Sarpkaya's coefficients. When Sarpkaya's coefficients were used, the calculations were performed using both Airy and Stokes' fifth order theories.

4.1.1 LR vs Sarpkaya (ω = 0.37 rad/s, t = 0.0)

Tables (24) and (25) show that:-

a. The percentage differences in the maximum axial force (N) ranged from -23.7% to 35.2% according to Sarpkaya (Airy). The fifth order theory gave differences ranging from 4.0% to 1078%.

b. The percentage differences in the maximum shearing force (F_y) ranged from -19.7% to 137% (Airy) and from -45.8% to

Member No	Max Axial Force N(N) x 10^{-6}					Max Shearing Force F_y(N) x 10^{-6}					Max Shearing Force F_z(N) x 10^{-6}				
	LR	Sarpkaya (Airy)	Sarpkaya (5th Ord)	Diff % Airy	Diff % 5th	LR	Sarpkaya (Airy)	Sarpkaya (5th Ord)	Diff % Airy	Diff % 5th	LR	Sarpkaya (Airy)	Sarpkaya (5th Ord)	Diff % Airy	Diff % 5th
1	2.0238	2.58	3.77	27.7	86.6	0.0551	0.0682	0.0734	23.8	33.2	-0.0099	-0.0131	0.0164	32.7	66.2
3	1.5964	2.01	2.92	25.6	82.5	0.0491	0.059	0.0596	20.2	21.4	-0.0201	-0.0285	-0.0347	41.8	92.6
5	1.2579	1.51	2.41	19.8	91.3	0.0403	0.0472	0.0502	17.1	24.6	-0.0227	-0.0347	-0.0410	52.9	80.6
7	0.2186	-1.167	0.777	-23.7	255	-0.0584	-0.0712	0.0922	21.9	57.9	-0.0372	-0.0537	-0.0844	44.4	127
8	2.2198	-2.86	-4.27	28.8	92.3	-0.0382	-0.0451	-0.0343	18.1	-10.2	-0.0114	-0.0154	-0.0188	33.9	63.5
10	1.7224	-2.23	-3.32	29.7	93.0	-0.0473	-0.0544	-0.0443	15.0	-6.3	-0.0225	-0.0318	-0.0387	41.3	72.0
12	1.3608	-1.75	-2.91	28.7	114	-0.0287	-0.0323	-0.0274	12.5	-4.5	-0.0181	-0.0323	-0.0407	78.5	125
14	-0.0663	-0.087	-0.781	31.2	1078	0.0055	-0.0079	0.0848	42.5	1434	-0.0128	-0.0265	-0.0583	107	356
15	2.4133	3.09	4.39	28.2	82.2	-0.0359	-0.0424	-0.0390	18.1	8.6	-0.0096	-0.0136	-0.0205	42.3	114
17	1.9958	2.55	3.59	27.5	79.5	0.0589	0.0688	0.0696	16.8	18.2	-0.0185	-0.0269	-0.0348	45.4	88.1
19	1.5746	2.00	3.15	27.4	101	0.0642	0.0761	0.0820	18.5	27.7	-0.0162	-0.0225	-0.0315	38.9	94.4
21	0.2329	0.28	1.06	20.2	355	-0.0350	-0.0426	0.181	21.7	417	-0.0115	-0.0174	-0.0597	51.3	419
85	0.0549	0.0604	0.0745	10.0	35.7	-0.0754	-0.085	-0.0409	12.6	-45.8	-0.0193	-0.0245	-0.0450	26.9	133
87	0.0374	0.0415	0.0693	11.0	85.3	0.1116	-0.120	-0.0963	7.1	-14.0	-0.0438	-0.0560	-0.0700	27.9	59.8
89	0.0354	0.0401	0.0418	13.3	18.1	0.0991	0.0954	0.0857	-3.7	-13.5	-0.0676	-0.0929	-0.101	37.4	49.4
91	-0.0447	-0.0408	0.0465	-8.7	4.0	0.1523	0.122	0.120	-19.7	-21.1	-0.1628	-0.208	-0.216	27.6	32.5
92	5.6889	7.05	12.3	23.9	116	-1.2904	-1.580	-2.21	22.5	71.3	0.8423	1.15	1.810	36.6	115
94	4.2529	5.28	9.57	24.2	125	-0.0782	-0.0948	-0.157	21.2	101	0.0556	0.0573	0.0905	3.1	62.8
96	2.2871	2.85	5.81	24.5	154	-0.0206	-0.0488	-0.0618	137	200	-0.0651	-0.0511	-0.0611	-21.5	-6.1
98	0.4545	0.614	2.04	35.2	349	0.0970	0.144	-0.391	48.5	303	-0.0251	-0.127	-0.267	406	964
106	-6.7743	-9.03	-14.3	33.4	111	0.9307	1.28	2.04	37.5	119	1.2281	1.480	2.09	20.3	69.9
108	-5.3918	-7.15	-11.5	32.7	113	0.0601	0.0858	0.149	42.8	148	0.1182	0.127	0.164	7.6	39.0
110	-3.1407	-4.14	-7.27	31.8	132	-0.078	-0.0647	-0.0805	-16.9	3.3	0.1165	0.106	0.109	-8.6	-6.0
112	-0.8714	-1.13	-2.72	29.6	212	0.1941	0.196	-0.276	1.0	42.3	0.2227	0.244	0.341	9.4	52.9

Table (24) Maximum Axial and Shearing Forces by LR & SARPKAYA (ω=0.37 rad/s, t=0.0)

Member No	Max Torsion Q (NM) x 10^{-6}					Max Bending Moment M_y(NM) x 10^{-6}					Max Bending Moment M_z(NM) x 10^{-6}				
	LR	Sarpkaya (Airy)	Sarpkaya (5th Ord)	Diff % Airy	Diff % 5th	LR	Sarpkaya (Airy)	Sarpkaya (5th Ord)	Diff % Airy	Diff % 5th	LR	Sarpkaya (Airy)	Sarpkaya (5th Ord)	Diff % Airy	Diff % 5th
1	0.0279	0.030	0.0250	7.5	-10.4	0.2193	0.297	0.392	35.6	79.0	-1.0487	-1.33	-1.73	26.7	64.8
3	0.0241	0.0307	0.0325	27.4	34.9	0.4280	0.616	-0.779	32.9	82.0	-0.5478	-0.674	-0.794	23.0	44.9
5	0.0179	0.0236	0.0255	31.8	42.5	0.4335	0.648	0.778	49.7	79.7	-0.2988	-0.364	-0.449	21.7	50.2
7	0.0226	0.0336	0.0440	48.7	94.7	-0.630	-0.941	-1.34	49.4	113	-0.3066	-0.393	-0.603	28.0	96.4
8	-0.0245	-0.0332	-0.0421	35.5	71.8	0.210	0.30	0.343	42.9	63.3	0.2417	0.198	0.357	23.1	47.5
10	-0.0601	-0.0921	-0.110	52.7	82.4	0.4805	0.709	0.835	47.7	74.0	0.2342	0.278	0.309	18.8	32.1
12	-0.0610	-0.0904	-0.113	48.2	85.2	0.3637	0.586	0.725	61.0	99.2	-0.1543	-0.183	-0.123	18.8	-20.1
14	-0.0629	-0.101	-0.140	60.6	123	0.2996	0.460	0.801	53.3	167	0.0829	0.113	0.315	36.5	280
15	-0.0497	-0.0714	-0.0983	43.7	97.8	-0.2464	-0.355	-0.529	44.3	115	-0.4608	-0.564	-0.654	22.3	41.9
17	-0.1408	-0.198	-0.250	40.4	77.3	-0.5206	-0.768	-0.984	47.4	88.9	-0.4310	-0.502	-0.560	16.5	29.9
19	-0.1162	-0.167	-0.214	44.0	84.5	-0.3809	-0.551	-0.746	44.6	95.8	-0.3705	-0.435	-0.494	17.3	33.2
21	-0.1511	-0.217	-0.294	43.7	94.7	-0.3399	-0.513	-0.964	50.9	184	0.0877	0.115	-0.887	31.1	911
85	0.0109	0.0145	0.0176	33.0	61.5	-0.3271	-0.410	-0.712	25.4	118	1.5649	1.82	1.17	15.9	-25.5
87	0.0144	0.0181	0.0207	25.7	43.8	-0.7492	-0.933	-1.10	24.6	46.9	1.8511	2.02	1.69	9.2	-8.6
89	0.0082	0.0102	0.0123	24.4	50.0	-0.9159	-1.24	-1.31	35.5	43.2	1.3619	1.31	1.26	-3.7	-7.4
91	0.0104	0.0160	0.003	53.8	-71.4	-1.8203	-2.30	-2.32	26.4	27.5	1.7165	1.35	1.33	-21.1	-22.2
92	-0.1769	-0.341	-0.458	92.7	159	-11.8838	-16.5	-26.0	38.7	119	-18.2431	-22.4	-31.10	23.1	70.9
94	-0.1448	-0.306	-0.493	111	240	-0.3962	-0.610	-1.21	54.0	206	-1.0341	-1.30	-2.06	26.2	100
96	-0.5441	-0.839	-1.16	54.2	113	0.4203	-0.459	-0.816	9.3	94.3	-0.3626	-0.536	-0.823	47.7	127
98	0.4372	0.539	0.412	23.3	-5.7	0.7474	0.961	1.66	28.6	122	-0.7561	-0.692	2.25	-8.5	198
106	-1.4184	-1.95	-2.91	37.3	105	-17.5444	-21.20	-30.0	21.1	71.4	13.1745	18.20	28.40	37.9	115
108	-1.0071	-1.49	-1.72	47.5	70.3	-1.2153	-1.44	-1.99	18.0	63.1	0.9831	1.29	1.86	31.2	89.2
110	-1.4134	-2.14	-2.68	51.8	90.1	-0.5169	-0.558	-0.736	7.9	42.4	0.8894	0.740	0.965	-16.8	8.5
112	-0.5393	-0.817	-2.26	51.3	319	1.6148	2.18	3.32	35.4	106	-2.1413	-1.96	-2.63	-8.4	22.9

Table (25) Maximum Torsion and Bending Moments by LR & SARPKAYA (ω=0.37 rad/s, t=0.0)

1434% according to the fifth order theory.

c. The percentage differences in the maximum shearing force (F_z) ranged from -21.5% to 406% according to Airy theory, and from -6.1% to 964% according to the fifth order theory.

d. The pecentage differences in the maximum torsion (Q) ranged from 7.5% to 111% according to Airy theory, and from -71.4% to 319% according to Stokes' fifth order theory.

e. The percentage differences in the maximum bending moment (M_y) ranged from 7.9% to 61.0% according to Airy theory, and from 27.5% to 206% according to Stokes' fifth order theory.

f. The percentage differences in the maximum bending moment (M_z) ranged from -21.1% to 47.7% according to Airy theory, and from -25.5% to 911% according to Stokes' theory.

4.1.2 LR vs Sarpkaya (ω = 0.37 rad/s, t = 0.3T)

Tables (26) and (27) show that:-

a. The percentage differences in the maximum axial force (N) ranged from -28.2% to 114% by Airy theory, and from -67.8% to 413% by Stokes' fifth order theory.

b. The percentage differences in the maximum shearing force (F_y) ranged from -9.9% to 54.3% by Airy theory, and from -45.8% to 42.3% by Stokes' theory.

c. The differences in the maximum shearing force (F_z) ranged from -11.3% to 218% by Airy theory, and from -15.0% to 196% by Stokes' theory.

Member No	Max Axial Force N(N) x 10^{-6}					Max Shearing Force F_y(N) x 10^{-6}					Max Shearing Force F_z(N) x 10^{-6}				
	LR	Sarpkaya (Airy)	Sarpkaya (5th Ord)	Diff % Airy	Diff % 5th	LR	Sarpkaya (Airy)	Sarpkaya (5th Ord)	Diff % Airy	Diff % 5th	LR	Sarpkaya (Airy)	Sarpkaya (5th Ord)	Diff % Airy	Diff % 5th
1	-4.74	-5.07	-5.10	7.0	7.6	-0.0881	-0.0946	-0.0963	7.4	9.3	0.0163	0.0248	0.0233	52.1	42.9
3	-3.07	-3.30	-3.09	7.5	0.7	-0.0389	-0.0455	-0.0361	17.0	-7.2	0.0261	0.0508	0.0490	94.6	87.7
5	-1.83	-1.99	-1.70	8.7	-7.1	-0.0426	-0.0577	-0.0487	35.4	14.3	0.0234	0.0564	0.0524	141	124
7	-0.205	-0.247	-0.349	20.5	70.2	0.0983	0.128	0.118	30.2	20.0	0.0376	0.100	0.0924	166	146
8	5.62	6.01	6.03	6.9	7.3	0.0278	0.0315	0.0387	13.3	39.2	0.0205	0.0308	0.0320	50.2	56.1
10	3.80	4.10	3.84	7.9	1.1	-0.0414	-0.0548	-0.0528	32.4	27.5	0.0272	0.0492	0.0477	80.9	75.4
12	2.44	2.69	2.28	10.2	-6.6	-0.0849	-0.108	-0.0973	27.2	14.6	0.0187	0.0595	0.0553	218	196
14	0.206	0.280	0.159	35.9	-22.8	-0.0406	-0.0509	0.022	25.4	-45.8	0.0118	0.0375	0.0230	218	94.9
15	-5.63	-6.02	-6.05	6.9	7.5	0.0331	0.0362	0.0449	9.4	35.6	0.0228	0.0277	0.0312	21.5	36.8
17	-3.77	-4.05	-3,80	7.4	0.8	-0.0228	-0.0218	-0.0283	-4.4	24.1	0.0309	0.0398	0.0408	28.8	32.0
19	-2.30	-2.48	-2.11	7.8	-8.3	0.0130	0.0126	0.0185	-3.1	42.3	0.0247	0.0287	0.0276	16.2	11.7
21	-0.0112	-0.008	0.0575	-28.2	413	0.0157	0.0180	0.0089	14.6	-43.1	0.0130	0.0146	0.0137	12.3	5.4
85	-0.0161	-0.0147	-0.0259	-8.7	60.9	0.0247	0.0251	0.0238	1.6	-3.6	0.0498	0.0650	0.0883	30.5	77.3
87	-0.0339	-0.0457	-0.0431	34.8	27.1	-0.0243	-0.0375	-0.0156	54.3	-35.8	0.0795	0.113	0.118	42.1	48.4
89	-0.0423	-0.0777	-0.0586	83.7	38.5	-0.0844	-0.124	-0.101	46.9	19.7	-0.0746	-0.126	-0.121	68.9	62.2
91	-0.0626	-0.134	-0.103	114	64.5	-0.250	-0.335	-0.283	34.0	13.2	-0.124	-0.240	-0.223	93.5	79.8
92	-13.10	-15.7	-14.20	19.8	8.4	2.78	3.17	3.22	14.0	15.8	-2.66	-2.63	-2.78	-1.1	4.5
94	-9.63	-11.7	-10.2	21.5	5.9	0.265	0.294	0.311	10.9	17.4	-0.175	-0.166	-0.179	-5.1	2.3
96	-5.09	-6.35	-5.24	24.8	2.9	0.231	0.239	0.240	3.5	3.9	0.168	0.157	0.159	-6.5	-5.4
98	-1.27	-1.70	-1.20	33.9	-5.5	0.365	0.396	0.343	8.5	-6.0	-0.275	-0.257	-0.240	-6.5	-12.7
106	12.0	11.80	11.0	-1.7	-8.3	-2.87	-2.86	-2.98	-	3.8	-2.63	-2.98	-3.09	13.3	17.5
108	8.43	8.19	7.39	-2.8	-12.3	-0.225	-0.221	-0.225	-1.8	-	-0.221	-0.228	-0.251	3.2	13.6
110	3.83	3.65	3.01	-4.7	-21.4	-0.173	-0.164	-0.170	-5.2	-1.7	-0.186	-0.165	-0.176	-11.3	-5.4
112	0.453	0.392	-0.146	-13.5	-67.8	0.313	0.282	0.300	-9.9	-4.2	-0.294	-0.280	-0.250	-4.8	-15.0

Table (26) Maximum Axial and Shearing Forces by LR & SARPKAYA (ω=0.37 rad/s, t=0.3T)

Member No	Max Torsion Q (NM) x 10^{-6}					Max Bending Moment M_y(NM) x 10^{-6}					Max Bending Moment M_z(NM) x 10^{-6}				
	LR	Sarpkaya (Airy)	Sarpkaya (5th Ord)	Diff % Airy	Diff % 5th	LR	Sarpkaya (Airy)	Sarpkaya (5th Ord)	Diff % Airy	Diff % 5th	LR	Sarpkaya (Airy)	Sarpkaya (5th Ord)	Diff % Airy	Diff % 5th
1	-0.0218	-0.0341	-0.0303	56.4	39.0	0.480	-0.614	0.680	27.9	41.7	-2.13	-2.29	-2.37	7.5	11.2
3	-0.0229	-0.0282	-0.0277	23.1	21.0	0.814	-1.06	-1.11	30.2	36.4	-0.651	-0.705	-0.636	8.3	-2.3
5	-0.0193	-0.0223	-0.0205	15.5	6.2	0.579	-0.864	-0.845	49.2	45.9	-0.333	-0.427	-0.380	28.2	14.1
7	-0.0173	-0.0684	-0.0627	295	262	0.782	-1.20	-1.15	53.5	47.1	-0.521	-0.690	-0.677	32.4	29.9
8	0.0515	0.0674	0.0912	30.9	77.1	-0.370	-0.517	-0.593	39.7	60.3	-0.662	-0.732	-0.761	10.6	15.0
10	0.0994	0.113	0.138	13.7	38.8	-0.568	-0.898	-0.929	58.1	63.6	-0.429	-0.509	-0.416	18.6	8.6
12	0.0608	0.0623	0.0722	2.5	18.8	-0.298	-0.703	-0.682	136	129	-0.520	-0.638	-0.562	22.7	8.1
14	0.0785	0.0839	0.0885	6.9	12.7	-0.254	-0.554	-0.506	118	99.2	-0.0793	0.105	0.111	32.4	40.0
15	0.0839	0.114	0.123	35.9	46.6	0.485	0.658	0.732	35.7	50.9	0.673	0.719	0.772	6.8	14.7
17	0.169	0.266	0.262	57.4	55.0	0.752	1.08	1.09	43.6	44.9	0.337	0.321	0.320	-4.7	-5.0
19	0.114	0.204	0.193	78.9	69.3	0.476	0.653	0.628	37.2	31.9	0.0947	0.071	0.0918	-25.0	-3.1
21	0.124	0.258	0.241	108	94.4	0.396	0.542	0.509	36.9	28.5	0.104	-0.127	-0.143	22.1	37.5
85	-0.0125	-0.0143	-0.0112	14.4	-10.4	0.751	0.976	1.360	30.0	81.1	-0.943	-0.883	-1.06	-6.4	12.4
87	-0.0052	-0.0056	-0.0039	7.6	-24.9	1.01	1.42	1.49	40.6	47.5	0.353	0.491	0.289	39.1	-18.1
89	-0.0015	-0.0013	-0.0010	-14.3	-33.3	0.871	1.48	1.42	69.9	63.0	0.964	1.47	1.18	52.5	22.4
91	-0.0016	-0.0015	0.0017	-3.8	3.8	1.21	2.41	2.24	99.2	85.1	2.70	3.65	3.06	35.2	13.3
92	1.30	1.45	2.06	11.5	58.5	38.1	37.8	39.40	-0.8	3.4	39.0	44.4	44.9	13.8	15.1
94	0.569	0.627	0.572	10.2	0.5	2.00	1.96	1.89	-2.0	-5.5	2.69	3.05	3.24	13.4	20.4
96	0.387	0.419	0.245	8.3	-36.7	0.745	0.742	0.643	-	-13.7	1.17	1.24	1.24	6.0	6.0
98	0.205	0.244	-0.0634	19.0	-69.1	-1.86	-1.70	-1.73	-8.6	-7.0	-2.74	-3.47	-2.98	26.6	8.8
106	2.49	3.51	3.85	41.0	54.6	37.3	42.5	43.6	13.9	16.9	-40.1	-40.1	-41.4	-	3.2
108	1.29	2.15	1.92	66.7	48.8	1.99	2.30	2.28	15.6	14.6	2.25	-2.24	-2.24	-	-
110	1.11	2.47	2.15	123	93.7	-1.08	-0.924	-1.06	-14.4	-1.9	0.702	0.761	0.822	8.4	17.1
112	0.533	1.39	1.19	161	123	-2.61	-2.65	-2.26	1.5	-13.4	-2.40	-3.23	-3.17	34.6	32.1

Table (27) Maximum Torsion and Bending Moments by LR & SARPKAYA (ω=0.37 rad/s, t=0.3T)

d. The percentage differences in the maximum torsion (Q) ranged from -14.3% to 295% by Airy theory, and from -69.1% to 262% by Stokes' theory.

e. The differences in the maximum bending moment (M_y) ranged from -14.4% to 136% by Airy theory, and from -13.7% to 129% by Stokes' theory.

f. The differences in the maximum bending moment (M_z) ranged from -21.1% to 47.7% by Airy theory, and from -25.5% to 911% by Stokes' theory.

4.1.3 LR vs Sarpkaya (ω = 0.37 rad/s, t = 0.6T)

Tables (28) and (29) show that:-

a. The percentage differences in the maximum axial force (N) ranged from -91.3% to 401% according to Airy theory, and from -85.2% to 540% according to Stokes' fifth order theory.

b. The differences in the maximum shearing force (F_y) ranged from -29.3% to 26.3% according to Airy theory, and from -59.6% to 286% according to Stokes' theory.

c. The differences in the maximum shearing force (F_z) ranged from -27.9% to 121% according to Airy theory, and from -39.0% to 486% according to Stokes' theory.

d. The differences in the maximum torsion (Q) ranged from -40.9% to 958% according to Airy theory, and from -22.3% to 110% according to Stokes' theory.

e. The differences in the maximum bending moment (M_y) ranged

Member No	Max Axial Force N(N) x 10^{-6}					Max Shearing Force F_y(N) x 10^{-6}					Max Shearing Force F_z(N) x 10^{-6}				
	LR	Sarpkaya (Airy)	Sarpkaya (5th Ord)	Diff %		LR	Sarpkaya (Airy)	Sarpkaya (5th Ord)	Diff %		LR	Sarpkaya (Airy)	Sarpkaya (5th Ord)	Diff %	
				Airy	5th				Airy	5th				Airy	5th
1	-1.3134	-1.02	-1.02	-22.1	-22.1	0.0410	0.0398	0.0262	-2.9	-36.1	-0.0095	-0.0107	-0.0099	12.5	4.1
3	-0.7088	-0.477	-0.442	-32.7	-37.7	0.0401	0.0457	-0.0342	14.0	-14.7	-0.0141	-0.0160	-0.0145	13.5	2.8
5	-0.3406	-0.181	-0.271	-46.9	-20.5	0.0406	-0.0509	-0.0457	25.4	12.6	0.0098	0.0145	0.0144	48.1	47.1
7	-0.1822	-0.150	-0.0968	-17.6	-46.8	0.0928	0.116	0.101	25.0	8.8	0.0147	0.0216	0.0169	46.9	15.0
8	-1.5540	-1.210	-1.10	-21.9	-29.0	-0.0352	-0.0397	-0.0340	12.8	-3.4	-0.0044	-0.0056	-0.0068	28.0	54.7
10	-0.8788	-1.612	-0.496	-30.4	-43.6	0.0584	0.0679	0.0617	16.3	5.7	0.0064	0.0068	0.0079	6.9	23.5
12	-0.3639	-0.172	-0.0537	-52.7	-85.2	0.0531	0.0624	0.0577	17.5	8.7	0.0084	0.0086	0.0091	1.8	7.6
14	-0.0730	-0.0967	0.0253	32.5	-65.3	0.0218	0.0257	-0.0842	17.9	286	0.0021	-0.0016	-0.0038	-25.5	78.3
15	1.3762	1.01	0.987	-26.8	-28.5	-0.0315	-0.0356	-0.0205	13.0	-34.9	-0.0049	-0.0038	0.0030	-23.6	-39.0
17	0.5998	0.281	0.190	-53.2	-68.3	-0.0512	-0.0638	0.0692	24.6	35.2	-0.0021	0.0042	0.0048	102	131
19	0.0786	-0.179	-0.272	128	246	-0.0806	-0.0994	-0.0992	23.3	23.1	0.0019	0.0041	0.0046	121	148
21	-0.1807	-0.221	-0.207	22.1	14.4	0.0411	0.0519	-0.0297	26.3	-27.7	-0.0010	0.0021	0.0058	106	486
85	-0.0447	-0.0501	-0.0557	12.1	24.6	-0.0656	-0.0726	-0.0265	10.7	-59.6	0.0336	0.0424	0.0529	26.2	57.4
87	-0.0314	-0.033	-0.0561	5.1	78.7	0.1096	-0.123	-0.0900	11.8	-18.2	0.0507	0.0692	0.0696	36.5	37.3
89	-0.0487	-0.0446	-0.0580	-8.4	19.1	-0.1248	-0.145	-0.126	16.0	0.8	0.0252	0.0460	0.0402	82.5	59.5
91	0.0136	0.0341	-0.0258	151	89.7	-0.2433	-0.271	-0.237	11.5	-2.5	0.0714	0.0688	0.0669	-3.6	-6.3
92	3.2416	3.15	2.36	-2.8	-27.2	-0.5796	-0.462	-0.520	-20.3	-10.3	0.9976	0.780	0.773	-21.8	-22.5
94	2.3678	2.37	1.72	-	-27.4	-0.1257	-0.115	-0.136	-8.7	7.9	0.1206	0.104	0.110	-14.0	-9.1
96	1.2587	1.36	0.889	7.9	-29.4	-0.1545	-0.136	-0.141	-12.3	-9.0	0.1375	0.122	0.124	-11.6	-10.1
98	0.4637	0.563	0.272	21.3	-41.4	-0.2478	-0.226	-0.175	-8.9	-29.4	-0.2008	0.145	0.129	-27.9	-35.8
106	-1.6533	0.144	0.539	-91.3	-67.3	0.9451	0.668	0.578	-29.3	-38.8	0.5735	0.521	0.555	-9.2	-3.3
108	-0.6670	0.734	1.11	10.0	66.4	0.0934	0.0789	0.0693	-15.5	-25.8	0.0264	0.0208	0.0230	-21.2	-12.9
110	0.1968	0.986	1.26	401	540	0.0751	0.0726	0.0656	-3.3	-12.6	-0.023	-0.0256	-0.0297	11.3	29.1
112	0.3491	0.531	0.680	52.1	94.8	0.1249	0.119	0.0806	-4.8	-25.5	-0.0557	-0.0968	-0.0806	73.8	44.7

Table (28) Maximum Axial and Shearing Forces by LR & SARPKAYA (ω=0.37 rad/s, t=0.6T)

Member No	Max Torsion Q (NM) x 10^{-6}					Max Bending Moment M_y(NM) x 10^{-6}					Max Bending Moment M_z(NM) x 10^{-6}				
	LR	Sarpkaya (Airy)	Sarpkaya (5th Ord)	Diff %		LR	Sarpkaya (Airy)	Sarpkaya (5th Ord)	Diff %		LR	Sarpkaya (Airy)	Sarpkaya (5th Ord)	Diff %	
				Airy	5th				Airy	5th				Airy	5th
1	-0.0190	-0.0155	-0.0123	-18.4	-35.3	-0.1889	-0.191	0.177	1.1	-6.3	0.7283	0.629	0.517	-13.6	-29.0
3	-0.0106	-0.0088	-0.010	-16.8	-5.8	0.2517	0.309	0.342	22.6	35.7	0.3470	0.346	0.242	-	-30.3
5	-0.0128	-0.0076	-0.0094	-40.9	-26.3	0.2097	0.232	0.235	10.5	11.9	0.2209	0.277	0.254	25.3	14.9
7	-0.0133	-0.0248	-0.0253	86.5	90.2	0.2347	0.257	0.360	9.4	53.2	0.4502	0.558	0.467	24.0	3.8
8	-0.0229	-0.0332	-0.0429	45.0	87.3	0.0960	0.129	0.180	34.4	87.5	0.3744	0.375	0.328	-	-12.3
10	-0.0450	-0.0550	-0.0622	22.2	38.2	0.1477	0.178	0.206	20.3	39.2	0.3908	0.427	0.394	9.2	0.8
12	-0.0166	-0.0181	-0.0178	9.0	7.2	0.1250	0.138	0.144	10.4	15.2	0.3077	0.355	0.338	15.3	9.7
14	-0.0477	-0.0568	-0.0454	19.1	-4.8	0.0434	0.0442	0.0614	1.8	41.5	0.0771	0.0861	-0.325	11.7	322
15	0.0009	0.0093	0.0200	958	2188	0.0417	0.0488	0.0745	16.7	78.2	0.1774	0.211	-0.109	19.2	-38.4
17	0.0445	0.0658	0.0841	47.9	89	0.0741	0.156	0.194	110	161	0.2823	0.357	0.414	26.6	46.8
19	0.0499	0.0668	0.0732	33.9	46.7	0.0754	0.1340	0.150	77.7	98.9	0.4357	0.541	0.545	24.1	25.0
21	0.0661	0.0778	0.0851	17.7	28.7	0.0647	0.119	0.194	83.9	200	-0.0977	-0.124	-0.151	26.9	54.6
85	-0.0091	-0.0163	-0.0179	78.9	96.5	-0.5807	-0.737	-0.912	26.9	57.0	-1.4042	-1.47	-0.609	5.0	-56.5
87	-0.0165	-0.0244	-0.0258	47.9	56.4	-0.8698	-1.20	-1.230	37.9	41.4	-1.7752	-1.97	-1.450	10.7	-18.5
89	-0.0111	-0.0166	-0.0162	49.5	45.9	-0.4084	-0.702	-0.636	72.1	55.9	-1.6724	-1.91	-1.640	14.4	-1.8
91	-0.0139	-0.0230	-0.0223	65.5	60.4	0.9833	1.010	0.964	2.7	-1.9	-2.7010	-2.94	-2.570	8.9	-4.8
92	-0.9779	-1.20	-1.540	22.7	57.5	-13.8774	-10.8	-10.3	-22.3	-25.9	-7.6502	-6.02	-6.60	-21.3	-13.7
94	-0.6134	-0.795	-0.589	29.7	-3.9	-0.9547	-0.788	-0.698	-17.5	-26.9	-0.8068	-0.748	-0.824	-7.3	2.1
96	-0.3350	-0.495	-0.245	47.8	-26.9	-0.5746	-0.581	-0.557	1.0	-3.1	0.8326	0.823	0.822	-1.2	-1.3
98	-0.7008	-0.906	-0.658	29.2	-6.1	-0.7268	-0.728	-0.587	-	-19.3	2.1731	2.68	2.00	23.5	-7.8
106	0.1441	0.365	0.779	154.	441	-8.1110	-7.37	-7.810	-9.1	-3.7	13.0305	9.10	8.040	-30.0	-38.2
108	0.3466	0.571	0.589	64.6	69.7	0.2413	0.228	0.222	-5.4	-7.9	-0.9754	-0.992	-0.791	1.7	-18.9
110	0.7488	0.983	0.875	31.2	16.8	0.3885	0.416	0.472	6.9	21.3	0.8244	-0.847	-0.782	2.8	-5.1
112	0.0718	-0.180	0.243	151	238	0.6477	-1.13	-0.944	74.4	45.7	2.5271	2.55	2.00	0.8	-20.9

Table (29) Maximum Torsion and Bending Moments by LR & SARPKAYA (ω=0.37 rad/s, t=0.6T)

from -22.3% to 110% according to Airy theory, and from -26.9% to 200% according to Stokes' theory.

f. The differences in the maximum bending moment (M_z) ranged from -30.0% to 26.9% according to Airy theory, and from -56.5% to 322% according to Stokes' theory.

4.1.4 LR vs Sarpkaya (ω = 0.56rad/s, t = 0.0)

Tables (30) and (31) show that:-

a. The differences in the maximum axial force (N) ranged from -14.4% to 37.6% in the case of Airy theory. Stokes' fifth order theory gave differences ranging from -30.8% to 999%

b. The differences in the maximum shearing force (F_y) ranged from -18.3% to 38.6% in the case of Airy theory. Stokes' theory gave differences ranging from -18.3% to 38.6%

c. The differences in the maximum shearing force (F_z) ranged from -32.7% to 214% in the case of Airy theory. Stokes' theory gave differences ranging from -9.9% to 579%.

d. The differences in the maximum torsion (Q) ranged from -16.5% to 76.6% in the case of Airy theory. Stokes' theory gave differences ranging from -52.8% to 126%.

e. The differences in the maximum bending moment (M_y) ranged from -7.3% to 84.0% in the case of Airy theory. Stokes' theory gave differences ranging from -15.8% to 279%.

f. The differences in the maximum bending moment (M_z) ranged from -4.2% to 39.2% in the case of Airy theory. Stokes' theory gave differences ranging from -70.0% to 878%.

Member No	Max Axial Force N(N) x 10^{-6} LR	Sarpkaya (Airy)	Sarpkaya (5th Ord)	Diff % Airy	Diff % 5th	Max Shearing Force F_y(N) x 10^{-6} LR	Sarpkaya (Airy)	Sarpkaya (5th Ord)	Diff % Airy	Diff % 5th	Max Shearing Force F_z(N) x 10^{-6} LR	Sarpkaya (Airy)	Sarpkaya (5th Ord)	Diff % Airy	Diff % 5th
1	0.533	0.678	0.946	27.2	77.5	0.0113	0.0141	0.0180	24.8	59.3	-0.0030	-0.0038	-0.0042	26.9	42.4
3	0.549	0.672	0.902	22.4	64.3	0.0146	0.0168	0.0203	15.1	39.0	-0.0071	-0.0094	-0.0101	32.0	42.5
5	0.766	0.877	1.09	14.5	42.3	0.0250	0.0284	0.0297	13.6	18.8	-0.0109	-0.0153	-0.0162	40.4	48.6
7	0.595	0.543	1.09	-8.7	83.2	-0.0844	-0.104	0.102	23.2	20.9	-0.0223	-0.0335	-0.0474	50.2	113
8	-0.587	-0.759	-1.07	29.3	82.3	-0.0076	-0.0091	-0.0109	18.6	42.9	-0.0011	-0.0014	-0.0018	28.4	67.0
10	-0.514	-0.664	-0.933	29.2	81.5	-0.0220	-0.0253	-0.0272	15.0	23.6	-0.0048	-0.0064	-0.0075	33.1	54.3
12	-0.549	-0.706	-1.00	28.6	82.1	-0.0424	-0.0496	-0.0485	17.0	14.4	-0.0074	-0.0098	-0.0106	32.8	43.6
14	0.0202	0.0197	-0.0718	-2.5	255	-0.0050	-0.0046	-0.0405	-8.3	704	-0.0045	-0.0140	-0.0303	214	579
15	0.619	0.794	1.10	28.3	77.7	-0.0069	-0.0074	-0.0079	7.4	15.0	-0.0036	-0.0047	-0.0054	28.4	48.5
17	0.612	0.776	1.06	26.8	73.2	0.0230	0.0267	0.0295	16.1	28.3	-0.0082	-0.0113	-0.0123	37.8	50.0
19	0.714	0.895	1.19	25.4	66.7	0.0455	0.0528	0.0536	16.0	17.8	-0.0088	-0.0128	-0.0141	45.1	59.9
21	0.215	0.258	0.524	20.0	144	-0.040	-0.0481	-0.175	20.3	338	-0.0029	-0.0053	-0.0066	81.7	127
85	0.0215	0.0224	0.0274	4.2	27.4	-0.0107	-0.0131	-0.0132	22.4	23.4	-0.0041	-0.0050	-0.0068	21.0	64.7
87	0.0471	0.0466	0.0468	-1.1	-0.6	-0.0321	-0.0372	-0.0421	15.9	31.2	-0.0149	-0.0177	-0.0194	18.8	30.2
89	0.123	0.118	0.0851	-4.1	-30.8	0.0636	0.0703	0.0722	10.5	13.5	-0.0286	-0.0367	-0.0375	28.3	31.1
91	0.114	0.116	0.205	1.8	79.8	0.223	0.223	0.212	-	-4.9	-0.161	-0.230	-0.208	42.9	29.2
92	1.93	2.38	3.74	23.3	93.8	-0.402	-0.492	-0.654	22.4	62.7	0.146	0.210	0.330	43.8	126
94	1.42	1.75	2.89	23.2	104	-0.0252	-0.0292	-0.0418	15.9	65.9	0.0295	0.0288	0.0360	-2.4	22.0
96	0.689	0.853	1.67	23.8	142	0.0860	0.0792	0.0835	-7.9	-2.9	0.0709	-0.0626	-0.0689	-11.7	-2.8
98	-0.0375	-0.0321	0.412	-14.4	999	0,234	0.203	0.112	-13.2	-52.1	0.211	0.142	-0.257	-32.7	21.8
106	-2.23	-3.21	-4.41	35.0	97.8	0.233	0.323	0.466	38.6	100	0.319	0.385	0.532	20.7	66.8
108	-1.89	-2.55	-3.77	34.9	99.5	-0.0263	-0.0215	0.0332	-18.3	26.2	0.0361	0.0362	0.0455	-	26.0
110	-1.27	-1.70	-2.60	33.9	105	-0.095	-0.0850	-0.0778	-10.5	-18.1	0.0802	0.0696	0.0723	-13.2	-9.9
112	-0.394	-0.542	-1.05	37.6	167	-0.231	0.195	0.300	-15.6	29.9	0.296	0.290	0.415	-2.0	40.2

Table (30) Maximum Axial and Shearing Forces by LR & SARPKAYA (ω=0.56 rad/s, t=0.0)

Member No	Max Torsion Q (NM) x 10^{-6} LR	Sarpkaya (Airy)	Sarpkaya (5th Ord)	Diff % Airy	Diff % 5th	Max Bending Moment M_y(NM) x 10^{-6} LR	Sarpkaya (Airy)	Sarpkaya (5th Ord)	Diff % Airy	Diff % 5th	Max Bending Moment M_z(NM) x 10^{-6} LR	Sarpkaya (Airy)	Sarpkaya (5th Ord)	Diff % Airy	Diff % 5th
1	0.0094	0.0103	0.0117	9.7	24.6	-0.0698	-0.0862	-0.0946	23.5	35.5	-0.244	-0.315	-0.426	29.1	74.6
3	0.0123	0.0161	0.0163	30.9	32.5	-0.179	-0.230	-0.243	28.5	35.8	-0.139	-0.179	-0.237	28.8	70.5
5	0.0089	0.0120	0.0129	35.6	45.8	-0.169	-0.224	-0.235	32.5	39.1	-0.139	-0.152	-0.187	9.4	34.5
7	0.0234	0.0316	0.0272	35.0	16.2	-0.295	-0.443	-0.562	50.2	90.5	-0.391	-0.489	-0.642	25.1	64.2
8	0.0070	0.0089	0.0096	27.5	37.8	-0.0302	-0.0358	-0.0395	18.5	30.8	0.0612	0.0774	0.102	26.5	66.7
10	0.0212	0.0243	0.0251	14.6	18.4	-0.103	-0.132	-0.141	28.2	36.9	0.105	0.127	0.152	21.0	44.8
12	0.0077	0.0064	0.0074	-16.5	-3.9	-0.104	-0.136	-0.140	30.8	34.6	-0.218	-0.254	-0.239	16.5	9.6
14	0.0379	0.0400	0.0456	5.5	20.3	0.0739	0.136	0.280	84.0	279	0.0727	0.0963	-0.291	32.5	300
15	-0.0191	-0.0251	-0.0270	31.4	41.4	-0.118	-0.153	-0.167	29.7	41.5	-0.104	-0.122	-0.152	17.3	46.2
17	-0.0754	-0.0992	-0.105	31.6	39.3	-0.273	-0.376	-0.397	37.7	45.4	-0.153	-0.181	-0.208	18.3	35.9
19	-0.0769	-0.108	-0.114	40.4	48.2	-0.220	-0.330	-0.355	50.0	61.4	-0.249	-0.288	-0.290	15.7	16.5
21	-0.104	-0.153	-0.161	47.1	54.8	-0.162	-0.261	-0.284	61.1	75.3	0.0901	0.111	-0.881	23.2	878
85	0.0099	0.0125	0.0141	26.5	42.7	0.104	0.127	0.150	22.1	44.2	0.248	0.314	0.343	26.6	38.3
87	0.0128	0.0158	0.0172	23.4	34.4	-0.349	-0.420	-0.453	20.3	29.8	0.544	0.636	0.725	16.9	33.3
89	0.0103	0.0130	0.0143	26.2	38.8	-0.461	-0.583	-0.602	26.5	30.6	0.850	0.932	0.978	9.6	15.1
91	0.0166	0.0225	0.0078	35.5	-52.8	-1.91	-2.67	-2.46	39.8	28.8	2.46	2.39	2.27	-2.8	-7.7
92	0.357	0.431	0.491	20.7	37.5	-2.04	-3.00	-4.71	47.1	131	-5.66	-6.96	-9.19	23.0	62.4
94	0.357	0.428	0.428	19.9	19.9	0.109	-0.138	-0.239	26.6	119	-0.322	-0.381	-0.524	18.3	62.7
96	0.290	0.334	0.367	15.2	26.6	0.322	0.300	0.2710	-6.8	-15.8	-0.598	-0.603	-0.720	0.8	20.4
98	0.528	0.679	0.865	28.6	63.8	1.00	0.927	3.040	-7.3	204	-1.82	-1.980	-0.546	8.8	-70.0
106	-0.721	-0.918	-1.01	27.3	40.1	-4.63	-5.61	-7.74	21.2	67.2	3.24	4.51	6.470	39.2	99.7
108	-0.698	-0.941	-0.975	34.8	39.7	-0.351	-0.409	-0.560	16.5	59.5	0.312	0.325	0.466	4.2	49.4
110	-1.11	-1.680	-1.780	51.4	60.4	-0.322	-0.322	-0.382	-	18.6	0.939	0.944	0.926	0.5	-1.4
112	-0.736	-1.30	-1.660	76.6	126	1.85	2.05	1.810	10.8	-2.2	-1.65	-1.58	1.73	-4.2	4.8

Table (31) Maximum Torsion and Bending Moments by LR & SARPKAYA (ω=0.56 rad/s, t=0.0)

4.1.5 LR vs Sarpkaya (ω = 0.56 rad/s, t = 0.3T)

Tables (32) and (33) show that:-

a. The percentage differences in the maximum axial force (N) ranged from -51.2% to 74.5% according to Airy theory, and from -38.7% to 158% according to Stokes' theory.

b. The differences in the maximum shearing force (F_y) ranged from -14.4% to 37.6% according to Airy theory, and from -94.4% to 34.8% according to Stokes' theory.

c. The differences in the maximum shearing force (F_z) ranged from -19.1% to 238% according to Airy theory, and from -21.6% to 120% according to Stokes' theory.

d. The differences in the maximum torsion (Q) ranged from -17.8% to 177% according to Airy theory, and from -91.3% to 143% according to Stokes' theory.

e. The differences in the maximum bending moment (M_y) ranged from -11.5% to 120% according to Airy theory, and from -24.1% to 88.5% according to Stokes' theory.

f. The differences in the maximum bending moment (M_z) ranged from -8.9% to 48.4% according to Airy theory, and from -29.0% to 71.5% according to Stokes' theory.

4.1.6 LR vs Sarpkaya (ω = 0.56 rad/s, t = 0.6T)

Tables (34) and (35) show that:-

a. The differences in the maximum axial force (N) ranged from -55.6% to 28.8% according to Airy theory. In the case of

Member No	Max Axial Force N(N) x 10^{-6} LR	Sarpkaya (Airy)	Sarpkaya (5th Ord)	Diff % Airy	Diff % 5th	Max Shearing Force F_y(N) x 10^{-6} LR	Sarpkaya (Airy)	Sarpkaya (5th Ord)	Diff % Airy	Diff % 5th	Max Shearing Force F_z(N) x 10^{-6} LR	Sarpkaya (Airy)	Sarpkaya (5th Ord)	Diff % Airy	Diff % 5th
1	-2.62	-2.70	-2.62	3.1	-	-0.0459	-0.048	-0.0464	4.6	1.1	0.0062	0.0070	0.0073	11.9	17.5
3	-2.11	-2.18	-2.06	3.3	-2.4	-0.0250	-0.0268	-0.0262	7.2	4.8	0.0108	0.0141	0.0151	30.6	39.8
5	-1.75	-1.83	-1.62	4.6	-7.4	-0.0192	-0.0201	-0.0187	4.7	-2.6	0.0127	0.0236	0.0237	85.8	86.6
7	-0.198	-0.199	-0.491	0.5	148	0.0947	0.126	0.117	33.1	23.5	0.0328	0.0794	0.0720	142	120
8	3.12	3.21	3.11	2.9	-	0.0110	0.0116	0.0113	5.5	2.7	0.0763	0.0086	0.0088	12.2	15.9
10	2.60	2.68	2.52	3.1	-3.1	-0.0047	-0.0045	-0.0041	-4.9	-14.0	0.0154	0.0183	0.0186	18.8	20.8
12	2.26	2.39	2.09	5.8	-7.5	-0.0210	-0.0289	-0.0283	37.6	34.8	0.0173	0.0330	0.0312	90.8	80.3
14	0.229	0.301	0.198	31.4	-13.5	-0.0395	-0.0491	0.0022	24.3	-94.4	0.0096	0.0323	0.0172	238	79.7
15	-3.13	-3.22	-3.12	2.9	-	0.0132	0.0135	0.0134	2.3	1.5	0.009	0.0102	0.0108	13.8	20.5
17	-2.62	-2.71	-2.56	3.4	-2.3	-0.0092	0.0092	-0.0112	-	22.3	0.0174	0.0220	0.0223	26.4	28.2
19	-2.25	-2.37	-2.08	5.3	-7.6	0.0163	0.0167	0.0188	2.5	15.3	0.0202	0.0255	0.0241	26.2	19.3
21	-0.0881	-0.0906	-0.0606	2.8	-31.2	0.0225	0.0256	0.0177	13.8	-21.3	0.0098	0.0092	0.0088	-5.7	-10.2
85	-0.0030	-0.0015	-0.0078	-51.2	158	0.0124	0.0125	0.0121	0.8	-2.4	0.0071	0.0085	0.0135	20.2	90.7
87	-0.0235	-0.0239	-0.0271	1.7	15.3	-0.0139	-0.0168	-0.0184	20.9	32.4	0.0250	0.0287	0.0337	14.8	34.8
89	-0.0602	-0.0677	-0.0476	12.5	-20.9	-0.0186	-0.0222	-0.0204	19.4	9.7	0.0461	0.0614	0.0636	33.2	38.0
91	-0.0596	-0.104	-0.121	74.5	103	-0.226	-0.309	-0.255	36.7	12.8	-0.163	-0.274	0.246	68.1	50.9
92	-9.24	-10.40	-9.36	12.6	1.3	1.530	1.650	1.600	7.8	4.6	-1.33	-1.290	-1.270	-3.0	-4.5
94	-7.21	-8.17	-7.250	13.3	0.6	0.119	0.129	0.1270	8.4	6.7	-0.0617	-0.0591	-0.0601	-4.2	-2.6
96	-4.19	-4.89	-4.17	16.7	-0.5	0.0907	0.0919	0.0950	1.3	4.7	0.0713	0.0691	0.0731	-3.1	2.5
98	-1.11	-1.43	-1.09	28.8	-1.8	-0.259	0.295	0.282	13.9	8.9	-0.251	-0.239	-0.237	-4.8	-5.6
106	8.58	8.28	7.71	-3.5	-10.1	-1.510	-1.47	-1.450	-2.6	-4.0	-1.370	-1.49	-1.440	8.8	5.1
108	6.57	6.32	5.79	-3.8	-11.9	-0.108	-0.103	-0.101	-4.6	-6.5	-0.0828	-0.0848	-0.0879	2.4	6.2
110	3.53	3.37	2.96	-4.5	-16.1	0.0933	0.0799	0.0822	-14.4	-11.9	-0.0834	-0.0675	-0.0797	-19.1	-4.4
112	0.537	0.477	0.329	-11.2	-38.7	0.379	0.337	0.370	-11.1	-2.4	-0.338	-0.314	-0.265	-7.1	-21.6

Table (32) Maximum Axial and Shearing Forces by LR & SARPKAYA (ω=0.56 rad/s, t=0.3T)

Member No	Max Torsion Q (NM) x 10^{-6} LR	Sarpkaya (Airy)	Sarpkaya (5th Ord)	Diff % Airy	Diff % 5th	Max Bending Moment M_y(NM) x 10^{-6} LR	Sarpkaya (Airy)	Sarpkaya (5th Ord)	Diff % Airy	Diff % 5th	Max Bending Moment M_z(NM) x 10^{-6} LR	Sarpkaya (Airy)	Sarpkaya (5th Ord)	Diff % Airy	Diff % 5th
1	-0.0118	-0.0169	-0.0169	43.2	43.2	-0.162	0.182	0.196	12.3	21.0	-1.16	-1.20	-1.17	3.4	0.9
3	-0.0123	-0.0170	-0.0181	38.2	47.2	0.302	0.378	0.405	25.2	34.1	0.402	-0.410	0.380	2.0	-5.5
5	-0.0126	-0.0150	-0.0146	19.0	15.9	0.333	-0.431	-0.425	29.4	27.6	-0.163	-0.164	-0.147	0.6	-9.8
7	-0.0247	-0.0684	-0.0600	177	143	0.676	-0.998	-0.910	47.6	34.6	-0.449	-0.605	-0.623	34.7	38.8
8	0.0125	0.0189	0.0199	51.2	59.2	-0.103	-0.123	-0.134	19.4	30.1	-0.321	-0.335	-0.330	4.4	2.8
10	0.0422	0.0536	0.0534	27.0	26.5	-0.293	-0.362	-0.367	23.5	25.3	-0.157	-0.155	-0.142	-1.3	-9.6
12	0.0459	0.0562	0.0518	22.4	12.9	-0.274	-0.437	-0.412	59.5	50.4	-0.160	-0.199	-0.189	24.4	18.1
14	0.0520	0.0581	0.0530	11.7	1.9	-0.208	-0.457	-0.392	120	88.5	-0.0768	0.114	0.0597	48.4	-22.3
15	0.0239	0.0287	0.0339	20.1	41.8	0.168	0.215	0.238	28.0	41.7	0.341	0.351	0.339	2.9	-0.6
17	0.0834	0.114	0.120	36.7	43.9	0.403	0.549	0.567	36.2	40.7	0.207	0.201	0.199	-2.9	-3.9
19	0.0862	0.130	0.1290	50.8	49.7	0.366	0.515	0.497	40.7	35.8	0.111	0.103	0.108	-7.2	-2.7
21	0.0980	0.191	0.185	94.9	88.8	0.326	0.394	0.384	20.9	17.8	0.118	0.143	0.180	21.2	52.5
85	-0.0121	-0.0125	-0.0132	3.3	9.1	-0.105	-0.127	0.194	21.0	84.8	-0.535	-0.526	-0.521	-1.7	-2.6
87	-0.0067	-0.0068	-0.0077	1.0	14.5	0.343	0.371	0.455	8.2	32.7	-0.241	-0.239	-0.246	-0.8	2.1
89	-0.0038	-0.0035	-0.0044	-9.4	15.1	0.552	0.709	0.752	28.4	36.2	0.128	0.139	0.127	8.6	-0.8
91	-0.0050	-0.0041	-0.0004	-17.8	-91.3	1.66	2.89	2.580	74.1	55.4	2.23	3.140	2.57	40.8	15.2
92	0.3100	0.350	0.385	12.9	24.2	19.40	18.90	18.50	-2.6	-4.6	21.6	23.40	22.60	8.3	4.6
94	0.3450	0.399	0.371	15.7	7.5	1.12	1.080	1.03	-3.6	-8.0	1.470	1.610	1.56	9.5	6.1
96	0.676	0.777	0.640	14.9	-5.3	0.685	0.702	0.636	2.5	-7.2	0.697	0.799	0.743	14.6	6.6
98	0.216	0.254	0.142	17.6	-34.3	-2.12	-2.04	-2.21	-3.8	4.2	-1.660	-2.08	-2.25	25.3	35.5
106	0.791	0.984	1.14	24.4	44.1	20.00	21.70	20.9	8.5	4.5	-21.20	-20.7	-20.4	-2.4	-3.8
108	0.833	1.120	1.16	34.5	39.3	1.190	1.30	1.22	9.2	2.5	-1.290	-1.260	-1.21	-2.3	-6.2
110	1.380	2.240	2.14	62.3	55.1	-0.330	0.292	-0.322	-11.5	-0.9	-0.642	-0.585	-0.456	-8.9	-29.0
112	1.290	2.480	2.14	92.2	65.9	-2.94	-2.88	-2.23	-2.0	-24.1	1.65	-2.250	-2.83	36.4	71.5

Table (33) Maximum Torsion And Bending Moments by LR & SARPKAYA (ω=0.56 rad/s, t=0.3T)

Member No	Max Axial Force N(N) $\times 10^{-6}$					Max Shearing Force F_y(N) $\times 10^{-6}$					Max Shearing Force F_z(N) $\times 10^{-6}$				
	LR	Sarpkaya (Airy)	Sarpkaya (5th Ord)	Diff % Airy	Diff % 5th	LR	Sarpkaya (Airy)	Sarpkaya (5th Ord)	Diff % Airy	Diff % 5th	LR	Sarpkaya (Airy)	Sarpkaya (5th Ord)	Diff % Airy	Diff % 5th
1	-1.01	-0.911	-0.976	-9.8	-3.4	0.0191	0.0178	0.0187	-6.8	-2.1	-0.0040	-0.0045	-0.0047	14.1	18.6
3	-0.822	-0.737	-0.757	-10.3	-7.9	0.0169	0.0171	0.0185	1.2	9.5	-0.0075	-0.0091	-0.0095	21.2	26.0
5	-0.750	-0.681	-0.634	-9.2	-15.5	0.0246	0.0269	0.0267	9.3	8.5	-0.0090	-0.0104	-0.0103	15.8	14.7
7	-0.600	-0.596	-0.331	-0.7	-44.8	0.102	0.131	0.120	28.4	17.6	-0.0170	-0.0285	-0.030	67.6	76.5
8	-1.19	-1.07	-1.13	-10.1	-5.0	-0.0077	-0.0083	-0.0097	7.8	25.6	-0.0039	-0.0041	-0.0045	6.2	16.0
10	-0.959	-0.857	-0.878	-10.6	-8.4	0.0206	0.0233	0.0260	13.1	26.2	-0.0057	-0.0063	-0.0065	10.2	13.4
12	-0.714	-0.643	-0.602	-9.9	-15.7	0.0464	0.0553	0.0534	19.2	15.1	-0.0058	-0.0093	-0.0082	58.7	41.0
14	-0.139	-0.179	-0.0323	28.8	-76.8	0.0288	0.0337	-0.0268	17.0	-6.9	-0.0025	-0.0070	-0.0081	181	228
15	1.16	1.04	1.110	-10.3	-4.3	-0.0082	-0.0082	-0.0675	-	-17.5	0.0017	0.0018	-0.0017	7.1	-
17	0.877	0.764	0.775	-12.9	-11.6	-0.0170	-0.0204	-0.0213	20.0	25.3	-0.0015	0.0018	-0.0021	23.5	37.6
19	0.554	0.454	0.414	-18.1	-25.3	-0.0417	-0.0516	-0.0491	23.7	17.7	-0.0025	-0.0017	-0.0027	-33.5	7.9
21	-0.168	-0.207	-0.189	23.2	12.5	0.0433	0.0540	-0.0317	24.7	-26.8	-0.0046	-0.0043	-0.0021	-7.4	-55.4
85	-0.0195	-0.0211	-0.0225	8.2	15.4	-0.0098	-0.0101	-0.010	3.2	2.1	0.0073	0.0088	0.0128	20.8	76.3
87	-0.033	-0.0314	-0.0336	-4.8	1.8	0.0306	0.0360	0.0396	17.6	29.4	0.0249	0.0295	0.0322	18.5	29.3
89	-0.0925	-0.0810	-0.0828	-12.4	-10.5	0.0631	0.0707	0.0709	12.0	12.4	0.0379	0.0499	0.0489	31.7	29.0
91	-0.0990	-0.0765	-0.0441	-22.7	-55.5	-0.283	-0.337	-0.294	19.1	3.9	0.0669	0.128	0.109	91.3	62.9
92	3.28	3.35	3.32	2.1	1.2	-0.467	-0.423	-0.476	-9.4	1.9	0.635	0.571	0.600	-10.1	-5.5
94	2.65	2.78	2.69	4.9	1.5	-0.0621	-0.0595	-0.0667	-4.2	7.4	0.0470	0.0414	0.0467	-11.9	-0.6
96	1.70	1.90	1.72	11.8	1.2	-0.130	-0.121	-0.124	-6.9	-4.6	-0.114	-0.0986	-0.0982	-13.5	-13.9
98	0.716	0.891	0.698	24.4	-2.5	-0.423	-0.425	-0.388	0.5	-8.3	-0.365	-0.320	-0.267	-12.3	-26.8
106	-2.69	-1.82	-1.91	-32.3	-29.0	0.628	0.517	0.570	-17.7	-9.2	0.471	0.473	0.491	-	4.2
108	-1.88	-1.17	-1.19	-37.8	-36.7	0.0511	0.0427	0.0463	-16.4	-9.4	0.0307	0.0297	0.0296	-3.3	-3.6
110	-0.788	-0.350	-0.317	-55.6	-59.8	0.0399	0.0389	0.0328	-2.5	-17.8	-0.0298	-0.0282	-0.0229	-5.4	-23.2
112	0.185	0.231	0.200	24.9	8.1	0.0993	0.0980	0.101	-1.3	1.7	0.101	-0.109	-0.0929	7.9	-8.0

Table (34) Maximum Axial and Shearing Forces by LR & SARPKAYA (ω=0.56 rad/s, t=0.6T)

Member No	Max Torsion Q (NM) $\times 10^{-6}$					Max Bending Moment M_y(NM) $\times 10^{-6}$					Max Bending Moment M_z(NM) $\times 10^{-6}$				
	LR	Sarpkaya (Airy)	Sarpkaya (5th Ord)	Diff % Airy	Diff % 5th	LR	Sarpkaya (Airy)	Sarpkaya (5th Ord)	Diff % Airy	Diff % 5th	LR	Sarpkaya (Airy)	Sarpkaya (5th Ord)	Diff % Airy	Diff % 5th
1	-0.0035	-0.0083	-0.0048	135	36.2	0.0698	0.0801	-0.0856	14.8	22.6	0.454	0.417	0.444	-8.1	-2.2
3	-0.0070	-0.0105	-0.0066	50.0	-5.1	0.155	0.199	0.183	28.4	18.1	0.178	0.172	0.180	-3.4	1.1
5	-0.0034	-0.0069	-0.0038	99.7	10.2	0.169	0.209	0.185	23.7	9.5	0.134	0.139	0.140	3.7	4.5
7	-0.0096	-0.0225	-0.0226	134	135	0.270	0.374	0.391	38.5	44.8	0.466	0.5930	0.556	27.3	19.3
8	-0.0154	-0.0223	-0.0230	44.8	49.4	0.0943	0.115	0.122	22.0	29.4	0.159	0.1520	0.166	-4.4	4.4
10	-0.0510	-0.0663	-0.0639	30.0	25.3	0.171	0.213	0.206	24.6	20.5	0.166	-0.174	0.189	4.8	13.9
12	-0.0412	-0.0546	-0.0485	32.5	17.7	0.111	0.162	0.141	45.9	27.0	0.258	-0.299	0.288	15.9	11.6
14	-0.0899	-0.115	-0.0945	27.9	5.1	0.0779	0.177	0.191	127	145	0.0590	0.0628	-0.139	6.4	136
15	0.0058	0.0094	0.0064	60.7	8.9	0.0308	0.0440	0.0289	42.9	-6.2	-0.0971	-0.0860	-0.0905	-11.4	-6.8
17	0.0312	0.0419	0.0320	34.3	2.6	0.0605	0.0971	0.0697	60.5	15.2	-0.115	-0.121	-0.120	5.2	4.3
19	0.0328	0.0453	0.0336	38.1	2.4	0.0635	0.0805	0.0704	26.8	10.9	0.194	0.245	0.238	26.3	22.7
21	0.0496	0.0569	0.0375	14.7	-24.4	0.0844	0.1130	0.0724	33.9	-14.2	-0.0793	-0.0968	-0.128	22.1	61.4
85	-0.0042	-0.0089	-0.0062	112	48.1	-0.143	-0.176	-0.237	23.1	65.7	-0.334	-0.320	-0.325	-4.2	-2.7
87	-0.0100	-0.0144	-0.0128	44.0	28.0	-0.468	-0.573	-0.595	22.4	27.1	-0.463	-0.508	-0.565	9.7	22.0
89	-0.0093	-0.0135	-0.0115	44.8	23.4	-0.567	-0.748	-0.712	31.9	25.6	-0.809	-0.922	-0.927	14.0	14.6
91	-0.0129	-0.0208	-0.0196	61.2	51.9	0.822	-1.29	-1.120	56.9	36.3	-3.16	-3.66	-3.200	15.8	1.3
92	-0.554	-0.664	-0.731	19.9	31.9	-9.18	-8.23	-8.590	-10.3	-6.4	-6.50	-5.87	-6.580	-9.7	1.2
94	-0.612	-0.768	-0.715	25.5	16.8	-0.597	-0.529	-0.544	-11.4	-8.9	-0.544	-0.523	-0.593	-3.9	9.0
96	-0.850	-1.15	-0.969	35.3	14.0	-0.639	-0.568	-0.510	-11.1	-20.2	0.651	-0.622	0.621	-4.5	-4.6
98	-0.903	-1.25	-0.957	38.4	6.0	1.08	-1.28	0.972	18.5	-10.0	2.86	3.26	3.140	14.0	9.8
106	0.339	0.486	0.363	43.4	7.1	-6.77	-6.78	-7.010	-	3.5	8.83	7.27	7.980	-17.7	-9.6
108	0.277	0.427	0.285	54.2	2.9	-0.331	-0.335	-0.334	1.2	0.9	0.489	0.393	0.422	-19.6	-13.7
110	0.457	0.711	0.472	55.6	3.3	0.155	0.143	0.160	-7.7	3.2	-0.579	-0.614	-0.632	6.0	9.2
112	0.191	0.282	0.226	47.6	18.3	0.822	0.583	0.505	-29.1	-38.6	2.23	2.31	2.370	3.6	6.3

Table (35) Maximum Torsion and Bending Moments by LR & SARPKAYA (ω=0.56 rad/s, t=0.6T)

Stokes' fifth order theory the differences ranged from -76.8% to 15.4%.

b. The differences in the maximum shearing force (F_y) ranged from -17.7% to 28.4%. In the case of Stokes' theory, the differences ranged from -26.8% to 29.4%.

c. The differences in the maximum shearing force (F_z) ranged from -33.5% to 181%. In the case of Stokes' theory, the differences ranged from -55.4% to 228%.

d. The differences in the maximum torsion (Q) ranged from 14.7% to 135% according to Airy theory, and from -24.4% to 135% by Stokes' theory.

e. The differences in the maximum bending moment (M_y) ranged from -29.1% to 127% according to Airy theory, and from -38.6% to 145% by Stokes' theory.

f. The differences in the maximum bending moment (M_z) ranged from -19.6% to 27.3% according to Airy theory, and from -13.7% to 136% by Stokes' theory.

4.2 Maximum Stresses on the Members

4.2.1 LR vs Sarpkaya ($\omega = 0.37$rad/s)

Tables (36) to (38) show that:-

a. When t = 0.0, the percentage differences in the maximum tensile or comprehensive stress (σ max) ranged from 6.2% to 51.2% according to Airy theory. Stokes' fifth order theory gave differences ranging from -13.9% to 271%. The differences in the maximum shearing stress (τ max) ranged from 6.2% to 51.1% in the case of Airy theory and from -13.5% to 257% in the case of Stokes' theory.

b. When t = 0.3T, the percentage differences in (σ max) ranged from -0.8% to 91.3% according to Airy theory. Stokes' theory gave differences ranging from -10.8% to 63.5%. The differences in the maximum shearing stress (τ max) ranged from 0.8% to 88.1% in the case of Airy theory and from -6.9% to 58.8% in the case of Stokes' theory.

c. When t = 0.6T, the differences in (σ max) ranged from -30.1% to 62.5% according to Airy theory. Stokes' theory gave differences ranging from -30.8% to 174%. The differences in (τ max) ranged from -30.3% to 54.7% according to Airy theory, and from -30.8% to 157% according to Stokes' theory.

4.2.2 LR vs Sarpkaya (ω = 0.56 rad/s)

Tables (39) to (41) show that:-

a. When t = 0.0, the percentage differences in the maximum tensile or compressive stress (σ max) ranged from 1.2% to 50.7% according to Airy theory. Stokes' fifth order theory gave differences ranging from 8.4% to 298%. The differences in the maximum shearing stress (τ max) ranged from -6.2% to 44.9% in the case of Airy theory, and from 8.8% to 275% in the case of Stokes' theory.

b. When t = 0.3T the differences in (σ max) ranged from -2.1% to 87.4% according to Airy theory. Stokes' theory gave differences ranging from -12.5% to 49.5%. The differences in (τ max) ranged from -6.7% to 85.6% in the case of Airy

Member No	Max Tensile (Compr) Stress $(N/m^2) \times 10^{-8}$					Max Shearing Stress $(N/m^2) \times 10^{-8}$				
	LR	Sarpkaya (Airy)	Sarpkaya (5th Ord)	Diff %		LR	Sarpkaya (Airy)	Sarpkaya (5th Ord)	Diff %	
				Airy	5th				Airy	5th
1	0.338	0.430	0.593	27.2	75.4	0.169	0.215	0.297	27.2	75.7
3	0.243	0.312	0.417	28.4	71.6	0.122	0.156	0.208	27.9	70.5
5	0.291	0.382	0.524	31.3	80.1	0.146	0.191	0.262	30.8	79.5
7	0.231	-0.320	0.515	38.5	123	0.116	0.161	0.258	38.8	122
8	0.231	-0.30	-0.425	29.9	84.0	0.116	0.150	0.212	29.3	82.8
10	0.227	-0.304	-0.413	33.9	81.9	0.114	0.152	0.206	33.3	80.7
12	0.263	-0.370	-0.530	40.7	102	0.131	0.185	0.265	41.2	102
14	-0.0996	-0.150	-0.341	51.2	244	0.0503	0.0754	0.172	51.1	245
15	0.280	0.358	0.492	27.9	75.7	0.140	0.179	0.246	27.9	75.7
17	0.271	0.355	0.475	31.0	75.3	0.136	0.178	0.238	30.9	75.0
19	0.326	0.422	0.603	29.4	85.0	0.163	0.211	0.302	29.4	85.3
21	0.135	0.193	0.501	43.0	271	0.0703	0.101	0.251	43.7	257
85	0.267	0.310	0.230	16.1	-13.9	0.133	0.155	0.115	16.5	-13.5
87	0.331	0.368	0.337	11.5	2.1	0.166	0.184	0.168	11.5	1.8
89	0.488	0.536	0.541	9.8	10.9	0.245	0.269	0.271	10.2	11.1
91	-0.744	-0.79	0.795	6.2	6.9	0.373	0.396	0.398	6.2	6.7
92	0.639	0.811	1.23	26.9	92.5	0.319	0.405	0.614	27.0	92.5
94	0.123	0.155	0.275	26.0	124	0.0617	0.0774	0.138	25.4	124
96	0.0663	0.0839	0.162	26.5	144	0.0336	0.043	0.0821	28.0	144
98	0.0374	0.0465	0.115	24.3	208	0.0198	0.0256	0.0602	29.3	204
106	-0.668	-0.860	-1.29	28.7	93.1	0.334	0.430	0.647	28.7	93.7
108	-0.161	-0.211	-0.330	31.1	105	0.0811	0.106	0.165	30.7	104
110	-0.101	-0.124	-0.202	22.8	100	0.0532	0.0658	0.104	23.7	95.5
112	-0.0827	-0.0951	-0.171	15.0	107	0.0414	0.0480	0.0919	15.9	122

Table (36) Maximum Stresses on the Members by LR & SARPKAYA (ω =0.37 rad/s, t=0.0)

Member No	Max Tensile (Compr) Stress $(N/m^2) \times 10^{-8}$					Max Shearing Stress $(N/m^2) \times 10^{-8}$				
	LR	Sarpkaya (Airy)	Sarpkaya (5th Ord)	Diff %		LR	Sarpkaya (Airy)	Sarpkaya (5th Ord)	Diff %	
				Airy	5th				Airy	5th
1	-0.739	-0.796	-0.814	7.7	10.1	0.370	0.398	0.407	7.6	10.0
3	-0.418	-0.474	-0.459	13.4	9.8	0.209	0.237	0.229	13.4	9.6
5	-0.393	-0.498	-0.455	26.7	15.8	0.197	0.249	0.228	26.4	15.7
7	-0.299	-0.435	-0.432	45.5	44.5	0.150	0.219	0.217	46.0	44.7
8	0.576	0.630	0.643	9.4	11.6	0.288	0.315	0.321	9.4	11.5
10	0.422	0.499	0.480	18.2	13.7	0.211	0.250	0.24	18.5	13.7
12	0.439	0.569	0.506	29.6	15.3	0.220	0.285	0.253	29.5	15.0
14	0.104	0.199	0.170	91.3	63.5	0.0537	0.101	0.0853	88.1	58.8
15	-0.589	-0.644	-0.661	9.3	12.2	0.295	0.322	0.331	9.2	12.2
17	-0.439	-0.511	-0.493	16.4	12.3	0.220	0.256	0.247	16.4	12.3
19	-0.391	-0.462	-0.417	18.2	6.6	0.196	0.232	0.210	18.4	7.1
21	0.126	-0.174	0.170	38.1	34.9	0.0648	0.092	0.0889	42.0	37.2
85	-0.199	-0.217	-0.285	9.0	43.2	0.0995	0.109	0.143	9.5	43.7
87	-0.178	-0.250	-0.252	40.4	41.6	0.0892	0.125	0.126	40.1	41.3
89	-0.388	-0.625	-0.553	61.1	42.5	-0.195	0.314	0.277	61.0	42.1
91	-0.881	-1.31	-1.13	48.7	28.3	0.442	0.657	0.569	48.6	28.7
92	-1.57	-1.72	-1.72	9.6	9.6	0.786	0.860	0.861	9.4	9.5
94	-0.299	-0.353	-0.323	18.1	8.0	0.150	0.176	0.161	17.3	7.3
96	-0.151	-0.181	-0.154	19.9	2.0	0.0763	0.0912	0.0777	19.5	1.8
98	-0.106	-0.130	-0.108	22.6	1.9	0.0533	0.0649	0.0540	21.8	1.3
106	1.56	1.63	1.66	4.5	6.4	0.786	0.818	0.829	5.1	6.6
108	0.264	0.265	0.246	-	-6.8	0.133	0.134	0.124	0.8	-6.8
110	0.120	0.119	0.107	-0.8	-10.8	0.0609	0.0633	0.0567	3.9	-6.9
112	0.0934	0.109	-0.0966	16.7	3.4	0.0468	0.0562	0.0495	20.1	5.8

Table (37) Maximum Stresses on the Members by LR & SARPKAYA (ω =0.37 rad/s, t=0.3T)

Member No	Max Tensile (Compr) Stress $(N/m^2) \times 10^{-8}$					Max Shearing Stress $(N/m^2) \times 10^{-8}$				
	LR	Sarpkaya (Airy)	Sarpkaya (5th Ord)	Diff % Airy	Diff % 5th	LR	Sarpkaya (Airy)	Sarpkaya (5th Ord)	Diff % Airy	Diff % 5th
1	-0.229	-0.190	-0.171	-17.0	-25.3	0.114	0.0948	0.0856	-16.8	-24.9
3	-0.127	-0.115	-0.104	-9.4	-18.1	0.0637	0.0573	0.0523	-10.0	-17.9
5	-0.127	-0.126	-0.131	-0.8	3.1	0.0638	0.0630	0.0656	-1.3	2.8
7	-0.170	-0.199	-0.186	17.1	9.4	0.0856	0.100	0.0941	16.8	9.9
8	-0.188	-0.162	-0.150	13.8	-20.2	0.0941	0.0812	0.0748	-13.7	-20.5
10	-0.140	-0.126	-0.114	-10.0	-18.6	0.070	0.0632	0.0574	-9.7	-18.0
12	-0.137	-0.131	-0.115	-4.4	-16.1	0.0690	0.0659	0.0576	-4.5	-16.5
14	-0.0365	-0.0416	0.100	14.0	174	0.0195	0.0221	0.0502	13.3	157
15	0.141	0.116	0.101	-17.7	-28.4	0.0703	0.0582	0.0505	-17.2	-28.2
17	0.0961	0.0865	0.0919	-10.0	-4.4	0.0480	0.0433	0.0468	-10.0	-2.7
19	0.139	-0.184	-0.196	32.4	41.0	0.0695	0.0919	0.0980	32.2	41.0
21	-0.0577	-0.0787	-0.0952	36.4	65.0	0.0307	0.0416	0.0478	35.5	55.7
85	-0.253	-0.273	-0.184	7.9	-27.3	0.126	0.137	0.0921	8.7	-26.9
87	-0.327	-0.381	-0.316	16.5	-3.4	0.164	0.190	0.158	15.9	-3.7
89	-0.512	-0.603	-0.525	17.8	2.5	0.256	0.302	0.263	18.0	2.7
91	0.849	0.921	-0.813	8.5	-4.2	0.425	0.461	0.407	8.5	-4.2
92	0.444	0.361	0.241	-18.7	-23.2	0.222	0.181	0.171	-18.5	-23.0
94	0.0842	0.081	0.0654	-3.8	-22.3	0.0425	0.0411	0.0331	-3.3	-22.1
96	0.0555	0.0579	0.0462	4.3	-16.8	0.0293	0.0306	0.0244	4.4	-16.7
98	0.0643	0.0823	0.0589	28.0	-8.4	0.0322	0.0435	0.0315	35.1	-2.2
106	-0.396	0.277	0.274	-30.1	-30.8	0.198	0.138	0.137	-30.3	-30.8
108	-0.0391	0.0416	0.0456	6.4	16.6	0.0198	0.0213	0.0233	7.6	17.7
110	0.0299	0.0486	0.0533	62.5	78.3	0.0170	0.0263	0.0282	54.7	65.9
112	0.0689	0.0775	0.0672	12.5	-2.5	0.0344	0.0389	0.0336	13.1	-2.3

Table (38) Maximum Stresses on the Members by LR & SARPKAYA (ω =0.37 rad/s, t=0.6T)

Member No	Max Tensile (Compr) Stress $(N/m^2) \times 10^{-8}$					Max Shearing Stress $(N/m^2) \times 10^{-8}$				
	LR	Sarpkaya (Airy)	Sarpkaya (5th Ord)	Diff % Airy	Diff % 5th	LR	Sarpkaya (Airy)	Sarpkaya (5th Ord)	Diff % Airy	Diff % 5th
1	0.0845	0.108	0.148	27.8	75.1	0.0423	0.0540	0.0738	27.7	74.5
3	0.0813	0.102	0.128	25.5	57.4	0.0407	0.0509	0.0641	25.1	57.5
5	0.147	0.174	0.205	18.4	39.5	0.0734	0.087	0.103	18.5	40.3
7	0.210	0.255	0.368	21.4	75.2	0.106	0.129	0.184	21.7	73.6
8	-0.0584	-0.075	-0.104	28.4	78.1	0.0292	0.0375	0.0519	28.4	77.7
10	-0.0656	-0.0836	-0.109	27.4	66.2	0.0329	0.0419	0.0547	27.4	66.3
12	-0.130	-0.161	-0.190	23.8	46.2	0.0653	0.0808	0.0950	23.7	45.5
14	0.0341	0.0514	-0.127	50.7	272	0.0178	0.0258	0.0636	44.9	257
15	0.0756	0.096	0.126	27.0	66.7	0.0379	0.0481	0.0628	26.9	65.7
17	0.101	0.131	0.159	29.7	57.4	0.0504	0.0656	0.0794	30.2	57.5
19	0.175	0.226	0.263	29.1	50.3	0.0876	0.113	0.132	29.0	50.7
21	0.0836	0.119	0.333	42.3	298	0.0448	0.0638	0.168	42.4	275
85	0.0458	0.0573	0.0636	25.1	38.9	0.0229	0.0286	0.0318	24.9	38.9
87	0.110	0.129	0.144	17.3	30.9	0.0549	0.0644	0.0720	17.3	31.1
89	0.298	0.337	0.348	13.1	16.8	0.149	0.169	0.174	13.4	16.8
91	0.932	1.07	1.01	14.8	8.4	0.467	0.538	0.508	15.2	8.8
92	0.185	0.232	0.327	25.4	76.8	0.0927	0.116	0.163	25.5	76.4
94	0.0408	0.0499	0.080	22.3	96.1	0.0208	0.0251	0.0401	20.7	92.8
96	0.0318	0.0370	0.0575	16.4	80.8	0.0160	0.0194	0.0294	21.3	83.8
98	-0.0496	-0.0524	0.0850	5.6	71.4	0.0249	0.0266	0.0442	6.8	77.5
106	-0.183	-0.237	-0.337	29.5	84.2	0.0919	0.119	0.169	29.5	83.9
108	-0.0562	-0.0728	-0.105	29.5	86.8	0.0290	0.0375	0.0530	29.3	82.8
110	-0.0578	-0.0703	-0.0901	21.6	55.9	0.0316	0.0392	0.0486	24.1	53.8
112	-0.0746	-0.0755	-0.100	1.2	34.0	0.0417	0.0391	0.0589	-6.2	41.2

Table (39) Maximum Stresses on the Members by LR & SARPKAYA (ω =0.56 rad/s, t=0.0)

Member No	Max Tensile (Compr) Stress (N/m^2) x 10^{-8} LR	Sarpkaya (Airy)	Sarpkaya (5th Ord)	Diff % Airy	Diff % 5th	Max Shearing Stress (N/m^2) x 10^{-8} LR	Sarpkaya (Airy)	Sarpkaya (5th Ord)	Diff % Airy	Diff % 5th
1	-0.403	-0.417	-0.405	3.5	0.5	0.202	0.208	0.202	3.0	-
3	-0.253	-0.267	-0.257	5.5	1.6	0.126	0.133	0.128	5.6	1.6
5	-0.298	-0.333	-0.307	11.7	3.0	0.149	0.167	0.153	12.1	2.7
7	-0.261	-0.370	-0.381	41.8	46.0	0.131	0.187	0.192	42.7	46.6
8	0.306	0.317	0.308	3.6	0.7	0.153	0.158	0.154	3.3	0.7
10	0.263	0.280	0.268	6.5	1.9	0.132	0.140	0.134	6.1	1.5
12	0.336	0.398	0.359	18.5	6.8	0.168	0.199	0.180	18.5	7.1
14	0.0923	0.173	0.138	87.4	49.5	0.0473	0.0878	0.0694	85.6	46.7
15	-0.314	-0.327	-0.319	4.1	1.6	0.157	0.163	0.159	3.8	1.3
17	-0.285	-0.314	-0.304	10.2	6.7	0.143	0.157	0.152	9.8	6.3
19	-0.356	-0.411	-0.375	15.4	5.3	0.178	0.206	0.188	15.7	5.6
21	-0.115	-0.141	-0.139	22.6	20.9	0.0592	0.0747	0.0728	26.2	23.0
85	-0.0896	-0.0889	-0.0918	-0.8	2.5	0.0448	0.0445	0.0459	-0.7	2.5
87	-0.0708	-0.0746	-0.0871	5.4	23.0	0.0355	0.0374	0.0437	5.4	23.1
89	-0.173	-0.220	-0.230	27.2	32.9	0.0866	0.110	0.115	27.0	32.8
91	-0.830	-1.27	-1.08	53.0	30.1	0.417	0.64	0.542	53.5	30.0
92	-0.889	-0.939	-0.896	5.6	0.8	0.445	0.469	0.448	5.4	0.7
94	-0.209	-0.233	-0.210	11.5	0.5	0.104	0.116	0.105	11.5	1.0
96	-0.120	-0.138	-0.120	15.0	-	0.0609	0.0699	0.0606	14.8	-0.5
98	-0.0921	-0.101	-0.0988	9.7	7.3	0.0479	0.0505	0.0494	5.4	3.1
106	0.876	0.891	0.858	1.7	-2.1	0.438	0.445	0.429	1.6	-2.1
108	0.192	0.188	0.174	-2.1	-9.4	0.0963	0.0944	0.0875	-2.0	-9.1
110	0.101	0.102	0.0884	1.0	-12.5	0.0520	0.0553	0.0479	6.3	-7.9
112	0.103	0.103	0.0975	-	-5.3	0.0585	0.0546	0.0517	-6.7	-11.6

Table (40) Maximum Stresses on the Members by LR & SARPKAYA (ω =0.56 rad/s, t=0.3T)

Member No	Max Tensile (Compr) Stress (N/m^2) x 10^{-8} LR	Sarpkaya (Airy)	Sarpkaya (5th Ord)	Diff % Airy	Diff % 5th	Max Shearing Stress (N/m^2) x 10^{-8} LR	Sarpkaya (Airy)	Sarpkaya (5th Ord)	Diff % Airy	Diff % 5th
1	-0.157	-0.143	-0.153	-8.9	-2.5	0.0783	0.0714	0.0763	-8.8	-2.6
3	-0.105	-0.102	-0.103	-2.9	-1.9	0.0524	0.0512	0.0515	-2.3	-1.7
5	-1.144	-0.147	-0.137	2.1	-4.9	0.0721	0.0737	0.0683	2.2	-5.3
7	-0.223	-0.271	-0.236	21.5	5.8	0.112	0.136	0.119	21.4	6.3
8	-0.126	-0.117	-0.125	-7.1	-0.8	0.0629	0.0586	0.0624	-6.8	-0.8
10	-0.116	-0.115	-0.117	-0.9	0.9	0.0583	0.0575	0.0587	-1.4	0.7
12	-0.160	-0.170	-0.160	6.3	-	0.0802	0.0855	0.0803	6.6	-
14	-0.050	-0.0812	-0.0746	62.4	49.2	0.0282	0.0439	0.038	55.7	34.8
15	0.110	0.0996	0.105	-9.5	-4.5	0.0551	0.0498	0.0523	-9.6	-5.1
17	0.0917	0.0869	0.0851	-5.2	-7.2	0.0459	0.0434	0.0426	-5.4	-7.2
19	0.120	0.125	0.118	4.2	-1.7	0.0598	0.0624	0.0588	4.3	-1.7
21	-0.0560	-0.0705	-0.0638	25.9	13.9	0.0299	0.0374	0.0320	25.1	7.0
85	-0.0612	-0.0616	-0.0677	0.7	10.6	0.0306	0.0308	0.0339	0.7	10.8
87	-0.111	-0.129	-0.138	16.2	24.3	0.0556	0.0646	0.0690	16.2	24.1
89	-0.301	-0.359	-0.354	19.3	17.6	0.151	0.180	0.177	19.2	17.2
91	-0.973	-1.15	-1.00	18.2	2.8	0.487	0.575	0.502	18.1	3.1
92	0.338	0.313	0.329	-7.4	-2.7	0.169	0.157	0.164	-7.1	-3.0
94	0.0805	0.0823	0.0813	2.2	1.0	0.0406	0.0417	0.0411	2.7	1.2
96	0.0620	0.0693	0.0604	11.8	-2.6	0.0318	0.0376	0.0313	18.2	-1.6
98	0.0930	0.103	0.093	10.8	-	0.0534	0.0518	0.050	-3.0	-6.4
106	-0.321	-0.274	-0.292	-14.6	-9.0	0.161	0.137	0.146	-14.9	-9.3
108	-0.0572	-0.0395	-0.0402	-30.9	-29.7	0.0287	0.0201	0.0202	-30.0	-29.6
110	-0.0336	-0.0265	-0.0244	-21.1	-27.4	0.0175	0.0151	0.0132	-13.7	-24.6
112	0.0608	0.0609	0.0611	-	0.5	0.0309	0.0304	0.0306	-1.6	-1.0

Table (41) Maximum Stresses on the Members by LR & SARPKAYA (ω =0.56 rad/s, t=0.6T) theory, and **from** -11.6% to 46.7% in the case of Stokes' theory.

c. When t = 0.6T the differences in (σ max) ranged from -30.9% to 62.4% according to Airy theory. Stokes' theory gave differences ranging from -29.7% to 49.2%. The differences in (τ max) ranged from -30.0% to 55.7% in the case of Airy theory and from -29.6% to 34.8% in the case of Stokes' theory.

4.3 Average Differences

Similarly to the results of Tables (22) and (23), Tables (42) and (43) show that the average percentage differences for the stresses decrease with the increase of time from t = 0.0 to t = 0.6T at both frequencies (ω=0.37 rad/s and 0.56 rad/s). The average percentage differences at ω= 0.37 rad/s are larger than the corresponding values at ω= 0.56 rad/s.

5. CLOSING DISCUSSION

As has been previously mentioned, the calculations of the maximum stresses were based on formulations from the basic principles of stress analysis and without considering safety factors (See Appendix E).

One may argue that if the stresses had been calculated according to the rules and strength formulation of each classification society (LR, DnV, BV), the percentage differences in the stresses would have been smaller and even negligible. To this point may be added the possibility that each classification society could have suggested different scantlings (diameter, wall thickness) for the

Forces Moment or Stress	SARPKAYA (Airy) Min Diff %	Member No	Max Diff %	Member No	Av Diff %	SARPKAYA (5th Order) Min Diff %	Member No	Max Diff %	Member No	Av Diff %
t = 0.0										
N	-23.7	7	35.2	98	22.2	4.0	91	1078	14	165
F_Y	-19.7	91	137	96	22.3	-45.8	85	1434	14	121
F_Z	-21.5	96	406	98	49.3	-6.1	96	964	98	135
Q	7.5	1	111	94	45.4	-71.4	91	319	112	85.5
M_Y	7.9	110	61.0	12	37.3	27.5	91	206	94	95.8
M_Z	-21.1	91	47.7	96	17.4	-25.5	85	911	21	95.0
σ max	6.2	91	51.2	14	27.4	-13.9	85	271	21	97.8
τ max	6.2	91	51.1	14	27.4	-13.5	85	257	21	97.4
t = 0.3T										
N	-28.2	21	114	91	16.7	-67.8	112	413	21	23.2
F_Y	-9.9	112	54.3	87	15.1	-45.8	14	42.3	19	6.4
F_Z	-11.3	110	218	12	54.8	-15.0	112	196	12	49.0
Q	-14.3	89	295	7	48.7	-69.1	98	262	7	39.6
M_Y	-14.4	110	136	12	37.9	-13.7	96	129	12	39.6
M_Z	-25.0	19	52.5	89	15.9	-18.1	87	40.0	14	12.5
σ max	-0.8	110	91.3	14	23.9	-10.8	110	63.5	14	17.5
τ max	0.8	108	88.1	14	24.3	-6.9	110	58.8	14	17.6
t = 0.6T										
N	-91.3	106	401	110	18.1	-85.2	12	540	110	22.2
F_Y	-29.3	106	26.3	21	6.7	-59.6	85	286	14	1.3
F_Z	-27.9	98	121	19	23.2	-39.0	15	486	21	45.3
Q	-40.9	5	958	15	80.6	-35.3	1	2188	15	147.9
M_Y	-22.3	92	110	17	23.6	-26.9	94	200	21	39.5
M_Z	-30.0	106	26.9	21	7.4	-56.5	85	322	14	7.6
σ max	-30.1	106	62.5	110	5.4	-30.8	106	174	14	5.0
τ max	-30.3	106	54.7	110	5.4	-30.8	106	157	14	3.9

Table (42) Percentage Differences of SARPKAYA Relative to LR (ω=0.37 rad/s)

Forces Moment or Stress	SARPKAYA (Airy) Min Diff %	Member No	Max Diff %	Member No	Av Diff %	SARPKAYA (5th Order) Min Diff %	Member No	Max Diff %	Member No	Av Diff %
t = 0.0										
N	-14.4	98	37.6	112	18.3	-30.8	89	999	98	126
F_Y	-18.3	108	38.6	99	10.0	-52.1	98	704	14	66.5
F_Z	-32.7	98	214	14	31.9	-9.9	110	579	14	666.5
Q	-16.5	12	76.6	112	28.3	-52.8	91	126	112	335.5
M_Y	-7.3	98	84.0	14	28.8	-15.8	96	279	14	63.4
M_Z	-4.2	112	39.2	106	16.8	-70.0	98	878	21	81.2
σ max	1.2	112	50.7	14	23.9	8.4	91	298	21	77.7
τ max	6.2	112	44.9	14	23.7	8.8	91	275	21	76.2
t = 0.3T										
N	-51.2	85	74.5	91	6.5	-38.7	112	158	85	10.4
F_Y	-14.4	110	37.6	12	8.6	-94.4	14	34.8	12	1.1
F_Z	-19.1	110	238	14	33.2	-21.6	112	120	7	29.5
Q	-17.8	91	177	7	35.2	-91.3	91	143	7	29.9
M_Y	-11.5	110	120	14	24.6	-24.1	112	88.5	14	26.0
M_Z	-8.9	110	48.4	14	10.8	-29.0	110	71.5	112	6.6
σ max	-2.1	108	87.4	14	14.9	-12.5	110	49.5	14	8.8
τ max	-6.7	112	85.6	14	14.7	-11.6	112	46.7	14	8.5
t = 0.6T										
N	-55.6	110	28.8	14	-5.8	-76.8	14	15.4	85	-15.5
F_Y	-17.7	99	28.4	7	6.3	-26.8	21	29.4	87	4.2
F_Z	-33.5	19	181	14	20.0	-55.4	21	228	14	22.7
Q	14.7	21	135	1	53.5	-24.4	21	135	7	21.5
M_Y	-29.1	112	127	14	23.9	-38.6	112	145	14	16.7
M_Z	-19.6	108	27.3	7	3.7	-13.7	108	136	14	13.0
σ max	-30.9	108	62.4	14	3.9	-29.7	108	49.2	14	1.3
τ max	-30.0	108	55.7	14	3.6	-29.6	108	34.8	14	-

Table (43) Percentage Differences of SARPKAYA Relative to LR (ω=0.56 rad/s) members for the same structure in such a way that, at the end, the maximum stresses estimated by the different societies would have been approximately the same.

However, one can justify the fairness of the method used to compare the results of the different societies on the grounds of the following facts:

a. To examine the effects of the different recommended coefficients (C_D, C_M) we must refer to a common base for comparison, ie, the same structure should be used. Otherwise, it would be impossible to compare wave loading results for two different jackets, each with different sets of C_D and C_M.

b. For fair comparison, the method of computing the stresses should also be the same in order to exclude any effect of the different safety factors inherent in the design codes of the different classification societies.

c. To say that applying the rules (wave loading and strength) of two different classification societies would, eventually, result in the same structure means that one of the two societies is adopting unnecessary or inadequate safety factors because the wave loadings, according to the two, are essentially different. There are also many doubts that the observed percentage differences in the loading can be balanced or remedied by larger safety factors.

d. The role of the classification societies has been mainly checking and approving ready-made designs, rather than designing structures. The structural drawings are submitted

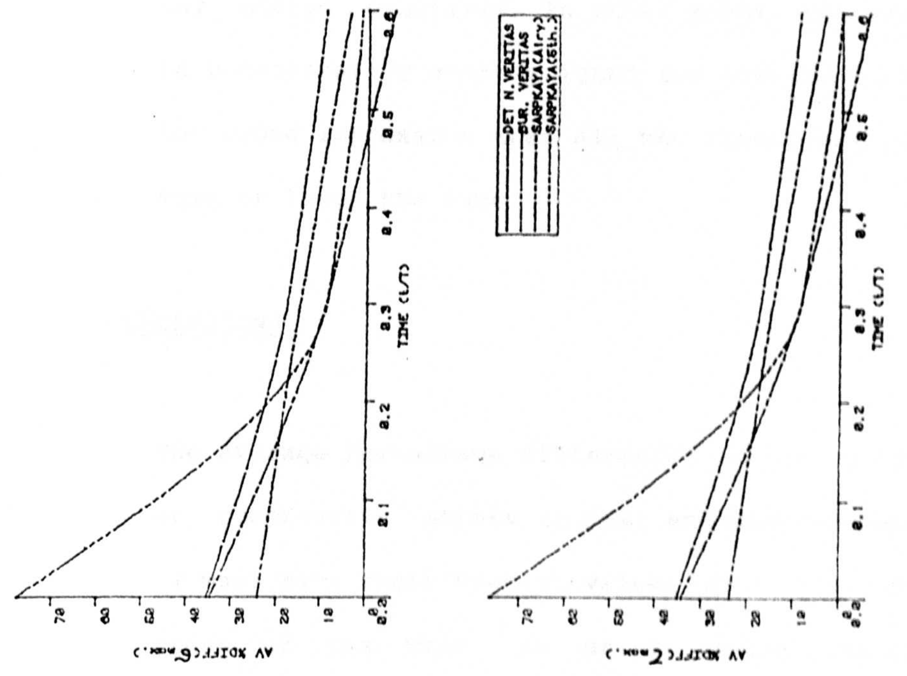

ω = 0.56 rad/s

FIG.(7) AVERAGE %DIFF. IN MAX. STRESSES VS. TIME

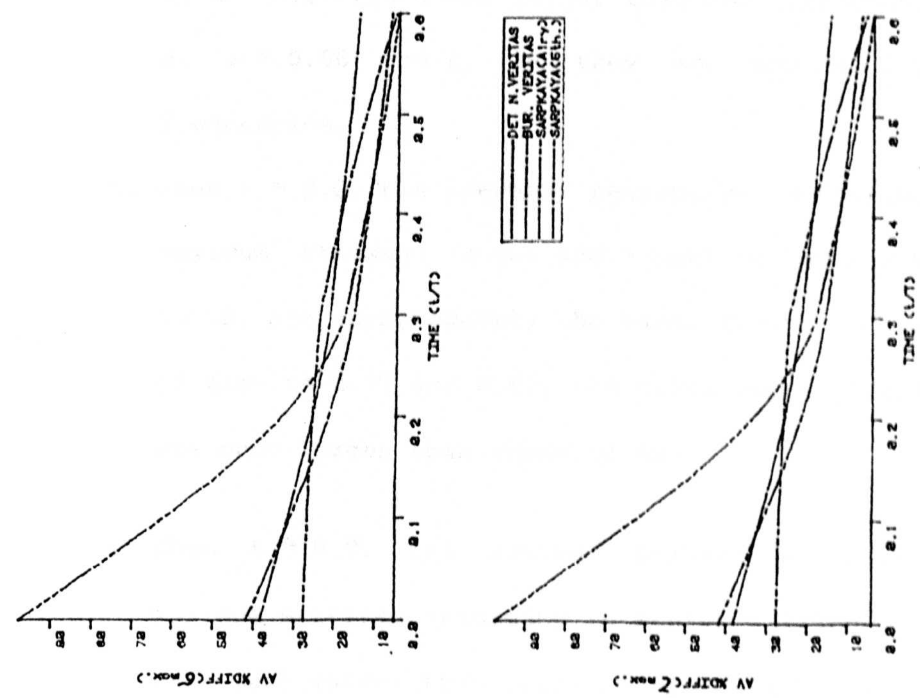

ω = 0.37 rad/s

FIG.(6) AVERAGE %DIFF. IN MAX. STRESSES VS. TIME by the client for approval and they usually meet (or are made to meet) the standards and requirements of any classification society due to the conservatism in present day design practices. In other words, the structure could be unnecessarily over-designed and uneconomical. This gives the wrong impression that all the classification rules are, more or less, the same.

6. CONCLUSIONS

a. The average percentage differences in the maximum tensile or compressive stress (σ max) and maximum shearing stress (τ max) have their highest values when t = 0.0, when the crest of the wave is at the centre-line of the jacket structure. The differences in the stresses decrease with the change of time from t = 0.0 to t = 0.6T.

b. The average percentage differences in the maximum stresses at ω = 0.37 rad/s are larger than the corresponding values at ω = 0.56 rad/s, ie they are smaller for the higher frequencies.

c. When t = 0.0, the average percentage differences in the maximum stresses (σ max and τ max) by DnV and BV, relative to LR, are approximately the same. However, with the change of time to 0.3T and 0.6T, the differences according to DnV are much larger than those of BV.

d. When t = 0.0, the average percentage differences in the maximum stresses according to Stokes' fifth order theory are much larger than those of Airy theory. With the change of time, the differences according to Stokes' theory decrease rapidly to values less than the corresponding values of Airy theory.

e. When using the coefficients recommended by LR, DnV and BV, Tables (16) to (21), the maximum absolute values of the stresses occurred at $t = 0.3T$ for $\omega = 0.37$ rad/s and at $t = 0.6T$ for $\omega = 0.56$ rad/s. When using Sarpkaya's coefficients, Tables (36) to (41), the maximum stresses occurred at $t = 0.3T$ for both frequencies, $\omega = 0.37$ and 0.56 rad/s.

REFERENCES

1. BATHE, K J, WILSON, E L, and PETERSON, F E, 'SAP IV - A Structural Analysis Program for Static and Dynamic Response of Linear Systems', Report No EERC 73-11, College of Engineering, University of California, Berkeley, 1974.

2. BUREAU VERITAS, 'Rules and Regulations for the Construction and Classification of Offshore Platforms', 1975.

3. DET NORSKE VERITAS, 'Rules for the Design, Construction and Inspection of Mobile Offshore Units', 1974.

4. DET NORSKE VERITAS, 'Rules for the Construction and Classification of Mobile Offshore Units', 1975.

5. DET NORSKE VERITAS, 'Rules for the Design, Construction and Inspection of Offshore Structures', Appendix B, 1977.

6. LLOYD'S REGISTER OF SHIPPING, 'Rules for the Construction and Classification of Mobile Offshore Units', 1972.

7. SARPKAYA, T, 'In-Line and Transverse Forces on Smooth and Sand-Roughened Cylinders in Oscillatory Flow at High Reynolds Numbers', Naval Postgraduate School, Technical Report No NPS-69SL76062, Monterey, CA, Jun 76.

8. SARPKAYA, T, 'Vortex Shedding and Resistance in Harmonic Flow about Smooth and Rough Circular Cylinders at High Reynolds Numbers', Naval Postgraduate School, Technical Report No NPS-59SL76021, Moneterey, CA, Feb 76.

9. SARPKAYA, T, 'In-Line and Transverse Forces on Cylinders in Oscillatory Flow at High Reynolds Numbers', OTC Paper No 2533, Houston, Texas, May 76.

10. SARPKAYA, T, 'Vortex Shedding and Resistance in Harmonic Flow about Smooth and Rough Circular Cylinders', BOSS '76, Trondheim, Vol I, 1976, pp220-235.

11. SARPKAYA, T, 'In-Line and Transverse Forces on Cylinders in Oscillatory Flow at High Reynolds Numbers', Jour of Ship Research, Vol 24, No 4, Dec 77, pp200-216.

12. SARPKAYA, T, 'The Hydrodynamic Resistance of Roughened Cylinders in Harmonic Flow', Trans RINA, Vol 120, 1978, pp41-55.

13. SARPKAYA, T, COLLINS, N J, and EVANS, S R, 'Wave Forces on Rough-Walled Cylinders at High Reynolds Numbers', OTC Paper No 2901, Houston, Texas, 1977.

14. SARPKAYA, T, and ISAACSON, M, 'Mechanics of Wave Forces on Offshore Structures', Van Nostrand Reinhold, New York, 1981.

15. SKJELBREIA, L, and HENDRICKSON, J A, 'Fifth Order Gravity Wave Theory', Proc 7th Coastal Eng Conf, The Hague, 1961, pp184-196.

16. VALIDAKIS J, 'On Joining a Wave Loading Program to 'SAPIV', (To be published).

CHAPTER 10

CHAPTER 10

RELIABILITY ANALYSIS IN THE DESIGN OF JACKET PLATFORMS

1. INTRODUCTION

Structural reliability theory is concerned with the rational treatment of uncertainties in structural design and with the methods for assessing the safety and serviceability of structures (46). The theory has developed rapidly over the last fifteen years (3-5, 19, 28, 30, 31). From the results of reliability analysis, it is possible to determine the relative importance of the different parameters regarding their effect on the safety of the structure, eg Refs (4-6, 23, 25, 41, 43, 45).

The concept of reliability analysis is also a valuable tool in the development of rational safety formats for design codes and for the evaluation of partial coefficients. The main potential for direct application is with structures having large failure consequences or where the use gives immediate savings in construction costs.

Within the fields of structural and offshore engineering, the practical application of reliability analysis has been mainly in the development of design codes to obtain optimal sets of partial coefficients, eg Refs (11, 34). This is partly because practical methods of reliability analysis are relatively recent and engineers and designers are not yet fully familiar with them and partly because the methods of analysis especially for complex systems with multiple failure modes need further improvements. Recently, reliability based design codes have been developed for fixed offshore platforms (32, 53) and tension leg platforms (9,16,29).

In this chapter the applicaton of the reliability analysis for jacket structures will be discussed with a special emphasis on the uncertainties in the environmental loadings.

2. METHODS OF RELIABILITY ANALYSIS

2.1 General

Methods of structural reliability analysis can be divided into two broad classes. These are (46):-

Level 3: (Full Probabilistic Approach): Methods in which calculations are made to determine the 'exact' probability of failure for a structure or structural component, making use of a full probabilistic description of the joint occurrence of the various quantities which affect the response of the structure and taking into account the true nature of the failure domain.

Level 2: (Semi-Probabilistic Approach): Methods involving certain approximate iterative calculation procedures to obtain an approximation to the failure probability of a structure or structural system, generally requiring an idealisation of failure domain and often associated with a simplified representation of the joint probability distributions of the variables.

In theory, both level 3 and level 2 methods can be used for checking the safety of a design or directly in the design process, provided a target reliability or reliability index has been specified.

However, for evaluating the partial coefficients or for use in design, level 2 methods are usually used for offshore structures.

2.2 Level 2 Method

The key step is the identification of a suitable mathematical model which defines failure in terms of a function (46):-

$$M = f(X_1, X_2 \ldots X_n) = f(\bar{X}) < 0$$

where $\bar{X}$ is a vector of basic random variables. For dynamically sensitive offshore structures the function f incorporates all the models for loading and response together with the failure criterion for the structural component under consideration (eg buckling, fatigue).

The reliability is given by:-

$$R = 1 - P_f = 1 - \underset{f(\bar{X}) < 0}{\int\int \ldots \int} f_{X_1, X_2, \ldots X_n}(x_1, x_2 \ldots x_n) dx_1, dx_2 \ldots dx_n$$

where $f_{X_1, X_2, \ldots X_n}(x_1, x_2, \ldots x_n)$ is the joint probability density function for the n variables X_i.

For complex failure functions involving spectral analysis, the following algorithm can be used (46) to apply level 2 method:-

a. Specification of the failure function f in terms of n basic random variables $\bar{X}$.

b. Creation of the failure surface in the n-dimensional space of the basic variables $\bar{X}$(x - space) by setting $f(\bar{X}) = 0$.

c. Defining the joint density function $f_{\bar{X}}$ for the n basic variables.

d. Mapping the failure surface in $\bar{X}$ - space to the space of n independent standard normal variables $\bar{Z}$ (z - space).

e. Finding the shortest distance, β, from the origin to the failure surface.

f. $R = 1 - P_f = 1 - \phi(-\beta)$

The methods of calculating R are described in Reference (46).

For any particular value of peak response (displacement) of the jacket, the forces and moments can be calculated for any member by linear analysis methods and the strength of the individual members of the jacket can be assessed against failure.

Knowing the probability distribution of the relevant basic variables and the uncertainties in strength models, it is possible to determine the probability of failure for any member for any given sea state and by integrating over all possible sea states, to evaluate the total probability of failure for any individual member throughout the assumed design life of the jacket

2.3 Reliability Analysis for Individual Members

2.3.1 Sensitivity analysis

Following the procedure presented in Reference (43), the method can be summarised as follows:-

a. The inline force per unit length of the cylinder is calculated by Morison's equation:-

$$F = \frac{\pi}{4}d^2.\rho.C_M\,\dot{U} + 0.5\rho d.C_D\,U\,|U| \qquad (1)$$

The length of cylinder is divided into a number of sections and the total force is calculated by numerical integration.

b. The force F is defined as a function g of the main variables: wave height (H), wave period (T), current velocity (V_s), drag coefficient (C_D), inertia coefficient (C_M) and wave kinematics U and $\dot{U}$.

$$F = g(H, T, V_s, C_D, C_M, U, \dot{U}) \tag{2}$$

c. The mean value is given by:-

$$\mu_F \simeq g(\mu_H, \mu_T, \mu_{V_s}, \mu_{C_D}, \mu_{C_M}, \mu_U, \mu_{\dot{U}}) \tag{3}$$

As an approximation, μ_F, is calculated from equation (1) by substituting for the variables by their mean values, μ_H, μ_T....etc.

d. The variance of F is given by the general relation:-

$$\sigma_F^{\,2} \simeq \sum_{i=1}^{7} \left(\frac{\partial g}{\partial x_i}\bigg|_{\mu_F}\right)^2 \sigma_{x_i}^{\,2} + \sum_{i=1}^{7} \sum_{\substack{j=1 \\ i \neq j}}^{7} \left(\frac{\partial g}{\partial x_i}\bigg|_{\mu_F}\right) \left(\frac{\partial g}{\partial x_j}\bigg|_{\mu_F}\right) \sigma_{x_i} \sigma_{x_j} \alpha_{ij} \tag{4}$$

where x_i is any variable in equation (2), (i=1-7)

σ_{x_i} is the standard deviation of variable x_i

σ_{x_j} is the standard deviation of variable x_j

α_{ij} is the correlation coefficient between variables i and j

$\left(\frac{\partial g}{\partial x_i}\bigg|_{\mu_F}\right)$ are the partial derivatives of the function g with respect to each variable, evaluated at its mean value

e. If the variables are assumed to be statistically independent, ie $\alpha_{ij} = 0.0$, equation (4) reduces to:-

$$\sigma_F^{\,2} \simeq \sum_{i=1}^{7} \left(\frac{\partial g}{\partial x_i}\bigg|_{\mu_F}\right)^2 \sigma_{x_i}^{\,2} \tag{5}$$

f. The partial derivatives $\left(\frac{\partial g}{\partial x_i}\bigg|_{\mu_F}\right)$ are evaluated numerically using equation (1).

g. The contribution of each variable to the final uncertainty is given by:-

$$\Delta_i = (\Delta\sigma_F^2)_i/\sigma_F^2$$

where

$(\Delta\sigma_F^2)_i$ is each of the i terms in equation (4) or (5).

2.3.2 Ultimate limit state of a cylindrical pile

Consider a steel cylindrical **pile of a diameter d and a wall** thickness t fixed at the sea bottom and piercing the water surface.

a. Assuming that the failure of the pile is to be caused by the wave overturning moment at the base, the reliability function **can be expressed (6) as:-**

$$z = M_p - M_{max} \tag{1}$$

where M_{max} = maximum overturning moment (due to the largest wave)

M_p = full plastic moment of the tube

$$M_p = td^2s_y \tag{2}$$

where s_y is the yield stress of the material

b. If the drag force is assumed to be negligible with respect to the inertia force, the overturning moment due to any wave of height H can be calculated by Morison's equation as follows:-

$$dF = \frac{\pi}{4}d^2\rho C_M\dot{U}_x.dy \tag{3}$$

$$\dot{U}_x = g.k.\frac{H}{2}\left|\frac{\cosh(k.y + k.D)}{\cosh(k.D)}\right|\cos\omega t \tag{4}$$

$$M = \int_0^{-D} (D - y)dF \tag{5}$$

where dF is the inline force on an element dy of the cylinder at distance y below surface

C_M is the inertia coefficient

$\dot{U}_x$ is the horizontal acceleration of the water particle by the linear wave theory.

D is the water depth

k is the wave number, $2\pi/L$

ω is the wave frequency (rad/s)

L is the wave length

Substituting (3) and (4) into (5) and putting $\cos\omega t = 1$ for maximum acceleration, we get (6):-

$$M = \frac{\pi}{4} d^2 \rho \; g \; C_M \frac{H}{2} \left| \frac{k\, D \sinh(k.D) - \cosh(k.D) + 1}{k \cosh(k.D)} \right| \tag{6}$$

c. Putting $H/L = \alpha$ where α is the wave steepness, the wave number can be written as:-

$$k = \frac{2\pi}{L} = \frac{2\pi\alpha}{H}$$

The maximum moment M_{max} is obtained by substituting for H the maximum wave height H_m occurring during the assumed working life of the structure. The reliability function (equation 1) can be written as:-

$$z = td^2 s_y - \frac{\pi d^2}{8} \rho \; g \; C_M H_m \left| \frac{\frac{2\pi\alpha D}{H_m} \sinh \frac{2\pi\alpha D}{H_m} - \cosh \frac{2\pi\alpha D}{H_m} + 1}{\frac{2\pi\alpha}{H_m} \cosh \frac{2\pi\alpha D}{H_m}} \right| \tag{7}$$

d. In the reliability analysis, D, d, ρ and g are deterministic variables while t, s_y, C_M, H_m and are treated as stochastic variables.

e. The mean value (μ_z) of the reliability function (z) is obtained by substituting the mean value for all the random variables into equation (7).

$$\mu_z = z(\mu_t, \mu_{s_y}, \mu_{C_M}, \mu_\alpha, \mu_{H_{max}}) \qquad (8)$$

The variance σ_z^2 is approximated by linearisation of z and evaluating the partial derivatives by substituting the mean values of the variables into them:-

$$\sigma_z^2 = \left(\frac{\partial z}{\partial t}\right)^2_{\mu_z} \sigma_t^2 + \left(\frac{\partial z}{\partial s_y}\right)^2_{\mu_z} \sigma s_y^2 + \ldots\ldots\ldots \qquad (9)$$

f. $$P_f = P\,|z < 0| = \phi(-\beta) \qquad (10)$$

where P_f = probability of failure

$$\beta = \frac{\mu_z}{\sigma_z}$$

ϕ = distribution function for normal (Gaussian) distribution.

2.4 Fatigue Analysis

A fatigue analysis can be described generally as a calculation procedure starting from a given sea state (waves) to determine at the end the fatigue damage occurring in the material or in the structural connections. The links between the wave data and the damage in the structure are formed by mathematical models for the wave forces, the structural behaviour and the material behaviour (7, 23, 28, 33, 47, 49, 51).

To carry out a reliability analysis for the fatigue of a jacket platform spectral and level 2 reliability techniques are combined (2, 6, 22, 27, 48, 50, 52). A general procedure for probabilistic reliability fatigue analysis can be summarised (22) as follows:-

a. The fatigue model is based on Miner's rule, which states that every stress cycle results in a degree of damage D_i given by:-

$$D_i = \frac{1}{N_i}$$

where N_i is the number of stress cycles at which failure occurs and is expressed by S - N (Stress-numbers) curves as (22):-

$$N_i = \left[\frac{2\hat{s}_i}{s_F}\right]^{-k}$$

where $\hat{s}_i$ is the stress amplitude and s_F and k are constants which can be determined from constant-amplitude fatigue tests.

b. The amplitudes of the stress cycles may be approximately assumed to conform to a Rayleigh distribution:-

$$f_{\hat{s}}(s) = \frac{s}{\sigma^2(s)} \exp\left[-\frac{s^2}{2\sigma^2(s)}\right]$$

where $\sigma_{(s)}$ is the standard deviation of the stress at the point under consideration in the structure.

c. The mean fatigue damage per cycle within one sea state can be determined (22) as:-

$$\bar{D}_i = \int_0^\infty D_i(s) f_{\hat{S}}(s) ds$$

$$= \int_0^\infty \left[\frac{2s}{s_F}\right]^k \cdot \frac{s}{\sigma^2(s)} \exp\left[-\frac{s^2}{2\sigma^2(s)}\right] ds$$

$$= (2\sqrt{2})^k \Gamma(1 + \frac{k}{2}) (\frac{\sigma(s)}{s_F})^k$$

where $\Gamma(..)$ is the gamma function.

d. The total damage $D_t = \Sigma D_i$ is obtained by summing the mean damage over the service life of the structure taking into account the long-term distribution for the sea states, see Ref. (22).

e. The reliability function z can be written as:-

$$z = D_f - D_t$$

with $z < 0$ corresponding to the fatigue failure,

or, preferably, $z = - \ln(D_F/D_t)$

where D_F is the value of total damage at which failure actually occurs.

f. Assuming that the reliability function z is a function of n mutually independent stochastic variables X_1, X_2, $...X_n$, the mean and standard deviation of z can be approximated by:-

$$\mu(z) = z\left[\mu(X_1), \mu(X_2) ... \mu(X_n)\right]$$

$$\sigma^2(z) = \sum_{i=1}^{n} \left[\frac{\partial z}{\partial x_i} \sigma(x_i)\right]^2$$

The derivatives $\frac{\sigma z}{\sigma_{x_i}}$ are evaluated at the mean values of the variables.

g. The probability of failure P_f is given by:-

$$P_f = P\left[z < 0\right] = \phi(-\beta)$$

where β is the reliability index = $\frac{\mu(z)}{\sigma(z)}$

3. UNCERTAINTIES IN JACKET STRUCTURES

The sources of uncertainty affecting the behaviour of jacket structures (14,15,18,46) are summarised in Fig. (1). These uncertainties, expressed by bias (B) and coefficient of variation (COV), are used in reliability analysis to predict the likelihood of each of a number of possible failure modes. With the knowledge of the consequences of the various failures, various decisions can be made about the overall safety of the structure and the strength of the individual members or components.

For modern deep-water jackets, the reliability analysis cannot be determined without a full dynamic analysis because they are likely to experience significant dynamic response due to wave loading in severe environments. The main structural and loading variables and the parameters of the wave spectra are treated as random quantities.

3.1 Types of Errors

The sources of structural failure of offshore stuctures may be associated with design, choice or use of material, workmanship and maintenance and operation of the structure. These failures are caused by accidental non-compliance with criteria for safe design, construction or operation. This non-compliance may be caused by errors that can be classified (19)as:- a) gross errors (blunders); b) systematic errors; and c) random errors, as shown in Fig. (2).

3.2 Gross Errors (Blunders)

It has been estimated that only 10-25% of all failures occur because the design loads exceed the strength of the structure. The majority of failures occur due to blunders. These errors may be caused by wrong assumptions concerning loads, ie omitting certain types of loading, errors in the design process, eg ignoring fatigue in a structure subject to fluctuating loads and errors in construction, eg using low-grade steel when high-grade steel is specified.

The only way to eliminate gross errors is with extensive supervision and inspection of all activities in the process of design, construction, maintenance and operation of the structure. The expenditure of time and money for these activities contributes more to structural safety than large safety factors (19). No safety factor, however large, will guarantee adequate protection against the effect of gross errors.

3.3 Systematic Errors

They are associated with empirical relationships between visual wave records compared with significant wave heights (wave spectra) recognised design formulae based on incomplete theory or experiment (Morison's equation, Miner's rule), strength properties determined from destructive tests. Systematic errors reduce safety

SOURCES OF UNCERTAINTIES

Environmental Loading

Spectral models of sea state

- extreme windspeed
- H_s, T_z

Hydrodynamic loading

- Hydrodynamic coeff C_D, C_M, C_L
- wave kinematics
- linearisation of drag force

Current effect

Marine growth

Structural Response

Effect of soil properties on natural frequency

Variable deck load (natural frequency, static loads)

Structural and hydrodynamic damping

Modelling the 3-dimensional jacket response

The structural analysis

Selection of critical load effects for design

Component Strength

Material properties

Geometrical imperfections

Model uncertainties

System Behaviour

Ductility

Post-buckling strength of components

Fig. (1) Source of Uncertainties in the Design of Jacket Structures

E R R O R S

Gross Errors (Blunders)

- errors in design
- errors in construction

Systematic Errors Treated by Bias:

- Wave spectra
- Morison's equation
- Miner's rule
- Mechanical properties of material

Random Errors Treated by COV

Statistical Variability (Objective)

Modelling (Prediction)

Objective

- Morison's equation
- Hydrodynamic coefficients (C_D, C_M, C_L)

Subjective

- sea state

Fig. (2) Types of Errors

factors and are treated by a mean bias (B) defined as:-

$$\text{Bias (B)} = \frac{\text{observed or true behaviour}}{\text{predicted or modelled behaviour}}$$

3.4 Random Errors

They may be classified (15) into:-

a. Statistical Variability

This is a fundamental variability of natural processes and cannot be reduced by repeated observations, although choosing different variables may change it. It can be calculated and is, therefore, objective.

b. Modelling or Prediction Errors

These are due to incomplete information and can be reduced with improved knowledge and modelling and by the acquisition of additional data. Modelling errors can be divided into:-

1. Essentially Objective

The errors arising from the random components of the principal variables may be accounted for through the loading model (uncertainties in Morison's equation, C_D and C_M).

2. Essentially Subjective

There are insufficient data to apply statistical methods and yet they are significant and cannot be ignored. These errors have to be judged from experience and the available information (sea state uncertainty).

Random errors are treated by coefficients of variation (COV) defined as:-

$$\frac{\text{Standard deviation of the random variable}}{\text{Mean value of the random variable}}$$

4. UNCERTAINTIES IN ENVIRONMENTAL LOADING

4.1 Sea State Model

A number of spectral models for waves have been proposed, each with a few parameters. Two commonly used spectra are the Pierson-Moskowitz (40) and the JONSWAP (21).

For the reliability analysis of dynamically sensitive structures, the joint probability distribution of extreme wind speed and direction is required. For wave generation over a long fetch, the annual maximum average wind speed over 6-12 hours may be used and modelled by an extreme type I distribution.

For the North Sea, a typical value of the coefficient of variation of annual maximum mean-hourly extreme wind speeds is 12-13%.

When sufficient statistical data on wave heights and periods are available, P-M and JONSWAP spectra can be expressed in terms of the sea-state parameters H_s and T_z.

The selection of a particular spectrum, from the available spectra, therefore, involves some uncertainty besides the uncertainties associated with the parameter defining the spectrum, see for example Reference (44).

Schott (42) specifies some environmental uncertainties such as:-

a. There are uncertainties associated with extrapolating data (H,T) collected over a limited time interval (eg 3 years) to an extreme event such as the 100 year return period wave height.

b. Storm surge (water level setup) is correlated to the storm wind but the phase relationship is unknown.

c. The correlation and phasing between storm wind, storm surge and storm waves are not quite known. However, it is usually assumed that the independently estimated 100 year extremes all occur simultaneously and, thus, the likelihood of the event is further reduced. When the wave spectra are formulated in terms of the significant wave height (H_s) and the average zero-crossing period (T_z), the joint probability distribution for H_s and T_z is required.

The theoretical formulations for the joint probability of wave height and period are discussed and presented in References (1, 8, 26, 36-39).

Ochi (37) proposed the following formulation for the joint probability distribution of H_s and T_z:-

$$P(H_s,T_z) = \frac{1}{2\pi H_s T_z \sigma_{H_s} \sigma_{T_z} \sqrt{1 - \rho 2}} \text{EXP}\left(- \frac{X^2 - 2XY + Y^2}{2(1 - \rho^2)}\right) \qquad (1)$$

where σ_{H_s} = Standard deviation of ln H_s

σ_{T_z} = Standard deviation of ln T_z

$$X = \frac{\ln H_s - \mu_{H_s}}{\sigma_{H_s}}$$

$$Y = \frac{\ln T_z - \mu_{T_z}}{\sigma_{T_z}}$$

μ_{H_s} = Mean of ln H_s

μ_{T_z} = Mean of ln T_z

ρ = Correlation coefficient

Peters (39) determined the revised parameters of equation (1) suitable for the design wave heights and periods in the North Sea and Gulf of Mexico. These parameters are given in Table (1):-

Parameter	North Sea (m)	Gulf of Mexico (ft)
μ_{H_s}	0.861	1.181
μ_{T_z}	2.040	1.325
σ_{H_s}	0.597	0.614
σ_{T_z}	0.190	0.586
ρ	0.326	0.575

Table (1) Revised Parameters for the Bivariate Log-Normal Distribution, $P(H_s, T_z)$

Earle and Baer (12) assessed, by computer simulation, the relative effects of uncertainties due to record lengths, natural variability and measurement or hindcast errors on estimated extreme significant wave heights. They concluded that measurement or hindcasts uncertainties and sampling variability cause a positive bias so that calculated extreme wave heights are, on average, considerably greater than actual extreme wave heights. The positive bias increases with greater measurement or hindcast uncertainties and decreases with larger record lengths. Therefore, large uncertainties are expected when extrapolating from relatively short records or records with large uncertainties to long return periods.

Soares and Moan (43) estimated (for the North Sea) the model, measurement and statistical uncertainties (COV) for the wave height (H) as 11%, 9% and 8% respectively, giving a total COV of 16%.

For the wave period (T), the corresponding uncertainties are 10%, 10% and 5% and the total COV is 15%.

4.2 Hydrodynamic Loading

Loading uncertainties arise from the computational methods used to transfer the environmental data into forces and moments on the members of the structure (eg Morison's equation, C_D, C_M, etc) and also from the experimental methods used to calibrate and check the theoretical calculations (eg analysis of data, scaling problems, etc).

4.2.1 Drag, inertia, and lift coefficients (C_D, C_M, C_L)

Due to the considerable uncertainty in C_D and C_M, these coefficients are expressed as random variables and are usually assumed to have normal distribution.

Baker et al (5) suggested mean values for C_D and C_M of 0.75 and 1.8, respectively, with coefficient of variation (COV) between 25% and 35%.

Soares and Moan (43) assumes a COV of 10% for C_D and C_M when using Sarpkaya's experimental data.

Data from the ocean experiments showed large scatter in the coefficients of variation for C_D and C_M. For example, Evans (13) reported COVs of 74% and 54% for C_D and C_M, respectively, for all waves. For the higher waves the corresponding values were 54% and 60%. Kim (24) results showed COVs of 39% and 18% for C_D and C_M, respectively, while Nolte (35) suggests a value of less than 25% for the force coefficients.

From the above mentioned examples, it is clear that the present treatment of the drag and inertia coefficients (C_D, C_M) as random variables in the reliability analysis is not satisfactory. It has been shown that variable hydrodynamic coefficients dependent on Reynolds and Keulegan-Carpenter numbers and surface roughness should be used in the wave loading calculations instead of the constant coefficients. Therefore, at the different levels of the jacket structure, different C_D and C_M values exist at the same instantaneous time. This distribution of C_D and C_M with depth below water surface is peculiar to a specific wave of certain height and period. For another wave, with different height and period, there is a new distribution for C_D and C_M with the depth because the values of Reynolds and Keulegan-Carpenter numbers would be different from the previous case.

Since the sea state model is expressed by a wave spectrum covering a range of wave heights and frequencies (or periods), there is a corresponding 'spectrum' for C_D and C_M at each level. Therefore, the uncertainty in C_D or C_M cannot be simply represented by a single value of COV (or a mean value and standard deviation). This, in fact, expresses the uncertainty for one level only.

Distribution or variation of C_D and C_M with depth should be obtained from sufficient and reliable data taking into account roughness and interference effects. Unfortunately, the required data are not available at the present time, as has been discussed in detail in Chapter 2.

When the information regarding the variation of C_D and C_M becomes available it would be possible to determine the probability distribution functions of C_D and C_M.

Another point which needs to be examined is the effect of the transverse or lift coefficients (C_L). At the present time, the effect of the lift forces is neglected completely. It has been shown that for jacket structures this part of wave loading is quite important (see Chapter 5), thus the lift coefficient should be treated in a similar way to C_D and C_M.

For a design wave of 30.0m height and 17 sec period (ω = 0.37 rad/s), the bias in the total forces and moments on the structure due to the effect of the lift forces (Chapter (5), Tables 15-18) is given in Table (2).

In the case of the lift force, the bias (B) is defined as:-

$$\frac{\text{force (moment) including lift force}}{\text{force (moment) without lift force}}$$

4.2.2 Kinematics of the wave particle

The spectral representation of the sea state and the spectral analysis of jacket structures are based on the linear wave theory (Airy theory). However, for deep-water structures, Stokes 5th order theory is recommended for estimating the velocities and accelerations of the water particles. As has been shown in Chapter 6, the differences between Airy and Stokes 5th order theory in estimating the velocities and accelerations and the wave loading are large. This may be treated as a systematic error by a bias (B) in the wave loading model or as a modelling error (COV) in Morison's equation.

Table (2) gives the bias in the total forces and moments when comparing the results (using Sarpkaya's data) of Stokes 5th order theory with Airy theory (Chapter 6, Tables 11-14). In this case the bias is defined as:-

$$\frac{\text{force (moment) by Stokes 5th ord theory}}{\text{force (moment) by Airy theory}}$$

There is also uncertainty associated with the use of Stokes 5th order theory. The estimated COVs is about 25%, Reference (20).

4.2.3 Linearisation of Drag Force

The method of spectral analysis, which is based on linear superposition implies that non-linear loads, such as drag forces, must be small in comparison to the linear loads such as the inertia forces. This is not the case for jacket structures since the drag (and lift) forces represent a significant proportion of the total load.

The least squares linearisation of Morison's equation introduces uncertainty in the representation of the drag component. The linearization overestimates the drag force when the water particle velocities are less than $\sqrt{8/\pi}$ times the root mean square velocity values and underestimates it for higher velocities (45).

Dao and Penzien (10) concluded that, for a single harmonic wave, the linearized method of representing drag forces produces structural response amplitudes which can be in error by as much as 20% for H/d > 20. For random waves the linearized method produces extreme values of structural response which are generally considered lower than those produced by the non-linear method.

4.3 Current Speed

Current is composed mainly of a wind generated component varying linearly with depth under water surface and a tidal component which varies exponentially. There is a considerable uncertainty in modelling current kinematics. However, tidal currents may be modelled reasonably by a zero mean normal probability distribution (5)

The bias in the total forces and moments due to the effect of 1 m/s current (Chapter 8, Tables 3,4) is given in Table (2). The bias is defined as:-

$$\frac{\text{force (moment) with current}}{\text{force (moment) without current}}$$

For the North Sea, the mean combined current speed (at surface) may be taken as 1.25m/s with a COV of 35% (43).

4.4 Marine Growth

For the overall structural response, the mean thickness of marine growth at the different levels below the water surface is considered. The thickness at the mean waterline may be assumed to have a normal distribution. The variation of the thickness with depth may be assumed linear and diminishing at about 120m depth below water surface. The uncertainty in the fouling thickness is estimated by a COV of 38%, Reference (5), to 45%, Reference (43).

The bias in the total forces and moments due to roughness effects on the hydrodynamics coefficients (Chapter 5, Tables 19,20) is given in Table (2). In this case the bias is defined as:

$$\frac{\text{force (moment) for rough cylinders}}{\text{force (moment) for smooth cylinders}}$$

5. UNCERTAINTIES IN STRUCTURAL RESPONSE

For determining the dynamic response, the jacket structure may be idealised by a number of lumped masses, particularly for the first mode of vibration which dominates the overall response to wave loading (46). The uncertainties in the mass of the jacket, due to additional equipment or structural modifications should be taken into account.

The overall stiffness of the jacket can be considered a deterministic function of Young's modulus (E) and the member dimensions because the uncertainty in E for steel is very small. The total uncertainty in the stiffness can be neglected (46).

The deck loads and the wind loads on the superstructure can be neglected.

The remaining sources of uncertainty (18) may be summarised as follows:-

a. The effect of soil properties (foundation stiffness).

$\omega = 0.37$ rad/s, $H = 30.0$m, $T = 17$ sec	Lift Force		Surface Roughness		Wave Kinematics		Current	
	Bias		Bias		Bias		Bias	
	$\beta = 0.0$	$\beta = \pi/4$	$\beta = 0.0$ SR = 1/800	$\beta = 0.0$ SR = 1/200	$\beta = 0.0$	$\beta = \pi/4$	$V_s = 1.0$m/s $\Theta = 0.0$	$V_s = 1.0$m/s $\Theta = \pi/4$
Surge Force	1.06	1.11	1.43	1.56	1.20	1.27	1.16	1.11
Heave Force	0.98	0.98	1.60	1.88	0.87	0.81	1.03	1.02
Sway Force	11.7	1.10	7.55	7.54	0.82	1.22	1.37	19.17
Rolling Moment	8.9	1.09	6.27	6.27	0.81	1.37	1.34	12.77
Yawing Moment	3.71		15.10	15.03	1.48		1.16	13.57
Pitching Moment	1.06	1.08	1.61	1.75	1.35	1.44	1.22	1.14

Table (2) Bias in Total Forces and Moments

b. Structural and hydrodynamic damping.

c. Modelling the complicated three-dimensional jacket response including wave-structure interaction, lumped mass assumptions, etc.

d. The structural analysis, eg modelling the complex structure by a set of simplified members having rigid joints, uniform properties, neglect of secondary members, etc.

e. The transformation of internal nominal loads in a component to load effects or field stresses on structural elements.

f. The distributional assumptions for load effects.

g. The selection of the most critical of these simultaneously acting load effects for designing the shell, stiffening and connections.

6. UNCERTAINTIES IN COMPONENT STRENGTH

The probability of failure of any member of the structure depends on the magnitude of the loads acting on it and the member strengths. The strength depends on the mechanical properties of the material, especially the yield stress, dimensions and geometric imperfections.

The uncertainty in the actual magnitude of imperfection and the structural dimensions has little effect on the reliability of the component (5).

The reliability of the members can be enhanced very considerably by using steel with a high mean yield stress. The yield stress can be represented by a log-normal distribution with a COV of 5-7%.

For the ultimate strength uncertainties, see for example References (17,18).

7. CONCLUSIONS

As far as the uncertainties in the wave loading are concerned the following may be concluded:-

a. The present treatment of the drag and inertia coefficients as random variables for reliability analysis is not satisfactory. Experimental works are required to obtain variable hydrodynamic coefficients dependent on the flow particulars (K, R_e) and taking into consideration the surface roughness and interference effects. When these data become available it will be possible to represent the coefficients reasonably with much less uncertainty.

b. The effect of the lift (transverse) forces cannot be neglected. This effect may be treated by bias in the wave loading model (Morison's Equation). For smooth cylinders, bias in the total forces in the direction of wave propagation (surge forces) was approximately 1.1. However, in the perpendicular direction (sway forces) the bias was about 12.

c. The effects of non-linear loads resulting from the drag and lift forces and also when using Stokes fifth order theory to produce wave kinematics should be taken into consideration. The results have shown that the bias in the total forces and moments due to the fifth order theory may vary between 0.8 and 1.4.

REFERENCES

1. ARHAU, M, CAVANIC, A, and EZRATY, 'Determination of the Period Range Associated with the Design Wave, 'OTC Paper No 3643, Houston, Texas, 1979.

2. ARULIAH, P, 'Fatigue Dynamics and Design', 2nd Intl Symp on Ocean Engineering and Ship Handling, Gothenburg, 1983.

3. BAKER, M J, and FLINT, A R, 'Safety Approaches for Structures Subject to Stochastic Loads', Symp on Integrity of Offshore Structures, IESS, Glasgow, Apr 78.

4. BAKER, M J, and WYATT, T A, 'Methods of Reliability Analysis for Jacket Platforms', BOSS '79, London, Vol 2, 1979, pp499-520.

5. BAKER, M J, and RAMACHANDRAN, K, 'Reliability Analysis as a Tool in the Design of Fixed Offshore Platforms', 2nd Intl Symp on Inetegrity of Offshore Structures', Glasgow, Jul 81.

6. BUOMA, A L, MONNIER, T, and VRONWENVELDER, A, 'Probabilistic Reliability Analysis', BOSS '79, London, Vol 2, 1979, pp521-542.

7. BROUWERS, J J H, and VERBEEK, P H J, 'Expected Fatigue Damage and Expected Extreme Response for Morison-Type Wave Loading', Applied Ocean Research, Vol 5, No 3, 1983, pp129-133.

8. CAVANIC, A, ARHAU, M, and EZRATY, R, 'A Statistical Relationship Between Individual Heights and Periods of Storm Waves, 'BOSS '76, Trondheim, Vol 2, 76.

9. CHEN, Y N, LIU, D, and SHIN, Y S, 'Probabilistic Analysis of Environmental Loading and Motion of a Tension Leg Platform for Reliability-Based Design', Marine Safety Conf, University of Glasgow, Sep 83.

10. DAO, B V, and PENZIEN, J, 'Comparison of Treatments of Non-Linear Drag Forces Acting on Fixed Offshore Platforms', Applied Ocean Research, Vol 4, No 2, 1982.

11. DET NORSKE VERITAS, 'Rules for the Design, Construction and Inspection of Offshore Structures', Oslo, 1977.

12. EARLE, M D, and BAER, L, 'Effects of Uncertainties on Extreme Wave Heights', Jour of the Waterway, Port, Coastal and Ocean Div, ASCE, Vol 108, No WW4, Nov 82.

13. EVANS, D J, 'Analysis of Wave Force Data', Jour of Petroleum Technology, Mar 70.

14. FAULKNER, D, 'Loading Uncertainties - Some Thoughts and Recommendations', Rule Case Committee, Paper No RCC(b), 03/DF, Mar 82.

15. FAULKNER, D, 'Loading Uncertainties - Further Thoughts', Rule Case Committee, Paper No RCC(b), 15/DF, Sep 82.

16. FAULKNER, D, BIRRELL, N D and STIANSEN, S G, 'Development of a Reliability Based Design Code for the Structure of Tension Leg Platforms', OTC Paper No 4648, Houston, Texas, 1983.

17. FAULKNER, D, 'On Selecting a Target Reliability for Deep Water Tension Leg Platforms', 11th IFIP Conf on System Modelling and Optimisation (Modelling of Offshore Structures), Copenhagen, Jul 83.

18. FAULKNER, D, 'Reliability of Offshore Structures', Keynote Address to SERC Marine Technology Seminar, London, Apr 84.

19. FIELD, S, 'Reliability of Offshore Structures', Jour of Petroleum Technology, Oct 78.

20. FORRISTAL, G Z, WARD, E G, CARDENE, V J, and BORGMAN, L E, 'The Directional Spectra and Kinematics of Surface Gravity Waves in Tropical Storm Delia', Jour of Phys Oceanography, Vol 8, 1978.

21. HASSELMANN, K, et al, 'Measurements of Wind-Wave Growth and Swell Decay During the Joint North Sea Wave Project (JONSWAP)', Deutches Hydrographisches Zeitschrift, Hamburg, Reihe A(8) Nr 12, 1973.

22. KARADENIZ, H, VAN MANEN, S and VROUWENVELDER, A, 'Probabilistic Reliability Analysis for the Fatigue Limit State of Gravity and Jacket-Type Structures', BOSS '82, Vol II, pp147-165.

23. KAWAMOTO, J, SUNDER, S S, and CONNOR, J J, 'An Assessment of Uncertainties in Fatigue Analyses of Steel Jacket Offshore Platforms', Applied Ocean Research, Vol 4, No 1, 1982.

24. KIM, Y Y, and HIBBARD, H C, 'Analysis of Simultaneous Wave Force and Water Particle Velocity Measurements', OTC Paper No 2192, Houston, Texas, 1975.

25. KRIGER, G, PIERMATTEI, WHITE, J D, and KING, R W, 'Risk Analysis Applied to Offshore Platforms During the Unpiled Installation Phase', OTC Paper No 4442, Houston, Texas, 1983.

26. LONGUET-HIGGINS, M S, 'On the Joint Distribution of the Periods and Amplitudes of Sea Waves', Jour of Geophysical Research, Vol 80, No 18, 1975.

27. MANNERS, W, and BAKER, M J, 'Reliability Analysis in Fatigue', 2nd Intl Symp on Integrity of Offshore Structure, Glasgow, Jul 81.

28. MARSHALL, P W, 'Failure Modes for Offshore Platforms', BOSS '76, Trondheim, Vol 2, 1976.

29. Model Code for Structural Design of Tension Leg Platforms (Draft), CONOCO/ABS TLP Rule Case Committee, ABS, New York, Nov 83.

30. MOSES, F, 'Reliability of Structural Systems', BOSS '76, Trondheim, Vol 1, 1976.

31. MOSES, F, and STAHL, B, 'Reliability Analysis Format for Offshore Structures', OTC Paper No 3046, Houston, Texas, 1978.

32. MOSES, F, 'Utilising a Reliability-Based API RP2A Format', Final Report, API PRAC Project 82-22, API, Dallas, Texas, Nov 83.

33. MUKHOPADHYAY, A, ITOH, Y, and BOUWKAMP, J G, 'Fatigue Behaviour of Tubular Joints in Offshore Structures', OTC Paper No 2207, Houston, Texas, 1975.

34. New Code for the Design of Steel Bridges, Part 3, BS 5400, London, 1982.

35. NOLTE, K G, 'The Effect of Uncertainty in Wave Force Coefficients for Offshore Structures', OTC Paper No 3066, Houston, Texas, 1978.

36. NOLTE, K G, 'Joint Probability of Wave Period and Height', Jour of the Waterway, Port, Coastal and Ocean Div, ASCE, Vol 105, No WW4, Nov 79.

37. OCHI, M K, 'Wave Statistics for the Design of Ships and Ocean Structures', SNAME Trans, Vol 86, 1978, pp47-76.

38. OCHI, M K, 'Stochastic Analysis and Probabilistic Prediction of Random Seas', Report No UFL/COEL-TR/042, Coastal and Oceanographic Engineering Dept, University of Florida, Jun 80.

39. PETERS, D H, 'Environmental Data Input for CONOCO-ABS Rules Case Committee on the Design Codes', Paper No RCC(b) 11/DJHP, Aug 82.

40. PIERSON, W J, and MOSKOWITZ, L, 'A Proposed Spectral Form for Fully Developed Wind Seas Based on the Similarity Theory of S A Kitaigordskii', Jour of Geophysical Research, Vol 69, No 24, Dec 64.

41. PLANEIX, J M, CIOLINA, J, DELUEIL, J, DORIS, C G, and HEAS, J Y, 'Are Offshore Structures Over-Designed? Relative Influence of Environmental Parameters', OTC Paper No 3387, Houston, Texas, 1979.

42. SCHOTT, W E, 'Overview of the Loading Problem', Rule Case Committee, Paper No RCC(b), 01/WES, Jan 82.

43. SOARES, C G, and MOAN, T, 'On the Uncertainties Related to the Extreme Hydrodynamic Loading of a Cylindrical Pile', Reliability Theory and Its Application in Structural and Soil Mechanics, P Thoft-Christensen (Editor), Martinus Nijhoff Pub, The Hague, 1982.

44. SPIDSOE, N, and SIGBJORUSSON, R, 'On the Reliability of Standard Wave Spectra in Structural Response Analysis', Eng Struct, Vol 2, Apr 80, pp123-135.

45. SUNDER, S S, and CONNOR, J J, 'Sensitivity Analyses for Steel Jacket Offshore Platforms', Applied Ocean Research, Vol 3, No 1, 1981.

46. THOFT-CHRISTENSEN, P, and BAKER, M J, 'Structural Reliability Theory and Its Applications', Springer-Verlag, Berlin, 1982.

47. TOMKINS, B, 'Fatigue DEsign Rules for Steel Welded Joints in Offshore Structures', OTC Paper No 4403, Houston, Texas, 1982.

48. VUGHTS, J H, and KINRA, R K, 'Probabilistic Fatigue Analysis of Fixed Offshore Structures', OTC Paper No 2608, Houston, Texas, 1976.

49. WALKER, S, and BRAZIER, S G, 'Vortex-Shedding Forces and the Fatigue Analysis of Offshore Structures', Paper No EUR 253, European Offshore Petroleum Conf and Exhibition, London, 1980.

50. WALLIS, J R, BAYAZITOG, Y O, CHAPMAN, F M, and MANGIAVACCHI, A, 'An Approach to Probabilistic Fatigue Analysis of Offshore Structures', OTC Paper No 3379, Houston, Texas, 1979.

51. WILLIAMS, A K, and RINNE, J E, 'Fatigue Analysis of Steel Offshore Structures', Proc Inst of Civil Engineers, Part 1, 60, Nov 76.

52. WIRSCHING, P H, 'Fatigue Reliability in Welded Joints of Offshore Structures', OTC Paper No 3380, Houston, Texas, 1979.

53. WIRSCHING, P H, 'Forward to Fatigue and Fracture Reliability: A State-of-the-Art-Review', Proc ASCE, J Str Div, Vol 108, No STI, Jan 82.

54. WIRSCHING, P H, 'Probability Based Fatigue Design Criteria for Offshore Structures', Final Report, API PRAC Project 81-15, API, Dallas, Texas, Jan 83.

CHAPTER 11

CHAPTER 11

CONCLUSIONS AND RECOMMENDATIONS

Each chapter in this study contains its own main conclusions given at the end. However, within each chapter and from the analysis of the large amount of data presented, many other conclusions can be drawn. In fact, the percentage differences in the forces or moments for a particular condition may be considered, themselves, as secondary or sub-conclusions. From the available data, the reader can also draw his own conclusions.

However, the main conclusions and recommendations for the design of jacket platforms may be summarised as follows:-

1. In the design process of jacket platforms, the area of wave loading estimation may be considered the weakest link in the chain which still contains major uncertainties starting from the determination of the environmental conditions for design and translating them into forces and moments on the structure. Although the main concepts in the wave loading calculations are well known and generally agreed upon, it appears that there exists several interpretations of the correct method of application of these concepts. This is felt to be worrying because, as will be indicated later, any misinterpretation or neglect of certain aspects in the wave loading calculation could lead to serious discrepancies and errors in the final results.

2. To start with, the present state of choosing and using the hydrodynamic coefficients (C_D, C_M, C_L) is of major concern.

The big question as to what are the most suitable coefficients has yet to be answered. The influence of the hydrodynamic coefficients on the wave loading have been clearly demonstrated beyond any doubt and need no further comment except to hope that people will be aware of the level of percentage differences which could result if unsuitable coefficients were chosen. In this respect, there are good reasons to state that constant coefficients should not be used any more if a reasonable loading estimation is required. Variable local coefficients should be used depending on Reynolds number, Keulegan-Carpenter number and the surface roughness of the member. In the absence of more accurate data and until they become available, Sarpkaya's experimental results for C_D, C_M and C_L can be used by integrating them into wave loading computer programs but the differences between these results and some measurements in waves must be borne in mind.

3. When applying Morison's equations it is important to consider the relative positions of the different members in space and time when the wave passes through the jacket. It is equally important to consider the phase differences between the velocities and accelerations of the wave particles. This approach will determine accurately the total forces (surge, heave, sway) and moments (rolling, yawing, pitching) on the complete structure at any interval of time within the wave cycle, from which the maximum values of the total forces and moments can be determined. Similarly, the total force on any individual member at any time can be determined as well as the maximum force in a cycle. The results have shown that less than 40% of the

total number of members in the jacket had their maximum forces occurring at the same time.

4. The lift or transverse forces represent a significant percentage of the total wave loading, especially the total sway force and rolling and yawing moments at the base of the structure. The lift force should be seen as a complementary part for Morison's equation which must be taken into consideration when evaluating the wave loading.

5. Similarly to the case of the constant hydrodynamic coefficients, using coefficients related to smooth cylinders is not realistic because the effect of surface roughness on the coefficients is quite significant even for small relative roughness. The results have shown that the total forces (surge, heave, sway) and the total moments (rolling, yawing, pitching) were greatly increased due to roughness compared with the case of smooth cylinders. The effect of marine roughness on wave loading due to the increased diameter of the member is less important than the effect of roughness on the values of the hydrodynamic coefficients. Besides, estimating the relative roughness accurately is not so essential. The more important thing is to take the roughness into consideration by specifying a reasonable or average value for the marine growth preferably at the different levels below surface. The results have shown that the differences in the wave loading between the smooth cylinder case (SR = 0.0) and the rough cylinders of 1/800 are much larger than the differences between the two roughnesses of 1/800 and 1/200, although the differences in the relative roughness in the second

case is three times the first case.

6. Although it has been generally accepted that for deep water waves Stoke's fifth order theory (or stream function theory) should be used to evaluate the flow kinematics, the non-deterministic analyses of jacket structures are based on linear (Airy) wave theory. The results of the variations of the wave velocities and accelerations at the mean water line and below it have shown that the differences in predicting the wave kinematics by Airy and Stoke's theories are large. As a natural result, the wave forces on the individual members as well as the total forces and moments on the complete structure calculated by the fifth order theory, showed large discrepancies when compared with the results based on Airy theory.

7. The interference problem between the members, although studied theoretically and experimentally, is hardly mentioned when talking about the wave loading and there are strong doubts whether it has ever been taken into account when calculating the wave loading in practice. This is because the available experimental data are not sufficient to help designers incorporate interference effects in the calculation of wave loading. Reliable tank tests with models consisting of groups of members resembling the various configurations found in practice are much needed to provide the required information. Whether the net result will be a decrease or increase in the wave loading of the jacket is difficult to speculate from the presently available data.

8. When estimating the hydrodynamic loading on jacket

platforms, sited in areas of strong currents, it is necessary to compute the total water particle velocities of the combined wave-current flow field. The drag and lift forces are proportional to the square of this total fluid velocity. Since the drag and lift forces represent a significant percentage of the wave loading, the increase in the forces and moments due to current cannot be neglected.

9. The differences in the wave loading estimation due to using different hydrodynamic coefficients, eg by LR, DnV and BV, or when applying different wave theories will show again as differences in the maximum stresses on the members when the structural analysis is performed. The percentage differences in the stresses may be somehow different from the original percentage differences in the wave loading due to the redistribution of the loads throughout the jacket. However, there are no sound arguments to suggest that the initial differences in the loads will eventually be minimised when applying different design codes which have different strength formulation and safety factors.

10. Within the area of the uncertainties in the environmental loading the modelling of the wave loading for the purpose of the reliability analysis needs further improvements. Present modelling of the drag and inertia coefficients is not accurate enough. Further experimental data are needed which express the coefficients in relation to the main flow parameters, eg R_e, K and taking into account the surface roughness and the interference effects between the members of the jacket. The effect of the lift forces should be allowed for in the wave loading model.

Since the Stochastic analysis of jacket structures is based on linear superposition, the effects of the non-linear loads due to the drag and lift forces or due to non-linear wave theories, eg Stokes fifth order theory should be taken into consideration.

11. The method of computing the hydrodynamic loading for jacket platforms which has been presented in this study is believed to be accurate, comprehensive and flexible. The various computer programs developed constitute a good computing package to deal with the different aspects of the wave loading. Although the computer programs are sophisticated internally they are easy to run since they are presented in the interactive format. The only thing the user has to do is to answer a few questions for minimum input data to get very detailed output information. The programs are designed in such a way that it would be very simple to change the subroutines, for example, when better experimental data for the hydrodynamic coefficients or the interference effect become available. Thus, the programs can always be updated without any major changes.

12. There is a great need now for a large testing facility or wave tank where regular and irregular waves of sufficient size can be generated to simulate as near as possible the flow conditions for full scale structures. Large scale jacket models can be tested and the various problems relating to the wave loading can be examined and assessed.

In fact, if such a facility were available many of the arguments and conclusions drawn throughout the present study could have been assessed and verified.

APPENDICES

APPENDIX A

1. The Starting and End Points

The co-ordinates of the starting and end points of the members are calculated by Program XYZ using the following convention. This convention is arbitrary, and any other system may be used.

(i) for all bracing members of faces (1) and (2), when looking at the structure from direction x-x, the starting point of a member is the left hand side point and the end point is the right hand side point.

(ii) for all bracing members of faces (3) and (4), when looking from direction y-y, the starting point of a member is the left hand side point while the end point is the right hand side point.

(iii) for any horizontal diagonal, the starting point is the left hand side point and the end point is the right hand side point.

(iv) for the main columns, the starting point for any member is the lower point while the end point corresponds to the upper point of the member.

2. Length Corrections

To determine the actual length of a member (Program XYZ), the nodal points are first calculated and then corrections are made to get the actual starting and end points from which the actual length can be calculated. The corrections are made as given below using the following definitions:

X_s, Y_s, Z_s: co-ordinates of the starting point of member.
X_E, Y_E, Z_E: co-ordinates of the end point of member.

(Cont'd)

XN_s, YN_s, ZN_s	:	co-ordinates of the nodal point at start.
XN_E, YN_E, ZN_E	:	co-ordinates of the nodal point at end.
S_1	:	length correction for horizontal members.
S_2, S_3	:	length corrections for inclined bracing members.
S_4, S_5	:	length corrections for horizontal diagonals.
R_C	:	radius of main column.
R_B	:	radius of horizontal member.
LN	:	length of member between nodes.
SE	:	actual length of member.

From Fig. (A.1)

$$\tan\theta = \frac{(A - B)}{2H} \quad , \quad \cos\theta = \frac{2H}{\sqrt{(A - B)^2 + 4H^2}}$$

$$S_1 = \frac{Rc}{\cos\theta}$$

$$\sin\Psi = \frac{(YN_E - YN_S)}{LN}$$

$$\alpha = 180^\circ - (\Psi + \phi) = 180^\circ - \Psi - (90^\circ - \theta)$$

$$= 90^\circ + \phi - \Psi$$

$$S_2 = \frac{Rc}{\sin\alpha} \quad , \quad S_3 = \frac{R_B}{\sin\Psi}$$

(i) Horizontal Members

$$X_E = XN_E - S_1$$

$$X_S = - X_E$$

$$SE = LN - 2S_1$$

(ii) Inclined Members

for the starting point

$$\frac{(XN_E - XN_S)}{LN} = \frac{(X_S - XN_S)}{S_3}$$

then $$X_S = \frac{(XN_E - XN_S)}{LN} \times S_3 + XN_S \; ,$$

$$Y_S = \frac{(YN_E - YN_S)}{LN} \times S_3 + YN_s \; ,$$

$$Z_S = \frac{(ZN_E - ZN_S)}{LN} \times S_3 + ZN_s$$

for the end point

$$\frac{(XN_E - XN_S)}{LN} = \frac{(X_E - XN_S)}{(LN - S_2)}$$

then $$X_E = \frac{(XN_E - XN_S) \times (LN - S_2)}{LN} + XN_S,$$

$$Y_E = \frac{(YN_E - YN_S) \times (LN - S_2)}{LN} + YN_S,$$

$$Z_E = \frac{(ZN_E - ZN_S) \times (LN - S_2)}{LN} + ZN_S,$$

$$SE = LN - (S_2 + S_3)$$

(iii) Horizontal Diagonals

$$\sin\gamma = \frac{A}{\sqrt{(A^2 + C^2)}} \qquad \cos\gamma = \frac{C}{\sqrt{(A^2 + C^2)}}$$

$$S_4 = R_c \times \sin\gamma$$
$$S_5 = R_c \times \cos\gamma$$

$$X_E = XN_E - S_4 \ , \quad X_s = - X_E$$

$$Z_E = ZN_E - S_5 \ , \quad Z_s = - Z_E$$

$$SE = LN - 2R_c$$

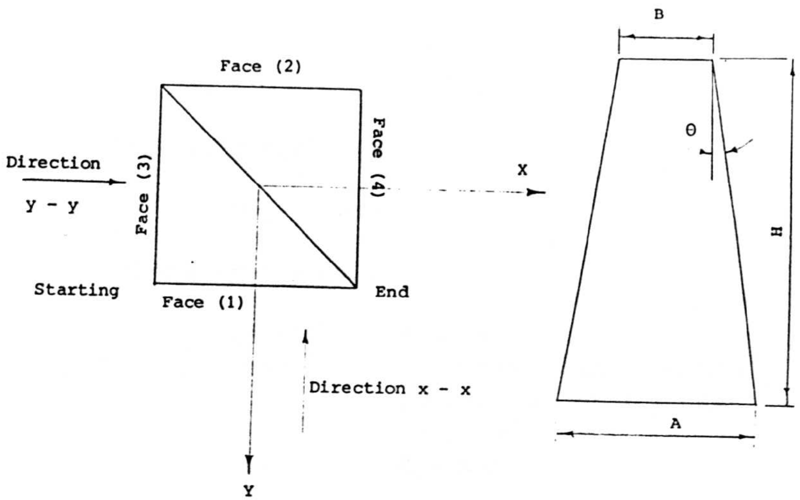

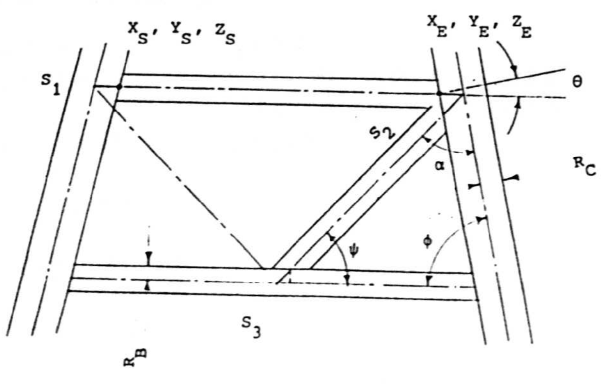

Horizontal and Inclined Members

Fig. (A.1) Length Corrections

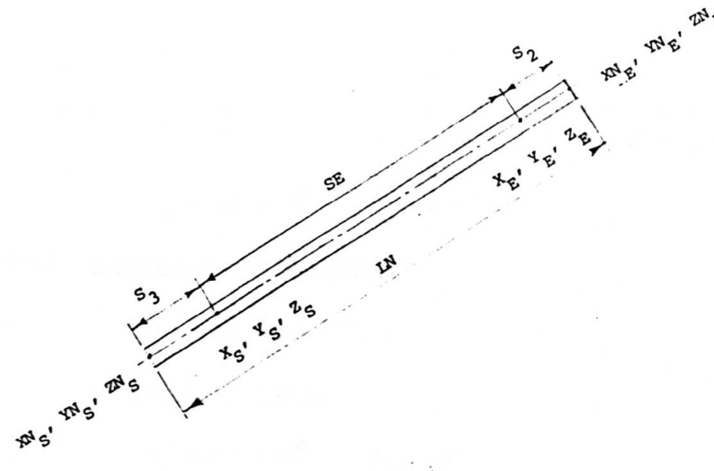

Inclined Members

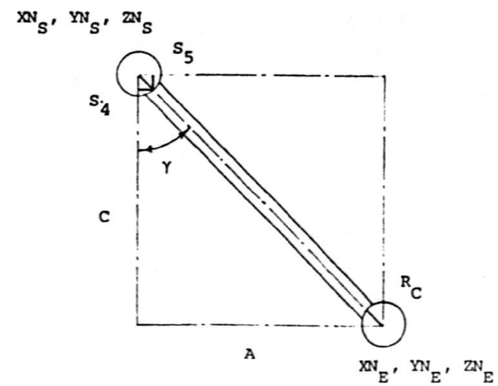

Horizontal Diagonals

Fig. (A.2) Length Corrections

APPENDIX B

POLYNOMIAL EQUATIONS OF C_D, C_M, AND C_L

1. HYDRODYNAMIC COEFFICIENTS C_D AND C_M FOR K = 20

(i) Smooth cylinders SR = 0.0

$X = \text{Log}_{10}\,(Re \times 10^{-4})$

(a) drag coefficient C_D

$R_e < 1.5 \times 10^4$	$C_D = 1.9$
$1.5 \times 10^4 \leq R_e \leq 7 \times 10^5$	$C_D = 1.7256 + 2.1586\,X - 9.5967\,X^2 + 8.9131\,X^3 - 2.0318\,X^4 - 0.8045\,X^5 + 0.3145\,X^6$
$R_e > 7 \times 10^5$	$C_D = 0.68$

(b) inertia coefficient C_M

$R_e < 2 \times 10^4$	$C_M = 1.0$
$2 \times 10^4 \leq R_e \leq 2 \times 10^5$	$C_M = 0.7362 + 1.654\,X - 5.0166\,X^2 + 10.4153\,X^3 - 8.3017\,X^4 + 2.1966\,X^5$
$R_e > 2 \times 10^5$	$C_M = 1.75$

(ii) Surface roughness SR = 1/800

$X = \text{Log}_{10}\,(Re \times 10^{-4})$

(a) drag coefficient C_D

$R_e < 2 \times 10^4$	$C_D = 1.74$
$2 \times 10^4 \leq R_e \leq 2.5 \times 10^5$	$C_D = 3.925 - 19.8921\,X + 75.6837\,X^2 - 152.9393\,X^3 + 153.7288\,X^4 - 72.3454\,X^5 + 12.6207\,X^6$
$R_e > 2.5 \times 10^5$	$C_D = 1.34$

(b) inertia coefficient C_M

$R_e < 2 \times 10^4$	$C_M = 1.0$
$2 \times 10^4 \leq R_e \leq 2.5 \times 10^4$	$C_M = 1.0 + 1.1932\,(X - 0.301)$
$2.5 \times 10^4 < R_e \leq 3.0 \times 10^5$	$C_M = 8.6273 - 48.7038\,X + 115.6757\,X^2 - 124.2483\,X^3 + 62.9534\,X^4 - 13.1331\,X^5 + 0.5086\,X^6$
$R_e > 3.0 \times 10^5$	$C_M = 1.315$

(iii) Surface roughness SR = 1/400

$X = \text{Log}_{10}\,(R_e \times 10^{-4})$

(a) drag coefficient C_D

$R_e < 1.5 \times 10^4$	$C_D = 1.83$
$1.5 \times 10^4 \leq R_e \leq 1.5 \times 10^5$	$C_D = 3.5141 - 22.8488\,X + 115.83\,X^2 - 299.1383\,X^3 + 381.5178\,X^4 - 230.0091\,X^5 + 52.4433\,X^6$
$1.5 \times 10^5 < R_e \leq 5 \times 10^5$	$C_D = -5.1607 + 13.4523\,X - 9.0622\,X^2 + 2.0311\,X^3$
$R_e > 5 \times 10^5$	$C_D = 1.5$

(b) inertia coefficient C_M

$R_e < 1.7 \times 10^4$	$C_M = 1.0$
$1.7 \times 10^4 \leq R_e \leq 2.5 \times 10^4$	$C_M = 1.1 + 1.1932\,(X - 0.301)$
$2.5 \times 10^4 < R_e \leq 2 \times 10^5$	$C_M = 8.6353 - 61.9813\,X + 191.2561\,X^2 - 280.6898\,X^3 + 212.5766\,X^4 - 80.4719\,X^5 + 12.0728\,X^6$
$R_e > 2 \times 10^5$	$C_M = 1.275$

(iv) Surface roughness SR = 1/200

$X = \text{Log}_{10}\,(R_e \times 10^{-4})$

(a) drag coefficient C_D

Range	Coefficient
$R_e < 1.5 \times 10^4$	$C_D = 1.8$
$1.5 \times 10^4 \leq R_e \leq 0.7 \times 10^5$	$C_D = 2.9021 - 18.4083\,X + 119.1318\,X^2 - 429.3721\,X^3 + 786.3064\,X^4 - 689.1391\,X^5 + 231.0379\,X^6$
$0.7 \times 10^5 < R_e \leq 0.5 \times 10^6$	$C_D = -1.3251 + 6.3516\,X - 4.5415\,X^2 + 1.0771\,X^3$
$R_e > 0.5 \times 10^6$	$C_D = 1.62$

(b) inertia coefficient C_M

Range	Coefficient
$R_e < 1.5 \times 10^4$	$C_M = 1.0$
$1.5 \times 10^4 \leq R_e \leq 2 \times 10^5$	$C_M = 2.274 - 17.2238\,X + 81.2434\,X^2 - 159.7727\,X^3 + 152.5198\,X^4 - 70.4223\,X^5 + 12.6269\,X^6$
$R_e > 2 \times 10^5$	$C_M = 1.24$

(v) Surface roughness SR = 1/100

$$X = \mathrm{Log}_{10}\,(R_e \times 10^{-4})$$

(a) drag coefficient C_D

Range	Coefficient
$R_e < 10^4$	$C_D = 1.9$
$10^4 \leq R_e \leq 0.8 \times 10^5$	$C_D = 1.8955 - 0.5555\,X - 16.9393\,X^2 + 58.9083\,X^3 - 67.5416\,X^4 + 26.4249\,X^5 - 0.3822\,X^6$
$0.8 \times 10^5 < R_e \leq 0.5 \times 10^6$	$C_D = 0.1587 + 3.5846\,X - 2.636\,X^2 + 0.645\,X^3$
$R_e > 0.5 \times 10^6$	$C_D = 1.8$

(b) inertia coefficient C_M

Range	Coefficient
$R_e < 1.2 \times 10^4$	$C_M = 1.0$
$1.2 \times 10^4 \leq R_e \leq 1.5 \times 10^5$	$C_M = 0.9321 + 0.3089\,X + 13.3233\,X^2 - 45.0771\,X^3 + 56.7973\,X^4 - 31.6124\,X^5 + 6.5367\,X^6$
$R_e > 1.5 \times 10^5$	$C_M = 1.22$

(vi) Surface roughness SR = 1/50

$$X = \mathrm{Log}_{10}\,(R_e \times 10^{-4})$$

(a) drag coefficient C_D

Range	Coefficient
$R_e < 10^4$	$C_D = 1.83$
$10^4 \leq R_e \leq 0.6 \times 10^5$	$C_D = 1.8165 - 1.096\,X - 12.8983\,X^2 + 89.4685\,X^3 - 191.1685\,X^4 + 173.4163\,X^5 - 57.6751\,X^6$
$R_e > 0.6 \times 10^5$	$C_D = 1.89$

(b) inertia coefficient C_M

Range	Coefficient
$R_e < 1.1 \times 10^4$	$C_M = 1.0$
$1.1 \times 10^4 \leq R_e \leq 10^5$	$C_M = 0.7759 + 5.7752\,X - 18.3352\,X^2 + 25.4062\,X^3 - 17.3108\,X^4 + 5.4295\,X^5 - 0.5522\,X^6$
$R_e > 10^5$	$C_M = 1.19$

2. HYDRODYNAMIC COEFFICIENTS C_D AND C_M FOR K = 30

(i) Smooth cylinders SR = 0.0

$$X = \mathrm{Log}_{10}\,(R_e \times 10^{-4})$$

(a) drag coefficient C_D

Range	Coefficient
$R_e < 10^4$	$C_D = 1.88$
$10^4 \leq R_e \leq 3 \times 10^5$	$C_D = 1.8832 - 1.0825\,X + 3.4185\,X^2 - 12.3079\,X^3 + 14.4804\,X^4 - 6.9104\,X^5 + 1.1739\,X^6$
$R_e > 3 \times 10^5$	$C_D = 0.5275 + 0.0798\,X$

(b) inertia coefficient C_M

Range	Coefficient
$R_e < 1.7 \times 10^4$	$C_M = 1.0$
$1.7 \times 10^4 \leq R_e \leq 5 \times 10^4$	$C_M = 1.05 + 0.8794\,(X - 0.301)$
$5 \times 10^4 < R_e \leq 2.6 \times 10^5$	$C_M = 2.3574 - 3.8491\,X + 4.7817\,X^2 - 1.672\,X^3$
$R_e > 2.6 \times 10^5$	$C_M = 1.76$

(ii) Surface roughness SR = 1/800

$$X = \mathrm{Log}_{10}\,(R_e \times 10^{-4})$$

(a) drag coefficient C_D

$R_e < 2 \times 10^4$: $C_D = 1.7$

$2 \times 10^4 \leq R_e \leq 0.9 \times 10^5$: $C_D = 3.5474 - 13.8\,X + 41.7627\,X^2 - 70.3953\,X^3 + 56.041\,X^4 - 16.5085\,X^5$

$0.9 \times 10^5 < R_e \leq 3 \times 10^5$: $C_D = -772.2103 + 3931.2556\,X - 8216.0859\,X^2 + 9029.9328\,X^3 - 5506.6197\,X^4 + 1768.2549\,X^5 - 233.8422\,X^6$

$R_e > 3 \times 10^5$: $C_D = 1.23$

(b) inertia coefficient C_M

$R_e < 1.5 \times 10^4$: $C_M = 1.0$

$1.5 \times 10^4 \leq R_e \leq 2 \times 10^4$: $C_M = 1.0 + 0.64\,(X - 0.176)$

$2 \times 10^4 < R_e \leq 9.5 \times 10^4$: $C_M = 8.9538 - 78.8988\,X + 315.2314\,X^2 - 643.833\,X^3 + 716.1433\,X^4 - 409.3919\,X^5 + 93.6241\,X^6$

$9.5 \times 10^4 < R_e \leq 3 \times 10^5$: $C_M = -90.8112 + 367.8923\,X - 596.2698\,X^2 + 507.2148\,X^3 - 240.1542\,X^4 + 60.2236\,X^5 - 6.2636\,X^6$

$R_e > 3 \times 10^5$: $C_M = 1.47$

(iii) Surface roughness SR = 1/400

$$X = \mathrm{Log}_{10}\,(R_e \times 10^{-4})$$

(a) drag coefficient C_D

$R_e < 1.5 \times 10^4$: $C_D = 1.7$

$1.5 \times 10^4 \leq R_e \leq 0.6 \times 10^5$: $C_D = 0.4754 + 16.1283\,X - 73.2685\,X^2 + 139.3703\,X^3 - 123.7983\,X^4 + 34.905\,X^5 + 8.2109\,X^6$

$0.6 \times 10^5 < R_e \leq 2.5 \times 10^5$: $C_D = 307.8188 - 1601.9417\,X + 3434.1288\,X^2 - 3882.6034\,X^3 + 2448.1148\,X^4 - 817.5191\,X^5 + 113.0713\,X^6$

$R_e > 2.5 \times 10^5$: $C_D = 1.4$

(b) inertia coefficient C_M

$R_e < 1.5 \times 10^4$: $C_M = 1.0$

$1.5 \times 10^4 \leq R_e \leq 5.2 \times 10^4$: $C_M = 1.4 + 1.2613\,(X - 0.477)$

$5.2 \times 10^4 < R_e \leq 2.1 \times 10^5$: $C_M = -112.4852 + 540.4984\,X - 1000.9108\,X^2 + 902.4195\,X^3 - 389.0481\,X^4 + 56.7747\,X^5 + 4.2475\,X^6$

$R_e > 2.1 \times 10^5$: $C_M = 1.4$

(iv) Surface roughness SR = 1/200

$$X = \mathrm{Log}_{10}\,(R_e \times 10^{-4})$$

(a) drag coefficient C_D

$R_e < 1.5 \times 10^4$: $C_D = 1.65$

$1.5 \times 10^4 \leq R_e \leq 2.2 \times 10^5$: $C_D = 1.4053 + 4.5608\,X - 28.0866\,X^2 + 51.5116\,X^3 - 38.6309\,X^4 + 11.0831\,X^5 - 0.5\,X^6$

$R_e > 2.2 \times 10^5$: $C_D = 1.5$

(b) inertia coefficient C_M

$R_e < 1.3 \times 10^4$: $C_M = 1.0$

$1.3 \times 10^4 \leq R_e \leq 4 \times 10^4$: $C_M = 1.25 + 1.4205\,(X - 0.301)$

$4 \times 10^4 < R_e \leq 1.5 \times 10^5$: $C_M = -6.9944 + 50.1523\,X - 114.2464\,X^2 + 131.7396\,X^3 - 82.5748\,X^4 + 26.8954\,X^5 - 3.5715\,X^6$

$R_e > 1.5 \times 10^5$: $C_M = 1.36$

(v) Surface roughness SR = 1/100

$$X = \mathrm{Log}_{10}\,(R_e \times 10^{-4})$$

(a) drag coefficient C_D

$R_e < 1.5 \times 10^4$: $C_D = 1.6$

$1.5 \times 10^4 \leq R_e \leq 10^5$: $C_D = 2.304 - 11.2783\,X + 63.9175\,X^2 - 197.2985\,X^3 + 316.2447\,X^4 - 246.0261\,X^5 + 73.7019\,X^6$

$10^5 < R_e \leq 2 \times 10^5$: $C_D = 1.56 + 0.1993\,(X - 1.0)$

$R_e > 2 \times 10^5$: $C_D = 1.635$

(b) inertia coefficient C_M

$R_e < 1.2 \times 10^4$: $C_M = 1.0$

$1.2 \times 10^4 \leq R_e \leq 3 \times 10^4$: $C_M = 1.16 + 1.3626\ (x - 0.1761)$

$3 \times 10^4 < R_e \leq 1.5 \times 10^5$: $C_M = -3.6451 + 32.0369\ X - 76.6507\ X^2 + 92.3105\ X^3 - 60.3585\ X^4 + 20.5029\ X^5 - 2.8387\ X^6$

$R_e > 1.5 \times 10^5$: $C_M = 1.32$

(vi) Surface roughness SR = 1/50

$$X = \mathrm{Log}_{10}\ (R_e \times 10^{-4})$$

(a) drag coefficient C_D

$R_e < 1.5 \times 10^4$: $C_D = 1.56$

$1.5 \times 10^4 \leq R_e \leq 1.1 \times 10^5$: $C_D = 0.2816 + 18.4547\ X - 102.6756\ X^2 + 264.2445\ X^3 - 342.3534\ X^4 + 219.2551\ X^5 - 55.4296\ X^6$

$R_e > 1.1 \times 10^5$: $C_D = 1.8$

(b) inertia coefficient

$R_e < 10^4$: $C_M = 1.0$

$10^4 \leq R_e \leq 2.1 \times 10^4$: $C_M = 1.0 + 1.4286\ X$

$2.1 \times 10^4 < R_e \leq 10^5$: $C_M = -1.2506 + 21.0487\ X - 61.7196\ X^2 + 90.1363\ X^3 - 70.9904\ X^4 + 28.8371\ X^5 - 4.7394\ X^6$

$R_e > 10^5$: $C_M = 1.3$

3. HYDRODYNAMIC COEFFICIENTS C_D & C_M FOR K = 40

(i) Smooth Cylinders SR = 0.0

$$X = \mathrm{Log}_{10}\ R_e - 4.1761$$

(a) drag coefficient

$R_e < 1.5 \times 10^4$: $C_D = 1.71$

$1.5 \times 10^4 \leq R_e \leq 3.6 \times 10^5$: $C_D = 1.7095 - 0.702\ X - 0.2239\ X^2 - 3.2124\ X^3 + 4.504\ X^4 - 1.5255\ X^5$

$R_e > 3.6 \times 10^5$: $C_D = 0.5018 + 0.0533\ X$

(b) inertia coefficient C_M

$R_e < 1.5 \times 10^4$: $C_M = 1.0$

$1.5 \times 10^4 \leq R_e \leq 4 \times 10^5$: $C_M = 1.0002 + 0.3198\ X + 0.9029 X^2 - 0.5155\ X^3$

$R_e > 4 \times 10^5$: $C_M = 1.785$

(ii) Surface roughness SR = 1/800

$$X = \mathrm{Log}_{10}\ R_e - 4.1761$$

(a) drag coefficient C_D

$R_e < 4 \times 10^4$: $C_D = 1.4$

$4 \times 10^4 \leq R_e \leq 10^5$: $C_D = -14.894 + 141.2792\ X - 475.8207\ X^2 + 777.8457\ X^3 - 628.5346\ X^4 + 202.071\ X^5$

$10^5 < R_e \leq 4.5 \times 10^5$: $C_D = 86.4261 - 365.1992\ X + 605.5795\ X^2 - 490.4459\ X^3 + 195.1838\ X^4 - 30.6519\ X^5$

$R_e > 4.5 \times 10^5$: $C_D = 1.3$

(b) inertia coefficient C_M

$R_e < 2 \times 10^4$: $C_M = 1.0$

$2. \times 10^4 \leq R_e \leq 4 \times 10^4$: $C_M = 1.0 + 1.0628\ (X - 0.1249)$

$4 \times 10^4 < R_e \leq 10^5$: $C_M = 2.1879 - 5.9812\ X + 11.871\ X^2 - 6.1145\ X^3$

$10^5 < R_e \leq 5 \times 10^5$: $C_M = 2.8727 - 1.6573\ X + 0.6909\ X^2 - 0.075\ X^3$

$R_e > 5 \times 10^5$: $C_M = 1.7$

(iii) Surface roughness SR = 1/400

$$X = \mathrm{Log}_{10}\ Re - 4.1761$$

(a) drag coefficient C_D

$R_e < 2 \times 10^4$: $C_M = 1.56$

$2 \times 10^4 \leq R_e \leq 7 \times 10^4$: $C_D = 0.5581 + 16.8662X - 94.5351\ X^2 + 218.51228\ X^3 - 240.6813\ X^4 + 104.4497\ X^5$

$7 \times 10^4 < R_e \leq 7 \times 10^5$: $C_D = 9.3991 - 44.4711\ X + 83.4044\ X^2 - 71.8745\ X^3 + 29.3887\ X^4 - 4.6322\ X^5$

$R_e > 7 \times 10^5$: $C_D = 1.4$

(b) inertia coefficient C_M

$R_e < 2 \times 10^4$	$C_M = 1.0$
$2 \times 10^4 \leq R_e \leq 3 \times 10^4$	$C_M = 1.0 + 1.3061\,(X - 0.1249)$
$3 \times 10^4 < R_e \leq 7 \times 10^4$	$C_M = 1.4285 - 2.9769\,X + 9.6598\,X^2 - 6.5305\,X^3$
$7 \times 10^4 < R_e \leq 4 \times 10^5$	$C_M = 1.1164 + 3.31\,X - 5.1036\,X^2 + 2.9125\,X^3 - 0.5698\,X^4$
$R_e > 4 \times 10^5$	$C_M = 1.56$

(iv) Surface roughness SR = 1/200

$$X = \mathrm{Log}_{10}\,R_e - 4.1761$$

(a) drag coefficient C_D

$R_e < 2 \times 10^4$	$C_D = 1.55$
$2 \times 10^4 \leq R_e \leq 4 \times 10^4$	$C_D = 2.0475 - 11.3039\,X + 104.1955\,X^2 - 643.7928\,X^3 + 2181.5119\,X^4 - 3720.5278\,X^5 + 2507.7939\,X^6$
$4 \times 10^4 < R_e \leq 7 \times 10^5$	$C_D = 1.4615 - 3.6966\,X + 9.1219\,X^2 - 8.5953\,X^3 + 3.6699\,X^4 - 0.5971\,X^5$
$R_e > 7 \times 10^5$	$C_D = 1.5$

(b) inertia coefficient C_M

$R_e < 1.8 \times 10^4$	$C_M = 1.0$
$1.8 \times 10^4 \leq R_e \leq 2.5 \times 10^4$	$C_M = 1.05 + 1.931\,(X - 0.1249)$
$2.5 \times 10^4 < R_e \leq 4.15 \times 10^4$	$C_M = 1.4037 - 4.4352\,X + 21.3217\,X^2 - 22.4174\,X^3$
$4.15 \times 10^4 < R_e \leq 1.5 \times 10^5$	$C_M = 1.2509 + 3.8574\,X - 10.4905\,X^2 + 11.0347\,X^3 - 5.1845\,X^4 + 0.9129\,X^5$
$R_e > 1.5 \times 10^5$	$C_M = 1.38$

(v) Surface roughness SR = 1/100

$$X = \mathrm{Log}_{10}\,R_e - 4.1761$$

(a) drag coefficient C_D

$R_e < 2 \times 10^4$	$C_D = 1.41$
$2 \times 10^4 \leq R_e \leq 7 \times 10^5$	$C_D = 1.4866 - 2.309\,X + 6.8465\,X^2 - 7.8645\,X^3 + 4.3722\,X^4 - 1.1222\,X^5 + 0.0948\,X^6$
$R_e > 7 \times 10^5$	$C_D = 1.6$

(b) inertia coefficient C_M

$R_e < 1.5 \times 10^4$	$C_M = 1.04$
$1.5 \times 10^4 \leq R_e \leq 3.1 \times 10^4$	$C_M = 1.036 + 1.7503\,X - 0.0761\,X^2$
$3.1 \times 10^4 < R_e \leq 2 \times 10^5$	$C_M = 1.2829 + 2.6213\,X - 7.4473\,X^2 + 8.0337\,X^3 - 3.8519\,X^4 + 0.6905\,X^5$
$R_e > 2 \times 10^5$	$C_M = 1.33$

(vi) Surface roughness SR = 1/50

$$X = \mathrm{Log}_{10}\,R_e - 4.1761$$

(a) drag coefficient C_D

$R_e < 3 \times 10^4$	$C_D = 1.38$
$3 \times 10^4 \leq R_e \leq 7 \times 10^4$	$C_D = 1.0695 + 1.1795\,X - 0.5211\,X^2 + 0.0221\,X^3$
$7 \times 10^4 < R_e \leq 7 \times 10^5$	$C_D = 0.8594 + 2.0757\,X - 1.5825\,X^2 + 0.4015\,X^3$
$R_e > 7 \times 10^5$	$C_D = 1.78$

(b) inertia coefficient C_M

$R_e < 1.5 \times 10^4$	$C_M = 1.72$
$1.5 \times 10^4 \leq R_e \leq 2 \times 10^5$	$C_M = 1.716 - 0.6165\,X + 0.135\,X^2 + 0.0498\,X^3$
$R_e > 2 \times 10^5$	$C_M = 1.26$

4. HYDRODYNAMIC COEFFICIENTS C_D AND C_M FOR K = 60

(i) Smooth Cylinders SR = 0.0

$$X = \mathrm{Log}_{10}\,R_e - 4.301$$

(a) drag coefficient C_D

$R_e < 2 \times 10^4$: $C_D = 1.72$

$2 \times 10^4 \leq R_e \leq 1.4 \times 10^5$: $C_D = 1.705 - 1.254\,X - 0.0669\,X^2$

$1.4 \times 10^5 < R_e \leq 6 \times 10^5$: $C_D = -7.0747 + 31.4701\,X - 46.1048\,X^2 + 28.5675\,X^3 - 6.3577\,X^4$

$R_e > 6 \times 10^5$: $C_D = 0.655$

(b) inertia coefficient C_M

$R_e < 2.2 \times 10^4$: $C_M = 1.0$

$2.2 \times 10^4 \leq R_e \leq 2.35 \times 10^5$: $C_M = 0.9597 + 0.7729\,X - 0.0463\,X^2$

$2.35 \times 10^5 < R_e \leq 5 \times 10^5$: $C_M = 99.8992 - 318.9004\,X + 384.8811\,X^2 - 204.4853\,X^3 + 40.3659\,X^4$

$R_e > 5 \times 10^5$: $C_M = 1.76$

(ii) Surface roughness SR = 1/800

$$X = \text{Log}_{10} R_e - 4.301$$

(a) drag coefficient C_D

$R_e < 6 \times 10^4$: $C_D = 1.1$

$6 \times 10^4 \leq R_e \leq 1.1 \times 10^5$: $C_D = -19.4647 + 143.6034\,X - 361.6041\,X^2 + 388.5043\,X^3 - 152.1723\,X^4$

$1.1 \times 10^5 < R_e \leq 5 \times 10^5$: $C_D = 21.4083 - 95.1994\,X + 163.7244\,X^2 - 132.7213\,X^3 + 51.6068\,X^4 - 7.7754\,X^5$

$R_e > 5 \times 10^5$: $C_D = 1.315$

(b) inertia coefficient C_M

$R_e < 3 \times 10^4$: $C_M = 1.0$

$3 \times 10^4 \leq R_e \leq 6 \times 10^4$: $C_M = 1.0 + 1.8598\,(X - 0.1761)$

$6 \times 10^4 < R_e \leq 1.05 \times 10^5$: $C_M = 10.1958 - 59.7245\,X + 145.8719\,X^2 - 149.1043\,X^3 + 54.9952\,X^4$

$1.05 \times 10^5 < R_e \leq 4 \times 10^5$: $C_M = 2.4013 - 0.0866\,X - 1.3654\,X^2 + 1.132\,X^3 - 0.2576\,X^4$

$R_e > 4 \times 10^5$: $C_M = 1.74$

(iii) Surface roughness SR = 1/400

$$X = \text{Log}_{10} R_e - 4.301$$

(a) drag coefficient C_D

$R_e < 3 \times 10^4$: $C_D = 1.31$

$3 \times 10^4 \leq R_e \leq 7 \times 10^4$: $C_D = 0.7382 + 7.2392\,X - 27.2243\,X^2 + 25.6482\,X^3$

$7 \times 10^4 < R_e \leq 6 \times 10^5$: $C_D = 0.4946 - 0.8326\,X + 3.5183\,X^2 - 2.5449\,X^3 + 0.5544\,X^4$

$R_e > 6 \times 10^5$: $C_D = 1.4$

(b) inertia coefficient C_M

$R_e < 2.2 \times 10^4$: $C_M = 1.0$

$2.2 \times 10^4 \leq R_e \leq 4 \times 10^4$: $C_M = 1.2 + 1.6813\,(X - 0.1761)$

$4 \times 10^4 < R_e \leq 7 \times 10^4$: $C_M = 1.74 - 4.0624\,X + 6.1465\,X^2 + 24.3855\,X^3 - 39.3698\,X^4$

$7 \times 10^4 < R_e \leq 3 \times 10^5$: $C_M = 1.8282 + 0.9502\,X - 2.5193\,X^2 + 1.7691\,X^3 - 0.3906\,X^4$

$R_e > 3 \times 10^5$: $C_M = 1.62$

(iv) Surface roughness SR = 1/200

$$X = \text{Log}_{10} R_e - 4.301$$

(a) drag coefficient C_D

$R_e < 2 \times 10^4$: $C_D = 1.42$

$2 \times 10^4 \leq R_e \leq 4.3 \times 10^4$: $C_D = 1.4208 - 0.529\,X - 8.0382\,X^2 + 16.9846\,X^3$

$4.3 \times 10^4 < R_e \leq 7 \times 10^5$: $C_D = 0.543 + 1.4273\,X - 0.6829\,X^2 + 0.1385\,X^3 - 0.0158\,X^4 + 0.0174\,X^5$

$R_e > 7 \times 10^5$: $C_D = 1.52$

(b) inertia coefficient C_M

$R_e < 2 \times 10^4$: $C_M = 1.0$

$2 \times 10^4 \leq R_e \leq 3 \times 10^4$: $C_M = 1.0 + 1.7604\,X$

$3 \times 10^4 < R_e \leq 4.5 \times 10^4$: $C_M = -01075 + 24.0053\,X - 163.4284\,X^2 + 517.0602\,X^3 - 579.6197\,X^4$

$4.5 \times 10^4 < R_e \leq 3 \times 10^5$: $C_M = 1.8974 - 0.2003\,X - 0.7798\,X^2 + 0.7882\,X^3$

(v) Surface roughness SR = 1/100

$$X = \mathrm{Log}_{10} R_e - 4.301$$

(a) drag coefficient C_D

	$R_e < 2 \times 10^4$	$C_D = 1.38$
$2 \times 10^4 \leq$	$R_e \leq 6 \times 10^5$	$C_D = 1.3671 - 1.6618\,X + 4.9336\,X^2 - 5.205\,X^3 + 2.5167\,X^4 - 0.4698\,X^5$
	$R_e > 6 \times 10^5$	$C_D = 1.6$

(b) inertia coefficient C_M

	$R_e < 2 \times 10^4$	$C_M = 1.0$
$2 \times 10^4 \leq$	$R_e \leq 3 \times 10^4$	$C_M = 1.0 + 2.6689\,X$
$3 \times 10^4 <$	$R_e \leq 4 \times 10^4$	$C_M = 8.9199 - 147.6213\,X + 1048.7351\,X^2 - 3170.9163\,X^3 + 3491.8873\,X^4$
$4 \times 10^4 <$	$R_e \leq 2 \times 10^5$	$C_M = 1.8764 - 0.7949\,X + 0.2909\,X^2 + 0.1449\,X^3 - 0.0771\,X^4$
	$R_e > 2 \times 10^5$	$C_M = 1.46$

(vi) Surface roughness SR = 1/50

$$X = \mathrm{Log}_{10} R_e - 4.301$$

(a) drag coefficient C_D

	$R_e < 2 \times 10^4$	$C_D = 1.24$
$2 \times 10^4 \leq$	$R_e \leq 7 \times 10^5$	$C_D = 1.2423 + 0.6627\,X - 0.2815\,X^2 + 0.0195\,X^3$
	$R_e > 7 \times 10^5$	$C_D = 1.7$

(b) inertia coefficient C_M

	$R_e < 2 \times 10^4$	$C_M = 1.82$
$2 \times 10^4 \leq$	$R_e \leq 1.5 \times 10^5$	$C_M = 1.8148 - 0.8463\,X + 0.5304\,X^2 - 0.0999\,X^3$
	$R_e > 1.5 \times 10^5$	$C_M = 1.42$

5. HYDRODYNAMIC COEFFICIENTS C_D AND C_M FOR K = 100

(i) Smooth cylinders SR = 0.0

$$X = \mathrm{Log}_{10} R_e - 4.301$$

(a) drag coefficient C_D

	$R_e < 3 \times 10^4$	$C_D = 1.52$
$3 \times 10^4 \leq$	$R_e \leq 4 \times 10^5$	$C_D = 1.5519 + 0.1368\,X - 2.36\,X^2 + 1.2466\,X^3$
$4 \times 10^5 <$	$R_e \leq 10^6$	$C_D = 50.2861 - 126.7234\,X + 119.1963\,X^2 - 49.1534\,X^3 + 7.5184\,X^4$
	$R_e > 10^6$	$C_D = 0.66$

(b) inertia coefficients C_M

	$R_e < 3 \times 10^4$	$C_M = 1.0$
$3 \times 10^4 \leq$	$R_e \leq 2 \times 10^5$	$C_M = 0.8921 + 0.6541\,X + 0.0004\,X^2$
$2 \times 10^5 <$	$R_e \leq 15 \times 10^5$	$C_M = 2.6672 - 4.7262\,X + 6.0098\,X^2 - 2.8819\,X^3 + 0.474\,X^4$
	$R_e > 15 \times 10^5$	$C_M = 1.81$

(ii) Surface roughness SR = 1/800

$$X = \mathrm{Log}_{10} R_e - 4.301$$

(a) drag coefficient C_D

	$R_e < 6 \times 10^4$	$C_D = 1.4$
$6 \times 10^4 \leq$	$R_e \leq 1.4 \times 10^5$	$C_D = 11.5513 - 57.5105\,X + 125.0424\,X^2 - 127.4687\,X^3 + 49.5733\,X^4$
$1.4 \times 10^5 <$	$R_e \leq 8 \times 10^5$	$C_D = 60.8464 - 247.9907\,X + 394.674\,X^2 - 304.3779\,X^3 + 114.6302\,X^4 - 16.9443\,X^5$
	$R_e > 8 \times 10^5$	$C_D = 1.28$

(b) inertia coefficient C_M

$R_e < 4 \times 10^4$: $C_M = 1.0$

$4 \times 10^4 \leq R_e \leq 6 \times 10^4$: $C_M = 1.0 + 0.0763\,(X - 0.301)$

$6 \times 10^4 < R_e \leq 1.35 \times 10^5$: $C_M = 7.5633 - 31.5678\,X + 52.0747\,X^2 - 26.6835\,X^3$

$1.35 \times 10^5 < R_e \leq 6 \times 10^5$: $C_M = -2.6727 + 17.4755\,X - 23.5493\,X^2 + 13.4955\,X^3 - 2.8334\,X^4$

$R_e > 6 \times 10^5$: $C_M = 1.78$

(iii) Surface roughness SR = 1/400

$$X = \text{Log}_{10} R_e - 4.301$$

(a) drag coefficient C_D

$R_e < 4 \times 10^4$: $C_D = 1.4$

$4 \times 10^4 \leq R_e \leq 7.3 \times 10^4$: $C_D = -1.6801 + 24.4654\,X - 64.3408\,X^2 + 50.8865\,X^3$

$7.3 \times 10^4 < R_e \leq 8 \times 10^5$: $C_D = 0.4611 - 0.4058\,X + 2.6295\,X^2 - 1.9763\,X^3 + 0.4389\,X^4$

$R_e > 8 \times 10^5$: $C_D = 1.34$

(b) inertia coefficient C_M

$R_e < 3.6 \times 10^4$: $C_M = 1.0$

$3.6 \times 10^4 \leq R_e \leq 5 \times 10^4$: $C_M = 1.145 + 2.8351\,(X - 0.301)$

$5 \times 10^4 < R_e \leq 8 \times 10^4$: $C_M = 7.414 - 44.5966\,X + 103.9193\,X^2 - 74.8128\,X^3$

$8 \times 10^4 < R_e \leq 5 \times 10^5$: $C_M = 1.8944 + 0.4596\,X - 0.9598\,X^2 + 0.3869\,X^3$

$R_e > 5 \times 10^5$: $C_M = 1.73$

(iv) Surface roughness SR = 1/200

$$X = \text{Log}_{10} R_e - 4.301$$

(a) drag coefficient C_D

$R_e < 3 \times 10^4$: $C_D = 1.5$

$3 \times 10^4 \leq R_e \leq 5 \times 10^4$: $C_D = -1.5889 + 45.5435\,X - 253.5489\,X^2 + 576.4156\,X^3 - 468.0798\,X^4$

$5 \times 10^4 < R_e \leq 8 \times 10^5$: $C_D = 0.4747 + 1.4808\,X - 0.715\,X^2 + 0.0741\,X^3 + 0.0175\,X^4$

$R_e > 8 \times 10^5$: $C_D = 1.46$

(b) inertia coefficient C_M

$R_e < 2.7 \times 10^4$: $C_M = 1.0$

$2.7 \times 10^4 \leq R_e \leq 3.5 \times 10^4$: $C_M = 1.0 + 3.2823\,(X - 0.1304)$

$3.5 \times 10^4 < R_e \leq 5 \times 10^4$: $C_M = 3.2748 - 25.8909\,X + 101.8727\,X^2 - 115.1265\,X^3$

$5 \times 10^4 < R_e \leq 3 \times 10^5$: $C_M = 2.0283 - 0.4494\,X + 0.0089\,X^2 + 0.0933\,X^3$

$R_e > 3 \times 10^5$: $C_M = 1.68$

(v) Surface roughness SR = 1/100

$$X = \text{Log}_{10} R_e - 4.301$$

(a) drag coefficient C_D

$R_e < 2 \times 10^4$: $C_D = 1.08$

$2 \times 10^4 \leq R_e \leq 8 \times 10^5$: $C_D = 1.0761 + 0.1743\,X + 0.3714\,X^2 - 0.2266\,X^3 + 0.0253\,X^4$

$R_e > 8 \times 10^5$: $C_D = 1.55$

(b) inertia coefficient C_M

$R_e < 2 \times 10^4$: $C_M = 1.94$

$2 \times 10^4 \leq R_e \leq 4 \times 10^5$: $C_M = 1.9355 - 0.4978\,X + 0.1976\,X^2 - 0.0192\,X^3$

$R_e > 4 \times 10^5$: $C_M = 1.59$

(vi) Surface roughness SR = 1/50

$$X = \text{Log}_{10} R_e - 4.301$$

(a) <u>drag coefficient C_D</u>

$R_e < 2 \times 10^4$ $C_D = 1.24$

$2 \times 10^4 \leq R_e \leq 8 \times 10^5$ $C_D = 1.2366 + 0.0681 X + 0.6387 X^2 - 0.5203 X^3 + 0.1149 X^4$

$R_e > 8 \times 10^5$ $C_D = 1.6$

(b) <u>inertia coefficient C_M</u>

$R_e < 2 \times 10^4$ $C_M = 1.9$

$2 \times 10^4 \leq R_e \leq 5 \times 10^5$ $C_M = 1.8913 - 0.503 X + 0.1997 X^2 - 0.0162 X^3$

$R_e > 5 \times 10^5$ $C_M = 1.55$

6. <u>LIFT COEFFICIENT C_L</u>

(i) <u>Smooth cylinders SR = 0.0</u>

$$X = \mathrm{Log}_{10}\,(R_e \times 10^{-4})$$

<u>K = 10</u>

$10^4 \leq R_e \leq 2 \times 10^4$ $C_L = 3.4781 + 0.4302 X - 7.6394 X^2 + 39.6642 X^3 - 98.4265 X^4$

$2 \times 10^4 < R_e \leq 3 \times 10^4$ $C_L = 6.3965 - 10.7893 X$

$3 \times 10^4 < R_e \leq 6 \times 10^4$ $C_L = 54.3394 - 314.7259 X + 694.3959 X^2 - 680.9583 X^3 + 250.0169 X^4$

$R_e > 6 \times 10^4$ $C_L = 0.2$

<u>K = 15</u>

$10^4 \leq R_e \leq 3 \times 10^4$ $C_L = 3.1987 - 0.0288 X + 1.293 X^2 - 19.5107 X^3 + 57.7435 X^4 - 64.1787 X^5$

$3 \times 10^4 < R_e \leq 9 \times 10^4$ $C_L = 25.544 - 85.6351 X + 99.2644 X^2 - 38.4792 X^3$

$R_e > 9 \times 10^4$ $C_L = 0.2$

<u>K = 20</u>

$10^4 \leq R_e \leq 4 \times 10^4$ $C_L = 2.7496 + 0.0903 X - 8.4131 X^2 + 25.6204 X^3 - 27.307 X^4$

$4 \times 10^4 < R_e \leq 1.1 \times 10^5$ $C_L = 19.0144 - 50.5117 X + 36.4914 X^2 + 6.0396 X^3 - 10.3741 X^4$

$R_e > 1.1 \times 10^5$ $C_L = 0.2$

<u>K = 30</u>

$1.2 \times 10^4 \leq R_e \leq 7 \times 10^4$ $C_L = 1.7905 + 0.7651 X - 3.7887 X^2 + 1.3682 X^3$

$7 \times 10^4 < R_e \leq 6 \times 10^5$ $C_L = 2.3769 - 3.5486 X + 2.0205 X^2 - 0.4012 X^3$

$R_e > 6 \times 10^5$ $C_L = 0.2$

<u>K = 40</u>

$1.6 \times 10^4 \leq R_e \leq 3 \times 10^5$ $C_L = 1.1351 + 2.8439X - 9.2957 X^2 + 7.6833 X^3 - 2.0269 X^4$

$R_e > 3 \times 10^5$ $C_L = 0.2$

<u>K = 60</u>

$2.3 \times 10^4 \leq R_e \leq 2 \times 10^5$ $C_L = 1.2029 - 0.4827 X - 1.1772 X^2 + 0.7079 X^3$

$R_e > 2 \times 10^5$ $C_L = 0.185$

<u>$80 < K < 100$</u>

$3.2 \times 10^4 \leq R_e \leq 1.8 \times 10^5$ $C_L = 1.6247 - 2.6465 X + 1.533 X^2 - 0.3194 X^3$

$R_e > 1.8 \times 10^5$ $C_L = 0.18$

(ii) <u>Rough cylinders SR > 0.0</u>

$5 \leq K \leq 7$ $C_L = 0.8 - 0.485 K + 0.105 K^2$

$7 < K \leq 9$ $C_L = -8.3 + 2.425 K - 0.125 K^2$

$9 < K \leq 40$ $C_L = -0.8711 + 1.0478K - 0.0865K^2 + 3.0965 K^3 - 5.3508K^4 + 3.6631 K^5$

$40 < K \leq 100$ $C_L = 4.8704 - 0.1387 K + 1.5091 \times 10^{-3} K^2 - 5.7331 \times 10^{-6} K^3$

APPENDIX C

Velocity potential	$\phi = \dfrac{\pi H}{kT}\dfrac{\cosh(ks)}{\sinh(kd)}\sin\theta$
	$= \dfrac{gH}{2\omega}\dfrac{\cosh(ks)}{\cosh(kd)}\sin\theta$
Dispersion relation	$c^2 = \dfrac{\omega^2}{k^2} = \dfrac{g}{k}\tanh(kd)$
Surface elevation	$\eta = \dfrac{H}{2}\cos\theta$
Horizontal particle displacement	$\xi = -\dfrac{H}{2}\dfrac{\cosh(ks)}{\sinh(kd)}\sin\theta$
Vertical particle displacement	$\zeta = \dfrac{H}{2}\dfrac{\sinh(ks)}{\sinh(kd)}\cos\theta$
Horizontal particle velocity	$u = \dfrac{\pi H}{T}\dfrac{\cosh(ks)}{\sinh(kd)}\cos\theta$
Vertical particle velocity	$w = \dfrac{\pi H}{T}\dfrac{\sinh(ks)}{\sinh(kd)}\sin\theta$
Horizontal particle acceleration	$\dfrac{\partial u}{\partial t} = \dfrac{2\pi^2 H}{T^2}\dfrac{\cosh(ks)}{\sinh(kd)}\sin\theta$
Vertical particle acceleration	$\dfrac{\partial w}{\partial t} = -\dfrac{2\pi^2 H}{T^2}\dfrac{\sinh(ks)}{\sinh(kd)}\cos\theta$
Pressure	$p = -\rho gz + \dfrac{1}{2}\rho gH\dfrac{\cosh(ks)}{\cosh(kd)}\cos\theta$
Group velocity	$c_G = \dfrac{1}{2}\left[1 + \dfrac{2kd}{\sinh(2kd)}\right]c$
Average energy density	$E = \dfrac{1}{8}\rho gH^2$
Energy flux	$P = Ec_G$
Radiation stress	$S_{xx} = \left[\dfrac{1}{2} + \dfrac{2kd}{\sinh(2kd)}\right]E$
	$S_{xy} = S_{yx} = 0$
	$S_{yy} = \left[\dfrac{kd}{\sinh(2kd)}\right]E$

TABLE (C.1) Results of Airy (Linear) Wave Theory (Ref. 13)

	Shallow Water	Deep Water
Range of validity	$kd < \dfrac{\pi}{10}$	$kd > \pi$
	$\dfrac{d}{L} < \dfrac{1}{20}$	$\dfrac{d}{L} > \dfrac{1}{2}$
	$\dfrac{d}{gT^2} < 0.0025$	$\dfrac{d}{gT^2} > 0.08$
Velocity potential	$\phi = \dfrac{\pi H}{k^2 Td}\sin\theta$	$\phi = \dfrac{\pi H}{kT}e^{kz}\sin\theta$
	$= \dfrac{gH}{2\omega}\sin\theta$	$= \dfrac{gH}{2\omega}e^{kz}\sin\theta$
Dispersion relation	$c^2 = \dfrac{\omega^2}{k^2} = gd$	$c^2 = c_0^2 = \dfrac{\omega^2}{k^2} = \dfrac{g}{k}$
Wave length	$L = T\sqrt{gd}$	$L = L_0 = gT^2/2\pi$
Surface elevation	$\eta = \dfrac{H}{2}\cos\theta$	$\eta = \dfrac{H}{2}\cos\theta$
Horizontal particle displacement	$\xi = -\dfrac{H}{2kd}\sin\theta$	$\xi = -\dfrac{H}{2}e^{kz}\sin\theta$
Vertical particle displacement	$\zeta = \dfrac{H}{2}\left(1 + \dfrac{z}{d}\right)\cos\theta$	$\zeta = \dfrac{H}{2}e^{kz}\cos\theta$
Horizontal particle velocity	$u = \dfrac{\pi H}{T(kd)}\cos\theta$	$u = \dfrac{\pi H}{T}e^{kz}\cos\theta$
Vertical particle velocity	$w = \dfrac{\pi H}{T}\left(1 + \dfrac{z}{d}\right)\sin\theta$	$w = \dfrac{\pi H}{T}e^{kz}\sin\theta$
Horizontal particle acceleration	$\dfrac{\partial u}{\partial t} = \dfrac{2\pi^2 H}{T^2(kd)}\sin\theta$	$\dfrac{\partial u}{\partial t} = \dfrac{2\pi^2 H}{T^2}e^{kz}\sin\theta$
Vertical particle acceleration	$\dfrac{\partial w}{\partial t} = -\dfrac{2\pi^2 H}{T^2}\left(1 + \dfrac{z}{d}\right)\cos\theta$	$\dfrac{\partial w}{\partial t} = -\dfrac{2\pi^2 H}{T^2}e^{kz}\cos\theta$
Pressure	$p = -\rho gz + \frac{1}{2}\rho gH\cos\theta$	$p = -\rho gz + \frac{1}{2}\rho gH e^{kz}\cos\theta$
Group velocity	$c_G = c$	$c_G = \frac{1}{2}c$
Average energy density	$E = \frac{1}{8}\rho gH^2$	$E = \frac{1}{8}\rho gH^2$
Energy flux	$P = Ec$	$P = \frac{1}{2}Ec$
Radiation stress	$S_{xx} = \frac{3}{2}E$	$S_{xx} = \frac{1}{2}E$
	$S_{xy} = S_{yx} = 0$	$S_{xy} = S_{yx} = 0$
	$S_{yy} = \frac{1}{2}E$	$S_{yy} = 0$

TABLE (C.2) Shallow and Deep Water Approximations to Linear Wave Theory (Ref. 13)

Velocity potential	$\phi = \frac{\pi H}{kT}\frac{\cosh(ks)}{\sinh(kd)}\sin\theta + \frac{3}{8}\frac{\pi H}{kT}\left(\frac{\pi H}{L}\right)\frac{\cosh(2ks)}{\sinh^4(kd)}\sin 2\theta$
Dispersion relation	$c^2 = \frac{\omega^2}{k^2} = \frac{g}{k}\tanh(kd)$
Surface elevation	$\eta = \frac{H}{2}\cos\theta + \frac{H}{8}\left(\frac{\pi H}{L}\right)\frac{\cosh(kd)}{\sinh^3(kd)}[2+\cosh(2kd)]\cos 2\theta$
Horizontal particle displacement	$\xi = -\frac{H}{2}\frac{\cosh(ks)}{\sinh(kd)}\sin\theta + \frac{H}{8}\left(\frac{\pi H}{L}\right)\frac{1}{\sinh^2(kd)}\left[1-\frac{3\cosh(2ks)}{2\sinh^2(kd)}\right]\sin 2\theta + \frac{H}{4}\left(\frac{\pi H}{L}\right)\frac{\cosh(2ks)}{\sinh^2(kd)}(\omega t)$
Vertical particle displacement	$\zeta = \frac{H}{2}\frac{\sinh(ks)}{\sinh(kd)}\cos\theta + \frac{3H}{16}\left(\frac{\pi H}{L}\right)\frac{\sinh(2ks)}{\sinh^4(kd)}\cos 2\theta$
Horizontal particle velocity	$u = \frac{\pi H}{T}\frac{\cosh(ks)}{\sinh(kd)}\cos\theta + \frac{3}{4}\frac{\pi H}{T}\left(\frac{\pi H}{L}\right)\frac{\cosh(2ks)}{\sinh^4(kd)}\cos 2\theta$
Vertical particle velocity	$w = \frac{\pi H}{T}\frac{\sinh(ks)}{\sinh(kd)}\sin\theta + \frac{3}{4}\frac{\pi H}{T}\left(\frac{\pi H}{L}\right)\frac{\sinh(2ks)}{\sinh^4(kd)}\sin 2\theta$
Horizontal particle acceleration	$\frac{\partial u}{\partial t} = \frac{2\pi^2 H}{T^2}\frac{\cosh(ks)}{\sinh(kd)}\sin\theta + \frac{3\pi^2 H}{T^2}\left(\frac{\pi H}{L}\right)\frac{\cosh(2ks)}{\sinh^4(kd)}\sin 2\theta$
Vertical particle acceleration	$\frac{\partial w}{\partial t} = -\frac{2\pi^2 H}{T^2}\frac{\sinh(ks)}{\sinh(kd)}\cos\theta - \frac{3\pi^2 H}{T^2}\left(\frac{\pi H}{L}\right)\frac{\sinh(2ks)}{\sinh^4(kd)}\cos 2\theta$
Pressure	$p = -\rho g z + \frac{1}{2}\rho g H\frac{\cosh(ks)}{\cosh(kd)}\cos\theta + \frac{3}{4}\rho g H\left(\frac{\pi H}{L}\right)\frac{1}{\sinh(2kd)}\left[\frac{\cosh(2ks)}{\sinh^2(kd)}-\frac{1}{3}\right]\cos 2\theta - \frac{1}{4}\rho g H\left(\frac{\pi H}{L}\right)\frac{1}{\sinh(2kd)}[\cosh(2ks)-1]$
Average energy density	$E = \frac{1}{8}\rho g H^2\ (+0[\epsilon^4])$
Energy flux	$P = \frac{1}{16}\rho g H^2 c\left(1+\frac{2kd}{\sinh(2kd)}\right)(+0[\epsilon^4])$

TABLE (C.3) Results of Stokes Second Order Wave Theory (Ref. 13)

Velocity potential, ϕ	$\frac{k\phi}{c} = \sum_{n=1}^{5}\phi'_n\cosh(nks)\sin(n\theta)$
Wave celerity, c	$\frac{c^2}{gd} = \frac{\tanh(kd)}{kd}[1+\lambda^2 C_1+\lambda^4 C_2]$
Surface elevation, η	$k\eta = \sum_{n=1}^{5}\eta'_n\cos(n\theta)$
Horizontal particle velocity, u	$\frac{u}{c} = \sum_{n=1}^{5} n\phi'_n\cosh(nks)\cos(n\theta)$
Vertical particle velocity, w	$\frac{w}{c} = \sum_{n=1}^{5} n\phi'_n\sinh(nks)\sin(n\theta)$
Horizontal particle acceleration, $\partial u/\partial t$	$\frac{\partial u/\partial t}{\omega c} = \sum_{n=1}^{5} n^2\phi'_n\cosh(nks)\sin(n\theta)$
Vertical particle acceleration, $\partial w/\partial t$	$\frac{\partial w/\partial t}{\omega c} = -\sum_{n=1}^{5} n^2\phi'_n\sinh(nks)\cos(n\theta)$
Temporal derivative of ϕ	$\frac{\partial\phi/\partial t}{c^2} = -\sum_{n=1}^{5} n\phi'_n\cosh(nks)\cos(n\theta)$
Pressure, p	$\frac{p}{\rho g d} = 1-\frac{s}{d}-\frac{c^2}{gd}\left\{\frac{\partial\phi/\partial t}{c^2}+\frac{1}{2}\left[\left(\frac{u}{c}\right)^2+\left(\frac{w}{c}\right)^2\right]\right\}$

where

$\phi'_1 = \lambda A_{11}+\lambda^3 A_{13}+\lambda^5 A_{15},\ \phi'_2 = \lambda^2 A_{22}+\lambda^4 A_{24},$
$\phi'_3 = \lambda^3 A_{33}+\lambda^5 A_{35},\ \phi'_4 = \lambda^4 A_{44},\ \phi'_5 = \lambda^5 A_{55},$
$\eta'_1 = \lambda,\ \eta'_2 = \lambda^2 B_{22}+\lambda^4 B_{24},\ \eta'_3 = \lambda^3 B_{33}+\lambda^5 B_{35},$
$\eta'_4 = \lambda^4 B_{44},\ \eta'_5 = \lambda^5 B_{55}.$

The coefficients A, B, C are known functions of kd only, given by Skjelbreia and Hendrickson (1960).

TABLE (C.4) Results of Stokes Fifth Order Wave Theory (Ref. 13)

$$A_{11} = 1/s$$

$$A_{13} = \frac{-c^2\ (5c^2+1)}{8s^5}$$

$$A_{15} = \frac{-(1184c^{10}-1440c^8-1992c^6+2641c^4-249c^2+18)}{1536s^{11}}$$

$$A_{22} = \frac{3}{8s^4}$$

$$A_{24} = \frac{(192c^8-424c^6-312c^4+480c^2-17)}{768s^{10}}$$

$$A_{33} = \frac{(13-4c^2)}{64s^7}$$

$$A_{35} = \frac{(512c^{12}+4224c^{10}-6800c^8-12{,}808c^6+16{,}704c^4-3154c^2+107)}{4096s^{13}\ (6c^2-1)}$$

$$A_{44} = \frac{(80c^6-816c^4+1338c^2-197)}{1536s^{10}\ (6c^2-1)}$$

$$A_{55} = \frac{-(2880c^{10}-72{,}480c^8+324{,}000c^6-432{,}000c^4+163{,}470c^2-16{,}245)}{61{,}440s^{11}\ (6c^2-1)(8c^4-11c^2+3)}$$

$$B_{22} = \frac{(2c^2+1)}{4s^3}c$$

$$B_{24} = \frac{c(272c^8-504c^6-192c^4+322c^2+21)}{384s^9}$$

$$B_{33} = \frac{3(8c^6+1)}{64s^6}$$

$$B_{35} = \frac{(88{,}128c^{14}-208{,}224c^{12}+70{,}848c^{10}+54{,}000c^8-21{,}816c^6+6264c^4-54c^2-81)}{12{,}288s^{12}\ (6c^2-1)}$$

$$B_{44} = \frac{c(768c^{10}-448c^8-48c^6+48c^4+106c^2-21)}{384s^9\ (6c^2-1)}$$

$$B_{55} = \frac{(192{,}000c^{16}-262{,}720c^{14}+83{,}680c^{12}+20{,}160c^{10}-7280c^8)}{12{,}288s^{10}\ (6c^2-1)(8c^4-11c^2+3)} +$$

$$+ \frac{(7160c^6-1800c^4-1050c^2+225)}{12{,}288s^{10}\ (6c^2-1)(8c^4-11c^2+3)}$$

$$C_o^{\,2} = g\cdot \tanh(k\,d)$$

$$C_1 = \frac{(8c^4-8c^2+9)}{8s^4}$$

$$C_2 = \frac{(3840c^{12}-4096c^{10}+2592c^8-1008c^6+5944c^4-1830c^2+147)}{512s^{10}\ (6c^2-1)}$$

$$C_3 = -\frac{1}{4sc}$$

$$C_4 = \frac{(12c^8+36c^6-162c^4+141c^2-27)}{192cs^9}$$

where

$s = \mathrm{Sinh}(2\pi d/L)$

$c = \mathrm{Cosh}(2\pi d/L)$

TABLE (C.5) Coefficients of Stokes Fifth Order Theory (Ref. 13)

APPENDIX D

POLYNOMIAL EQUATIONS OF C_t AND C_s

1. Subroutine AHDCY

$SPR = S/d$

Flow Direction →

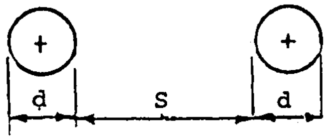

$X = SPR - 1.0$

If $1.0 < SPR < 1.85$ $\quad C_t = 0.4941\,SPR - 0.5441$

If $1.85 < SPR < 5.0$ $\quad C_t = -\,0.9412 + 3.4964\,x - 3.5486X^2 - 1.8833X^3 - 0.5487X^4 + 0.0835X^5 - 5.1803X10^{-3}X^6$

IF $5.0 < SPR < SPR <$ &.5 $\quad C_t = 0.2357SPR - 0.5321$

2. Subroutine SIDECY

$SPR = S/d$

Flow Direction →

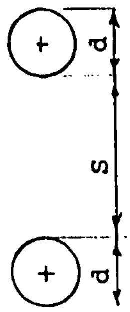

If $0.1 < SPR < 0.2$ $\quad C_s = 1.64 - 3SPR$

If $0.2 < SPR < 0.35$ $\quad C_s = 1.04$

If $0.35 < SPR < 0.65$ $\quad C_s = 1.3784 - 0.9667SPR$

If $0.65 < SPR < 1.3$ $\quad C_s = -\,54.3454 + 308.0627SPR - 676.1191SPR^2 + 726.6224SPR^3 - 381.7293SPR^4 + 78.5059SPR^5$

If $1.3 < SPR < 4.3$ $\quad C_s = 0.6691 + 1.0081SPR - 0.8218SPR^2 + 0.2992SPR^3 - 0.0516SPR^4 + 3.4402X10^{-3}SPR^5$

If $SPR > 4.3$ $\quad C_s = 1.0$

APPENDIX E

COMBINED STRESSES

Consider a cylindrical member of outer diameter 'd' and a wall thickness 't' under the action of the forces (N, F_y and F_z) and moments (Q, M_y and M_z) as shown in Fig.(E.1).

Inner diameter $\quad di = d - 2t$

Cross sectional area $\quad A = \frac{\pi}{4}(d^2 - di^2)$

Moment of inertia $\quad I = \frac{\pi}{64}(d^4 - di^4)$

Modulus of section for bending $\quad Z_b = \frac{I}{d/2} = \frac{\pi}{32}\frac{(d^4 - di^4)}{d}$

Polar moment of inertia $\quad J = \frac{\pi}{32}(d^4 - di^4)$

Modulus of section for torsion $\quad Z_p = \frac{J}{d/2} = \frac{\pi}{16}\frac{(d^4 - di^4)}{d}$

Direct stress (tension or compression) $\quad \sigma_n = \frac{N}{A}$

Shear stress due to torsion $\quad \tau_t = \frac{Q}{Z_p}$

a. Points of Maximum Bending Stresses (1 and 2)

Resultant bending moment $\quad M_R = M_y^2 + M_z^2$

$$\cos\theta = \frac{M_z}{M_R} \quad , \quad \sin\theta = \frac{M_y}{M_R}$$

At points (1) and (2), bending stress $\sigma_b = \pm \frac{M_R}{Z_b}$

Component of the shearing forces in direction of M_R producing maximum shearing stresses at point (1) or (2):-

$$F_s = F_z \cos\theta + F_y \sin\theta$$

The maximum shearing stress due to F_s is given by:-

$$\tau_f = \frac{F_s}{2It} \times M.O.A$$

where M.O.A. is the first moment of area for the semi-ring

$$M.O.A = 2\int_o^{\pi/2} r d\phi . t . r \sin\phi = 2tr^2 \int_o^{\pi/2} \sin\phi d\phi$$

$$= 2tr^2 \Big[-\cos\phi\Big]_o^{\pi/2} = 2tr^2$$

$$r = di/2$$

$$\therefore \tau_f = \frac{F_s}{2It} \cdot 2tr^2 = \frac{F_s di^2}{4I}$$

The total tension or compression stress $\sigma = \pm \sigma_b + \sigma_n$

The total shearing stress $\tau = \tau_t + \tau_f$

Hoop (Circumferential) Stresses

If the hoop stresses are to be considered they can be calculated by the formula:-

$$\sigma_h = \frac{\rho . g . H_s (d - t)}{2t}$$

$$= \frac{5.0276 H_s (d - t)}{t}$$

where H_s is the maximum static head of water below surface.

<u>Principal Stresses</u>

The principal stresses σ_1 and σ_2 and the maximum shearing stress τ can be calculated by the following equations:-

$$\sigma_1 = \tfrac{1}{2}\left[(\sigma - \sigma_h) + \sqrt{(\sigma - \sigma_h)^2 + 4\tau^2}\right]$$

$$\sigma_2 = \tfrac{1}{2}\left[(\sigma - \sigma_h) - \sqrt{(\sigma - \sigma_h)^2 + 4\tau^2}\right]$$

$$\tau_c = \tfrac{1}{2}(\sigma_1 - \sigma_2)$$

b. Points of Maximum Shearing Stresses (3 and 4)

Resultant shearing force $F_R = \sqrt{F_y^2 + F_z^2}$

$$\cos\phi = \frac{F_z}{F_R} \quad , \quad \sin\phi = \frac{F_y}{F_R}$$

At points (3) and (4) the shearing stress $\tau_f = \dfrac{F_R \cdot d_i^2}{4I}$

Components of the bending moments (M_y and M_z producing maximum bending stresses at points (3) and (4):-

$$M_c = M_z \cos\phi + M_y \sin\phi$$

The bending stress $\sigma_b = \pm \dfrac{M_c}{Z_b}$

The principal stresses σ_1 and σ_2 and τ_{max} can now be calculated as mentioned before.

Finally, from the results of case (a) and case (b), the overall maximum tension or compression stress σ_{max} and maximum shearing stress τ_{max} can be determined.

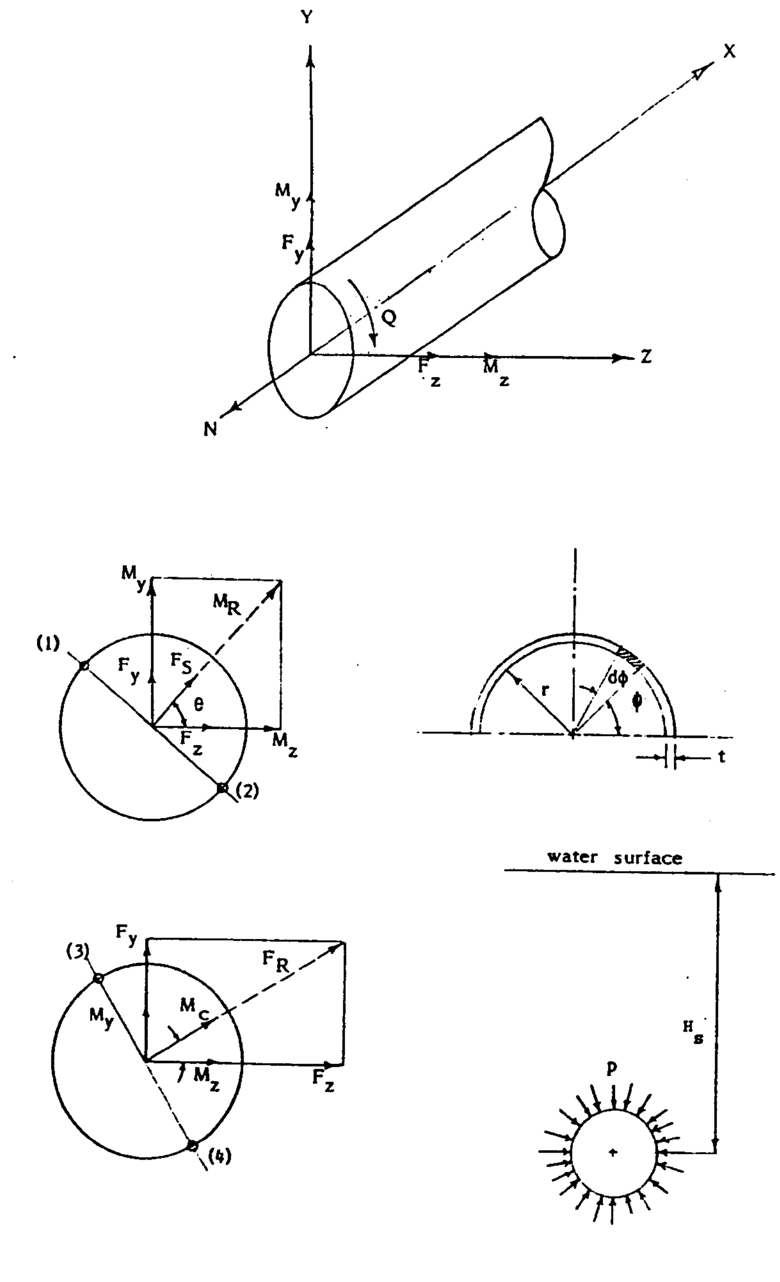

Fig. (E.1) Forces and Moments on Members